Bulletin of the
Geological Society
of Denmark

DGF

Chief editor

Ole Bennike, Geological Survey of Denmark and Greenland (GEUS), Øster Voldgade 10, DK-1350 Copenhagen K. Tel: 91333527; obe@geus.dk

Co-editors: Lotte Melchior Larsen [lml@geus.dk] and *Gunver Krarup Pedersen* [gkp@geus.dk], both Geological Survey of Denmark and Greenland (GEUS), Øster Voldgade 10, DK-1350 Copenhagen K.

Scientific editors

Lars B. Clemmensen, Department of Geosciences and Natural Resource Management, University of Copenhagen, Øster Voldgade 10, DK-1350 Copenhagen K. Tel: 35322449; E-mail: larsc@ign.ku.dk (clastic sedimentology, sedimentary basins and palaeoclimatology).

Nicolaj Krog Larsen, Globe Institute, University of Copenhagen, Øster Voldgade 5–7, DK-1350 Copenhagen K, Denmark. Tel: 20693350; E-mail: nicl@sund.ku.dk (Quaternary geology).

Jesper Milàn, Geomuseum Faxe, Østsjællands Museum, Østervej 2, DK-4640 Faxe. Tel: 23319488; E-mail: jesperm@oesm.dk (palaeontology).

Lars Nielsen, Department of Geosciences and Natural Resource Management, University of Copenhagen, Øster Voldgade 10, DK-1350 Copenhagen K. Tel: 35322454; E-mail: ln@ign.ku.dk (geophysics).

Stig Schack Pedersen, Geological Survey of Denmark and Greenland (GEUS), Øster Voldgade 10, DK-1350 Copenhagen K. Tel: 21252733; E-mail: sasp@geus.dk (structural geology and tectonics).

Jan Audun Rasmussen, Museum Mors, Fossil- og Molermuseet, Skarrehagevej 8, DK-7900 Nykøbing Mors. Tel: 42149792; E-mail: jan.rasmussen@museummors.dk (palaeontology).

Mette Elstrup Steeman, Museum Sønderjylland, Naturhistorie og Palæontologi, Lergravsvej 2, DK-6510 Gram. Tel: 73820909; E-mail: mese@museum-sonderjylland.dk (palaeontology)

Erik Thomsen, Department of Geoscience, University of Aarhus, Høegh-Guldbergs Gade 2, DK-8000 Aarhus C. Tel: 87156443; E-mail: erik.thomsen@geo.au.dk (palaeontology and stratigraphy).

Henrik Tirsgaard, Total Upstream Danmark A/S, Amerika Plads 29, DK-2100 Copenhagen Ø. Tel: 61209140; E-mail: Henrik.tirsgaard@total.com (carbonate sedimentology, petroleum geology and sedimentary basins).

Tod Waight, Department of Geosciences and Natural Resource Management, University of Copenhagen, Øster Voldgade 10, DK-1350 Copenhagen K. Tel: 35 32 24 82; E-mail: todw@ign.ku.dk (igneous petrology and geochemistry).

Cover photo: During the Danish Bicentenary Jubilee Expedition North of Greenland 1920–1923 Lauge Koch, Ittukusuk, Inuuteq and Nukagpiaanguaq reached the northern point of Greenland, Kap Morris Jesup, in May 1921. *Fieldaspis*? *iubilaei* is named in commemoration of the Jubilee Expedition. See this volume pp. 1–33: Peel, J.: Trilobite fauna of the Telt Bugt Formation (Cambrian Series 2–Miaolingian Series), western North Greenland (Laurentia).

Trilobite fauna of the Telt Bugt Formation (Cambrian Series 2–Miaolingian Series), western North Greenland (Laurentia)

JOHN S. PEEL

DGF

Trilobites dominantly of middle Cambrian (Miaolingian Series, Wuliuan Stage) age are described from the Telt Bugt Formation of Daugaard-Jensen Land, western North Greenland (Laurentia), which is a correlative of the Cape Wood Formation of Inglefield Land and Ellesmere Island, Nunavut. Four biozones are recognised in Daugaard-Jensen Land, representing the Delamaran and Topazan regional stages of the western USA. The basal *Plagiura–Poliella* Biozone, with *Mexicella* cf. *robusta*, *Kochiella*, *Fieldaspis*? and *Plagiura*?, straddles the Cambrian Series 2–Miaolingian Series boundary. It is overlain by the *Mexicella mexicana* Biozone, recognised for the first time in Greenland, with rare specimens of *Caborcella arrojosensis*. The *Glossopleura walcotti* Biozone, with *Glossopleura*, *Clavaspidella* and *Polypleuraspis*, dominates the succession in eastern Daugaard-Jensen Land but is seemingly not represented in the type section in western outcrops, likely reflecting the drastic thinning of the formation towards the north-west. The *Ehmaniella* Biozone, with *Ehmaniella*, *Clappaspsis*, *Blainia* and *Blainiopsis*, is the youngest recognised biozone. The presence of Drumian Stage strata reported elsewhere in North Greenland and adjacent Ellesmere Island has not been confirmed in Daugaard-Jensen Land. Lower beds of the Cass Fjord Formation, which directly overlie the Telt Bugt Formation, are assigned to the Guzhangian Stage. New species: *Fieldaspis*? *iubilaei*, *Ehmaniella tupeqarfik*.

Keywords: Cambrian, Miaolingian (Wuliuan), trilobites, North Greenland, Laurentia.

John S. Peel, [john.peel@pal.uu.se], Department of Earth Sciences (Palaeobiology), Uppsala University, Villavägen 16, SE-75236 Uppsala, Sweden.

On 11th August 1921, the Danish explorer, cartographer and geologist Lauge Koch (1892–1964) and three Inughuit (North Greenlandic) companions fixed tent cloth to their dog sledge and sailed before the wind down Humboldt Gletscher (Glacier) in North Greenland to safety, thus narrowly escaping death by starvation while crossing the Inland Ice (Fig. 1). A glimpse of the dramatic descent of Humboldt Gletscher in Koch's own words was presented by Dawes (2016, vol. 1, p. 41–42). The group of four left the glacier in south-western Daugaard-Jensen Land, south of Telt Bugt (Fig. 2), reaching a previously established food cache on the small island of Pullassuaq [Putlersuak of Koch 1929, pl. 3] on the next day. The three Inughuit expedition members were named as Etukussuk, Inu-

iterk and Nugapiinguak by Koch (1926). Dawes (2016, vol. 2, p. 3–4) provided portrait photographs and gave their names as Ittukusuk, Inuuteq and Nukagpiaanguaq. As members of the Danish Bicentenary Jubilee Expedition North of Greenland 1920–23 (Jubilæumsekspeditionen Nord om Grønland 1920–23), the four had survived a harrowing journey of more than 600 km across the Inland Ice, ascending the ice cap at Independence Fjord in eastern North Greenland (Fig. 1B) on 26th June after journeying around the northern coast of Greenland. For much of the homeward journey across the ice they were sustained by eating their sledge dogs, none of which survived the transect.

During subsequent evacuation to a small pre-arranged Inughuit camp at Nunatami in southern
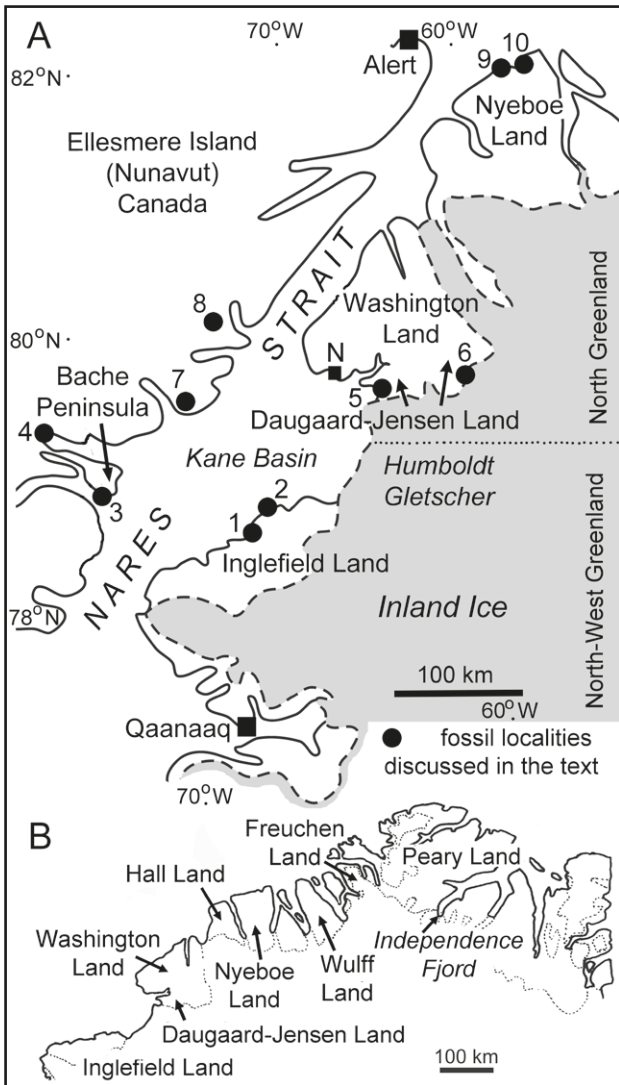
Washington Land (Fig. 1A, locality N), Koch (1929) recognised three units that comprise the geological succession between Humboldt Gletscher and Kap Clay (Fig. 2). Yellow saccharoidal dolomites, indicated as Thule Formation on the accompanying map (Koch 1929, pl. 3), are overlain by limestones that he claimed resembled the Cape Wood Formation of Inglefield Land (Poulsen 1927), and above these is the extensive outcrop of Cass Fjord Formation with its beds of intra-formational limestone conglomerates. No fossils were found in the lower two units, but a poorly preserved assemblage from the uppermost part of the Cass Fjord Formation at Kap Clay yielded an Early Ordovician fauna that was described by (Poulsen 1927). The dolomites are now referred to the Kastrup Elv Formation, equivalent to Cambrian (Series 2) carbonates in Inglefield Land (Henriksen & Peel 1976; Peel & Christie 1982; Dawes *et al*. 2000; Fig. 3), whereas the overlying limestones, which were correctly compared by Koch

◄ **Fig. 1. A:** The Nares Strait area showing fossil localities discussed in the text. 1, Kap Russell and Marshall Bugt; 2, Blomsterbækken, Kap Frederik VII, Kap Wood and Kap Kent; 3, Bache Peninsula; 4, head of Copes Bay; 5, Telt Bugt; 6, Romer Søer; 7, north of Dobbin Bay; 8, north of Scoresby Bay; 9, Hand Bugt; 10, Frankfield Bugt. N, location of Inughuit camp at Nunatami. **B:** Geographical map of northern Greenland.

▼ **Fig. 2.** Outcrops of the Telt Bugt Formation in Daugaard-Jensen Land showing the derivation of GGU samples. RS, the three lakes referred to collectively as Romer Søer.
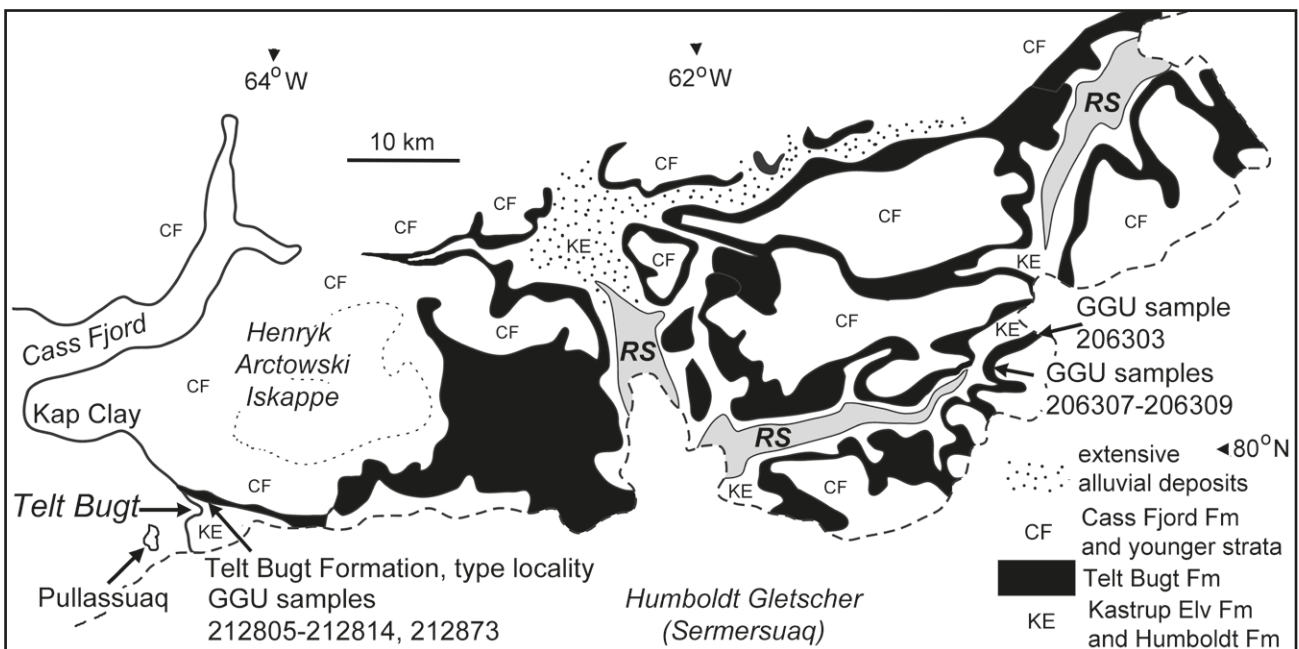
(1929) to the Cape Wood Formation, are assigned to the Telt Bugt Formation (Henriksen & Peel 1976; Peel 2020a), the subject of the present paper.

In this centenary year of their epic journey around the coast of North Greenland and the arduous return journey across the Inland Ice to the Telt Bugt area, it is appropriate to recall the many geological and cartographical successes of the expedition, and the logistic and scientific contributions of its members (Koch 1926 and numerous subsequent publications by various authors in Meddelelser om Grønland volumes 70–73; Dawes 1991). In describing the Cambrian (Miaolingian Series) trilobite fauna of the Telt Bugt Formation in southern Daugaard-Jensen Land, the present paper acknowledges these achievements in proposing *Fieldaspis*? *iubilaei* sp. nov., in commemoration.

The Telt Bugt Formation fauna is of Laurentian inner craton aspect and its trilobites are assigned to four biozones comprising the Wuliuan Stage of the Miaolingian Series: *Plagiura–Poliella* (in part), *Mexicella mexicana*, *Glossopleura walcotti* and *Ehmaniella* biozones (Fig. 4). These biozones are equivalent to the Delamaran and Topazan stages of western North America usage, for review see Babcock *et al.* (2011). The *Mexicella mexicana* Biozone is recognised for the first time in Greenland, but trilobites from the other three biozones have been described from Inglefield Land, Daugaard-Jensen Land and Bache Peninsula (Nunavut), around Kane Basin (Fig. 1A), by C. Poulsen (1927, 1946), his son V. Poulsen (1964) and Peel (2020a,b).

Geological background

Nares Strait, named after Captain Sir George Nares who led the British Expedition of 1875–1876, separates western North Greenland from easternmost Ellesmere Island, Nunavut (Fig. 1A) and provided a conduit for early ship-borne expeditions exploring the high Arctic (Christie & Dawes 1991; Dawes 2012, 2016).

Nares Strait is also the proposed site of a prominent strike–slip complex, the interpretation of which is of fundamental importance to the understanding of the evolution of the seaways between Greenland and Canada, and the placement through geological time of Greenland relative to the Laurentian mainland (Dawes & Kerr 1982; Harrison 2006; Pulvertaft & Dawes 2011; Oakey & Chalmers 2012; Frisch & Dawes 2014; Gosen *et al.* 2019). The nature, timing and magnitude of the supposed displacements along the zone are highly controversial, with estimates of the lateral displacement of Greenland relative to the rest of Laurentia ranging from as much as 350 km to 25 km or less. However, Oakey & Chalmers (2012) presented a model that attempted to accomodate both extremes, with large-scale movements between Greenland and Baffin Island – Labrador in the south, but only small displacement between eastern Ellesmere Island and Greenland in the north. The latter was advocated by geologists familiar with local stratigraphy and tectonics (Dawes & Kerr 1982; Pulvertaft & Dawes

		Inglefield Land	Bache Peninsula	Daugaard-Jensen Land	North-east Ellesmere Island (de Freitas)	(Dewing *et al.*)	Nyeboe Land
ORDOV.							
CAMBRIAN	Furong.	Cass Fjord Formation	Cass Fjord Formation	Cass Fjord Formation	Cass Fjord Formation	Cass Fjord Formation	Kap Stanton Formation
	Miaolingian						Henson Gletscher Formation
		Cape Wood Formation		TELT BUGT FORMATION	Parrish Glacier Formation		
	Series 2	Cape Kent Fm Wulff River Fm	Cape Kent Fm Police Post Fm	Kastrup Elv Fm	Scoresby Bay Formation		Aftenstjernesø Formation
		Cape Ingersoll & Cape Leiper Fms					
		Dallas Bugt Formation		Humboldt Fm			

Fig. 3. Cambrian stratigraphy around Nares Strait. Furongian and Ordovician are abbreviated. Terminology in North-east Ellesmere Island derives from de Freitas (1998a,b,c) and Dewing *et al.* (2001).

2011; Frisch & Dawes 2014). Oakey & Chalmers (2012) followed Harrison (2006) in envisaging essentially structural continuity between Inglefield Land and the area from Bache Peninsula southwards on Ellesmere Island (Fig. 1A), the Bache Peninsula arch or Inglefield Land High, the latter regarded as part of the Greenland Plate. The main zone of lateral displacement of the strike–slip complex was located on the Canadian side of the present strait and passed around the Inglefield Land High on its western side. Thus, localities 4, 7 and 8 in eastern Ellesmere Island (Fig. 1A) lie within this mobile belt. Detailed analysis of early Palaeogene faults in eastern Nunavut by Gosen *et al.* (2019) indicated some post-Mesozoic tectonism affecting the Palaeozoic outcrops, but displacement of older geological markers by this is minimal.

Cambrian strata in the Inglefield Land, Bache Peninsula and Daugaard-Jensen Land areas (Fig. 1A) were deposited on the southern inner shelf of the transarctic Franklinian Basin and their similarity confirms the integrity of the Inglefield Land High. Siliciclastic sediments of the Dallas Bugt and Humboldt formations (Fig. 3) deposited during the original Cambrian transgression are overlain by a succession dominated by carbonates that forms the lower part of the Ryder Gletscher Group (Higgins *et al.* 1991a,b; Ineson & Peel 1997; Dawes *et al.* 2000; Dawes 2004; Watt 2019; Peel 2020a). Dawes (2004) presented an overview of the geology of the Humboldt Gletscher area of Greenland, including a 1:500 000 geological map.

Christian Poulsen (1927) described Cambrian stratigraphy and faunas from Inglefield Land on the basis of collections made by Lauge Koch between 1916 and 1923. Subsequent field work by Johannes C. Troelsen during 1939–1941 resolved several lithostratigraphic problems arising from the initial surveying (Troelsen 1950) and provided new fossil collections, which were described by C. Poulsen (1958), his son V. Poulsen (1964) and Peel (2020a,b).

Peel (2020a) noted that Cambrian fossils were not discovered in Daugaard-Jensen Land on the northern margin of Humboldt Gletscher until 1969 (Dawes 1976; Palmer & Peel 1981). The fossil assemblages described in the present paper, and material documented by Palmer & Peel (1981) and Peel (2020a,b), were collected during field work carried out by Grønlands Geologiske Undersøgelse (GGU) during 1975–1977 (Henriksen & Peel 1976; Palmer & Peel 1981; Peel 2020a). Regional geological investigations on both sides of Humboldt Gletscher by the Geological Survey of Denmark and Greenland (GEUS) were resumed in 1999 (Dawes *et al.* 2000; Dawes 2004), but additional collections of Cambrian fossils were not forthcoming.

The Telt Bugt Formation was formally described by Peel (2020a) on the basis of its original naming by

Henriksen & Peel (1976) and is lithostratigraphically equivalent to the Cape Wood Formation of Inglefield Land and Bache Peninsula (Christie 1967; Peel & Christie 1982; Fig. 3).

Peel (2020b) described the trilobites *Glossopleura* and *Polypleuraspis*, originally described by Poulsen (1927), from Miaolingian (Wuliuan Stage; *Glossopleura walcotti* Biozone) strata of the Cape Wood Formation in Inglefield Land and on Bache Peninsula, Ellesmere Island (Fig. 1A), and from the lower Telt Bugt Formation in Daugaard-Jensen Land. Slightly younger trilobite assemblages (Miaolingian Series, Wuliuan Stage; *Ehmaniella* Biozone) from the Telt Bugt Formation were described by Peel (2020a). These studies are integrated into the present description of the trilobite fauna of the Telt Bugt Formation as a whole.

Biostratigraphy and correlation

In discussing the biostratigraphy of the middle Cambrian of Inglefield Land, V. Poulsen (1964, pl. 4) used the scheme with five biozones employed by Lochman-Balk & Wilson (1958) in Laurentia (Fig. 4), but only three of these biozones were recognised from collections available to him: *Plagiura–Poliella* Biozone, *Glossopleura* Biozone, and *Bathyuriscus–Elrathina* Biozone. The original five zones comprise the Delamaran, Topazan and the lower part of the Marjuman stages of some subsequent North American regional usage, the last stage also including the *Cedaria* and *Crepicephalus* biozones of the former Dresbachian Stage in addition to the zones recognised by V. Poulsen (1964). In terms of the global standard, most of this stratigraphic interval is now assigned to the Wuliuan, Drumian and Guzhangian Stages of the Miaolingian Series, the third series of the Cambrian (Babcock *et al.* 2011; Robison & Babcock 2011; Peng *et al.* 2012; Geyer 2019; Zhao *et al.* 2019; Fig. 4).

Robison (1976, 1984) introduced a biostratigraphic zonation that recognised ecological and lithological differences among trilobites from the Great Basin (mostly Utah), western USA, complementing the scheme presented by Lochman-Balk & Wilson (1958; Fig. 4). Separate zonal patterns were recognised for restricted shelf polymerids, open shelf polymerids, and open shelf agnostoids. Agnostoids from outer shelf and shelf margin environments enable worldwide correlation (Robison 1976, 1984; Babcock *et al.* 2011, 2017; Robison & Babcock 2011; Peng *et al.* 2012). Sundberg (1994, 2005), Sundberg & McCollum (2003a,b) and McCollum & Sundberg (2007) introduced a biostratigraphic scheme with speciesbased biozones for mainly inner shelf environments of the western

Great Basin (mostly Nevada) as a replacement for the previous genus-based biostratigraphy of the Delamaran and Topazan regional stages (Fig. 4). In particular, the *Plagiura–Poliella* Biozone was subdivided into three biozones, and also a number of subzones (assemblages) was proposed (Sundberg & McCollum 2003a,b; McCollum & Sundberg 2007; Fig. 4). Open shelf strata were assigned to the internationally recognised *Oryctocephalus indicus* Biozone (McCollum & Sundberg 2007).

Robison (1984) and Robison and Babcock (2011) defined six agnostoid intervalzones in middle Cambrian strata (Fig. 4). Agnostoids have not been collected from the Telt Bugt Formation but are well documented in North Greenland from Miaolingian strata in northern Nyeboe Land (Fig. 1A, localities 9, 10) and outcrops to the east (Robison 1984, 1988, 1994).

As with polymeroid zonations from elsewhere, the biozonal scheme from the western USA is based mainly on species endemic to the craton, and the refined subdivision established in that area through detailed study is not immediately applicable outside of the western USA. Rasetti (1951) described an equivalent zonation in British Columbia. While noting the close overall similarity to the Great Basin, Pratt & Bordonaro (2014) suggested a combined *Amecephalus arrojosensis–Eokochaspis nodosa* Biozone in the Precordillera of Argentina and did not record the *Poliella denticulata* Biozone. In the present context, an undivided *Plagiura–Poliella* Biozone is employed, largely on account of the scarcity of material.

As a consequence of the definition of the base of the Miaolingian Series and the Wuliuan Stage at the base of the *Oryctocephalus indicus* Biozone (Zhao *et al.* 2019), the two lowest biozones of the Delamaran regional stage recognised in the western USA by Sundberg (2018 and earlier literature) were re-assigned to Cambrian Series 2, Stage 4 (Geyer 2019; Sundberg *et al.* 2020; Fig. 4). Thus, trilobite assemblages from the Telt Bugt Formation described herein range in age from Cambrian Series 2, Stage 4 through the Wuliuan Stage of the Miaolingian.

One of the main areas of uncertainty regarding Cambrian biostratigraphy in Inglefield Land that remains after the studies of Poulsen (1927, 1958), Troelsen (1950) and V. Poulsen (1964) concerns the relationship between the historic lower and middle Cambrian (Cambrian Series 2 and 3), the latter roughly corresponding to the Miaolingian Series (Geyer 2019; Zhao *et al.* 2019). Poulsen (1927) recorded two new trilobite genera, *Kochiella* and *Dolichometopsis*, which occurr together with olenelloids in the Cape Kent Formation, referred to Cambrian Series 2 (Fig. 3). Both Poulsen (1927) and V. Poulsen (1964) were firm in their interpretation of the Cape Kent Formation as of early Cambrian age (Cambrian Series 2), but the apparent restriction of *Kochiella* to supposed middle Cambrian (Early Delamaran) in western North

	Stages	USA stages	Sundberg (2005) McCollum & Sundberg (2007)		Lochman-Balk & Wilson (1958) V. Poulsen (1964)	Robison (1984) Robison & Babcock (2011)	
SERIES	Guzhangian	Marjuman			*Crepicephalus*		*Cedaria*
					Cedaria	*Proagnostus bulbus*	
	Drumian				*Bolaspidella*	*Lejopyge laevigata*	*Bolaspidella*
						Ptychagnostus punctuosus	
						Ptychagnostus atavus	
MIAOLINGIAN	Topazan		*Ehmaniella*		*Bathyuriscus - Elrathina*	*Ptychagnostus gibbus*	
	Wuliuan	Delamaran	*Glossopleura walcotti*		*Glossopleura*	*Ptychagnostus praecurrens*	*Oryctocephalus*
			Mexicella mexicana	*Oryctocephalus indicus*	*Albertella*		
			Poliella denticulata		*Plagiura - Poliella*		
Cambrian Series 2			*Amecephalus arrojosensis Eokochaspis nodosa*				

Fig. 4. Miaolingian biostratigraphic schemes.

America prompted Sundberg & McCollum (2002) to suggest that the mainly talus-based collections from the Cape Kent Formation available to Poulsen (1927) could indicate the presence in the formation of separate faunas of early and middle Cambrian age, the latter with *Kochiella* but without olenelloids. However, Sundberg & McCollum (2003b) described a possible kochaspid occurring together with olenelloids in the basal Emigrant Formation at Split Mountain, Nevada. In current formal international nomenclature, these occurrences of *Kochiella* in western USA are derived from strata now referred in part to Cambrian Series 2, Stage 4 (Geyer 2019; Fig. 4). Resser (1933, p. 744) had previously suggested that this supposedly post-olenelloid *Kochiella* zone might be middle Cambrian in age, and Norford (1968) described *Kochiella* from strata in the District of MacKenzie interpreted as early middle Cambrian in age. The issue was discussed by Rasetti (1951, p. 85) who noted written confirmation from Christian Poulsen of the occurrence of *Kochiella* with olenelloids in the Cape Kent Formation, a position restated by V. Poulsen (1964, p. 60).

The Cape Kent Formation is overlain by the Cape Wood Formation in Inglefield Land and this has yielded a *Glossopleura* assemblage of middle Cambrian age (Miaolingian Series, Wuliuan Stage) first described by Poulsen (1927, see also V. Poulsen 1964). Faunas from the latest part of Cambrian Stage 4 and the earliest Wuliuan Stage were not identified between the Cape Kent Formation and the *Glossopleura* horizons of the Cape Wood Formation, possibly due to the sporadic nature of collection. However, V. Poulsen (1964) subsequently identified rare trilobites from clasts within a conglomerate apparently derived from the basal Cape Wood Formation, which he interpreted as a *Plagiura–Poliella* Biozone fauna.

It has not been possible to examine collections in Copenhagen made by Lauge Koch or J.C. Troelsen from Inglefield Land, with the exception of some type specimens. V. Poulsen (1964) commented on substantial extra material of several taxa in Troelsen's collections from Inglefield Land in general, but presented few illustrations, and the possibility to assess variation within previously described taxa is limited. Such examination would prove valuable to the understanding of the ontogeny and relationships of several Cambrian trilobite genera proposed by Poulsen (1927) from Inglefield Land, as well as providing increased insight into the biostratigraphy. Thus, no new information is offered here concerning the age range of the Cape Kent Formation and the composition of its fauna. The formation is not recognised in Daugaard-Jensen Land and presumed equivalent uppermost beds of the Kastrup Elv Formation (Dawes *et al.* 2000; Fig. 3) have not yielded fossils. There is no reason to question

the opinions of Christian and Valdemar Poulsen that *Kochiella* occurs together with olenelloids in Inglefield Land. However, *Kochiella* is reported herein in a small assemblage without olenelloids described from the basal Telt Bugt Formation of Daugaard-Jensen Land, on the north side of Humboldt Gletscher at Romer Søer (Fig. 2, GGU sample 206307; Fig. 5), although this description does not invalidate its reported occurrence with olenelloids in the Cape Kent Formation. The assemblage is attributed to the *Plagiura–Poliella* Biozone, which straddles the Cambrian Series 2–Miaolingian Series boundary, and it is succeeded in the Telt Bugt Formation by assemblages referred to the *Mexicella mexicana*, *Glossopleura walcotti* and *Ehmaniella* Biozones (Miaolingian Series, Wuliuan Stage; Figs 5–12). Drumian Stage assemblages (Fig. 4) have not been recognised. Faunas attributed to the Guzhangian Stage and Furongian Series from the overlying Cass Fjord Formation in Daugaard-Jensen Land were partly described by Palmer & Peel (1981).

Correlation in Daugaard-Jensen Land

The trilobite faunas described herein are derived from the Telt Bugt Formation in two areas, namely the type area around Telt Bugt, and at Romer Søer some 75 km to the east (Fig. 2). Peel (2020a) noted that the Telt Bugt Formation attained a thickness of about 45 m at Telt Bugt, increasing to approximately 100 m at Romer Søer. The formation, however, thins rapidly to the north and north-west; it is only about 5 m thick at the head of Cass Fjord but no fossils are known from that area. The available faunas from the two fossiliferous outcrops share no common taxa. The *Plagiura–Poliella* Biozone is recognised in both areas, but the *Glossopleura walcotti* Biozone is only recognised at Romer Søer. At Telt Bugt the *Plagiura–Poliella* Biozone is followed by the *Mexicella mexicana* Biozone and the *Ehmaniella* Biozone (Fig. 5). Particularly noteworthy is the absence of *Glossopleura* and related taxa from the Telt Bugt area, whereas *Glossopleura* occurs through at least 30 m of strata at Romer Søer. It is uncertain to what extent the faunal differences reflect lithostratigraphic and facies variation between the two areas witnessed by the substantial thickness variation. Available fossil collections are mainly sporadic in nature and generally small, such that gaps in collecting may accommodate unrecognised assemblages to some extent.

Plagiura–Poliella Biozone
This biozone is recognised in one small sample (GGU sample 206307) from 2 m above the base of the Telt Bugt Formation at Romer Søer (Fig. 1A, locality 6; Figs 2, 5) and in GGU sample 212806 at Telt Bugt, about 13 m above the base of the formation. GGU sample 206307

has yielded *Kochiella* sp. associated with *Fieldaspis*? *iubilaei* and *Plagiura*? sp. (Figs 5, 6). Their presence suggests comparison with the Mount Whyte Formation of British Columbia (Rasetti 1951) but also the *Plagiura–Poliella* Biozone of the Carrara Formation in the southern Great Basin (Palmer & Halley 1979), although *Kochiella* was not recorded from the latter. Norford (1968) described the morphologically similar *Kochiella mackenziensis* from the District of Mackenzie in association with *Fieldaspis* cf. *F. superba*, *Fieldaspis*? *nahanniensis* and *Inglefieldia* sp. in an association also interpreted as *Plagiura–Poliella* Biozone. *Fieldaspis*? *nahanniensis* compares well with *Fieldaspis*? *iubilaei*. *Fieldaspis* species are also well represented in strata from Nevada referred to the *Poliella denticulata* Biozone by Sundberg & McCollum (2003a), corresponding to the upper *Plagiura–Poliella* Biozone (Fig. 4).

GGU sample 212806 contains *Mexicella* cf. *robusta*, suggesting correlation with the *Amecephalus arrojosensis* Biozone of Nevada (Sundberg & McCollum 2000, p. 624), equivalent to the basal *Plagiura–Poliella* Biozone (Fig. 4). Following the international standard, the *Eoko-chaspis nodosa* Biozone is pre-Miaolingian, assigned to uppermost Stage 4 of Cambrian Series 2 (Geyer 2019).

The *Plagiura–Poliella* Biozone was recognised in Inglefield Land by V. Poulsen (1964) on the basis of three loose-lying specimens in clasts within a conglomerate considered to have been deposited at the base of the Cape Wood Formation. The fragment of a pygidium attributed to *Fieldaspis* by V. Poulsen (1964) is reminiscent of specimens identified as *Fieldaspis bilobata* by Sundberg & McCollum (2003a), but has a narrower and longer axis. Rasetti's (1951) material from the Mount Whyte Formation is wider, with more axial rings and prominent furrowing on the pleural areas than both of these. Although similar in general morphology to *Kochiella* sp., the co-occurring *Amecephalus troelseni* has narrower interocular areas, which slope away from the glabella rather than towards it, a longer (sag.), more convex, preglabellar area passing into a narrower border, and robust eye ridge (V. Poulsen 1964).

Mexicella mexicana Biozone

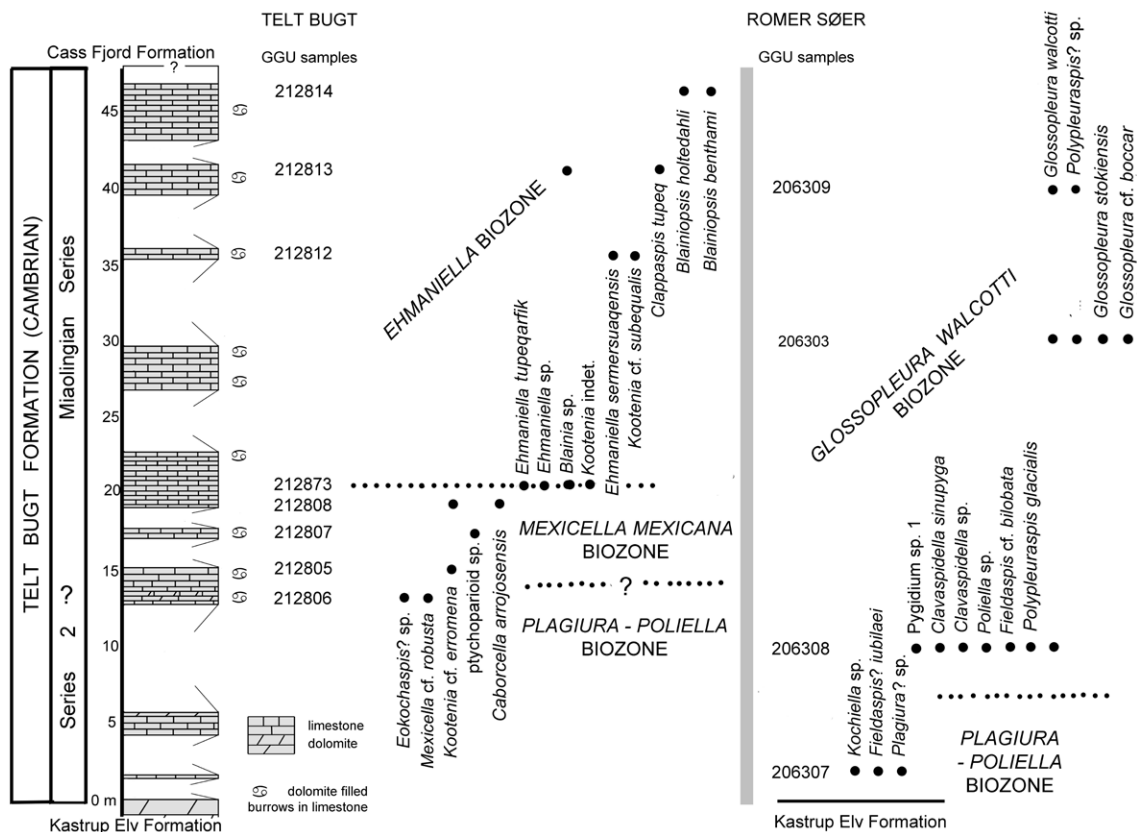GGU sample 212808 (Figs 5, 7) from Telt Bugt yielded

Fig. 5. Distribution of trilobites in the Telt Bugt Formation of Daugaard-Jensen Land at the type locality at Telt Bugt and at Romer Søer (Fig. 2). Lithological details are not available from Romer Søer, although the section height of GGU samples was recorded. Samples are located on the same vertical scale as the type section at Telt Bugt but no correlation is implied from stratigraphic thicknesses.

rare *Caborcella arrojosensis*, originally described from the Arrojos Formation of Sonora, northern Mexico (Lochman 1948). These are associated with sclerites compared to *Kootenia erromena*, described by Deiss (1939) from the Damnation Limestone (*Glossopleura walcotti* Biozone) of Montana. This *Mexicella mexicana* Biozone (or its equivalent *Albertella* Biozone) is recognised extensively in western North America (Resser 1939a; Rasetti 1951; Fritz 1968; Campbell 1974; Palmer & Halley 1979) but this is the first record from Greenland. It has not been recognised in the Romer Søer area.

Glossopleura walcotti Biozone

V. Poulsen (1964) noted almost 20 trilobite species from the *Glossopleura walcotti* Biozone in Inglefield Land, but few of these have been found in the available small samples from the Telt Bugt Formation (Fig. 5). At least 30 m of section at Romer Søer have yielded rare *Glossopleura*, including *Glossopleura walcotti*, *Clavaspidella* and *Polypleuraspis* (Figs 8–10), the last described by Peel (2020b), but the *Glossopleura walcotti* Biozone is not recognised at Telt Bugt (Fig. 5). The fauna from GGU sample 206308 at Romer Søer contains elements suggesting both the *Plagiura–Poliella* Biozone (Sundberg &
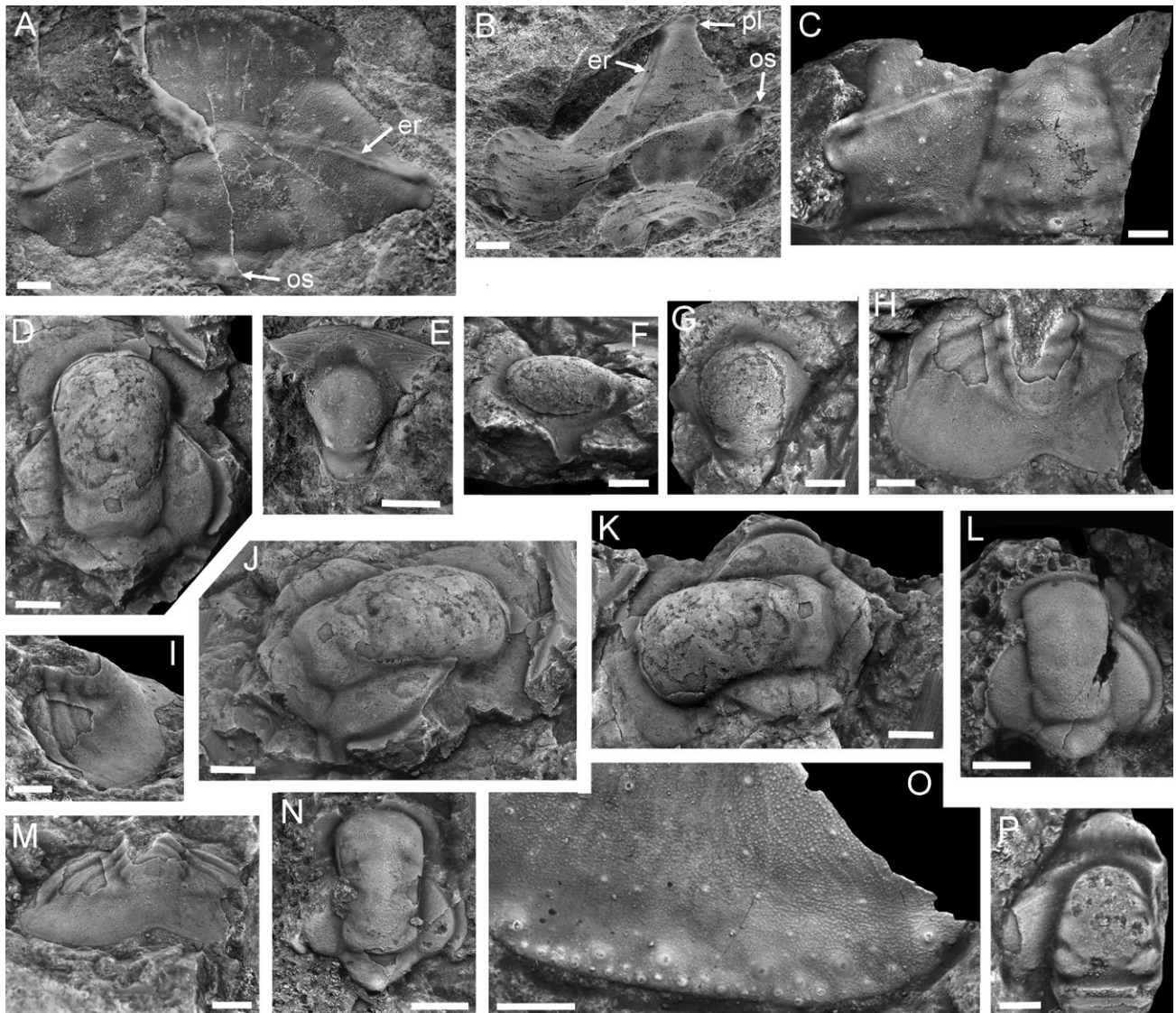

Fig. 6. Trilobites of the *Plagiura–Poliella* Biozone, Telt Bugt Formation, GGU sample 206307, Romer Søer, Daugaard-Jensen Land. **A–C**, **O**: *Kochiella* sp. **A**, **B**: MGUH 33473, digitally prepared cast of external mould of incomplete cranidium. **C**: MGUH 33474, fragment of cranidium. **O**: MGUH 33475, fragment of free cheek border. er, eye ridge; os, occipital spine; pl, palpebral lobe. **D–N**: *Fieldaspis*? *iubilaei* sp. nov. **D**, **J**, **K**: MGUH 33476, holotype, cranidium showing the flattened preglabellar field in dorsal (**D**) and oblique views. **E–G**: hypostomes. **E**: MGUH 33477. **F**, **G**: MGUH 33478. **N**, **L**: MGUH 33479 and MGUH 33480, cranidia of small individuals. **H**, **I**, **M**: MGUH 33481, pygidium. **P**: *Plagiura*? *sp.*, PMU 33482, fragment of cranidium. Scale bars: 1 mm (L, P); otherwise 2 mm.

McCollum 2003a) and the *Glossopleura walcotti* Biozone, but is referred to the latter on account of the incoming of *Clavaspidella sinupyga*.

GGU sample 212873 from Telt Bugt yielded *Ehmaniella tupeqarfik* and *Ehmaniella* sp. (Fig. 11) indicating the *Ehmaniella* Biozone. Immediately underlying strata (GGU sample 212808) contain a fauna assigned to the *Mexicella mexicana* Biozone (Fig. 7). The apparent disappearance of the *Glossopleura walcotti* Biozone from Romer Søer to Telt Bugt is likely due to regional thinning.

V. Poulsen (1964) recognised an upper *Clavaspidella* faunule and a lower *Glossopleura* faunule within the *Glossopleura* [*walcotti*] Biozone in Inglefield Land, but evidence for this separation was not unequivocal and it is not supported here. At Romer Søer, *Clavaspidella* appears before *Glossopleura*, together with species that are reminiscent of the underlying *Plagiura–Poliella* Biozone.

Ehmaniella Biozone

Trilobites indicative of the *Ehmaniella* Biozone (Figs 5, 12) were described from the upper half of the Telt Bugt Formation at Telt Bugt by Peel (2020a) and the range of the zone is extended downwards by some 15 m to include GGU sample 212873 (Figs 5, 11). The biozone has not been recognised at Romer Søer, where the upper part of the formation is talus covered.

Blainiopsis benthami, *Blainiopsis holtedahli* and *Blainia* occur in the Cape Wood Formation of Inglefield Land in a fauna referred by V. Poulsen (1964, p. 66) to the *Bathyuriscus–Elrathina* zone [= *Ehmaniella* Biozone].

Correlation in North Greenland

Miaolingian fossils were first described from northern Nyeboe Land (Fig. 1A, locality 9) by V. Poulsen (1969) on the basis of collections made by P.R. Dawes in 1966 as part of a joint Canadian–Danish project, Operation Grant Land 1965–1966. Early Cambrian fossils were recognised in the same series of collections by Peel (1974) and Dawes & Peel (1984). V. Poulsen (1969) referred the agnostoids to the *Pychagnostus punctuosus* Biozone, Drumian Stage (Fig. 4) and therefore younger than the Wuliuan Stage faunas described herein from Daugaard-Jensen Land, which lack agnostoids.

Collections from northern Nyeboe Land made during 1985 by J.S. Peel (Fig. 1A, locality 9) and A.K. Higgins (Fig. 1A, locality 10) were described by Babcock (1994a,b) and Robison (1994) who documented faunas from the *Glossopleura walcotti*, *Ptychagnostus gibbus*, *Ptychagnostus atavus* and *Ptychagnostus punctuosus* biozones (late Wuliuan and Drumian Stages; Fig. 4) from the Henson Gletscher and Kap Stanton formations (Fig. 3). The absence of other biozones may

reflect the sparse nature of collecting, not least since no fossils were available from the lowest 80 m of the Henson Gletscher Formation at this locality, but the Henson Gletscher Formation is strongly diachronous in North Greenland (Ineson & Peel 1997). The oldest assemblage in northern Nyeboe Land contains *Glossopleura walcotti* associated with *Kootenia*, *Ogygopsis*, *Syspacephalus* and undetermined ptychoparioids, but only the first of these is recognised in the Telt Bugt Formation (Figs 5, 9). In westernmost Peary Land (Fig. 1B), the lower part of the Henson Gletscher Formation is of Cambrian Series 2, Stage 4 age (Blaker & Peel 1997; Ineson & Peel 1997; Geyer & Peel 2011). The occurrence of a single specimen of *Oryctocephalus* cf. *indicus* in the upper part of the formation indicates the base of both the Miaolingian Series and the Wuliuan Stage, above an uppermost Cambrian Series 2 assemblage with *Ovatoryctocara granulata* (Geyer & Peel 2011). However, immediately overlying strata yield a *Ptychagnostus gibbus* Biozone assemblage indicating that much of the Wuliuan Stage is missing; *Glossopleura* is not recorded from this area.

Ineson & Peel (1997, p. 116) reported sparse late Miaolingian fossils from the Blue Cliffs Formation of the Ryder Gletscher Group in southern Wulff Land (Fig. 1B), likely correlative with the Cass Fjord Formation of western outcrops. Peel (in press) described an *Eldoradia* assemblage from the basal Blue Cliffs Formation in southern Wulff Land indicating a Guzhangian age (Fig. 4).

Correlation with eastern Nunavut

Poulsen (1946) recognised the similarity of Cambrian stratigraphy and faunas from Inglefield Land and Bache Peninsula (Fig. 1A, locality 3), and Troelsen (1950) and V. Poulsen (1964) presented an integrated stratigraphy. The Cape Wood Formation of Inglefield Land and Bache Peninsula is the direct equivalent of the upper Telt Bugt Formation (Peel & Christie 1982; Peel 2020a,b) and has yielded a lower assemblage with *Glossopleura* and *Polypleuraspis*, and an upper assemblage with *Blainiopsis*, which Poulsen (1946) referred to as the *Blainiopsis* horizon. V. Poulsen (1964) correlated this horizon with strata assigned to the *Bathyuriscus–Elrathina* Biozone [=*Ehmaniella* Biozone] at Blomsterbækken in Inglefield Land (Fig. 1A, locality 2). Peel (2020a) described *Blainiopsis holtedahli* and *B. benthami* from the uppermost of three fossiliferous horizons (GGU samples 212812–212814) referred to the *Ehmaniella* Biozone in the Telt Bugt Formation (Figs 5, 12), in which *Ehmaniella sermersuaqensis*, *Clappaspis tupeq*, *Blainia* and *Kootenia* also occur.

The Parrish Glacier Formation was correlated with the Cape Wood and Telt Bugt formations by de Freitas & Fritz (1995), although Dewing *et al.* (2001) integrated

the Parrish Glacier Formation into the overlying Cass Fjord Formation. Fossil collections were reported, but not described, from several localities by de Freitas (1998a–c). *Glossopleura* assemblages were noted by de Freitas (1998a) from the type section of the Parrish Glacier Formation at the head of Copes Bay (Fig. 1A, locality 4). To the north-east, at Dobbin Bay (Fig. 1A, locality 7), de Freitas (1998b) commented that the base of the Parrish Glacier Formation was dated to the *Ehmaniella* Biozone, and thus younger than the age at its type section. This observation may be relevant given the apparent absence of the underlying *Glossopleura walcotti* Biozone in the Telt Bugt Formation in its westernmost exposures, at Telt Bugt (Fig. 1A, locality 5).

Farther to the north (Fig. 1A, locality 8), de Freitas (1998c) reported highly fossiliferous limestone beds yielding diverse faunas assigned to the *Ptychagnostus gibbus* Biozone; associated assemblages were assigned to the stratigraphically older *Albertella* and *Glossopleura* Biozones. A stratigraphically younger assemblage was referred to the *Bolaspidella* Biozone (Drumian Stage). The diversity of these assemblages from locality 8 and the presence of agnostoids, eodiscoids, *Ogygopsis* and *Oryctocephalus* indicates more open shelf conditions than those present during deposition of the Telt Bugt Formation, and the faunas are more closely comparable with those in northern Nyeboe Land and western Peary Land (Babcock 1994a; Robison 1994; Blaker & Peel 1997; Geyer & Peel 2011).

Derivation of samples

With the exception of the large collection from GGU sample 212812, most of the available samples (Figs 2, 5) are small and most of the specimens are illustrated. No macrofossils other than trilobites were observed.

GGU sample 206303 was collected by J.S. Peel on 15th July 1976 from 30 m above the base of the Telt Bugt Formation, which is about 100 m thick in this section. The locality lies near the eastern extremity of the southernmost of three large lakes in Daugaard-Jensen Land, collectively referred to as Romer Søer (80°5.6′N, 60°23′W; Fig. 1A, locality 6; Fig. 2).

GGU samples 206307–206309 were collected from the Romer Søer area (80°03′N, 60°41′W; Fig. 2) by J.S. Peel on 16th July 1976 from 2 m, 10 m and 40 m, respectively, above the base of the Telt Bugt Formation, of which about 70 m are exposed in this section (Fig. 5). The boundary with the overlying Cass Fjord Formation is talus covered.

GGU samples 212805–212814 and GGU 212873 were collected by J.S. Peel on 6th–18th July 1975 from the type section of the Telt Bugt Formation (Fig. 1a, locality 5; Figs 2, 5), north-east of Telt Bugt, Daugaard-Jensen Land (79°56.3′N, 60°15′W).

Methods. Following mechanical preparation, specimens were coated with black colloidal carbon and then whitened with ammonium chloride sublimate prior to photography using a Lumenera Infinity X32 digital camera and MicroNikkor 55 mm lens. Images were assembled in Adobe Photoshop CS4; some images were stacked using Helicon Focus.

Systematic palaeontology

Repositories and abbreviations. Type and figured specimens are deposited in the type collection of the Natural History Museum of Denmark, Copenhagen (MGUH prefix) and in the palaeontological type collection of the Museum of Evolution, Uppsala University, Uppsala, Sweden (PMU prefix). GGU prefix indicates a sample made during regional geological campaigns of Grønlands Geologiske Undersøgelse (Geological Survey of Greenland), Copenhagen, Denmark (now GEUS). In the following descriptions, sagittal and transverse measurements are abbreviated to (sag.) and (trans.), denoting dimensions measured parallel and transverse to the longitudinal axis, respectively.

This published work and the nomenclatural acts it contains have been registered in ZooBank: http://zoobank.org:pub:D33C7C2A-05EA-4ED8-B93C-FA0E8BEF6392

Class Trilobita Walch 1771

Order Corynexochida Kobayashi 1935

Family Dorypygidae Kobayashi 1935

Genus *Kootenia* Walcott 1889

Type species. Bathyuriscus (Kootenia) dawsoni Walcott 1889.

Discussion. Sundberg (1994) clarified the distinction between *Kootenia* Walcott 1889, *Olenoides* Walcott 1889 and *Dorypyge* Dames 1883.

Dorypyge resseri Poulsen 1927 and *Dorypyge obliquespina* Poulsen 1927 from the Cape Wood Formation of Inglefield Land were referred to *Kootenia* by Resser (1937) and V. Poulsen (1964). V. Poulsen (1964) also recorded the latter from the *Glossopleura* Biozone of Bache Peninsula (Fig. 1A, locality 3) and described, as *Kootenia* cf. *billingsi* Rasetti 1948, a pygidium from the upper part of the Cape Wood Formation at Blomsterbækken (Fig. 1A, locality 2). An indeterminate fragment of *Kootenia* is recorded from GGU sample 212873 (Fig. 5).

Kootenia **cf.** *erromena* Deiss 1939
Fig. 7A–G, J–M

Figured material. Cranidia: MGUH 33483 and MGUH 33488 from GGU sample 212805; MGUH 33486 from GGU sample 212808. Hypostomes: MGUH 33484 and MGUH 33485 from GGU sample 212805. Pygidia: MGUH 33487 from GGU sample 212805; MGUH 33489 and MGUH 33490 from GGU sample 212808. Telt Bugt Formation, Telt Bugt. Miaolingian Series, Wuliuan Stage, *Mexicella mexicana* Biozone.

Description. Small cranidium is wider than long, with posterior limb of fixigenae as wide as maximum transverse width (*c*. 4 mm) at the front of the slightly concavesided glabella (Fig. 7G). Palpebral lobe terminating at just anterior of mid-length (sag.) of glabella. Frontal areas of fixigenae with concave brim, reduced to a narrow groove and rim in front of the shallowly convex effaced glabella.

Large cranidium with parallel-sided glabella rather strongly curved from the occipital ring almost to the anterior margin. Axial furrow broad, shallowing slightly at the anterior limbs of the fixigenae and narrowing, as does the brim, as it passes in front of the glabella. Glabella and fixigenae uniformly convex, the latter sloping down steeply as the distal margins of the posterior fixigenae are approached. Occipital furrow broad, deeper laterally. Occipital ring posteriorly extended, probably with a short, blunt spine or node.

Thorax and librigenae not known. Hypostome with parallel sides and truncated posterior (Fig. 7C); anterior margin uniformly convex in plan view with flattened, stout, anterior wings passing in front of the oval anterior lobe of the median body as a shallowly concave border. Anterior lobe separated from posterior lobe by a shallow, posteriorly convex, transverse furrow, which joins laterally with a broad marginal furrow that extends from close to the anterior wings around the posterior margin. Junction between lateral margins and posterior margin sharply angular, with minute incipient spine, two more of which may be located equidistantly on the lateral margins posterior to the transverse furrow.

Length of pygidium about three quarters of its maximum transverse width, including spines, with maximum anterior width of axis greater than pleural area. Axis strongly convex, tapering posteriorly with three prominent rings delimited by transverse furrows and a fourth ring grading into the terminal piece, the latter terminating just prior to the posterior margin of the border. Pleural areas with well defined pleural and interpleural furrows terminating at abrupt transition to the shallowly convex border. Margin with five or six pairs of needle-shaped spines arising from

flattened triangular bases; spines forming the sixth pair short, about half the length of those forming the fifth pair, or absent.

Smooth, or with ornamentation of fine pits in a dimpled pattern.

Discussion. *Kootenia erromena* Deiss 1939 was described from the Damnation Limestone of north-western Montana where it forms part of a *Glossopleura–Kootenia* assemblage (Deiss 1939) of early Wuliuan age; it has a slightly narrower axis than specimens from the Telt Bugt Formation. Pygidia of *Kootenia* cf. *erromena* are also distinguished from those of *Kootenia resseri* (Poulsen 1927), *K. obliquespina* (Poulsen 1927) and *K.* cf. *billingsi* of V. Poulsen (1964) from the Cape Wood Formation of Inglefield Land by the greater width of their axis. In specimens of *Kootenia* cf. *erromena* from the Telt Bugt Formation, the maximum transverse width of the pygidial axis is also greater than each pleural area whereas it is narrower in species described by Poulsen (1927) and V. Poulsen (1964).

Specimens of *Kootenia* cf. *erromena* from GGU sample 212805 are otherwise similar to *K. resseri* in that the pygidium usually has six pairs of spines, an axis with three rings and long tail piece (the latter includes an incipient fourth ring in *K.* cf. *erromena*), and a well-developed border; cranidia of *K. resseri* were not described by Poulsen (1927) nor by V. Poulsen (1964). Poulsen's (1927) figures of *Kootenia obliquespina* are too small to permit precise comparison, but four axial rings appear to be present. An associated but poorly preserved cranidium seems comparable to those from Telt Bugt. *Kootenia* cf. *billingsi* of V. Poulsen (1964, pl. 1, fig. 8) is similar to *Kootenia* cf. *erromena* in preserving six pairs of pygidial spines, with the spines forming the sixth, most posterior, pair being greatly reduced in length. This is a feature of specimens from GGU sample 212805 (Fig. 7E,L) but also of other described species of *Kootenia*, e.g. *Kootenia quadriceps* (Hall & Whitfield 1877) and *Kootenia quebecensis* Rasetti 1948. However, three pygidia of *Kootenia* cf. *erromena* from GGU sample 212808, and a single specimen from GGU sample 212873, possess only five pairs of shorter spines (Fig. 7M) or just a rudimentary sixth pair (Fig. 7J).

Pygidia of *Kootenia* cf. *erromena* resemble a poorly preserved specimen, reportedly with six pairs of spines, from the *Glossopleura walcotti* Biozone figured by Sundberg (2005, fig. 6.15) from the Chisholm Formation, Drum Mountains, Utah, in the proportions of the axis, but the spines in the latter are more robust and pleural furrowing is less distinct. *Kootenia quadriceps*, as illustrated by Palmer (1954, pl. 14, figs 1–4) from the Ute Limestone of Blacksmith Fork, Utah, has longer pygidial spines but its axis is narrower than *Kootenia* cf. *erromena*. Both *Kootenia quadriceps* and *Kootenia* cf.

erromena have a parallel-sided glabella but the eyes are located more posteriorly in the latter, whereas the border in front of the anterior fixigenae is more strongly upturned in *Kootenia quadriceps*.

***Kootenia* cf. *subequalis* Deiss 1939**
Fig. 12E

2020a *Kootenia* cf. *subequalis*; Peel, p. 6, fig. 3K.

Figured material. Cranidium, PMU 35702 from GGU sample 212812, Telt Bugt Formation, Telt Bugt. Miaolingian Series, Wuliuan Stage, *Ehmaniella* Biozone.

Discussion. This poorly preserved glabella is similar to *Kootenia subequalis* Deiss 1939 from the Pentagon Shale (Miaolingian) of Montana, but the posterior fixed cheeks are shorter in the Telt Bugt specimen.

Family Dolichometopidae Walcott 1916

Genus *Poliella* Walcott 1916
Type species. Bathyuriscus (Poliella) anteros Walcott 1916.
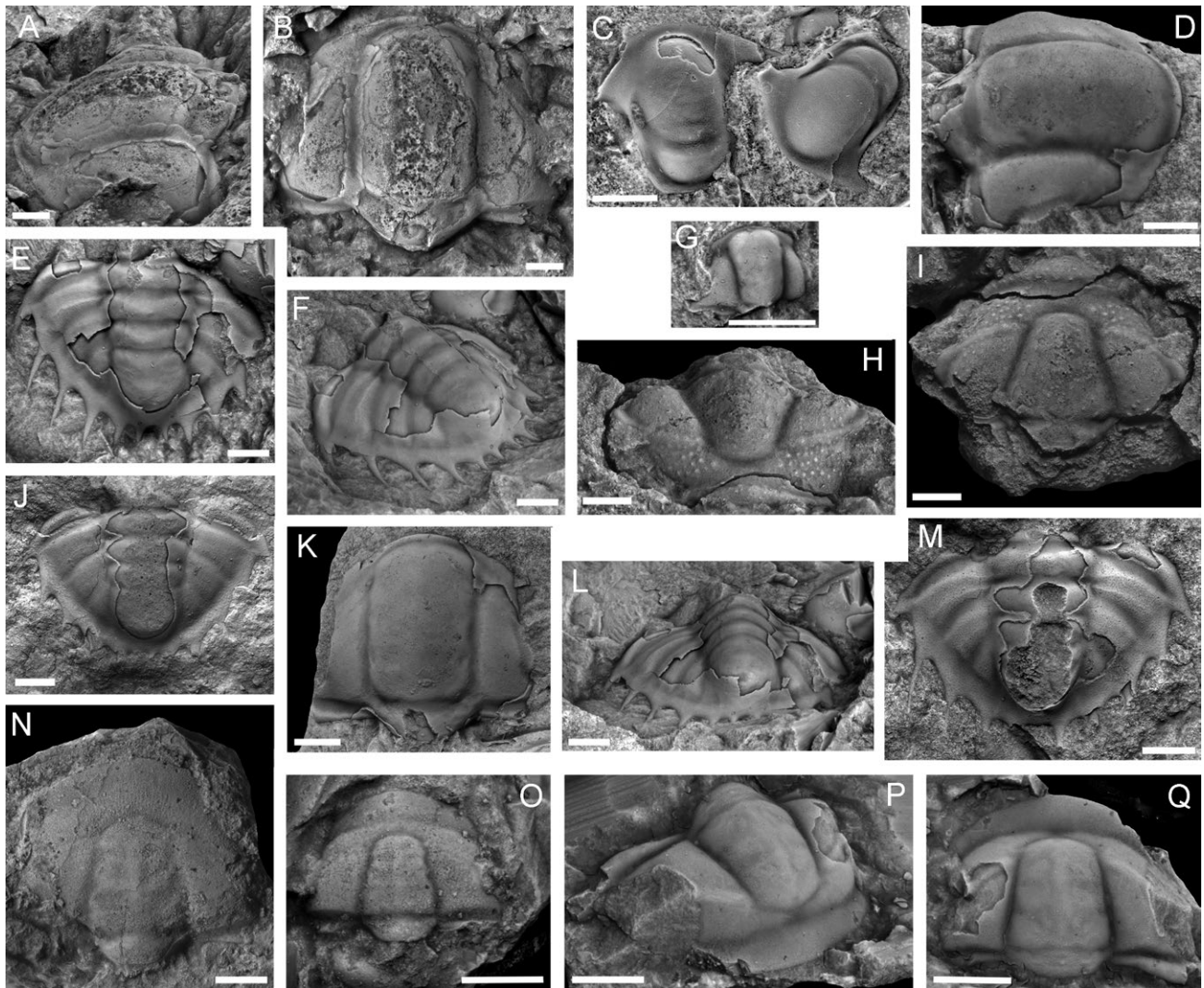
***Poliella*? sp.**
Fig. 8A

Fig. 7. Trilobites of the *Mexicella mexicana* Biozone, Telt Bugt Formation, GGU samples 212805–212808, Telt Bugt, Daugaard-Jensen Land. **A–G, J–M:** *Kootenia* cf. *erromena* Deiss 1939. **A, B:** MGUH 33483, cranidium, GGU sample 212805. **C:** MGUH 33484 and MGUH 33485, hyperstomes, GGU sample 212805. **D, K:** MGUH 33486, cranidium, GGU sample 212808. **E, F, L:** MGUH 33487, pygidium, GGU sample 212805. **G:** MGUH 33488, small cranidium, GGU sample 212805. **J:** MGUH 33489, pygidium, GGU sample 212808. **M:** MGUH 33490, pygidium, GGU sample 212808. **H, I:** *Caborcella arrojosensis* Lochman 1948, MGUH 33491, cranidium, GGU sample 212808. **N:** *Mexicella* cf. *mexicana* Lochman 1948, MGUH 33492, cranidium, GGU sample 212806. **O:** *Eokochaspis*? sp., MGUH 33493, cranidium, GGU sample 212806. **P, Q:** ptychoparioid sp., MGUH 33494, cranidium, GGU sample 212807. Scale bars: 2 mm.

Figured material. Cranidium, MGUH 33495 from GGU sample 206308. Telt Bugt Formation, Romer Søer. Miaolingian Series, Wuliuan Stage, *Glossopleura walcotti* Biozone.

Discussion. The single fragmentary cranidium has a glabella with almost parallel sides, a broad occipital furrow and four pairs of glabellar furrows, which are effaced medially. The axial furrow shallows anteriorly, almost disappearing at S4, but re-appearing as a broad, shallowly concave, preglabellar field. A shallowly convex brim anterior to this preglabellar furrow widens as it passes laterally into the anterior lobes of the fixigenae. The palpebral lobes are broad, uniformly convex in transverse profile and with a well-defined broad furrow on their axial side delimiting shallowly convex interocular areas from the axial furrow. The palpebral lobes terminate anteriorly at the axial furrow. The occipital ring is seemingly broad (sag.); posterior lobes of fixigenae and other skeletal elements are not known. The surface is ornamented with an irregular cellular pattern of fine ridges in which individual cells become elongated, passing into terrace ridges parallel to the margin on the frontal area. The ornamentation is only weakly expressed on the palpebral lobes and in the glabellar furrows.

The cranidium can be compared to a specimen from the Mount Whyte Formation (early Miaolingian) of British Columbia, which Rasetti (1951, pl. 12, fig. 10) assigned to *Poliella prima* Walcott 1916, in terms of the narrowness of the glabella and the shape of the frontal area, although the glabella expands slightly towards the anterior in that specimen. It differs in terms of its cellular ornamentation, with the Canadian material reportedly smooth (Rasetti 1951), and its glabellar furrows being equally developed.

Poliella? sp. differs from the co-occurring *Fieldaspis*? *iubilaei* sp. nov. in the form of the axial groove around the front of the glabella in the latter species. Its ornamentation is finely granular in contrast to the cellular pattern on the cranidium of *Poliella*? sp. Cranidia of *Fieldaspis bilobata* illustrated by Rasetti (1951) are distinguished by the anterior brim being turned up, in contact with the front of the glabella, and the corresponding very narrow anterior groove.

The cranidium of *Poliella*? sp. occurs together with two pygidia in GGU sample 206308, each of which could be referred to *Poliella*? sp. One of these (Fig. 9K–M) is described herein as *Fieldaspis* cf. *bilobata* Rasetti 1951 but the presence of similar ornamentation around the border may suggest reference to *Poliella*? sp. The second pygidium (Pygidium sp. 1; Fig. 9G,I,J) is similar in shape to pygidia of *Poliella* species illustrated by Sundberg & McCollum (2003a, fig. 10). It differs from these in having a greater number of axial rings, in which respect it is similar to *Fieldaspis* cf. *bilobata*.

Genus *Clavaspidella* Poulsen 1927

Type species. *Clavaspidella sinupyga* Poulsen 1927 from the Cape Wood Formation, Marshall Bugt, Inglefield Land.

Discussion. Poulsen (1927) assigned three species from Inglefield Land to his new genus *Clavaspidella*. The material was collected from boulders at Kap Frederik VII and assigned to the Cape Frederik VII Formation, erroneously thought at that time to be of Lower Ozarkian(?) age (Poulsen 1927). Resser (1935, 1939a,b) applied the generic name to a number of North American species, considering the genus to be a senior synonym of *Athabaskia* Raymond 1928, an opinion not shared by Kobayashi (1942). Lochman *in* Cooper *et al.* (1952, p. 128) also rejected the synonymy, following comparison of type material, concluding that all species from the Cordilleran region should be assigned to *Athabaskia* and confirming the opinion of Kobayashi (1942). Bordonaro (2014) referred material from Argentina previously assigned to *Clavaspidella* to *Athabaskia*. V. Poulsen (1964) accepted the conclusions of Lochman *in* Cooper *et al.* (1952) noting, as did Kobayashi (1942), that *Clavaspidella* was probably restricted to North-West Greenland. He observed that *Clavaspidella* occurred in the *Glossopleura* Biozone of Inglefield Land, following Troelsen's (1950) inclusion of the Cape Frederik VII Formation within the Cape Wood Formation, and described an additional species, *Clavaspidella ovaticauda* V. Poulsen 1964, based on four pygidia.

Clavaspidella was tentatively reported from Bache Peninsula by Poulsen (1946), from the Hawke Bay Formation of western Newfoundland (Knight & Boyce 1987) and from the Parrish Glacier Formation of eastern Ellesmere Island (de Freitas 1998a).

Poulsen *in* Harrington *et al.* (1959, p. O224) noted the well-defined eye ridges as characteristic of *Clavaspidella*, a feature not mentioned by Lochman *in* Cooper *et al.* (1952) or V. Poulsen (1964) but evident in the illustration of the lectotype figured by Poulsen (1927, pl. 17, fig. 19; not holotype as stated by V. Poulsen 1964, p. 23). Lochman *in* Cooper *et al.* (1952) stressed the greater width of the fixigenae in *Clavaspidella* relative to *Athabaskia* and differences in the shape of the posterior glabella. V. Poulsen (1964) emphasized the presence in pygidia of *Clavaspidella* of the axial indentation, a morphological feature not seen in *Athabaskia*.

Clavaspidella sinupyga Poulsen 1927
Fig. 8P–S

1927 *Clavaspidella sinupyga* Poulsen, p. 277, pl. 17, figs. 21–22.

Figured material. Pygidia: MGUH 33498 and MGUH 33499 from GGU sample 206308, Telt Bugt Formation, Romer Søer. Miaolingian Series, Wuliuan Stage, *Glossopleura walcotti* Biozone.

Discussion. Two large exfoliated pygidia display the characteristic narrow axis and broad, concave brim, which is indented medially at the posterior margin. The transition from the pleural areas to the brim is abrupt and angular, but without a furrow. Pleural furrows are deeper at this transition, producing a pitted appearance. *Clavaspidella ovaticauda* V. Poulsen 1964 from the Cape Wood Formation at Kap Frederik VII (Fig. 1A, locality 2) differs in its wider axis and more backwards curved pleurae.
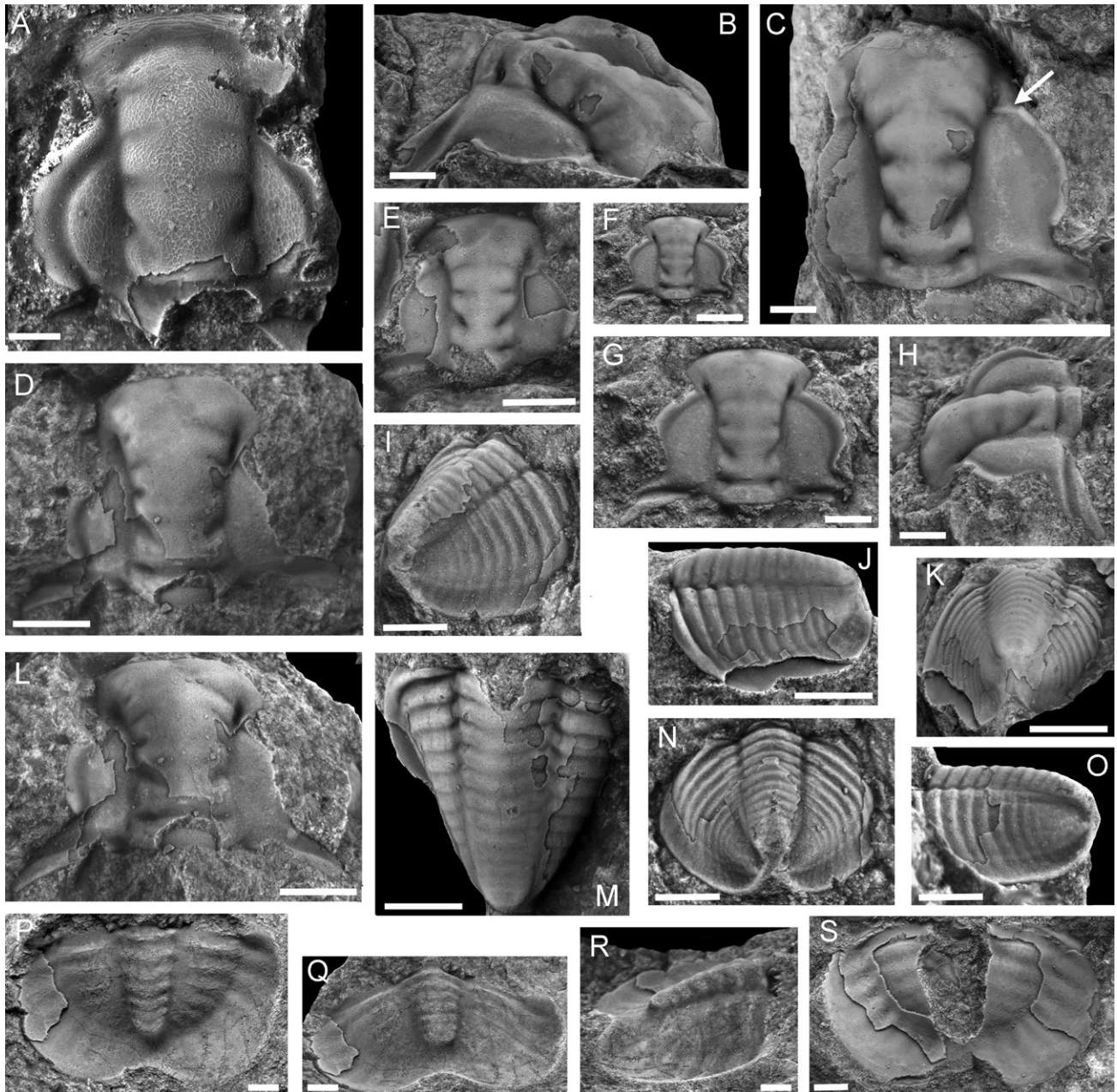

Fig. 8. Trilobites of the *Glossopleura walcotti* Biozone, Telt Bugt Formation, GGU sample 206308, Romer Søer, Daugaard-Jensen Land. **A**: *Poliella*? sp., MGUH 33495, cranidium with prominent honeycomb-like ornamentation. **B, C, F–H**: *Clavaspidella* sp., **B**, **C**: MGUH 33496, cranidium with arrow indicating eye ridge. **F–H**: MGUH 33497, small cranidium (**F** at same scale as **C**). **D, E, I–O**: *Polypleuraspis glacialis* Peel 2020b. **D, L**: PMU 35037, cranidium. **E**: PMU 35039, cranidium. **I, N, O**: PMU 35038 (.14), holotype, pygidium. **J, K, M**: PMU 35040 (.16), pygidium. **P–S**: *Clavaspidella sinupyga* Poulsen 1927. **P–R**: MGUH 33498 (.12), internal mould of pygidium. **S**: MGUH 33499, exfoliated, broken pygidium. Scale bars: 1 mm (**A**), otherwise 2 mm.

Clavaspidella sp.
Fig. 8B, C, F–H

Figured material. Cranidia: MGUH 33496 and MGUH 33497 from GGU sample 206308, Telt Bugt Formation, Romer Søer. Miaolingian Series, Wuliuan Stage, *Glossopleura walcotti* Biozone.

Discussion. While the rapidly expanding glabella with concave sides, wide fixigenae and transverse eye ridge (Fig. 8C, arrrow) indicate assignment to *Clavaspidella*, the narrowness of the glabella in *Clavaspidella* sp. is not characteristic of any of the three species described by Poulsen (1927) and invites comparison with *Polypleuraspis solitaria* Poulsen 1927, as illustrated by Peel (2020b). The latter, however, has narrower interocular areas and eye ridges that curve in gradually to meet the axial furrow. The posterior limb of the fixed cheeks in *Clavaspidella* sp. is shorter (trans.) than in *Polypleuraspis*, relative to the width of the interocular area (Fig. 8C).

The ratio of glabellar length (sag.) to glabellar maximum width (trans.) is about 1.25 in the lectotype of the type species *Clavaspidella sinupyga* and in *Clavaspidella platyrrhina* Poulsen 1927, but about 1.75 in the largest available specimen of *Clavaspidella* sp. from GGU sample 206308 (Fig. 8B,C). The same ratio is 1.5 in the single cranidium described as *Clavaspidella quinquesulcata* Poulsen 1927, but the nature of the palpebral lobes and eye ridges (if present) is not clear from the single tiny illustration (Poulsen 1927, pl. 17, fig. 23).

Eye ridges are not seen in small specimens of *Clavaspidella* sp. which are placed here on account of the perpendicular relationship between the anterior end of the palpebral lobes and the lateral margin of the anterior fixigenae (Fig. 8F–H). In these, the anterior margin is more shallowly convex than in the illustrated large specimen (Fig. 8C), shown at the same scale, a feature which Poulsen (1927) considered characteristic of *Clavaspidella platyrrhina*. However, the lectotype of that species, here designated as the specimen illustrated as Poulsen (1927, pl. 17, fig. 24), has well developed eye ridges.

V. Poulsen (1964) did not discuss *Clavaspidella platyrrhina* and *Clavaspidella quinquesulcata*, although the names were retained in his faunal list (Poulsen 1964, p. 64). In view of the variation in glabellar form in the available small sample, the current material from Daugaard-Jensen Land is not assigned at species level. However, *Clavaspidella* sp. occurs in the same sample as pygidia that are referred to *Clavaspidella sinupyga* (Fig. 8P–S).

Genus *Glossopleura* Poulsen 1927

Type species. Dolichometopus boccar Walcott 1916 from the Stephen Formation, Miaolingian Series, British Columbia.

Glossopleura walcotti Poulsen 1927
Fig. 9A–F, H; Fig. 10K–M

1927 *Glossopleura walcotti* Poulsen, p. 268, pl. 16, figs 20–30.
1964 *Glossopleura walcotti*, Poulsen, p. 25, pl. 1, figs 2–4, text-fig. 3–4.
1979 *Glossopleura walcotti*, Palmer & Halley, p. 79, pl. 16, figs 6–8, 11–19.
1994 *Glossopleura walcotti*, Babcock, 1994a, p. 94, fig. 12.
2018 *Glossopleura walcotti*, Sundberg, p. 19, fig. 13.1–13.7.
2020b *Glossopleura walcotti*, Peel, fig. 3A–G.

Figured material. Cranidium, PMU 35046; free cheek, MGUH 33500; pygidium, PMU 35047; hypostome, MGUH 33501, all from GGU sample 206308. Cranidia: MGUH 33512 and MGUH 33513; pygidia: MGUH 33510 and MGUH 33511, all from GGU sample 206309. Telt Bugt Formation, Romer Søer, Miaolingian Series, Wuliuan Stage, *Glossopleura walcotti* Biozone.

Discussion. Following its original description, *Glossopleura walcotti* Poulsen 1927 was fully described by V. Poulsen (1964), Palmer & Halley (1979) and Foglia & Vaccari (2010). It was described from the Henson Gletscher Formation in northern Nyeboe Land (Fig. 1A, locality 9), North Greenland, by Babcock (1994a) and illustrated by Peel (2020b) from the Cape Wood Formation of Inglefield Land and Bache Peninsula, and the Telt Bugt Formation of Daugaard-Jensen Land. A *Glossopleura* Biozone has been widely recognised for many years but McCollum & Sundberg (2007) refined this to the *Glossopleura walcotti* Zone, the *Glossopleura walcotti/Ptychagnostus praecurrens* Zone of Sundberg (2018).

Glossopleura stokiensis Rasetti 1951
Fig. 10H

1951 *Glossopleura stokiensis* Rasetti, p. 166, pl. 23, figs 6–10.

Figured material. Pygidium with thoracic segments, MGUH 33506 from GGU sample 206303, Telt Bugt Formation, Romer Søer. Miaolingian Series, Wuliuan Stage, *Glossopleura walcotti* Biozone.

Discussion. This distinctive pygidium is known as an external mould with parts of five pleural segments

and is illustrated as a digital cast, corresponding to the outer surface (Fig. 10H). A second example is associated with a *Polypleuraspis solitaria* specimen designated MGUH 2305 (Peel 2020b, fig. 2D) from the Cape Wood Formation of Blomsterbækken in Inglefield Land (Fig. 1A, locality 2). The pleural segments are sharply pointed with a fine proximal tuberculation and prominent terrace lines distally.

The pygidium is elliptical, with length about two thirds of width. The axis is broad with five rings, the most posterior of which grades into a slightly raised terminal piece. The articulating half ring is sharply delimited by a complete furrow. The three following axial furrows are broad, shallow and only weakly expressed medially, and become indistinct posteriorly. Pleural fields are each about half the width of the axis and lack furrows. They steepen in profile before passing abruptly, but without a delimiting furrow, onto a flat border, which is equal in width to the maximum transverse width of the axis and terminates in a shallow median excavation. Ornamentation consists of fine meandering ridges, which are most prominent on the axis, and numerous small pores. On the border, the ridges pass distally into an increasingly coarser, sub-parallel pattern of terrace ridges.

Glossopleura stokiensis Rasetti 1951 was originally described from the Cathedral Limestone of British Columbia by Rasetti (1951) who considered it to be closely related to *Glossopleura walcotti.* However, pygidia of *Glossopleura walcotti* from Daugaard-Jensen Land differ in having a narrower axis, a less curved anterior margin, welldeveloped pleural furrows and a narrower border (Fig. 9E). *Glossopleura expansa* Poulsen 1927 also has a narrow axis and was placed in synonymy of *Glossopleura walcotti* by V. Poulsen (1964) and by Babcock (1994a, in part).

A similar specimen from the Spence Shale of Antimony Canyon, northern Utah, was illustrated by Campbell (1974, pl. 6, figs 7,8) as *Glossopleura* sp. undet. 1. The latter differs in having a border which becomes wider posteriorly and in preserving traces of furrows on the pleural fields not seen in the Greenland specimen. The pygidium of *Glossopleura yatesi* Robison & Babcock 2011 is closely similar to the Greenland
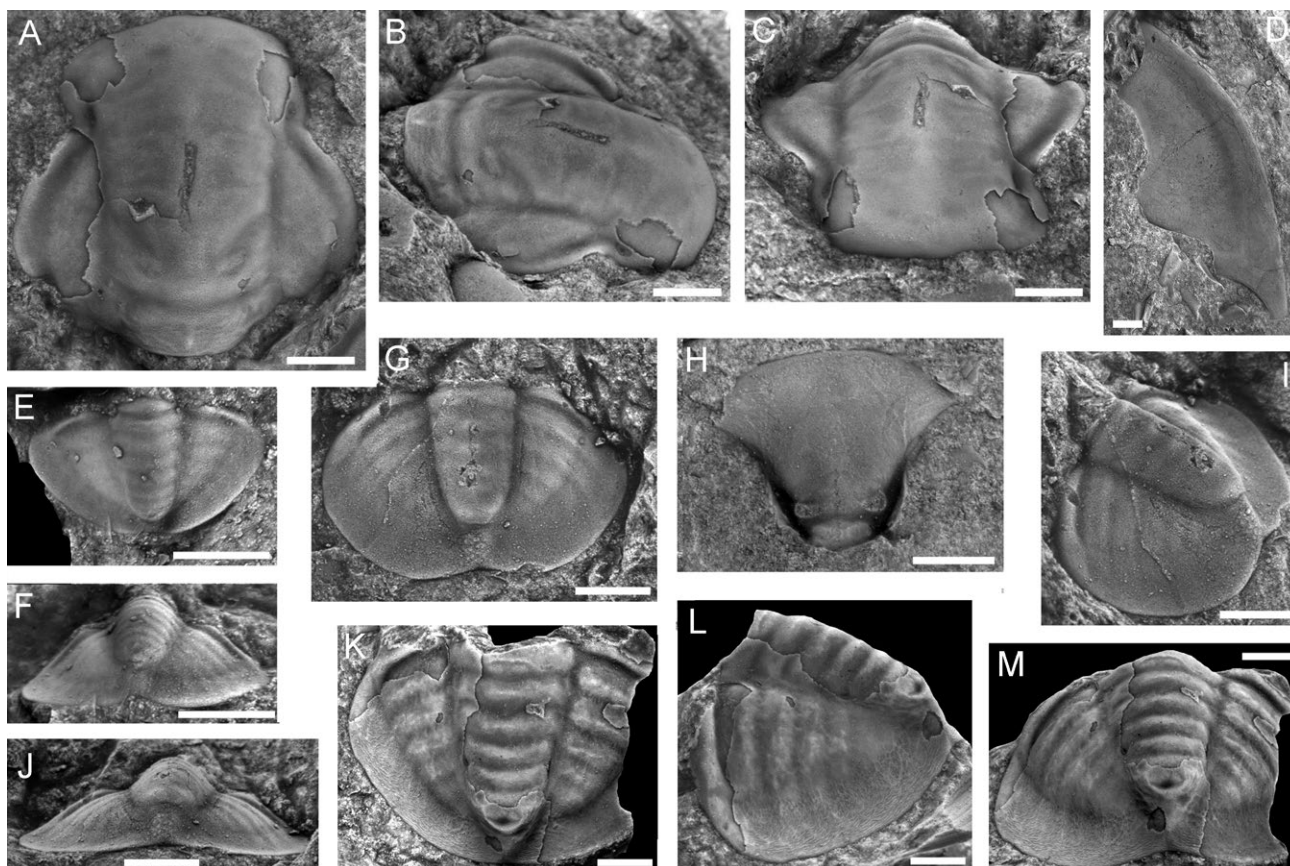

Fig. 9. Trilobites of the *Glossopleura walcotti* Biozone, Telt Bugt Formation, GGU sample 206308, Romer Søer, Daugaard-Jensen Land. **A–F, H**: *Glossopleura walcotti* Poulsen 1927. **A–C**: PMU 35046, testate cranidium. **D**: MGUH 33500, librigena. **E, F**: PMU 35047, pygidium. **H**: MGUH 33501 hyperstome. **G, I, J**: Pygidium sp. 1, MGUH 33502. **K–M**: *Fieldaspis* cf. *bilobata* Rasetti 1951. Pygidium, MGUH 33503. Scale bars: 2mm.

material but this species from the Spence Shale of the Wellsville Mountains of Utah is readily distinguished by the long medial spines on axial rings in the thorax (Robison & Babcock 2011, fig. 6).

Glossopleura cf. *boccar* Walcott 1916
Fig. 10A–C, G, J

Figured material. Cranidium, MGUH 33504, and pygidium, MGUH 33505, both from GGU sample 206303, Telt Bugt Formation, Romer Søer. Miaolingian Series, Wuliuan Stage, *Glossopleura walcotti* Biozone.

Discussion. The cranidium is narrower, with shallowly concave sides, and interocular areas are of similar width to cranidia referred to *Glossopleura walcotti* (Fig. 9A), but with slightly more deeply incised palpebral furrows. Glabellar furrows are weakly expressed, except for the obliquely directed pair of posterior fur-

rows (Fig. 10A,B,J), and the slightly sinuous palpebral lobes contact the glabella at an acute angle, as is the case in *Glossopleura walcotti* (Fig. 10L). The palpebral lobes terminate posteriorly at the posterior glabellar furrows (Fig. 10J) but closer to the occipital ring in *Glossopleura walcotti* (Fig. 10L).

The pygidium is semicircular, with length (sag.) about three quarters of width (Fig. 10G); it is inflated, with only a narrow, ill-defined, border. Its maximum width is at the lateral angulations, at about one third of the distance from the anterior to the posterior margins. The axis is slightly shorter than pygidial length; its width slightly less than that of the upper surface of the pleural areas. There are six axial rings with deep pits at the junction betweeen the axial furrows and the axial border furrow. Pleural surfaces are smooth between broad, shallow, pleural furrows, although traces of furrowing can be seen as the pleural areas pass onto the border.
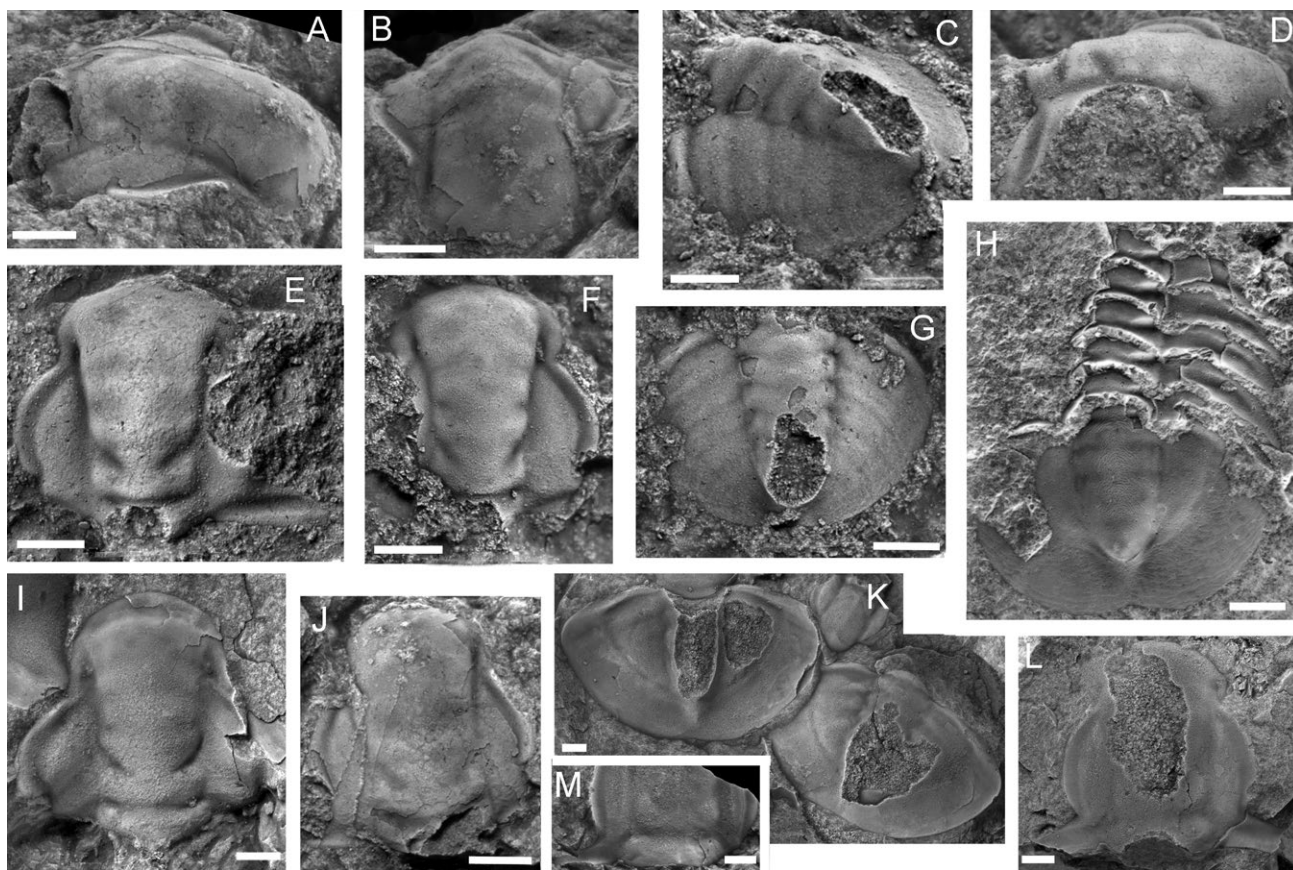

Fig. 10. Trilobites of the *Glossopleura walcotti* Biozone, Telt Bugt Formation, GGU sample 206303 and 206309. Romer Søer, Daugaard-Jensen Land. **A–C**, **G**, **J**: *Glossopleura* cf. *boccar* Walcott 1916, from GGU sample 206303. **A**, **B**, **J**: cranidium, MGUH 33504 from GGU sample 206303. **C**, **G**: pygidium, MGUH 33505 from GGU sample 206303. **H**: *Glossopleura stokiensis* Rasetti 1951, pygidium with thoracic segments, MGUH 33506 from GGU sample 206303. **D–F**, **I**: *Polypleuraspis*? sp., from GGU sample 206303. **D**, **E**, cranidium, MGUH 33507. **F**: cranidium, MGUH 33508. **I**: MGUH 33509 from GGU sample 206309, cranidium. **K–M**: *Glossopleura walcotti* Poulsen 1927, from GGU sample 206309. **K**: pygidia, MGUH 33510 and MGUH 33511. **L**: cranidium, MGUH 33512. **M**: occipital area of cranidium, MGUH 33513. Scale bars: 1 mm (C–G, I), 2 mm (A, B, H, J–M).

Most pygidia illustrated as *Glossopleura boccar* by Rasetti (1951, pl. 24, figs 2,4,5) from the Mount Whyte Formation of British Columbia are similar in terms of the width of the axis but they are less inflated and transversely wider on account of the greater breadth of the border. Pygidia from the Great Basin referred to *G. boccar* by Sundberg (2005, figs 6.13,6.14) have a shorter axis and wider border. Pygidia of *Glossopleura arrecta* Resser 1939a from the Wasatch Mountains of western USA (Resser 1939a; Campbell 1974) are inflated, with a similar broad axis, but have a wider border and obscure furrowing. Pygidia of *Glossopleura walcotti* from Telt Bugt, and from the Cape Wood Formation of Inglefield Land and Bache Peninsula, are readily distinguished by their narrower axis, more lenticular form, and well-developed wide border (Fig. 9E,F,J; Fig. 10K).

Genus *Polypleuraspis* Poulsen 1927

Type species. Polypleuraspis solitaria Poulsen 1927 from the lower Cape Wood Formation, Kap Kent, Inglefield Land.

Discussion. Polypleuraspis Poulsen 1927 was originally described from a single pygidium from the lower Cape Wood Formation, Kap Kent, Inglefield Land (Fig. 1A, locality 2). V. Poulsen (1964) referred cranidia of *Glossopleura longifrons* Poulsen 1927 from boulders of the Cape Wood Formation at Kap Frederik VII, Inglefield Land to *Polypleuraspis solitaria* and the relationship to *Glossopleura longifrons* was re-evaluated by Peel (2020b). V. Poulsen (1964) referred, however, to abundant additional material from Bache Peninsula (Fig. 1A, locality 3).

Peel (2020b) revised *Polypleuraspis*, describing the type specimen of *Polypleuraspis solitaria* and additional material from the Cape Wood Formation of Inglefield Land and Bache Peninsula. The species was not recognised in Daugaard-Jensen Land, where a new species, *Polypleuraspis glacialis* Peel 2020b, was described from the Telt Bugt Formation.

A feature of *Polypleuraspis* and other similar cranidia is the relationship between the occipital ring and the interocular area. The axial boundary furrow is very shallow or even discontinuous at the posterior margin of the cranidium, such that the antero-lateral margins of the occipital ring continue as an arch into the interocular area at its postero-axial corner (Figs 6L, 8L). The prominent border furrow paralleling the posterior margin of the fixed cheeks is not continuous across the axis, via the occipital furrow, but curves as if to pass around the posterior margin of the occipital ring. Thus, the posterior border furrow consists of a distinct groove or channel on each fixed cheek, which

curves to join the posterior margin of the cranidium at the line of the axial groove.

***Polypleuraspis glacialis* Peel 2020b**
Figs 8D, E, I–O

2020b *Polypleuraspis glacialis* Peel, p. 22, fig. 2A–C, E–J, M,O,R.

Holotype. Pygidium, PMU 35038 from GGU sample 206308 (Fig. 8I,N,O), Telt Bugt Formation, Romer Søer. Miaolingian Series, Wuliuan Stage, *Glossopleura walcotti* Biozone.

Figured material. In addition to the holotype, cranidia: PMU 35037 and PMU 35039; pygidium, PMU 35040, all from GGU sample 206308, Telt Bugt Formation, Romer Søer. Miaolingian Series, Wuliuan Stage, *Glossopleura walcotti* Biozone.

Discussion. Polypleuraspis glacialis is known from about ten cranidia and fragments of several pygidia in GGU sample 206308. It differs from the type species *Polypleuraspis solitaria* in lacking axial nodes on its more elevated pygidium (Peel 2020b).

***Polypleuraspis*? sp.**
Fig. 10D–F, I

Material. Cranidia: MGUH 33507 and MGUH 33508 from GGU sample 206303; MGUH 33509 from GGU sample 206309. Telt Bugt Formation, Romer Søer. Miaolingian Series, Wuliuan Stage, *Glossopleura walcotti* Biozone.

Discussion. The three specimens placed here are not associated with pygidia of *Polypleuraspis* in the available small collections and differ from *Polypleuraspis glacialis* and *Polypleuraspis solitaria* in terms of glabellar characters. The glabella is more slowly expanding, with straight (Fig. 10E) or shallowly concave sides (Fig. 10F). The anterior margin of the glabella passes abruptly into a narrow anterior border (Fig. 10F) with a convex anterior margin (Fig. 10I), in which respect it is similar to *Bathyuriscus* Meek 1873, whereas the transition in *Polypleuraspis glacialis* and *Polypleuraspis solitaria* is less sharply defined. The palpebral lobes are more uniformly convex (Fig. 10E) than in both these described species.

Family Zacanthoididae Swinnerton 1915

Genus *Fieldaspis* Rasetti 1951

Type species. Fieldaspis furcata Rasetti 1951 from the

Mount Whyte Formation (Miaolingian) of British Columbia.

Discussion. The dificulties of delimiting dolichometopine and zacanthoidean genera on the basis of the cranidium alone are well known (Rasetti 1951; Palmer & Halley 1979). Reference of disarticulated sclerites from GGU sample 206307 to *Fieldaspis* relies heavily on the characters of the weakly bilobed pygidium, although similar, less strongly bilobed, lenticular pygidia with fewer rings are present in *Poliella* Walcott 1916 (Sundberg & McCollum 2003a).

Fieldaspis? iubilaei sp. nov.
Fig. 6D–N

Derivation of name. From the latin, iubilaeum, meaning jubilee year, commemorating *Jubilæumsekspeditionen Nord om Grønland 1920–23* (Danish Bicententary Jubilee Expedition North of Greenland 1920–23), 100 years after its expedition members arrived in the Telt Bugt area of Daugaard-Jensen Land.

Holotype. MGUH 33476 from GGU sample 206307. Telt Bugt Formation, Romer Søer. Miaolingian Series, Wuliuan Stage, *Plagiura–Poliella* Biozone.

Figured material. In addition to the holotype: cranidia: MGUH 33479 and MGUH 33480; pygidium: MGUH 33481; hypostomes: MGUH 33478 and MGUH 33477. All from GGU sample 206307, Telt Bugt Formation, Romer Søer. Miaolingian Series, Wuliuan Stage, *Plagiura–Poliella* Biozone.

Diagnosis. Glabella with poorly defined glabellar furrows; occipital ring extended posteriorly, with low posterior spine. Anterior border narrower in front of glabella; strongly convex in small specimens, becoming wider (sag.) and flattened in large specimens. Pygidium about twice as wide as long, with maximum width reached at about two thirds of distance from anterior to posterior margin; bilobed with broad, distinct, medial notch in posterior margin. Axis prominent with three rings and terminal axial piece; pleural furrows well marked, effaced on broad border.

Description. The cranidium is sub-trapezoidal in shape with its overall length (sag.) about four-fifths of width (trans.) and the glabella occupying almost all of the cranidial length. Glabella parallel-sided at its posterior, expanding slightly at about mid-length from the occipital ring to the front border; the anterior is uniformly convex (Fig. 6D). However, in a small specimen (Fig. 6L), the glabella is almost parallel-sided at all stages and the transition to the convex anterior is abrupt. In transverse profile, the glabella is uniformly convex and raised above the shallowly convex interocular areas and especially the anterior areas of the fixed cheeks. Three pairs of obscure short glabellar furrows are present, of which the posteriormost pair is strongly oblique. The occipital furrow is broad and shallow (Fig. 6K), curved towards the anterior medially, but deeper and narrower in the small specimen (Fig. 6L). The occipital ring expands medially and terminates in a prominent node or short spine (Fig. 6N). The axial border furrow is narrow and deep, particularly anterior to the eye ridges where the interocular surface steps down abruptly to the anterior fixed cheek (Fig. 6J,K), and where a fossula is developed on each side of the glabella. At the occipital ring, the axial border furrow is shallow as the interocular area and the occipital ring are conjoined.

The anterior area is broad and shallowly convex between the axial border furrow and the anterior margin (Fig. 6D), although it is narrow and more strongly convex in the small specimen (Fig. 6L). Preocular areas are wide, with sutures curving in to join the eye ridge–palpebral lobe at almost half of the transverse width of the interocular area. Interocular areas, at their point of maximum width, are about two thirds width (trans.) of the glabella. Deep, wide palpebral furrows narrow anteriorly before joining the anterior border furrows (Fig. 6J). The anterior limit of the palpebral lobes is not well known, but seemingly close to the axial border furrow; in the small specimen (Fig. 6L) the lobes are of uniform curvature and width and extend from close to the axial border furrow to their posterior termination at the occipital furrow. Posterior fixed cheek narrow (sag.), lateral extent not known, border furrow terminating against the conjoined occipital ring and interocular area (Figs 6J,L,N).

Free cheeks and thorax are not known. Hyperstome triangular with broadly extended uniformly convex anterior margin delimited from anterior lobe by a deep groove that is excavated medially. Anterior border shallowly convex, sloping in towards anterior border groove (Fig. 6F). Lateral border areas narrow adjacent to middle furrows, with tubercles developed at posterior of anterior lobe. Small, triangular posterior lobe separated from globose anterior lobe by broad shallow transverse furrow (Fig. 6G).

Pygidium elliptical, with maximum transverse width almost twice length (sag.), and reached at about two thirds of distance from anterior to posterior margin. Anterior margin with almost perpendicular junction between pleural areas and lateral margin sloping towards point of maximum transverse width. Axis prominent, wide, convex, about half of length (sag.) of pygidium, with three axial rings and short tail piece. Pleural areas triangular, with prominent

furrows and, distally, weakly marked pleural grooves. Posterior border with broad medial notch.

Ornamentation of fine pits and granules, the latter conspicuous on the small specimen (Fig. 6L).

Discussion. The few available specimens suggest that the development of the broad and unusually flattened frontal area of *Fieldaspis*? *iubilaei* is ontogenetically controlled. A small specimen (Fig. 6L, length 3.3 mm) shows a convex rim separated from the front of the glabella by a groove of similar width. The rim is less strongly convex in a larger specimen (Fig. 6N, length about 6.4 mm) and only shallowly convex in the holotype (Fig. 6D, length about 13.1 mm).

The type species and other species of *Fieldaspis* described by Rasetti (1951) differ from *Fieldaspis*? *iubilaei* in that their upturned anterior border is almost in contact with the front of the glabella, which consequently has a rather angular transition to the glabellar sides. A distinct anterior border furrow is present in small specimens assigned to *Fieldaspis*? *iubilaei*, but the glabellar front in the holotype is more rounded and slightly overhangs the flattened preglabellar area. The presence of a definite border in *Fieldaspis*? *nahanniensis* Norford 1968 from the Nahanni River of the District of Mackenzie caused Norford (1968) to question the assignment to *Fieldaspis*, as is also the case here.

Fieldaspis? *nahanniensis* is similar to *Fieldaspis*? *iubilaei* in the broad and deep palpebral furrows but has a more strongly expressed occipital furrow and a long occipital spine. Its anterior border is wide (sag.) and shallowly convex, although it may be broken away in some specimens figured by Norford (1968, pl. 4, fig. 3) and appear to be acutely upturned, thereby resembling *Fieldaspis* from Mount Whyte. In *Fieldaspis*? *iubilaei* the border in front of the glabella is flattened, only shallowly convex. The pygidium of *Fieldaspis*? *iubilaei* is similar to that of *Fieldaspis bilobata* Rasetti 1951 from the Mount Whyte Formation of British Columbia and *Fieldaspis* cf. *bilobata* from GGU sample 206308 but has fewer rings and a wider brim. The brim is also wide in the pygidium of *Fieldaspis*? *nahanniensis* from the Nahanni River of the District of Mackenzie but this has one fewer axial ring and more steeply sloping, straight, furrows crossing the pleural surfaces.

Poliella lomataspsis Palmer *in* Palmer & Halley 1979 from the *Plagiura–Poliella* Biozone (*Poliella denticulata* Biozone of McCollum & Sundberg 2007; Sundberg 2011) of the Carrara Formation in Nevada, has a more lenticular pygidium with a similar wide brim, but fewer rings. The frontal area in the holotype cranidium of *Poliella lomataspsis* is narrow with an upturned rim (Palmer & Halley 1979, pl. 6, fig. 2), unlike the flat preglabellar area in the holotype of *Fieldaspis*? *iubilaei* (Fig. 6D,J,K). The frontal area of the cranidium

of *Poliella leipalox* Fritz 1968, from the Pioche Shale of Nevada, is flattened, as in *Fieldaspis*? *iubilaei*, but not strongly delimited from the front of the glabella.

Fieldaspis cf. *bilobata* Rasetti 1951
Fig. 9K–M

Material. Pygidium, MGUH 33503 from GGU sample 206308. Telt Bugt Formation, Romer Søer, Daugaard-Jensen Land. Miaolingian, Wuliuan Stage, *Glossopleura walcotti* Biozone.

Discussion. The length (sag.) of this single specimen is about two thirds of its maximum width (trans.), the latter occurring just anterior of mid-length. The anterior margin is convex, angled at the margin of the pleural areas; the posterior margin is uniformly convex (Fig. 4K) but arched medially (Fig. 4L,M). The axis is strongly convex, wider than the pleural areas, seemingly consisting of five rings and a small tail piece, with a low triangular ridge persisting across the border. The pleural areas steepen abruptly with passage onto the outward-sloping, broad, but shallowly concave border. Furrows are broad and deep, but hardly discernible except on the anterior parts of the border (Fig. 9L).

In terms of shape and strong expression of the rings and furrows, the pygidium is close to *Fieldaspis bilobata* Rasetti 1951 from the Mount Whyte Formation of British Columbia, although the latter shows greater curvature of the furrows on the pleural areas and has one less axial ring. The border and distal portions of the pleural areas of the pygidium (Fig. 9L) show the same cellular ornamentation as the single cranidium described here as *Poliella*? sp. (Fig. 8A), suggesting that the two may represent the same taxon. The latter, however, shows a much longer (sag.) preglabellar area and more prominent border than the narrow, abruptly upturned anterior margin of *Fieldaspis bilobata* illustrated by (Rasetti 1951), while the pygidium shows a greater number of axial rings than described *Poliella* species (Rasetti 1951; Sundberg & McCollum 2003a).

Specimens from the Pioche Shale assigned to *Fieldaspis bilobata* by Sundberg & McCollum (2003a) have a more angulated anterior margin, shorter axis, fewer axial rings and a much more pronounced lobation of the border than either Rasetti's (1951) material from British Columbia or the specimen from Romer Søer.

Fieldaspis cf. *bilobata* differs from the pygidium of *Fieldaspis*? *iubilaei* (Fig. 6H) in terms of its greater number of rings and furrows, the axis extending almost to the posterior margin and the narrower border without a substantial median indentation. The morphological differences are substantial but not greater than those encompassed in species within the concept originally applied to *Fieldaspis* by Rasetti (1951).

V. Poulsen (1964, pl. 1, fig. 9) assigned a fragment of a pygidium from the basal Cape Wood Formation Blomsterbækken, Inglefield Land, (Fig. 1A, locality 2) to *Fieldaspis* in which the margin from anterior to posterior is uniformly convex, the border lobes long (sag.) and only two rings are present on the axis. In these aspects it is more closely similar to the specimens illustrated by Sundberg & McCollum (2003a), and unlike the material from the Telt Bugt or Mount Whyte formations.

Order Ptychopariida Swinnerton 1915

Suborder Ptychopariina Richter 1932

Family Ptychopariidae Matthew 1887

Genus *Kochiella* Poulsen 1927

Type species. *Kochiella tuberculata* Poulsen 1927 from the Cape Kent Formation (Cambrian Series 2), Inglefield Land, North-West Greenland.

Discussion. Poulsen (1927) assigned four species from the Cape Kent Formation to *Kochiella*, which is a ptychoparioid characterised by a rather flat cephalon with extended lateral areas and a distinctive ornament of scattered, large tubercles. He distinguished *Kochiella* from *Amecephalus* Walcott 1924 by the way in which the frontal groove in *Kochiella* curves back towards the glabella as it crosses the axial plane, while it remains parallel to the anterior margin in the latter genus. No pygidia were assigned originally to *Kochiella,* but Resser (1935) referred a pygidium described as *Crepicephalus* cf. *cecinna* Walcott 1917 by Poulsen (1927, pl. 16, figs 17 and 18) to the type species. Rasetti (1951) questioned the certainty of this assignment but V. Poulsen (1964) accepted Resser's (1935) action, considering the scattered tubercles on the bilobed pygidium to indicate its assignment to *Kochiella*. V. Poulsen (1964) also referred to *Kochiella* a bilobate pygidium illustrated but not described by Poulsen (1927, pl. 16, fig. 19), although this action seems questionable. Sundberg & McCollum (2002) considered the pygidium that Poulsen (1927, pl. 16, figs 17 and 18) referred to *Crepicephalus* cf. *cecinna* Walcott 1917 to belong probably in their new genus *Hadrocephalites,* but noted that cranidia of this had not been identified in material illustrated by Poulsen (1927).

Kochiella, as originally described by Poulsen (1927), was revised by V. Poulsen (1964) who reduced the four original species from the Cape Kent Formation (Cambrian Stage 2) to three, but he gave no additional illustrations. V. Poulsen (1964) concluded that

Kochiella? *maxeyi* Rasetti 1951, the type species of *Eiffelaspis* Chang 1963, should be placed in a new genus, although Sundberg & McCollum (2002) regarded it as a junior synonym of *Kochiella*. V. Poulsen (1964) also excluded *Kochiella crito* (Walcott 1917) of Resser (1935), *Kochiella*? *pennsylvanica* Resser 1938 and *Kochiella fitchi* (Walcott 1887) of Lochman (1956) from *Kochiella* but Sundberg & McCollum (2002) commented that poor preservation prevented proper generic assignment.

Sundberg & McCollum (2002) emended *Kochiella* in reviewing species from western North America, which they noted were restricted to early Delamaran strata (late Stage 4) and Miaolingian. Pratt & Bordonaro (2014) reviewed *Kochiella* in describing Miaolingian trilobites from the Precordillera of western Argentina. Much of the discussion of *Kochiella* by these authors and V. Poulsen (1964) has centred on the nature of the pygidium. No relevant pygidia occur in the small collection from GGU sample 206307 from the Telt Bugt Formation.

Kochiella sp.
Fig. 6A–C, O

Figured material. Cranidia: MGUH 33473 and 33474, and fragment of free cheek, MGUH 33475 from GGU sample 206307, Telt Bugt Formation, Romer Søer. *Plagiura–Poliella* Biozone.

Description. This species is represented by three cephalic fragments, of which an external mould, illustrated as a digitally produced cast (Fig. 6A,B), is the most complete. In this, the posterior fixigenae are not preserved but the transverse (trans.) distance between the outer margins of the palpebral lobes is 1.5 times the length of the cranidium. The glabella, including occipital ring, comprises about 60 % of the cranidial length (15 mm), measured along the axial plane. The cranidial profile in lateral perspective shows the shallowly convex glabella curving along the sagittal line from the short occipital spine (Fig. 6B, os) to the frontal area, where it becomes uniformly concave towards the anterior margin. A border furrow is hardly discernible in the preglabellar field (Fig. 6A) but appears laterally at the junction between the preocular area and the border.

The glabella is broad, length inclusive occipital ring equal to width, tapering forward with straight or shallowly inflected (Fig. 6C) sides from the occipital ring to about half its width at the rounded anterior margin. The axial border furrow around the glabella is narrow and shallow, obscure in front of the glabella. The occipital furrow is shallow, but complete; there are three pairs of shallow glabellar furrows. The occipital ring is narrow (sag.) with a

median tubercle. Each shallowly convex inner ocular area, measured at the outer margin of the palpebral lobe, is somewhat wider (trans.) than the glabella at the same point. The surfaces slope in towards the axial border furrow such that the palpebral lobes are strongly elevated (Fig. 6B, pl). The palpebral lobes are short, much less than half the length (sag.) of the glabella, raised, and strongly crescentic (Fig. 6C). An eye ridge consisting of two narrow ridges joins the anterior margin of each palpebral lobe to the axial border furrow in front of the glabella (Fig. 6A). Posterior limb of fixigenae poorly known in terms of its lateral extent; its posterior margin straight with the border furrow curving posteriorly to join the posterior margin rather than joining the axial border furrow. Thorax and pygidium not known, librigenae represented by a fragment of the border with well preserved ornamentation (Fig. 6O).

Ornamentation finely granular, the individual granules sometimes arranged in lines in an anastomising pattern (Fig. 6O). Tubercles of two size orders are scattered over the surface, but concentrated around the sclerite margins (Fig. 6O), where large tubercles are surrounded by a granule-free collar and may be perforate.

Discussion. Although fragments, the three available specimens of *Kochiella* sp. preserve exquisite details of the ornamentation of tubercles set against a background of fine granules (Fig. 6A–C,O).

Of particular note in the two cranidial fragments is the structure of the eye ridges, each of which consists of two parallel, narrow, rounded ridges, of which the posterior one is slightly more prominent (Fig. 6A,B, er). A similar structure has not been discerned in illustrations of Poulsen (1927), Sundberg & McCollum (2002) or Pratt & Bordonaro (2014) where the eye ridges are single and broader. Similar double eye ridges were described in *Pianaspis sors* (Öpik 1961) from the Miaolingian of Queensland and Tasmania by Öpik (1961, pl. 15, fig. 2) and by Bentley & Jago (2014). Öpik (1967, pl. 17, figs 1–3; pl. 18, fig. 3; fig. 89) also described double eye ridges in *Pagodia (Idamea) baccata* Öpik 1967 from the Mindyallan of Quensland, while Palmer (1968, pl. 5, fig. 9) illustrated similar double ridges in *Prohedinia brevifrons* Palmer 1968 from the Miaolingian of Akaska. Their presence may be inferred in an internal mould referred to *Amecephalus arrojosensis* (Lochman *in* Cooper *et al.* 1952) illustrated by Sundberg & McCollum (2000, figs 5.1,5.2) from the Comet Shale Member of the Pioche Shale of Nevada.

In terms of the concavity of the frontal area and lack of differentiation of the preglabellar area, *Kochiella* sp. resembles *Kochiella mackenziensis* Norford

1968 from the *Plagiura–Poliella* faunule of the District of MacKenzie, but the latter has more deeply incised glabellar furrows and more dense tuberculation (Norford 1968).

The type species, *Kochiella tuberculata* Poulsen 1927 from the Cape Kent Formation of Inglefield Land, and other species described by Poulsen (1927) and Poulsen (1964) have a clearly marked border, as do specimens attributed to *Kochiella* by Sundberg & McCollum (2002). Half way between the front of the glabella and the anterior margin, a comarginal groove curves shallowly towards the posterior as it crosses the axial plane, a feature discussed both by Poulsen (1927) and V. Poulsen (1964), but this groove is medially obscure in the Telt Bugt specimen (Fig. 6A) and in most of the specimens illustrated by Norford (1968).

Amecephalus troelseni V. Poulsen 1964 from the Cape Wood Formation at Blomsterbækken, Inglefield Land (Fig. 1A, locality 2) lacks the tuberculation seen in *Kochiella* sp. It differs also in having a distinct axial border furrow in front of the glabella, with a longer (sag.) and shallowly convex preglabellar area; its eye ridges are convex towards the anterior (V. Poulsen 1964, pl. 2, figs 10–11), as distinct from straight in *Kochiella* sp. The only specimen of *Amecephalus troelseni* was derived from a loose pebble from the basal conglomerate of the *Glossopleura* Zone, which he interpreted as *Plagiura–Poliella* Zone (V. Poulsen 1964).

Genus *Caborcella* Lochman 1948

Type species. Caborcella arrojosensis Lochman 1948 from the middle Cambrian of Sonora, northern Mexico.

***Caborcella arrojosensis* Lochman 1948**
Fig. 7H, I

1948   *Caborcella arrojosensis* Lochman, p. 461, pl. 70, figs 19–21.

Figured material. Cranidium, MGUH 33491 from GGU sample 212808, Telt Bugt Formation, Telt Bugt, Daugaard-Jensen Land. Miaolingian, Wuliuan Stage, *Mexicella mexicana* Biozone.

Discussion. This species is known from the illustrated specimen and an additional broken cranidium, both from GGU sample 212808. The width of the illustrated cranidium is about one third greater than its length. It is characterised by the conical glabella, which decreases in transverse width by half from posterior to anterior, and is almost as wide at its posterior as it is long (Fig. 7I). Glabellar furrows are weakly impressed and the occipital furrow is deep laterally but

shallow axially, whereas it is of more uniform depth in the Mexican material figured by Lochman (1948). Ornamentation is finely granulose; large tubercles are scattered over the entire cranidium, most densely on the border and most weakly on the anterior part of the glabella and the preglabellar area.

Genus *Eokochaspis* Sundberg & McCollum 2000

Type species. Eokochaspis nodosa Sundberg & McCollum 2000 from the Comet Shale Member, Pioche Shale, of Nevada. Miaolingian, *Poliella denticulata* Biozone.

Eokochaspis? sp.
Fig. 7O

Figured material. Cranidium, MGUH 33493 from GGU sample 212806, Telt Bugt Formation, Telt Bugt. Miaolingian, Wuliuan, *Plagiura–Poliella* Biozone.

Discussion. This single cranidium from GGU sample 212806 has a tapering glabella with almost straight sides and effaced glabellar furrows. The occipital furrow is deep laterally and shallow medially. The occipital ring is trapezoidal in plan view, narrowing towards the posterior and seemingly with a low median node. The front margin is slightly arched medially. The frontal area is divided by a broad and shallow furrow into a steepened preglabellar field and a shallow convex border, which is more than twice the length (sag.) medially of the preglabellar field (Fig. 7O). Fixigenae are of similar transverse width to the corresponding glabellar width. The palpebral lobes are small and located at mid-length (sag.) of the glabella. The prominent posterior border furrows are essentially continuous with the occipital furrow; posterior limbs of the fixigenae appear to be short and robust. The surface is slightly weathered, but seemingly a wrinkled granular ornamentation was developed on the glabella and fixigena.

In general proportions, the cranidium resembles *Eokochaspis*? *cabinensis* Sundberg & McCollum 2003a from the Log Cabin Member (Wuliuan Stage, *Poliella denticulata* Biozone) of the Pioche Shale, although the glabella narrows more rapidly and the anterior fixigenae are proportionately slightly wider in that species. It is also similar to a small cranidium of *Mexicella robusta* Sundberg & McCollum 2000 from the *Eokochaspis nodosa* Biozone, although the anterior brim is more elliptical, and the posterior border furrows more strongly defined.

Genus *Mexicella* Lochman 1948

Type species. Mexicella mexicana Lochman 1948, from the Arrojos Formation of Sonora, northern Mexico.

Mexicella cf. *robusta* Sundberg & McCollum 2000
Fig. 7N

Figured material. Cranidium, 33492 from GGU sample 212806, Telt Bugt Formation, type locality, Telt Bugt, Daugaard-Jensen Land. *Plagiura–Poliella* Biozone.

Discussion. The only known specimen is a partially exfoliated cranidium that compares with specimens illustrated by Sundberg & McCollum (2000, fig. 13) from the Pioche Shale (*Amecephalus arrojosensis* Biozone) in Nevada in terms of the shape of the glabella. The glabella is more strongly tapering, with shallowly convex sides, in the type species *Mexicella mexicana* Lochman *in* Cooper *et al.* (1952) from the Arrojos Formation in Sonora, Mexico. Additionally, the frontal slope is less steep in the Greenland specimen than in some illustrated specimens of *Mexicella mexicana* from Mexico (Lochman *in* Cooper *et al.* 1952). The cranidium from the Telt Bugt Formation is about 9.5 mm long, about two thirds of the size of the largest Sonora specimens, but about the same size as specimens of *Mexicella robusta* from Nevada. The fine radial venation is expressed most clearly in the preglabellar area. Scattered coarse granules noted by Palmer & Halley (1979, p. 109) in specimens from Mexico and the Carrara Formation in Nevada and California (*Albertella* Biozone), and a central tubercle on the occipital ring have not been observed. *Mexicella granulata* Eddy & McCollum 1998 from the Pioche Shale (*Albertella* Zone) of south-eastern Nevada has a more pointed anterior margin and longer (sag.) pre-frontal field.

Mexicella robusta occurs in the *Amecephalus arrojosensis* Biozone of Nevada, equivalent to the middle *Plagiura–Poliella* Biozone (Fig. 4). In terms of the international standard (Geyer 2019), the biozone is pre-Miaolingian, assigned to uppermost Stage 4 of Cambrian Series 2.

Genus *Plagiura* Resser 1935

Type species. Ptychoparia? *cercops* Walcott 1917 from the Mount Whyte Formation, British Columbia.

Plagiura? sp.
Fig. 6P

Figured material. Cranidium, 33482 from GGU sample 206307, Telt Bugt Formation, Romer Søer. *Plagiura–Poliella* Biozone.

Discussion. Three broken cranidia from GGU sample 206307 are referred to an undetermined species, which is only questionably referred to *Plagiura* on account of its longer palpebral lobes. The illustrated

specimen (Fig. 6P) has a narrower glabella, with less rapidly tapering sides and more rounded front than specimens from the Mount Whyte Formation of British Columbia, referred by Rasetii (1951, 1957) to *Plagiura cercops* (Walcott 1917), or from species described from the Carrara Formation (Palmer & Halley 1979) and the Log Cabin Member of the Pioche Shale (Sundberg & McCollium 2003a) of Nevada.

Family Alokistocaridae Resser 1939b

Genus *Ehmaniella* Resser 1937

Type species. *Crepicephalus* (*Loganellus*) *quadrans* Hall & Whitfield 1877, from the Spence Shale (Miaolingian) of Utah, USA.

Ehmaniella sermersuaqensis Peel 2020a
Fig. 12A, C, D, I

2020a *Ehmaniella sermersuaqensis* Peel, p. 6, fig. 3A–J, L.

Holotype. Cranidium, PMU 35701 (212812.20 D) from GGU sample 212812, Telt Bugt Formation, Telt Bugt. Miaolingian, Wuliuan Stage, *Ehmaniella* Biozone.

Figured material. In addition to the holotype, cranidium, PMU 35698; pygidia: PMU 35693 and PMU 35700, all from GGU sample 212812. Telt Bugt Formation, Telt Bugt.

Discussion. *Ehmaniella sermersuaqensis* is characterised by its narrow (sag.), convex preglabellar field, without a sharply defined border furrow, passing into a broad (sag.), concave border (Peel 2020a). The transversely elliptical pygidium has five or six rings and a well-developed concave border, which differentiates it from other previously described species of *Ehmaniella* (Sundberg 1994).

Ehmaniella tupeqarfik sp. nov.
Fig. 11A, D–I

Holotype. Cranidium, MGUH 33515, from GGU sample 212873, Telt Bugt Formation, Telt Bugt. Miaolingian, Wuliuan Stage, *Ehmaniella* Biozone.

Figured material. In addition to the holotype, cranidia: MGUH 33514, MGUH 33516; pygidia: MGUH 33517, MGUH 33518, all from GGU sample 212873, Telt Bugt Formation, Telt Bugt. Miaolingian, Wuliuan Stage, *Ehmaniella* Biozone.

Derivation of name. From the Greenlandic word *tu-*

peqarfik, meaning tent place (Danish: teltplads), referring to the locality at Telt Bugt with numerous palaeoeskimo archaeological remains (Peel & Frykman 1975).

Diagnosis. Pygidium transversely elliptical, with lateral angulations lying at about half of its length (sag.). Axis strongly convex with five? or six axial rings. Pleural areas becoming steeply convex before passage into the wide concave border, with furrows strongly incised at transition to border, extending well into the border area, and a narrow groove on the pleural surfaces. Anterior cranidial area with narrow preglabellar field separated from shallowly convex, outward sloping brim by a well-defined but shallow groove which curves forward in front of glabella.

Description. Cranidium sub-trapezoidal with length (sag.) almost three quarters of width (trans.); frontal margin uniformly convex with crescentic brim. Axial border furrow well defined, deep, shallowing in front of glabella. Glabella conical, with straight sides and rather angular transition to the shallowly convex front. Glabella with three pairs of broad, shallow furrows that may be effaced; the posterior glabellar furrows are strongly oblique. Occipital ring narrow laterally, trapezoidal and broadly convex, with small node; occipital furrow broad, wave-formed in dorsal view (Fig. 11D). Frontal area divided into the shallowly convex, outward sloping brim and convex anterior preglabellar field by a well defined but shallow groove that shallows slightly and curves forward in front of the glabella. Preocular areas usually slightly narrower (trans.) than anterior glabella; sutures curving in to meet palpebral lobes at right angles.

Broad, shallowly convex eye ridges terminate anteriorly at the axial border furrow and continue posteriorly into palpebral lobes, which increase in relief posteriorly. Palpebral lobes long, extending over two thirds of glabellar length from the point where the anterior branches of the suture contact the eye ridges to just anterior of occipital furrow. Palpebral furrows broad and shallow. Interocular areas convex, sloping in towards axial furrow, their maximum transverse width about half of corresponding glabellar width. The interocular areas are strongly elevated above the palpebral furrow at the posterior of palpebral lobe (Fig. 11E), but shallow forwards. Posterior fixigenae stout, triangular and somewhat shorter (trans.) than corresponding glabellar width (Fig. 11D); posterior furrow prominent. Thorax and free cheeks not known.

The pygidium is transversely elliptical, with length (sag.) about half of width (Fig. 11G,I). The lateral angulations, at the point of maximum width (trans.), lie at about half the length (sag.). Axis strongly convex with five? or six axial rings, becoming less clearly

defined towards the posterior termination. Pleural areas are initially shallowly convex before becoming steeply convex with passage into the wide concave border. Furrows strongly incised, slightly channelled, deepened to form pits at the transition to border, and extending well into the border area. Pleurae with shallow groove near posterior margin (Fig. 11I).
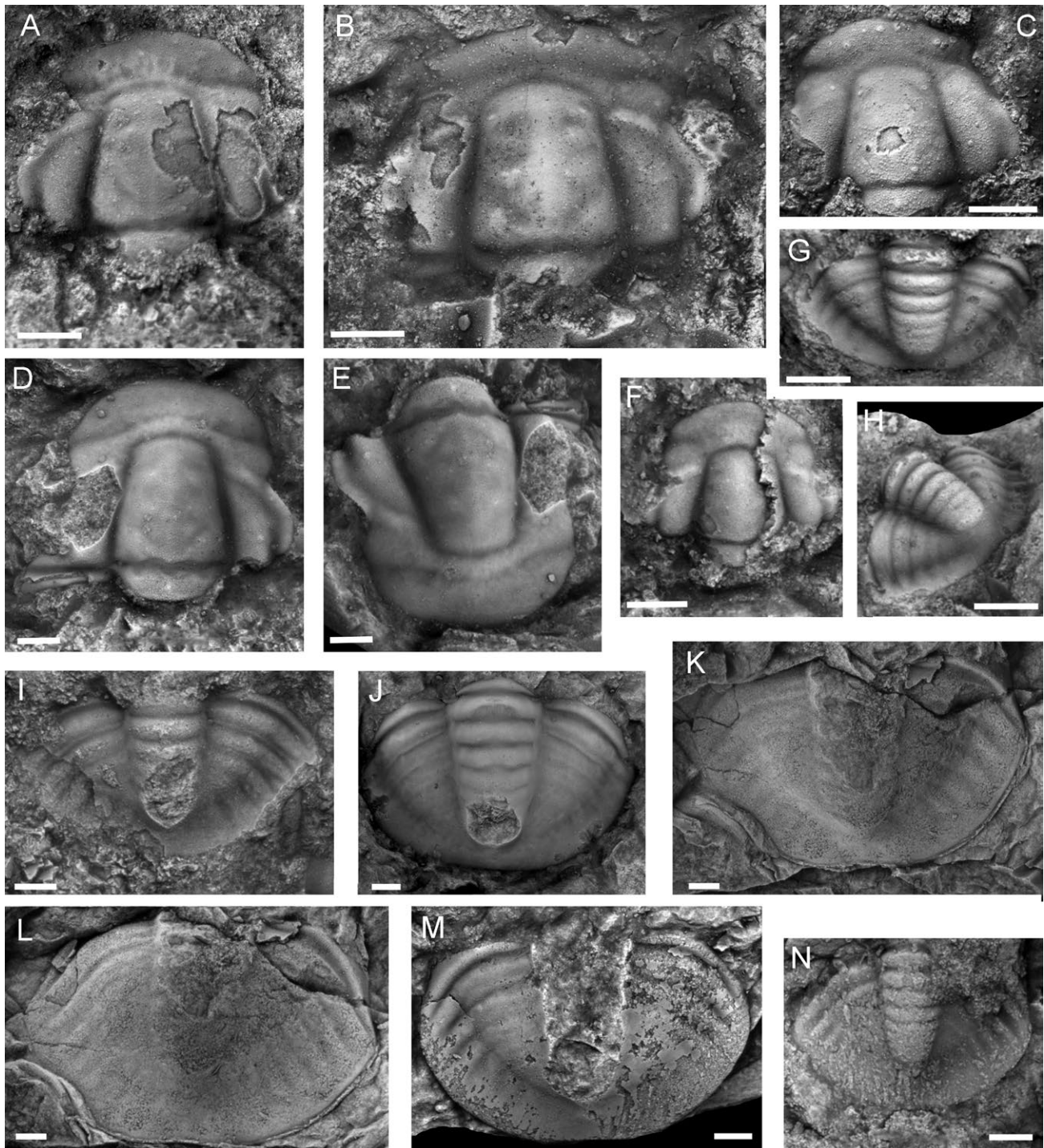
Ornamentation usually consists of fine granules.

Fig. 11. Trilobites of the *Ehmaniella* Biozone, Telt Bugt Formation, GGU sample 212873, Telt Bugt, Daugaard-Jensen Land. **A**, **D–I**: *Ehmaniella tupeqarfik* sp. nov., **A**: cranidium, MGUH 33514. **D**, **E**: cranidium, holotype, MGUH 33515. **F**: cranidium, MGUH 33516. **G**, **H**: pygidium, MGUH 33517. **I**: pygidium, MGUH 33518. **B**, **C**: *Ehmaniella* sp., **B**: cranidium, MGUH 33519. **C**: cranidium with tuberculate ornamentation, MGUH 33520. **J?**, **K–N**: *Blainia* sp., **J**: tentatively assigned pygidium, MGUH 33521. **K**, **L**: pygidium, MGUH 33522. **M**: pygidium, MGUH 33523. **N**: pygidium, MGUH 33524. Scale bars: 1 mm.

Discussion. Cranidia of *Ehmaniella tupeqarfik* sp. nov. are quite common in GGU sample 212873. *Ehmaniella tupeqarfik* and *Ehmaniella sermersuaqensis* Peel 2020a are distinguished from species of *Ehmaniella* described by Sundberg (1994) from Utah and Nevada by the lenticular pygidium with its concave border. *Ehmaniella tupeqarfik* differs from *Ehmaniella sermersuaqensis* in that the axis is less tapering and the furrows on the pleural areas tend to be deepened at the transition to the border. The border furrow in the frontal area of cranidia in *Ehmaniella tupeqarfik* is more strongly delimited and tends to swing forward in front of the glabella (Fig. 11D). The brim in *Ehmaniella sermersuaqensis* is concave whereas it is shallowly convex and sloping outwards in *Ehmaniella tupeqarfik*. Ornamentation in the latter is dominated by fine granules of similar size, whereas coarser granules are characteristic of the occipital ring and central glabella of *Ehmaniella sermersuaqensis* (Fig. 12C,D).

Ehmaniella sp.
Fig. 11B, C

Figured material. Cranidia: MGUH 33519 and MGUH 33520, from GGU sample 212873, Telt Bugt Formation, Telt Bugt. Miaolingian, Wuliuan Stage, *Ehmaniella* Biozone.

Discussion. A few cranidia in GGU sample 212873 develop an upturned, shallowly convex border with scattered coarse tubercles on the border and posterior glabella and fixigenae.

Genus *Clappaspis* Deiss 1939

Type species. Clappaspis typica Deiss 1939 from the Pentagon Shale of Montana.

Discussion. Clappaspis was regarded as a junior syno-
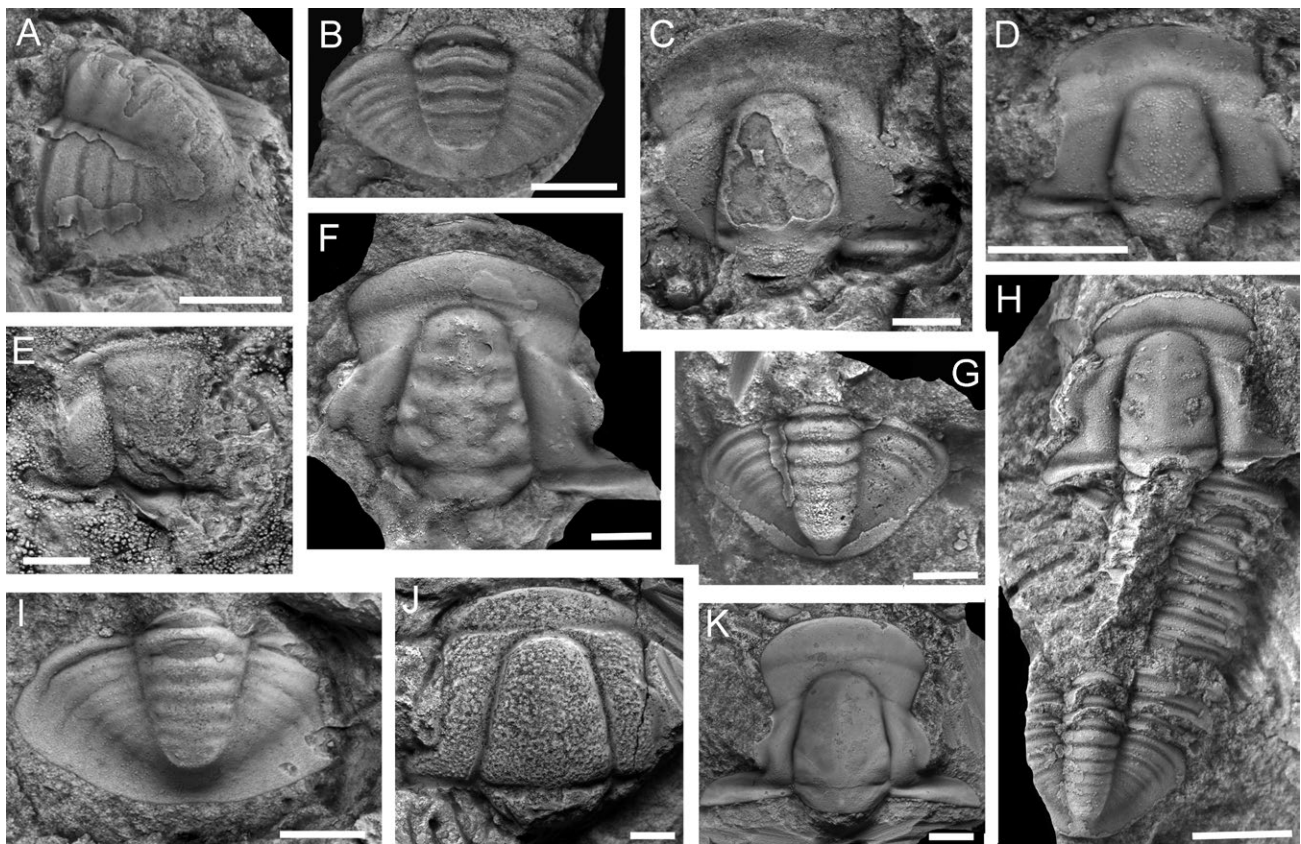
Fig. 12. Trilobites of the *Ehmaniella* Biozone, Telt Bugt Formation, Telt Bugt. Daugaard-Jensen Land. **A**, **C**, **D**, **I**: *Ehmaniella sermersuaqensis* Peel 2020a from GGU sample 212812. **A**: pygidium, PMU 35693. **C**: cranidium, PMU 35698. **D**: cranidium, PMU 35701, holotype. **I**: pygidium, PMU 35700. **B**, **J**: *Clappaspis tupeq* Peel 2020a from GGU sample 212813. **B**: pygidium, PMU 35703. **J**: cranidium, holotype, PMU 35705. **E**: *Kootenia* cf. *subequalis* Deiss 1939, cranidium, PMU 35702, from GGU sample 212812. **F**: *Blainiopsis holtedahli* Poulsen 1946, cranidium, PMU 35715 from GGU sample 212814. **G**, **H**: *Blainiopsis benthami* Poulsen 1946 from GGU sample 212814. **G**: pygidium, PMU 35714. **H**: damaged articulated specimen, PMU 35713. **K**: *Blainia* sp., cranidium, PMU 35710 from GGU sample 212813. Scale bars: 2 mm.

nym of *Ehmaniella* by Rasetti (1951) and Harrington *et al.* (1959) but Peel (2020a) employed it for *Clappaspis tupeq* Peel, 2020a on account of the occluded preglabellar field, straight anterior border furrow and relatively coarse granular ornamentation of the Telt Bugt material.

Classaspis tupeq Peel 2020a
Fig. 12B, J

2020a *Classaspis tupeq* Peel, p. 7, fig. 4A–J, M.

Holotype. Cranidium: PMU 35706 from GGU sample 212813, Telt Bugt Formation, Telt Bugt, Daugaard-Jensen Land.

Figured material. In addition to the holotype, pygidium, PMU 35703 from GGU sample 212813, Telt Bugt Formation, Telt Bugt. Miaolingian, Wuliuan Stage, *Ehmaniella* Biozone.

Ptychoparioid sp. indet.
Fig. 7P, Q

Figured material. Cranidium, MGUH 33494 from GGU sample 212807, Telt Bugt Formation, Telt Bugt. Miaolingian, Wuliuan Stage, *Mexicella mexicana* Biozone.

Discussion. This single cranidium, the only specimen preserved in GGU sample 212807, is noteworthy on account of its steeply inclined anterior area, with the transition between the palpebral lobes and the anterior fixigenae being close to perpendicular. Additionally, the border furrow is joined to the axial furrow in front of the glabella by a short sagittal furrow. The preglabellar area is thus divided at the median line, in which character it is reminiscent of Ehmaniellinae sp. indet. of Sundberg (1994, fig. 56) from the Eldorado Formation of Nevada. Specimens attributed to *Achlysopsis liokata* Fritz 1968 by Sundberg (2018, fig. 23) from the *Glossolpeura walcotti*/*Ptychagnostus praecurrens* Biozone of Split Mountain, Nevada, have an undivided, short, steep preglabellar field, but this is less steep than in the narrower Telt Bugt specimen.

Superfamily Asaphiscoidea Raymond 1924

Family Asaphiscidae Raymond 1924

Genus *Blainia* Walcott 1916

Type species. *Asaphiscus (Blainia) gregarius* Walcott 1916 from the Conasauga Formation of Alabama, USA.

Discussion. *Blainia* was described by Walcott (1916) from the Conasauga Formation of Alabama as a subgenus of *Asaphiscus* Meek 1873 and revised by Resser (1935, 1938) and Schwimmer (1989). Bordonaro *et al.* (2013) placed *Glyphaspis* Poulsen 1927 as a junior subjective synonym of *Blainia*, which was followed by Peel (2020a) with reservations concerning the extensive synonymy proposed by Bordonaro *et al.* (2013) on the basis of material just from Argentina. The small amount of material from the Telt Bugt Formation does not contribute to the solution of this problem.

Glyphaspis perconcava Poulsen 1927 was proposed for a single cranidium and a few pygidia from boulders of the Cape Wood Formation in Inglefield Land. V. Poulsen (1964) reported, but neither illustrated nor described, numerous additional cranidia and pygidia. V. Poulsen (1964) described *Glyphaspis parkensis* Rasetti 1951, originally described from the Stephen Formation (Miaolingian) of British Columbia, occurring together with *Glyphaspis perconcava*, proposing derivation from the *Bathyuriscus–Elrathina* Biozone.

Blainia sp.
Fig. 11J, K–N, Fig. 12K

2020a *Blainia* sp., Peel, p.10, fig. 4K, L, N–Q.

Figured material. Cranidium, PMU 35710 from GGU sample 212813. Pygidia: MGUH 33521–MGUH 33524, from GGU sample 212873. Telt Bugt Formation, Telt Bugt. Miaolingian, Wuliuan Stage, *Ehmaniella* Biozone.

Discussion. Three cranidia from GGU sample 212813 described by Peel (2020a), corresponding to cranidial morphotype 2 of Bordonaro *et al.* (2013), closely resemble *Glyphaspis dearbornensis* as illustrated by Deiss (1939, pl. 16, fig. 22) from the Steamboat Limestone (Miaolingian, Marjumian Stage) of Dearborn Canyon, Montana. No pygidia from sample 212813 have been assigned to the same genus.

Pygidia assigned to *Blainia* sp. are common in GGU sample 212873 from Telt Bugt (Fig. 11J–N); they are smooth to finely granulose. Corresponding cranidia have not been recognised. The available sample of pygidia shows a high degree of morphological variation, as described by Bordonaro *et al.* (2013) in samples from Argentina attributed to *Blainia gregarius* Walcott 1916, and they are treated collectively here.

Their length (sag.) is about two thirds of width, and in plan view they vary from lenticular (Fig. 11L,N), with maximum width (trans.) at about mid-length, to oval with the maximum width closer to the anterior (Fig. 11M). The anterior margin is angulated close to the transition from the pleural areas to the border. The posterior margin is uniformly convex, slightly flat-

tened behind the axis. The axis is prominent (weathered in Fig. 11K–M) and variable in width; it is usually broad, equal in width to each pleural area (Fig. 11J), but less frequently somewhat narrower (Fig. 11N). The axis is of variable length, slowly tapering, with six or seven rings with deep furrows that are prominent anteriorly but fade towards a short tail piece. Pleural areas are convex towards their abrupt, steepened, transition to the border; furrowing of the pleural areas curves strongly towards the posterior, but fades posteriorly; the anteriormost furrow is prominent. The pygidial border is of variable width (trans.), often as wide as each pleural area, with several furrows conspicuous anteriorly. The furrows are deepened near the steep transition from the pleural areas to the shallowly convex, outwards sloping border, but fade towards the margin and also posteriorly. In some specimens, a narrow groove parallels the posterior margin of each pleura (Fig. 11J).

Deiss (1939) described similar pygidia from the Steamboat Limestone of Dearborn Canyon, Montana, as *Glyphaspis dearbornensis* and *Glyphaspis similis*, assigned to *Blainia* by Bordonaro *et al.* (2013). *Glyphaspis perconcava*, *Glyphaspis parkensis* Rasetti 1951 of V. Poulsen (1964, pl. 3, fig. 9) from the Cape Wood Formation of Inglefield Land (Fig 1A, localities 1,2), and Rasetti's (1951) original specimens from the Stephen Formation have a narrower pygidial axis.

Genus *Blainiopsis* Poulsen 1946

Type species. Blainiopsis holtedahli Poulsen 1946 from the Cape Wood Formation of Bache Peninsula, Ellesmere Island, Nunavut (Fig. 1A, locality 3).

Discussion. Poulsen (1946) described *Blainiopsis* from the Cape Wood Formation of Bache Peninsula. V. Poulsen (1964) reported *Blainiopsis holtedahli* Poulsen 1946 and *B. benthami* Poulsen 1946 from west of Blomsterbækken in Inglefield Land (Fig. 1A, locality 2), suggesting a late *Bathyuriscus–Elrathina* Zone age [= *Ehmaniella* Biozone] for the upper Cape Wood Formation. Peel (202a) reported about ten specimens of *Blainiopsis* in GGU sample 212814 from the Telt Bugt Formation at Telt Bugt, where both species seem to be present. *Blainiopsis* has been recorded also from western Newfoundland (Boyce 1979) and from the Cambrian of San Juan, Argentina (Bordonaro 1980).

Blainiopsis holtedahli Poulsen 1946
Fig. 12F

1946   *Blainiopsis holtedahli* Poulsen, p. 313, pl. 19, figs 10–15.
2020a   *Blainiopsis holtedahli*, Peel, p. 11, fig. 5B,D,E,H.

Figured material. Cranidium, PMU 35715 from GGU sample 212814, Telt Bugt Formation, Telt Bugt. Miaolingian, Wuliuan Stage, *Ehmaniella* Biozone.

Discussion. Blainiopsis holtedahli is represented by five cranidia in GGU sample 212814 from the upper Telt Bugt Formation at Telt Bugt (Peel 2020a).

Blainiopsis benthami Poulsen, 1946
Fig. 12G, H

1946   *Blainiopsis benthami* Poulsen, p. 314, pl. 19, fig. 16, pl. 20, figs 1–2.
2020a   *Blainiopsis benthami*, Peel, p. 12, fig. 5A,C,F,G,I,J.

Figured material. Partially articulated specimen, PMU 35713 and pygidium, PMU 35714 from GGU sample 212814, Telt Bugt Formation, Telt Bugt. Miaolingian, Wuliuan Stage, *Ehmaniella* Biozone.

Discussion. Blainiopsis benthami differs from *Blainiopsis holtedahli* in the greater curvature of the anterior margin, greater curvature of the anterior part of the facial suture and the greater curvature of the palpebral lobes. In addition, the glabella has shallowly convex sides and a less conical form than the tapering glabella of *B. holtedahli*.

Pygidium sp. 1
Fig. 9G, I, J

Material. Pygidium, MGUH 33502 from GGU sample 206308. Telt Bugt Formation, Romer Søer. Miaolingian, Wuliuan Stage, *Glossopleura walcotti* Biozone.

Discussion. This pygydium is oval in shape, with its greatest width (trans.) at mid-length (sag.) and overall length about two thirds of width; the posterior margin has a shallow median indentation. The prominent axis is about the same width (trans.) as the upper surfaces of the pleural fields before they pass across a shallow furrow onto the downward sloping border area, which becomes slightly concave as the margin is approached. The axis is about two thirds the length (sag.) of the pygidium and terminates abruptly at the posterior end, although a broad low ridge continues to the margin. Five axial rings and a short tail piece are defined by broad, shallow furrows, with four segments on the pleural areas rapidly fading as they pass into the border. It is ornamented with a fine dimpled pattern.

The pygidium is similar in shape and curvature of the pleural furrowing to pygidia of *Poliella* species illustrated by Sundberg & McCollum (2003a, fig. 10), but differs in having a greater number of axial rings. Rasetti (1951) reported only two rings and a tail piece

in *Poliella prima*, where furrowing also extends more prominently onto the narrower border. A similar number of axial rings is present in the co-occurring pygidium *Fieldaspis* cf. *bilobata* (Fig. 9K–M) but this is distinguished by its more tapering axis, stronger delimitation of the border and more pronounced furrowing.

Acknowledgements

References

Babcock, L.E. 1994a: Systematics and phylogenetics of polymeroid trilobites from the Henson Gletscher and Kap Stanton Formations (Middle Cambrian), North Greenland. Bulletin Grønlands Geologiske Undersøgelse 169, 79–127.

Babcock, L.E. 1994b: Biogeography and biofacies patterns of Middle Cambrian polymeroid trilobites from North Greenland: palaeogeographic and palaeo-oceanographic implications. Bulletin Grønlands Geologiske Undersøgelse 169, 129–147.

Babcock, L.E., Robison, R.A. & Peng, S.C. 2011: Cambrian stage and series nomenclature of Laurentia and the developing global chronostratigraphic scale. Museum of Northern Arizona Bulletin 67, 12–26.

Babcock, L.E., Peng, S. & Ahlberg, P. 2017: Cambrian trilobite biostratigraphy and its role in developing an integrated history of the Earth system. Lethaia 50, 381–399. https:// doi. org/10.1111/let.12200

Bentley, C.J. & Jago, J.B. 2014: A Cambrian Series 3 (Guzhangian) trilobite fauna with *Centropleura* from Christmas Hills, northwestern Tasmania. Memoirs of the Association of Australasian Palaeontologists 45, 267–296.

Blaker, M.R. & Peel, J.S. 1997: Lower Cambrian trilobites from North Greenland. Meddelelser om Grønland, Geoscience 35, 1–145.

Bordonaro, O.L. 1980: El Cámbrico en la quebrada de Zonda, provincia de San Juan. Revista de la Asociación Geológica Argentina 35, 26–40.

Bordonaro, O.L. 2014: Nuevos datos sobre *Athabaskia anax* (Walcott, 1916) (Trilobita, Corynexochida) del Cámbrico Medio de la Precordillera de Mendoza, Argentina. Instituto Geológico y Minero de España, Boletín Geológico y Minero 125, 561–571.

Bordonaro, O.L., Pratt, B.R. & Robledo, V. 2013: Systematic, morphometric and palaeobiogeographic study of *Blainia gregaria* Walcott, 1916 (Trilobita, Ptychopariida), Middle Cambrian of the Precordillera of western Argentina. Geological Journal 48, 126–141. https://doi.org/10.1002/gj.1344

Boyce, W.D. 1979: Further developments in western Newfoundland Cambro-Ordovician biostratigraphy. Newfoundland Department of Mines and Energy, Mineral Development Division, Report of Activities for 1979, Report 1979-1, 7–9.

Campbell, D.P. 1974: Biostratigraphy of the *Albertella* and *Glossopleura* Zones (lower Middle Cambrian) of northern Utah and southern Idaho. Unpublished M.S. thesis, University of Utah, Salt Lake City, 295 pp.

Chang, W.T. 1963: A classification of Cambrian trilobites from north and northeastern China, with description of new families and new genera. Acta Palaeontologica Sinica 11, 447–487.

Christie, R.L. 1967: Bache Peninsula, Ellesmere Island, Arctic Archipelago. Geological Survey of Canada, Memoir 347, 1–63. https://doi.org/10.4095/100534

Christie, R.L. & Dawes, P.R. 1991: Geographic and geologic exploration. In: Trettin (ed.), Geology of the Innuitian Orogen and Arctic Platform of Canada and Greenland, Geology of Canada 3, 7–25. Geological Survey of Canada, Ottawa. https://doi.org/10.1130/dnag-gna-e.5

Cooper, G.A., Arellano, A.R.V., Johnson, J.H., Okulitch, V.J., Stoyanow, A. & Lochman, C. 1952: Cambrian stratigraphy and paleontology near Caborca, northwestern Sonora, Mexico: Smithsonian Miscellaneous Collections 119, 1, 184 pp.

Dames, W. 1883: Cambrische Trilobiten von Liau-Tung, In: Richthofen, F. von (ed.), China, 1–33. D. Reimer, Berlin.

Dawes, P.R. 1976: Precambrian to Tertiary of northern Greenland. In: Escher, A. & Watt, W. S. (eds), Geology of Greenland, 248–303. Geological Survey of Greenland, Copenhagen.

Dawes, P.R. 1991: Lauge Koch: pioneer geo-explorer of Greenland's far north. Earth Sciences History 10, 130–153. https://doi.org/10.17704/eshi.10.2.333584781u008431

Dawes, P.R. 2004: Explanatory notes to the geological map of Greenland, 1:500 000. Humboldt Gletscher sheet 6. Geological Survey of Denmark and Greenland Map Series 1, 1–48. https://doi.org/10.34194/geusb.v1.4615

Dawes, P.R. 2012: The Koch family papers. Part 1: new insight into the life, work and aspirations of Greenland geo-explorer Lauge Koch (1892–1964). Copenhagen, Geological Survey of Denmark and Greenland, 220 pp.

Dawes, P.R. 2016: The Koch family papers. Part 2: drawings and maps from the 2nd Thule and Bicentenary Jubilee Expeditions 1916–1923 and the mapping of northern Greenland (Avannaarsua). Volume 1: Background to the expeditions

and a catalogue, 250 pp. Volume 2: mapping from Baffin to Koch and the role of Greenlanders. Copenhagen, Geological Survey of Denmark and Greenland, 242 pp.

Dawes, P.R. & Kerr, J.W. (eds) 1982: Nares Strait and the drift of Greenland: a conflict in plate tectonics. Meddelelser om Grønland, Geoscience 8, 392 pp.

Dawes, P.R. & Peel, J.S. 1984: Biostratigraphic reconnaissance in the Lower Palaeozoic of western North Greenland. Rapport Grønlands Geologiske Undersøgelse 121, 19–51.

Dawes, P.R. *et al.* 2000: Kane Basin 1999: mapping, stratigraphic studies and economic assessment of Precambrian and Lower Palaeozoic provinces in north-western Greenland. Geology of Greenland Survey Bulletin 186, 11–28. https://doi.org/10.34194/ggub.v186.5211

de Freitas, T. 1998a: New observations on the geology of eastern Ellesmere Island, Canadian Arctic, part II: Cambro-Ordovician stratigraphy of the Parrish Glacier region. Geological Survey of Canada, Current Research 1998-E, 31–40. https://doi.org/10.4095/209951

de Freitas, T. 1998b: New observations on the geology of eastern Ellesmere Island, Canadian Arctic, part III: Cambro-Ordovician stratigraphy of the Dobbin Bay, Scoresby Bay, and Franklin Pierce Bay areas. Geological Survey of Canada, Current Research 1998-E, 41–50. https://doi.org/10.4095/209951

de Freitas, T. 1998c: New observations on the geology of eastern Ellesmere Island, Canadian Arctic, Part IV: Cambro-Ordovician stratigraphy of the Rawlings Bay area and nunataks of the Agassiz Ice Cap. Geological Survey of Canada, Current Research 1998-E, 51–61. https://doi.org/10.4095/209951

de Freitas, T. & Fritz, W.H. 1995: Age and stratigraphy of the Cass Fjord Formation, Arctic Canada. Geological Survey of Canada, Current Research 1995-E, 97–104. https://doi.org/10.4095/205193

Deiss, C.F. 1939: Cambrian stratigraphy and trilobites of north-western Montana. Geological Society of America, Special Papers 18, 135 pp. https://doi.org/10.1130/spe18-p1

Dewing, K, Harrison, J.C. & Mayr, U. 2001: Stratigraphy of the Cass Fjord Formation (Middle and Upper Cambrian), northeast Ellesmere Island, Nunavut. Geological Survey of Canada, Current Research 2001–B4, 1–9. https://doi.org/10.4095/212118

Eddy, J.D. & McCollum, L.B. 1998: Early Middle Cambrian *Albertella* Biozone trilobites of the Pioche Shale, south-eastern Nevada. Journal of Paleontology 72, 864–887. https://doi.org/10.1017/s0022336000027207

Foglia, R.D. & Vaccari, N.E. 2010: Delamaran trilobites from the La Laja Formation, San Juan, Argentina. Ameghiniana 47, 431–445.

Frisch, T. & Dawes, P.R. 2014: Discussion: The rotations opening the Central and Northern Atlantic Ocean: compilation, drift lines, and flow lines (Int J Earth Sci 102: 1357–1376). International Journal of Earth Sciences 103, 967–969. http://dx.doi.org/10.1007/s00531-013-0981-6

Fritz, W.H. 1968: Lower and early Middle Cambrian trilobites from the Pioche Shale, eastcentral Nevada, U.S.A. Palaeon-tology 11, 183–235.

Geyer, G. 2019: A comprehensive Cambrian correlation chart. Episodes 42, 4, 1–12. https://doi.org/10.18814/epiiugs/2019/019026

Geyer, G. & Peel, J.S. 2011: The Henson Gletscher Formation, North Greenland, and its bearing on the global Cambrian Series 2–Series 3 boundary. Bulletin of Geosciences 86, 465–534. https://doi.org/10.3140/bull.geosci.1252

Gosen, W. von, Piepjohn, K., Gilotti, J.A., McClelland, W.C. & Reinhardt, L. 2019: Structural evidence for sinistral displacement on the Wegener Fault in southern Nares Strait, Arctic Canada. Geological Society of America Special Paper 541, 367–396. https://doi.org/10.1130/2018.2541(18)

Hall, J. & Whitfield, R.P. 1877: Paleontology part 2: Report of the geological exploration of the fortieth parallel 4, 197–302. United States Geological Survey. https://doi.org/10.3133/70039230

Harrington, H.J. *et al.* 1959: Arthropoda 1. In: Moore, R.C. (ed) Treatise on Invertebrate Paleontology part O, 560 pp. Geological Society of America and University of Kansas Press. https://doi.org/10.17161/dt.v0i0.5604

Harrison, J.C. 2006: In search of the Wegener Fault: re-evaluation of strike-slip displacements along and bordering Nares Strait. Polarforschung 74, 129–160.

Henriksen, N. & Peel, J.S. 1976: Cambrian–Early Ordovician stratigraphy in south-western Washington Land, western North Greenland. Rapport Grønlands Geologiske Undersøgelse 80, 17–23.

Higgins, A.K., Ineson, J.R., Peel, J.S., Surlyk, F. & Sønderholm, M. 1991a: Lower Palaeozoic Franklinian Basin of North Greenland. Grønlands Geologiske Undersøgelse Bulletin 160, 71–139.

Higgins. A.K., Ineson, J.R., Peel, J.S. Surlyk, F.S. & Sønderholm, M. 1991b: Cambrian to Silurian basin development and sedimentation, North Greenland. In: Trettin, H.P. (ed.) Geology of the Innuitian Orogen and Arctic Platform of Canada and Greenland. Geology of Canada 3, 109–161. Geological Survey of Canada. https://doi.org/10.1130/dnag-gna-e.109

Ineson, J.R. & Peel, J.S. 1997: Cambrian shelf stratigraphy of North Greenland. Geology of Greenland Survey Bulletin 173, 120 pp. https://doi.org/10.34194/ggub.v173.5024

Knight, I. & Boyce, W.D. 1987: Lower to Middle Cambrian terrigenous-carbonate rocks of Chimney Arm, Canada Bay: Lithostratigraphy, preliminary biostratigraphy and regional significance. Current Research (0987) Newfoundland Department of Mines and Energy, Mineral Development Division, Report 87-1, 359–365.

Kobayashi, T. 1935: The Cambro–Ordovician formations and faunas of South Chosen. Paleontology, pt. III. Cambrian Faunas of South Chosen with special study on the Cambrian trilobite genera and families. Journal of the Faculty of Science Imperial University of Tokyo 4, 49–344.

Kobayashi, T. 1942: On the Dolichometopinae. Journal of the Faculty of Science Imperial University of Tokyo, Section II, 6 (10), 141–206.

Koch, L. 1926: Report on the Danish Bicentenary Jubilee Expedition North of Greenland 1920–23. Meddelelser om Grønland 70, 1, 1, 232 pp.

Koch, L. 1929: The geology of the south coast of Washington Land. Meddelelser om Grønland 73, 1, 1, 39 pp.

Lochman, C. 1948: New Cambrian trilobite genera from northwest Sonora, Mexico. Journal of Paleontology 22, 451–464.

Lochman, C. 1952: Trilobites. In: Cooper, G.A., Arellano, A.R.V., Johnson, J.H., Okulitch, V.J., Stoyanow, A. & Lochman, C.: Cambrian stratigraphy and paleontology near Caborca, northwestern Sonora, Mexico. Smithsonian Miscellaneous Collections 119, 60–162.

Lochman, C. 1956: Stratigraphy, paleontology, and paleogeography of the *Elliptocephala asaphoides* strata in Cambridge and Hoosick quadrangles, New York. Bulletin of the Geological Society of America 67, 1331–1396. https://doi.org/10.1130/0016-7606(1956)67[1331:spapot]2.0.co;2

Lochman-Balk, C. & Wilson, J.L. 1958: Cambrian Biostratigraphy in North America. Journal of Paleontology 32, 312–350.

Matthew, G.F. 1887: Illustrations of the fauna of the St. John Group, number 4, part 2. The smaller trilobites with eyes (Ptychoparidae and Ellipsocephalidae). Transactions and Proceedings of the Royal Society of Canada, series 2, 5, 39–66.

McCollum, L.B. & Sundberg, F.A. 2007: Cambrian trilobite biozonation of the Laurentian Delamaran Stage in the southern Great Basin, U.S.A.: implications for global correlations and defining a Series 3 global boundary stratotype. Memoirs of the Association of Australasian Palaeontologists 34, 147–156.

Meek, F.B. 1873: Preliminary palaeontology report, consisting of list and descriptions of fossils, with remarks on the age of the rocks in which they are found. Annual Report of the United States Geological Survey of Territories 6, 429–518.

Norford, B.F. 1968: A Middle Cambrian *Plagiura–Poliella* faunule from southwest District of MacKenzie. Geological Survey of Canada Bulletin 163, 29–38.

Oakey, G.N. & Chalmers, J.A. 2012: A new model for the Paleogene motion of Greenland relative to North America: plate reconstructions of the Davis Strait and Nares Strait regions between Canada and Greenland. Journal of Geophysical Research 117, B10401, 28 pp. doi:10.1029/2011JB008942

Öpik, A.A. 1961: Cambrian geology and palaeontology of the headwaters of the Burke River, Queensland. Bureau of Mineral Resources, Geology and Geophysics (Australia) Bulletin 53, 249 pp.

Öpik, A.A. 1967: The Mindyallan Fauna of north-western Queensland. Bureau of Mineral Resources, Geology and Geophysics (Australia), Bulletin 74, vol. 1, 404 pp; vol. 2, 167 pp.

Palmer, A.R. 1954: An appraisal of the Great Basin Middle Cambrian trilobites described before 1900. United States Geological Survey Professional Paper 264-D, 53–86. https://doi.org/10.3133/pp264d

Palmer, A.R. 1968: Cambrian trilobites of East-Central Alaska: United States Geological Survey Professional Paper 559-B, 115 pp. https://doi.org/10.3133/pp559B

Palmer, A.R. & Halley, R.B. 1979: Physical stratigraphy and trilobite biostratigraphy of the Carrara Formation (Lower and Middle Cambrian) in the southern Great Basin: United States Geological Survey Professional Paper 1047, 131 pp. https://doi.org/10.3133/pp1047

Palmer, A.R. & Peel, J.S. 1981: Dresbachian trilobites and stratigraphy of the Cass Fjord Formation, western North Greenland. Bulletin Grønlands Geologiske Undersøgelse 141, 46 pp.

Peel, J.S. 1974: Lower Cambrian fossils from Nyeboe Land, North Greenland fold belt. Rapport Grønlands Geologiske Undersøgelse 65, 17 (only).

Peel, J.S. 2020a: Middle Cambrian trilobites (Miaolingian, *Ehmaniella* Biozone) from the Telt Bugt Formation of DaugaardJensen Land, western North Greenland. Bulletin of the Geological Society of Denmark 68, 1–14. https://doi.org/10.37570/bgsd-2020-68-01

Peel, J.S. 2020b: *Polypleuraspis* (Arthropoda,Trilobita) from the middle Cambrian (Miaolingian) around Kane Basin (Nunavut and Greenland). Canadian Journal of Earth Sciences 57, 16–24. https://doi.org/10.1139/cjes-2019-0011

Peel, J.S. in press: *Eldoradia* and *Acrocephalops* (Trilobita: Bolaspididae) from the middle Cambrian (Miaolingian) of northern Greenland (Laurentia). GFF.

Peel, J.S. & Christie, R.L. 1982: Cambrian–Ordovician platform stratigraphy: correlations around Kane Basin. Meddelelser om Grønland, Geoscience 8, 117–135.

Peel, J.S. & Frykman, P. 1975: Archaeological observations in southern Washington Land, July–August 1975. Report and accompanying chert flakes and bone fragments presented to the National Museum, October 1975. Grønlands Geologiske Undersøgelse Intern Rapport, 25 pp.

Peng, S.C., Babcock, L.E. & Cooper, R.A. 2012: The Cambrian Period. In: Gradstein, F.M., Ogg, J.G., Schmitz, M.D. & Ogg, G.M. (eds.), The Geologic Time Scale 2012, 437–488. Elsevier BV, Amsterdam. https://doi.org/10.1016/C2011-1-08249-8

Poulsen, C. 1927: The Cambrian, Ozarkian, and Canadian faunas of northwest Greenland. Meddelelser om Grønland 70, 233–343.

Poulsen, C. 1946: Notes on the Cambro-Ordovician fossils collected by the Oxford University Ellesmere Land expedition. Quarterly Journal of the Geological Society of London 102, 299–337. https://doi.org/10.1144/gsl.jgs.1946.102.01-04.15

Poulsen, C. 1958: Contribution to the palaeontology of the Lower Cambrian Wulff River formation. Meddelelser om Grønland 162, 27 pp.

Poulsen, V. 1964: Contribution to the Lower and Middle Cambrian Palaeontology and stratigraphy of Northwest Greenland. Meddelelser om Grønland 164, 105 pp.

Poulsen, V. 1969: An Atlantic Middle Cambrian fauna from North Greenland. Lethaia 2, 1–14. https://doi.org/10.1111/j.1502-3931.1969.tb01248.x

Pratt, B.R. & Bordonaro, O.L. 2014: Early middle Cambrian trilobites from the La Laja Formation, Cerro El Molle, Pre-

cordillera of western Argentina. Journal of Paleontology 88, 906–924. http://doi.org/10.1666/13-083

Pulvertaft, T.C.R. & Dawes, P.R. 2011: North Atlantic spreading axes terminate in the continental cul-de-sacs of Baffin Bay and the Laptev Sea. Canadian Journal of Earth Sciences 48, 593–601. https://doi.org/10.1139/E11-004

Rasetti, F. 1948: Middle Cambrian Trilobites from the Conglomerates of Quebec (Exclusive of the Ptychopariidea). Journal of Paleontology 22, 315–339.

Rasetti, F. 1951: Middle Cambrian stratigraphy and faunas of the Canadian Rocky Mountains. Smithsonian Miscellaneous Collections 116, 277 pp.

Rasetti, F. 1957: Additional fossils from the Middle Cambrian Mount Whyte Formation of the Canadian Rocky Mountains. Journal of Paleontology 31, 955–972.

Raymond, P.E. 1924: New Upper Cambrian and Lower Ordovician trilobites from Vermont. Proceedings of the Boston Society of Natural History 37, 389–466.

Raymond, P.E. 1928: Two new Cambrian trilobites. American Journal of Science 5, 309–313. https://doi.org/10.2475/ajs.s5-15.88.309

Resser, C.E. 1933: Preliminary generalized Cambrian time scale. Geological Society of America Bulletin 44, 735–756. https://doi.org/10.1130/gsab-44-735

Resser, C.E. 1935: Nomenclature of some Cambrian trilobites. Smithsonian Miscellaneous Collections 93, 5, 46 pp.

Resser, C.E. 1937: Third contribution to nomenclature of Cambrian trilobites. Smithsonian Miscellaneous Collections 95, 22, 29 pp.

Resser, C.E. 1938: Cambrian system (restricted) of the Southern Appalachians. Geological Society of America, Special Papers 15, 140 pp. https://doi.org/10.1130/SPE15

Resser, C.E. 1939a: The *Ptarmigania* strata of the northern Wasatch Mountains. Smithsonian Miscellaneous Collections 98, 72 pp.

Resser, C.E. 1939b: The Spence Shale and its fauna. Smithsonian Miscellaneous Collections 97, 12, 29 pp.

Richter, R. 1933: Crustacea (Paläontologie). In: Dittler, R., Joos, G., Korschelt, E., Linek, G., Oltmanns, F. & Schaum, K. (eds), Handwörterbuch der Naturwissenschaften (2nd edition), 840–864. Gustav Fischer, Jena.

Robison, R.A. 1976: Middle Cambrian trilobite biostratigraphy of the Great Basin. Brigham Young University Geology Studies 23(2), 93–109.

Robison, R.A. 1984: Cambrian Agnostida of North America and Greenland. Part I, Ptychagnostidae. University of Kansas Paleontological Contributions Paper 109, 59 pp.

Robison, R.A. 1988: Trilobites of the Holm Dal Formation (late Middle Cambrian), central North Greenland. Meddelelser om Grønland, Geoscience 20, 23–103.

Robison, R.A. 1994: Agnostoid trilobites from the Henson Gletscher and Kap Stanton formations (Middle Cambrian), North Greenland. Bulletin Grønlands Geologiske Undersøgelse 169, 25–77.

Robison, R.A. & Babcock, L.E. 2011: Systematics, paleobiology,

and taphonomy of some exceptionally preserved trilobites from Cambrian Lagerstätten of Utah. Kansas University Paleontological Contributions 5, 47 pp.

Schwimmer, D.R. 1989: Taxonomy and biostratigraphic significance of some Middle Cambrian trilobites from the Conasauga Formation in western Georgia. Journal of Paleontology 63, 484–494. https://doi.org/10.1017/S0022336000019703

Sundberg, F.A. 1994: Corynexochida and Ptychopariida (Trilobita, Arthropoda) of the *Ehmaniella* Biozone (Middle Cambrian), Utah and Nevada. Natural History Museum of Los Angeles County, Contributions in Science 446, 137 pp.

Sundberg, F.A. 2005: The Topazan Stage, a new Laurentian stage (Lincolnian Series—"Middle" Cambrian). Journal of Paleontology 79, 63–71. https://doi.org/10.1666/0022-3360(2005)079<0063:ttsanl>2.0.co;2

Sundberg, F. 2011: Delamaran biostratigraphy and lithostratigraphy of Southern Nevada. Museum of Northern Arizona Bulletin 67, 174–185.

Sundberg, F.A. 2018: Trilobite biostratigraphy of the Cambrian 5 and Drumian stages, Series 3 (Laurentian Delamaran, Topazan, and Marjuman stages, Lincolnian Series) of the lower Emigrant Formation at Clayton Ridge, Esmeralda County, Nevada. Journal of Paleontology 92, Memoir 76, 1–44. https://doi.org:10.1017/jpa.2017.130

Sundberg, F.A. & McCollum, L.B. 2000: Ptychopariid trilobites of the lower–middle Cambrian boundary interval, Pioche Shale, south-eastern Nevada. Journal of Paleontology 74, 604–630. https://doi.org/10.1666/0022-3360(2000)074<0604:ptotlm>2.0.co;2

Sundberg, F.A. & McCollum, L.B. 2002: *Kochiella* Poulsen, 1927, and *Hadrocephalites* new genus (Trilobita: Ptychopariida) from the early Middle Cambrian of western North America. Journal of Paleontology 76, 76–94. https://doi.org/10.1666/0022-3360(2002)076<0076:kpahng>2.0.co;2

Sundberg, F.A. & McCollum, L.B. 2003a: Trilobites of the lower Middle Cambrian *Poliella denticulata* Biozone (new) of southeastern Nevada. Journal of Paleontology 77, 331–359. https://doi.org/10.1666/0022-3360(2003)077<0331:totlmc>2.0.co;2

Sundberg, F.A. & McCollum, L.B. 2003b: Early and Mid Cambrian trilobites from the outer-shelf deposits of Nevada and California, USA. Palaeontology 46, 945–986. https://doi.org/10.1111/1475-4983.00328

Sundberg, F.A. *et al.* 2020: Asynchronous trilobite extinctions at the early to middle Cambrian transition. Geology 48, 441–445. https://doi.org/10.1130/G46913.1

Swinnerton, H.H. 1915: II.– Suggestions for a revised classification of trilobites. Geological Magazine 2, 538–545. https://doi.org/10.1017/S0016756800203737

Troelsen, J.C. 1950: Contributions to the geology of Northwest Greenland, Ellesmere Island and Axel Heiberg Island. Meddelelser om Grønland 149, 86 pp.

Walch, J.E.I. 1771: Die Naturgeschichte der Versteinerungen, zur Erläuterung der Knorrischen Sammlung von Merkwürdigkeiten der Natur, 4, 3, 184 pp. Paul Jonathan Felstecker, Nürnberg.

Walcott, C.D. 1887: Fauna of the "upper Taconic" of Emmons, in Washington County, New York. American Journal of Science 34, 187–199. https://doi.org/10.2475/ajs.s3-34.201.187

Walcott, C.D. 1889: Description of new genera and species of fossils from the Middle Cambrian. U. S. National Museum Proceedings 11, 441–446. https://doi.org/10.5479/si.00963801.11-738.441

Walcott, C.D. 1916: Cambrian geology and paleontology III, no. 5, Cambrian trilobites. Smithsonian Miscellaneous Collections 64, 303–456.

Walcott, C.D. 1917: Cambrian geology and paleontology 3, Fauna of the Mount Whyte formation. Smithsonian Miscel-laneous Collections 67, 3, 61–114.

Walcott, C.D. 1924: Cambrian and Ozarkian trilobites. Smith-sonian Miscellaneous Collections 75, 53–60.

Watt, W.S. 2019: Stratigraphic lexicon for Greenland. Nomencla-ture of stratified successions in current use, 327 pp. Geologi-cal Survey of Denmark and Greenland, Copenhagen. https://doi.org/10.22008/geusbook/strat-lex-greenland

Zhao, Y. *et al.* 2019: Global Standard Stratotype-Section and Point (GSSP) for the conterminous base of the Miaolin-gian Series and Wuliuan Stage (Cambrian) at Balang, Jianhe, Guizhou, China. Episodes 42, 165–184. https://doi.org 10.18814/epiiugs/2019/019013

A tale from the middle Paleocene of Denmark: A tube-dwelling predator documented by the ichnofossil *Lepidenteron mortenseni* n. isp. and its predominant prey, *Bobbitichthys* n. gen. *rosenkrantzi* (Macrouridae, Teleostei)

WERNER SCHWARZHANS, JESPER MILÀN & GIORGIO CARNEVALE

DGF

Geological Society of Denmark
https://2dgf.dk

The ichnofossil *Lepidenteron* provides a unique taphonomic window into the life habits of a tube-dwelling predator, probably an eunicid polychaete, and its fish prey. Here we describe a new tube-like ichnofossil *Lepidenteron mortenseni* n. isp. from the Kerteminde Marl (100–150 m palaeo-water depth) from the Gundstrup gravel pit near Odense, Fyn, Denmark. 110 individual tubes were examined which contain fish remains, including a variety of disarticulated bones and otoliths, by far dominated by a single gadiform taxon referred herein to as *Bobbitichthys* n. gen. The isolated otoliths here associated with disarticulated gadiform bones have previously been described, from the time equivalent Lellinge Greensand exposed in the Copenhagen area, as *Hymenocephalus rosenkrantzi*, a grenadier fish (family Macrouridae). The abundance of associated bones and otoliths in the examined tubes allowed us to reconstruct part of the cranial configuration of *Bobbitichthys rosenkrantzi* and to tentatively interpret it as a stem macrourid. *Bobbitichthys rosenkrantzi* represents the earliest grenadier known in the fossil record. Additional, although considerably less abundant, skeletal remains and otoliths have been tentatively referred to a long-fin bonefish (family Pterothrissidae, *Pterothrissus? conchaeformis*), a viviparous brotula (family Bythitidae, *Bidenichthys? lapierrei*), a conger eel (family Congridae, possibly belonging to *Rhynchoconger angulosus*), and another unidentified gadiform.

Keywords: Predatory polychaete; Macrouridae; *Lepidenteron* tube; otolith; osteology; Kerteminde Marl; Paleocene; Selandian.

Werner Schwarzhans [wwschwarz@aol.com], Ahrensburger Weg 103, D-22359 Hamburg, Germany; also Natural History Museum of Denmark, Universitetsparken 15, DK-2100 Copenhagen Ø, Denmark. http://orcid.org/0000-0003-4842-7989. Jesper Milàn [jesperm@oesm.dk], Geomuseum Faxe, Østsjællands Museum, Rådhusvej 2, DK-4640 Faxe, Denmark. https://orcid.org/0000-0002-9556-3177. Giorgio Carnevale [giorgio.carnevale@unito.it], Dipartimento di Scienze della Terra, Università degli Studi di Torino, Via Valperga Caluso 35, I-10125 Torino, Italy. http://orcid.org/0000-0002-3433-4127.

Corresponding author: Jesper Milàn

Skeletal elements documenting predator–prey interactions offer a unique opportunity to study specific palaeoecological relationships in deep time (McAllister 2003). Here we investigate fish skeletal remains found in the tubular trace fossils of the ichnogenus *Lepidenteron* from the middle Paleocene (Selandian) Kerteminde Marl (Clemmensen & Thomsen 2005; Schnetler & Nielsen 2018), coming from the gravel pit at Gundstrup, north of Odense, Fyn, Denmark (Fig. 1). The *Lepidenteron* tubes of the Kerteminde

Marl, which represent a new ichnospecies described herein, are remarkable for their abundance (a total of 110 tubes have been retrieved) and the contained skeletal elements which mostly belong to a single gadiform species hitherto known only from isolated otoliths and originally referred to as *Hymenocephalus rosenkrantzi* Schwarzhans 2003, a grenadier fish, from the time-equivalent Lellinge Greensand exposed in the Copenhagen area.

The associated otoliths and bones of the fishes found in the tubes of the new *Lepidenteron* ichnospecies from the Kerteminde Marl provide an opportunity to review the systematic position of *Hymenocephalus rosenkrantzi*, leading to the establishment of the fossil genus *Bobbitichthys* n. gen. A specimen each of the extant *Hymenocephalus italicus* and *Euclichthys polynemus* were dissected for a direct comparison

with the fossil bones, to test two alternative phylogenetic attributions that have been discussed in past literature. Only a few other fish taxa were identified from the *Lepidenteron* tubes of the Kerteminde Marl, including (in order of abundance) the viviparous brotula *Bidenichthys*? *lappierrei*, the longfin-bonefish *Pterothrissus*? *conchaeformis*, a second unidentifiable gadiform, a single otolith of a conger eel possibly belonging to *Rhynchoconger angulosus* and, finally, a single otolith of *Centroberyx integer*, which was found outside of a *Lepidenteron* tube. The majority of the otoliths of *Bidenichthys*? *lappierrei* were found in two discrete tubes and their associated bones did not yield any useful taxonomic information. In the case of *Pterothrissus*? *conchaeformis* a rare instance of a partially articulate oral jaw was found in a single tube and a large maxilla in another.
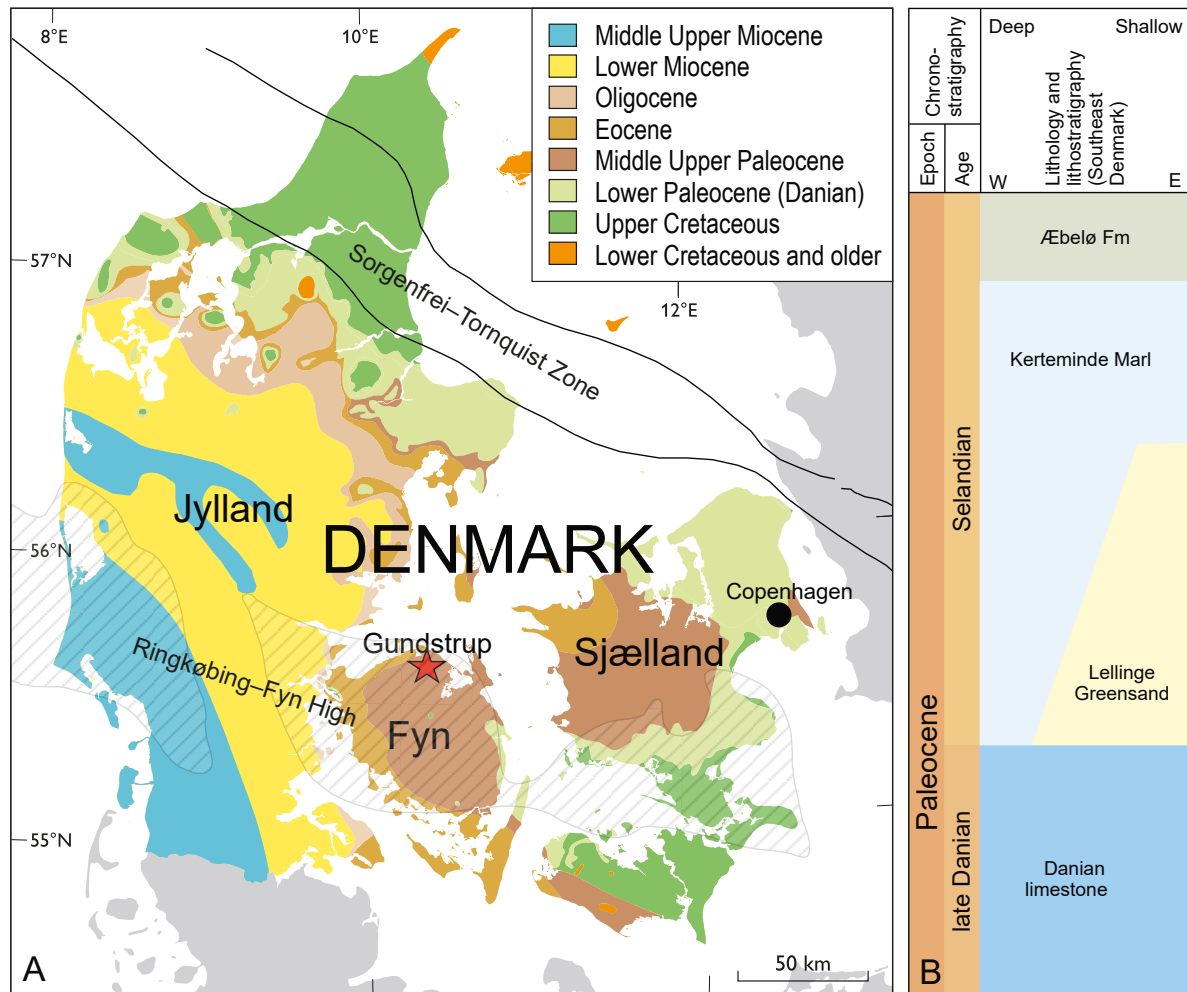

Fig. 1. A: Pre-Quaternary map of Denmark indicating the location of the Gundstrup gravel pit in the middle upper Paleocene deposits on the island of Fyn (55.56°N, 10.35°E). Modified from Håkansson & Pedersen (1992). **B:** Schematic representation of the Upper Danian – Selandian stratigraphy of south-eastern Denmark. Modified from Clemmensen & Thomsen (2005).

Geological setting and location

The Paleocene sedimentation in the Danish Basin started as carbonate dominated during the Danian. The carbonate deposition ended at the end of the Danian as a consequence of a major regression that took place at about 61.6 Ma (Vandenberghe *et al.* 2012), resulting in an extensive erosional unconformity at the boundary to the overlying Selandian deposits (e.g. Thomsen & Heilmann-Clausen 1985; Clemmensen & Thomsen 2005). The succeeding Selandian transgression resulted in a different depositional regime dominated by siliciclastic sedimentation, as documented by the Kerteminde Marl and its lateral equivalent the Lellinge Greensand (Clemmensen & Thomsen 2005). While the Danian carbonates were deposited in a subtidal shelf palaeoenvironment situated at a depth down to a few hundred metres, the Selandian Kerteminde Marl is interpreted as being deposited in an offshore shelf environment at about 100–150 m depth (Clemmensen & Thomsen 2005; Heilmann-Clausen & Surlyk 2006). The overlying Selandian – Thanetian Æbelø Formation is predominantly clay and represents a progressively deeper depositional environment (Clemmensen & Thomsen 2005). The thickness of the Kerteminde Marl is up to 150 m, thinnest over the Ringkøbing–Fyn High and thickest northward towards the Sorgenfrei–Tornquist Zone (Sorgenfrei & Buch 1964; Clausen & Huuse 1999; Clemmensen & Thomsen 2005). The Selandian depocentre of the Kerteminde Marl is located on western Sjælland (Clemmensen & Thomsen 2005).

So far only the mollusc fauna of the Kerteminde Marl has been the focus of systematic studies, revealing a diverse assemblage of 133 species (Schnetler & Nielsen 2018). Vertebrates are known in the form of abundant skeletal remains of teleost fishes (King 1994), and several undescribed chondrichthyan teeth exist in the collection of the Natural History Museum of Denmark. Turtles are known in the form of a plastron showing traces of predation by sharks and crocodilians (Myrvold *et al.* 2018). In addition, ostracods, sponges and fragments of echinoderms are also mentioned by King (1994).

Material and methods

The Gundstrup gravel pit contains numerous fossil-rich, glacially derived fragments of the Kerteminde Marl which range in size from boulders to cobbles and pebbles. A total of 110 such samples with *Lepidenteron* tubes from the Kerteminde Marl, collected by amateur geologist Peter Tang Mortensen in the Gundstrup gravel pit, have been examined together with two otoliths found outside of tubes. Overall, 529 otoliths have been recognized, of which 361 are identifiable. Of the identified otoliths, 320 belong to *Bobbitichthys* n. gen. *rosenkrantzi*, the remainder to five different species (see below for details). Considering the abundance of otoliths referred to a single species, it is reasonable to attribute a large part of the isolated fish bones to the same taxon, i.e., *Bobbitichthys rosenkrantzi*. In fact, many of the isolated identifiable fish bones are readily recognizable as belonging to a single gadiform species. Also, a quantitative evaluation of the measured otoliths shows that most of the fish remains located in the tubes are derived from specimens of similar size. Based on these observations we felt able to reliably reconstruct an idealized portion of the skull of *Bobbitichthys rosenkrantzi* from the individual bones.

The specimens were studied and drawn with a stereo-microscope equipped with a camera lucida drawing tube. Photographs were taken with a digital camera adapted to a Wild M400 photomacroscope and remotely controlled from a computer. Sets of photographs of differing fields of depth of individual specimens were stacked using the HeliconFocus software of HeliconSoft and were then digitally retouched with Adobe Photoshop for sand grains or minor inconsistencies, as far as doing so did not alter the morphology of the photographed specimens. Mirror imaged figures are indicated in the captions as 'reversed'. All the investigated and figured specimens are housed at the collection of Geomuseum Faxe, Østsjællands Museum (OESM) in Faxe, Denmark. Extant fishes of the species *Hymenocephalus italicus* and *Euclichthys polynemus* used for morphological comparisons are housed in the collection of the Natural History Museum of Denmark (ZMUC).

This published work and the nomenclatural acts it contains have been registered in Zoobank: http://zoobank.org/NomenclaturalActs/06ADB39E-D932-4098-91DE-1D033FB9B720 and http://zoobank.org/NomenclaturalActs/0c0777f5-899d-412c-a935-d4664921cc59

Systematic palaeontology

Ichnogenus *Lepidenteron* Frič 1878
***Lepidenteron mortenseni* n. isp.**
Fig. 2

Holotype. OESM 10971, Kerteminde Marl, middle Paleocene (Selandian), gravel pit at Gundstrup, north of Odense, Fyn, Denmark. Fig. 2A.

Paratypes. five specimens, OESM 10969, 10996–10999, same data as holotype.

Further material. 104 specimens, same data as holotype.

Diagnosis. Long, straight, un-branched, sediment-filled tube up to at least 20 cm in length, with oval cross section and with an average 2 cm width across the longest diameter (range 1.5–2.5 cm), embedded in clayey marlstone without apparent bedding orientation. Tube outline defined by fish debris lining the entire tube perimeter with about 1 mm thickness; no further evidence of tube walls. Tube filling is a homogeneous sediment of the same composition as the surrounding sediment.

Description. The tube segments are straight and of variable lengths. The longest tube segment found is
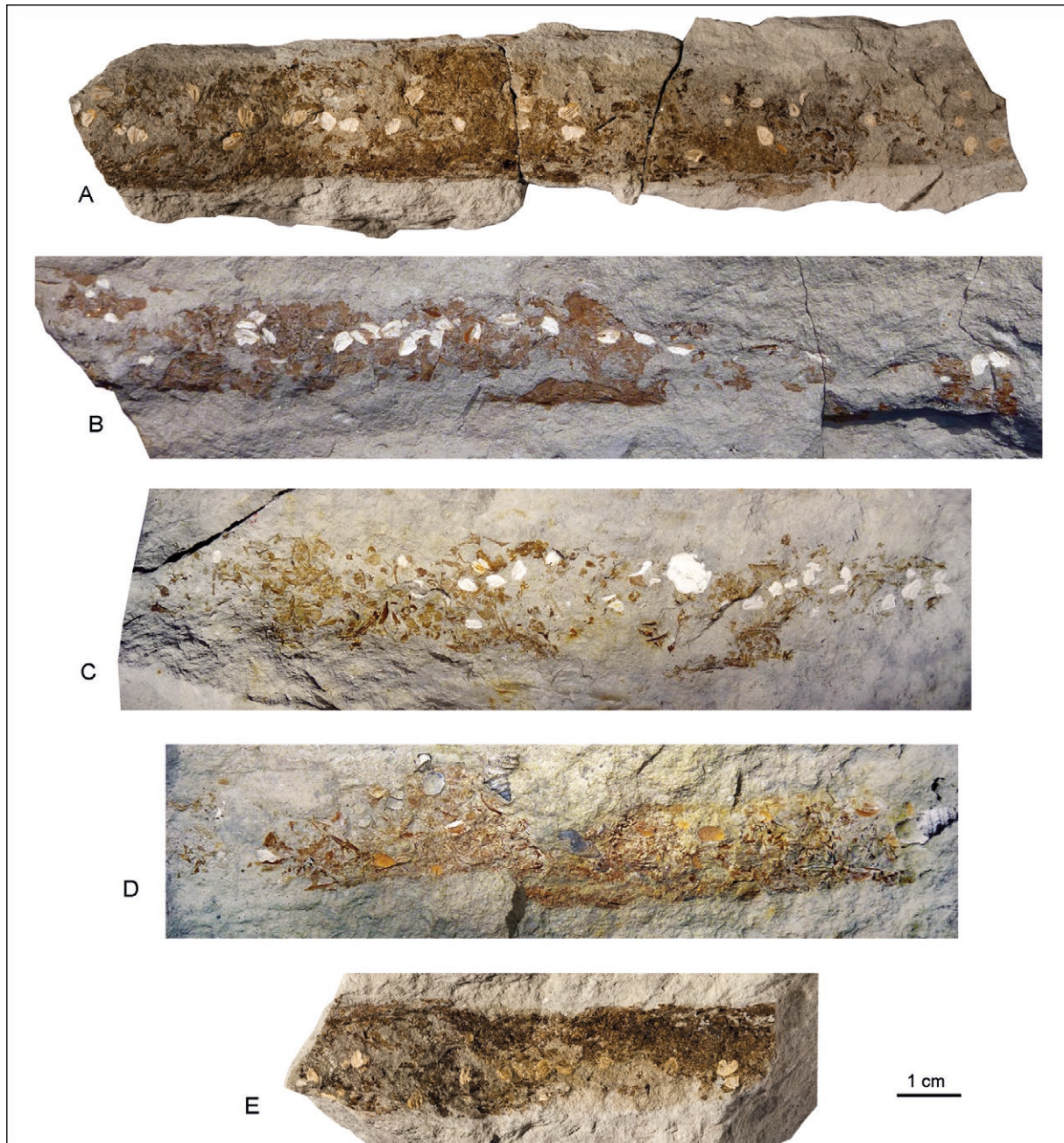
Fig. 2. *Lepidenteron mortenseni* n. isp. tubes. **A:** OESM 10971, holotype. **B:** OESM 10969, paratype. **C:** OESM 10997, paratype. **D:** OESM 10998, paratype, note tectonically induced displacement. **E:** OESM 11000. Otoliths have light colours; bones and scales have dark colours.

20 cm long and is still incomplete. The tube diameters are 1.5 to 2.5 cm across the longest direction (average 2.0 cm) and 1.0 to 1.3 cm across the shortest one. The oval diameter is probably a result of a mild degree of compaction. No termination or opening of tubes is known. The tube walls are marked by debris of about 1 mm thickness composed of fish bones, scales and otoliths. The fish debris is almost always completely disarticulated and individual bones are commonly also broken into smaller fragments. However, some tubes contain less abundant fish debris and then individual bones are preserved and identifiable. Only in two cases partially articulated fish bones have been observed. The tubes are embedded in the clayey marlstone of the Kerteminde Marl (middle Paleocene) deposited on the lower shelf well below wave base, and the embedding lithology does not differ from the tube filling sediment. In cases of moderate debris content the exact outline of the tube is not continuously discernable. The composition of the fish debris along the tube walls is of a mixed nature in the majority of tubes, although apparently stemming almost totally from two fish species only. A few tube segments have been observed with dominantly scales, or otoliths, or bones accumulated along the walls.

Discussion. Four different species are currently recognized of the ichnogenus *Lepidenteron*, identified according to the different composition of the tube walls (Suhr 1988; Jurkowska & Uchman 2013; Niebuhr & Wilmsen 2016). These are *L. lewesiensis* (Mantell 1822) with fish bones, *L. mantelli* (Gleinitz 1849) with plant remains, *L. cancellata* (Bather 1911) with sedimentary debris, and *L. variabilis* Suhr 1988 with varying compositions of litho- and bioclasts. *Lepidenteron mortenseni* is similar to *L. lewesiensis* because the wall lining components are exclusively composed of fish debris. It differs from *L. lewesiensis* in being always straight and with a constant diameter; different diameters observed in *L. mortenseni* may relate to tube dwellers of different sizes and do not show any variation of diameter along the preserved segments. A typical feature of *Lepidenteron lewesiensis* appears to be the concentration of bioclasts close to the lower margin of the burrow (Jurkowska & Uchman 2013), while in *L. mortenseni* the bioclasts may vary in composition and density of distribution but are not concentrated as in *L. lewesiensis*. In addition, *Lepidenteron mortenseni* further differs from *L. lewesiensis* in the composition of the embedding sediment (clayey marl versus chalk) and geological age (Paleocene versus late Cretaceous).

The tracemaker of the ichnofossil *Lepidenteron* is unknown. Potential body fossils related to the tracemaker have not been observed in any of its tubes, including the newly discovered ones described here

from the Kerteminde Marl. A variety of potential candidates have been hypothesized for the tube dwelling organism. Bather (1911) hypothesized a terebelloid polychaete as the most probable tracemaker, a possibility also reported by Suhr (1988), although anguilliform fishes and stomatopod crustaceans have also been considered (see discussion in Jurkowska & Uchman 2013). Jurkoska & Uchman (2013) considered predatory eunicid polychaete worms as the most probable candidates, although no scolecodont jaw elements have been found in association with *Lepidenteron* tubes. However, scolecodonts have recently been described from upper Danian sediments of southern Sweden (Bergman & Eriksson 2003), indicating that potential predator polychaetes occurred in the vicinity in time and space.

Bieńkowska-Wasiluk *et al.* (2015) described fish remains belonging to ten different taxa retrieved from tubes of *Lepidenteron lewesiensis* and concluded that "the preservation of fish remains suggests that the fishes were pulled down into the burrow", "probably by eunicid polychaetes." *Lepidenteron mortenseni* is remarkable for containing abundant otoliths associated with other fish remains, which allow a detailed identification of the fish taxa occurring within these tubes. Of the 529 otoliths found, 361 are identifiable and belong to species previously described from time-equivalent strata in the Copenhagen area (Lellinge Greensand, Schwarzhans 2003). Of the otoliths found in the *Lepidenteron* tubes, 320 belong to a single species, which was originally described as *Hymenocephalus rosenkrantzi* Schwarzhans 2003 (now *Bobbitichthys* n. gen. *rosenkrantzi*, see below), based on isolated otoliths, while another 28 specimens belong to *Bidenichthys*? *lappierrei* (Nolf 1978). Moreover, there are six specimens belonging to an unidentified additional gadiform taxon, five specimens referred to *Pterothrissus*? *conchaeformis* (Koken 1885), and a single specimen of a conger eel plus a single specimen of *Centroberyx integer* (Koken 1885), the last-named found outside of a *Lepidenteron* tube. The otoliths of *Bobbitichthys rosenkrantzi* are highly diagnostic because of their very specific outline and sulcus morphology (Schwarzhans 2003). The majority of the remains of the 168 unidentifiable otoliths, which are mostly represented by small fragments, likely also belong to *Bobbitichthys rosenkrantzi*. We do not assume that the hypothesized eunicid polychaete was prey selective to such an extent as required for the composition of the observed fish debris, but that it rather acted as an opportunistic predator. The overwhelming abundance of remains of *Bobbitichthys rosenkrantzi* is taken to indicate that this fish was abundant and relatively easy to catch for a tube-dwelling and hiding ambush hunter like an eunicid polychaete. Thus, our observations

are fully consistent with the hypothesis proposed by Bieńkoska-Wasiluk *et al.* (2015).

Etymology. Named after Peter Tang Mortensen (Odense), who collected all the specimens of *Lepidenteron* described here.

Description of fish remains in the tubes of *Lepidenteron mortenseni* that can be associated with otoliths

Order Albuliformes Jordan 1923

Family Pterothrissidae Gill 1893

Genus *Pterothrissus* Hilgendorf 1877

Pterothrissus? conchaeformis (Koken 1885)
Fig. 3

Material. Five otoliths, OESM 10974, 10997, 10999; a single partially articulated oral jaw exposed in medial view and consisting of the premaxilla, maxilla (part), dentary and angular (part), OESM 10994 (Fig. 3A–B); a single maxilla, OESM 10981 (Fig. 3C); Kerteminde Marl, middle Paleocene (Selandian), gravel pit at Gundstrup, north of Odense, Fyn, Denmark.

Description of skeletal remains. The partially articulated oral jaw consists of a well-preserved stout premaxilla, which is characterized by a lobate, simple anterior articulatory facet and a relatively long, tapering alveolar process bearing a single row of widely spaced, sharp and pointed conical teeth. The maxilla is long and robust, slightly curved with a long anterior process that articulates with the premaxilla; it bears numerous sharp, moderately long teeth arranged in a single row. The maxillary teeth appear to be slightly smaller than the premaxillary ones. The dentary is massive, broad, almost v-shaped, bearing a large but incompletely preserved coronoid process; the coronoid process is situated in the posterior half of the mandible. The dentary teeth are similar to those of the premaxilla. The angular is only partially preserved.

Discussion. The partially articulated oral jaw represents one of two cases of articulated bones found in the *Lepidenteron* tubes of the Kerteminde Marl. The premaxilla with its simple anterior articulatory facet, the overall morphology of the long and toothed maxilla, and the mandible with a well-developed coronoid process are indicative of elopomorphs belonging to the family Pterothrissidae (Forey 1973). As mentioned above, five otoliths referred to *Pterothrissus? conchaeformis* have been observed in the examined *Lepidenteron* tubes of the Kerteminde Marl. This otolith-based species has been associated with the genus *Pterothrissus* Hilgendorf 1877 or with the related fossil otolith-based genus *Pteralbula* Stinton 1973. *Pteralbula* has been redefined and restricted to species of Aptian and Albian age (Schwarzhans 2018), while the Paleocene species was assigned to the
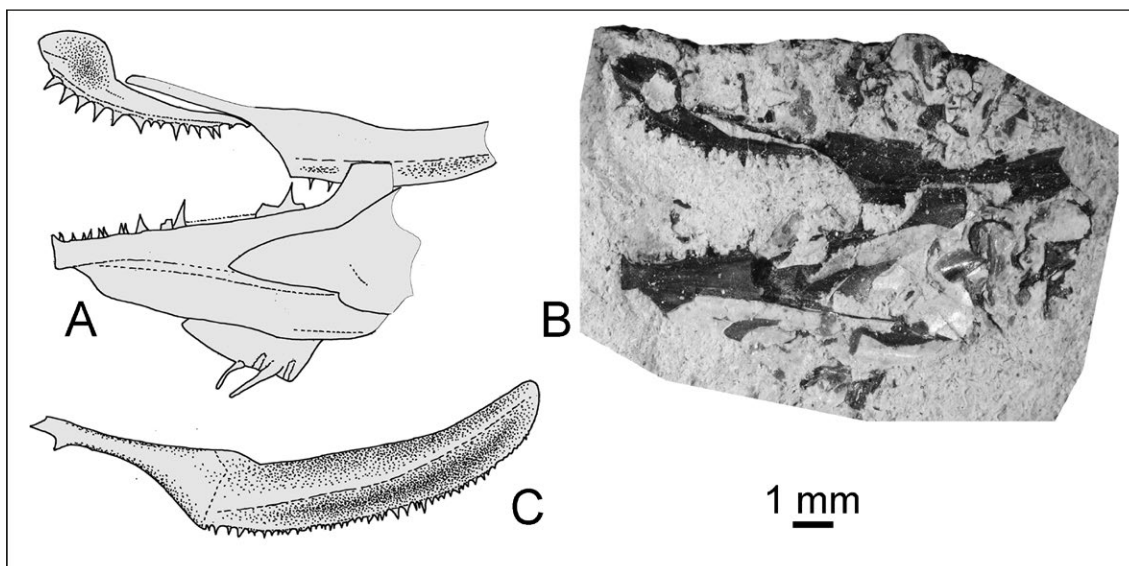

Fig. 3. *Pterothrissus? conchaeformis* (Koken 1885). **A, B:** OESM 10994, partly right articulated jaws, including premaxilla, maxilla, dentary and fragmentary angular, plus anterior ceratohyal and a few branchiostegal rays, medial view (A: interpretative drawing, B: photograph); **C:** OESM 10981, right maxilla, medial view.

genus *Pterothrissus*. However, the large conical teeth, long maxilla, relatively long alveolar process of the premaxilla and large and posteriorly located coronoid process of the dentary are considerably different from those of the extant *P. gissu* Hilgendorf 1877 or the late Cretaceous fossil genus *Istieus* Agassiz 1844 (see Forey 1973) and could indicate the presence of a further fossil genus of the Pterothrissidae. Therefore, the allocation within the genus *Pterothrissus* remains tentative in the present study. *Pterothrissus? conchaeformis* is a long-ranging species known from the late Maastrichtian to the late Paleocene, although there is evidence that would possibly extend its record to the middle Eocene (Schwarzhans & Stringer 2020). It has been identified as one of a small group of potentially post-disaster opportunists following the K–Pg boundary extinction event (Schwarzhans & Milàn 2017; Schwarzhans & Stringer 2020).

Order Gadiformes Goodrich 1909

Family Macrouridae Bonaparte 1832

Genus *Bobbitichthys* n. gen.

Type species. Hymenocephalus rosenkrantzi Schwarzhans 2003 by subsequent designation and monotypy.

Remarks. The definition and description of *Bobbitichthys rosenkrantzi* are mostly based on isolated otoliths associated with disarticulated bones in the *Lepidenteron mortenseni* tubes. The otoliths of *Bobbitichthys rosenkrantzi* represent more than 60% of all the otoliths found in the tubes and 88.5% of the identifiable ones. As discussed above, the other identifiable otoliths belong to the viviparous brotula *Bidenichthys? lappierrei* (7.5% of identifiable otoliths) and, very rarely, to *Pterothrissus? conchaeformis* and a second, unidentifiable gadiform. The skeletal elements referred herein to *Bobbitichthys* are easily recognizable due to their thin and light texture and exhibit numerous gadiform characters. Moreover, they derive from tubes where no other gadiform otoliths have been observed. Schwarzhans (2003) described three different otolith-based taxa belonging to the Macrouridae from the Selandian of Denmark, which would represent the earliest geological records of the family. Their allocation within the family Macrouridae was criticized by Nolf (in Kriwet & Hecht 2008 and in Nolf 2013), who assigned two species to the Merlucciidae in open generic nomenclature and considered the third, *Hymenocephalus rosenkrantzi* as an indeterminate member of the Euclichthyidae, a basal gadiform family nowadays containing a single genus, *Euclichthys*, with three

species inhabiting the seas off southern Australia, New Zealand and New Caledonia (Last & Pogonoski 2020). Nolf (2013) further commented that one of the paratypes of *Hymenocephalus rosenkrantzi* would not belong to the same taxon but rather represents a species of *Coelorinchus*, "apparently as a Neogene downfall pollution in the bore hole". The latter hypothesis is unsustainable because the closest Miocene sediments preserved in the Danish subsurface are situated more than 150 km west of the original locality (Håkansson & Pedersen 1992). Thus, the otoliths referred herein to *Bobbitichthys rosenkrantzi* were originally assigned by Schwarzhans (2003) to the macrourid genus *Hymenocephalus* and later to an indeterminate euclichthyid by Nolf (2013). In order to clarify the potential affinities of the gadiform bones associated with the otoliths of *Bobbitichthys rosenkrantzi*, we compared them with those of the grenadier *Hymenocephalus italicus* Giglioli 1884 and the Eucla cod *Euclichthys polynemus* McCulloch 1926.

Diagnosis. Otoliths with droplet-like outline, anteriorly rounded, posteriorly pointed and with broad and distinctly expanded predorsal lobe. Otolith length to otolith height ranges from 1.50 to 1.65. Sulcus distinctly homosulcoid, reaching close to anterior and posterior tips of the otolith. Colliculi clearly separated, caudal colliculum posteriorly not reaching the posterior rim of sulcus, about as long as ostial colliculum or slightly longer. Collum moderately wide with distinct ventral pseudocolliculum.

Moreover, there are certain additional skeletal features that appear to be diagnostic of *Bobbitichthys*, including: vomer with relatively narrow anterior head and long caudal section, edentulous; premaxilla with long and slender ascending and articular processes separated by a wide and deep v-shaped gap; paddle-like postmaxillary process of the premaxilla emerging at about middle of the alveolar process, large, with distinct posterior notch [gadoid notch; Rosen & Patterson (1969) and Patterson & Rosen (1989)]; oral jaw teeth very small, uniformly villiform; palatine short, diamond-shaped with maxillary prong ventrally directed at about 45°, prominent longitudinal ridge and short medial ethmoid wing; hyomandibula with distinct preopercular process; cleithrum with short posterodorsal process located in its upper fourth of its height along the posterior margin; scales cycloid.

Discussion. The morphology of the recognized skeletal elements referred to *Bobbitichthys* seems to suggest that this Paleocene genus should be regarded as a basal member of the family Macrouridae. The preopercular process of the hyomandibula and the peculiar aspect of the palatine are both regarded as distinctive characters of the family Macrouridae (Okamura 1970;

Howes 1987; Howes & Crimmen 1990; Endo 2002). The postmaxillary process of the premaxilla emerging at the mid-length of the alveolar process and involving a well-developed posterior notch are shared with the Bathygadidae (Okamura 1970; Howes & Crimmen 1990) as well as the possession of unornamented (cycloid) scales (Okamura 1970; Endo 2002); the scales are usually spinoid in macrourids, with very few exceptions (e.g., Okamura 1970; Iwamoto 1989). The position of the postmaxillary process was considered a synapomorphy of bathygadids by Okamura (1970), a point of view not followed by Howes & Crimmen (1990), who solely recognized non-skeletal potential synapomorphies for the Bathygadidae. Extant bathygadid otoliths exhibit strongly reduced colliculi and a wide collum, which could be regarded as a derived character, and which are not developed like that in *Bobbitichthys*. Although the otoliths of *Euclichthys* are in many ways similar to those of *Bobbitichthys*, *Euclichthys* unquestionably differs in certain skeletal characters from *Bobbitichthys*. These differences are primarily the highly specialized shape of the cleithrum with a low insertion of the posterodorsal process, absence of a preopercular process in the hyomandibula, and the different shape of the palatine with a well-developed ventral ethmoid wing.

We therefore interpret *Bobbitichthys* as most likely representing a macrourid, but neither a representative of the genus *Hymenocephalus* nor an euclichthyid as was suggested by Nolf (2013) based on otolith morphology alone. It should be noted, however, that the time equivalent Lellinge Greensand of Copenhagen has also yielded macrourid otoliths, which appear somewhat more advanced and have been tentatively associated with the genera *Coelorinchus* – *C. balticus* (Koken 1885) – and *Coryphaenoides* – *C. amager* Schwarzhans 2003. In any case, *Bobbitichthys rosenkrantzi* represents the earliest evidence of a grenadier fish in the fossil record indicated independently by otoliths and skeletal elements.

Etymology. Named after the common name 'bobbit-worm' for the extant predatory polychaete *Eunice aphroditois*, referring to the fishes representing the most common prey of the presumed voracious polychaete responsible for the tubular ichnofossil *Lepidenteron mortenseni*.

Bobbitichthys rosenkrantzi (Schwarzhans 2003)
Figs. 4–16

2003   *Hymenocephalus rosenkrantzi* – Schwarzhans: fig. 26.
2013   "? *Euclichthyida*" *rosenkrantzi* (Schwarzhans 2003) – Nolf: pl. 88, no fig. numbers.

Material. 320 otoliths from *Lepidenteron mortenseni* tubes; referred skeletal remains from at least 17 tubes; OESM 10967–10981, 10984–10991, 10993, 10995–10998; Kerteminde Marl, middle Paleocene (Selandian), gravel pit at Gundstrup, north of Odense, Fyn, Denmark.

Remarks on otoliths. For description of otoliths see Schwarzhans (2003) and diagnosis of genus *Bobbitichthys* above (Fig. 4). Due to the internal leaching resulting in a hollow internal part, otoliths are rarely well preserved at the Gundstrup location. However, a few well preserved specimens exposed from the inner face allow a reliable identification and also allow us to attribute the majority of the split-up otoliths because of the highly diagnostic outline with the prominent predorsal lobe, the proportions (otolith length to otolith height 1.5 to 1.65) and the shape of the sulcus and colliculi, which is commonly recognizable even in split specimens. Figure 4 is composed to document the different preservation forms of these otoliths.

Description of skeletal remains. Of the neurocranium only a few elements have been identified, including three vomers (Fig. 5A–B), a single frontal and two basioccipitals (Fig. 5E). The vomer has a narrow head, long posterior shaft and is edentulous; overall, the vomer length is more than 2.5 times its width. The basioccipital shows a very regular lobate anterior margin, similar to that of extant macrourids (Okamura 1970), including *Hymenocephalus italicus* (Fig. 5G); the anterior margin is bilobate in *Euclichthys polynemus* (Fig. 5F).

The structure and morphology of the jaws can be properly interpreted thanks to several isolated remains. There are five isolated and nearly complete premaxillae, three exposed in lateral view (Fig. 6A–E) and two in medial view (Fig. 6F); the ascending and articular processes are long, narrow, straight, nearly equally long and forming a broad and deep v-shaped gap between each other; the alveolar process is long and bears a large laminar paddle-like postmaxillary process emerging at its mid-length, which forms a distinctly large posterior (gadoid) notch; the teeth are very small, uniformly villiform, densely packed, and arranged in two to three rows. The overall configuration of the premaxilla is similar to that of *Euclichthys polynemus* (Fig. 6G), although the anterior processes are similar to those of certain grenadiers, including *Hymenocephalus italicus* (Fig. 6H; see also Okamura 1970). There are two incomplete narrow maxillae solely represented by their expanded anterior articular portion (Fig. 7). The mandible can be restored based on two dentaries and two anguloarticulars (Fig. 8). Both the recognized dentaries are incomplete, one exposed in lateral view and the other exposed in medial view; overall, the dentary is v-shaped, broad

posteriorly, apparently without a wide mental channel, as is the case in *Hymenocephalus,* and bearing a slender coronoid process in a similar way to other macrourids (see also Okamura 1970); the coronoid process is much enlarged in *Euclichthys*. The teeth are very small, villiform throughout like in the premaxilla but apparently arranged in a single row. The anguloarticular has a broad anterior process, a slender ascending process, and a posteroventral laminar plate with rounded profile.

A single well-preserved palatine has been recognized (Fig. 9A, B); it is short, diamond-shaped, with a distinct longitudinal ridge and a reduced ethmoid wing, like other macrourids (Fig. 9F; Howes 1987), whereas *Euclichthys polynemus* exhibits a distinct ethmoid wing (Fig. 9D). Anteriorly, the palatine shows a distinct maxillary prong forming an angle of about 45° with the main axis of the bone, similar to bathygadids and *Euclichthys* (Howes 1987). Only an incomplete posterior portion of an ectopterygoid is preserved (Fig. 9C). Two partially complete controlateral fan-shaped quadrates are observed close to each other in one tube (Fig. 10C). The symplectic has not been observed in any of the examined tube. Only two hyomandibulae have been observed in the examined tubes, of which one is almost complete (Fig. 10A–B), rather stout and characterized by a long opercular process and a distinct preopercular process similar to that observed in extant macrourids (Fig. 10G; Okamura 1970) but not in *Euclichthys* (Fig. 10D).

A single poorly preserved crescent-shaped preopercle can be recognized (Fig. 11A). Two small opercles (Fig. 11 B–C) and several, mostly incomplete sub- and interopercles have been identified (Fig. 11D–E). The
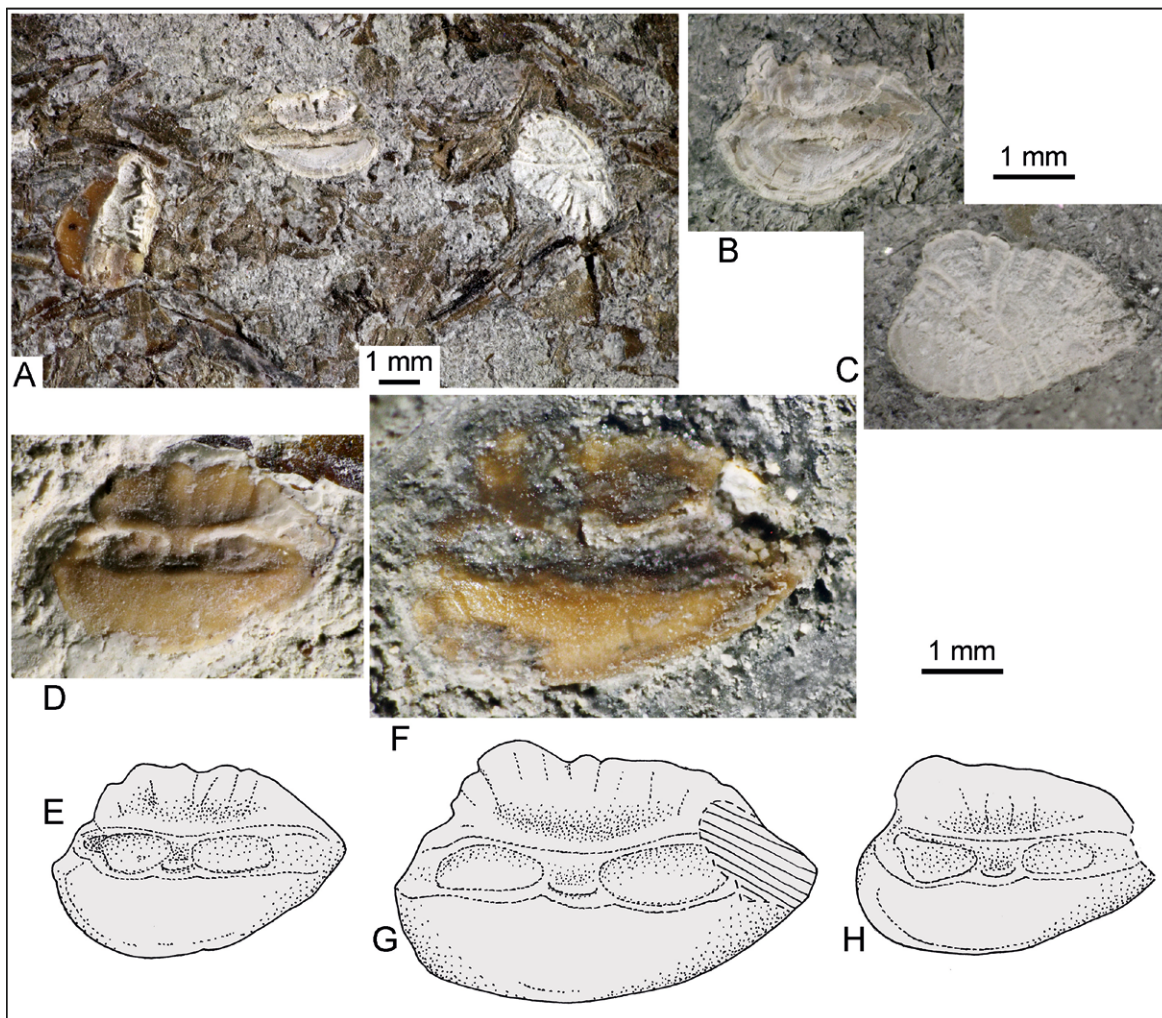
Fig. 4. Otoliths, *Bobbitichthys* n. gen. *rosenkrantzi* (Schwarzhans 2003). **A**: OESM 10969, composite expression of three partly preserved otoliths typical of a *Lepidenteron* tube. **B–C**: OESM 10967, otoliths split along the long axis. **B**: view into inner face. **C**: view into outer face. **D–H**: Otoliths; **D–E**: OESM 10972 (**D** photograph, **E** interpretative drawing). **F–G**: OESM 10975 (**F** photograph of moistened specimen, **G** interpretative drawing). **H**: OESM 10969 (interpretative drawing, specimen destructed during preparation).
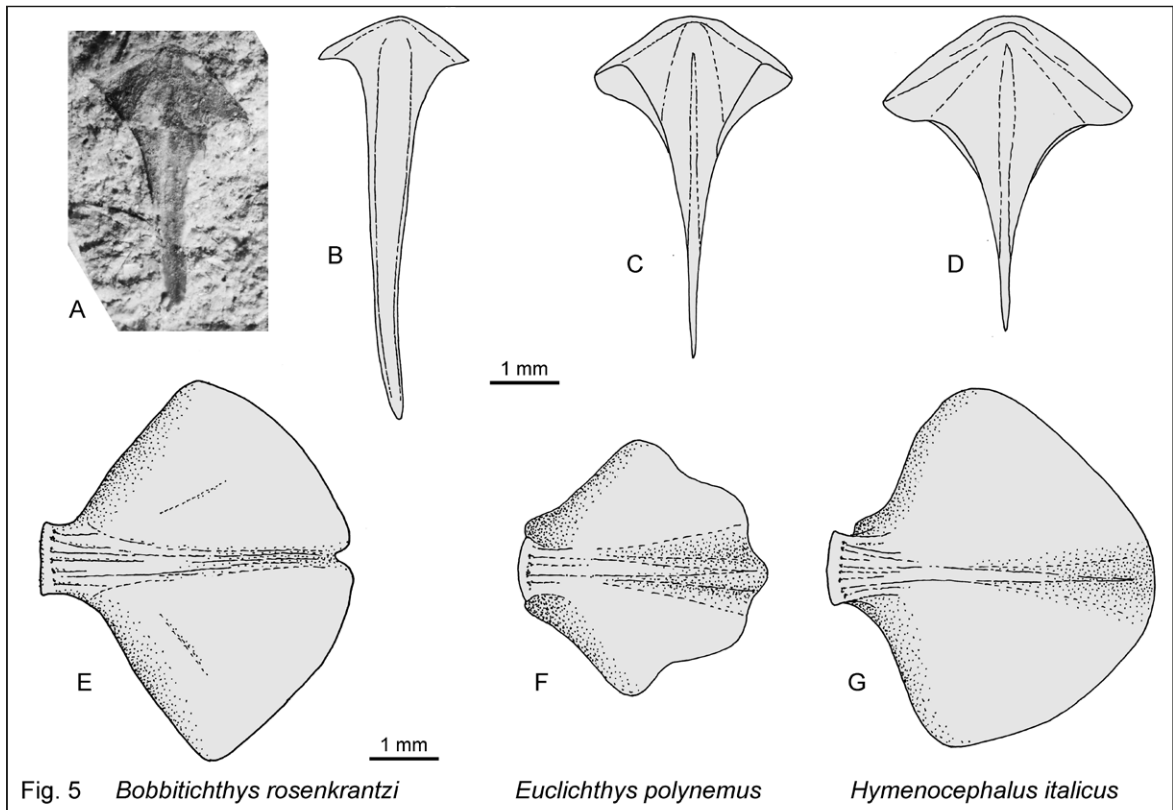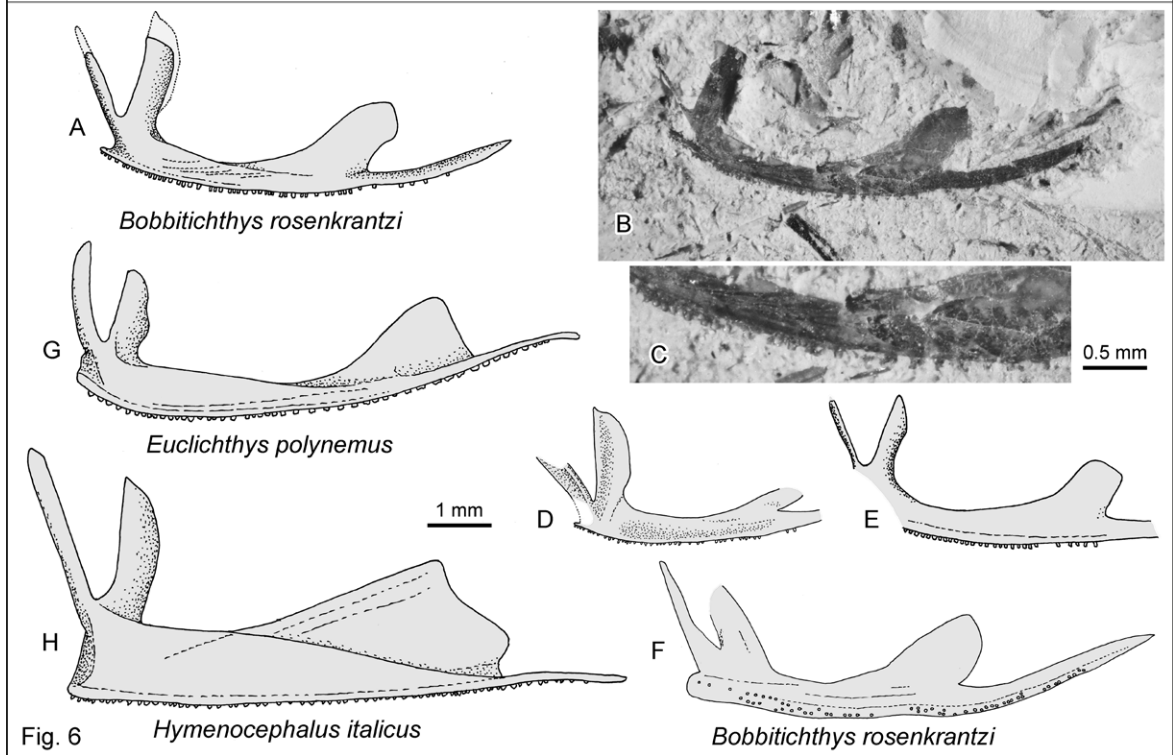
Fig. 5. Vomer and basioccipital. **A–D**: Vomer; **A–B**: *Bobbitichthys* n. gen. *rosenkrantzi* (Schwarzhans 2003) (A: OESM 10968; B: OESM 10998). **C**: *Euclichthys polynemus* McCulloch 1926, ZMUC P2397027. **D**: *Hymenocephalus italicus* Giglioli 1884, ZMUC P373414. **E–G**: Basioccip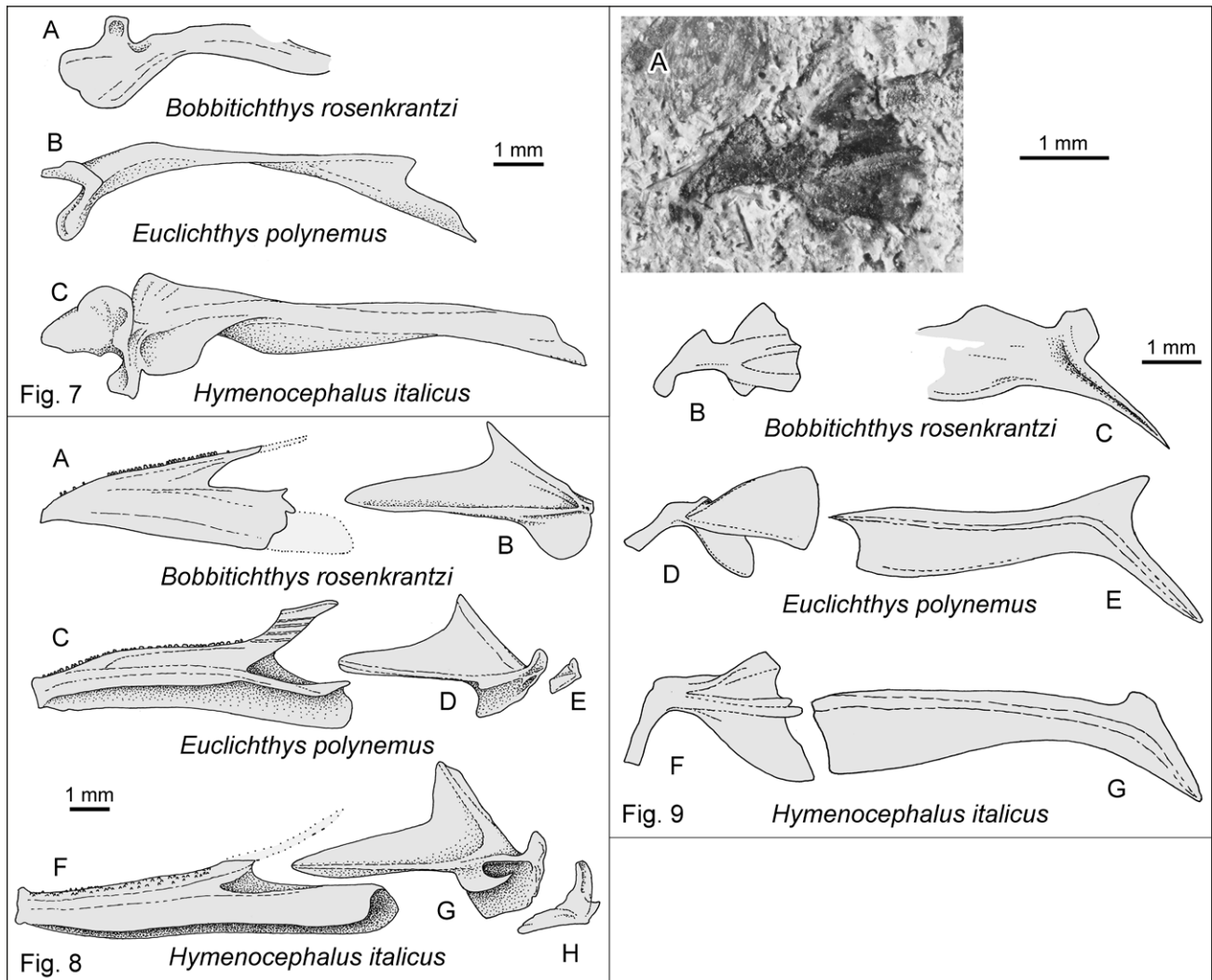ital: **E**: *Bobbitichthys* n. gen. *rosenkrantzi* (Schwarzhans 2003), OESM 10991. **F**: *Euclichthys polynemus* McCulloch 1926; ZMUC P2397027. **G**: *Hymenocephalus italicus* Giglioli 1884; ZMUC P373414.

Fig. 6. Premaxilla. **A–F**: *Bobbitichthys* n. gen. *rosenkrantzi* (Schwarzhans 2003). **A–C**: OESM 10985, lateral view (**A**: interpretative drawing, **B**: photograph, **C**: detail of dentition). **D**: OESM 10967, lateral view. **E**: OESM 10998, lateral view. **F**: OESM 10976, medial view. **G**: *Euclichthys polynemus* McCulloch 1926, ZMUC P2397027. **H**: *Hymenocephalus italicus* Giglioli 1884, ZMUC P373414.

opercle is fan-shaped and bears two posterior pointed spines. The subopercle and interopercle are thin, laminar and ovoid in outline, the subopercle being larger compared to the much slender interopercle.

At least two anterior ceratohyals have been recognized, of which one was found partially articulated with the lower part of the opercular series and fragments of three branchiostegal rays. A single articulated branchiostegal ray shows a broadly expanded and irregular base and is regarded to represent the fourth element of the series. The ventrally expanded rear part of one of the anterior ceratohyals shows insertion traces of branchiostegal rays (Fig. 12A–E), probably the fourth to sixth rays, which is similar to the pattern found in macrourids and *Euclichthys* (Fig. 12F–K). Two triangular posterior ceratohyals are also preserved; the posteriormost (seventh) branchiostegal ray may have articulated with these bones.

Fig. 7. Maxilla. **A**: *Bobbitichthys* n. gen. *rosenkrantzi* (Schwarzhans 2003), OESM 10995, medial view. **B**: *Euclichthys polynemus* McCulloch 1926, ZMUC P2397027. **C**: *Hymenocephalus italicus* Giglioli 1884, ZMUC P373414.

Fig. 8. Lower jaw. **A–B**: *Bobbitichthys* n. gen. *rosenkrantzi* (Schwarzhans 2003). **A**: OESM 10996, dentary, lateral view. **B**: OESM 10987, anguloarticular, lateral view. **C–E**: *Euclichthys polynemus* McCulloch 1926, ZMUC P2397027. **C**: dentary. **D**: anguloarticular. **E**: retroarticular. **F–H**: *Hymenocephalus italicus* Giglioli 1884, ZMUC P373414. **F**: dentary, **G**: anguloarticular. **H**: retroarticular.

Fig. 9. Palatine and ectopterygoid. **A–B**, **D**, **F**: Palatine. **A–B**: *Bobbitichthys* n. gen. *rosenkrantzi* (Schwarzhans 2003), OESM 10977 (**A**: photograph with rock background brightened; **B**: interpretative drawing). **D**: *Euclichthys polynemus* McCulloch 1926, ZMUC P2397027. **F**: *Hymenocephalus italicus* Giglioli 1884, ZMUC P373414. **C**, **E**, **G**: Ectopterygoid. **C**: *Bobbitichthys* n. gen. *rosenkrantzi* (Schwarzhans 2003), OESM 10998. **E**: *Euclichthys polynemus* McCulloch 1926, ZMUC P2397027. **G**: *Hymenocephalus italicus* Giglioli 1884, ZMUC P373414.

A tube-dwelling predator and its prey from the middle Paleocene of Denmark · 45

A number of vertebral fragments have been recognized, and only a single caudal vertebra is nearly complete and shows the bases of the neural and haemal spines.

The pectoral girdle is represented by three cleithra and a single furcate posttemporal (Fig. 13A–B). The cleithrum is slender, moderately curved, with a distinct dorsal spine and a weak posterodorsal process emerging in the upper fourth of its height along the posterior border. This character state is similar to the condition observed in *Hymenocephalus italicus* (Fig. 13F–G) and differs from that characteristic of *Euclichthys polynemus* (Fig. 13C–E) in which the posterodorsal process emerges at about the mid-length of the posterior border. No supracleithrum and postcleithrum have been recognized.

Many unornamented cycloid scales of variable size have been observed (Fig. 14); spinoid scales, which are considered characteristic for macrourids (Endo 2002), were not observed. A single small, probably lateral scale showing a wide central pore has also been recognized (Fig. 14D). Unornamented scales are widespread among gadiforms, including *Euclichthys* and certain macrourid species of the genera *Coryphaenoides*, *Hymenogadus*, and *Nezumia* in which this condition is considered as a secondary loss (Iwamoto 1989).

Discussion. A quantitative analysis of the length of the *Bobbitichthys rosenkrantzi* otoliths found in the *Lepidenteron mortenseni* tubes shows that they stem mostly from a narrow size spectrum with a variation not exceeding 20% (Fig. 15). For this reason, an adjustment
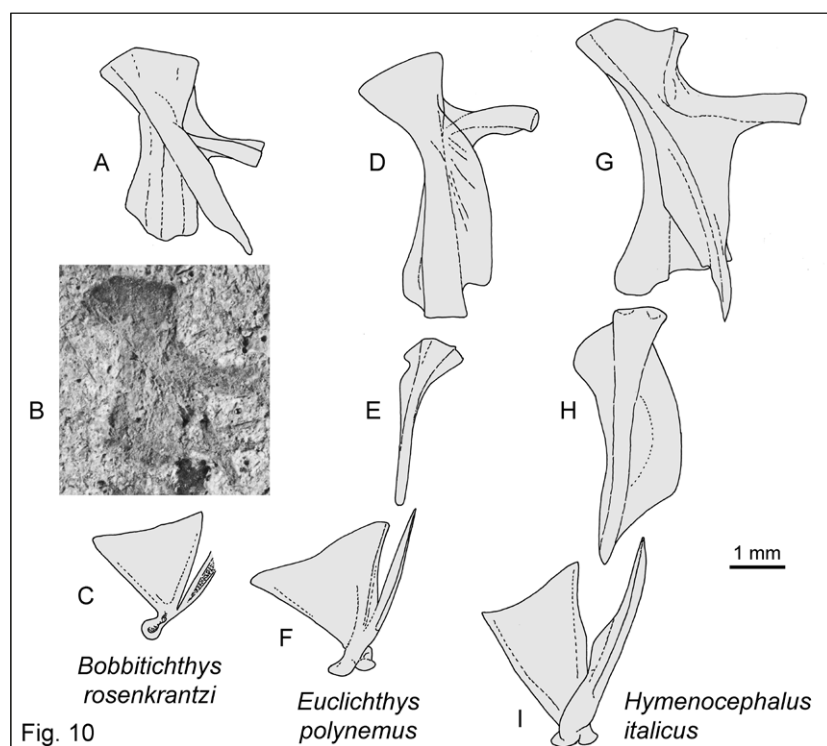
Fig. 10. Suspensorium (selected elements). **A–C**: *Bobbitichthys* n. gen. *rosenkrantzi* (Schwarzhans 2003). **A–B**: OESM 10977, hyomandibula (**A**: interpretative drawing, **B**: photograph). **C**: OESM 10968, quadrate. **D–F**: *Euclichthys polynemus* McCulloch 1926, ZMUC P2397027. **D**: hyomandibula. **E**: symplectic. **F**: quadrate. **G–I**: *Hymenocephalus italicus* Giglioli 1884, ZMUC P373414. **G**: hyomandibula. **H**: symplectic. **I**: quadrate.
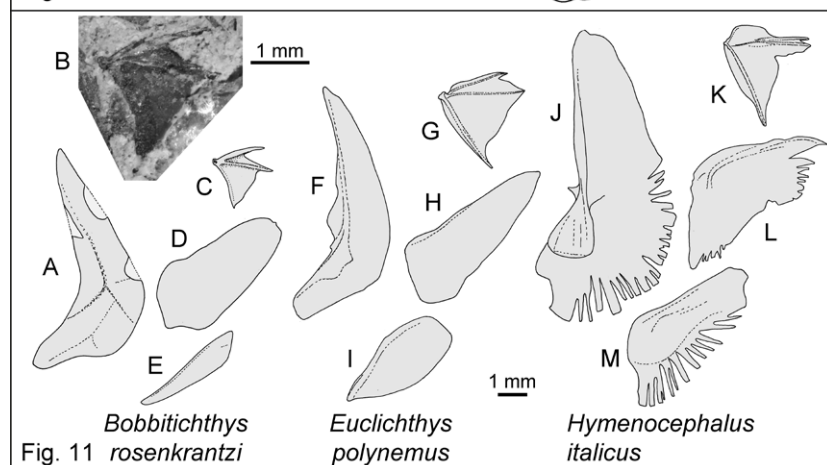
Fig. 11. Opercular series. **A–E**: *Bobbitichthys* n. gen. *rosenkrantzi* (Schwarzhans 2003). **A**: OESM 10989, preopercle. **B–C**: OESM 10998, opercle (**B**: photograph with rock background brightened, **C**: interpretative drawing). **D**: OESM 10976, subopercle. **E**: OESM 10987, interopercle. **F–I**: *Euclichthys polynemus* McCulloch 1926, ZMUC P2397027. **F**: preopercle. **G**: opercle. **H**: subopercle. **I**: interopercle. **J–M**: *Hymenocephalus italicus* Giglioli 1884, ZMUC P373414. **J**: preopercle. **K**: opercle. **L**: subopercle. **M**: interopercle.

not exceeding 20% has been used, when necessary, to reconstruct the skull of *B. rosenkrantzi* based on the identified bones (Fig. 16). The otoliths of *B. rosenkrantzi* found isolated in the Lellinge Greensand do not exceed the sizes observed in the specimens obtained from the *Lepidenteron* tubes but show a wider range including much smaller specimens. We conclude that *Bobbitichthys rosenkrantzi* was a small species probably not exceeding 100 to 120 mm SL (standard length) and characterized by rather thin and delicate bones. Its very small, uniform and densely patterned teeth on dentary and premaxilla indicate that its diet was mostly based on small benthic invertebrates, especially crustaceans.

Isolated otoliths in the tubes of *Lepidenteron mortenseni* that cannot be associated with fish bones

As discussed above, other otoliths identified from the same locality and, with one exception, within the *Lepidenteron mortenseni* tubes, have been referred to as *Bidenichthys? lappierrei* (Nolf 1978; Fig. 17, 28 specimens), an unidentifiable additional gadiform taxon (six specimens), a conger eel possibly belonging to *Rhynchoconger angulosus* (Schwarzhans 2003), and outside of a tube *Centroberyx integer* (Koken 1885). *Bidenichthys? lappierrei* represents the second most
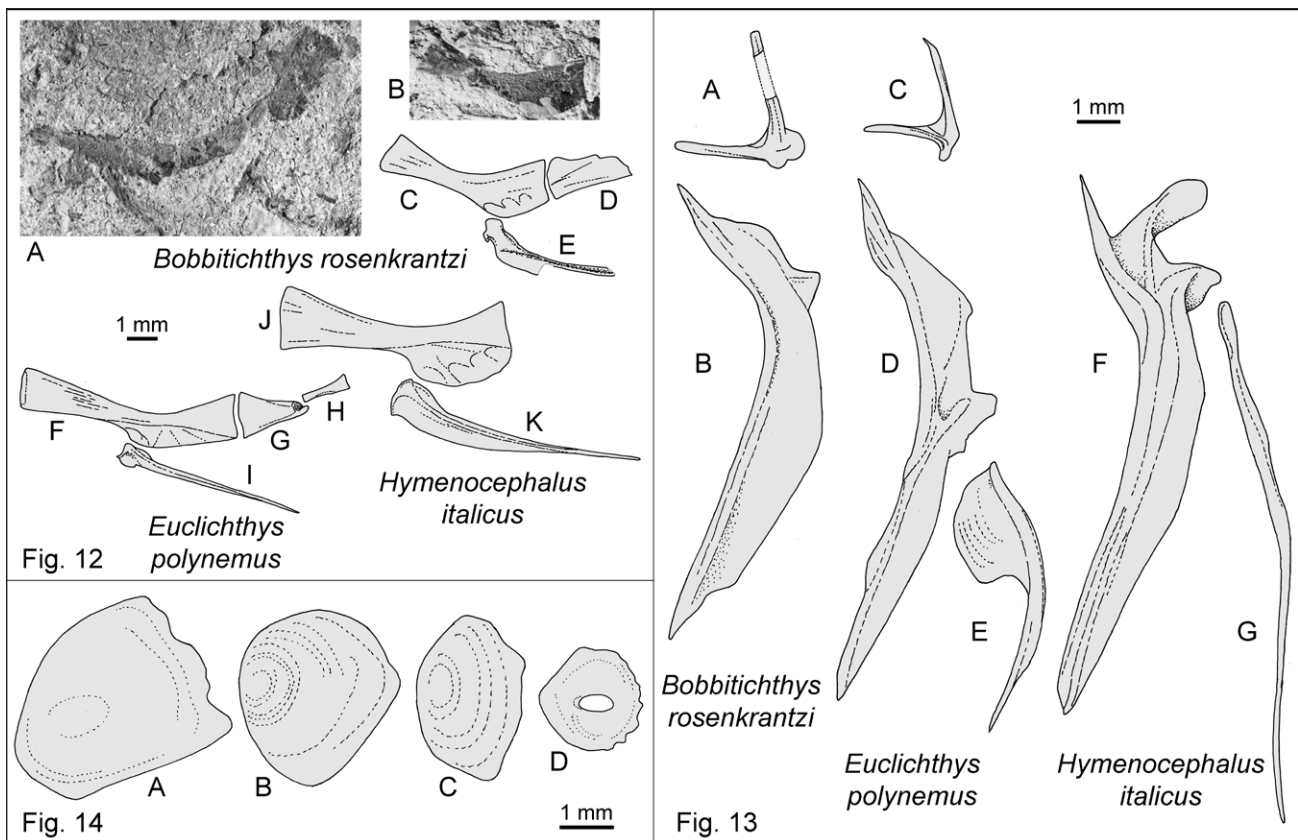
Fig. 12. Hyoid arch (selected elements). **A–E**: *Bobbitichthys* n. gen. *rosenkrantzi* (Schwarzhans 2003). **A**: OESM 10977, partly articulated hyoid arch, left to right anterior ceratohyal with articulated fragment of 4th branchiostegal ray, posterior ceratohyal, ?interhyal fragment, subopercle fragment (photograph with rock background brightened). **B**: OESM 10995, anterior ceratohyal showing three insertion traces of branchiostegal rays ventrally at widened rear part (photograph with brightened rock background). **C–E**: Hyoid arch reconstruction drawing composed from: **C**: OESM 10995, anterior ceratohyal. **D**: OESM 10976, posterior ceratohyal. **E**: OESM 10967, branchiostegal ray (supposed 4th ray). **F–I**: *Euclichthys polynemus* McCulloch 1926, ZMUC P2397027. **F**: anterior ceratohyal. **G**: posterior ceratohyal. **H**: interhyal. **I**: 4th branchiostegal ray. **J–K**: *Hymenocephalus italicus* Giglioli 1884, ZMUC P373414. **J**: anterior ceratohyal. **K**: 4th branchiostegal ray.

Fig. 13. Pectoral girdle (selected elements). **A–B**: *Bobbitichthys* n. gen. *rosenkrantzi* (Schwarzhans 2003); **A**: OESM 10977, posttemporal; **B**: OESM 10967, cleithrum. **C–E**: *Euclichthys polynemus* McCulloch 1926, ZMUC P2397027; **C**: posttemporal; **D**: cleithrum; **E**: postcleithrum. **F–G**: *Hymenocephalus italicus* Giglioli 1884, ZMUC P373414; **F**: cleithrum; **G**: postcleithrum.

Fig. 14. Scales of *Bobbitichthys* n. gen. *rosenkrantzi* (Schwarzhans 2003); **A**, **D**: OESM 10991; **B–C**: OESM 10973.

common species identified based on otoliths in the *Lepidenteron* tubes, and contrary to the otoliths of *Bobbitichthys rosenkrantzi* they are robust and mostly well preserved as documented in Fig. 17. They were found in five distinct tubes and, in two of them, as

the dominant fish prey taxon, with 18 and 8 otoliths, respectively. *Bidenichthys*? *lappierrei* belongs to a persisting lineage of basal bythitid fishes that were first observed in the late Campanian to at least the early Eocene (Schwarzhans & Stringer 2020). Their placement to *Bidenichthys* remains tentative and it is likely that they represent an extinct stem taxon of the Bythitoidei (Møller *et al.* 2016).
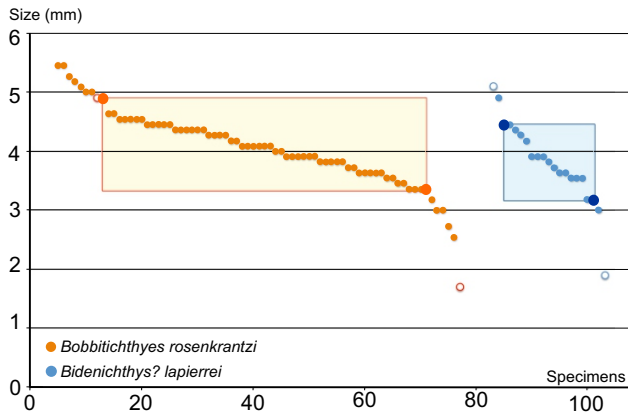
Fig. 15. Otolith size abundance plot of *Bobbitichthys* n. gen. *rosenkrantzi* (Schwarzhans 2003) and *Bidenichthys*? *lappierrei* (Nolf 1978). Full circles represent values of otoliths from *Lepidenteron* tubes; open circles represent maximal and minimal sizes of isolated otoliths; rectangles mark 80% ranges with upper and lower cut-off values marked by darker and larger circles.

Life reconstruction for the middle Paleocene Kerteminde Marl (Fig. 18)

The Kerteminde Marl represents the outer neritic facies equivalent and overlies the inner neritic Lellinge Greensand of middle Paleocene Selandian age (King 2016). The Lellinge Greensand has yielded a rich otolith-based teleost fauna that was described by Schwarzhans (2003). A water depth of about 100 to 150 m has been estimated for the Kerteminde Marl depositional environment in the Storebælt area (Clemmensen & Thomsen 2005), as well as in the Gundstrup gravel pit where the *Lepidenteron* tubes were collected
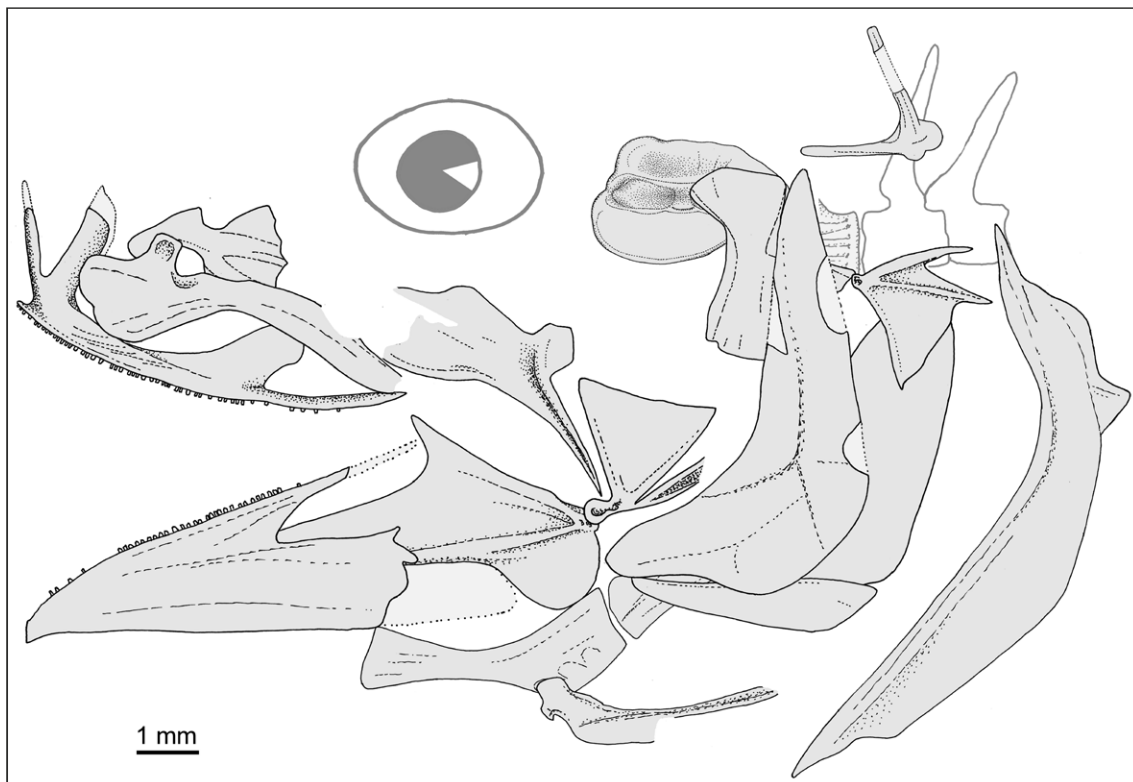

Fig. 16. Reconstruction of the skull of *Bobbitichthys* n. gen. *rosenkrantzi* (Schwarzhans 2003) based on selected skeletal elements found in the *Lepidenteron* tubes. Eye and first two vertebrae hypothetical. Scale based on premaxilla; other bones adjusted in size for optimal fit up to a maximum of 20%.

(Schnetler & Nielsen 2018). Presumably, an eunicid-like polychaete tube-dwelling predator inhabited the soft ground of the Kerteminde Marl sea bottom. The traces left behind by the predator are described here as the ichnofossil *Lepidenteron mortenseni*. The abundance and distribution of the tube-dwelling predator is unknown, but given the total number of retrieved tubes may have been locally significant.

As described above, the tube-dwelling predator responsible for the *Lepidenteron* ichnofossil preyed primarily on a single fish species, i.e. *Bobbitichthys rosenkrantzi*. We presume that the predator hiding in the soft mud was not prey selective but likely an opportunistic ambush hunter similar to the extant *Eunice* spp. Consequently, the marine environment of the Kerteminde Marl facies sampled in the Gundstrup gravel pit must have been favorable for *B. rosenkrantzi* that was characterized by a lifestyle that would bring it easily into contact with the tube-dwelling predator. *Bobbitichthys rosenkrantzi* is relatively uncommon in the inner neritic Lellinge Greensand of the Copenhagen area but occurred more commonly in the slightly deeper environment of the Kongedyb wells (Schwarzhans 2003) indicating an uneven, environmentally driven distribution pattern. Probably, *B. rosenkrantzi* was a benthopelagic fish that commonly occurred over soft bottom on the outer shelf, possibly feeding on small benthic crustaceans, similar to many extant grenadier or Eucla cod species. The narrow size range of otoliths of *B. rosenkrantzi* preyed upon by the tube-dwelling predator could indicate that it lived in schools or occupied different environments ontogenetically, similar to the extant *Euclichthys* (Last & Pogonoski 2020). Its size of presumably less than 120 mm SL and the reduced thickness of its bones was probably favorable for the predator. Other fishes that may have occurred near the bottom and within the reach of the tube-dwelling predator were probably uncommon and some of them rather large or robust and therefore less suitable as prey, such as for instance *Pterothrissus*? *conchaeformis* and *Centroberyx integer*. Two of the 110 investigated *Lepidenteron* tubes primarily contained otoliths of *Bidenichthys*? *lapierrei*. Even though no skeletal details are available for this early, presumable stem bythitid, it appears likely that this Paleocene species was adapted to a benthic life like its extant relatives. The abundance of isolated otoliths of *Bidenichthys*? *lappierrei* is extremely variable; it is the second most common species in the Danian chalk of Faxe but extremely rare in the Lellinge Greensand. Its very uneven distribution in the *Lepidenteron* tubes indicates that their distribution in the Kerteminde environment was probably patchy, but locally abundant.

Schnetler & Nielsen (2018) described a rich mollusc fauna from the Gundstrup gravel pit. They observed that almost all the gastropod species were carnivores,
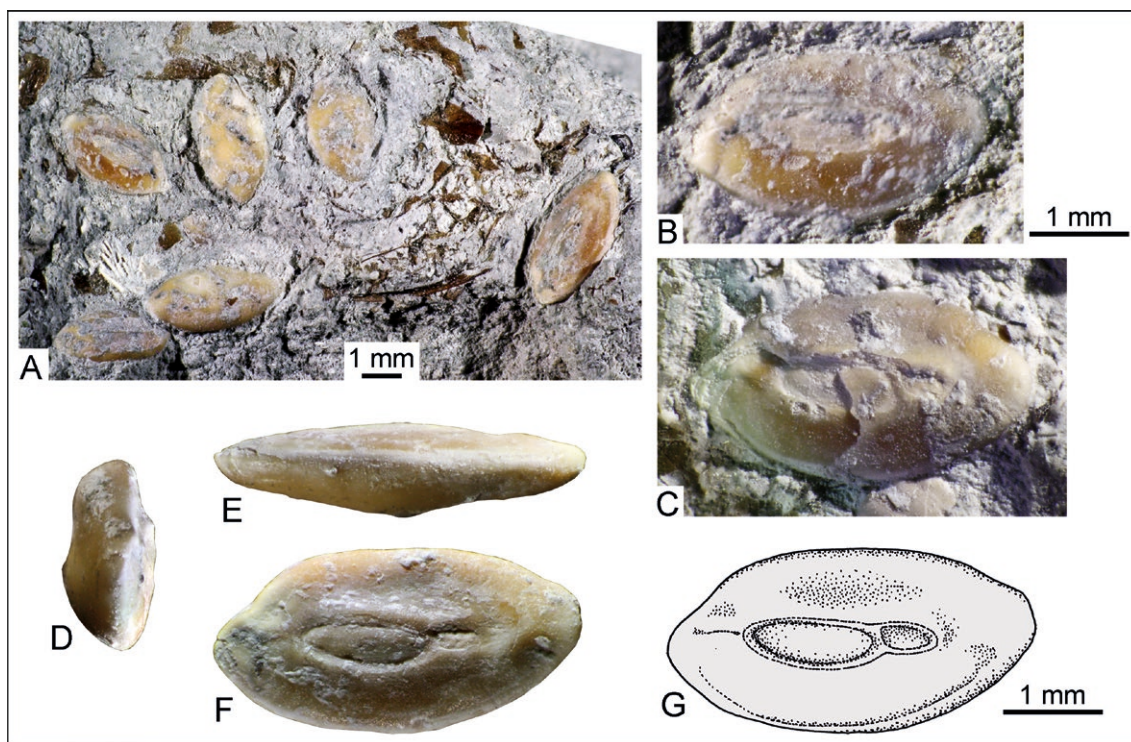

Fig. 17. Otoliths, *Bidenichthys*? *lappierrei* (Nolf 1978), OESM 10970. **A**: Composite expression of six otoliths in a *Lepidenteron* tube; **B–G**: Individual otoliths; **B**, **C**, **F**, **G**: inner faces (**G**: interpretative drawing of F); **D**: anterior view; **E**: ventral view.

Fig. 18. An artistic expression of the life scenery in the Middle Paleocene Kerteminde sea of Denmark, depicting polychaetes thought to have been the constructors of the *Lepidenteron mortenseni* n. isp. hiding in tubes in the soft sea bottom in ambush for *Bobbitichthys* n. gen. *rosenkrantzi* fishes swimming close to the ground in search for small benthonic crustaceans on the sea floor. The extant *Eunice* has been used as model for the polychaete and the extant *Hymenocephalus* for *Bobbitichthys* n. gen. Illustration by Amanda McKeewer.

and that occasionally specific molluscs were found concentrated in lumps, some of which were associated with sunken driftwood likely accumulated by palaeocurrents. The hypothesized environmental setting was located in the deep neritic zone, at depths of about 100–150 m, and consisted of a soft bottom rich in trophic resources. Clemmensen & Thomsen (2005) assumed a high sedimentation rate due to a considerable input of reworked chalk, a well-ventilated bottom water with low current activity, and a low planktonic production. Such a context would have favored specialized off-benthic feeders such as *Bobbitichthys* and *Bidenichthys*? and ambush predators hiding in tubes in the soft bottom.

Conclusions

110 specimens of the tubelike tracefossil *Lepidenteron mortenseni* n. isp. were examined for their contents of skeletal remains and fish otoliths. *Lepidenteron mortenseni* is interpreted to be made by eucinid

polychaete worms. The bone and otolith assemblage from the burrows were by far dominated by a single gadiform taxon, i.e., *Bobbitichthys* n. gen. *rosenkrantzi* (Schwarzhans 2003). The abundance of associated bones and otoliths in the examined tubes has allowed us to reconstruct part of the cranial configuration of *Bobbitichthys rosenkrantzi* and to tentatively interpret it as a stem macrourid. *Bobbitichthys rosenkrantzi* represents the earliest grenadier fish known in the fossil record.

Acknowledgements

one of us of its nature and providing photos of the specimens. The senior author cordially thanks Jørgen Nielsen and Peter Møller (Natural History Museum of Denmark, Copenhagen) for making a specimen of *Hymenocephalus italicus* and John Pogonoski (CSIRO, Hobart) for making a specimen of *Euclichthys polynemus* available for dissection. Amanda McKeewer is thanked for her skillful reconstruction of the dramatic life on the Selandian seafloor. Finally, we thank Alexander Bannikov (Moscow) and Hiromitsu Endo (Kochi, Japan) for their constructive reviews of the article.

References

Note: References to taxa authorities are omitted from the list below which includes only the works referred to in the text.

Bather, F.A. 1911: Upper Cretaceous terebelloids from England. Geological Magazine, new series, decade V, vol. VIII, No. XI, 481–487.

Bergman, C.F. & Eriksson, M.E. 2003: Scolecodonts from the Upper Danian (Paleocene) of Skåne, Sweden. GFF 125, 163–167. https://doi.org/10.1080/11035890301253163

Bieńkowska-Wasiluk, M., Uchman, A. & Jurkowska, A. 2015: The trace fossil *Lepidenteron lewesiensis*: a taphonomic window on diversity of Late Cretaceous fishes. Paläontologische Zeitschrift 89, 795–806. https://doi.org/10.1007/s12542-015-0260-x

Clausen, O.R. & Huuse, M. 1999: Topography of the Top Chalk surface, on- and offshore Denmark. Marine and Petroleum Geology 16, 677–691. https://doi.org/10.1016/S0264-8172(99)00003-3

Clemmensen, A. & Thomsen, E. 2005: Palaeoenvironmental changes across the Danian–Selandian boundary in the North Sea Basin. Palaeogeography Palaeoclimatology Palaeoecology 219, 351–394. https://doi.org/10.1016/j.palaeo.2005.01.005

Endo, H. 2002: Phylogeny of the order Gadiformes (Teleostei, Paracanthopterygii). Memoirs of the Graduate School of Fisheries Sciences, Hokkaido University 49, 75–149.

Forey, P.L. 1973: A revision of the elopiform fishes, fossil and recent. Bulletin of the British Museum (Natural History), Geology, supplement 10, 222 pp.

Heilmann-Clausen, C. & Surlyk, F. 2006: Koralrev og lerhav. In: Larsen, G. (ed.): Naturen i Danmark. Geologien, 181–226, Gyldendal.

Håkansson, E. & Pedersen, S.A.S. 1992: Geologisk kort over den danske undergrund. VARV [Special publication]. København: Tidsskriftet VARV.

Howes, G.J. 1987: The palatine bone and its associations in gadoid fishes. Journal of Fish Biology 31, 625–637. https://doi.org/10.1111/j.1095-8649.1987.tb05267.x

Howes, G.J. & Crimmen, O.A. 1990: A review of the Bathygadi-

dae (Teleostei: Gadiformes). Bulletin of the British Museum Natural History (Zoology) 56, 155–203.

Iwamoto T. 1989: Phylogeny of grenadiers (suborder Macrouroidei): Another interpretation. In: Cohen, D.M. (ed.): Papers on the systematics of gadiform fishes. Science Series, Natural History Museum of Los Angeles County, No. 32, 159–173.

Jurkowska, A. & Uchman, A. 2013: The trace fossil *Lepidenteron lewesiensis* (Mantell 1822) from the Upper Cretaceous of southern Poland. Acta Geologica Polonica 63, 611–623. https://doi.org/10.2478/agp-2013-0026

King, C. 1994: Late Paleocene microfaunas of the Harre borehole (North Jylland, Denmark). In: Nielsen, O.B. (ed.): Lithostratigraphy and biostratigraphy of the Tertiary sequence from Harra Borehole, Denmark. Aarhus Geoscience 1, 65–72.

King, C. (eds. Gale, A.S. & Barry, T.L.) 2016: A revised correlation of Tertiary rocks in the British Islands and adjacent areas of NW Europe. Geological Society Special Report 27, 719 pp. https://doi.org/10.1144/SR27

Koken, E. 1885: Otolithen. In: von Koenen, A.V.: Über eine Palaeocene Fauna von Kopenhagen. Abhandlungen der Königlichen Gesellschaft der Wissenschaften zu Göttingen 32, 113–116.

Kriwet, J. & Hecht, T. 2008: A review of early gadiform evolution and diversification: first record of a rattail fish skull (Gadiformes, Macrouridae) from the Eocene of Antarctica, with otoliths preserved in situ. Naturwissenschaften 95, 899–907. https://doi.org/10.1007/s00114-008-0409-5

Last, P.R. & Pogonoski, J.J. 2020: Revision of the fish family Euclichthyidae (Pisces: Gadiformes) with the description of two new species from the West Pacific. Zootaxa 4758, 231–256. https://doi.org/10.11646/zootaxa.4758.2.2

McAllister J. 2003: Predation of fishes in the fossil record. In: Kelley K.H., Kowalewski M. & Hansen T.A. (eds): Predator–prey interactions in the fossil record, 303–324. New York: Kluwer Academic/Plenum Publishers.

Møller, P.R., Knudsen, S.W., Schwarzhans, W. & Nielsen, J.G. 2016: A new classification of viviparous brotulas (Bythitidae) – with family status for Dinematichthyidae – based on molecular, morphological and fossil data. Molecular Phylogenetics and Evolution 100, 391–408. https://doi.org/10.1016/j.ympev.2016.04.008

Myrvold, K.S., Milàn, J. & Rasmussen, J.A. 2018: Two new finds of turtle remains from the Danian and Selandian (Paleocene) deposits of Denmark with evidence of predation by crocodilians and sharks. Bulletin of the Geological Society of Denmark 66, 211–218. https://doi.org/10.37570/bgsd-2018-66-11

Niebuhr, B. & Wilmsen, M. 2016: Ichnofossilien. Geologica Saxonica 62, 181–238.

Nolf, D. 1978: Les otolithes de téléostéens des Formations de Landen et de Heers (Paléocène de la Belgique). Geologica et Palaeontologica 12, 223–234.

Nolf, D. 2013: The diversity of fish otoliths, past and present. Operational Directorate "Earth and History of Life", 581 pp. Brussels: The Royal Belgian Institute of Natural Sciences.

Okamura, O. 1970: Studies on the macruroid fishes of Japan; morphology, ecology and phylogeny. Reports of the USA Marine Biological Station 17, 179 pp.

Patterson, C. & Rosen, D.E. 1989: The Paracanthopterygii revisited: Order and disorder. In: Cohen, D.M. (ed.): Papers on the systematics of gadiform fishes. Science Series, Natural History Museum of Los Angeles County 32, 5–39.

Rosen, D.E. & Patterson, C. 1969: The structure and relationships of the paracanthopterygian fishes. Bulletin of the American Museum of Natural History 141, 357–474.

Schnetler, K.I. & Nielsen, M.S. 2018: A Palaeocene (Selandian) molluscan fauna from boulders of Kerteminde Marl in the gravel-pit at Gundstrup, Fyn, Denmark. Cainozoic Research 18, 3–81.

Schwarzhans, W. 2003: Fish otoliths from the Paleocene of Denmark. Geological Survey of Denmark and Greenland Bulletin 2, 94 pp. https://doi.org/10.34194/geusb.v2.4696

Schwarzhans, W. 2018: A review of Jurassic and early Cretaceous otoliths and the development of early morphological diversity in otoliths. Neues Jahrbuch für Geologie und Paläontologie Abhandlungen 287, 75–121. https://doi.org/10.1127/njgpa/2018/0707

Schwarzhans, W. & Milàn, J. 2017: After the disaster: Bony fish remains (mostly otoliths) from the K/Pg boundary section at Stevns Klint, Denmark, reveal consistency with teleost faunas from later Danian and Selandian strata. Bulletin of the Geological Society of Denmark 65, 59–74. https://doi.org/10.37570/bgsd-2017-65-05

Schwarzhans, W. & Stringer, G.L. 2020: Fish otoliths from the late Maastrichtian Kemp Clay (Texas, USA) and the early Danian Clayton Formation (Arkansas, USA) and an assessment of extinction and survival of teleost lineages across the K-Pg boundary based on otoliths. Rivista Italiana di Paleontologica e Stratigrafia 126, 395–446. https://doi.org/10.13130/2039-4942/13425

Sorgenfrei, T. & Buch, A. 1964: Deep tests in Denmark 1935–1959. Danmarks Geologiske Undersøgelse III. Række, Vol. 36, 146 pp.

Stinton, F.C. 1973: Fish otoliths from the English Cretaceous. Palaeontology 16, 293–305.

Suhr, P. 1988: Taxonomie und Ichnologie fossiler Wohnröhren terebelloider Würmer. Freiberger Forschungshefte 419, 81–87.

Thomsen, E. & Heilmann-Clausen, C. 1985: The Danian-Selandian boundary at Svejstrup with remarks on the biostratigraphy of the boundary in western Denmark. Bulletin of the Geological Society of Denmark 33, 341–362.

Vandenberghe, N., Hilgen, F.J. & Speijer, R.J. 2012: The Paleogene period. In: Gradstein, F.M., Ogg, J.G., Schmitz, M. & Ogg, G. (eds): The geologic time scale 2012, 855–921, Amsterdam: Elsevier.

Prognathodon (Squamata, Mosasauridae) from the Maastrichtian chalk of Denmark

TOM J. GILTAIJ, JESPER MILÀN, JOHN W.M. JAGT & ANNE S. SCHULP

DGF

Geological Society of Denmark
https://2dgf.dk

Two mosasaur tooth crowns collected from the Maastrichtian chalk sequences of Stevns Klint and Møns Klint are here assigned to *Prognathodon*, a mosasaur genus hitherto unknown from Denmark. Together with previous records of the mosasaurs *Plioplatecarpus*, *Mosasaurus* and *Carinodens*, these new finds of *Prognathodon* document the coexistence of four mosasaurid genera in the Danish chalk and underscore similarities to coeval assemblages from the Maastrichtian type area in the Netherlands and Belgium.

Tom J. Giltaij [tom.giltaij@live.nl], Faculty of Science, Vrije Universiteit Amsterdam, De Boelelaan 1085, 1081 HV Amsterdam, the Netherlands; also Geologisch Museum Hofland, Hilversumseweg 51, 1251 EW Laren, the Netherlands; and Faculty of Geosciences, Utrecht University, P.O. Box 80115, 3508 TC Utrecht, the Netherlands. Jesper Milàn [jesperm@oesm.dk], Geomuseum Faxe/Østsjællands Museum, Rådhusvej 2, 4640 Faxe, Denmark. John W.M. Jagt [john.jagt@maastricht.nl], Natuurhistorisch Museum Maastricht, De Bosquetplein 6-7, 6211 KJ Maastricht, the Netherlands. Anne S. Schulp [anne.schulp@naturalis.nl], Naturalis Biodiversity Center, P.O. Box 9517, 2300 RA Leiden, the Netherlands; also Faculty of Science, Vrije Universiteit Amsterdam, Faculty of Geosciences, Utrecht University, and Natuurhistorisch Museum Maastricht.

Corresponding author: Jesper Milàn

Mosasaurs were the apex predators of the Late Cretaceous seas, and their fossil remains have been recorded from all continents (Polcyn *et al.* 2014). In spite of the numerous outcrops of Upper Cretaceous (Maastrichtian) marine sedimentary rocks in northern and eastern Denmark, and the countless hours of dedicated field work by a vibrant community of citizen scientists and professionals alike, the Danish mosasaur record is comparatively poor. Only recently has a third mosasaur taxon, *Carinodens*, been recognised from the Danish Chalk (Milàn *et al.* 2018), and this record is based on a single tooth crown only. Here we describe and illustrate a fourth mosasaur genus from the Maastrichtian of Denmark, *Prognathodon*, on the basis of two isolated tooth crowns.

Material

Institutional abbreviation: NHMD: Natural History Museum of Denmark (Statens Naturhistoriske Museum), Copenhagen, Denmark.

The material consists of two isolated tooth crowns: one from Møns Klint, initially identified as *Mosasaurus hoffmanni* Mantell, 1829 and collected in 2004 by amateur palaeontologist Mette Hofstedt, and another from Mandehoved, Stevns Klint, collected by amateur palaeontologist Peter Bennicke in the spring of 2019. Both specimens have been declared Danekræ (a rare or extremely well-preserved fossil found in Denmark with unique scientific value) with Danekræ numbers DK-740 and DK-1049, respectively, and are now housed

in the collections of the Natural History Museum of Denmark (NHMD-188119 and NHMD-633422, respectively).

Geological setting

The Upper Cretaceous (Maastrichtian) chalk in Denmark is most prominently exposed in the coastal cliffs of Stevns Klint (Stevns peninsula) and Møns Klint (island of Møn, eastern Denmark), and to a lesser degree at inland quarries in the northern part of Jylland (Fig. 1A). The Maastrichtian chalk of Denmark is assigned to the upper portion of the Boesdal Member of the Campanian–Maastrichtian Mandehoved Formation and to the overlying Møns Klint Formation, which is subdivided into four members (Fig. 1B). The lowermost of these is the Hvidskud Member, which stratigraphically spans the lower to middle upper Maastrichtian. This particular unit is exposed in the glacial thrust sheets that form the coastal cliffs at Møns Klint and has also been recognised in the borehole cores Stevns-1 and Stevns-2 (Surlyk *et al.* 2013). The Hvidskud Member is overlain by the Rørdal Member, which is exposed at Rørdal quarry (Ålborg, northern Jylland) and has also been recorded in cores Stevns-1 and Stevns-2, Kalslunde-1 and in boreholes to the south and west of Copenhagen (Surlyk *et al.* 2013). Topping

the Rørdal Member is the Sigerslev Member, which is prominently exposed along the coastal cliffs of Stevns Klint and in boreholes in eastern Sjælland. There are also outcrops of this unit in small quarries south of Ålborg in northern Jylland. The Sigerslev Member is topped by a thick nodular flint band and two incipient hardgrounds, which, in turn, are overlain by a few metres of mounded bryozoan-rich chalk of the uppermost Maastrichtian Højerup Member (Fig. 1). The age of the Højerup Member is difficult to determine precisely because its basal level predates the terminal cooling event at ~200,000 years prior to the Cretaceous/Palaeogene boundary. The base of the member is represented by an incipient hardground, which reflects a hiatus of unknown duration. Due to the complex stratigraphy of Stevns Klint, the top of the Højerup Member is either an erosive surface or is overlain by the Fiskeler Member of the lower Danian Rødvig Formation (Surlyk *et al.* 2006). Based on the average sedimentation rate during the Late Maastrichtian, the Højerup Member must represent a time span of about 50,000 to 60,000 years (Thibault *et al.* 2016; Thibault & Husson 2016). The Cretaceous/Palaeogene (K/Pg) boundary is exposed in the upper part of the cliff where the basal Fiskeler and *Cerithium* Limestone Members of the Rødvig Formation occur in small depressions topped by an erosional hardground and overlain by lower Danian bryozoan limestone mounds of the Stevns Klint Formation (Surlyk *et al.*
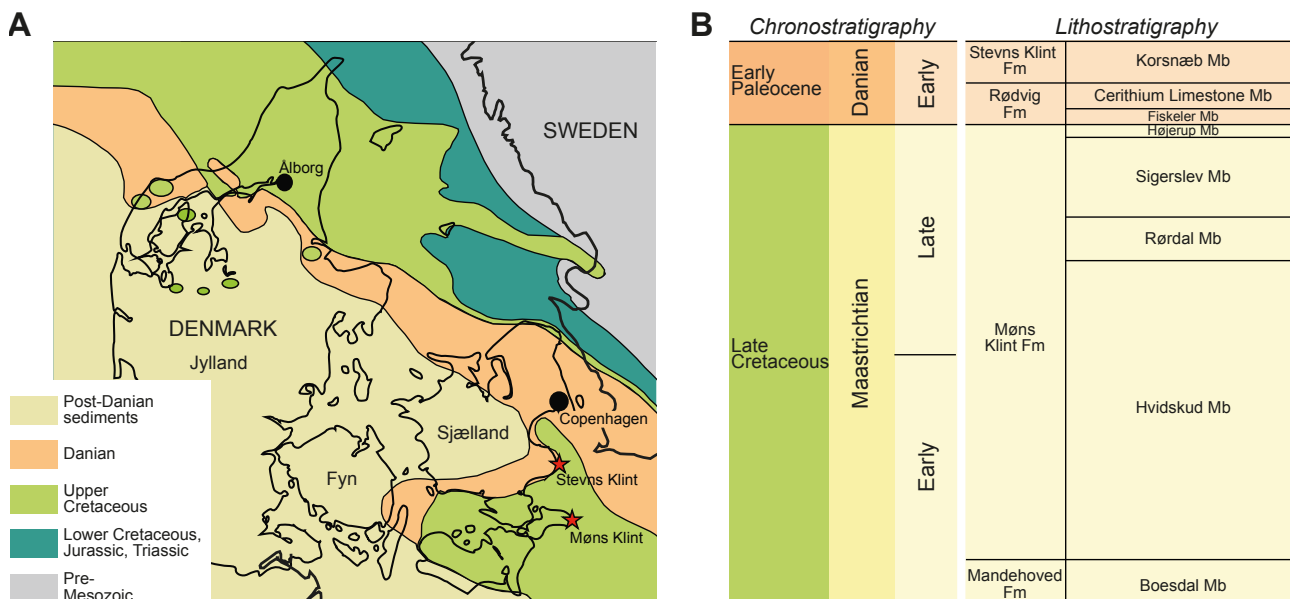

Fig. 1. A: Pre-Quaternary map of Denmark, modified from Thomsen (1995). The mosasaur tooth crowns recorded herein originate from the cliffs at Møns Klint and the UNESCO World Heritage Site of Stevns Klint. **B:** Schematic representation of the Maastrichtian–lower Danian stratigraphy of Denmark, modified from Lauridsen *et al.* (2012) and Surlyk *et al.* (2013). Specimen NHMD 633422 stems from either the Sigerslev or Højerup Member (Møns Klint Formation), while NHMD 188119 is from the Hvidskud Member (Møns Klint Formation).

2006, 2013). The strata at Møns Klint are heavily disturbed by glacial tectonics; they are assigned to the Hvidskud Member (Møns Klint Formation) in their entirety.

Description

Specimen NHMD 188119 (Fig. 2A–D) is a medium-sized tooth crown; as preserved, total crown height is 36 mm. The base measures 25 mm anteroposteriorly and 18 mm labiolingually. There are no conspicuous prisms or fluting on the labial and lingual enamel surfaces. The enamel surface is macroscopically smooth and shows a weak texturing from a microscopic perspective. At about one-third of crown height, posterior recurvature commences, with a near-straight carinal section underneath. The base of the crown is slightly swollen over the root (root not preserved) and elliptical in cross section. Both carinae carry serrations of about 0.2 × 0.2 mm. The absence of prisms (which are characteristic of *Mosasaurus*), the macroscopically smooth enamel surface, the inconspicuous, yet characteristic inflexion in the posterior carina at about one-third of crown height ('pinched' condition; Bardet *et al.* 2013), the aspect ratio, the serration-carrying carinae and the slightly swollen base all favour assignment of NHMD 188119 to *Prognathodon* (compare Dortangs *et al.* 2002, Bardet *et al.* 2005, 2013; Schulp *et al.* 2008; Grigoriev 2013). On a final note, both *Eremiasaurus* and *Gnathomortis* can be excluded from consideration here, too. In comparison with *Eremiasaurus* (LeBlanc *et al.* 2012), the aspect ratio of NHMD 188119 only leaves anterior teeth of *Eremiasaurus* for consideration, but these lack the posterior curvature seen in the Danish material. The teeth of *Gnathomortis* (Lively 2020) (formerly known as *Prognathodon stadtmani*) are wider labiolingually compared to NHMD 188119, the curvature of the posterior carina lacks the characteristic 'pinch' (Bardet *et al.* 2013) with a smooth, continuous curvature instead (pers. obs. AS), and the inflation of the basal tooth crowns is missing (Lively 2020).

Similar considerations apply to the much smaller NHMD 633422 (Fig. 2E–H). Crown height as preserved is 10.5 mm, but only the topmost part is preserved. Anteroposterior dimensions are 7.5 mm as preserved, but a part of the enamel is missing on the lower part on the anterior edge. Labiolingually, the thickest part preserved is 6.1 mm. Enamel thickness increases markedly towards the apex. The tooth has carinae both anteriorly and posteriorly. Posterior recurvature of the preserved section of the crown is similar to NHMD 188119. The sediment adhering to the tooth crown contains abundant bryozoan fragments.

Discussion

Vertebrate palaeobiodiversity
Currently, the Maastrichtian vertebrate fauna of Denmark comprises 31 species of neoselachians, all based on isolated teeth (Adolfssen & Ward 2014), with additional evidence in the form of coprolites (Milàn *et al.* 2015). Teleosteans are represented by at least eight taxa, documented by skeletal remains and otoliths (Bonde *et al.* 2008; Bonde & Leal 2017; Schwarzhans & Milàn 2017). Remains of marine reptiles are comparatively rare; to date, isolated tooth crowns of thoracosaurine crocodilians (Gravesen & Jakobsen 2012), and a single carapace fragment of a chelonioid turtle (Karl & Lindow 2009) have been recorded. Mosasaurs are hitherto known from finds of mainly isolated tooth crowns and isolated elements of the appendicular skeleton of *Mosasaurus hoffmanni*, *Plioplatecarpus* sp. (Lindgren & Jagt 2005) and the durophagous mosasaur *Carinodens minalmamar* Schulp *et al.*, 2010 (Milàn *et al.* 2018). Recognition of *Prognathodon* adds the fourth mosasaur genus to the Danish faunal assemblage and increases the similarity to the mosasaur faunas of the Maastrichtian type area in the south-east Netherlands and north-east Belgium, where representatives of these four genera are known. Based on the dimensions of the two tooth crowns, and the recurvature suggesting a position somewhat posteriorly in the dental ramus, a body length of close to 7.5 and 4 m, respectively, can be extrapolated (Fig. 2I) (compare Giltaij *et al.* 2021).

Stratigraphical age of the specimens
The Danish mosasaur finds are important as they represent some of the stratigraphically youngest mosasaur records worldwide, with both *Mosasaurus* and *Plioplatecarpus* being found within the highest Maastrichtian levels (Lindgren & Jagt 2005). A single find of the durophageous mosasaur *Carinodens* has been assigned to the Højerup Member (Møns Klint Formation), placing it within the latest 50,000 years of the Cretaceous (Milàn *et al.* 2018). The larger tooth crown described here (NHMD 188119) was found loose at Møns Klint, where the Lower–Upper Maastrichtian Hvidskud Member (Møns Klint Formation) is exposed. The exact position within the member is not possible to determine. The small specimen (NHMD 633422) was found loose on the beach in a small rockfall below Mandehoved (Stevns Klint), where the top of the Sigerslev Member and the entire Højerup Member (both Stevns Klint Formation) are exposed. At Mandehoved, the Højerup Member is approximately 1.5 m thick (Surlyk *et al.* 2006). At the locality which yielded NHMD 633422, the Højerup Member is the main cliff-forming unit, together with the overlying Danian Stevns Klint Formation, but as the tooth crown
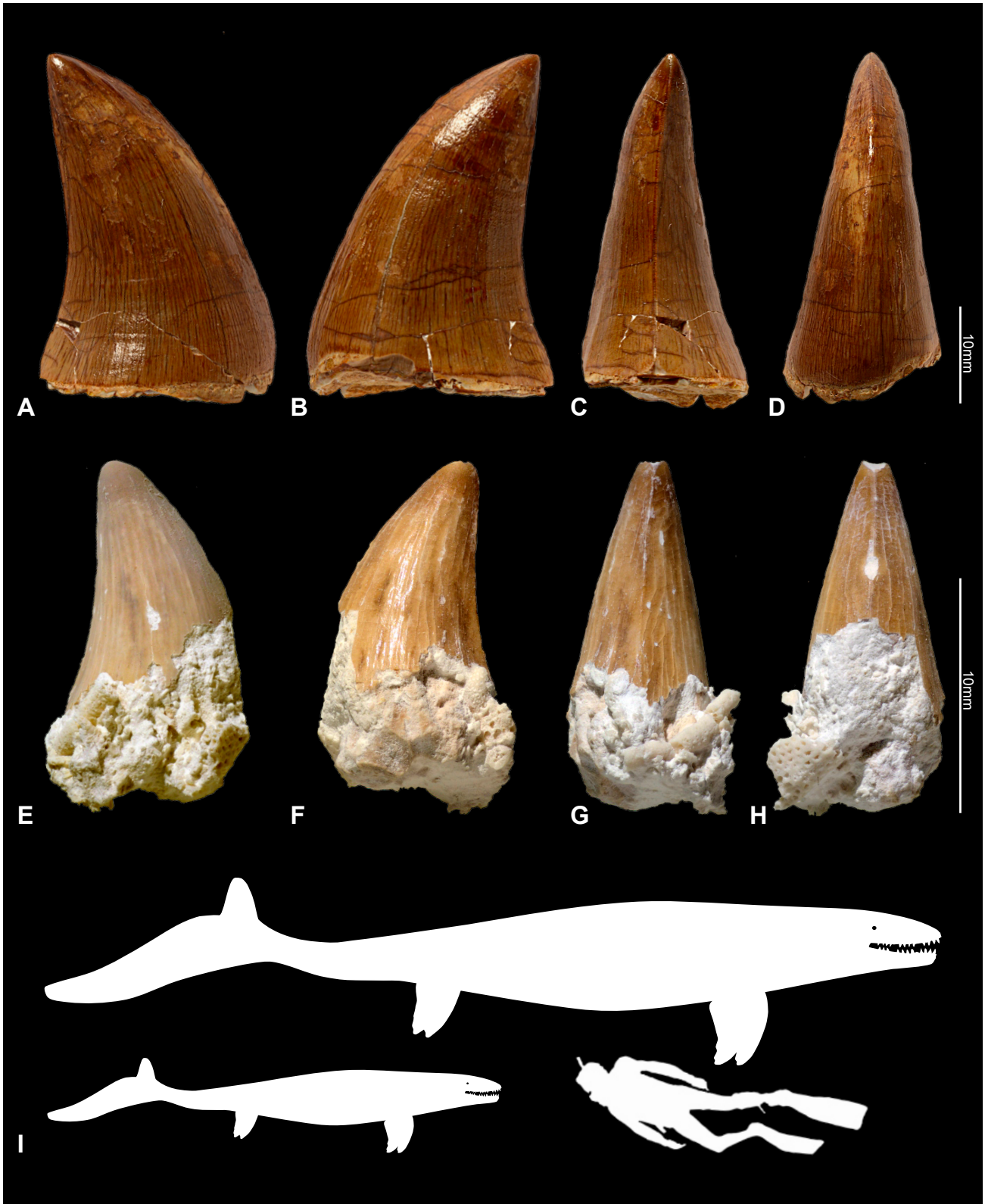
Fig. 2. *Prognathodon* sp.; **A–D:** NHMD 188119, from Møns Klint, in labial, lingual, posterior and anterior views, respectively. **E–H:** NHMD 633422, from Stevns Klint in labial, lingual, posterior and anterior views, respectively. Scale bars equal 10 mm. Note the abundant bryozoan fragments in the sediment below the crown. Photos: Sten Lennart Jakobsen. **I:** Silhouettes of two *Prognathodon* scaled to the approximate overall body size on the basis of the two isolated tooth crowns (Giltaij *et al.* 2021); human diver for scale. Mosasaur silhouettes follow tail flukes as documented by Lindgren *et al.* (2013).

was not found *in situ*, it could also have originated from the uppermost section of the Sigerslev Member. The presence of abundant bryozoan fragments in the sediment below the tooth crown suggests that NHMD 633422 originates from the Højerup Member and thus represents one of the youngest records of *Prognathodon* worldwide.

Conclusions

The presence of *Prognathodon* in the Danish chalk brings the diversity of latest Cretaceous (Maastrichtian) mosasaurs to four genera, which is in accordance with the mosasaur diversity known from the type Maastrichtian. Stratigraphically, the Danish mosasaurs rank amongst the youngest finds, showing a high mosasaur diversity right up to the K/Pg boundary.

Acknowledgements

References

Adolfssen, J.S. & Ward, D.J. 2014: Crossing the boundary: an elasmobranch fauna from Stevns Klint, Denmark. Palaeontology 57, 591–629. https://doi.org/10.1111/pala.12079

Bardet, N., Pereda Suberbiola, X., Iarochène, M., Amalik, M. & Bouya, B. 2005: Durophagous Mosasauridae (Squamates) from the Upper Cretaceous phosphates of Morocco, with description of a new species of *Globidens*. In: Schulp, A.S. & Jagt, J.W.M. (eds): Proceedings of the first Mosasaur meeting. Netherlands Journal of Geosciences 84, 167–175. https://doi.org/10.1017/s0016774600020953

Bardet, N., Baeza-Carratalá, J.F., Díez-Díaz, V., Carbonell, A., García-Ávila, M. & Giner, V. 2013: First occurrence of Mosasauridae (Squamata) in the Maastrichtian (latest Cretaceous) of Alicante (Valencia Community, Eastern Spain). Estudios Geológicos 69(1), 97–104. https://doi:10.3989/egeol.40792.169

Bonde, N. & Leal, M.E.C. 2017: Danian teleosteans of the

North Atlantic region – compared with the Maastrichtian. Research & Knowledge 3, 50–54.

Bonde, N., Andersen, S., Hald, N. & Jakobsen, S.L. 2008: Danekræ – Danmarks bedste fossiler, 225 pp. Copenhagen: Gyldendal. https://doi.org/10.7146/gn.v0i3.3458

Dortangs, R.W., Schulp, A.S., Mulder, E.W.A., Jagt, J.W.M., Peeters, H.H.G. & de Graaf, D.T. 2002: A large new mosasaur from the Upper Cretaceous of The Netherlands. Netherlands Journal of Geosciences 81, 1–8. https://doi.org/10.1017/s0016774600020515

Giltaij, T.J., Van der Lubbe, H.J.L., Lindow, B.E.K., Schulp, A.S. & Jagt, J.W.M. 2021: Carbon isotope trends in north-west European mosasaurs (Squamata; Late Cretaceous). Bulletin of the Geological Society of Denmark 69, 59–70. https://doi.org/10.37570/bgsd-2021-69-04

Gravesen, P. & Jakobsen, S.L. 2012: Skrivekridtets fossiler, 153 pp. Copenhagen: Gyldendal.

Grigoriev, D.V. 2013: Redescription of *Prognathodon lutugini* (Squamata, Mosasauridae). Proceedings of the Zoological Institute RAS 317, 246–261.

Karl, H.-V. & Lindow, B.E.K. 2009: First evidence of a Late Cretaceous marine turtle (Testudines: Chelonioidea) from Denmark. Studia Geologica Salmanticensia 45, 175–180.

Lauridsen, B.W., Bjerager, M. & Surlyk, F. 2012: The middle Danian Faxe Formation – new lithostratigraphic unit and a rare taphonomic window into the Danian of Denmark. Bulletin of the Geological Society of Denmark 60, 47–60. https://doi.org/10.37570/bgsd-2012-60-04

LeBlanc, A.R.H., Caldwell, M.W. & Bardet, N. 2012: A new mosasaurine from the Maastrichtian (Upper Cretaceous) phosphates of Morocco and its implications for mosasaurine systematics. Journal of Vertebrate Paleontology 32, 82–104. https://doi.org/10.1080/02724634.2012.624145

Lindgren, J. & Jagt, J.W.M. 2005: Danish mosasaurs. In: Schulp, A.S. & Jagt, J.W.M. (eds): Proceedings of the first Mosasaur meeting. Netherlands Journal of Geosciences 84, 315–320. https://doi.org/10.1017/s0016774600021090

Lindgren, J., Kaddumi, H.F. & Polcyn, M.J. 2013: Soft tissue preservation in a fossil marine lizard with a bilobed tail fin. Nature Communications 4, 1–8. https://doi.org/10.1038/ncomms3423

Lively, J.R. 2020: Redescription and phylogenetic assessment of '*Prognathodon*' *stadtmani*: Implications for Globidensini Monophyly and Character Homology in Mosasaurinae. Journal of Vertebrate Paleontology 40(3), e1784183. https://doi.org/10.1080/02724634.2020.1784183

Mantell, G.A. 1829: A tabular arrangement of the organic remains of the country of Sussex. Transactions of the Geological Society of London 2(3), 201–216. https://doi.org/10.1144/transgslb.3.1.201

Milàn, J., Hunt, A.P., Adolfssen, J.S., Rasmussen, B.W. & Bjerager, M. 2015: First record of a vertebrate coprolite from the Upper Cretaceous (Maastrichtian) chalk of Stevns Klint, Denmark. New Mexico Museum of Natural History and Science Bulletin 67, 227–229.

Milàn, J., Jagt, J.W.M., Lindgren, J. & Schulp, A.S. 2018: First record of *Carinodens* (Squamata, Mosasauridae) from the uppermost Maastrichtian of Stevns Klint, Denmark. Alcheringa 42, 597–602. https://doi.org/10.1080/03115518.2017.1391878

Polcyn, M.J., Jacobs, L.L., Araújo, R., Schulp, A.S. & Mateus, O. 2014: Physical drivers of mosasaur evolution. Palaeogeography, Palaeoclimatology, Palaeoecology 400, 17–27. https://doi.org/10.1016/j.palaeo.2013.05.018

Schulp, A.S., Polcyn, M.J., Mateus, O., Jacobs, L.L. & Morais, M.L. 2008: A new species of *Prognathodon* (Squamata, Mosasauridae) from the Maastrichtian of Angola, and the affinities of the mosasaur genus *Liodon*. In: Everhart, M. (ed.): Proceedings of the second Mosasaur meeting. Fort Hays Studies, Special Issue 3, 1–12.

Schulp, A.S., Bardet, N. & Bouya, B. 2010: A new species of the durophagous mosasaur *Carinodens* (Squamata, Mosasauridae) and additional material of *Carinodens belgicus* from the Maastrichtian phosphates of Morocco. Netherlands Journal of Geosciences 88, 161–167. https://doi.org/10.1017/s0016774600000871

Schwarzhans, W. & Milàn, J. 2017: After the disaster: bony fish remains (mostly otoliths) from the K/Pg boundary section at Stevns Klint, Denmark, reveal consistency with teleost faunas from later Danian and Selandian strata. Bulletin of the Geological Society of Denmark 65, 59–74. https://doi.org/10.37570/bgsd-2017-65-05

Surlyk, F., Damholt, T. & Bjerager, M. 2006: Stevns Klint, Denmark: uppermost Maastrichtian chalk, Cretaceous–Tertiary boundary, and lower Danian bryozoan mound complex. Bulletin of the Geological Society of Denmark 54, 1–48. https://doi.org/10.37570/bgsd-2006-54-01

Surlyk, F., Rasmussen, S.L., Boussaha, M., Schiøler, P., Schovsbo, N.H., Sheldon, E., Stemmerik, L. & Thibault, N. 2013: Upper Campanian-Maastrichtian holostratigraphy of the eastern Danish Basin. Cretaceous Research 46, 232–256. https://doi.org/10.1016/j.cretres.2013.08.006

Thibault, N. & Husson, D. 2016: Climatic fluctuations and sea-surface water circulation patterns at the end of the Cretaceous era: calcareous nannofossil evidence. Palaeogeography, Palaeoclimatology, Palaeoecology 441, 152–164. https://doi.org/10.1016/j.palaeo.2015.07.049

Thibault, N., Harlou, R., Schovsbo, N.H., Stemmerik, L. & Surlyk, F. 2016: Late Cretaceous (late Campanian–Maastrichtian) sea-surface temperature record of the Boreal Chalk Sea. Climate of the Past 12, 429–438. https://doi.org/10.5194/cp-12-429-2016

Thomsen, E. 1995: Kalk og kridt i den danske undergrund. In: Nielsen, O.B. (ed.): Danmarks geologi fra Kridt til i dag. *Århus Geokompendier 1,* 31–68.

Carbon isotope trends in north-west European mosasaurs (Squamata; Late Cretaceous)

TOM J. GILTAIJ, JEROEN H.J.L. VAN DER LUBBE, BENT E.K. LINDOW, ANNE S. SCHULP & JOHN W.M. JAGT

DGF

The carbon stable isotope composition ($\delta^{13}C$) of tooth enamel in mosasaurid squamates reflects aspects of their diet and diving behaviour. Here we present new $\delta^{13}C$ data for such marine squamates from the Maastrichtian of Denmark and compare these with results obtained in previous studies from the lower-latitude type area of the Maastrichtian Stage (latest Cretaceous; 72.1–66.0 Ma) in the south-east Netherlands and north-east Belgium. For the Danish samples, there is a weak correlation between mosasaur body size and $\delta^{13}C$ values, with larger-sized taxa having lower $\delta^{13}C$ values, comparable to what has previously been observed for mosasaurs from the Maastrichtian type area.

Tom Giltaij [tom.giltaij@live.nl], Faculty of Science, Vrije Universiteit Amsterdam, De Boelelaan 1085, 1081HV Amsterdam, the Netherlands; also Geologisch Museum Hofland, Hilversumseweg 51, 1251EW Laren, the Netherlands; and Faculty of Geosciences, Utrecht University, PO Box 80115, 3508TC Utrecht, the Netherlands. Jeroen van der Lubbe [h.j.l.vander.lubbe@vu.nl], Faculty of Science, Vrije Universiteit Amsterdam; also School of Earth and Ocean Sciences, Cardiff University, Park Place, Cardiff CF10 3AT, United Kingdom. Bent Lindow [lindow@snm.ku.dk], Statens Naturhistoriske Museum, Københavns Universitet, Universitetsparken 15, 2100 København Ø, Denmark. Anne Schulp [anne.schulp@naturalis.nl], Naturalis Biodiversity Center, PO Box 9517, 2300RA Leiden, the Netherlands; also Faculty of Science, Vrije Universiteit Amsterdam, Faculty of Geosciences, Utrecht University, and Natuurhistorisch Museum Maastricht. John W.M. Jagt [john.jagt@maastricht.nl], Natuurhistorisch Museum Maastricht, De Bosquetplein 6–7, 6211KJ Maastricht, the Netherlands.

Corresponding author: Tom Giltaij

Mosasaurs were a diverse, highly successful clade of marine squamates that were secondarily adapted to an aquatic life and were widely distributed during the last ~30 million years of the Cretaceous (Polcyn *et al.* 2014). These medium- to large-sized, agile predators fed on an extensive range of macroscopic prey, as is reflected in the wide variety of tooth morphologies. Although tooth morphology (e.g. Massare 1987; Schulp 2005), bite marks (e.g. Neumann & Hampe 2018), dental microwear (e.g. Holwerda *et al.* 2013), stomach contents (Martin & Fox 2007; Konishi *et al.* 2011) and eye size (Yamashita *et al.* 2015) may provide indirect or even direct evidence of hunting behaviour and dietary preferences, additional independent lines of evidence in reconstructing diet and trophic relationships are desirable.

Stable carbon and oxygen isotopes in tooth enamel have been used for evaluation of diet and other aspects of mosasaur palaeobiology (e.g. Robbins *et al.* 2008; Schulp *et al.* 2013). In the present contribution, we discuss the carbon isotope ($\delta^{13}C$) signatures recovered from tooth enamel of mosasaur teeth from the Maastrichtian of Denmark and compare these data with the pattern observed in the lower-latitude, but roughly coeval, type Maastrichtian ecosystem in the south-east Netherlands and north-east Belgium, as well as sites elsewhere.

Mosasaur teeth were continuously replaced, taking up to almost two years for each to form fully (Gren & Lindgren 2013). Tooth enamel is predominantly composed of hydroxyapatite, $Ca_{10}(PO_4)_6(OH)_2$, which contains less than 5 % by weight of carbonate (e.g. Koch *et al.* 1997). This structurally bound carbonate is precipitated in isotopic equilibrium with body fluids, which, prior to the formation of tooth enamel, becomes fractionated due to respiration (in which the lighter ^{12}C-isotope preferentially becomes liberated from the body pool) and during the formation of new enamel (DeNiro & Epstein 1978). Of this carbonate fraction, the stable isotope composition of carbon and oxygen ($\delta^{18}O$) can be measured. Robbins *et al.* (2008) and Schulp *et al.* (2013) noted that mosasaurs of larger body sizes generally had relatively low $\delta^{13}C$ values in comparison to smaller taxa, with juveniles having relatively higher values compared to conspecific adults. These $\delta^{13}C$ values mainly reflect diet, metabolic and physiological processes, whereas the $\delta^{18}O$ values would have been affected by temperature and the $\delta^{18}O$ values of ambient seawater. As such, the $\delta^{13}C$ and $\delta^{18}O$ signatures can be used to infer biological aspects of extinct squamates.

Schulp *et al.* (2013) focused their research on mosasaur teeth from the Upper Maastrichtian of the Netherlands and Belgium, while Robbins *et al.* (2008) used mosasaurid teeth from the Upper Cretaceous of Texas (USA) and Angola. Here we present the $\delta^{13}C$ signature from teeth of the full range of mosasaur genera represented in the Upper Cretaceous of D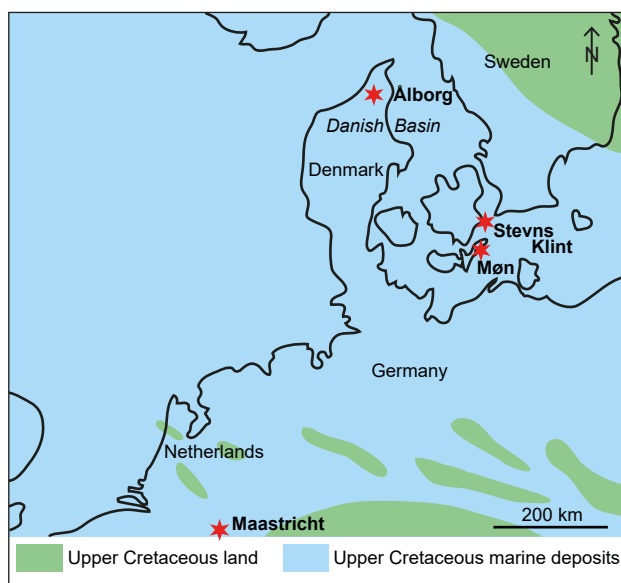enmark, namely *Mosasaurus*, *Plioplatecarpus*, *Carinodens* and *Prognathodon*. On account of the similarities in assemblage between coeval faunas from Denmark and the Maastricht area, the present study aims to investigate whether a similar trend towards lower $\delta^{13}C$ in larger-sized mosasaurs exists in the Danish material. As this study constitutes a new data set from a more northern palaeolatitude, it also expands the latitudinal record of $\delta^{13}C$ signatures from mosasaur teeth.

Material and methods

Institutional abbreviations
NHMD: Natural History Museum of Denmark (Statens Naturhistoriske Museum), Copenhagen, Denmark; NHMM: Natuurhistorisch Museum Maastricht, Maastricht, the Netherlands; OESM: Østsjællands Museum, Store Heddinge, Denmark.

Geographical setting
During the Maastrichtian, the area of present-day Denmark was covered by a shallow (100–250 m deep) epicontinental sea (Lindgren & Jagt 2005; Einarsson 2018) in which mosasaurs ranked amongst the top predators. Since 1964, mosasaur tooth crowns have been recognized from Maastrichtian sedimentary rocks of Denmark (Lindgren & Jagt 2005; Fig. 1), corresponding to palaeolatitudes of ~44°N (reference frame from Van Hinsbergen *et al.* 2015; www.paleolatitude.org). Additional mosasaur material from the type Maastrichtian (south-east Netherlands, north-east Belgium; Mulder 2004) studied here corresponds to a palaeolatitude of *c.* 40°N during the latest Cretaceous (Van Hinsbergen *et al.* 2015; www.paleolatitude.org).

Localities, stratigraphy and specimens
The mosasaur teeth from Denmark analysed in the present study (Table 1) were collected at three localities: Stevns Klint, Møns Klint and Ålborg. In order to expand the existing data set from Schulp *et al.* (2013), additional material from the Maastrichtian type area around Maastricht, the Netherlands (Fig. 1), was assessed as well.

The majority of the Danish teeth examined in the present study originate from the Møns Klint Formation (Surlyk *et al.* 2013), previously referred to the Tor Formation (Surlyk *et al.* 2006). This unit is characterized by thick sequences of marine chalk (Lindgren & Jagt 2005), as observed at Stevns Klint, that formed at water depths of ~100–200 m (Noe-Nygaard 1975) along the south-eastern margin of the Danish Basin. Stevns Klint comprises one of the best-preserved and most extensively studied records of Cretaceous–Palaeogene boundary sections and has therefore been recognized
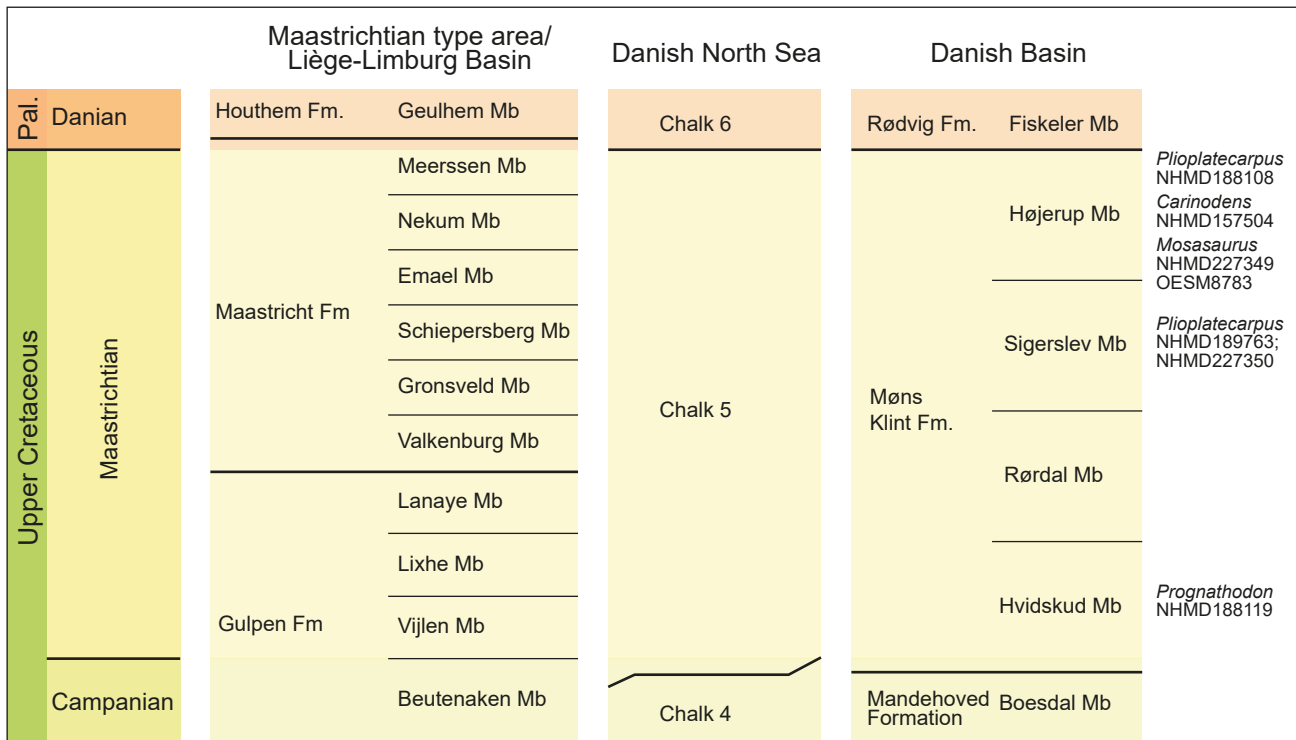

Fig. 1. Palaeogeography of north-west Europe during the Late Cretaceous, adapted from Blakey (2012), with indication of the localities of mosasaur teeth and tooth crowns analysed in the present study.

Stratigraphy of the Danish Basin and the Maastrichtian type area (Liège-Limburg Basin) as well as lithostratigraphic scheme for the Danish North Sea.

Age	Maastrichtian type area / Liège-Limburg Basin		Danish North Sea	Danish Basin		Specimens
Pal. — Danian	Houthem Fm.	Geulhem Mb	Chalk 6	Rødvig Fm.	Fiskeler Mb	
Upper Cretaceous — Maastrichtian	Maastricht Fm	Meerssen Mb	Chalk 5	Møns Klint Fm.	Højerup Mb	*Plioplatecarpus* NHMD188108; *Carinodens* NHMD157504; *Mosasaurus* NHMD227349 OESM8783
		Nekum Mb				
		Emael Mb			Sigerslev Mb	*Plioplatecarpus* NHMD189763; NHMD227350
		Schiepersberg Mb				
		Gronsveld Mb			Rørdal Mb	
		Valkenburg Mb				
	Gulpen Fm	Lanaye Mb			Hvidskud Mb	*Prognathodon* NHMD188119
		Lixhe Mb				
		Vijlen Mb				
Campanian		Beutenaken Mb	Chalk 4	Mandehoved Formation	Boesdal Mb	

Fig. 2. Stratigraphy of the Danish Basin and the Maastrichtian type area (Liège-Limburg Basin) as well as lithostratigraphic scheme for the Danish North Sea (compare Lieberkind *et al.* 1982; Isaksen & Tonstad 1989; Van Adrichem Boogaert & Kouwe 1994; Niebuhr *et al.* 2007 and Surlyk *et al.* 2013). The record of *Prognathodon* NHMD 188119 is discussed by Giltaij *et al.* (2021).

as a UNESCO World Heritage Site (UNESCO website, accessed August 2020). The Møns Klint Formation spans the uppermost Maastrichtian up to the Cretaceous–Palaeogene boundary and has yielded several tooth crowns of at least three species of mosasaur (Bonde & Christiansen 2003).

The Møns Klint Formation can be subdivided into four members (Fig. 2). The basal unit, the Hvidskud Member, is of early Maastrichtian age and consists of alternating white chalk and darker, slightly marly chalk beds. At Møns Klint, these beds yielded a diverse fossil assemblage, including sponges, bivalves and echinoids and, at several levels in the upper part of the member, bryozoans and foraminifera (Surlyk *et al.* 2013). At Store Stejlebjerg on Møns Klint, an isolated tooth crown (NHMD 188119) assigned to the genus *Prognathodon* Dollo, 1889 (Giltaij *et al.* 2021) was found loose in scree; this stems from the Hvidskud Member.

Overlying the Hvidskud Member is the Rørdal Member, which lacks the white chalk beds. Its reference section is at the Rørdal quarry near Ålborg (Surlyk *et al.* 2013). It is overlain by the Sigerslev Member, which comprises benthos-rich chalk in mounded bedding with nodular flint deposited below storm wave base in the sub-photic zone with oxygenated bottom waters (Hansen & Surlyk 2014). This is followed by a benthos- and flint-poor chalk horizon

with near-horizontal bedding suggestive of a very weak bottom current, overlain by a marker band of flint associated with a sea level drop (Surlyk *et al.* 2006; Hansen & Surlyk 2014; Milàn *et al.* 2018). Two specimens, both referred to the genus *Plioplatecarpus* Dollo, 1882, originate from the Sigerslev Member. One is a 28-mm-tall tooth crown from the cliff at Sigerslev at Stevns Klint (NHMD 189763; Fig. 3A–D), the other is a 12-mm-tall tooth crown from Stevns Kridtbrud, Stevns Klint (NHMD 227350; Fig. 3M). Both specimens are here referred to as *Plioplatecarpus* sp. on the basis of their relatively small size, marked recurvature and finely striated basal enamel surface.

The uppermost unit of the formation, the Højerup Member, consists of bryozoan-rich wackestone in southward-trending, asymmetrical mounds up to 35 m in length, deposited after the return of suberosive currents and a sea-level rise (Hansen & Surlyk 2014). This unit is about five metres in thickness at the southern end of Stevns Klint and becomes gradually thinner towards the north (Surlyk *et al.* 2006; Milàn *et al.* 2018). One shed tooth crown of *Carinodens minalmamar* (NHMD 157504) has been collected from the uppermost metre of this member at Mandehoved, Stevns Klint (Milàn *et al.* 2018).

A marginal tooth crown, referred to as *Plioplatecarpus* sp. (NHMD 188108) by Lindgren & Jagt (2005),

was recovered from a loose block of limestone on the beach north of Stevns Kridtbrud, Stevns Klint. The block had fallen from a section of the cliff only a few metres below the Cretaceous–Palaeogene boundary and can be assigned either to the Højerup Member or to the Sigerslev Member, making it possibly the youngest representative of *Plioplatecarpus* known to date (Bonde *et al.* 2008). It should be noted that Lindgren & Jagt (2005) erroneously noted this specimen to have been collected from the locality of Holtug Kridtbrud. Two additional teeth (OESM 8783 and NHMD 227349), both referred to the genus *Mosasaurus* (Conybeare,

1822), also stem from either the Højerup Member or the Sigerslev Member at Stevns Klint. OESM 8783 has recently been illustrated by Milàn *et al.* (2018), who assigned it to *M. hoffmanni* (Mantell, 1829). Although fragmentary, NHMD 227349 (Fig. 3I–L) is referred to as *Mosasaurus* with confidence on account of its relatively large size, slightly conical shape, coarse faceting of the enamel and the presence of a significant anterior carina.

Finally, one large tooth crown referred to as *Mosasaurus* cf. *hoffmanni* (NHMD 226499) stems from the Møns Klint Formation *sensu lato* near Ålborg. How-
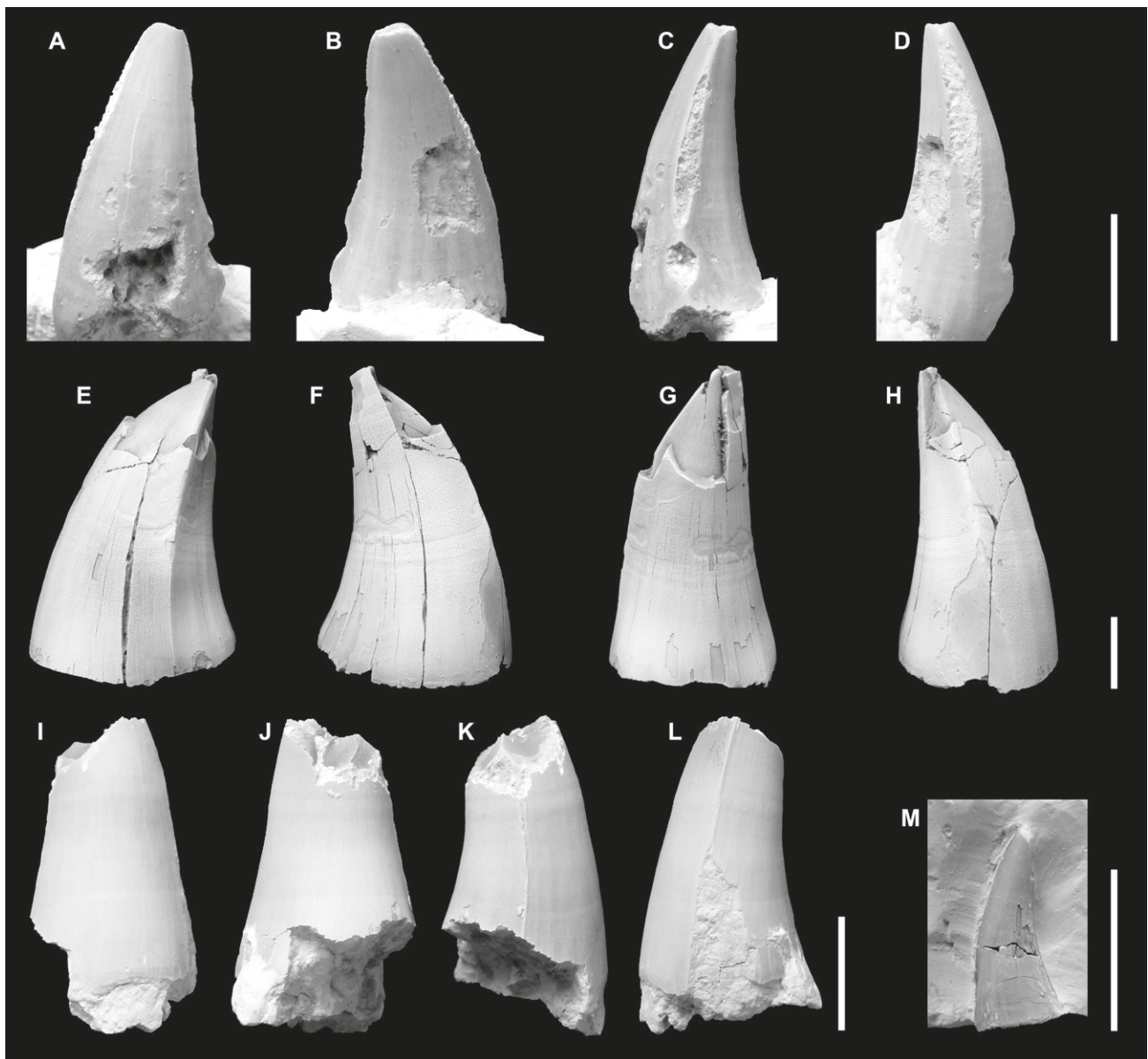

Fig. 3. Isolated mosasaurid tooth crowns. NHMD 189763, *Plioplatecarpus* sp. in labial (**A**), lingual (**B**), posterior (**C**) and anterior (**D**) views. NHMD 226499, *Mosasaurus* cf. *hoffmanni* in labial (**E**), lingual (**F**), posterior (**G**) and anterior (**H**) views. NHMD 227349, *Mosasaurus* sp. in labial (**I**), lingual (**J**), posterior (**K**) and anterior (**L**) views. NHMD 227350, *Plioplatecarpus* sp. in matrix (**M**). Scale bars equal 10 mm.

ever, the exact stratigraphic position is unknown (Lindgren & Jagt 2005; Fig. 3E–H).

The mosasaur teeth and tooth crowns from the Maastrichtian type area that have been analysed for the present study stem from the Maastricht and Gulpen Formations (Jagt & Jagt-Yazykova 2012; Schulp *et al.* 2013; Keutgen 2018; Fig. 2). While the Maastrichtian type locality is renowned for the historical discovery of the holotype of *Mosasaurus hoffmanni* in October 1778 (Pieters 2009; Homburg 2015), other species of mosasaur recovered from the uppermost strata include *Prognathodon sectorius* (Cope, 1871), *Prognathodon saturator* Dortangs *et al.* 2002, *Plioplatecarpus marshi* Dollo, 1882 and *Carinodens belgicus* (Woodward, 1891) (compare Jagt 2005; Schulp *et al.* 2013).

Tooth morphology
Mosasaurs are typically considered secondary con-

sumers up to apex predators, having fed on ammonites, bony and cartilaginous fish, plesiosaurs, turtles and even other mosasaurs (Massare 1987; Schulp *et al.* 2013; Miedema *et al.* 2019). In addition to stable isotopes, tooth morphology can also be used as a proxy for mosasaur diet. Most mosasaurs had a more or less homodont type of dentition with conical teeth (Massare 1987; Lingham-Soliar 1995; Caldwell 2007; Robbins *et al.* 2008). Some species, such as *Carinodens*, had a more heterodont type of dentition, which indicates a more specialised foraging repertoire (Schulp 2005; Mulder *et al.* 2013). Prey with a hard shell or external armour required stout, low teeth, while more slippery prey called for more slender, sharp teeth for piercing and handling. The diversity in tooth morphology enables reconstruction of prey preferences; Massare (1987) divided tooth crowns into 'guilds', based on tooth morphology (Fig. 4); this division is followed here.
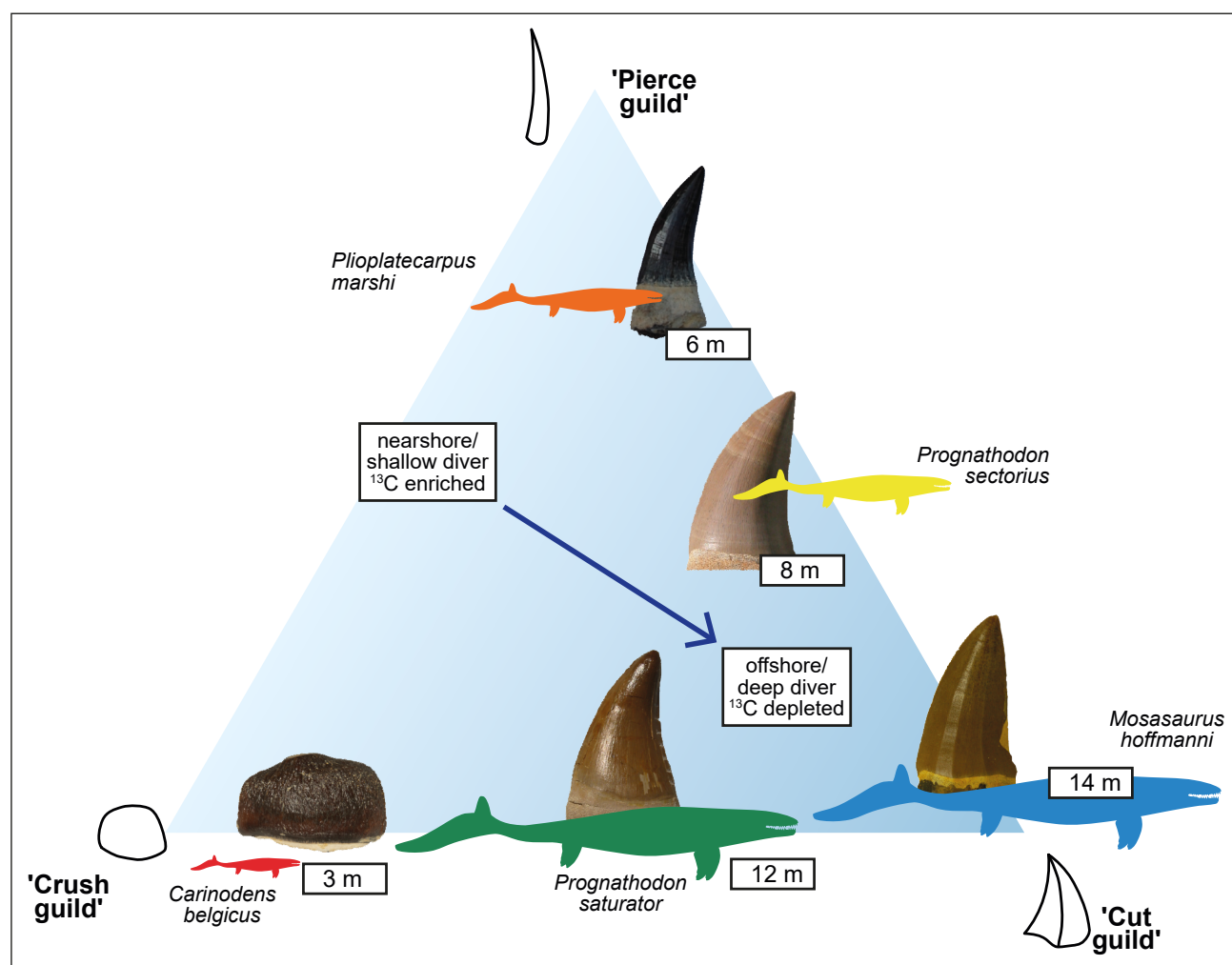

Fig. 4. Feeding strategies in mosasaurs, based on tooth morphology following Massare (1987), with the general ^{13}C isotope nearshore/offshore gradient (Robbins *et al.* 2008; Schulp *et al.* 2013) superimposed. Placement of mosasaur taxa follows Schulp *et al.* (2013); body lengths and example tooth images are based on assemblages from the Maastrichtian type area (Schulp *et al.* 2013); mosasaur silhouettes follow tail flukes as documented by Lindgren *et al.* (2013).

Body length reconstruction
As the dentition of mosasaurs is mostly homodont in nature, the body length of the individuals sampled could be roughly approximated using a linear relationship between tooth length and body length. As all the analysed teeth are detached from the jaws, we assume the teeth to be in either the seventh or eighth developmental stage (*sensu* Caldwell 2007). Body lengths (Table 1) were reconstructed following Russell (1967), Dortangs *et al.* (2002), Schulp *et al.* (2013) and Milàn *et al.* (2018).

Stable isotope analysis
Carbonate ions substitute into bioapatite in enamel, dentine and bone. Enamel is less porous, contains only a few percent of organic matter, and has larger and more stable crystals (*c.* 1000 × 130 × 30 nm) in comparison to bone or dentine (Cerling & Sharp 1996; Koch *et al.* 1997; Kohn *et al.* 1999; Koch 2007), which makes enamel less sensitive to diagenesis and therefore the preferred material for stable isotope analysis.

Prior to sampling, teeth were cleaned using ethanol in order to remove possible dirt, grease, and any residual flakes of sediment or glues and other residues from the enamel surface. Under an Olympus SZ60 optical microscope equipped with an Olympus Highlight 3000 fibre optic light source, tiny flakes (about 1 × 1 mm) of enamel were chipped off using a scalpel and put into vials after inspection for (and removal of) any remaining adhering dentine. Tooth crowns registered as NHMD 226499 and NHMM 1984089-1 were sampled in multiple locations in order to assess intra-tooth variability, and some samples of dentine were also included in order to document diagenesis. Samples of adhering matrix were taken to determine a background signal and examine possible diagenetic alteration. All samples are listed in Table 1. The structural carbonate in the enamel of mosasaur teeth was analysed using a Gasbench II connected to a Finnigan Delta+ mass spectrometer following the standard protocol at the Vrije Universiteit (Amsterdam) Earth Science stable isotope laboratory: samples were reacted with concentrated phosphoric acid (H_3PO_4) at 45°C for 24 hours to produce CO_2. Mixed with He, CO_2 was introduced to the mass spectrometer. Five samples of CO_2 monitor gas and ten subsamples of produced CO_2 were routinely analysed of each sample. A mean value of the samples was based on the last nine measurements. To monitor the accuracy of the analysis, ten samples with each a single grain of the VICS (VU In-house Carbonate Standard) were analysed in the same run as the samples and the international isotope standard IAEA-603. For the carbonate standards, the standard deviation (1σ) of the standard measurements is 0.08 ‰ and 0.14 ‰ for $\delta^{13}C$ and $\delta^{18}O$, respectively.

For the individual enamel samples, the standard deviations of both averaged $\delta^{13}C$ and $\delta^{18}O$ values are below 0.4 ‰. The standard deviations of the measured $\delta^{13}C$ and $\delta^{18}O$ values of specimens NHMD 188119 and NHMM 001456 are larger than 0.5 ‰ and are therefore omitted from the dataset for interpretations. The $\delta^{13}C$ and $\delta^{18}O$ for the analysed bioapatite samples have a standard deviation ranging between 0.1 and 0.4 ‰ (Table 1). Hereafter, all reported results are reported as $\delta^{13}C$ and $\delta^{18}O$ values against the V-PDB scale.

Results

Isotope values
Table 1 shows the results of $\delta^{13}C$ and $\delta^{18}O$ analysis for structural carbonates of the tooth enamel as well as for the adhering matrix from Denmark. The $\delta^{13}C$ values in the Danish samples range from –11.1 to 0.2 ‰, whereas the $\delta^{18}O$ values range from –3.4 to –2.5 ‰.

The adhering carbonate sediments have $\delta^{13}C$ values between 0.1 and 2 ‰ and $\delta^{18}O$ values between –2.1 and –1.6 ‰. In case some of the adhering sediments would have remained, analysis of these samples would lead to considerably higher $\delta^{13}C$ values. This is less obvious for oxygen isotopes, which occur more or less in comparable ranges. Given the excess of oxygen in water, $\delta^{18}O$ values are expected to be more vulnerable to isotopic alteration than carbon isotopes during recrystallisation (Van Baal *et al.* 2013). Complementary to the Danish isotope data listed in Table 1 are $\delta^{13}C$ and $\delta^{18}O$ isotope analyses for structural carbonates in teeth from the Maastrichtian type area; $\delta^{13}C$ values range from –11.6 to –7 ‰ and $\delta^{18}O$ values range from –4.0 to –2.4 ‰.

The $\delta^{13}C$ values are plotted against the reconstructed body lengths of the sampled mosasaurs from Denmark and the Maastrichtian type area for the present study (Fig. 5). For comparison, these data have been plotted together with previously published datasets from the type Maastrichtian, USA and Angola (Schulp *et al.* 2013; Robbins *et al.* 2008). The $\delta^{13}C$ data show a negative relation with respect to body length, showing larger mosasaurs to have systematically lower $\delta^{13}C$ values. By combining both datasets from the Maastrichtian type area, we obtain a significant regression between reconstructed body length and $\delta^{13}C$ values, with a slope of –0.36 ‰ per metre body length. Some teeth considered to be from juvenile and subadult ontogenetic stages (indicated 'J' in Fig. 5) have not been included in the calculation of the regression line.

For the limited Danish mosasaur data (n = 6, juvenile specimen excluded), their reconstructed body

Table 1. Results of δ¹³C and δ¹⁸O stable isotope analysis for structural carbonates of the teeth sampled and of adhering matrix from Denmark and reconstructed body length.

Registration number	Species	Provenance	Member	δ¹³C	δ¹⁸O	Body length (m)
NHMD 157504	*Carinodens minalmamar*	Stevns Klint	Sigerslev	−6.28±0.13	−3.12±0.15	2
NHMD 227349	*Mosasaurus* sp.	Stevns Klint		−11.13±0.18	−2.48±0.18	10
OESM 8783	*Mosasaurus* sp.	Stevns Klint		−8.61±0.10	−2.62±0.14	8
OESM 8783	*Mosasaurus* sp.	Stevns Klint		−0.09±0.09	−2.05±0.16	[matrix]
NHMM 1984089-1	*Mosasaurus hoffmanni*	Maastricht		−10.32±0.29	−2.71±0.43	12
NHMM 1984089-1	*Mosasaurus hoffmanni*	Maastricht		−8.97±0.14	−3.38±0.18	12
NHMD 226499	*Mosasaurus* cf. *hoffmanni*	Ålborg		−6.94±0.37	−2.83±0.27	10
NHMD 226499	*Mosasaurus* cf. *hoffmanni*	Ålborg		−11.03±0.16	−2.74±0.15	10
NHMD 227350	*Plioplatecarpus* sp. juv.	Stevns Klint	?Sigerslev	0.24±0.30	−3.42±0.36	2.5
NHMD 189763	*Plioplatecarpus* sp.	Stevns Klint	?Sigerslev	−9.54±0.21	−2.82±0.19	5.5
NHMD 189763	*Plioplatecarpus* sp.	Stevns Klint	?Sigerslev	1.95±0.06	−1.61±0.09	[matrix]
NHMM 1997289	*Plioplatecarpus marshi*	Maastricht		−6.95±0.19	−2.40±0.23	5.5
NHMM 1997289	*Plioplatecarpus marshi*	Maastricht		−7.85±0.33	−4.01±0.27	5.5
NHMM 1998141-11	*Prognathodon saturator*	Maastricht	Upper Lanaye	−10.90±0.21	−2.67±0.18	12
NHMM 1998141-7	*Prognathodon saturator*	Maastricht	Upper Lanaye	−11.59±0.13	−2.52±0.06	12

length and δ¹³C values follow a trend comparable to the larger (n = 30) Maastrichtian type area dataset. These trends from north-west Europe show a gentler slope compared to the trend observed by Robbins *et al.* (2008) based on mosasaurs from USA and Angola.

Discussion

The limited number of data points from Danish mosasaurs fall to a certain extent within the pattern previously observed in the relationship between reconstructed body length and δ¹³C values; however, the relatively large spread in data suggests that other factors besides body length likely played a role in the measured δ¹³C values of the specimens examined. Here we review possible factors that may have been influential on the measured δ¹³C values.

Diet
According to Kohn (1996), Koch *et al.* (1997), Kohn *et al.* (1999) and Koch (2007), an individual's diet primarily affects δ¹³C apatite values. Based on the blunt shape of the teeth (Fig. 4), the diet of the smallest mosasaur in our data set, *Carinodens*, presumably consisted of hard-shelled prey such as oysters, other bivalves and decapod crustaceans in (near) coastal environments, while the large-sized *Prognathodon saturator* may have fed on marine turtles, plesiosaurs, large-sized saurodontid teleosts and other mosasaurs farther offshore (Schulp & Jagt 2015). Medium-sized mosasaurs, such as *Plioplatecarpus marshi*, would have occupied an intermediate trophic position between these two habitats, feeding on more slippery prey such as fish and squid (Schulp 2005). The largest mosasaurs, such as *Mosasaurus hoffmanni*, could have eaten virtually everything, opportunistically including other mosasaurs (e.g. Lingham-Soliar 1995). In general, δ¹³C values in tooth enamel increase by ~1‰ per trophic level (DeNiro & Epstein 1978; Polcyn *et al.* 2014); contrastingly, as previously observed by Robbins *et al.* (2008), Schulp *et al.* (2013) and the present study, larger mosasaurs have generally lower δ¹³C values. Teeth from juvenile and subadult ontogenetic stages would have occupied lower trophic levels, possibly more nearshore.

The negative trend of δ¹³C values towards larger mosasaurs such as *Prognathodon saturator* and *Mosasaurus hoffmanni* may be explained by a more lipid-rich diet of the larger mosasaurs (Post *et al.* 2007), which would tend to lower the overall δ¹³C values incorporated into bioapatite. Interestingly, coeval shark teeth from the Maastrichtian type area yield significantly higher δ¹³C values than mosasaurs, even though they would have occupied comparably high trophic levels (Schulp *et al.* 2013). The latter further supports that enamel largely preserves *in vivo* δ¹³C values and that, besides diet, other factors determine the δ¹³C signatures of the studied mosasaurs, such as habitat and migration.

Habitat
Robbins *et al.* (2008), Schulp *et al.* (2013) and Schulp & Jagt (2015) suggested that a habitat differentiation can be regarded as an important factor contributing to the δ¹³C signatures of mosasaurs, considering
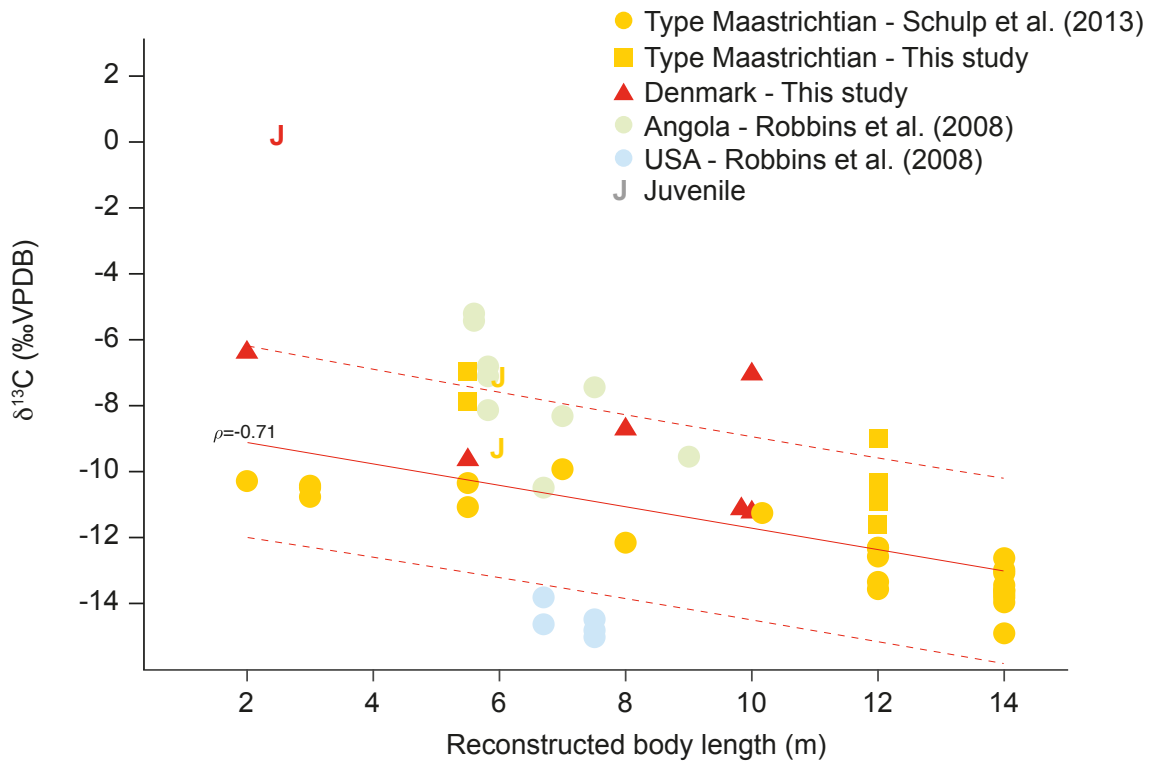
Fig. 5. Reconstructed mosasaur body length plotted against δ¹³C, with data from the Maastrichtian type area (Schulp *et al.* 2013), USA and Angola (Robbins *et al.* 2008), and analyses from the present study with material from Denmark and additional samples from the Maastrichtian type area. The red line represents a linear regression with a 99 % prediction interval (dashed lines) and Pearson's correlation coefficient of −0.71. Juveniles are not included in the regression line.

the higher δ¹³C values nearshore compared to more offshore marine ecosystems (Vennemann *et al.* 2001; Koch 2007). Consequently, larger-sized mosasaurs such as *Prognathodon* that preferred more offshore habitats would have lower δ¹³C values than taxa that were associated with more nearshore, shallow-water settings. *Mosasaurus* has slightly higher δ¹³C values in comparison to *Prognathodon*, which would place it in a more nearshore setting (Schulp *et al.* 2013). In accordance, skeletal remains of *Mosasaurus* outnumber those of *Prognathodon* by orders of magnitude, indicating that they were abundantly present in the shallow-marine ecosystem of the type Maastrichtian (Schulp & Jagt 2015). Furthermore, Mulder *et al.* (1998), Mulder (2003) and Jagt (2005) have previously noted that as fully nektic animals mosasaurs, including *Mosasaurus hoffmanni*, could have easily migrated through the Cretaceous Boreal Sea during the Late Cretaceous. A migratory behaviour of *Prognathodon* could cause isotopic signatures that differ greatly from the environment a specimen is buried in (e.g. Kohn *et al.* 1999).

The recent addition of *Prognathodon* to the Danish mosasaur record (Giltaij *et al.* 2021) underscores the resemblance between the Danish and Dutch fossil

faunal assemblages, previously evident from other mosasaur taxa, which were situated ~4° latitude apart during the late Maastrichtian (Milàn *et al.* 2018). The Danish isotope data fall largely in the δ¹³C trend of the mosasaurs from the Maastrichtian type area (Fig. 5), highlighting the possible similarity between both mosasaur populations. The expected latitudinal effect on the δ¹³C values in marine ecosystems (~0.02 ‰ per degree latitude; Rau *et al.* 1982; Fang *et al.* 2016), is indeed too small to cause a significant difference in the isotope signatures of the Danish and type Maastrichtian mosasaurs.

Respiratory physiological effects

Beside the dietary and habitat influences, the observed δ¹³C trend can be further attributed to respiratory physiological effects. Prolonged and rapid repeated breath-hold diving of extant and extinct Squamata and marine turtles elevates the CO_2 pressure in blood, leading to lower δ¹³C values in the skeletal material (the so-called Bohr effect; Biasatti 2004; Robbins *et al.* 2008; Van Baal *et al.* 2013; Schulp *et al.* 2013; Janssen 2017). Consequently, mosasaurs that hunted for prey further offshore or at greater depths would have needed to make more prolonged or frequent dives,

which would be expressed by lower $\delta^{13}C$ signatures. Larger divers store more oxygen relative to their consumption rate, due to their lower mass-specific metabolic rates (Verberk *et al.* 2020). Intensive diving behaviour of some mosasaur genera is also supported by independent lines of evidence, such as the occurrence of avascular necrosis and reconstructions of mosasaur eyes (Martin & Rothschild 1989; Schulp *et al.* 2013 and references therein; Yamashita *et al.* 2015). The obtained relationship between $\delta^{13}C$ values and body size is less steep as observed by Robbins *et al.* (2008) in two distinct mosasaur populations from USA and Angola, which therefore might have been more strongly affected by the aforementioned factors related to diet and habitat than those in the present study.

Conclusions

The inverse relationship between $\delta^{13}C$ values of mosasaur tooth enamel and their reconstructed body length is complemented by the new data from the Maastrichtian type area. For the Danish samples, there is only a weak correlation between mosasaur body size and $\delta^{13}C$ values. This trend can be partly attributed to environmental and biological factors, such as diet and habitat differentiation, but the Bohr effect appears to be a dominant factor. The obtained relationship between $\delta^{13}C$ in tooth enamel and body size seems to be less affected by other factors than that found by Robbins *et al.* (2008), who analysed mosasaurs from very different settings. The weak correlation for the Danish mosasaurs can partly be attributed to the low sample number (n = 6) compared to the type Maastrichtian dataset (n = 30). Future research with a more extensive dataset would expand the knowledge about these similar mosasaur populations.

Acknowledgements

References

Biasatti, D.M. 2004: Stable carbon isotopic profiles of sea turtle humeri: implications for ecology and physiology. Palaeogeography, Palaeoclimatology, Palaeoecology, 206(3–4), 203–216. https://doi.org/10.1016/j.palaeo.2004.01.004

Blakey, R. 2012: Global paleogeography maps, library of paleogeography. Colorado Plateau Geosystems Inc., Arizona, USA.

Bonde, N. & Christiansen, P. 2003: New dinosaurs from Denmark. Comptes Rendus Palevol 2, 13–26. https://doi.org/10.1016/s1631-0683(03)00009-5

Bonde, N., Andersen, S., Hald, N., & Jakobsen, S.L. 2008: Danekræ – Danmarks bedste fossiler, 225 pp. Copenhagen: Gyldendal. https://doi.org/10.7146/gn.v0i3.3458

Caldwell, M.W. 2007: Ontogeny, anatomy and attachment of the dentition in mosasaurs (Mosasauridae: Squamata). Zoological Journal of the Linnean Society 149, 687–700. https://doi.org/10.1111/j.1096-3642.2007.00280.x

Cerling, T.E. & Sharp, Z.D. 1996: Stable carbon and oxygen isotope analysis of fossil tooth enamel using laser ablation. Palaeogeography, Palaeoclimatology, Palaeoecology 126, 173–186. https://doi.org/10.1016/s0031-0182(96)00078-8

Conybeare, W.D. 1822: p. 298. In: Parkinson, J. (ed.): Outlines of oryctology: an introduction to the study of fossil organic remains, especially those found in the British strata; intended to aid the student in his enquiries respecting the nature of fossils, and their connection with the formation of the earth, 298 pp. London: The author. https://doi.org/10.5962/bhl.title.22356

Cope, E.D. 1871: Supplement to the "Synopsis of the extinct Batrachia and Reptilia of North America". Proceedings of the American Philosophical Society 12, 41–52. https://doi.org/10.5962/bhl.title.60499

DeNiro, M.J. & Epstein, S. 1978: Influence of diet on the distribution of carbon isotopes in animals. Geochimica et Cosmochimica Acta 42(5), 495–506. https://doi.org/10.1016/0016-7037(78)90199-0

Dollo, L. 1882: Note sur l'ostéologie des Mosasauridæ. Bulletin du Musée d'Histoire naturelle de la Belgique 1, 55–80.

Dollo, L. 1889: Note sur les vertébrés récemment offerts au Musée de Bruxelles par M. Alfred Lemonnier. Bulletin de la Société belge de Géologie, de Paléontologie et d'Hydrologie 3, 181–182.

Dortangs, R.W., Schulp, A.S., Mulder, E.W.A., Jagt, J.W.M., Peeters, H.H.G. & de Graaf, D.T. 2002: A large new mosasaur from the Upper Cretaceous of The Netherlands. Netherlands Journal of Geosciences 81, 1–8. https://doi.org/10.1017/s0016774600020515

Einarsson, E. 2018: Palaeoenvironments, palaeoecology and

palaeobiogeography of Late Cretaceous (Campanian) faunas from the Kristianstad Basin, southern Sweden, with applications for science education. Litholund Theses, Lund University, Faculty of Science, Department of Geology, Lithosphere and Biosphere Science 32, 35–40.

Fang, Z., Thompson, K., Jin, Y., Chen, X. & Chen, Y. 2016: Preliminary analysis of beak stable isotopes (δ^{13}C and δ^{15}N) stock variation of neon flying squid, *Ommastrephes bartramii*, in the North Pacific Ocean. Fisheries Research 117, 153–163. https://doi.org/10.1016/j.fishres.2016.01.011

Giltaij, T.J., Milàn, J., Jagt, J.W.M. & Schulp, A.S. 2021: *Prognathodon* (Squamata, Mosasauridae) from the Maastrichtian chalk of Denmark. Bulletin of the Geological Society of Denmark 69, 53–58. https://doi.org/10.37570/bgsd-2021-69-03

Gren, J.A. & Lindgren, J. 2013: Dental histology of mosasaurs and a marine crocodilian from the Campanian (Upper Cretaceous) of southern Sweden: incremental growth lines and dentine formation rates. Geological Magazine 151, 1–10. https://doi.org/10.1017/s0016756813000526

Hansen, T. & Surlyk, F. 2014: Marine macrofossil communities in the uppermost Maastrichtian chalk of Stevns Klint, Denmark. Palaeogeography, Palaeoclimatology, Palaeoecology 399, 323–344. https://doi.org/10.1016/j.palaeo.2014.01.025

Holwerda, F.M., Beatty, B.L. & Schulp, A.S. 2013: Dental macro- and microwear in *Carinodens belgicus*, a small mosasaur from the type Maastrichtian. Netherlands Journal of Geosciences 92, 267–274. https://doi.org/10.1017/s0016774600000202

Homburg, E. 2015: Wetenschapsbeoefening, 1750–1950. In: Tummers, P. (ed.): Limburg. Een geschiedenis, vanaf 1800: pp. 355–394. Koninklijk Limburgs Geschied- en Oudheidkundig Genootschap (LGOG), Maastricht.

Isaksen, D. & Tonstad, K. 1989: A revised Cretaceous and Tertiary lithostratigraphic nomenclature for the Norwegian North Sea. Norwegian Petroleum Directorate Bulletin 5, 1–59.

Jagt, J.W.M. 2005: Stratigraphic ranges of mosasaurs in Belgium and the Netherlands (Late Cretaceous) and cephalopod-based correlations with North America. Netherlands Journal of Geosciences 84, 283–301. https://doi.org/10.1017/s0016774600021065

Jagt, J.W.M. & Jagt-Yazykova, E.A. 2012: Stratigraphy of the type Maastrichtian – a synthesis. In: Jagt, J.W.M., Donovan, S.K. & Jagt-Yazykova, E.A. (eds): Fossils of the type Maastrichtian (Part 1). Scripta Geologica, Special Issue 8, 5–32. https://doi.org/10.1016/j.cretres.2017.05.022

Janssen, R. 2017: Isotope records in vertebrate fossils from Cretaceous seas to Quaternary Sundaland. PhD Thesis, Vrije Universiteit Amsterdam, 142 pp.

Keutgen, N. 2018: A bioclast-based astronomical timescale for the Maastrichtian in the type area (southeast Netherlands, northeast Belgium) and stratigraphic implications: the legacy of P.J. Felder. Netherlands Journal of Geosciences 97, 229–260. https://doi.org/10.1017/njg.2018.15

Koch, P.L. 2007: Isotopic study of the biology of modern and fossil vertebrates. In: Michener, R. & Lajtha, K. (eds): Stable isotopes in ecology and environmental science, second edition, 99–154. Malden: Blackwell Publishing. https://doi.org/10.1002/9780470691854.ch5

Koch, P.L., Tuross, N. & Fogel, M.L. 1997: The effects of sample treatment and diagenesis on the isotopic integrity of carbonate in biogenic hydroxylapatite. Journal of Archaeological Science 24, 417–429. https://doi.org/10.1006/jasc.1996.0126

Kohn, M.J. 1996: Predicting animal δ^{18}O: Accounting for diet and physiological adaptation. Geochimica et Cosmochimica Acta 60, 4811–4829. https://doi.org/10.1016/s0016-7037(96)00240-2

Kohn, M.J., Schoeninger, M.J. & Barker, W.W. 1999: Altered states: Effects of diagenesis on fossil tooth chemistry. Geochimica et Cosmochimica Acta 63, 2737–2747. https://doi.org/10.1016/s0016-7037(99)00208-2

Konishi, T., Brinkman, D., Massare, J.A. & Caldwell, M.W. 2011: New exceptional specimens of *Prognathodon overtoni* (Squamata, Mosasauridae) from the upper Campanian of Alberta, Canada, and the systematics and ecology of the genus. Journal of Vertebrate Paleontology 31, 1026–1046. https://doi.org/10.1080/02724634.2011.601714

Lieberkind, K., Bang, I., Mikkelsen, N. & Nygaard, E. 1982: Late Cretaceous and Danian limestone. In: Michelsen, O. (ed.): Geology of the Danish Central Graben. Danmarks Geologiske Undersøgelse B8, 49–62.

Lindgren, J. & Jagt, J.W.M. 2005: Danish mosasaurs. Netherlands Journal of Geosciences 84, 315–320. https://doi.org/10.1017/s0016774600021090

Lindgren, J., Kaddumi, H.F. & Polcyn, M.J. 2013: Soft tissue preservation in a fossil marine lizard with a bilobed tail fin. Nature Communications 4, 1–8. https://doi.org/10.1038/ncomms3423

Lingham-Soliar, T. 1995: Anatomy and functional morphology of the largest marine reptile known, *Mosasaurus hoffmanni* (Mosasauridae, Reptilia) from the Upper Cretaceous, Upper Maastrichtian of The Netherlands. Philosophical Transactions of The Royal Society B 347, 155–180. https://doi.org/10.1098/rstb.1995.0019

Mantell, G.A. 1829: A tabular arrangement of the organic remains of the country of Sussex. Transactions of the Geological Society of London 2(3), 201–216. https://doi.org/10.1144/transgslb.3.1.201

Martin, J.E. & Fox, J.E. 2007: Stomach contents of *Globidens*, a shell-crushing mosasaur (Squamata), from the Late Cretaceous Pierre Shale Group, Big Bend area of the Missouri River, central South Dakota. Special Papers, Geological Society of America 427, 167–176. https://doi.org/10.1130/2007.2427(12)

Martin, L.D. & Rothschild, B.M. 1989: Paleopathology and diving mosasaurs. American Scientist 77, 460–467.

Massare, J. 1987: Tooth morphology and prey preference of Mesozoic marine reptiles. Journal of Vertebrate Paleontology 2, 121–137. https://doi.org/10.1080/02724634.1987.10011647

Miedema, F., Schulp, A.S., Jagt, J.W.M. & Mulder, E.W.A. 2019: New plesiosaurid material from the Maastrichtian type area, the Netherlands. Netherlands Journal of Geosciences, 98, e3. https://doi.org/10.1017/njg.2019.2

Milàn, J., Jagt, J.W.M., Lindgren, J. & Schulp, A.S. 2018: First record of *Carinodens* (Squamata, Mosasauridae) from the uppermost Maastrichtian of Stevns Klint, Denmark. Alcheringa 42, 597–602. https://doi.org/10.1080/03115518.2017.1391878

Mulder, E.W.A. 2003: On latest Cretaceous tetrapods from the Maastrichtian type area. Publicaties van het Natuurhistorisch Genootschap in Limburg 44, 1–188.

Mulder, E.W.A. 2004: Maastricht Cretaceous finds and Dutch pioneers in vertebrate palaeontology. In: Touret, J.L.R. & Visser, R.P.W. (eds): Dutch pioneers of the earth sciences, 165–176. Royal Netherlands Academy of Arts and Sciences (KNAW), Amsterdam.

Mulder, E.W.A., Jagt, J.W.M., Kuypers, M.M.M., Peeters, H.H.G. & Rompen, P. 1998: Preliminary observations on the stratigraphic distribution of Late Cretaceous marine and terrestrial reptiles from the Maastrichtian type area. Oryctos 1, 55–64.

Mulder, E.W.A., Formanoy, P., Gallagher, W.B., Jagt, J.W.M. & Schulp, A.S. 2013: The first North American record of *Carinodens belgicus* (Squamata, Mosasauridae) and correlation with the youngest *in situ* examples from the Maastrichtian type area: palaeoecological implications. Netherlands Journal of Geosciences 92, 145–152. https://doi.org/10.1017/s001677460000007x

Neumann, C. & Hampe, O. 2018: Eggs for breakfast? Analysis of a probable mosasaur biting trace on the Cretaceous echinoid *Echinocorys ovata* Leske, 1778. Fossil Record 21, 55–66. https://doi.org/10.5194/fr-21-55-2018

Niebuhr, B., Hiss, M., Kaplan, U., Tröger, K.-A., Voigt, S., Voigt, T., Wiese, F. & Wilmsen, M. 2007: Lithostratigraphie der norddeutschen Oberkreide. Schriftenreihe der Deutschen Gesellschaft für Geowissenschaften 55, 1–136. https://doi.org/10.1127/sdgg/83/2014/73

Noe-Nygaard, A. 1975: Erratics of the Danish Maastrichtian and Danian Marine Limestones. Bulletin of the Geological Society of Denmark 24, 75–81.

Pieters, F.F.J.M. 2009: Natural history spoils in the Low Countries in 1794/95: the looting of the fossil *Mosasaurus* from Maastricht and the removal of the cabinet and menagerie of stadholder William V. Berliner Schriften zur Museumsforschung 27, 55–72.

Polcyn, M.J., Jacobs, L.L., Araújo, R., Schulp, A.S. & Mateus, O. 2014: Physical drivers of mosasaur evolution. Palaeogeography, Palaeoclimatology, Palaeoecology 400, 17–27. https://doi.org/10.1016/j.palaeo.2013.05.018

Post, D.M., Layman, C.A., Arrington, D.A., Takimoto, G., Quattrochi, J. & Montaña, C.G. 2007: Getting to the fat of the matter: models, methods and assumptions for dealing with lipids in stable isotope analyses. Oecologia 152, 179–189. https://doi.org/10.1007/s00442-006-0630-x

Rau, G.H., Sweeney, R.E. & Kaplan, I.R. 1982: Plankton ^{13}C:^{12}C ratio changes with latitude: differences between northern and southern oceans. Deep-Sea Research 29, 1035–1039. https://doi.org/10.1016/0198-0149(82)90026-7

Robbins, J.A., Ferguson, K.M., Polcyn, M.J. & Jacobs, L.L. 2008: Application of stable carbon isotope analysis to mosasaur ecology. In: Everhart, M. (ed.): Proceedings of the second Mosasaur meeting, Fort Hays Studies, Special Issue 3, 123–130.

Russell, D.A. 1967: Systematics and morphology of American Mosasaurs. Peabody Museum of Natural History, Yale University, Bulletin 23, 1–241.

Schulp, A.S. 2005: Feeding the mechanical Mosasaur: what did *Carinodens* eat? Netherlands Journal of Geosciences 84, 345–357. https://doi.org/10.1017/s0016774600021132

Schulp, A.S. & Jagt, J.W.M. 2015: New material of *Prognathodon* (Squamata, Mosasauridae) from the type Maastrichtian of the Netherlands. Netherlands Journal of Geosciences 94, 19–21. https://doi.org/10.1017/njg.2014.15

Schulp, A.S., Vonhof, H.B., van der Lubbe, H.J.L., Janssen, R. & van Baal, R.R. 2013: On diving and diet: resource partitioning in type-Maastrichtian mosasaurs. Netherlands Journal of Geosciences 92, 165–170. https://doi.org/10.1017/s001677460000010x

Surlyk, F., Damholt, T. & Bjerager, M. 2006: Stevns Klint, Denmark: Uppermost Maastrichtian chalk, Cretaceous-Tertiary boundary, and lower Danian bryozoan mound complex. Bulletin of the Geological Society of Denmark 54, 1–48. https://doi.org/10.37570/bgsd-2006-54-01

Surlyk, F., Rasmussen, S.L., Boussaha, M., Schiøler, P., Schovsbo, N.H., Sheldon, E., Stemmerik, L. & Thibault, N. 2013: Upper Campanian–Maastrichtian holostratigraphy of the eastern Danish Basin. Cretaceous Research 46, 232–256. https://doi.org/10.1016/j.cretres.2013.08.006

Van Adrichem Boogaert, H.A. & Kouwe, W.F.P. 1994: Stratigraphic nomenclature: section H - Upper Cretaceous and Danian (Chalk Group). Mededelingen Rijks Geologische Dienst 50 (sections paginated independently).

Van Baal, R.R., Janssen, R., van der Lubbe, H.J.L., Schulp, A.S., Jagt, J.W.M. & Vonhof, H.B. 2013: Oxygen and carbon stable isotope records of marine vertebrates from the type Maastrichtian, The Netherlands and northeast Belgium (Late Cretaceous). Palaeogeography, Palaeoclimatology, Palaeoecology 392, 71–78. https://doi.org/10.1016/j.palaeo.2013.08.020

Van Hinsbergen, D.J.J., de Groot, L.V., van Schaik, S.J., Spakman, W., Bijl, P.K., Sluijs, A., Langereis, C.G. & Brinkhuis, H. 2015: A paleolatitude calculator for paleoclimate studies (model version 2.1). PLoS ONE 10(6), e0126946. https://doi.org/10.1371/journal.pone.0126946

Vennemann, T.W., Hegner, E., Cliff, G., & Benz, G.W. 2001: Isotopic composition of recent shark teeth as a proxy for environmental conditions. Geochimica et Cosmochimica Acta 65(10), 1583–1599. https://doi.org/10.1016/s0016-7037(00)00629-3

Verberk, W.C.E.P., Calosi, P., Brischoux, F., Spicer, J., Garland, T.J., & Bilton, D. 2020: Universal metabolic constraints shape the evolutionary ecology of diving in animals. Proceedings Royal Society B 287, 20200488. https://doi.org/10.1098/rspb.2020.0488

Woodward, A.S. 1891: Note on a tooth of an extinct alligator (*Bottosaurus belgicus*, sp. nov.) from the Lower Danian of Ciply, Belgium. Geological Magazine, new series 8(321), 114–115. https://doi.org/10.1017/s0016756800186236

Yamashita, M., Konishi, T. & Sato, T. 2015: Sclerotic rings in mosasaurs (Squamata: Mosasauridae): structures and taxonomic diversity. PLoS ONE 10(2), e0117079. https://doi.org/10.1371/journal.pone.0117079

A possible phytosaurian (Archosauria, Pseudosuchia) coprolite from the Late Triassic Fleming Fjord Group of Jameson Land, central East Greenland

JESPER MILÀN, OCTÁVIO MATEUS, MALTE MAU, ARKA RUDRA, HAMED SANEI & LARS B. CLEMMENSEN

DGF

A large, well-preserved vertebrate coprolite was found in a lacustrine sediment in the Malmros Klint Formation of the Late Triassic Fleming Fjord Group in the Jameson Land Basin, central East Greenland. The size and internal and external morphology of the coprolite is consistent with that of crocodilian coprolites and one end of the coprolite exhibits evidence of post-egestion trampling. As the associated vertebrate fauna of the Fleming Fjord Group contains abundant remains of pseudosuchian phytosaurs, the coprolite is interpreted as being from a large phytosaur.

Jesper Milàn [jesperm@oesm.dk], Geomuseum Faxe, Østsjællands Museum, Rådhusvej 2, DK-4640 Faxe, Denmark. Octávio Mateus [omateus@fct.unl.pt], GEOBIOTEC, Departamento de Ciências da Terra, FCT-UNL Faculdade de Ciências e Tecnologia, Universidade Nova de Lisboa, Portugal & Museu da Lourinhã, Portugal. Malte Mau [malm@ign.ku.dk], Department of Geosciences and Natural Resource Management, University of Copenhagen, Øster Voldgade 10, DK-1350 Copenhagen K, Denmark. Arka Rudra [arudra@geo.au.dk], Lithospheric Organic Carbon (L.O.C) group, Department of Geosciences, Aarhus University, Aarhus, Denmark. Hamed Sanei [sanei@geo.au.dk], Lithospheric Organic Carbon (L.O.C) group, Department of Geosciences, Aarhus University, Aarhus, Denmark. Lars B. Clemmensen [larsc@ign.ku.dk], Department of Geosciences and Natural Resource Management, University of Copenhagen, Øster Voldgade 10, DK-1350 Copenhagen K, Denmark.

Coprolites are important palaeoecological indicators and are frequently included in fauna analyses, as they can provide important, additional information about extinct animals and their diet, in the form of preserved inclusions of undigested prey remains (e.g. Thulborn 1991; Hunt *et al.* 1994; Northwood 2005; Prasad *et al.* 2005; Chin 2007; Souto 2008; Eriksson *et al.* 2011; Milàn 2012; Milàn *et al.* 2012; Hansen *et al.* 2016). Coprolites are regarded as ichnofossils and were first recognized as fossil faeces by Rev. William Buckland (1835) who coined the term coprolite. Today vertebrate coprolites are known from the Silurian to the present (Hunt & Lucas 2012; Hunt *et al.* 2012).

During the 2018 expedition to the Lepidopteriselv area at Carlsberg Fjord in Jameson Land (central East Greenland; Fig. 1), a very large coprolite was found in a loose sediment slab belonging to the middle part of the Malmros Klint Formation of the Fleming Fjord Group (Clemmensen *et al.* 2020). The aim of this paper is to describe the newfound coprolite and to discuss its possible affiliation within the known Late Triassic vertebrate fauna of the Jameson Land Basin.

Geological Setting

Late Triassic sediments occur in the Jameson Land Basin, which is located in central East Greenland at about 71 °N at the present-day land areas of Jameson Land and Scoresby Land (Fig. 1; Clemmensen *et al.* 2016, 2020). Particularly well-exposed mountain slopes
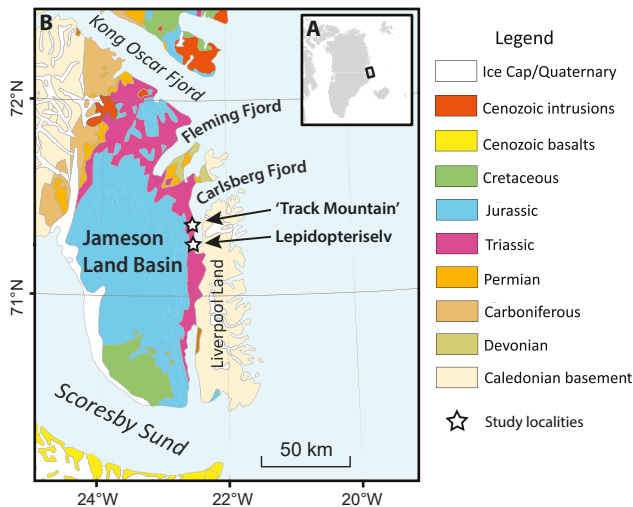
Fig. 1. A: Map of Greenland with Jameson Land indicated by a rectangle. **B:** Geological map of central East Greenland showing Triassic exposures in the Jameson Land Basin. The locations of Lepidopteriselv and 'Track Mountain' are indicated by stars. Modified from Guarnieri *et al.* (2017) and Clemmensen *et al.* (2020).

with Late Triassic sediments are present along the western shores of Carlsberg Fjord. These sediments belong to the uppermost Pingo Dal, Gipsdalen and Fleming Fjord Groups (Clemmensen *et al.* 2020) with the latter unit forming spectacular cliff sides at many localities. The Fleming Fjord Group consists of three units: Edderfugledal, Malmros Klint and Ørsted Dal Formations (Clemmensen *et al.* 2020). In the study area, the Edderfugledal Formation is about 50 m thick and characterized by cyclically bedded greenish grey mudstone and yellowish grey dolostone including stromatolitic limestone overlain by cyclically bedded grey quartz sandstone, red sandstone and siltstone, green mudstone and rare stromatolitic limestone. The Malmros Klint Formation is 135 m thick and composed of cyclically bedded brownish red to greyish red mudstone and fine-grained sandstone. The Ørsted Dal Formation is 125 m thick and composed of a cyclically bedded succession of red structureless mudstone associated with thin greenish grey siltstone and fine-grained sandstone of the Carlsberg Fjord Member overlain by poorly exposed light grey carbonate/marlstone and dark grey mudstone of the Tait Bjerg Member (Fig. 2).

The Fleming Fjord Group has until recently been considered to be of late Carnian, Norian and early Rhaetian age (Clemmensen 1980; Jenkins *et al.* 1994; Clemmensen *et al.* 2020). New magnetostratigraphic work, however, indicates that the group is of Norian age and spans a time interval between 220 and 209 Ma (Kent & Clemmensen 2021). The vertebrate fauna of the Fleming Fjord Group comprises a diverse as-

semblage, some of which was recently described, containing chondrichthyans and actinopterygian fishes, dipnoi such as *Ceratodus tenuensis* (Agnolin *et al.* 2018), theropod and sauropodomorph dinosaurs, temnospondyls such as *Cyclotosaurus naraserluki*, turtles, aetosaurs, phytosaurs and pterosaurs (Jenkins
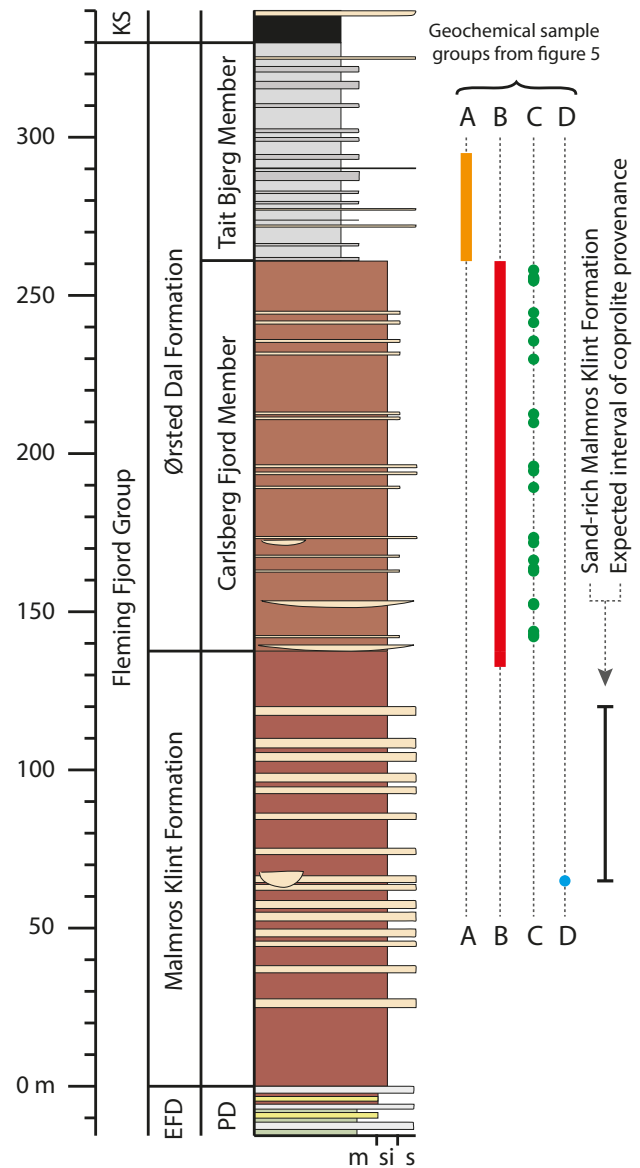

Fig. 2. Simplified lithological log of the Malmros Klint Formation and the Ørsted Dal Formation along Carlsberg Fjord. Geochemical sample groups are used to identify the original stratigraphic position of the coprolite-bearing rock slab. The stratigraphic levels of the geochemical samples are illustrated with the following letters: **A:** Samples from the lower part of the Tait Bjerg Member. **B:** Samples from the Carlsberg Fjord Member and upper part of the Malmros Klint Formation. **C:** Sandstone/siltstone samples from the Carlsberg Fjord Member. **D:** Samples from the phytosaur bone bed.

et al. 1994; Sulej *et al.* 2014; Clemmensen *et al.* 2016; Hansen *et al.* 2016; Marzola *et al.* 2017a, 2018; Agnolin *et al.* 2018). Furthermore, the fauna includes both teeth and skeletal elements of the mammaliforms *Haramiyavia clemmenseni, Brachyzostrodon,* and *Kuehneotherium* (Jenkins *et al.* 1994; Jenkins *et al.* 1997). Trace fossil evidence show the presence of abundant small theropod dinosaurs, sauropodomorphs, sauropods, and other achosaurs (Sulej *et al.* 2014; Clemmensen *et al.* 2016; Klein *et al.* 2016; Lallensack *et al.* 2017). The Malmros Klint Formation is less rich in vertebrate material compared to the overlying Carlsberg Fjord Member, but a quarry, nicknamed Mateus quarry, lying 65 m above the base of the Malmros Klint Formation at the Lepidopteriselv site contains a rich skeleton material of phytosaurs ascribed to *Mystriosuchus* as well as rarer bones tentatively ascribed to theropod dinosaurs (Clemmensen *et al.* 2016; Marzola *et al.* 2017b; 2018).

In the Late Triassic (late Norian-early Rhaetian), the Jameson Land Basin was located at 43°N on the northern part of the supercontinent Pangaea (Kent & Clemmensen 2021). This position placed the basin with lake and fluvial sediments in a transition zone between the relatively dry interior of the supercontinent Pangaea and the more humid peripheral part of this continent (Clemmensen *et al.* 1998; Sellwood & Valdes 2006), or well inside the humid temperate belt (Kent *et al.* 2014).

Material and methods

A well-preserved coprolite preserved in a slab of greyish sandstone (Fig. 3) was found in 2018 on a mountain slope close to Lepidopteriselv at Carlsberg Fjord (Fig. 1). The loose slab was found in a small meltwater stream, situated in a stratigraphic level that equals the middle part of the Malmros Klint Formation and is found about 100 m south of the quarry with phytosaur remains. The slab had very likely been transported downwards by modern stream action or by solifluction.

The internal morphology of the coprolite and surrounding sediment was investigated, and two samples of the sediment were examined by X-ray fluorescence (XRF) to characterize its geochemical composition. The obtained result was compared with a large geochemical database from the uppermost Malmros Klint Formation and overlying Carlsberg Fjord Member and the main part of the Tait Bjerg Member at the Lepidopteriselv site and a nearby site to the north.

To study the organic matter preservation, the top dark part of the coprolite sample was crushed in clean agate-mortar and pestle. Approximately, 50 mg of the coprolite sample and a sample from the base sandstone was studied using Rock-Eval® analysis method, applied on Hawk Pyrolysis and TOC instrument, Wildcat Technologies. The pyrolysis cycle starts with an iso-temperature at 300 °C for 3 minutes followed by a temperature ramp up to 650 °C, at 25 °C per minute. Hydrocarbons released during pyrolysis; S1 and S2 (mg HC/g TOC) are detected by online Flame Ionization Detector. The CO_2 released during pyrolysis of oxygen-bearing organic compounds (S3; mg CO_2/g of sample) is measured by online Infrared (IR) detectors. The oxidation phase starts with an isothermal stage at 300 °C (for 1 minute) to 850 °C at 25 °C/minute, with 5 minutes hold time. The CO and CO_2 released during combustion of residual organic carbon (S4; mg CO–CO_2/g of sample) is measured by online (IR) detector (Lafargue *et al.* 1998; Strunk *et al.* 2020). The pyrolysis parameters were calibrated with standards having <0.1 % standard deviation from the actual value (Table 1).

A sample of the sediment was prepared for dinocyst analysis, but the sediment contained no recognizable microfossils. Rock samples used for statistical analyses, were rinsed with demineralized water, dried at 50 °C and crushed with a vibratory ball mill before any analysis. XRF analyses were performed with a fixed Olympus Delta Premium DP-6000 XRF analyzer. Each sample was analyzed for 2 × 120 seconds with a 10 kV beam and a 30 kV beam. The samples were covered with a thin Mylar film to improve the detection limit of the lightest elements. The accuracy was regularly tested by re-analyzing samples and by analyzing PACS-3 and SiO_2 standards. Three Pb measurements showed values below the detection limit (LOD). These missing values were replaced with the LOD value. Ele-

Table 1. Rock-eval analyses of the coprolite and sediment.

Sample	S1 mgHC/g	S2 mgHC/g	S3 mgCO$_2$/g	Pyrolysable labile organic carbon wt%	Residual organic carbon wt%	TOC* wt%
Sediment	0.02	0.04	0.74	15 %	81 %	0.26
Coprolite	0.6	0.38	0.98	39 %	61 %	0.33

* Total organic carbon

ments (variables) with a high number of LOD values were discarded from the multivariate analyses. The XRF data points were log-transformed with the natural logarithm before statistical analyses to normalize the data. This is done because Hotelling's T-squared test assumes normality. Furthermore, normality ensures more robust results when using compositional data such as geochemical data and likewise ensures more robust results from the principal component analysis (Gazley *et al.* 2015). Normality was validated with normal quantile plots and lagged residual plots. Principal component analyses (PCAs) were performed with the pca function in Matlab. Hotelling's two-sample T-squared tests were performed with the R

package Hotelling (Curran 2018). The test assumes that samples are independently drawn from two independent multivariate normal distributions with the same covariance and tests the hypothesis of equal means. Using this statistical test, samples from the coprolite-bearing rock slab were tested against four data groups defined by stratigraphical and lithological characteristics. The Hotelling R package includes a permutation test used to estimate the non-parametric P-value for the hypothesis test. The permutation test determines the statistical significance by computing a test statistic on the dataset for many random permutations. This provides a more robust test by building a permutation distribution. Therefore, the assumption of normal

Fig. 3. Photos of coprolite NHMD 875622. **A:** Complete specimen partly prepared out of matrix. Constricted zone indicated by arrows. **B:** Oblique view highlighting the trampled part of the coprolite, indicated by arrows. **C:** Cross section of the trampled part of the coprolite revealing the layered internal structure, as well as prominent deformation of the sediments below the trampled part of the coprolite, indicated by arrows.

distribution is not strictly needed. The permutation p-values were based on 10,000 permutations. The coprolite is now part of the collection of the Natural History Museum of Denmark (NHMD 875622).

Description

The specimen is 2/3 prepared out of the original matrix from the slab it was found in (Fig. 3). The specimen is 125 mm long and is flattened with a largest diameter of 49 mm and a flattened diameter of 24 mm. A prominent constricted zone is present in the widest part pf the specimen locally reducing the widest diameter to 39 mm (Fig. 3A). One end is partly broken, suggesting a larger original total length. The specimen tapers towards the other end, before turning sharply to the side and revealing a rounded flattened zone in the bent part (Fig. 3B). Internally, the specimens consist of three concentric layers 1-2 mm thick, wrapped around a more structureless core. Each layer appears structureless in composition (Fig. 3C). The specimen contains no prey remains either in the form of bones, scales or plant fragments. The surface is smooth, with occasional small pits, grooves and irregularities.

The coprolite-bearing rock slab measures 5.5 cm in thickness and consists of a dark-grey fine sandstone with a light-grey colour in the topmost few centimetres. The internal structures are strongly deformed but show horizontal lamination and some horizons with poorly developed wave ripple lamination. The light-coloured top shows a very fine millimetre-scale horizontal lamination. There are no indications of trace fossils on the sole of the slab. The lack of trace fossils is typical for sandstones found in the Malmros Klint Formation. On the contrary, sandstones and siltstones from the Ørsted Dal Formation have sharp junctions with the mudstone below and therefore usually show interface preservation of trace fossils on the soles (Bromley *et al.* 1979). Sandstone beds are rare in the Ørsted Dal Formation but are more common in the Malmros Klint Formation. Coarse-grained beds in the Ørsted Dal Formation generally consist of siltstone and are less than 5 cm thick (Clemmensen *et al.* 1998).

To identify the source of the coprolite-bearing slab, the geochemical signature of the slab is compared to the geochemical distribution of a large quantity of samples from the stratigraphic units above the level where the coprolite was found. Unfortunately, no samples from the Kap Stewart Group or the main part of the Malmros Klint Formation were available for this analysis. The geochemical signature is based on XRF measurements of 16 chemical elements in the top and the bottom of the slab. These two samples are compared to 116 samples from the Tait Bjerg Member (group A), 557 samples from the Carlsberg Fjord Member and the uppermost Malmros Klint Formation (group B), 27 samples from sandstone and siltstone from the Carlsbarg Fjord Member (group C), and 4 samples from a phytosaur bone bed in the middle of the Malmros Klint Formation (group D; Fig. 2). For the initial assessment, we use principal component analysis (PCA) to reduce the 16 variables into a few principal components, which convey the most variation in the dataset. This provides a measure of how each sample is related to the chemical elements and which samples are alike. When performing PCAs for each data group, biplots of the two most important principal components show that samples from the coprolite-bearing slab plot well away from the rest of the samples (Fig. 4). This indicates that the geochemical composition of the slab is different from all four groups. Group A shows three outliers plotting in the lower left corner of the PCA biplot. These geochemical signatures represent green siltstone beds with low Pb concentrations (< LOD) which are most likely a result of diagenetic flushing of Pb and other elements like Fe giving them a greenish colour. To further test if the coprolite-bearing slab could origin from one of the sample groups, we use a multivariate statistic two-sample Hotelling's T-squared test combined with permutation testing. This tests the null-hypothesis that the slab mean and sample group mean are equal for all response variables (geochemical elements). The result of the statistic tests are significant permutation p-values (p = 0) for sample group A, B and C meaning that the geochemical signature of the slab is significantly different from the units above the sand-rich Malmros Klint Formation. The few samples from the phytosaur bone bed (group D) does not allow for a test on the 16 geochemical variables. Instead, Hotelling's T-squared test with 10,000 permutations is performed on principal component one and two accounting for 96.7 % of the variance in the group. This gives a non-statistically significant p-value of 0.0666. However, this high p-value is likely a result of the small sample size. Using the asymptotic distribution of the T-squared test gives a p-value of 0.0007419. Thus, like group A, B, and C the geochemical signature of the slab is significantly different from rock samples from the phytosaur bone bed.

In conclusion, assuming the coprolite-bearing rock slab has travelled down slope since deposition the lithological and chemical characteristics of the slab place the original level of deposition between the stratigraphic level of the phytosaur bone bed, and the uppermost muddy interval in the Malmros Klint Formation. This corresponds to the interval between 65 m and 120 m above the base of the Malmros Klint Formation (Fig. 2).
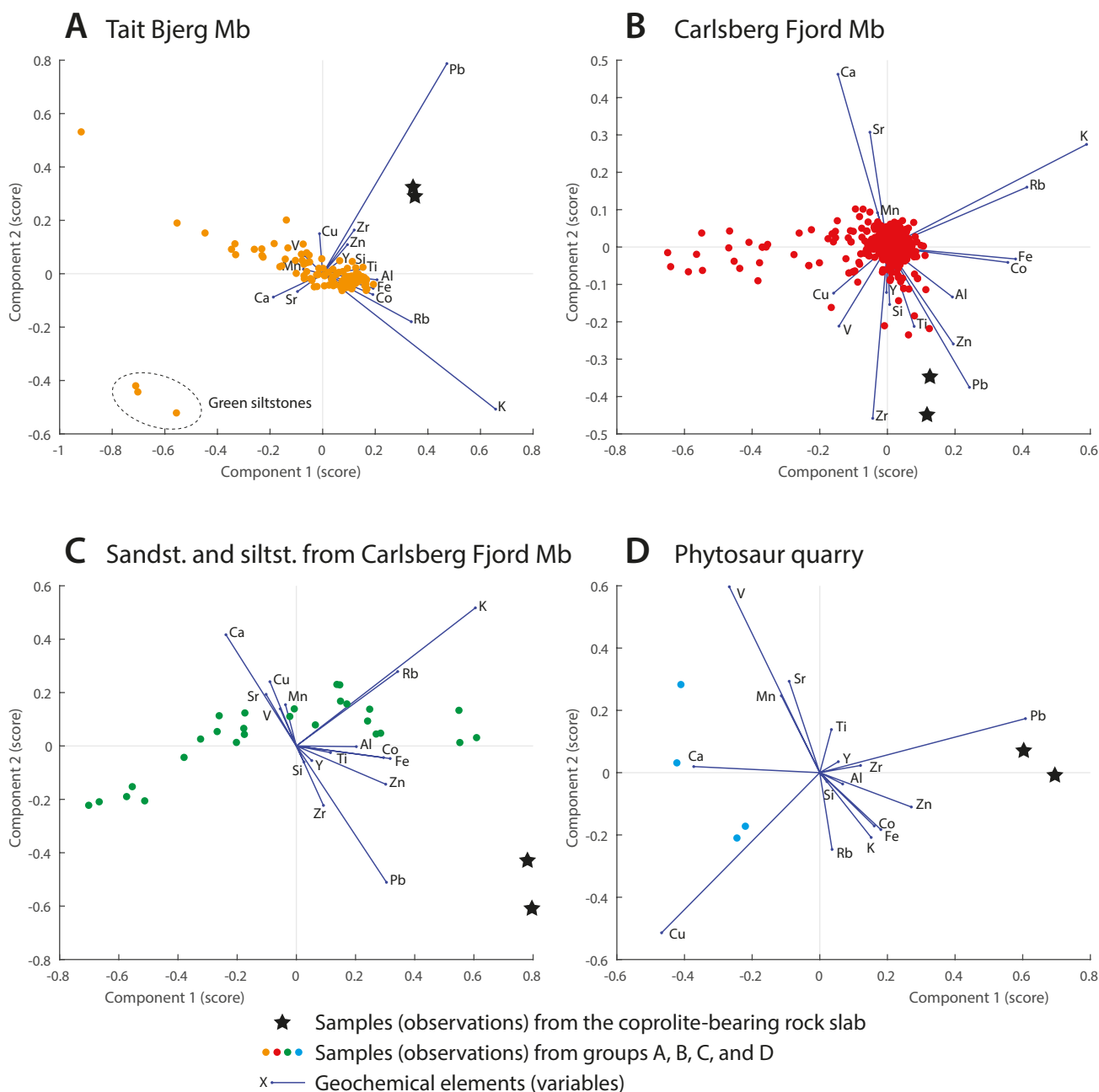
Fig. 4. PCA biplots for the four sample groups based on principal component one and two. The plots provide a measure of how each sample is related to the chemical elements and which samples are alike. Samples from the coprolite-bearing slab plot well away from the rest of the samples indicating that the slab is chemical different from all four sample groups. Thus, the slab is likely originating from this sandstone-rich part of the Malmros Klint Formation (i.e. between 65 m and 120 m above the base of the Malmros Klint Formation (Fig. 2)). The first two principal components explain 73.8 %, 88.3 %, 77.8 %, and 96.7 % of the variance in group A, B, C, and D respectively. **A:** Bulk sample group from the lower part of the Tait Bjerg Member (Ørsted Dal Formation). Outliers are encircled with dashed lines. **B:** Bulk sample group from the Carlsberg Fjord Member (Ørsted Dal Formation). **C:** Samples from sandstone and siltstone from Carlsberg Fjord Member. **D:** Samples from a phytosaur quarry in the middle of the Malmros Klint Formation.

Discussion

Identifying the faeces-maker

To precisely identify the producer of a coprolite, is at best a challenging task, with many uncertainties. This is because faeces form several unrelated groups of animals, can share the same morphology, due to similarities in diet of the producer and mode of egestion. This gets further complicated as faeces from the same individual can show a wide range of morphological variation as well (e.g. McAllister 1985; Lewin 1999; Chin 2002; Chame 2003; Milàn 2012).

The dimensions of the coprolite, with a maximum flattened diameter of 49 mm and a length of at least 125 mm suggest the producer to be among the larger archosaurs from the formation. While mammals have been reported from the formation (Jenkins *et al.* 1994, 1997; Sulej *et al.* 2020), they can quickly be excluded as possible producers as all Triassic mammals have a body-size significantly smaller than the length and width of the herein described specimen. Assuming that the coprolite stratigraphically belongs to the middle to upper part of the Malmros Klint Formation likely producers include the herbivorous dinosaur *Plateosaurus* and theropod dinosaurs (Clemmensen *et al.* 2016) and the phytosaurs (Jenkins *et al.* 1994; Clemmensen *et al.* 2016; Niedzwiedzki & Sulej 2020).

Coprolites from herbivores are generally scarcer in the fossil records than coprolites from carnivores, because the phosphate contents of the latter, originating from the soft tissue and bones from prey animals predispose them to mineralization (Thulborn 1991; Gill & Bull 2012). The herein studied specimen is well-preserved and well-mineralized and is interpreted as a carnivore coprolite. The theropods reported form the Fleming Fjord Formation, both inferred from tracks and skeletal material are all small sized animals (Jenkins *et al.* 1994; Clemmensen *et al.* 2016; Niedzwiedzki & Sulej 2020).

Despite the abundance of coprolites in Triassic sediments (e. g. Hunt *et al.* 2007), no coprolites have so far been convincingly been attributed to phytosaurs, despite phytosaurs being abundant elements in Late Triassic ecosystems. Umamaherawan *et al.* (2019), suggested that large coprolites from the Upper Triassic Maleri Formation, India, could be made by small to medium sized semi aquatic predators, and suggest phytosaurs as one of the possible makers. The Late Triassic coprolite ichnogenus *Alococoprus* (Hunt *et al.* 2007) comprises elongated, sub-rounded coprolites, with longitudinal striations, and has been assigned to basal arcosauromorphs.

Crocodylian coprolites are generally sausage shaped and circular in cross section with few structures visible on their outer surface except occasional longitudinal striations, or traces from coprophageous organisms (Souto 2010; Milàn 2012). A study of the morphological variation within fresh faeces from 10 species of extant crocodilians demonstrated that a commonly occurring feature of crocodilian faeces is circumferal constriction marks and a bend between 120–150°, and their internal structure is composed of concentric layers of various thickness around a central core of more homogenous mass (Milàn & Hedegaard 2010; Milàn 2012). Crocodilian faeces are devoid of any bone or shell remains as the digestive system of crocodilians effectively dissolves any bone or shell remains of their prey (Fischer 1981), leaving only hair and feathers behind (Milàn 2012). The external and internal morphology of the herein described specimen, being elongated, with a subrounded cross-section, composed of several concentric layers around a homogenous core, and devoid of prey remains, and with a prominent constrained zone around its circumference, is in accordance with the morphology of crocodilian coprolites (Milàn & Hedegaard 2010; Milàn 2012). The phylogenetic hypotheses of the position of Phytosauria and its relationships with other archosaurs such as crocodylomorphs has changed over the years. In the most updated exhaustive analysis (Ezcurra 2016) phytosaurs are pseudosuchians, sister taxa of Suchia, which include crocodylomorphs (Fig. 5). Moreover, phytosaurs and crocodylomorphs share a number of anatomical convergences, general morphology, similar lifestyle, diet, and comparable sizes. Phylogenetically, similar faeces are also to be expected.

The total body length of a crocodile can be estimated from the diameter of the faeces (Milàn 2012). In this case, a diameter of 49 mm corresponds to a crocodylomorph with a body length of around 300 cm (Milàn 2012). Assuming that this ratio is true for Triassic crocodylomorphs, and pseudosuchians with their very similar body proportions, this estimated length falls within the sizes of phytosaurs skeletons found in the nearby quarry (Clemmensen *et al.* 2016).
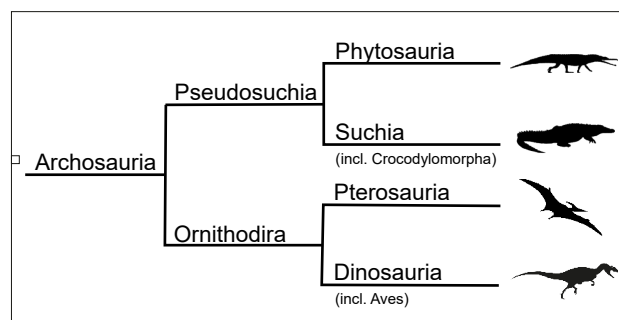

Fig. 5. Schematic representation of the main archosaurian groups. Phytosaurs appear as a sister group to Suchia, which include the modern crocodiles. Based on Ezcurra (2016).

Organic content

The coprolite sample has S1 0.6 mgHC/g rock, S2 0.38 mgHC/g rock and 0.33% total organic carbon (TOC), with 39 % reactive and 61 % residual organic carbon. This suggests that the sample has lighter degradable hydrocarbons (S1) as well as preserved macromolecular organic carbon (S2). In contrast, the host sandstone has negligible S1 and S2 fractions of hydrocarbons, 0.26% TOC with 81% residual OC (Table 1). The S1 fraction represents the labile proto-hydrocarbon fractions, probably derived from the original egested by-product, combined by the microbial decay of the macromolecules in the coprolites in the depositional site. Higher S2 in the coprolite than the sandstone indicates the preservation of the stable organic carbon in the coprolite. These hydrocarbon compounds might represent the remnants of the egested food material by the phytosaur combined by post-egestion changes in the coprolite depositional sites. The chemical composition further excludes the possibility that the specimen should be an inorganic concretion.

Trampling

The distorted area in one end of the coprolite, is rounded in the bottom, and in the exposed broken edge of the flattened area, it is evident that the coprolite has been deformed to a bowl-shaped cross section (Fig. 3B, C), contrary to the oval cross section in the undeformed rest of the coprolite. Further, the flattened area is depressed down into the surrounding sediment, relative to the rest of the coprolite, suggesting the deformation is the result of a significant force exercised on this part of the coprolite. Similar deformations are observed in Miocene mammalian coprolites from Portugal, where even identifiable footprints are found preserved depressed into coprolites. These footprints are interpreted as being formed by post egestion trampling of the coprolite before it dried up (Antunes *et al.* 2005). Based on the similarity to the depressions in the Portuguese coprolites, and the observation that the deformed parts of the coprolite is pushed down into the sediment in a very similar way to what is observed when examining subsurface deformation below theropod tracks in cross section, from the same formation (Milàn *et al.* 2004, 2006), we interpret the deformed part of NHMD 875622 to be the result of trampling by either the maker of the coprolite or another vertebrate animal inhabiting the area.

Conclusion

A large well-preserved coprolite from the middle to upper part of the Malmros Klint Formation (65-120 m above the base of the formation at the study site), Fleming Fjord Group of Jameson Land, central East Greenland is interpreted as being from a phytosaur, based on its size, internal and external morphology and stratigraphical context. This is the first record of a convincing phytosaur coprolite from the Late Triassic globally. Geochemical examinations of the coprolite reveal preservation of organic carbon, which might represent degraded food residues egested by the organism/phytosaur. Furthermore, the coprolite shows evidence of trampling by either the producer of the coprolite or another individual from the associated Late Triassic fauna of East Greenland.

References

Agnolin, F.L., Mateus, O., Milàn, J., Marzola, M., Wings, O., Adolfssen, J.S. & Clemmensen, L.B. 2018: *Ceratodus tunuensis*, sp. nov., a new lungfish (Sarcopterygii, Dipnoi) from the Upper Triassic of central East Greenland. Journal of Vertebrate Paleontology 38, e1439834. https://doi.org/10.1080/02724634.2018.1439834

Antunes, M.G., Ausenda C. Balbino, A.C. & Ginsburg, L. 2005: Miocene mammalian footprints in coprolites from Lisbon, Portugal. Annales de Paléontologie 92, 13–30. https://doi.org/10.1016/j.annpal.2005.09.002

Bromley, R. & Asgaard, U. 1979: Triassic freshwater ichnocoenoses from Carlsberg Fjord, east Greenland. Palaeogeography, Palaeoclimatology, Palaeoecology 28, 39–80. https://doi.

org/10.1016/0031-0182(79)90112-3

Buckland, W. 1835: On the discovery of coprolites, or fossil faeces, in the Lias at Lyme Regis, and in other formations. Transactions of the Geological Society of London 3, 223–238. https://doi.org/10.1144/transgslb.3.1.223

Chame, M. 2003: Terrestrial mammal feces: a morphometric summary and description. Memoirs Instituto Oswaldo Cruz, Rio de Janeiro 98 (Supplement I), 71–94. https://doi.org/10.1590/s0074-02762003000900014

Chin, K. 2002: Analyses of coprolites produced by carnivorous vertebrates. Paleontological Society Papers 8, 43–50. https://doi.org/10.1017/s1089332600001042

Chin, K. 2007: The paleobiological implications of herbivorous dinosaur coprolites from the Upper Cretaceous Two Medicine Formation of Montana: Why eat wood? Palaios 22, 554–566. https://doi.org/10.2110/palo.2006.p06-087r

Clemmensen, L.B. 1980: Triassic lithostratigraphy of East Greenland between Scoresby Sund and Kejser Franz Josephs Fjord. Grønlands Geologiske Undersøgelse Bulletin 139, 56 pp. https://doi.org/10.34194/bullggu.v139.6681

Clemmensen, L.B., Kent, D.V. & Jenkins, F.A., Jr. 1998: A Late Triassic lake system in East Greenland: facies, depositional cycles and palaeoclimate. Palaeogeography, Palaeoclimatology, Palaeoecology 140, 135–159. https://doi.org/10.1016/s0031-0182(98)00043-1

Clemmensen, L.B., Milàn, J., Adolfssen, J.S., Estrup, E.J., Frobøse, N., Klein, N., Mateus, O. & Wings, O. 2016: The vertebrate-bearing Late Triassic Fleming Fjord Formation of central East Greenland revisited: stratigraphy, palaeoclimate and new palaeontological data. Geological Society of London Special Publications 434, 31–47. https://doi.org/10.1144/sp434.3

Clemmensen, L.B., Kent, D.V., Mau, M., Mateus, O. & Milàn, J. 2020: Triassic lithostratigraphy of the Jameson Land basin (central East Greenland), with emphasis on the new Fleming Fjord Group. Bulletin of the Geological Society of Denmark 68, 95–132. https://doi.org/10.37570/bgsd-2020-68-05

Curran, J. 2018: Hotelling's T^2 test and variants. R package Hotelling version 1.0-5.

Eriksson, M.E., Lindgren, J., Chin, K. & Månsby, U. 2011: Coprolite morphotypes from the Upper Cretaceous of Sweden: novel views on an ancient ecosystem and its implications for coprolite taphonomy. Lethaia 44, 455–468. https://doi.org/10.1111/j.1502-3931.2010.00257.x

Ezcurra, M. D. 2016: The phylogenetic relationships of basal archosauromorphs, with an emphasis on the systematics of proterosuchian archosauriforms. PeerJ 4, e1778. https://doi.org/10.7717/peerj.1778

Fischer, D.F. 1981: Crocodilian scatology, microvertebrate concentrations, and enamel-less teeth. Paleobiology 7, 262–275. https://doi.org/10.1017/s0094837300004048

Gazley, M.F., Collins, K.S., Roberston, J., Hines, B.R., Fisher, L.A. & McFarlane, A. 2015: Application of principal component analysis and cluster analysis to mineral exploration and mine geology. AusIMM New Zealand Branch Annual Conference, 131–139. Dunedin, New Zealand.

Gill, F.L. & Bull, I.D. 2012: Lipid analysis of vertebrate coprolites. New Mexico Museum of Natural History and Science Bulletin 57, 93–98.

Guarnieri, P., Brethens, A. & Rasmussen, T.M. 2017: Geometry and kinematics of the Triassic rift basin in Jameson Land (East Greenland). Tectonics 36, 602–614. https://doi.org/10.1002/2016tc004419

Hansen, B.B., Milàn, J., Clemmensen, L.B., Adolfssen, J.S., Estrup, E.J., Klein, N., Mateus, O. & Wings, O. 2016: Coprolites from the Late Triassic Kap Steward Formation, Jameson Land, East Greenland: Morphology, classification and prey inclusions. Geological Society of London Special Publications 434, 49–69. https://doi.org/10.1144/sp434.12

Hunt, A.P. & Lucas, S.G. 2012: Classification of vertebrate coprolites and related trace fossils. New Mexico Museum of Natural History and Science, Bulletin 57, 137–146.

Hunt, A.P., Chin, K. & Lockley, M.G. 1994: The paleobiology of vertebrate coprolites. In: Donovan, S., (ed.): The palaeobiology of trace fossils, 221–240. London: John Wiley and Sons.

Hunt, A.P., Lucas, S.G., Milàn, J. & Spielmann, J.A. 2012: Vertebrate coprolites: status and prospectus: New Mexico Museum of Natural History and Science, Bulletin 57, 5–24.

Hunt, A.P., Lucas, S.G., Spielmann, J.A. & Lerner, A.J. 2007: A review of vertebrate coprolites of the Triassic with descriptions of new Mesozoic ichnotaxa. New Mexico museum of Natural History and Science Bulletin 41, 88–107.

Jenkins, F.J., Shubin, N.H., Amarel, W.W., Gatesy, S.M., Schaff, C.R., Clemmensen, L.B., Downs, W.R., Davidson, A.R., Bonde, N.C. & Osbaeck, F. 1994: Late Triassic continental vertebrates and depositional environments of the Fleming Fjord Formation, Jameson Land, East Greenland. Meddelelser Om Grønland, Geoscience 32, 25 pp.

Jenkins, F.A., Jr., Gatesy, S.M., Shubin, N.H. & Amaral, W.W. 1997: Haramiyids and Triassic mammalian evolution. Nature 385, 715–718. https://doi.org/10.1038/385715a0

Kent, D.V. & Clemmensen, L.B. 2021. Northward dispersal of dinosaurs from Gondwana to Greenland at the mid-Norian (215-212 Ma, Late Triassic) dip in atmospheric pCO2. PNAS 118. https://doi.org/10.1073/pnas.2020778118.

Kent, D.V., Malnis, P.S., Colombi, C.E., Alcober, O.A. & Martínez, R.N. 2014: Age constraints on the dispersal of dinosaurs in the Late Triassic from magnetochronology of the Los Colorados Formation (Argentina). PNAS 111, 7958-7963. https://doi.org/10.1073/pnas.1402369111

Klein, H., Milàn, J., Clemmensen, L.B., Frobøse, N., Mateus, O., Klein, N., Adolfssen, J.S., Estrup, E. & Wings, O. 2016: Archosaur footprints (cf. *Brachychirotherium*) with unusual morphology from the Upper Triassic Fleming Fjord Formation (Norian–Rhaetian) of East Greenland. Geological Society of London Special Publications 434, 71–85. https://doi.org/10.1144/sp434.1

Lafargue, E.,Marquis, F. & Pillot, D. 1998: Rock–Eval 6 applications in hydrocarbon exploration, production, and soil contamination studies. Oil Gas Science Technology Review

53, 421–437. https://doi.org/10.2516/ogst:1998036

Lallensack, J.N., Klein, H., Milan, J., Wings, O., Mateus, O. & Clemmensen, L.B. 2017: Sauropodomorph dinosaur trackways from the Fleming Fjord Formation of East Greenland: Evidence for Late Triassic Sauropods. Acta Palaeontologica Polonica 64, 833–843. https://doi.org/10.4202/app.00374.2017

Lewin, R.A. 1999: Merde, excursions into scientific, cultural and socio-historical coprology, 164 pp. London: Aurum Press.

Marzola, M., Mateus, O., Shubin, N.H. & Clemmensen, L.B. 2017a: *Cyclotosaurus naraserluki*, sp. nov., a new Late Triassic cyclotosaurid (Amphibia, Temnospondyli) from the Fleming Fjord Formation of the Jameson Land Basin (East Greenland). Journal of Vertebrate Paleontology 37, e1303501. https://doi.org/10.1080/02724634.2017.1303501

Marzola, M., Mateus, O., Milàn, J. & Clemmensen, L.B. 2017b: The 2016 Dinosaur Expedition to the Late Triassic of the Jameson Land Basin, East Greenland, 249–253. Abstract book of the XV Encuentro de Jóvenes Investigadores en Paleontología, Pombal.

Marzola, M., Mateus, O., Milàn, J., Clemmensen L.B. 2018: A review of Palaeozoic and Mesozoic tetrapods from Greenland. Bulletin of the Geological Society of Denmark 66, 21–46. 46. https://doi.org/10.37570/bgsd-2018-66-02

McAllister, J.A. 1985: Re-evaluation of the formation of spiral coprolites. University of Kansas, Paleontological Contributions 144, 1–12.

Milàn, J., Clemmensen, L.B., Adolfssen, J.S., Estrup, E.J., Frobøse, N., Klein, N., Mateus, O. & Wings, O. 2012a: A preliminary report on coprolites from the Late Jurassic part of the Kap Steward Formation, Jameson Land, East Greenland. New Mexico Museum of Natural History and Science Bulletin 57, 203-205.

Milàn, J. 2012: Crocodylian scatology – a look into morphology, internal architecture inter- and intraspecific variation and prey remains in extant crocodylian feces. New Mexico Museum of Natural History and Science, Bulletin 57, 65–71.

Milàn, J. & Hedegaard, R. 2010: Interspecific variation in tracks and trackways from extant crocodylians. New Mexico Museum of Natural History and Science, Bulletin 51, 15–29

Milàn, J., Clemmensen, L.B. & Bonde, N. 2004: Vertical sections through dinosaur tracks (Late Triassic lake deposits, East Greenland) – undertracks and other subsurface deformation structures revealed. Lethaia 37, 285–296. https://doi.org/10.1080/00241160410002036

Milàn, J., Avanzini, M., Clemmensen, L.B, Garciá-Ramos, J.C. & Piñuela, L. 2006: Theropod foot movement recorded from Late Triassic, Early Jurassic and Late Jurassic fossil footprints. New Mexico Museum of Natural History and Science Bulletin 37, 352–364.

Milàn, J., Rasmussen, B.W. & Lynnerup, N. 2012: A coprolite in the MDCT-scanner – internal architecture and bone contents revealed. New Mexico Museum of Natural History and Science Bulletin 57, 99–103.

Niedzwiedzka, G. & Sulej, T. 2020: Theropod dinosaur fossils from the Gipsdalen and Flemming fjord formations (Carnian-Norian, Upper Triassic), East Greenland. Abstracts and Proceedings of the Geological Society of Norway, p. 151, 34th Nordic Geological Winter Meeting, 8–10 January 2020, Oslo, Norway. Available at https://geologi.no/images/NGWM20/Abstractvolume_NGWM20.pdf

Northwood, C. 2005: Early Triassic coprolites from Australia and their palaeobiological significance. Palaeontology 48, 49–68. https://doi.org/10.1111/j.1475-4983.2004.00432.x

Prasad, V., Caroline, A.E., Stromberg, C.A.E., Alimohammadian, H. & Sahni, A. 2005: Dinosaur coprolites and the early evolution of grasses and grazers. Science 310, 1177–1180. https://doi.org/10.1126/science.1118806

Sellwood, B.W. & Valdes, P. J. 2006: Mesozoic climates: General circulation models and the rock record. Sedimentary Geology 190, 269–287. https://doi.org/10.1016/j.sedgeo.2006.05.013

Souto, P.R.F. 2008: Coprólitos do Brazil – Principais occorências e studio, 93 pp. Rio de Janeiro: Publit.

Souto, P.R.F. 2010: Crocodylomorph coprolites from the Bauru basin, Upper Cretaceous, Brazil. New Mexico Museum of Natural History and Science, Bulletin 51, 201–208.

Strunk, A., Olsen, J., Sanei, H., Rudra, A. & Larsen, N.K. 2020: Improving the reliability of bulk sediment radiocarbon dating. Quaternary Science Reviews 242, 1–13. 13. https://doi.org/10.1016/j.quascirev.2020.106442

Sulej, T., Wolniewicz, A., Bonde, N., Błazejowski, B., Niedz´wiedzki, G. & Tałanda, M. 2014: New perspectives on the Late Triassic vertebrates of East Greenland: preliminary results of a Polish–Danish palaeontological expedition. Polish Polar Research 35, 541–552. https://doi.org/10.2478/popore-2014-0030

Sulej, T., Krzesinski, G., Talanda, M., Wolniewicza, A.S., Blazejowski, B., Bonde, N., Gutowski, P., Sienkiewicz, M. & Niedwiedzki, G. 2020. The earliest-known mammaliaform fossil from Greenland sheds light on origin of mammals. PNAS 117, 26861–26867. https://doi.org/10.1073/pnas.2012437117

Thulborn, R.A. 1991: Morphology, preservation, and palaeobiological significance of dinosaur coprolites. Palaeogeography, Palaeoclimatology, Palaeoecology 83, 341–366. https://doi.org/10.1016/0031-0182(91)90060-5

Umamaheswaran, R., Prasad, G.V.R., Rudra, A. & Dutta, S. 2019: Biomarker signatures in Triassic coprolites. Palaios 34, 458–467. https://doi.org/10.2110/palo.2019.023

Claus Heinberg (1945–2021) – Trace fossils, Greenland expeditions and bivalves of the K–T boundary strata

FINN SURLYK, ECKART HÅKANSSON & PEDER W. AGGER

DGF

The eminent palaeontologist and Greenland explorer Claus Heinberg was born in 1945 and died in 2021 after prolonged illness. His scientific production was focused on two remarkably different subjects: the bivalve fauna of the Cretaceous–Palaeogene (K–T) boundary beds and the Mesozoic geology and stratigraphy of eastern North Greenland. He was employed at Roskilde University during most of his career until he retired in 2012. He was part of a cross disciplinary collaborative environment, comprising biologists, geographers, geologists, sociologists, civil engineers and architects. He was a highly engaged social debater of a wide spectrum of societal subjects throughout his life. He was a fine person, a good colleague and friend.

Finn Surlyk [finns@ign.ku.dk], Department of Geosciences and Natural Resource Management, University of Copenhagen, Øster Voldgade 10, DK-1350 Copenhagen K, Denmark. Eckart Håkansson [eckart.hakansson@uwa.edu.au], Centre for Energy Geoscience, School of Earth Science, University of Western Australia, 35 Stirling Highway, Crawley WA 6009, Australia. Peder W. Agger [pa@ruc.dk], Amaliegade 32,4, DK-1256 Copenhagen K, Denmark.

Claus Heinberg was born on 21 August 1945 in Ordrup north of Copenhagen, Denmark and died in Copenhagen on 19 February 2021. His father, Hugo Heinberg (1898–1988) was a journalist, an editor and worked for a relief organization under the United Nations. His mother, Johanne Heinberg (1916–2003) was a weaver and a housewife.

Claus attended primary school first at Skovshoved Skole north of Copenhagen (Fig. 1) followed by high school at Ordrup Gymnasium where he graduated (STX) in 1965. He was a partner with Misja Keiding in the years 1971–1985. They had two children, Nana (born 1975) and Mads (born 1977).

After a short period associated with 'Kana', one of the more persistent Danish communal collectives, Claus found an alternative abode, more suitable for his approach to communal living in 'Brumleby', in København (Copenhagen) – a tightly knit community of two-story blocks with numerous, *very* small apartments. Build in the mid-1800s, as a social experiment, it was now housing a rather colourful mixture of people, and since this was the time of the hippies, it was colourful in all aspects of the word. Claus was an active participant in the community life. Thus, he was instrumental in reviving the good heathen tradition of celebrating winter solstice with a candle-lit procession through the community, carrying a precise replica of the Trundholm Sun Chariot, which is perhaps the most iconic of all archaeological finds from the Nordic early Bronze Age – and the replica was made by Claus, of course!

Study years

Soon after moving into Brumleby, Claus was enrolled as a geology student at the University of Copenhagen in 1965. Most of his study took place at a department named Institute for Historical Geology and Palaeontology, which was part of the Geological Central Institute. He earned his cand. scient (M.Sc.) degree

Fig. 1. Claus in 5th grade, primary school 1956 (far right, in the back row), Skovshoved Skole north of Copenhagen. (With permission from Gentofte Lokalarkiv).

with a thesis dealing with trace fossils from the Jurassic of Milne Land in East Greenland (Fig. 2). Trace fossil studies were a new and exciting subject at the time and Claus was the first Danish palaeontologist to specialise in this field. He was a talented draftsman and his 3D diagrams of the trace fossils from Milne Land heralded a new way of illustrating this type of fossils (Fig. 3). His first paper on trace fossils was published as early as 1970.

Then as now, most students held various jobs to finance their activities. Claus's first job was to check tickets in a small booth at Ordrup train station, which gave him plenty of time to read. However, he soon landed a geology-relevant student job, processing large numbers of 10–30 kg bulk samples of chalk collected as base for a major investigation of the Danish chalk brachiopods and later also bryozoans.

He continued his studies as a Ph.D. student at the same department, changing his subject to the bivalve fauna in the Cretaceous–Palaeogene (K–T) boundary strata at Stevns Klint. He was awarded his Ph.D. degree with a thesis on bivalves in the cemented layers below and above the K–T boundary at Stevns Klint. The study was made possible because a large,

otherwise unknown fauna of aragonite-shelled bivalves, which are normally not preserved in chalk was beautifully preserved as moulds and casts due to early lithification of the boundary strata. This offered an unrivalled opportunity to study the fate of this important faunal group across a major event in Earth history, and his first publication about the aragonitic bivalves from the topmost Maastrichtian appeared in 1976. He continued his studies of the K–T bivalves for the rest of his career, starting as a Postdoc at the same department.

Geologist at Nordjyllands Amt

His first 'real' job after his Postdoc years started in the spring of 1978, when he was employed as a geologist in Nordjyllands Amt – the administrative unit responsible for the northern county of Jylland (for some reasons termed Jutland in English). He was recommended for this position by Erik Heller (State Geologist) and Jens Morten Hansen (Head of administrative Secretariat) both at the DGU (the Geological

Survey of Denmark). During his employment here, which lasted for 1½ year Claus and his family lived away from Brumleby, in a small house at Rebild, in a clearing in one of the largest forests in Denmark.

Claus was not the typical administrator of gravel pits, groundwater and other environmental issues. However, he used the opportunity to hire several graduate students from the University of Copenhagen to undertake sedimentological and other geological studies in the region. Two of these students, Lars Henrik Nielsen and Peter Johannessen located a well-preserved Pleistocene spit, which was preserved in 3D due to isostatic uplift after the ice melted away. Claus visited the outcrop and agreed in the interpretation and strongly supported their further study of the locality. This resulted in a now classic study of this otherwise little-known sedimentary environment (Nielsen *et al.* 1988).

Teaching at Roskilde University (RUC)

Claus obtained his first permanent academic position as an assistant professor at Roskilde University Centre (RUC) about 40 km west of Copenhagen, where he was employed from 1979 until retirement in 2012. RUC was commonly referred to as an experimental university, and a number of disciplines which had not previously been part of a classic university curriculum was introduced there. Through the more than 30 years Claus worked at RUC his ability to look at every topic in a broader and more societal context was essential to his contribution to teaching. At the Institute of Environmental Technology and Society (today the Institute for Man and Society) he was part of a strong, cross disciplinary collaborative environment, comprising biologists, geographers, geologists, sociologists, civil engineers and architects. His broad approach also found its way into teaching, be it courses or projects, in keeping with the RUC tradition that every course or student project involved more than one teacher, typically one from natural sciences and one from social sciences. This gave Claus the possibility to draw on his specific competence within palaeontology, his deep interest in scientific theory and philosophy as well as his strong engagement in all aspects of the environmental debate – preferably involving field-based elements. To Claus, science and politics were inextricably linked.

Claus had the capacity to discuss and inspire both as a scientist and as a teacher. With his love for nature, he opened the eyes of both colleagues and students for the values one had to protect, as a person or – more

formally as an environmental planner. He taught his students in a straightforward language how the Earth was formed, how it can enrich our lives in a sustainable way, and how we can destroy the very foundation for our existence if ignorance and greed reign.

In addition to the references in the Bibliography his engagement resulted in a large amount of internal teaching material, as well as letters to newspapers, notably to the daily newspaper Information, and numerous public lectures at Vestjyllands Højskole and Folkeuniversitetet.

Expeditions to East Greenland

During his study, and in the following years, Claus participated in several expeditions to central East Greenland, most notably to Milne Land in 1970 with Tove Birkelund, EH and Peter Willumsen in 1970 (Fig. 2; Håkansson *et al.* 1971), in 1977 where the team now included Tove Birkelund, John Callomon, Franz Fürsich and Stefan Piasecki (Fürsich & Heinberg 1983; Birkelund *et al.* 1984) and later to Jameson Land with Tove Birkelund (Heinberg & Birkelund 1984). During field work he obtained an excellent trace fossil collection from the Upper Jurassic – lowermost Cretaceous succession exposed on the steep cliff forming the east coast of Milne Land. This material formed the basis for his MSc thesis and for excellent publications (Heinberg 1973, 1974). In his first paper from 1973, he described the internal structure of the trace fossils *Gyrochorte* and *Curvolithus* from the uppermost Jurassic – lowermost Cretaceous Hartz Fjeld Formation (Fig. 3). The whole trace fossil assemblage was illustrated in a block diagram, giving an excellent picture of both the internal structures and bedding plane morphology of

Fig. 2. Milne Land 1970. Relaxing in the neighbouring team camp (Tove Birkelund, right and Peter Willumsen, middle) after a long hike over the top of Hartz Fjeld.

these two trace fossils supplemented with *Planolites* and *Siphonites*. This assemblage is characteristic for most of the shallow marine Jurassic sandstones in East Greenland. His talent for 3D-type drafting of complicated trace fossils is well displayed in this and later papers.

Then followed a detailed description of the new trace fossil genus *Ancorichnus* from 1974, again, accompanied by a block diagram, now also including the trace fossil *Muensteria*. He developed sophisticated models for the movements of the trace maker in the act of producing an *Ancorichnus* trace. The early trace fossil works were followed up in 1984 with a comprehensive study with Birkelund on the ichnology of the shallow marine Pelion Formation in Jameson Land, East Greenland. This study was again accompanied with detailed block diagrams now also including *Diplocraterion habichi* (now referred to the ichnogenus *Tisoa*), *Monocraterion tentaculatum*, *Ophiomorpha nodosa*, *Rhizocorallium irregulare*, *Thalassinoides suevica*, and *Phoebichnus trochoides*. In contrast to the earlier studies the trace fossils were referred not only to ichnogenus but also to ichnospecies – this concept was vividly discussed in the literature, mainly reflecting that an 'ichnospecies' was neither an animal nor the remain of an animal such as a shell, but traces recording the movements of the animal on or through the sediment. The paper includes numerous somewhat simplistic sedimentological logs, which formed the basis for the recognition of the spatial distribution of the trace fossil assemblages or ichnocoenoses throughout the formation (Heinberg & Birkelund 1984).
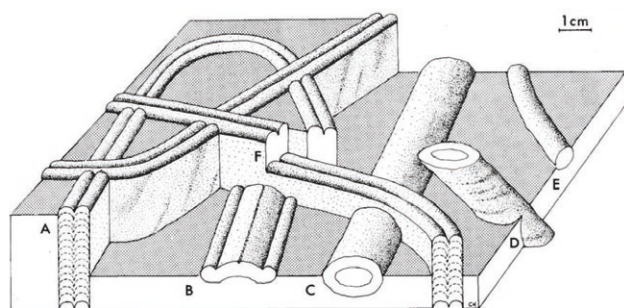

Fig. 3. One of Claus' characteristic block diagrams showing the trace fossil assemblage from the middle Volgian – Valanginian Hartz Fjeld Formation, Milne Land, East Greenland. The main emphasis is on the traces *Gyrochorte* (A) and *Curvolithus* (B) and the diagram shows both the bedding plane expression of the traces and their internal structures. From Heinberg (1973).

Expeditions to eastern North Greenland

In the years 1976 to 2009 Claus participated in a number of expeditions to eastern North Greenland mainly together with EH with the primary purpose of mapping the Wandel Sea Basin, a largely unknown succession of Late Palaeozoic to Palaeogene deposits covering the junction between the East Greenland Caledonian fold belt and the North Greenland Ellesmerian fold belt (Figs 4, 5). In combination with a number of other participants, including Lars Stemmerik, Tove Birkelund and Stig Schack Pedersen. This work gradually led to the first attempts of unravelling the complicated tectonic and stratigraphic relations in this remote, poorly known region. This was completed with a plate tectonic analysis of the area.

Claus' first expedition to North Greenland was shambolic. Code-named 'Brilliant Ice' it was a joint military operation with the purpose of testing the operation capabilities under extreme conditions of the Danish Air Force Sikorsky 61 helicopters. For political reasons the Geological Survey of Greenland (GGU) had been granted two slots – including all logistic support – to test the helicopter-based working conditions in Peary Land. The GGU team, consisting of Claus and EH only got into the field in eastern Peary Land at the very day when everybody was supposed to arrive back in Copenhagen. But once in the field, it was magic – until rain and sleet took over. Fourteen hours investigating a Lower Triassic succession was the meagre accomplishment of his first effort in North Greenland (Håkansson & Heinberg 1977).

Claus' next expedition to North Greenland, in 1980, as part of the large-scale GGU mapping program, was as it should be – lots of exiting geology with abundant fossils, from the Lower Carboniferous to the Palaeogene, scattered across much of the north-eastern corner of Greenland, covered by two teams of two in about seven weeks. For the first part of the season Claus, together with Lars Stemmerik, was focusing on the Late Palaeozoic successions exposed in a series of impressive, richly fossiliferous cliffs along the east coast of Kronprins Christian Land. Later in the season a helicopter reconnaissance stop at Kilen rekindled Claus' previous focus on the Jurassic–Cretaceous sediments on his first expeditions to East Greenland. The isolated elongate semi-nunatak Kilen is deeply incised into the Flade Isblink ice cap in Kronprins Christian Land. The few geological overview maps had offered different interpretations – 'very old', mainly gneisses, or 'old', Caledonian fold belt rocks – based on aerial assessments during a couple of pioneering overflights.

The first stop revealed intensely folded sediments

with absolutely no signs of being 'old', let alone 'very old'. But with no fossils to actually give an indication of the age the team proceeded to another ground-stop, this time with folded sediments of a different type and – heureka! – Claus found a small concretion containing a handful of scaphitid ammonites that, then and there, allowed establishing the age as Late Cretaceous – the first unequivocal record of rocks of

Fig. 4. A: Departure of the Danish Air force S-61 helicopter after unloading the camp gear in Kim Fjelde, Peary Land, 1976. **B:** Iconic site in northern East Greenland: the Mallemuk Fjeld exposing the Upper Carboniferous sandstones and limestones of the Foldedal and Kim Fjelde Formations investigated by Claus a.o. in 1980. Photo courtesy Lars Stemmerik. **C:** Claus posing after a hard fight to get his Honda out of a near bottomless quagmire in Kilen, 1985. **D:** On the road again, on his fifth and last expedition to eastern Peary Land in 2009. Note the upgrade in transport – a 4-wheel Honda. **E:** The first of many concretions with scaphitid ammonites from the inner part of Kilen, providing the first conclusive evidence of Upper Cretaceous strata in North Greenland. From Håkansson & Heinberg (2003). **F:** Party at Station Nord in 2008 during Claus' second last field season in Greenland. Photo courtesy Jesper Milàn.

that age in North Greenland (Fig. 4E). After a brief conference with the GGU base camp, it was decided to bring in the rest of the team (LS and the botanist Per Mølgaard) and set up a couple of camps for a more comprehensive reconnaissance. These few extra days of investigation strongly indicated that Kilen exposed a number of substantial successions of various Mesozoic sediments.

Having completed the geological mapping of the eastern part of North Greenland at the end of the 1980 season, GGU moved its three-year old basecamp farther to the west, and with no rocks of 'our' age in that region, the group studying the Wandel Sea Basin was left to fend for itself trying to get back to all the very interesting problems raised through the regional mapping program. Over the next good many years, a string of smaller expeditions targeted the main areas of interest revealed through the mapping, supported by various funds, as well as GGU, with Claus as a frequent participant. With its newly discovered, near total Mesozoic successions, Kilen was the target for the first follow-up expedition. Without the usual helicopter support alternative ways to cover the substantial, ice-free area in Kilen was necessary, and the solution was motorcycles. Six people (Claus plus EH, Tove Birkelund, Stig Schack Pedersen, Christian Hjort and PM), two 3-wheeled Hondas plus a single luggage trailer facilitated investigations and camp shifts, covering most of the area, and the net result was documentation of a composite Jurassic and Cretaceous succession, more than 3.5 km thick, not matching anything else recorded in North Greenland (Håkansson et al. 1993). Next step in revisiting the main Mesozoic localities was back to Peary Land. Eight people covered the Kim Fjelde area – just under 2000 km² – again with two Honda MC's and two trailers working out of, and in between, three base depots established with
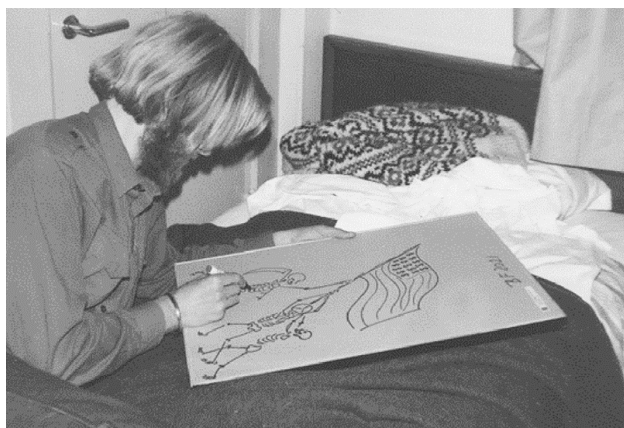

Fig. 5. Claus re-decorating a guest room at the US Air Base at Søndre Strømfjord, West Greenland on the way back from field work in Peary Land in 1976.

help from the Twin-Otter STOL plane chartered by GGU. The work was summarized in a voluminous report to Energistyrelsen (Håkansson 1994) with Claus contributing to five of the reports included, all with a Mesozoic aspect.

In recent years Claus's work in North Greenland with EH formed the basis for renewed studies during an intensive field campaign by geologists from GEUS, the now combined Geological Surveys for Greenland and Denmark (Hovikoski et al. 2018; Bjerager et al. 2019, 2020).

Claus' last visits to Greenland

Claus' last two trips to Greenland were different in many ways, and this time he was working directly for GEUS. In 2008 GEUS had a request from an oil company whether it would be possible to demonstrate the presence of further Mesozoic basins under the Greenland ice sheet in East Greenland. Clever planning resulted in a change to the demobilization route for a long-ranging Super Puma helicopter already in North Greenland, allowing a couple of GEUS glaciologists, and Claus, to work without fuel depots all the way between Station Nord and Mestersvig. Claus' task was to collect sedimentary rocks from glaciogenic deposits along the margin of the ice sheet, to possibly reveal the existence of such basins. As it turned out, the samples provided no conclusive evidence to that effect – but for Claus, it was a truly memorable trip, connecting all the areas of Greenland he had worked in.

The following year, 2009, was his final expedition to Greenland – back to the Wandel Sea Basin together with EH. The objective was the collection of sediments from east Peary Land, Kilen and Holm Land to extend the GEUS based provenance data base. The expedition was without helicopter support and relied on the well tested model combining a fixed-wing Twin-Otter STOL aircraft and two Honda motorcycles.

Bivalves from the K–T boundary strata at Stevns Klint

Over his last many years, the Department of Geosciences and Natural Resource Management, University of Copenhagen offered Claus office space in the ground floor facing the back yard. Most of Claus' published scientific work was on palaeontological subjects. Almost from the outset of his scientific career his main studies were focused on the K–T boundary at Stevns Klint south of Copenhagen. 'K–T' stands
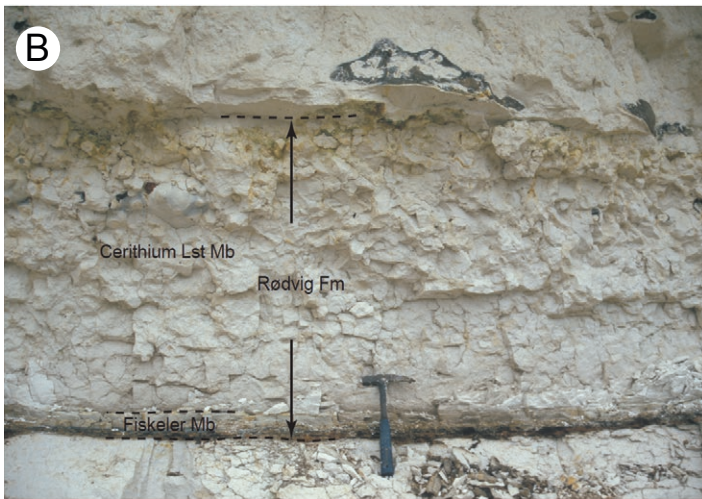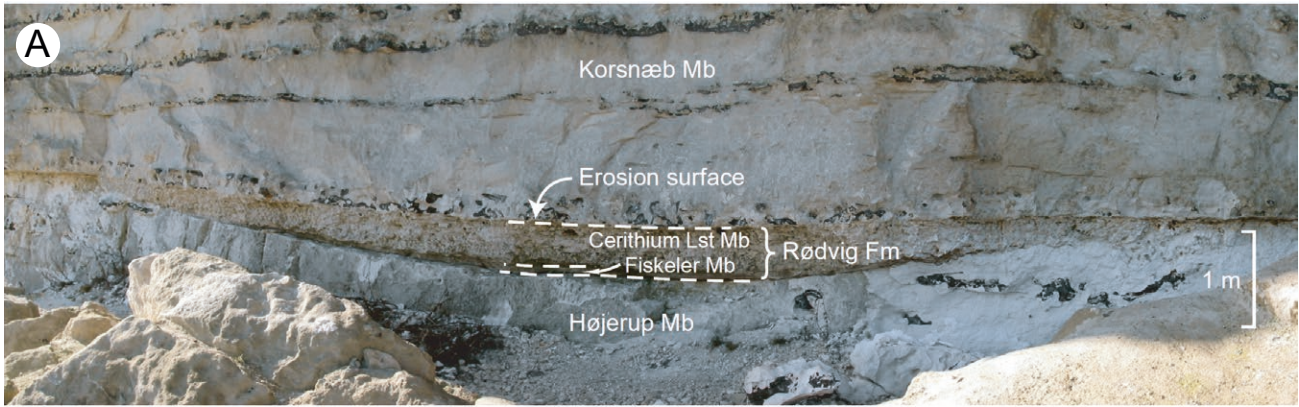
Fig. 6. A: Stevns Klint, UNESCO World Heritage Site for the K–T boundary. The bivalve faunas studied by Claus were collected from the lithified topmost Højerup Member seen to the right in the picture at the top of the 1 m scale bar, and from the Cerithium Limestone Member. **B:** Close-up of the boundary strata at Stevns Klint, Showing the topmost Maastrichtian part of the Højerup Member, the basal Danian Fiskeler Member, overlain by the Cerithium Limestone Member. Claus' studies of the bivalves from the K–T boundary strata were focused on the lithified top of the Højerup Member and the Cerithium Limestone Member. From Surlyk et al. (2006).

for the 'Cretaceous–Tertiary', but the Tertiary has unfortunately later been split into the Palaeogene and Neogene, but the K–T abbreviations is still in common use. The 15 km long sea-cliff of Stevns Klint forms a continuous exposure of a Maastrichtian–Danian succession, including one of the most complete transitions across the important K–T boundary anywhere in the World. Being easily accessible this has, over the years, allowed multiple detailed studies of the biota across the boundary which marks an important mass extinction and for this reason the cliff was included in UNESCO's 'World Heritage List' in 2014 (Fig. 6). Claus' studies were focused on the aragonite-shelled bivalves which are not normally preserved in the chalk, but early cementation of the top of the Maastrichtian chalk and the lowermost Danian Cerithium Limestone resulted in preservation, as moulds, casts and imprints, of a rich bivalve fauna, comprising mainly mm-sized species.

Claus spent endless hours in the field hammering at big blocks of limestone and subsequently examining the fragments under a hand lens to locate the minute bivalves. Back in the lab the fossils were photographed in the SEM, allowing even the finest details to be shown. This resulted in a fine series of papers on the bivalve fauna from the boundary strata. The first of these from 1976 dealt with the Limopsidae. He introduced the study as follows: "This paper is intended
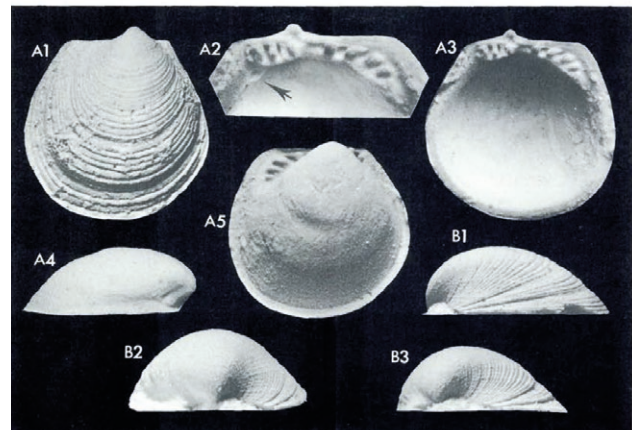

Fig. 7. The aragonitic bivalve *Limposis ravni* from the lithified topmost Maastrichtian chalk of the Højerup Member, Stevns Klint. Latex casts of valve imprints. Note the excellent preservation of the valve sculpture and hinge details. Maximum width 3.9 mm. From Heinberg (1976).

Claus Heinberg (1945–2021) · 87

to be the first in a series with descriptions of about 40 new species of aragonitic bivalves from the white chalk (Maastrichtian of Denmark)". This was quite a brave introduction, but Claus managed to live up to it in a series of papers published over the years from 1976 to 1999. In the paper on the Limopsidae Claus described no less than eight new species, and the excellent preservation of the casts of these small bivalves were very well illustrated (Fig. 7). This paper was followed by a paper on the Arcoida in 1978, where another eight new species were described (Fig. 8; Heinberg 1978). In a paper on Cuspidariidae from 1979 Claus described seven species, six of which were new (Fig. 9). The material illustrated in these three papers records the finest details of the surface ornamentation and hinge structure.

However, his paper on the evolutionary ecology of nine sympatric species of *Limopsis*, also published in 1979 is undoubtedly the most detailed and penetrating of Claus' works. These bivalves all lived in the mounded bryozoan-rich chalk of the topmost Maastrichtian Højerup Member at Stevns Klint, and detailed analysis allowed the recognition of two independent lines of limopsids, a non-byssate lineage represented by a single burrowing species, and a byssate lineage comprising eight species, seven of which represent a morphocline, interpreted as reflecting adaptations along an environmental gradient, possibly related to substrate size and water flow. As usual, this work is very well illustrated by his own drawings, some of which are almost too complicated to be easily comprehended (Fig. 10). After a pause of ten years he continued his studies of the chalk bivalves with number IV in his series of taxonomic publications of aragonite-shelled bivalves from the lithified K–T boundary layers, this time on the Nuculoida. He
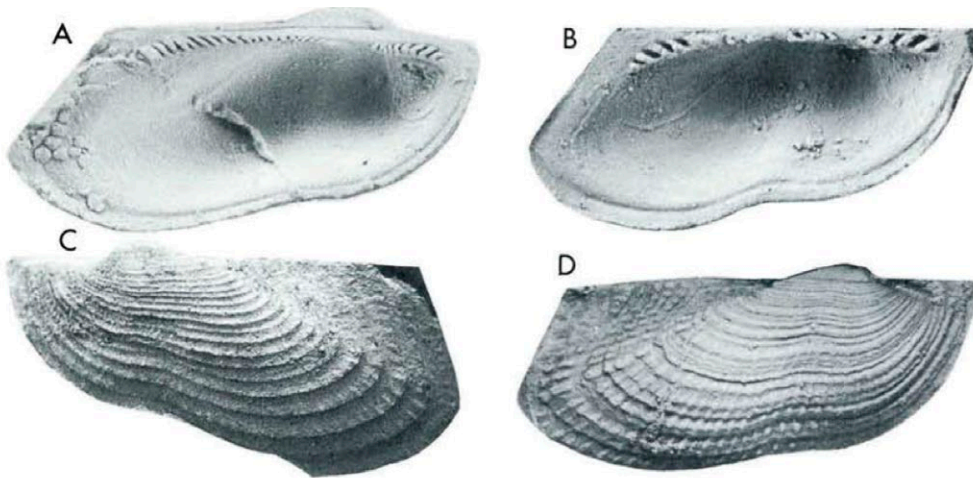

Fig. 8. The aragonitic bivalve *Barbatia* (*Acar*) *hennigi* from the lithified topmost Maastrichtian chalk of the Højerup Member, Stevns Klint. Maximum width about 6 mm. From Heinberg (1979a).
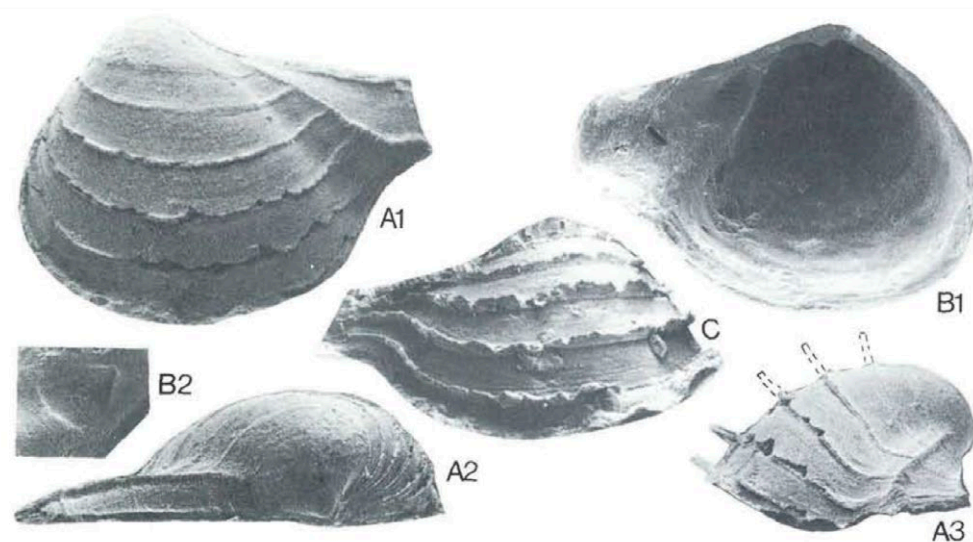

Fig. 9. The aragonitic bivalve *Cuspidaria* (*C.*) *lisbethae* from the lithified topmost Maastrichtian chalk of the Højerup Member, Stevns Klint. Maximum width 5 mm. From Heinberg (1979b).

recognized six species, four of which were new.

In 1993 he erected a new genus *Birkelundita* of the Carditidae, named in honour of Professor Tove Birkelund who had died in 1986 (Fig. 11). This paper not only describes the morphology of the new genus in great detail but offers a beautifully illustrated highly comprehensive analysis of its mode of life and ecology.

His last scientific paper which was co-authored with the late Richard Bromley was published in 2006. The subject was attachment strategies of organisms to hard substrates (Bromley & Heinberg 2006). It differs fundamentally from Claus' previous work. It is a literature review and does not contain any independent analytical work. One may perhaps wonder why Claus involved himself in this study.

In addition to his work at Stevns Klint, Claus undertook field work in the Upper Cretaceous chalk throughout northern Europe, notably the Netherlands, Belgium and France much of it with both Danish and foreign colleagues.
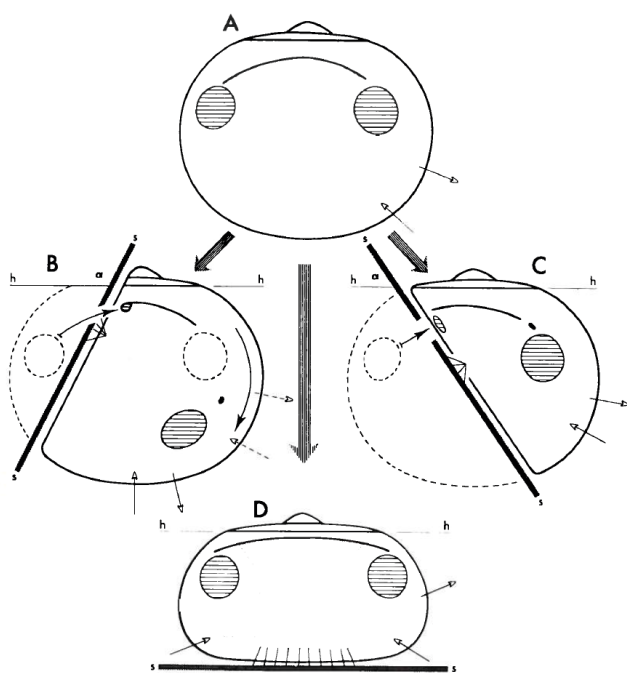

Fig. 10. Diagrams illustrating the complex distortion in position and size of the fundamental functional elements in the shells of the aragonitic bivalve *Limopsis* associated with three evolutionary lineages (broad arrows) leading to the presence of nine sympatric species of *Limopsis* in the lithified top 30 cm of the Maastrichtian at Stevns Klint, Denmark. The diagram is characteristic of Claus' sometimes quite elaborate illustrations. h-h = hinge line; s-s = substrate; α = hinge/sole angle; open headed arrows = inhalant and exhalant currents; black headed arrows = transposition of elements from the '*Glycimeris* stage' (A); adductor muscles hatched horizontally; posterior pedal retractor is black.

As a final note on Claus' work on the chalk it may be mentioned that he in 2000 published a comprehensive, 48 page long and well-illustrated popular science account in Danish entitled 'Livet i Kridthavet' ('The life in the Chalk Sea'; Heinberg 2000). It suffers – as does many similar accounts – from a lack of references in the text or a list of 'Papers recommended for further reading'. This is a pity because it includes some of Claus' interesting and original ideas, while much of the text is clearly based on the work of others.

Claus and the K–T boundary

The nature of the changes in the bivalve fauna across the K–T boundary was presented in great detail in 1999 based on Claus' extensive work on Stevns Klint. Claus concluded that the faunal changes were caused by environmental changes rather than an abrupt mass extinction (Heinberg 1999). This view was prevalent at the Institute of Historical Geology and Palaeontology at that time, and in hindsight Claus' analysis of the shift appears to be somewhat influenced by an attempt to see the faunal change as more insignificant than it actually was.

His account of the bivalve recovery in the earliest Danian after the K–T mass extinction, was a logical conclusion to his work on the bivalves from the boundary strata. He found that the bivalves of the lowermost Danian Cerithium Limestone represented an early recovery fauna, showing a gradual recovery from zero

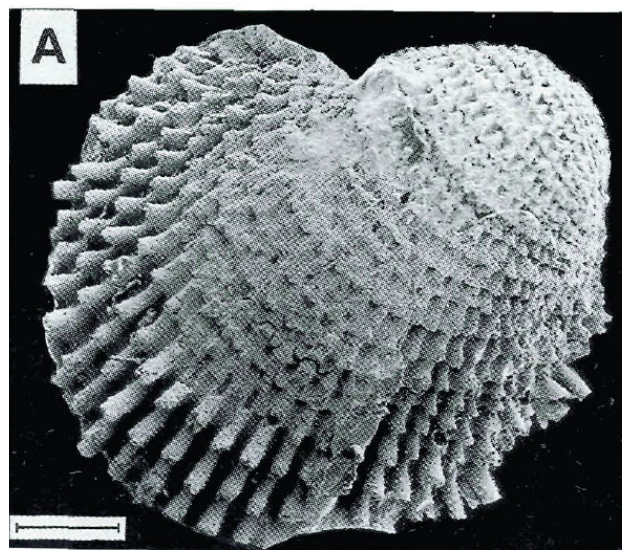

Fig. 11. The new bivalve genus *Birkelundita* named by Claus in honour of the late professor Tove Birkelund. This specimen is from the Campanian of Belgium. The genus ranges from the Turonian to the upper Maastrichtian. From Heinberg (1993).

species at the base to a rather constant level of about 20 species through the upper half of the thin limestone unit. The lowest assemblages are characterized by the extreme dominance of a single 'disaster species' followed by a rapid increase in species numbers.

It was Claus's dream to conclude his work on the bivalves from the K–T boundary strata with a Dr. scient. thesis – the classical European senior doctorate which is normally based on many years of independent work by a mature scientist without any kind of supervision. However, increasingly bad health conditions during his later years did not allow this dream to come through.

Other interests and activities

Throughout his life Claus maintained a very broad spectrum of interests, many of which dated back to his schooldays. All things nature was close to his heart, always with an ecological angle, and with particular emphasis on fossils and plants. His interest in geology and especially palaeontology was founded during his childhood where he spent many summer holidays on the island of Mors in northern Jylland. An Eocene diatomite, the Fur Formation is well exposed on the island and contains beautifully preserved fossils of fish and insects. Art and history were other elements of interest, ranging from early Nordic to modern political history. It also included a deep fascination of the Danish village churches and the rich archive of Medieval murals adorning many of their walls – all in spite of his strictly non-religious approach to life. And, importantly, he read 'everything' about Arctic exploration – particularly about the Danish explorers in the north-eastern part of Greenland.

Claus was strongly engaged in left-wing political work and debates. Especially in his younger years he was active on the extreme left wing, however, from a personal, rather than strictly dogmatic, platform. During the student revolts in the years between 1968 and 1970 he held flaming political talks from the central stairs leading up to the imposing door of the main university building in central Copenhagen, and also from the lectern of the University central hall (Fig. 12). Later he abandoned his most radical style, claiming that it was because it resulted in painful ulcers. However, he remained a highly engaged social debater throughout his life, active in a wide range of political, grassroot work and social issues, notably climate, nuclear power plants, environmental and ecological subjects, consistently drawing on his scientific experience. Key figures in his political network were Niels Frölich, Henning Prins and Ejvind Larsen – with the latter he shared a deep interest in Grundtvig, a Danish author, theologists, debater and schoolman. Unfortunately, he never ventured into publishing his highly original – and often highly controversial – thoughts in English.

As would be expected, Claus was strongly engaged in the debates concerning introduction of nuclear power in Denmark around 1980. However, his most

Fig. 12. Claus standing on the lectern in the main hall of the University of Copenhagen during the student revolts and occupation of the Vice-chancellor's office on 9 March 1970 (Lars Hansen/Ritzau Scanpics). This photo and the following (Fig. 13) span virtually all of Claus' geological career.

prominent effort was centred about the very problematic location of the Swedish nuclear powerplant Barsebäck less than 20 km from the Town Hall in Copenhagen, the Danish capital. Together with Jens Morten Hansen, Claus ventured into an investigation of the neotectonic activity of the major fault zone separating the Scandinavian Shield from the Danish Basin, and in the process, they published a summary of the legislation regulating the necessary investigations and demands to potential sites for placing of both radioactive waste products and nuclear power plants in the USA. The report was published by DGU (Hansen & Heinberg 1980) and included an appendix applying this level of scrutiny to Barsebäck. Based on a neotectonic overview of Scania and Sjælland it was made quite evident, that Barsebäck could *not* have been constructed in this position in the USA, a finding that created quite a stir and no small irritation in the ministerial departments. Nevertheless, the very positioning of Barsebäck so close to a major metropolis *and* on top of a complex fault-zone soon became key arguments in the Danish government's prolonged attempts to persuade Sweden to close down this nuclear powerplant. Just before the turn of the millennium decommission finally commenced.

Claus' broad engagement was a clear reflection of his personal preferences, and most were well established already during his high school years. Although an atheist from his teenage years, he maintained a deep interest in art inspired by religion, such as the wonderful early Medieval murals that adorn many walls in Danish village churches, culminating in a – sadly unsuccessful submission headed by PWA – of a proposal to get *'The Danish Village Church'* to be included in UNESCOs 'World Heritage List'. On the other hand, his strong interest in the Vikings and their times, was – at least in part – connected to his political philosophy reflected in the early democratic elements in Viking society.

He commonly gave lectures in a former dairy store in Brumleby, called 'ismejeriet', advertised with his own posters and illustrated with slides, pictures and artefacts. These sessions were very popular among the residents of Brumleby. He had a somewhat strange taste for heroic persons, counting among others Winston Churchill, Clint Eastwood and Vikings in general, exemplified by his collection of videos and books.

In connection with his North Greenland work Claus became friends with the late count Eigil Knuth who had undertaken fundamental studies of the remains of the oldest Inuit cultures in North Greenland, from Thule in the west to Eskimonæs in the east. At first, their relation was not particularly friendly, but a real friendship started to develop when they ran into each

Fig. 13. Claus on a botanical and ornithological field trip in March 2015 with botanist Ib Johnsen and PWA at Østerild Plantation near the field station of Aarhus University at Klim in northern Jylland, Denmark. It served as the base for several week-long courses on 'Nature Management and Nature Politics' from RUC.

other on a street in Copenhagen and Knuth learned that Claus lived in Brumleby, the small community in the city for which Knuth had warm feelings. Claus' solstice ceremony in Brumleby further strengthened their relation, as Knuth was also strongly inclined towards paganism and Nordic mythology. Knuth, who was quite eccentric, decided that Claus was the man to produce the film about himself and his work, despite the fact that Claus had never done anything like that before and others had already started on this project! Courageously, Claus accepted the challenge, and with full cooperation from Knuth he ventured into this prolonged project – including a trip to film Knuth in Greenland. Knuth never saw the final result. The 46 minutes long film was completed in 2000 and was entitled: 'Eigil Knuth – Billedhugger, forfatter og polarforsker' (Eigil Knuth – Sculptor, author and polar explorer).

The words renaissance person or polyhistor have commonly been used to describe Claus. His gradually deteriorating health eventually interfered with his capacity to carry on his research work, and after one last couple of glorious trips to North and East Greenland in 2008 and 2009 his strength faded rapidly. Over the last 5–6 years he was physically restrained, but still managed with the support and companionship of PWA, to revisit most of the art galleries, museums and Medieval churches around Copenhagen as well as other sentimental journeys (Fig. 13).

In memory of Claus Heinberg – a fine person, a good colleague and friend.

Acknowledgements

References

Birkelund, T., Callomon, J.H. & Fürsich, F.T. 1984: The stratigraphy of the Upper Jurassic and Lower Cretaceous sediments of Milne Land, central East Greenland. Grønlands Geologiske Undersøgelse Bulletin 147, 56 pp.

Bjerager, M., Alsen, P., Hovikoski, J., Lindström, Pilgaard, A.

Stemmerik, L. & Therkelsen, J. 2019: Triassic lithostratigraphy of the Wandel Sea Basin, North Greenland. Bulletin of the Geological Society of Denmark 67, 83–105. https://doi.org/10.37570/bgsd-2019-67-06

Bjerager, M., Alsen, Bojesen-Koefoed, J., Fyhn, M.B.W., Hovikoski, J., Ineson, J.R., Nøhr-Hansen, H., Nielsen, L.H., Piasecki, S. & Vosgerau, H. 2020: Cretaceous lithostratigraphy of North-East Greenland. Bulletin of the Geological Society of Denmark 68, 37–93. https://doi.org/10.37570/bgsd-2020-68-04

Bromley, R.G. & Heinberg, C. 2006: Attachment strategies of organisms on hard substrates: A palaeontological view. Palaeogeography, Palaeoclimatology, Palaeoecology 232, 429–53. https://doi.org/10.1016/j.palaeo.2005.07.007

Fürsich, F.T. & Heinberg, C. 1983: Sedimentology, biostratinomy, and palaeoecology of an Upper Jurassic offshore sand bar complex. Bulletin of the Geological Society of Denmark, 32, 67–95.

Håkansson, E. ed. 1994: Wandel Sea Basin: Basin analysis. Unpublished Report, University of Copenhagen, 290 pp.

Håkansson, E. & Heinberg, C. 1977: Reconnaissance work in the Triassic of the Wandel Sea Basin, Peary Land, North Greenland. Rapport Grønlands geologiske Undersøgelse 85, 11–15.

Håkansson, E., Birkelund, T., Heinberg, C. & Villumsen, P. 1971: Preliminary results of mapping the Upper Jurassic and Lower Cretaceous sediments of Milne Land. Rapport Grønlands geologiske Undersøgelse 37, 32–41. https://doi.org/10.34194/rapggu

Håkansson, E., Birkelund, T., Heinberg, C., Hjort, C., Mølgaard, P. & Pedersen, S.A.S. 1993: The Kilen Expedition 1985. Bulletin of the Geological Society of Denmark 40, 9–32.

Heinberg, C. 1973: The internal structure of the trace fossils *Gyrochorte* and *Curvolithos*. Lethaia 6, 227–238. https://doi.org/10.1111/j.1502-3931.1973.tb01196.x

Heinberg, C. 1974: A dynamic model for a meniscus filled tunnel (*Ancorichnus* n. ichnogen,) from the Jurassic Pecten Sandstone of Milne Land, East Greenland. Rapport Grønlands geologiske Undersøgelse 62, 20 pp. https://doi.org/10.34194/rapggu

Heinberg, C. 1976: Bivalves from the white chalk (Maastrichtian) of Denmark: Limopsidae. Bulletin of the Geological Society of Denmark 25, 57–70.

Heinberg, C. 1978: Bivalves from the white chalk (Maastrichtian) of Denmark, II: Arcoida. Bulletin of the Geological Society of Denmark 27, 105–116.

Heinberg, C. 1979a: Bivalves from the white chalk (Maastrichtian) of Denmark, III: Cuspidariidae. Bulletin of the Geological Society of Denmark 28, 39–45.

Heinberg, C. 1979b: Evolutionary ecology of nine sympatric species of the pelecypod *Limopsis* in Cretaceous chalk. Lethaia 12, 325–340. https://doi.org/10.1111/j.1502-3931.1979.tb01018.x

Heinberg, C. 1993: *Birkelundita*, a new genus (Bivalvia, Cardiacea) from the Upper Cretaceous white chalk of Europe. Bulletin of the Geological Society of Denmark 40, 185–195.

Heinberg, C. 2000: Livet i Kridthavet. Varv 4, 47 pp.

Heinberg, C. 1999: Lower Danian bivalves, Stevns Klint, Denmark: Continuity across the K/T boundary. Palaeogeography, Palaeoclimatology, Palaeoecology 154, 87–106. https://doi.org/10.1016/s0031-0182(99)00088-7

Heinberg, C. & Birkelund, T. 1984: Trace-fossil assemblages and basin evolution of the Vardekløft Formation (Middle Jurassic, central East Greenland). Journal of Paleontology 56, 362–397.

Hovikoski, J., Pedersen, G.K., Alsen, P., Lauridsen, B.W., Svennevig, K., Nøhr-Hansen, H., Sheldon, E., Dybkjær, K., Bojesen-Koefoed, J., Piasecki, S., Bjerager, M. & Ineson, J. 2018: The Jurassic–Cretaceous lithostratigraphy of Kilen, Kronprins Christian Land, eastern North Greenland. Bulletin of the Geological Society of Denmark 66, 61–112. https://doi.org/10.37570/bgsd-2018-66-04

Nielsen, L.H., Johannessen, P.N. & Surlyk, F. 1988: A Late Pleistocene coarse-grained spit-platform sequence in northern Jylland, Denmark. Sedimentology 35, 915–937. https://doi.org/10.1111/j.1365-3091.1988.tb01738.x

Surlyk, F., Damholt, T. & Bjerager, M. 2006: Stevns Klint, Denmark: Uppermost Maastrichtian chalk, Cretaceous–Tertiary boundary, and lower Danian bryozoan mound complex. Bulletin of the Geological Society of Denmark 54, 1–48. https://doi.org/10.37570/bgsd-2006-54-01

Appendix

Bibliography

Peer-reviewed journal papers

Heinberg, C. 1970: Some Jurassic trace fossils from Jameson Land (East Greenland). In: T.P. Crimes & J.C. Harper (eds): Trace fossils, 227–234. Geological Journal Special Issue 3.

Håkansson, E., Birkelund, T., Heinberg, C. & Villumsen, P. 1971: Preliminary results of mapping the Upper Jurassic and Lower Cretaceous sediments of Milne Land. Rapport Grønlands geologiske Undersøgelse 37, 32–41.

Heinberg, C. 1973: The internal structure of the trace fossils *Gyrochorte* and *Curvolithos*. Lethaia 6, 227–238.

Heinberg, C. 1974: A dynamic model for a meniscus filled tunnel (*Ancorichnus* n. ichnogen,) from the Jurassic Pecten Sandstone of Milne Land, East Greenland. Rapport Grønlands geologiske Undersøgelse 62, 20 pp.

Birkelund, T. & Heinberg, C. 1975: Facies variation and trace fossil assemblages of the Vardekløft and Olympen Formations of Jameson Land and Scoresby Land, central East Greenland. Rapport Grønlands geologiske Undersøgelse 75, 100–103.

Heinberg, C. 1976: Bivalves from the white chalk (Maastrichtian) of Denmark: Limopsidae. Bulletin of the Geological Society of Denmark 25, 57–70.

Håkansson, E. & Heinberg, C. 1977: Reconnaissance work in the Triassic of the Wandel Sea Basin, Peary Land, North Greenland. Rapport Grønlands geologiske Undersøgelse 85, 11–15.

Håkansson, E., Heinberg, C. & Stemmerik, L. 1981: The Wandel Sea Basin from Holm Land to Lockwood Ø, eastern North Greenland. Rapport Grønlands geologiske Undersøgelse 106, 47–63.

Heinberg, C. 1978: Bivalves from the white chalk (Maastrichtian) of Denmark, II: Arcoida. *Bulletin* of the Geological Society of Denmark 27, 105–116.

Heinberg, C. 1979: Evolutionary ecology of nine sympatric species of the pelecypod *Limopsis* in Cretaceous chalk. Lethaia 12, 325–340.

Heinberg, C. 1979: Bivalves from the white chalk (Maastrichtian) of Denmark, III: Cuspidariidae. Bulletin of the Geological Society of Denmark 28, 39–45.

Hansen, J.M. & Heinberg, C. 1980: Geologiske kriterier for placering af A-kraftværker. Et resumé af USA's lovgivning og dens anvendelsesmuligheder på danske forhold. Danmarks Geologiske Undersøgelse, Årbog 1979, 107–123.

Håkansson, E., Heinberg, C. & Stemmerik, L. 1981: The Wandel Sea Basin from Holm Land to Lockwood Ø, eastern North Greenland. Rapport Grønlands geologiske Undersøgelse 106, 47–63.

Fürsich, F.T. & Heinberg, C. 1983: Sedimentology, biostratinomy, and palaeoecology of an Upper Jurassic offshore sand bar complex. Bulletin of the Geological Society of Denmark, 32, 67–95.

Heinberg, C. & Birkelund, T. 1984: Trace-fossil assemblages and basin evolution of the Vardekløft Formation (Middle Jurassic, central East Greenland). Journal of Paleontology 56, 362–397.

Heinberg, C. 1989: Bivalves from the white chalk (Maastrichtian) of Denmark, IV: Nucoloida. Bulletin of the Geological Society of Denmark 37, 227–236.

Håkansson, E., Heinberg C. & Stemmerik, L. 1991: Mesozoic and Cenozoic history of the Wandel Sea Basin area, North Greenland. Bulletin Grønlands geologiske Undersøgelse 160, 153–164.

Pedersen, S.A.S., Håkansson, E., Heinberg, C. & Madsen, L. 1992: Variations in the regional stress field through the Carboniferous to Tertiary development in North Greenland. Norsk Geologisk Tidsskrift 72, 137–138.

Håkansson, E., Birkelund, T., Heinberg, C., Hjort, C., Mølgaard, P. & Pedersen, S.A.S. 1993: The Kilen Expedition 1985. Bulletin of the Geological Society of Denmark 40, 9–32.

Heinberg, C. 1993: *Birkelundita*, a new genus (Bivalvia, Carditacea) from the Upper Cretaceous white chalk of Europe. Bulletin of the Geological Society of Denmark 40, 185–195.

Heinberg, C. 1999: Lower Danian bivalves, Stevns Klint, Denmark: Continuity across the K/T boundary. Palaeogeography, Palaeoclimatology, Palaeoecology 154, 87–106.

Dypvik, H., Håkansson, E. & Heinberg, C 2002: Jurassic and Cretaceous paleogeography in the North Greenland - Svalbard region. Polar Research 21, 91-108.

Machalski, M. & Heinberg, C. 2005: Evidence for ammonite survival into the Danian (Paleogene) from the Cerithium Limestone at Stevns Klint, Denmark. Bulletin of the Geological Society of Denmark 52, 97–111.

Dypvik, H., Plado, J., Heinberg, C., Håkansson, E., Pesonen, L., Schmitz, B. & Raiskila, S. 2008:ett Impact structures and events – a Nordic perspective. Episodes 31, 1, 107–114.

Hart, M.B., Feist, S.E., Håkansson, E., Heinberg, C., Price, D.G., Leng, M.J. & Watkinson, M.P. 2005. The Cretaceous-Paleogene boundary succession at Stevns Klint, Denmark: Foraminifers and stable isotope stratigraphy. Palaeogeography, Palaeoclimatology, Palaeoecology 224, 6–26.

Rasmussen, J.A., Heinberg, C. & Håkansson, E. 2005: Planktic foraminiferid biostratigraphy of the lowermost Danian strata at Stevns Klint, Denmark. Bulletin of the Geological Society of Denmark 52, 113–132.

Heinberg, C. 2005: Morphotype biostratigraphy, diachronism, and bivalve recovery in the earliest Danian of Denmark. Bulletin of the Geological Society of Denmark 52, 81–95.

Bromley, R.G. & Heinberg, C. 2006: Attachment strategies of organisms on hard substrates: A palaeontological view. Palaeogeography, Palaeoclimatology, Palaeoecology 232, 429–53.

Machalski, M., Jagt, J.W.M., Heinberg, C., Landman, N.H. & Håkansson, E. 2009: Danske amonity – obecny stan wiedzy i perspektywy badan (Danian ammonites – The present state of knowledge and perspective for future research). Przeglad Geologiczny 57, 6, 486–493.

Abstracts

Håkansson, E., Heinberg, C. & Pedersen, S.A.S. 1986: The Upper Cretaceous of Kilen. Palæontologisk Klub, Tove Birkelund mindemøde, 1 p.

Heinberg, C. & Håkansson, E. 1990: Syntectonic clastic outer shelf sedimentation in the Wandel Hav Strike-Slip Mobile Belt, North Greenland. 19. Nordiske Geologiske Vintermøde, Abstracts. 2 pp.

Pedersen, S.A.S., Håkansson, E., Heinberg, C. & Madsen, L. 1990: Variations in the regional stress field through the Carboniferous-Tertiary development in North Greenland. Symposium on Post-Devonian tectonic evolution of Svalbard, Oslo. Abstracts. 1 p.

Dypvik, H., Håkansson, E. & Heinberg, C. 1992: Jurassic–Cretaceous depositional history of the North Greenland-Svalbard region. International Conference on Arctic Margins, Anchorage, Sept. 1992, Abstracts.

Dypvik, H., Håkansson, E. & Heinberg, C. 1993: Avsetningshistorie og paleogeografi Jura/Kritt i Nord Grønland-Svalbard området. Geonytt 20, 1, 20.

Heinberg, C. 1996: The first post-K/T bivalve fauna – a Maastrichtian remnant. Sixth North American Paleontological convention. The Paleontological Society Special Publications 8, 169.

Heinberg, C. & Håkansson, E. 1999: Selective loss of low-Mg calcitic organisms at the K–T boundary in Denmark. ESF – Impact, Scientific programme, 3rd Workshop, Esperanza, France, Sept. 1999. Abstracts.

Heinberg, C., Rasmussen, J.A & Håkansson, E. 1999: Lithology, biostratigraphy and faunal distribution across the K–T boundary in Denmark. ESF – Impact, Scientific programme, 3rd Workshop, Esperanza, France, Sept. 1999. Abstracts.

Heinberg, C. & Håkansson, E. 2000: Selektiv K–T uddøen af organismer med lav-Mg calcit skelet i det Danske Bassin. Nordisk Geologisk Vintermøde, Trondheim, Jan. 2000.

Heinberg, C., Rasmussen, J.A. & Håkansson, E. 2001: Planktic foraminifera from the lowermost type Danian of Stevns Klint, Denmark. Palaeontological Association, 45th Annual Meeting, Geological Museum, Copenhagen. Abstracts, 15.

Heinberg, C. & Håkansson, E. 2008: Strange or Strangelove Ocean conditions before and after the K–T event in the Danish Basin. 28th Nordic Geological Winter Meeting, January 7-10, 2008, Aalborg – Denmark. Abstract Volume, 127.

Håkansson, E., Machalski, M., Heinberg, C. & Jagt, J.W.M. 2008: The ammonite fauna of the type Danian (Denmark) and adjacent areas. 33rd International Geological Congress, 6-14 August, Oslo, Norway. Abstracts CD-ROM.

Unpublished reports

Håkansson, E., Heinberg, C., Madsen, L., Mølgaard, S., Piasecki, S., Rasmussen, J.A., Stemmerik, L. & Zinck-Jørgensen, K. 1992: Wandel Sea Basin: basin analysis - a status report. Unpublished report, University of Copenhagen, 12 pp.

Heinberg, C. & Håkansson, E. 1994: Late Jurassic - Early Cretaceous stratigraphy and depositional environment. Unpublished Report, University of Copenhagen, 22 pp.

Håkansson, E., Heinberg, C. & Pedersen. S.A.S. 1994: Geology of Kilen. Unpublished Report, University of Copenhagen, 13 pp.

Håkansson, E., Heinberg, C., Madsen, L., Mølgaard, S., Pedersen, S.A.S., Piasecki, S., Rasmussen, J.A., Stemmerik, L. & Zinck-Jørgensen, K. 1994: WANDEL SEA BASIN: Basin Analysis-Project Summary. Unpublished Report, University of Copenhagen, 13 pp.

Mølgaard, S., Heinberg, C., Håkansson, E. & Piasecki, S. 1994: Triassic stratigraphy and depositional environment of eastern Peary Land. Unpublished Report, University of Copenhagen, 11 pp.

Outreach

Predominantly in Danish, and predominantly on eco-politics. Quite a few letters to newspapers, notably the newspaper Information are not included in the Bibliography.

Håkansson, E. & Heinberg, C. 1975: Milne Land - en ø i Østgrønland. Naturens Verden

Heinberg, C. 1974: Koralrev. Naturens Verden 1974/5, 165–173.

Heinberg, H. & Heinberg, C. 1978: Snegle og muslinger fra havet. Translation and adaption from Lellák, J.: Muscheln und Wasserschnecken, 184 pp. Fremad.

Heinberg, C. 1978/79: Værs'go at bore. Politisk Revy 16/346, 13–14.

Heinberg, C. 1978/79: Eventyr – for hvem. Politisk Revy årgang 16, nr. 346, 15–16.

Heinberg, C., Andersen, H.L., Ringberg, B. & Hansen, J.M. 1980: Hvad er Barsebäck bygget på? Politikens Kronik, 12 March 1980.

Hansen, J.M. & Heinberg, C. 1980: Geologiske kriterier for placering af A-kraftværker: Et resumé af USAs lovgivning og dens anvendelsesmuligheder på danske forhold. Danmarks geologiske Undersøgelse, Årbog 1979, 107–123.

Heinberg, C. 1981: Brumleby. BoligRevy 3, 84–93.

Heinberg, C. 1984: Dinosaurer og dialektik. Naturkampen 32, 30–33.

Heinberg, C. 1987: Evolutionen kan ikke gentages. Naturkampen 43, 12–19.

Heinberg, C. 1987: Mellem himmel og jord: bidrag til den fortsatte debat om holisme: mens vi venter på det store paradigmeskift. Naturkampen 45, 12–4.

Heinberg, C. 1987: Monumentet over is-ørkenens ofre. Politiken, 6 September 1987

Bonde, N. & Heinberg, C. 1987: Kritik af Neo-Darwinismen.

Gradualisme kontra punktualisme. In: Bonde, N., Hoffmeyer, J. & Stangerup, H. (eds): Naturens Historiefortællere. Bind II: Fra Darwins syntese til nutidens krise, 182–195. Copenhagen: G.E.C. Gads Forlag.

Heinberg, C. 1987: Kritik af Neo-Darwinismen. En videnskab om forandring. In: Bonde, N., Hoffmeyer, J. & Stangerup, H. (eds): Naturens Historiefortællere. Bind II: Fra Darwins syntese til nutidens krise, 196–202. Copenhagen: G.E.C. Gads Forlag.

Heinberg, C. 1987: Økosystemet, struktur og evolution. In: Bonde, N, Hoffmeyer, J. & Stangerup, H. (eds): Naturens Historiefortællere. Bind II: Fra Darwins syntese til nutidens krise, 252–287. Copenhagen: G.E.C. Gads Forlag.

Heinberg, C. 1988: Holismen er totalitær, 1. Naturkampen 47, 26–29.

Heinberg, C. 1988: Holismen er totalitær, 2. Naturkampen 48, 28–31.

Heinberg, C. 1988: Moskusokser, mudder og motorcykler. Ud & se 11, 24–26.

Heinberg, C. 1989: Post-modernismens biologiske grundlag. Naturkampen 51, 24–26.

Heinberg, C. 1991: Friheden er en bøjet ske. Naturkampen, 59, 7–9.

Heinberg, C. 1994: Om entropi og entropisme: en kritik af det misantrope menneskesyn. Salt 3/1, 23–26.

Heinberg, C. 1994: En snegl i vejen. Salt 3/7, 2–5.

Heinberg, C. 1995: Sprog og miljø, et par truede arter. In: Geertsen, U. (ed.): Afskaf økologisk Mælk, 194–210. Det økologiske Råd, Årsrapport.

Heinberg, C. 1995: Kærlighed til naturen er had til verden. Kredsen: teologi, æstetik, filosofi, 7–41.

Heinberg, C. & Haaland, T. 1995: Den som har kroner og ører vil høre: forsikringsbranchen i alarmberedskab. In: Anonymous (ed.):75–81. Hvor går grænsen? Samleren.

Heinberg, C. 1996: Det tomme køleskab. Salt 5/1, 19–21.

Heinberg, C. 1996: Økologi er en død sild. Miljøsk 7, 8–23.

Heinberg, C. 1996: Passivisering. Salt 5, p. 1.

Heinberg, C. 1996: Sprog og miljø: to truede arter. Jord og Viden 141-4, 24–27.

Heinberg, C. 1996: Politisk Økologi: hinsides miljøpolitikken. Efterskrift. In: Roussopoulos, D.I. (ed.): Politisk økologi: mere end miljøbevægelse. Politisk Revy.

Heinberg, C. 1996: Tumpeland?! Global Økologi 3, p. 2

Heinberg, C. 1996: Hvem beskytter demokratiet mod parlamentet? Salt 5, p. 1.

Heinberg, C. 1996: Godt landmandskab? Global Økologi 3, p. 2

Heinberg, C. 1997: Tanker ved en videnskab. Psyke & Logos 18, 486-498.

Heinberg, C. 1997: Skal tumperne redde verden – når nu de kloge ikke vil? In: Geertsen, I. (ed.): Livet i drivhuset, 180–202. Det Økologiske Råds Årsrapport.

Heinberg, C. 1997: Råstofferne, landskabet og friheden. In:

Agger, P. & Land, B. (ed.): Råstoferfaringer, Roskilde Universitetsforlag, 13–26.

Heinberg, C. 1998: Tunpeland eller Trøjborg. Salt 7/6, 33–36.

Heinberg, C. 1998: Solhverv. Salt 6/7, 28–31.

Heinberg, C. 1998: Kære Helge. Salt 7/5, 27–28.

Heinberg, C. 1998: At kalde en spade ved sit rette navn. In: Madslund, S. (ed.): Bevar bønderne, 44–68. Det Økologiske Råds Årsrapport.

Heinberg, C. 1999: Det er hovedet og ikke hjertet, den er gal med - ikke regnemaskinen Miljøsk 18, 37–40.

Heinberg, C. 1999: Den nye miljøpolitiske dagsorden. In: Nielsen, K.A. (ed.): Risiko, politik og miljø i det moderne samfund, 316–336. Københavns Universitet.

Heinberg, C. 1999: Risiko, teknologi og refleksivitet. In: Hansen, B.S., Holm, J. & Breck, T. (eds): Risikosamfundet – afvikling eller udvikling, 41–46.

Heinberg, C. 1999: Økologisk eksperimentelle zoner. In: Myrtue-Nielsen-N. & Bramming (eds): Hovedland, 245–272.

Heinberg, C. 1999: Ånden i maskinen. Vestjyllands højskole. Årsskrift.

Heinberg, C. 2000: Et par argumenter omkring GMO. Salt 9/5, 22–24.

Heinberg, C. 2000: Uden politik – ingen miljøpolitik. Salt 9/6, 28–29.

Agger, P.W., Nielsen, K.A. & Heinberg, C. 2000: Democratic challenges in risk society. Proceedings of the international transdisciplinarity 2000 conference, Zürich, 224–228.

Heinberg, C. 2000: Livet i Kridthavet. Varv 4, 47 pp.

Heinberg, C. & Ingemann, J.H. 2001: Visionen om det bæredygtige landbrug. Salt 10/6, 18–20.

Heinberg, C. 2001: Økologiske eksperimentelle zoner: samfundets husholdningsskole og udviklingsafdeling. In: Ingemann, J.H. (ed.): Samfundets udviklingsafdeling: bæredygtig udvikling gennem eksperimenter, 31–58. Aalborg Universitetsforlag.

Heinberg, C. 2003: Rejsen til Peary Land. In: Martens, G. et al. (eds): Peary Land, 35–57. Nuuk: Utuagkat.

Håkansson, E. & Heinberg, C. 2003: Da Nordamerika og Asien mødtes i Peary Land – en geologisk ekspeditionsberetning. In: Martens, G. et al. (eds): Peary Land, 189–209. Nuuk: Utuagkat.

Heinberg, C. 2009: Undermålernes sejrsmarch – mod en ny og social darwinisme? Information, 12 February 2009.

Heinberg, C. 2013: Das Leben im Kreidemeer, 72 pp. Stevns Museum/Østsjællands Museum.

Heinberg, C. 2013: Filmen om Eigil Knuth-samlingen: sådan blev den til. Grønland 61, 196–201.

Movies

Heinberg, C. 2000: Eigil Knuth - Billedhugger, forfatter og polarforsker. Doccumentary. Director: Claus Heinberg. 46 min.

Stratigraphy and petrophysical characteristics of Lower Paleocene cool-water carbonates, Faxe quarry, Denmark

JENS MARTIN HVID, FRANS VAN BUCHEM, FRANK ANDREASEN, EMMA SHELDON
& IDA LYKKE FABRICIUS

DGF

The Faxe limestone quarry in eastern Denmark exposes Danian (Lower Paleocene) cool-water carbonate deposits. They constitute remnants of an apparent build-up that covers about 12 km² today. The Danian deposits at Faxe are conspicuous due to their pronounced thickness of coral limestone relative to the regional carbonate system. In the Faxe quarry, scleractinian corals are uniquely exposed in up to 30 m high mounds. The rapid accumulation of scleractinians combined with induration of the mounds may locally have protected the limestone from Quaternary glacial erosion and created a Danian thickness anomaly at Faxe. The position of Faxe above a local fault-bounded basement high and the extent of coral limestone has been better defined by new mapping. A mapped lithostratigraphic surface in the quarry reveals the large-scale organisation of nested bryozoan mounds on three elongated ridges striking NW–SE. The main scleractinian coral mounds are located above this horizon. Data for reservoir characterisation, mainly of the bryozoan mounds, were collected as photographs of the outcrop, petrophysical and petrographical data from cored boreholes, and as ground-penetrating radar sections. Old boreholes and measured sections were used to reconstruct the build-up, and new nannofossil data allow a discussion of stratigraphy and accumulation rate. The petrophysical data show that common mound-building bryozoan packstone has higher permeability and lower capillary entry pressure than chalk, whereas less commonly occurring grain-dominated packstone and grainstone deposits from local higher-energy sites of the mound complex were found to have reduced amounts of coccolith mud, significantly higher permeability and a higher degree of lithification. Based on biostratigraphic age constraints, correlation of flint – limestone couplets and recognised hierarchical patterns, we develop a cyclostratigraphy for the middle Danian and suggest that cyclicity in lithology and petrophysical characteristics of bryozoan limestone are controlled by precession and eccentricity of the orbit of the Earth.

Jens Martin Hvid [jens.martin.hvid@lyse.net], Technical University of Denmark, Department of Civil Engineering, DK-2800 Kgs. Lyngby, Denmark; present address: Vågedalsveien 43, 4020 Stavanger, Norway. Frans van Buchem [fransvanbuchem@gmail.com], King Abdullah University of Science and Technology (KAUST), Thuwal 23955, Saudi Arabia. Frank Andreasen [radarteknik@yahoo.com], Nakskovvej 16, DK-4000 Roskilde, Denmark. Emma Sheldon [es@geus.dk], Geological Survey of Denmark and Greenland, Øster Voldgade 10, DK-1350, Copenhagen K, Denmark. Ida Lykke Fabricius [ilfa@byg. dtu.dk], Technical University of Denmark, Department of Civil Engineering, DK-2800 Kgs. Lyngby, Denmark.

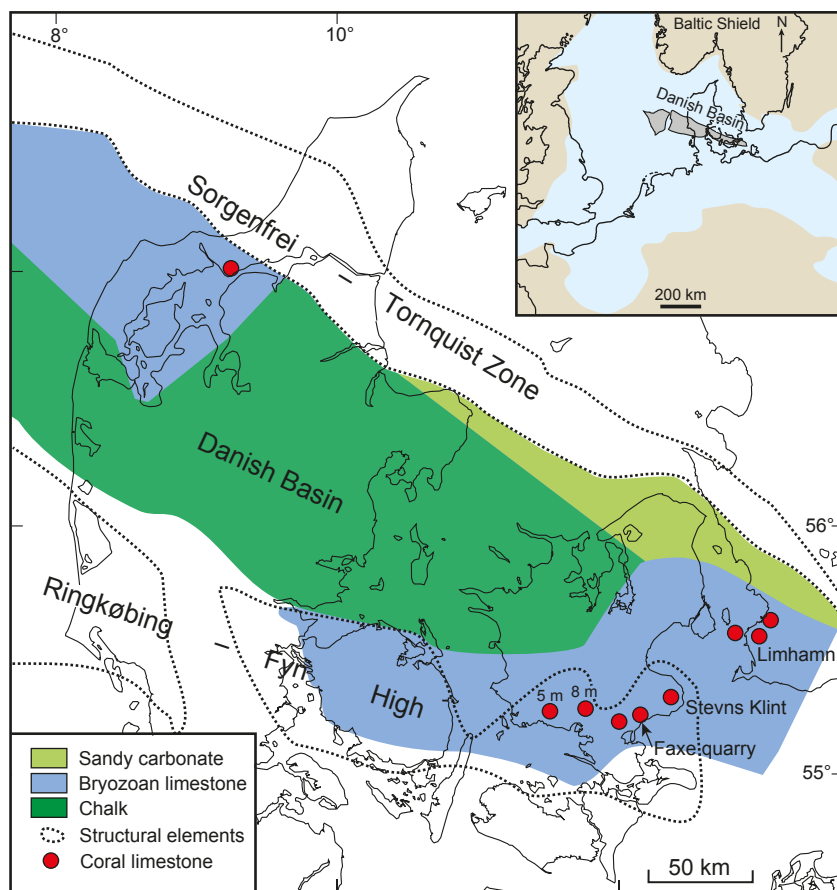*Corresponding author: Ida Lykke Fabricius.*

Fig. 1. Map showing the location of Faxe quarry, main facies distribution and occurrences of middle Danian cool-water coral limestone in the Danish Basin. The inset palaeogeographic map of the late middle Danian of northwest Europe is modified after Bjerager *et al.* (2017).

In the North Sea Basin, Upper Cretaceous – Lower Paleocene (Danian) chalk form reservoirs for oil and gas (e.g. Andersen 1995; van Buchem *et al.* 2018). It is noteworthy that in the adjacent Danish Basin, the Danian chalk grades into bryozoan limestone towards the south-east (Thomsen 1995). These coarse-grained bryozoan limestones have better reservoir properties than the North Sea chalks, however the Danish Basin is not a hydrocarbon province. The bryozoan limestone is found at shallow depths in many areas of Denmark and south-western Sweden and is exposed at several localities, most conspicuously in the coastal cliffs of Stevns Klint and in the Faxe limestone quarry (Fig. 1). The Limhamn quarry in south-western Sweden exposes limestones of lower, middle and upper Danian age (Brotzen 1959; Nielsen *et al.* 2009). Faxe quarry and Stevns Klint (Desor 1846) comprise the classical type localities of the Danian.

The Danian limestone at Faxe constitutes biogenic deposits of bryozoan limestone and coral limestone interpreted to have been deposited in a cool sea at water depths of 200–300 m (Bernecker & Weidlich 1990, 2005). The middle Danian bryozoan limestone at Faxe is part of the Stevns Klint Formation (Surlyk *et al.* 2006), whereas the coral limestone makes up the Faxe Formation defined by Lauridsen *et al.* (2012; Fig.

2). During the last 150 years most geological literature concerning Faxe quarry has focused on palaeontological aspects of the limestone (Gravesen 2001; Schnetler & Milàn 2017; Schrøder & Surlyk 2019) and few studies have documented the general geology. These studies are mostly directed at the coral limestone (Johnstrup 1864; Floris 1979, 1980; Bernecker & Weidlich 1990, 2005; Willumsen 1995; Sigurdsson & Overgaard 1998; Lauridsen *et al.* 2012; Bjerager *et al.* 2017). A review of the geology of Faxe quarry was published by Surlyk & Håkansson (1999).

The closest modern analogue to the cool-water coral mounds at Faxe are mounds formed by the scleractinian coral *Lophelia pertusa* in siliciclastic and carbonate environments on continental shelves in the Straits of Florida and in the North Atlantic, particularly along shelf breaks (Hovland & Mortensen 1999; Freiwald *et al.* 2004; Buhl-Mortensen *et al.* 2015). However, modern or ancient massive cool-water coral limestone mounds intercalated with bryozoan limestone mounds, such as those at Faxe, have not been found outside the Danish Basin.

The purpose of this paper is to present the mound complex at Faxe from a reservoir geological perspective by providing a framework of depositional structures and middle Danian stratigraphic units

illustrated in maps and sections. Old and new data are integrated in order to map external and internal geometry of the limestone build-up, and petrophysical properties of Danian limestone deposits are integrated with petrographic data. The study has the potential to improve hydraulic modelling of Danian limestone aquifers and hydrocarbon exploration in Danian mounds in the North Sea Basin (Surlyk *et al.* 2003). The spatial organisation of the mound complex comprising coral and bryozoan limestone is addressed based on data from outcrops, boreholes and ground-penetrating radar. New biostratigraphic data combined with petrophysical data and correlation of flint horizons are used to investigate the cyclic stratigraphy of the bryozoan limestone.

Fig. 2. Maastrichtian and Danian lithostratigraphy of the Danish Basin (Stenestad 1976; Surlyk *et al.* 2006; modified after Lauridsen *et al.* 2012).

Regional geological setting

The Danish Basin developed as a NW–SE-trending Triassic rift basin, approximately 100 km by 200 km in size, bounded by the Baltic Shield to the north-east and the Ringkøbing–Fyn High to the south-west (Fig. 1). Deposition of mud, sand and carbonate continued until the end of the Early Cretaceous. The Danish Basin together with other north European basins accommodate the Upper Cretaceous – Lower Paleocene (Danian) carbonates (Gale 2002), mainly chalks of the Chalk Group (Knox & Holloway 1992; Johnson & Lott 1993; van Buchem *et al.* 2018). Outcrops towards the eastern margin of the Danish Basin (Fig. 1) contain cool-water calcareous benthic faunas dominated by bryozoans, molluscs and sponges, occasionally with cool-water coral limestone associated with bryozoan limestone and deposited below the photic zone (Bjerager & Surlyk 2007a, b). The siliceous spicular skeletons of the sponges were probably dissolved and re-precipitated as flint nodules parallel to the bedding (Bromley 1967; Surlyk 1997).

The Danian depocentre was situated in the central part of the Danish Basin, where limestone deposits, mainly of chalk are up to 300 m thick (Thomsen 1995). Danian limestone directly underlies Quaternary glacial deposits along the Sorgenfrei–Tornquist zone and on the eastern part of the Ringkøbing–Fyn High (Fig. 1). Outcropping Danian bryozoan limestone is commonly observed as 50–100 m wide asymmetric mounds with a vertical relief of 5–10 m. Asymmetric lower Danian bryozoan mounds are characterised by relatively thick beds and highly dipping southern flanks, probably reflecting southward migration of the bryozoan mounds against the direction of the marine current (Thomsen 1976, 1983; Bjerager & Surlyk 2007a, b). Middle Danian mounds exposed in horizontal sections at Hanstholm in north-western Jylland indicate a south-eastern direction of migration (Thomsen 1983, his fig. 3). The two localities show closely spaced bryozoan mounds with elliptical geometry in planar view, with their long axes on average striking 60° at Hanstholm and 110° at Stevns Klint.

Danian colonial corals have been found within bryozoan limestone at a number of localities in Denmark and south-western Sweden. The main locality is at Faxe quarry (Floris 1980; Bjerager *et al.* 2010; Fig. 1). The second largest concentration of coral limestone is located in the area of the Limhamn quarry, and nearby below the seabed in the Øresund strait a 20 m thick and 200 m wide coral limestone body was indicated on seismic data and sampled in boreholes (Bjerager *et al.* 2010). Observations of coral limestone are reported from 23 boreholes in southern Sjælland within a few tens of kilometres from Faxe quarry (Fig. 3; Table

1). In eight of the boreholes, drillers have described rock samples as coral limestone without scientific documentation (Table 1). The only occurrences of coral limestone confirmed from southern Sjælland outside the Faxe mound complex are those at Herlufsholm and Spjellerup (Ødum 1937). Rosenkrantz (1937) regarded blocks of coral limestone on the beach by the lighthouse at Stevns Klint as probably middle Danian in age (Fig. 3).

Regional modelling of the burial history of the Danish Basin suggests a Neogene exhumation of *c.* 500 m in southern Sjælland, possibly followed by minor Quaternary re-burial due to glaciations (Japsen & Bidstrup 1999). Observations of deformed and crushed flint bands in Faxe quarry indicate that glaciotectonic deformation has taken place (Surlyk & Håkansson 1999). The presence of fractures induced by exhumation and by glacial tectonics must have increased the permeability of the Danian limestone aquifer on a regional scale. This has been demonstrated near the small Karlstrup quarry 30 km north of Faxe, where the permeability is higher by two orders of magnitude in the upper 10 m of the limestone compared with deeper unfractured levels (Jakobsen *et al.* 1993).

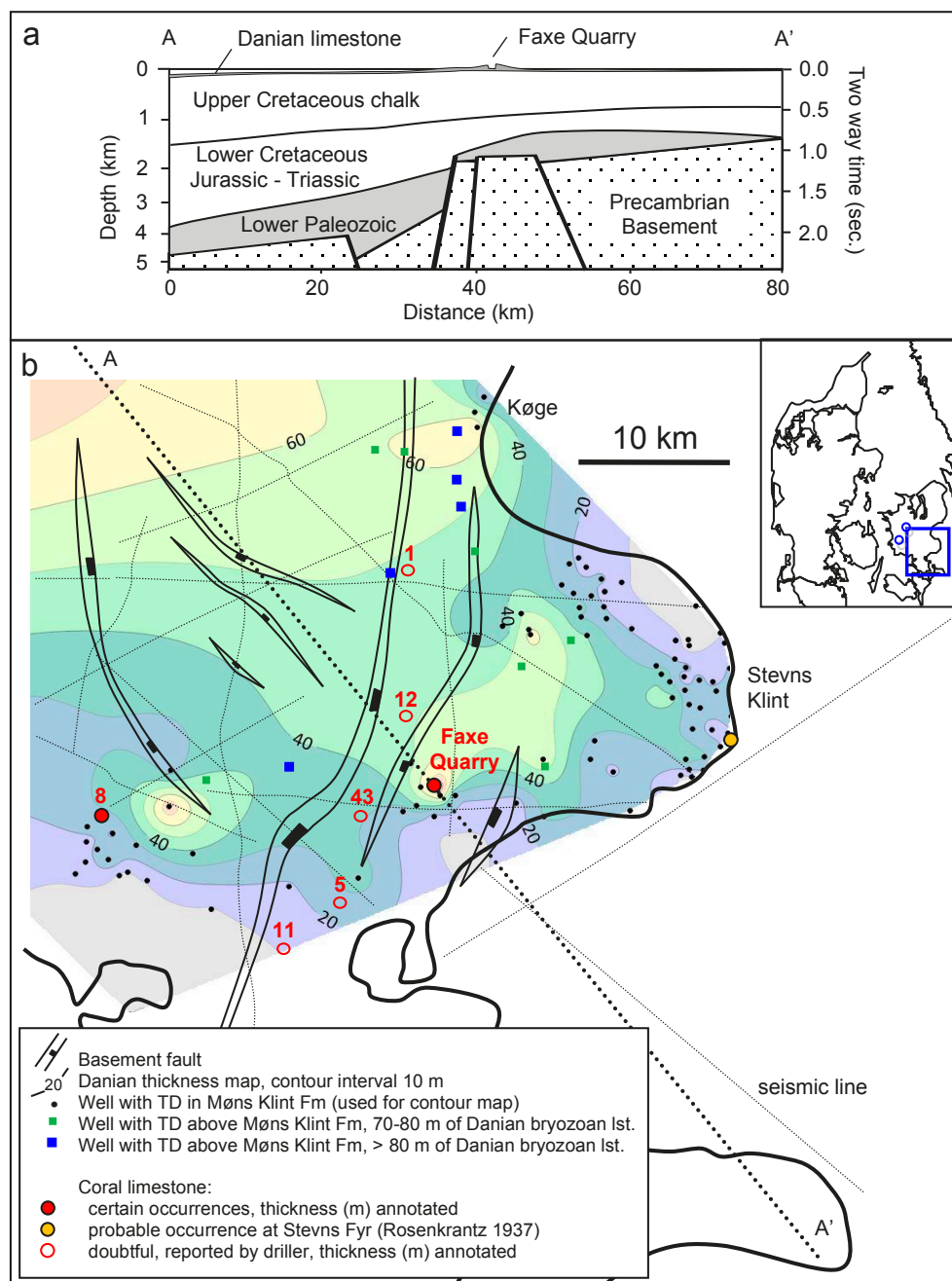**Fig. 3.** Danian thickness map of south-east Sjælland. **a:** Cross section showing Faxe quarry situated above a basement horst. The horizons: Base Upper Cretaceous, Top Pre-Zechstein and Top Precambrian were interpreted from seismic lines. **b:** Map showing basement faults, occurrences of hexacoral limestone, and thickness variation of Danian deposits gridded using wells with TD below the Rødvig Formation.

Table 1. Boreholes on southern Sjælland penetrating lithology reported as coral limestone

DGU borehole	Year drilled	Location	Approx. dist. direction from Faxe quarry	Coral limestone thickness (m)	Lithology above/ below coral limestone	Driller
220.3	1907	Spjellerup	37 km, west	5	clay/chalk	Unknown
220.4	1907	Spjellerup	37 km, west	5	clay/chalk	Unknown
221.52C	1918	Herlufsholm	25 km, west	8	brz. lst./brz. lst.	Unknown
217.26B	1936	Faxe brewery	0.5 km, NW	13	brz. lst./Cerithium lst.	Brøker-Sørensen
222.33	1939	Stubberup	0.5 km, SW	38*	clay/chalk	Brøker-Sørensen
217.178	1944	Viverup	5 km, NW	12*	brz. lst./brz. lst.	Christiansen
222.121	1950	near Faxe q.	0.2 km, SW	2	clay/brz. lst.	Christiansen
222.3f	1952	Hovby	1.5 km, SW	23*	lst./lst.	Anthonsen
217.26D	1954	Faxe brewery	0.5 km, NW	1	clay/brz. lst.	Brøker-Sørensen
217.233	1955	Sædder	20 km, NNW	1*	clay/end of well	Andersen
222.219	1960	Snesere	15 km, SW	11*	clay/chalk	Anthonsen
217.568	1970	within quarry	Faxe q. north	13	brz. lst./brz. lst.	Geoteknisk Inst.
217.569	1971	within quarry	Faxe q. NE	8	brz. lst./brz. lst.	Geoteknisk Inst.
217.570	1971	within quarry	Faxe q. north	32	brz. lst./brz. lst.	Geoteknisk Inst.
217.572	1971	within quarry	Faxe q. north	12	brz. lst./brz. lst.	Geoteknisk Inst.
217.576	1971	within quarry	Faxe q. NE	10	brz. lst./brz. lst.	Geoteknisk Inst.
217.578	1971	near Faxe q.	0.1 km, NE	8	brz. lst./brz. lst.	Geoteknisk Inst.
222.328	1972	Kongsted	5 km, WSW	43*	clay/end of well	Anthonsen
222.394	1976	Bækkerskov	10 km, SW	5*	clay/end of well	Anthonsen
222.401	1976	Hovby	2 km, SW	5*	clay/brz. lst.	Anthonsen
222.447	1986	at quarry wall	Faxe q. south	10	brz. lst./brz. lst.	Brøker-Sørensen
217.815	1994	within quarry	Faxe q. NE	11	brz. lst./brz. lst.	Faxe Kalk A/S
217.832	1996	within quarry	Faxe q. NE	28	top of well/end of well	Faxe Kalk A/S

Coordinates and reports for each borehole are available from Jupiter, the national well database (https://www.geus.dk/produkter-ydelser-og-faciliteter/data-og-kort/national-boringsdatabase-jupiter)
Coral limestone thickness is confirmed by geologists from the Geological Survey of Denmark and Greenland and described by borehole drillers.
*: Drillers' description of rock as coral limestone is considered unreliable.

The Faxe locality

Faxe quarry is located on the north-eastern flank of the Ringkøbing–Fyn High (Fig. 1). At this locality, as in southern Sjælland in general, the dominant Lower Paleocene lithology is bryozoan limestone in strata with a rather complete suite of nannofossil zones present in the lower and middle Danian (Thomsen 1995). The up to 40 m high walls bounding the Faxe quarry expose mounded limestone of middle Danian age (Surlyk & Håkansson 1999). Individual mounds are 50–100 m in diameter and are composed of either bryozoan limestone or cool-water coral limestone (Bernecker & Weidlich 1990, 2005). A cored groundwater well 217.26B from 1936 found Fiskeler Member and Cerithium Limestone Member above Maastrichtian chalk of the Møns Klint Formation and overlain by interbedded hexacoral and octocoral limestone of early Danian age (Rosenkrantz 1937). A hiatus above Cerithium Limestone as found at Stevns Klint (Rasmussen *et al.* 2005) could be present at Faxe.

Four main lithofacies have been distinguished in the quarry: (1) bryozoan limestone with flint, (2) cool-water hexacoral limestone, (3) cool-water octocoral limestone and (4) bryozoan grainstone without flint.

1. Bryozoan limestone with flint mainly has a packstone texture and forms asymmetrical mounds with lenticular or sheet-like flint horizons parallel to bedding. This limestone is cream coloured, weakly laminated or partly bioturbated (Floris 1979).

2. The term hexacoral limestone is used here for azooxanthellate scleractinian limestone developed as lithoherms (Willumsen 1995). It is a coral boundstone-rudstone forming mounds with geometry controlled by early lithification. Willumsen (1995) identified a cyclic pattern in the early lithification. The induration varies from unlithified to strongly cemented. Local leaching of corals has been interpreted as being caused by late meteoritic diagenesis (Weidlich & Bernecker 1991). Hexacoral limestone dominated the exposed deposits when the quarry was described at an early stage of excavation, and an older and

a younger coral limestone were distinguished by Johnstrup (1864). He observed a so-called 'bryozoan limestone' rich in coral fragments between the older and younger coral limestone and in small basins in marginal parts of the quarry. This coral-rich 'bryozoan limestone' was later described as a transitional
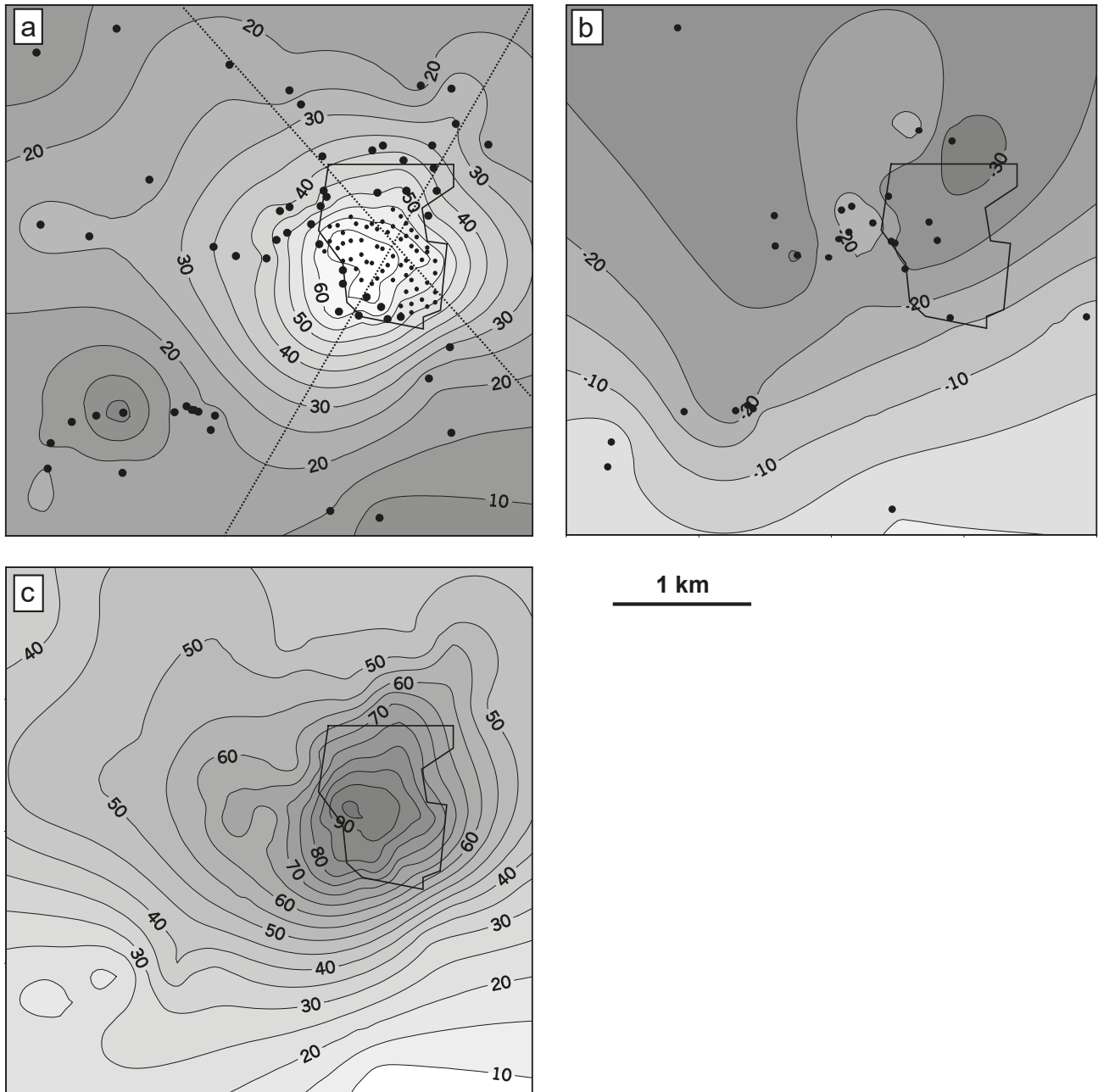

Fig. 4. Structural maps of the Faxe area, contoured using data from groundwater wells and measured sections. Faxe quarry in 1994 is outlined by a closed polygon on the maps. **a:** Top preserved Danian limestone reconstructed to its pre-excavation state using data from Johnstrup (1864) (small dots). Numbers are metres above mean sea level. The dotted lines show the locations of two cross sections in Fig. 5. **b:** Top Cretaceous structure map. A positive anomaly to the west of the quarry is constrained by groundwater wells. **c:** Isochore (m) map of Danian strata prior to excavation. **d:** An internal surface at the base of thick coral limestone corresponding to base of growth unit 2 in Bjerager *et al.* (2017). The geometries of three 700–1100 m long ridges of bryozoan limestone striking NW–SE are interpreted in red. **e:** Isochore (m) map of the strata between the top of bryozoan ridges and top Danian limestone. The locations of six cored boreholes are shown in blue. **f:** Aerial photograph of Faxe quarry in 2006 showing location and interpreted geometry of seven late middle Danian bryozoan mounds outcropping in the southern quarry wall. The location of a ground-penetrating radar section (Fig. 7b) is shown in the north-eastern part of the quarry.

type of coral limestone (Bernecker & Weidlich 1990, 2005).

3. Octocoral limestone, the 'white limestone' of Johnstrup (1864), is a very weakly lithified, white, chalky wackestone with fragments of octocorals and bryozans. Biogenic and sedimentary structures are weak or absent in the octocoral limestone, but nodules and thin layers of flint can occur. This limestone was deposited in troughs between bryozoan mounds (Surlyk & Håkansson 1999) and it is typically overlain by hexacoral limestone.

4. Coarse, cross-bedded bryozoan grainstone without flint was deposited in the northern part of Faxe quarry above an erosional surface developed as a hardground (Willumsen 1995). Sclerosponges and bryoliths found in this lithology indicate an origin in relatively shallow water (Surlyk & Håkansson 1999).
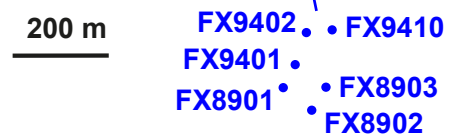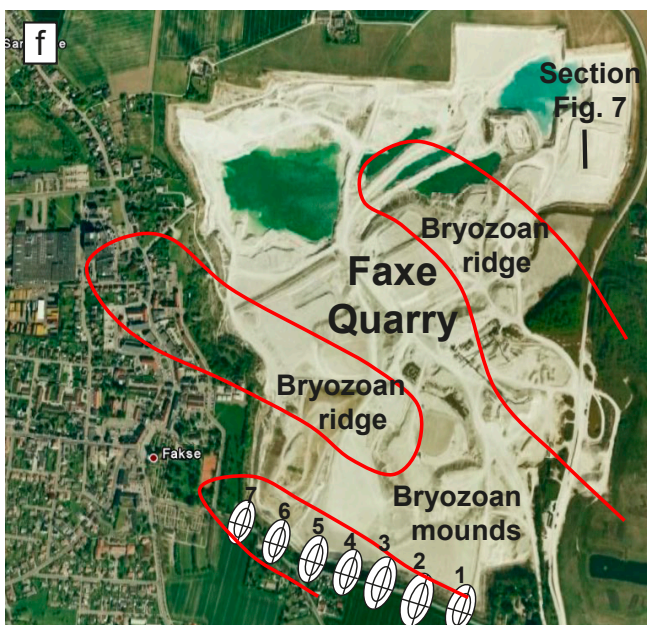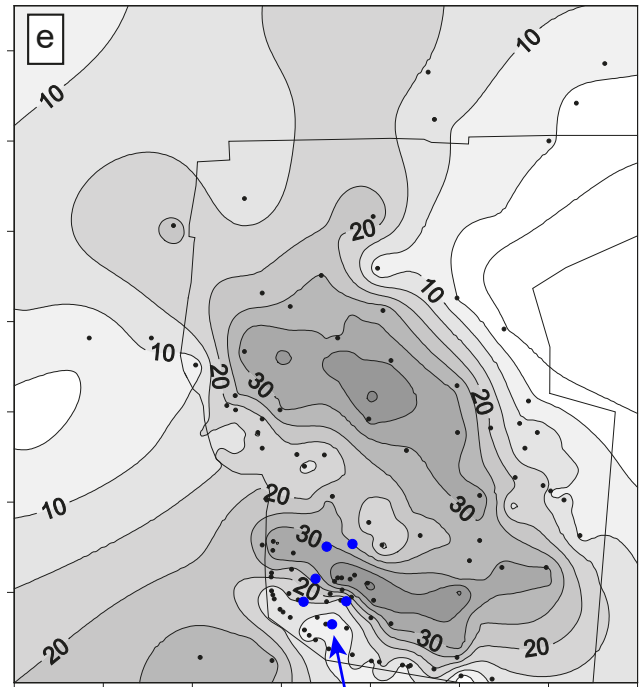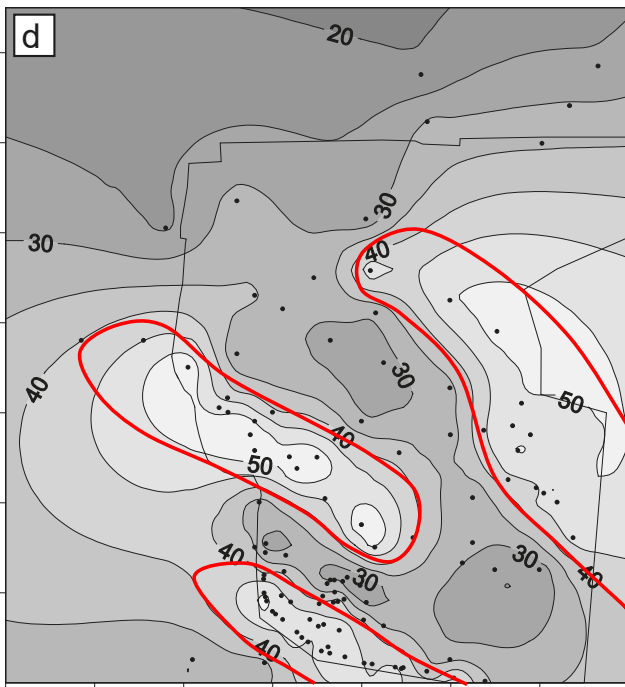
Data and methods

Most of the existing geological data from the Faxe quarry consist of sediment cores and 2D ground-penetrating radar (GPR) data acquired by Faxe Kalk A/S in order to identify the presence of the flint-free limestone desired for quarrying (Sigurdsson & Overgaard 1998).

A 37 m long core from the shallow borehole FX8901, located in the southern part of the quarry (Fig. 4) was extensively used in this study. Additional plug samples were drilled from other cores, from the outcrop walls and from larger blocks taken to the laboratory. He-porosity and Klinkenberg-corrected permeability were measured. Water drainage capillary pressure curves were obtained using the porous plate method (Andersen 1995). Descriptions of bryozoan limestone depositional texture follow Dunham (1962) with the modified definition of grain size less than 62 μm for carbonate mud (Wright 1992), and we distinguish between mud-dominated and grain-dominated fabric for packstones (Lucia 1995). After disintegration by freeze-thaw cycles, samples were used for grain size analysis by wet sieving. A set of 13 samples of mainly bryozoan limestone was taken from cores and outcrop in the southern part of the quarry for nannofossil biostratigraphy. The samples were dated using the nannofossil zonation of Varol (1998). Smear slides were prepared and basic presence/absence counting was used. Limestone blocks were abraded with a 50 bars water jet in order to remove coccolith matrix from the surface. The blocks were then examined for small-scale sedimentary structures and variation in depositional texture.

Ninety thin sections were prepared from the plugs after measurement of porosity and permeability. Texture, content of skeletal grains, visible porosity, intra-fossil porosity, and size of skeletal grains were estimated visually at low magnification (×2 – ×16) using reflected and transmitted light. Petrographic image analysis was carried out on six digital backscattered electron (BSE) images in order to calibrate the values estimated from thin section. Quantification of grains and pore space on all scales was undertaken using images representing 3 mm by 4 mm, 0.3 mm by 0.4 mm and 0.03 mm by 0.04 mm.

A 2D data set of fifteen 40–50 years old semi-regional seismic lines from south-east Sjælland was interpreted in order to clarify the deep structural setting at Faxe (Fig. 3). The Base Upper Cretaceous Chalk, Top pre-Zechstein and Top Precambrian basement horizons were interpreted with confidence on 14 seismic sections. Two deep wells, Slagelse-1 and Stenlille-1, located west and north-west of the mapped area, respectively, were used for mapping of horizons

(Fig. 3b inset map). The structure and thickness of the Danian limestone deposits in south-east Sjælland were mapped using data from several hundred groundwater wells. Wells with TD above Møns Klint Formation, represented by green and blue squares in Fig. 3, were not used for gridding. At Faxe quarry, the base and top surfaces of the Danian deposits and the basal surface of massive coral limestone were mapped by combined use of data from groundwater wells and cored slim boreholes, in addition to published sections of now excavated parts of the quarry (Johnstrup 1864; Rosenkrantz 1937; Floris 1979, 1980; Bernecker & Weidlich 1990, 2005; Willumsen 1995). The measured sections by Johnstrup (1864) were particularly useful for mapping the top surface and the internal surface at the base of massive coral limestone in the central part of the quarry, where early excavations had taken place. A subdivision of the massive coral limestone into units U2–U5 by Bjerager *et al.* (2017) has been used in this paper. Fischer plots were made to display variations in vertical thickness between flint horizons (Day 1997). A five point moving average was applied to core porosity data from borehole FX8901 to represent limestone porosity as a continuous curve with resolution similar to a well-log.

In the southern part of the quarry, photo mosaic and 2D GPR data were used to construct 2D sections, which together resolve individual flint horizons. GPR reflections result from changes in dielectric properties mainly related to contrasts in water content that can be caused by changing lithology and porosity (Bristow & Jol 2003). The GPR data were acquired using 40 MHz antennae carried at constant speed along the quarry edge, while recording thirty traces per second. Recorded 2D GPR data were combined to form longer sections which were filtered but not migrated. The electromagnetic wave velocity in the limestone was calibrated to 0.07 m/ns and used for depth conversion, giving imaging depths of up to 18–20 m.

Results and discussion

Danian carbonates of south-east Sjælland
Semi-regional mapping of Danian limestone thickness and underlying structures in south-east Sjælland reveals a broad picture of the structural setting of the limestone deposits near Faxe (Fig. 3), although mapping of limestone thickness and interpretation of thickness anomalies are hampered by glacial erosion and deformation (Jakobsen 1996) and clustering of groundwater wells in proximity to towns.

Base Upper Cretaceous Chalk is interpreted as an unfaulted NNW-dipping surface with a time-depth

of 570 ms two-way-travel-time (TWT) at Faxe. The Top pre-Zechstein surface dips NW with a >50 km long, NNE-striking basement fault located 6 km west of Faxe quarry, and a shorter sub-parallel basement fault located 2 km west of Faxe quarry. Lower Palaeozoic sediments are present at 850 ms TWT on a basement high below Faxe quarry (Fig. 3a) and are buried at depths of up to *c.* 5 km some 15 km west of Faxe. The basement high is bounded to the south-east by a third NNE-striking fault.

The mapped thickness of Danian strata is uncertain except in wells drilled into the underlying Upper Cretaceous Møns Klint Formation. Drillers observations of coral limestone are not confirmed (Fig. 3b). A continuous Danian thickness of >50 m to the north-east of Faxe quarry may be a mapping artefact. However, Danian strata more than 70 m thick is reported *c.* 10 km east and north-east of Faxe quarry without reaching the K/T boundary. Three groundwater wells penetrating >70

m of Danian deposits are located west of Faxe quarry towards Herlufsholm and Spjellerup and are proven localities of coral limestone (Figs 1, 3b). Danian strata >80 m thick are also located south of the town of Køge about 20 km to the north of Faxe. Spurious large thicknesses of bryozoan limestone could represent areas of glaciotectonic thrusting or lack of glacial erosion.

The Faxe mound complex

External and internal structures and main lithofacies of the entire mound complex at Faxe are shown in Figs 4 and 5. A reconstructed Top Danian limestone surface showing the geometry of the mound complex before limestone excavation started reaches a height of 70 m above mean sea level (Fig. 4a). Its relatively flat crest suggests an approximately 10 m higher elevation before erosion in the Quaternary or Neogene (Fig. 5a). The outer geometry of the mound complex is expressed
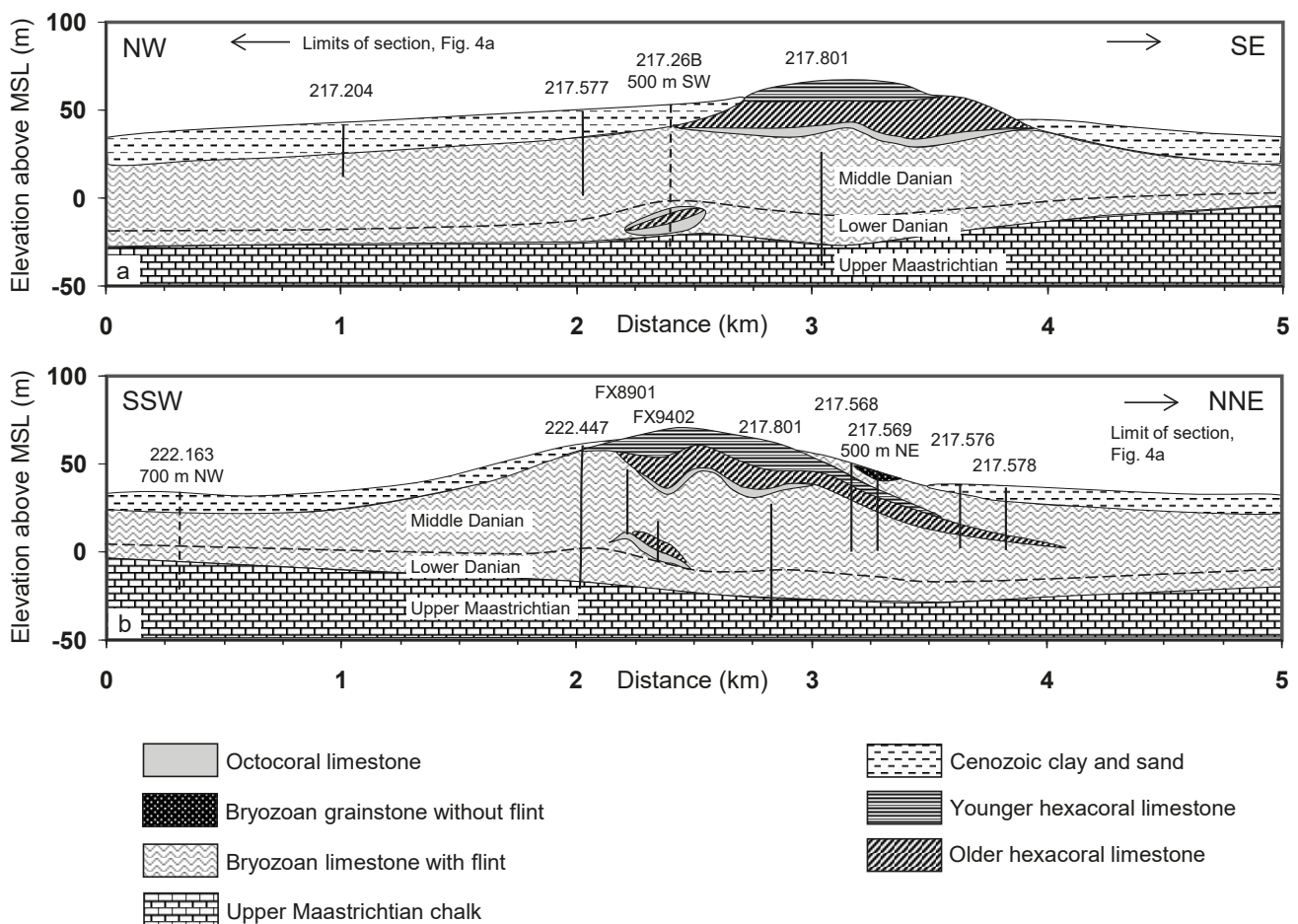
Fig. 5. Cross sections showing thickness variation in the Danian limestone at Faxe with main lithofacies and stratigraphy before excavation (for locations see Fig. 4a). **a:** NW–SE cross section along the northern trough between bryozoan ridges (Fig. 4d), showing thick coral limestone units overlying bryozoan limestone. **b:** Cross section perpendicular to the three bryozoan ridges (Fig. 4d). Note the occurrence of bryozoan grainstone to the north-east. Elevation above m.s.l. (present day mean sea level).

as a circular anomaly on the top Danian limestone surface and has a relief of 45 m, covering an area of approximately 4 km^2 (Fig. 4a).

The Top Cretaceous Chalk surface on which the Danian limestone was deposited is presently an irregular surface dipping to the north by 1% over 2.5 km with a vertical relief of 25 m (Figs 4b, 5). The shape of this surface and its overlying isochore of Danian limestone (Fig. 4c) may have been influenced by ice moving from the south-east during the Late Quaternary (Houmark-Nielsen 1988), but it can also be explained by syndepositional movements of underlying basement faults (Fig. 3), or more likely by erosive bottom currents (Lykke-Andersen & Surlyk 2004). The Danian

limestone deposits at Faxe had a maximum thickness of 97 m after uplift and removal of overlying sediments since the Neogene (Thomsen 1995; Japsen & Bidstrup 1999) and before excavations began (Fig. 4c).

A well-defined lithostratigraphic surface between the mounded middle Danian bryozoan limestone and the overlying thick cool-water coral limestone is found at and close to the quarry (Figs 4d, 5). This surface demonstrates three conspicuous ridges of more or less similar geometry. The bryozoan limestone ridges are characterised by elongated NW–SE striking bases at approximately 35 m above present mean sea level (m.s.l.) and reach 50 m above m.s.l. at their crests. Their lateral dimensions are 700–1100 m by 200–300 m at
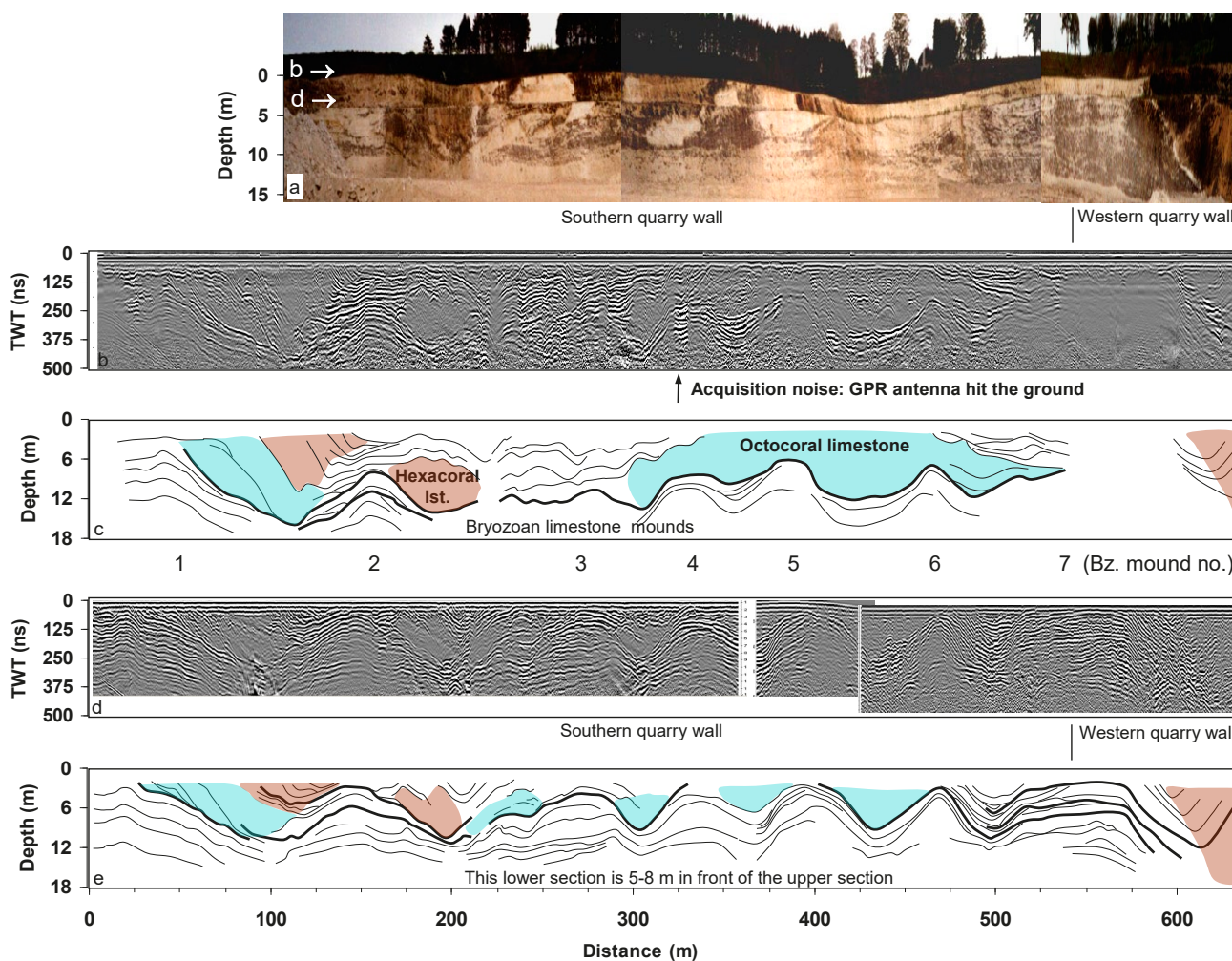
Fig. 6. a: Photomosaic, **b, d**: ground-penetrating radar (GPR) sections, and **c, e**: interpretations of GPR reflectors along the southern quarry wall. Two GPR sections separated by 5 m vertically and laterally were recorded and portray bryozoan mounds numbered 1–7, which make up the southern bryozoan ridge (Figs 4d, 4f). Interpreted reflectors are regarded as chronostratigrahic surfaces. The strongest and most continuous reflectors are interpreted with bold lines. The main upper bounding surface defining the bryozoan mounds is overlain by octocoral limestone (blue) or hexacoral limestone (brown), both of variable thickness. Limestone without colour is bryozoan limestone. Lateral changes in limestone facies occur along chronostratigraphic surfaces. A detailed geological description of the southern wall is given in Bjerager *et al.* (2017).

their bases with relief up to 15 m. The southern ridge is fully exposed in the southern quarry wall where its internal structure has been mapped by ground-penetrating radar (Fig. 6). The upper part of the ridge is composed of aligned bryozoan mounds separated and covered by octocoral limestone and hexacoral limestone (Figs 4f, 5).

The two troughs between the three bryozoan limestone ridges (Fig. 4d) are primarily filled with thick cool-water coral limestone representing Faxe Formation units U2–U6 of Bjerager *et al.* (2017), and locally by interfingering bryozoan limestone. The thickness of coral limestone from the base of the two troughs to the top Danian limestone surface amounts to *c.* 40 m (Fig. 4e). The coral limestone fill of the Faxe Formation grew to a higher elevation than the bryozoan limestone ridges (Fig. 5). Overgrowth by hexacoral limestone of individual bryozoan mounds is exposed in the southern quarry wall (Fig. 6c; Bjerager *et al.* 2017). The wider northern trough (Fig. 4d) is situated in the central part of the quarry and is mainly defined from sections measured by Floris (1980). Octocoral limestone, locally more than 10 m thick (Fig. 6), forms the deep fill of the troughs interfingering with, or more commonly overlain by, hexacoral limestone (Fig. 5). The octocoral limestone contains fragments of octocorals and bryozoans 'floating' in a coccolith matrix. Octocoral packstone has been observed in the trough between mounds 5 and 6 (Figs 4f, 6).

Bryozoan grainstone locality

An up to 9 m high and >100 m wide north-south section of mainly indurated bryozoan grainstone with large-scale cross-stratification that was excavated in the north-eastern part of Faxe quarry in 1996, was not found to contain flint and is characterised by a decreasing amount of carbonate mud upwards through beds and bundles of beds (Figs 4f, 5b, 7a). GPR data and interpretation support the observation of bedforms dominated by low-angle troughs, known as swaley cross-stratification (Allen & Underhill 1989), which has not been observed elsewhere in Faxe quarry (Figs 7b, 7c). The deepest and most mud-rich parts of the exposure are characterised by a grain-dominated packstone texture. The GPR data imaged deeper than the initially exposed section, including the northern flank of a bryozoan mound which was later exposed after further excavation (Figs 4f, 7b). From observations during excavation, the grainstone accumulation was estimated to cover at least 200 m by 200 m and was apparently deposited in a local depression. Elevation above present-day mean sea level of the exposure was estimated at 30–35 m (Fig. 5). The low content of carbonate mud could have been caused by a high-energy depositional environment
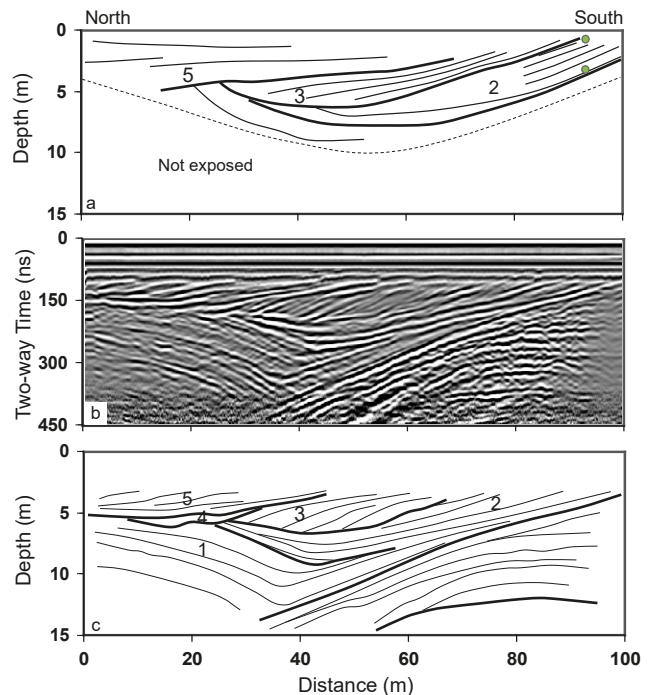
Fig. 7. A large accumulation of cross-bedded bryozoan grainstone without flint bands located in the north-eastern part of the quarry (Fig. 4f). **a:** Line drawing of bed boundaries measured in the field and adjusted using photos. An upwards reduction in carbonate mud and an upwards higher degree of induration was noticed in the field. Two end-member samples shown as green circles were examined for depositional texture, porosity and permeability. **b:** GPR profile along a wall section of bryozoan grainstone where reflections indicate contrasts in porosity. **c:** Interpretation of the GPR profile showing bedding structures. Bundles of grainstone beds numbered 1–5 are separated by interpreted breaks in sedimentation given by thick lines.

driven by bottom currents or a storm event (Rebesco *et al.* 2014). Similar mud-poor bryozoan grainstones of early middle Danian age found at Skillingsbro and Hammelev in eastern Jutland were probably related to shallow water depth (Thomsen 1995).

Stratigraphy in Faxe quarry

Lithostratigraphy
The succession of lithofacies found in Faxe quarry is shown in Fig. 5 in a cross section that covers the entire mound complex. Coral limestones of the Faxe Formation are found at three distinct stratigraphic levels: (1) In the lower Danian known only from well 217.26B (Fig. 5a; Rosenkrantz 1937), (2) from previously unpublished boreholes in the southern part of the quarry (Figs 4f, 5b, 8), and (3) the main exposed body

of up to 40 m thick middle Danian coral limestone (Johnstrup 1864; Floris 1980; Bernecker & Weidlich 1990, 2005; Willumsen 1995; Bjerager *et al.* 2017). At all stratigraphic levels coral limestone bodies consist of lithified hexacoral limestone underlain by or intercalated with chalky octocoral limestone and are vertically separated by regionally deposited bryozoan limestones of the Stevns Klint Formation (Surlyk *et al.* 2006). The southern bryozoan ridge is stratigraphically positioned between middle Danian octocoral limestone and hexacoral limestone (Figs 5b, 8). The limestone in the boreholes in Fig. 8 display flint and thin clay layers. A local accumulation of bryozoan grainstone is deposited stratigraphically above the thick coral limestone on the north-eastern flank of the mound complex (Figs 4f, 5b, 7).

The generally mound-forming and flint-bearing bryozoan limestone deposits (Figs 5, 6, 8), were cor-
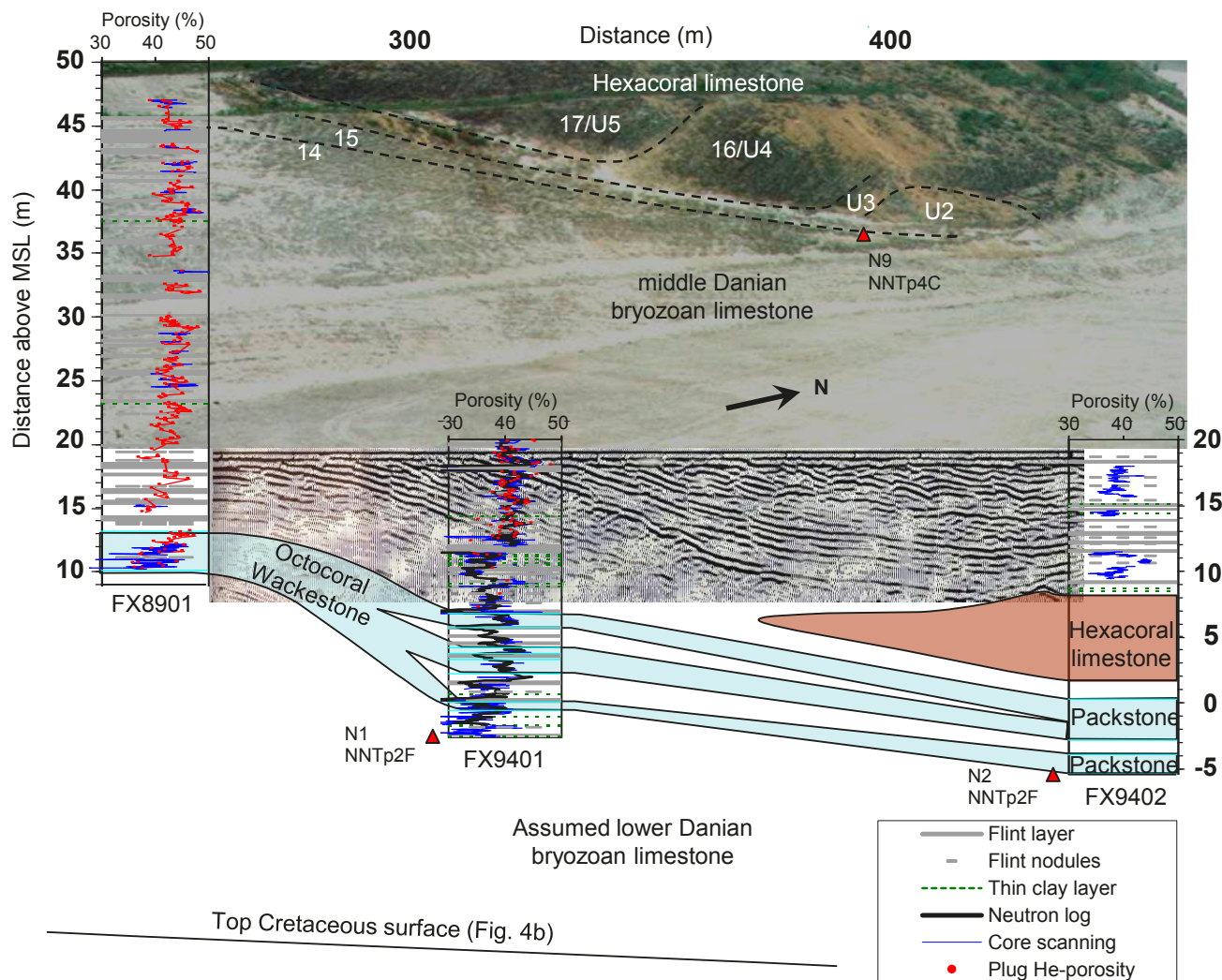
Fig. 8. South-western part of the Faxe quarry in 1995 with a GPR profile and data from cored boreholes (Fig. 4e) correlated by timelines. Borehole FX8901 was drilled before excavation down to 10 m above mean sea level (MSL). The photograph shows the north-western flank of the southern bryozoan ridge (Fig. 4d) overlain by a thin white octocoral limestone and a thick hexacoral limestone coloured dark brown by modern algae (Bernecker & Weidlich 1990, section G). The transition from bryozoan limestone into coral limestone is annotated with numerical units from this study and the U units of Bjerager *et al.* (2017). GPR reflectors are recognised to onlap a strong reflector that represents the top of a 30 cm thick outcropping flint layer. The GPR section shows normal faulting that can be traced to the western wall, and glaciotectonic deformation in the upper, northern part of the section. Locations of nannofossil samples N1, N2, and N9 are shown in red trinangles with their age (Table 2). The dip of the Maastrichtian chalk surface is found from mapping (Fig. 4b). The distances from FX8901, FX9401 and FX9402 to the lower part of the western wall are *c.* 30 m, 50 m and 70 m, respectively. Limestone porosity was derived from neutron logging (FX9401), core density scanning and Helium porosity measurements.

related in the southern and western quarry walls (Fig. 9) and with borehole FX8901, guided by measured depth and flint and limestone characteristics. Based on cycles in core porosity and permeability, which may be directly related to depositional cycles, the core of borehole FX8901 was subdivided into informal stratigraphic units numbered 1–15 which each laterally in the quarry walls correspond to up to five flint - bryozoan limestone couplets mostly bounded by thick, continuous flint layers and/or subtle unconformities (Figs 9, 10). The near-horizontal, layered units 3–7 exposed in the southern quarry wall (Fig. 9) comprise the deeper parts of the southern bryozoan ridge and are overlain by a middle section of units 8–10 with erosionally truncated flint-limestone couplets of variable thickness (Figs 9, 11). The ridge is topped by bryozoan mounds mostly displaying aggradational stacking (Figs 6, 9).

Borehole FX8901 reveals a low-porosity bryozoan limestone at stratigraphic unit boundaries, alternating with sections of higher porosity within units (Fig. 10). All flint horizons are drawn as continuous layers, but most are around 10 cm thick and consist of discontinuous nodules. The main lithology is bryozoan limestone, with zones of octocoral limestone at
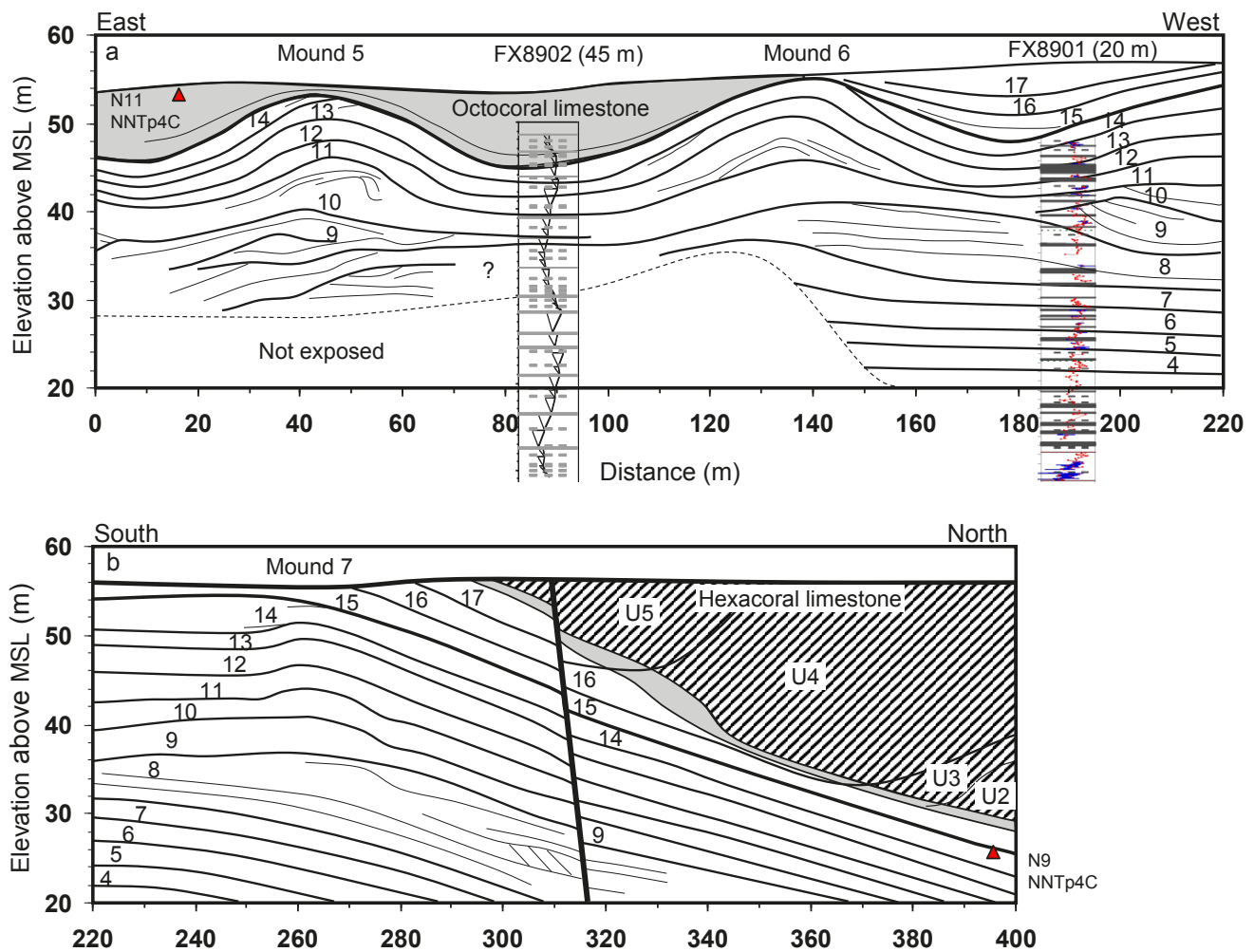
Fig. 9. Photography-based correlation of selected flint horizons in bryozoan limestone and main bedding planes in coral limestone are shown for **a**: a length section and **b**: a cross section of the southern bryozoan ridge (see Fig. 4f). Flint layers are shown as grey bands. Stratigraphic units of up to five flint-limestone couplets are numbered 1–17. Single truncated zones of bryozoan limestone and overlying flint are represented by units 8–10. Inclined zones in unit 8 at 310 m are interpreted as slumping. Borehole FX8901, located 20 m to the north of the section, shows porosity on a scale from 30 to 50% and flint. Borehole FX8902, located 45 m to the north of the section, displays the cumulative deviation from mean thickness of flint-limestone couplets (Day 1997), meaning that the curve deviates to the right when beds become thicker than average going upwards. The thick black line is a normal fault with a vertical throw of 1–2 m. The location of nannofossil samples N9 and N11 is shown in red triangles. Detailed geological descriptions of the coral limestone were published by Bernecker & Weidlich (1990, 2005), Lauridsen *et al.* (2012) and Bjerager *et al.* (2017).

depths of 34–35 m and at the top of the core. Unit 1 consists of a transition facies of octocoral limestone with upwards increasing amounts of bryozoans (Fig. 10) and an asymmetrical porosity cycle that becomes more symmetrical downflank in boreholes FX9401 and FX9402, where octocoral limestone interfingers with bryozoan limestone (Figs 8, 10). Unit 1 contains a thick flint layer a few tens of centimetres below its top, where pyrite also occurs. Unit 2 is 4 m thick and spans approximately five flint-limestone couplets and reveals a well-developed porosity cycle indicating no significant breaks in deposition (Fig. 10). The upper-most and lowermost 10–20 cm of unit 2 are strongly indurated, resulting in a porosity reduction of about five porosity units compared with the porosity in the middle of unit 2. The lithofacies at the boundaries

of unit 2 are more grain-rich than in its central part. Units 2 and 3 grade laterally into hexacoral limestone downflank in borehole FX9402 (Fig. 8). Units 4, 5 and 7 are also topped by 20–30 cm thick indurated bryozoan limestone zones, and units 4 and 5 were easily traced in the southern quarry wall (Fig. 10).

Zones of indurated bryozoan limestone with low porosity are most often zones with low amounts of coccolith mud and high permeability, as described below. The permeability variations over stratigraphic units 4–7 are large and vary between 3 and 10 mD for the most mud-rich samples and 100–200 mD for samples with low mud content (Figs 9, 10). A smoothed long-wave bounding curve for the permeability data spans the lower units 3–7 and upper units 11–14 in the upper part of the bryozoan ridge. There is a shortage of
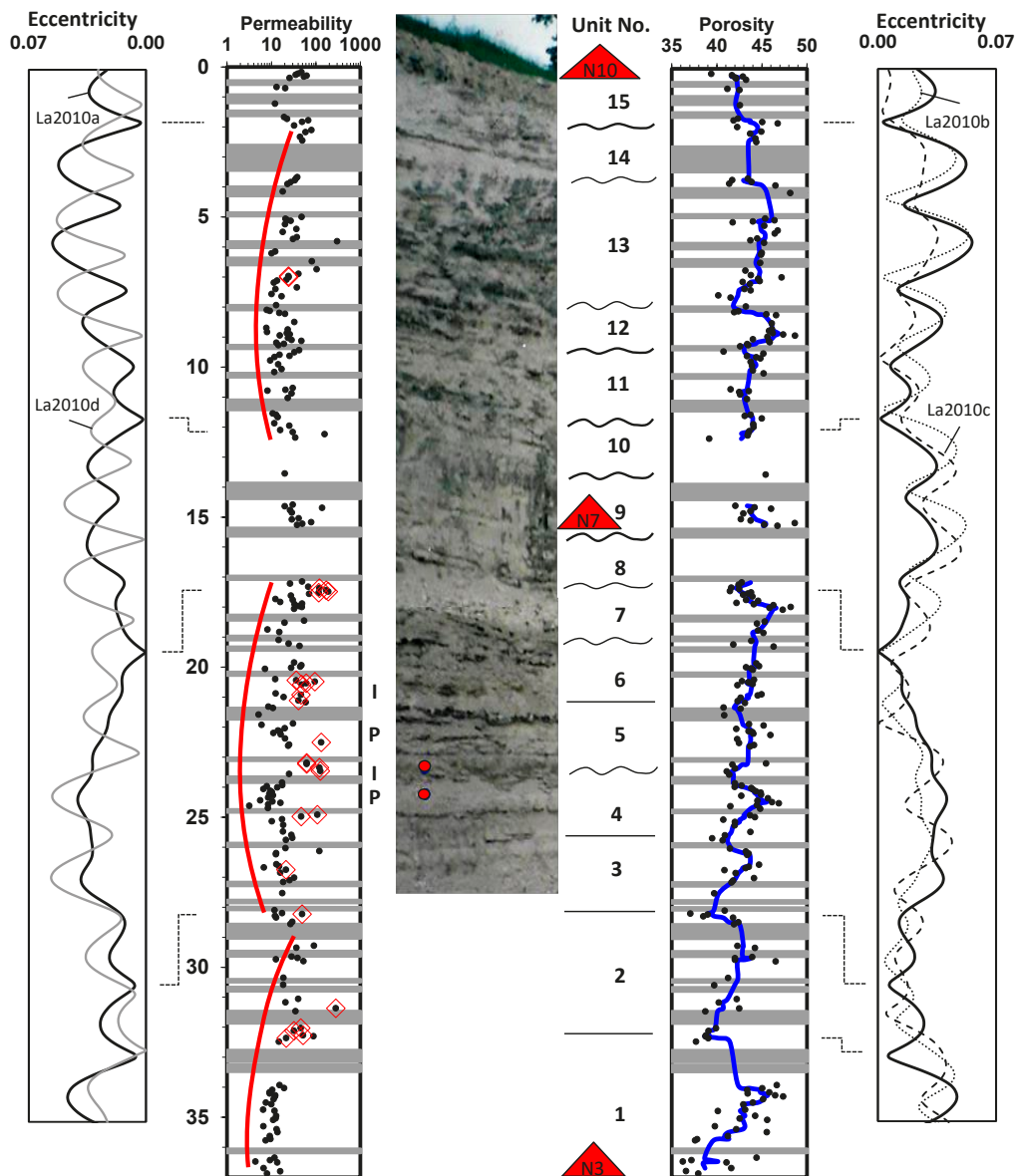
Fig. 10. Porosity and horizontal permeability of 248 core plugs from borehole FX8901 (Fig. 4e) plotted against depth. Flint layers are shown as grey bands. The most grain-rich core plugs are marked by red diamonds. Fifteen stratigraphic units with up to five flint-limestone couplets are laterally correlated into borehole FX8901 where they are characterised by cycles in porosity shown by an average curve in blue. Multiple units form longer cycles of permeability indicated in red. Indurated (I) bryozoan limestone alternating with more porous zones (P) of stratigraphic units 4–6 are shown. Porosity, permeability and depositional texture of plugs taken from the southern wall (red dots) confirmed the reservoir characteristics from borehole FX8901 situated 20 m to the north of the wall. The position of nannofossil samples is marked with red triangles. Calculated eccentricity curves La2010a-d are plotted for the time interval 63.5–64.9 Myr (Laskar *et al.* 2011).
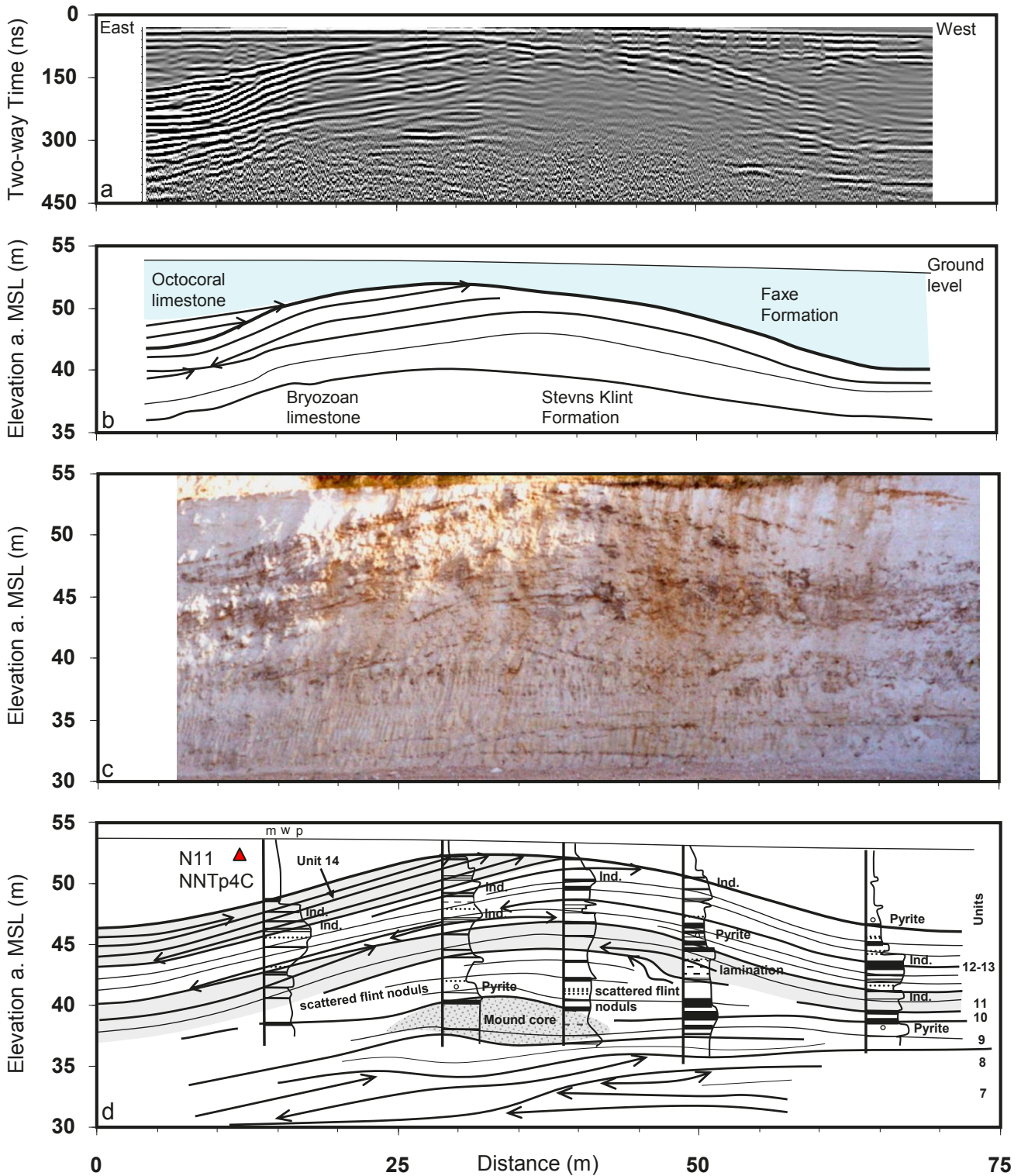
Fig. 11. Details of a typical bryozoan mound, also part of the Faxe S profile (Bjerager *et al.* 2017, Fig. 2). **a:** GPR section recorded along mound 5 (Figs 4f, 9). Strong reflections in the eastern part of the mound may indicate alternating indurated and soft subunits of onlapping flint-bryozoan limestone couplets as verified in the quarry wall. **b:** Interpretation of GPR reflections as lithological and chronostratigraphic surfaces with arrows indicating reflector terminations. **c:** Photo of mound 5 below white octocoral limestone with mound geometry outlined by flint bands. **d:** Details of mound 5 constructed using overlapping photographs and five measured sections, showing correlated flint horizons and their terminations (arrows). Interpreted stratigraphic units are numbered as in Fig. 9, and the main bounding unconformities are lines shown in bold. The depositional textures: mudstone (m), wackestone (w) and packstone (p) are indicated. Observed occurrences of indurated (Ind.) limestone zones, pyrite, and conspicuous lamination are given. The location of nannofossil sample N11 is shown.

data for units 8–10 due to truncated strata (Fig. 10). The top of unit 14 in borehole FX8901, above a thick and possibly amalgamated flint zone, is correlated towards the west and north along the south-western corner of the quarry, following a strongly indurated limestone zone downflank where the indurated top of unit 14 is sampled (Figs 8–10). Boundaries and individual flint-limestone couplets of units 15–17 are correlated from bryozoan limestone into much thicker, steeply dipping strata of hexacoral limestone and thinner strata of octocoral limestone, with a total stratigraphic thickness of around 60 m (Figs 8, 9).

Lithostratigraphy of a bryozoan mound
The position of flint horizons and the limestone depositional texture in a bryozoan mound is exemplified by mound 5 (Fig. 11). Below the mound, an unconformity truncates the thickly bedded, eastward migrating bryozoan limestone of units 8 and 9. A mound core in the upper part of unit 9 forms a 20 m wide and up to 2.5 m high structure upon which the bryozoan mound developed. The majority of the bryozoans in the mound core are peduncled cyclostomes with circular, flower-like morphology found in sieve fractions >1 mm. Unit 10 comprises westward migrating beds with strong vertical variation in depositional texture in the central part of the mound. Units 12–13 are thickest on the western and crestal parts of the mound where indurated beds occur. On the eastern mound flank units 12–13 are thin and subunits pinch out or have been truncated. Packstones with upwardly decreasing mud content are present. Unit 14 is separated from units 12–13 by a break in deposition, and unit 14 has strongly eastward migrating subunits. Most of the limestone zones in unit 14 are developed as indurated packstones which are truncated by an erosional unconformity at the crest of the mound, corresponding to the base of unit U2 of Bjerager *et al.* (2017). The truncated unit 14 causes mound 5 to have a weakly asymmetrical shape with a slightly steeper eastern flank. Unit 15 appears to be eroded above mound 5 but is present farther to the west (Figs 8–9).

Nannofossil biostratigraphy
The samples taken for nannofossil biostratigraphy represent an approximately 60 m almost complete middle Danian vertical section (subzones NNTp2F–4C of Varol 1998; Table 2). The sampled section includes stratigraphic units 1–14 of mainly bryozoan limestone and younger strata, intercalated with coral limestones. The oldest samples, N1 and N2, taken from below the octocoral limestone at the bottom of boreholes FX9401 and FX9402, immediately below 5 cm of clay, are dated as early middle Danian subzone NNTp2F and correlate with a level just below unit 1 in borehole FX8901 (Figs

8, 12). Compared to the more than 20 m thick section dated as early Danian zones 2–3 (Thomsen 1995) (= zones NNTp1A–NNTp2A of Varol 1998) at Stevns Klint (Surlyk *et al.* 2006), there is at Faxe a vertical thickness of 18 m from the location of samples N1 and N2 down to the mapped top Cretaceous surface (Figs 4b, 5) with nannofossil zones 1–4 preserved (Thomsen 1995). If rates of deposition at Stevns Klint and Faxe are similar, it is plausible that nannofossil zone 4 (Thomsen 1995), which is time equivalent to zone NNTp2E (Varol 1998) might be found a few metres below samples N1 and N2 (Fig. 12). Stratigraphic units 1–9 represent middle Danian subzones NNTp2G – NNTp3 (Table 2; Figs 9–12; Varol 1998). Sample N8 from unit 10 is probably assigned to either subzone NNTp4A or NNTp4B (Table 2). Units 14 and 15 sampled from indurated bryozoan limestone on the northern flank of the southern ridge (Figs 4f, 8–9) and at the top of core FX8901 (Fig. 10), are assigned to latest middle Danian nannofossil subzone NNTp4C based on *Prinsius martinii* (Table 2). Sample N11, from octocoral limestone (Figs 9, 11) which fills troughs between the bryozoan mounds forming the southern ridge, may also belong to subzone NNTp4C. Samples N12 and N13 from the uppermost western wall section are characterised by poor nannofossil recovery. Most or all of the upper Danian is missing at Faxe but the middle Danian is probably represented by all nannofossil zones NNTp2D–NNTp4C including the uppermost middle Danian zone NNTp4C which has not previously been identified at Faxe.

Based on our biostratigraphic data, we could correlate sequence boundary S3–S4 of Thomsen (1995) within his nannofossil zone 6 with the erosional truncation of bryozoan mounds of our unit boundary 14/15 (Figs 8–12). Progradation of unit 14 (Fig. 11) followed by termination and erosion of bryozoan mounds indicate a sea-level fall in the beginning of nannofossil zone NNTp4C (Figs 9, 12). However, based on a hardground found by Willumsen (1995, his hardground 2) with overlying coarse bryozoan grainstone, and based on a warming trend during deposition of coral limestones, as indicated by increasing abundance of *Coccolithus pelagicus* (Bjerager *et al.* 2017), we suggest keeping the S3–S4 boundary at the base of the younger hexacoral limestone (Figs 5, 12). Warm sea water is indicated by relatively high abundances of *Coccolithus pelagicus* in sample N2 of octocoral limestone and in samples N4, N6 and N8 of bryozoan limestone. In this study we find that sequence boundary S3–S4 has an age within nannofossil zone NNTp4C which is younger than previously stated (Thomsen 1995, his fig. 30).

Cyclostratigraphy
Bedding-parallel flint layers repeated approximately

every metre, and other evidence of cyclic stratigraphy from localities of Upper Cretaceous – Danian carbonates in the North Sea area, have been interpreted as a response of chalk sedimentation to orbital cycles (Hart 1987; Zijlstra 1994; Gale *et al.* 1999; Perdiou *et al.* 2016). With little or no ice at the poles during this time, cyclic chalk and limestone deposition may have been controlled by precession and eccentricity through hydrological cycles caused by the monsoon at low latitudes (Wang *et al.* 2017). Carbon and oxygen isotope data measured on benthic foraminifers from around the world have demonstrated long and short eccentricity cycles in Danian deep-sea carbonates (Westerhold *et al.* 2011).

Successful demonstration of Milankovitch cycles requires independent age control and recognition of a hierarchical stacking pattern (Strasser *et al.* 2006). We have sufficient age control for the upper limit of the upper long permeability cycle at a depth of 2 m in borehole FX8901 to make a tie to an astronomically calculated long eccentricity curve (Figs 10, 12). Nannofossil data (Table 2) show the appearance and increase in *Prinsius martini* (samples N9–11) indicating the presence and possibly the beginning of zone

NNTp4C in unit 14 (sample N10) at the top of the upper long permeability cycle with an age of 63.6 Ma (Agnini *et al.* 2014), when the age of the Cretaceous/Palaeogene boundary is corrected to 66.0 Ma (Renne *et al.* 2013). Our oldest nannofossil samples do not reach nannofossil zone NP2 (NNTp2E and older), however the age of the NP2/NP3 boundary is uncertain (Fig. 12; Agnini *et al.* 2014). Hence, the age correlation from our long permeability cycles to long eccentricity cycles relies on the assumption of relatively smooth rates of deposition. This implies that flint layers represent precession related cycles. We have chosen to compare all four calculated eccentricity solutions La2010a–d (Laskar *et al.* 2011) to porosity and permeability data in borehole FX8901 and to show one possible correlation between long permeability cycles and eccentricity solution La2010a (Figs 10, 12). We also make a tentative correlation between the well-developed porosity cycle of lithostratigraphic unit 2 and a short eccentricity cycle. The long permeability cycle spanning stratigraphic units 3–7 is supported by modulation of shorter cycles in porosity and permeability (Figs 10, 12). Short porosity cycles above unit 7 were recognised with low confidence

Table 2. Semi-quantitative counts of Danian nannofossil species from 13 samples from the southern part of Faxe quarry

				Danian nannofossils (counts)																				
Sample number	Sample location (well or quarry wall)	Stratigraphic unit	Sample elevation (m a.m.s.l.)	*Thoracosphaera* spp.	*Cyclagelosphaera alta*	*Zeugrhabdotus sigmoides*	*Cruciplacolithus primus*	*Cruciplacolithus asymmetricus*	*Cruciplacolithus tenuis*	*Cruciplacolithus intermedius*	Ch./Cr spp.	*Chiasmolithus inconspicuus*	*Coccolithus pelagicus*	*Prinsius coccosphere*	*Prinsius dimorphosus*	*Chiasmolithus danicus*	*Hornibrookina edwardsii*	*Prinsius tenuiculus*	*Prinsius martinii*	North Sea nannofossil Paleocene zonation (Varol 1998)	Calcareous nannofossil zone (Thomsen 1995)	Nannoplankton zonation (Martini 1971)	Sequence (Thomsen 1995)	Sequence (this paper)
N13	West	-	58	6	-	1	-	-	-	-	-	-	1	-	6	1	-	-	-	4C?	6			
N12	West	-	55	16	1	20	16	1	2	2	-	-	6	-	7	20	-	2	-	4C?	6			S4
N11	South	-	50	-	-	3	-	7	-	2	6	2	10	1	100	15	-	-	7	4C	6		S4	
N10	FX8901	14	47.0	100	3	7	6	6	-	-	1	-	10	-	4	4	-	-	4	4C	6			
N9	West	15	33	20	2	-	1	9	-	-	-	-	11	3	20	15	-	-	1	4C	6			
N8	South	10	39	100	3	10	1	3	-	1	-	-	15	1	100	3	-	-	-	4A-4B	5-6			
N7	FX8901	9	32.1	8	4	15	-	14	-	-	-	-	8	-	50	16	-	8	-	2G-3	5	NP3		
N6	South	6	26	28	-	10	2	14	-	-	-	-	25	7	25	18	-	2	-	2G-3	5			
N5	South	5	25	50	1	9	10	4	-	-	14	-	3	-	50	16	-	-	-	2G-3	5		S3	S3
N4	South	3	2	100	-	5	-	6	-	-	-	1	15	7	100	18	-	3	-	2G-3	5			
N3	FX8901	1	10.2	7	1	13	2	13	-	2	2	-	1	1	-	-	1?	24	-	2G-3	5			
N2	FX9402	1	-5.4	12	-	11	1	16	-	2	-	-	15	2	100	-	-	-	-	2F				
N1	X9401	-	-3.1	50	3	26	23	2	-	1	-	-	8	1	50	2	-	-	-	2F	5			

Samples N3 and N11 are from octocoral limestone whereas the other samples are from bryozoan limestone.
The North Sea Nannofossil Paleocene zonation of Varol (1998) was applied.
The boundary between regional sequences S3 and S4 was placed in nannofossil subzone NNTp4B by Thomsen (1995, his zone 6).

because of missing porosity data and unconformities in the middle and upper part of the southern bryozoan ridge (Fig. 9a).

We relate intervals of low porosity and high permeability near lithostratigraphic unit boundaries to nodes of interpreted low eccentricity as seen at the top of unit 7, which is characterised by a few decimetres of grain-dominated bryozoan packstone (Figs 10, 12). Zones of high porosity and reduced permeability are found between the nodes and relate to high amplitudes of short eccentricity (Fig. 10). Due to their cyclic content of coccolith mud, the alternating porous and permeable bryozoan limestone zones could express

cycles in primary productivity that may be related to insolation cycles (Burnett *et al.* 2000).

The placement of measured data into a geological time frame combined with the cyclic and hierarchical patterns in porosity, permeability and repeated flint-limestone couplets indicate orbital forcing as a significant depositional mechanism for Danian limestones at Faxe. For bryozoan limestone the rate of deposition for an expanded succession of stratigraphic units 2–14 is calculated to 40 m/1300 ka = 3.1 cm/ka, whereas the rate of deposition calculated from the base of the Stevns Klint Formation to the top of unit 14 is 62 m/2100 ka = 3.0 cm/ka. A much higher
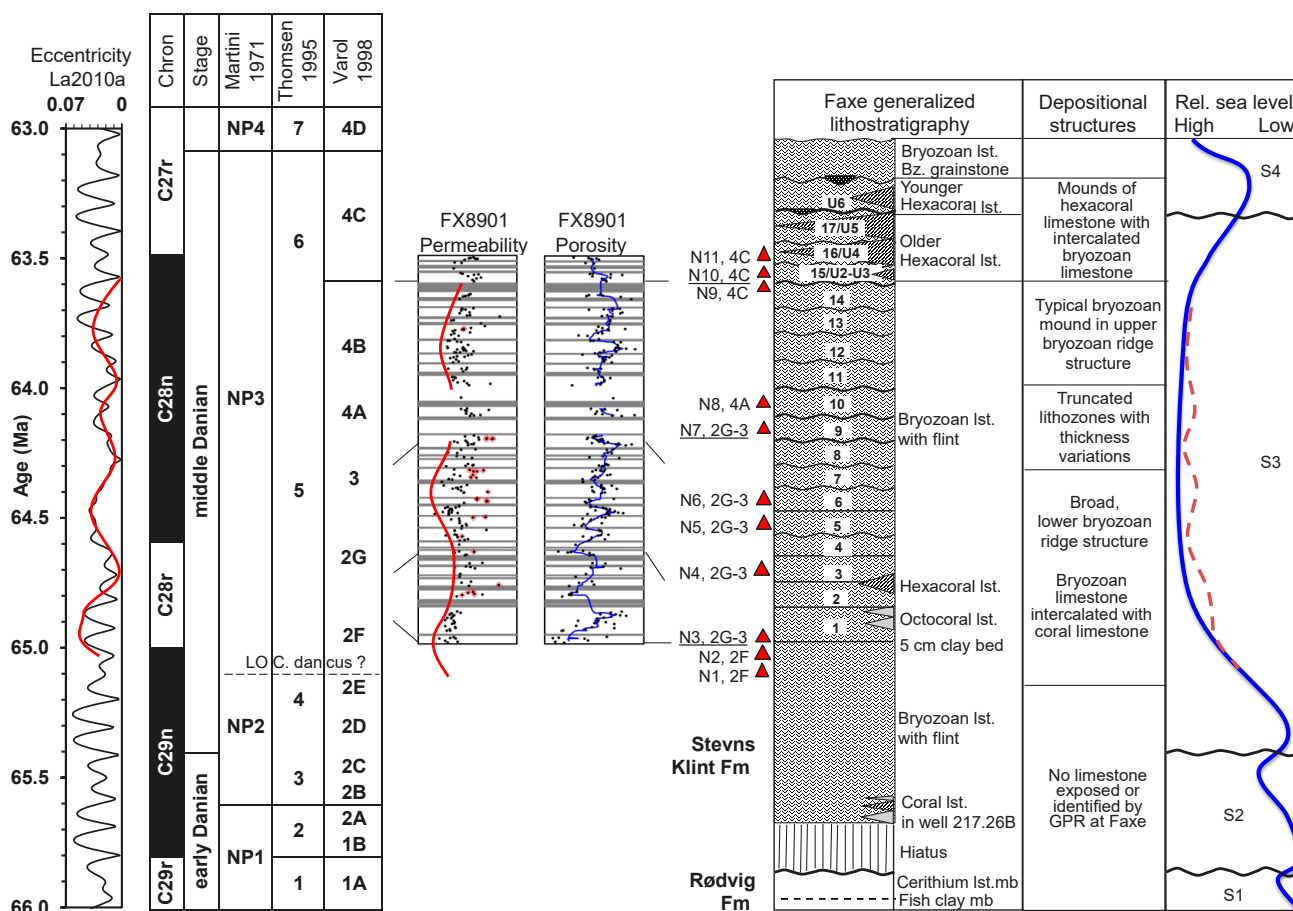

Fig. 12. Correlation of astrochronology, biostratigraphy, lithostratigraphy and porosity-permeability cycles from borehole FX8901 based mainly on data from the southern part of Faxe quarry. The timescale shows the astronomically calculated eccentricity La2010a of the earth's orbit (Laskar *et al.* 2011). The magnetostratigraphy is adopted from Cande & Kent (1995) and adjusted to a Cretaceous–Palaeogene boundary age of 66.0 Ma (Renne *et al.* 2013). Ages of nannofossil zones are adopted from Agnini *et al.* (2014). The dashed line dividing nannofossil zones NP2 and NP3 indicates an uncertainty in assigning an absolute age to the lowest occurrence of *Chiasmolithus danicus* (Agnini *et al.* 2014). The red trend line bounding the permeability data mirrors the long trends in calculated eccentricity. A generalised lithostratigraphic column shows the main limestone facies, stratigraphic units 1–17 (this study) and unit U2–U6 (Bjerager *et al.* 2017). Nannofossil samples N1–N11 (Table 2) are incorporated into the section using flint horizon correlation and GPR reflectors Thick wavy lines indicate surfaces of moderate to strong truncation. A division into depositional structures is included. The blue sea level curve is adopted from Thomsen (1995) and stretched to time, with sequence boundaries indicated. Possible eccentricity-driven sea-level fluctuations are shown using the red dashed curve.

depositional rate of 19 cm/ka is suggested for the 58 m stratigraphic thickness of coral limestone within stratigraphic units 15–17 (U2–U5) deposited during approximately 300 ka (Bjerager *et al.* 2017).

Lithofacies proportions, composition and petrophysical properties

Geological mapping allows the proportions of each of three dominant middle Danian limestone lithologies to be estimated within the central 1.5–2 km wide section of Faxe quarry (Figs 4, 5). Bryozoan limestone with flint, hexacoral limestone and octocoral limestone constitute *c.* 65%, 35% and 5% respectively of the rock volume, whereas matrix-poor bryozoan limestone deposits constitute a minor part (Table 3). The bryozoan grainstone accumulation mapped by GPR in the north-eastern part of the quarry constitute approximately 0.2 million m³, however at the time of mapping, the accumulation had been partly excavated. Reworked bryozoan grainstone within hexacoral limestone facies as described by Bjerager *et al.* (2017) may not be of volumetric significance.

Approximately one third of the bryozoan limestone observed in the quarry consists of sub-horizontally bedded bryozoan limestone that is not developed into the frequent 50–100 m wide mounds. Younger hexacoral limestone and older hexacoral limestone may have constituted similar amounts before excavation. Johnstrup (1864) noted a higher proportion of younger hexacoral limestone in his measured sections. Today coral limestone exposures are dominated by older hexacoral limestone.

Composition of limestones
The bryozoan limestone typically contains 30–50 wt% mud, defined as particles smaller than 63 μm (Table 3). Less carbonate mud is found in the indurated limestone at the crests of bryozoan mounds, at unit boundaries and in redistributed bryozoan grainstone (Fig. 13). As in a previous study based on petrographic analysis (Larsen 1961), we find bimodal grain size distribution of mud- and grain-dominated bryozoan packstones. Thin-section analysis reveals that the majority of investigated bryozoan limestone samples have grain-supported packstone texture, whereas wackestone or mudstone texture is predominant in octocoral limestones with mud-supported fragments of octocorals larger than 2 mm (Fig. 13). Local high concentrations of octocoral packstone has been observed at the base of troughs between bryozoan mounds (Fig. 9a) and in borehole FX9410 (Fig. 4e, M. Willumsen). The limestone at Faxe consists of more than 98% carbonate and almost entirely of calcite (Sigurdsson & Overgaard 1998) when flint is disregarded. The low content of 1–2% insoluble residue was confirmed by acid tests on sampled bryozoan limestone matrix to be mainly smectite and illite. Higher concentrations of clay were observed along barely visible bedding planes and on fracture surfaces. The amount of flint in the bryozoan limestone is estimated at 10% based on six boreholes in the southern part of the quarry, representing a total core length of 150 m (Fig. 4e). Flint layers and nodules vary in colour from light grey to black. Flint horizons are mostly located in burrows up to a few tens of centimetres below levels of indurated limestone with relatively low porosity (Fig. 10). Dolomite was previously present in the hexacoral limestone near to the crest of the mound complex (Johnstrup 1864), and dolomite occurs locally in the bryozoan limestone (Jørgensen 1988). Pyrite concretions are observed in zones of bryozoan limestone (Fig. 11) as indicated by red and yellow Fe-hydroxide staining in hexacoral limestone.

Table 3. Estimated proportions and composition of limestone lithologies characterised by depositional type and texture

Lithology	Bryozoan limestone				Hexacoral limestone	Octocoral limestone
Type of deposition or rock	Sub-horizontal bedding	Mound building	Indurated limestone	Redistributed limestone	Mound building	Valley deposits
Depositional texture	Packstone mud dom.	Packstone mud dom.	Packstone grain dom.	Grainstone	Variable	Mud-wacke-packstone
No. of samples	>50	>50	2	2	20	10
Proportion in Faxe quarry, %	30	30	<1	<1	35	<5
Porosity, %	40	43	28-38	46	15	37-44
Matrix permeability, mD	10-100	10-100	30-300	1000	variable	3-15
Carbonate mud < 63 μm, wt%	30-50	30-50	20	5-10	60-80	60-70

'Packstone mud dom.' refers to mud-dominated packstone, 'packstone grain dom.' refers to grain-dominated packstone (Lucia 1995). 'Mound building' and 'sub-horizontally bedded' bryozoan limestone refers to the upper and lower parts, respectively, of the southern bryozoan ridge (Figs 4d, 6, 12).
The lithological proportions of the Danian limestone are estimated from the reconstruction of Faxe quarry before excavation (Figs 4-5).
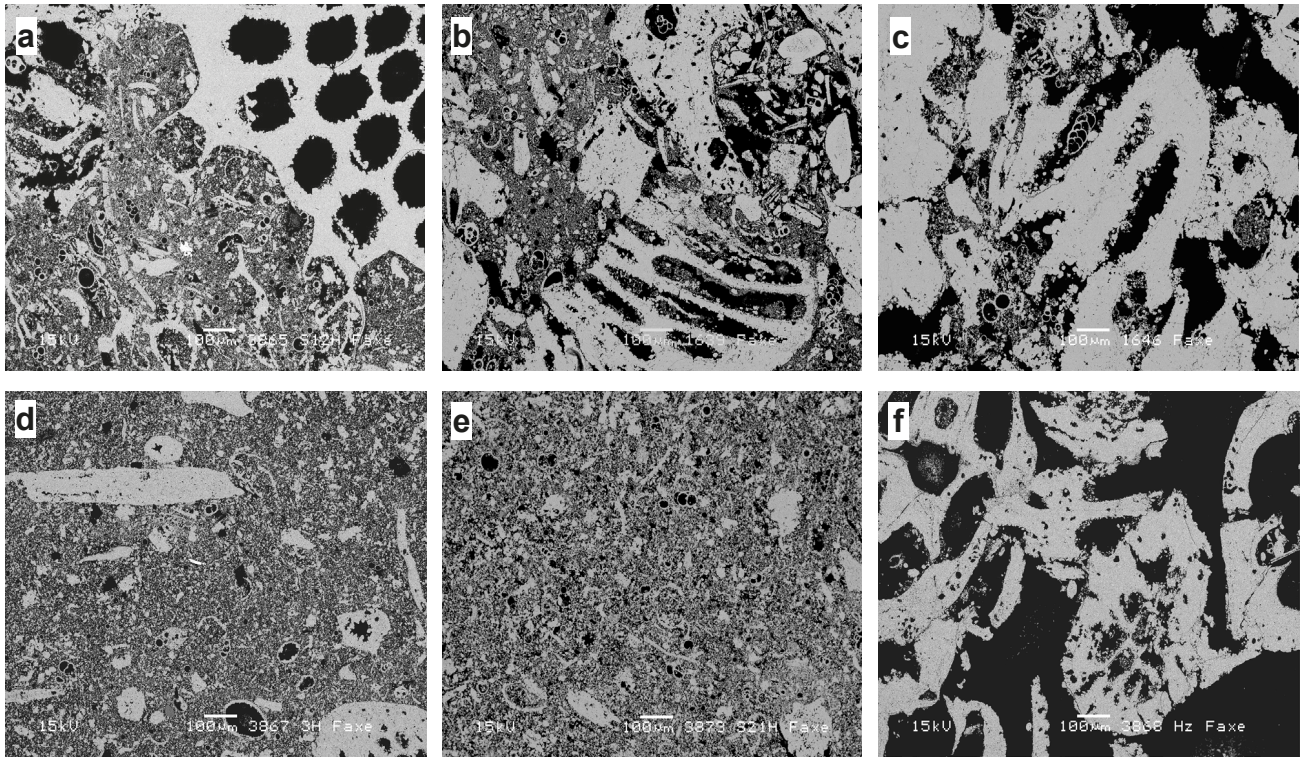
Fig. 13. Back-scattered electron micrographs of polished thin sections. Each picture represents a width of 1.3 mm and shows skeletal bryozoan debris, large foraminifers (lightest tone), mud (< 63 μm) comprising small foraminifers, coccoliths and skeletal fragments (grey) and pore space (black). **a:** Bryozoan packstone, porosity 37.9%, permeability 51.3 mD, unit 8 in quarry wall at 180 m (Fig. 9a). **b:** Indurated, bryozoan packstone, porosity 37.6%, permeability 103 mD, borehole FX8901, 21.5 m (Fig. 10). Calcite crystals are mainly seen on internal pore walls of bryozoans. **c:** Strongly indurated, grain dominated packstone, porosity 37.2%, permeability 228 mD, sample N9, unit 14 (Fig. 8). Large fragments of bryozoans are overgrown by calcite. **d:** Octocoral mudstone-wackestone, porosity 36.3% permeability 3.5 mD. The degree of skeletal fragmentation is high. **e:** Wackestone from a thin zone inter-bedded with typical mud-dominated bryozoan packstone, porosity 41.4%, permeability 12 mD. **f:** Indurated bryozoan grainstone, porosity 44.5%, permeability 966 mD, northeastern part of Faxe quarry (Fig. 7a, upper sample).

Petrophysical properties

Petrophysical properties vary among limestone lithologies (Table 3). The bryozoan limestone in general has high porosity and the permeability is over 10 mD, which indicates fair to good reservoir properties (Fig. 10, Table 3). Within the southern bryozoan ridge, data from core FX8901 show a gradual porosity increase from 35–40% at its base to around 45% near its top in the upper part of the ridge. The porosity declines near the top of the ridge, where indurated beds are present. The octocoral limestone is mud-dominated and has relatively low permeability (5 mD) in spite of relatively high porosity (Table 3). The hexacoral limestone has considerable amounts of cemented mud matrix in both older and younger hexacoral limestone. In this lithology, porosity has been calculated to around 15% from mass and bulk volume of hand specimens and from density data from geotechnical boreholes (Table 1), apart from the upper few metres of hexacoral limestone sections where porosity can reach around 30%.

Representative permeability of hexacoral limestone could not be measured because plug samples would be tight or only locally have large, connected pores. The bedded, older hexacoral limestone described by Willumsen (1995) is supposed to have high permeability anisotropy because mud-free beds of corals alternate with mud-rich beds. Sections measured by Bjerager *et al.* (2017) indicated high permeability only in rare octocoral packstone interbedded with cemented hexacoral limestone.

In core from borehole FX9401 between 12 and 13 m above mean sea level (Figs 4e, 8), a 5–10 cm thin zone of grain dominated packstone was observed. It has a porosity of 28% and a permeability of around 40 mD (Fig. 14b) and forms the lower part of a 0.50 m thick succession with increasing mud content towards the top, where typical porosity and permeability of 42% and 30 mD is measured.

The permeability of the limestones at Faxe correlates positively with decreasing carbonate mud content (Fig.

14a) and also with porosity (Fig. 14b). The permeability of a mixture of small and large grains varies theoretically with the fraction of fine grains with minimum permeability for mud-dominated packstone with complete packing (Glover & Luo 2020). The dashed line through our data (Fig. 14a) shows how limestone permeability at Faxe is controlled by depositional texture, with mud-dominated bryozoan packstone reaching a low permeability of 8–10 mD for a mud fraction of around 0.40. Octocoral limestone shows relatively low porosity and permeability values, the bryozoan limestone plots as a cloud with porosity of 0.35-0.48 and permeabilities of 3–300 mD, whereas mud-poor samples of indurated bryozoan packstone and grainstone deposits with permeability up to 2324

mD show high values indicating an open pore structure (Fig. 14b). Indurated zones of bryozoan limestones (Figs 10, 13b, 13c) can however, have 3–6 times higher permeability than the 30 mD that characterize the data cloud (Fig. 14b). Permeability anisotropy of bryozoan limestone was found by comparing permeability of 43 pairs of adjacent samples taken perpendicular to bedding (kv) and parallel to bedding (kh). The resulting small kv/kh anisotropy factor of 2.0 can be explained by the presence of a weak lamination on a mm scale, observed to be more or less randomly distributed in about half of the bryozoan limestone samples. A range of typical bryozoan limestone samples from Faxe, with permeability from 12 mD to 70 mD reveal capillary pressure drainage curves with a larger
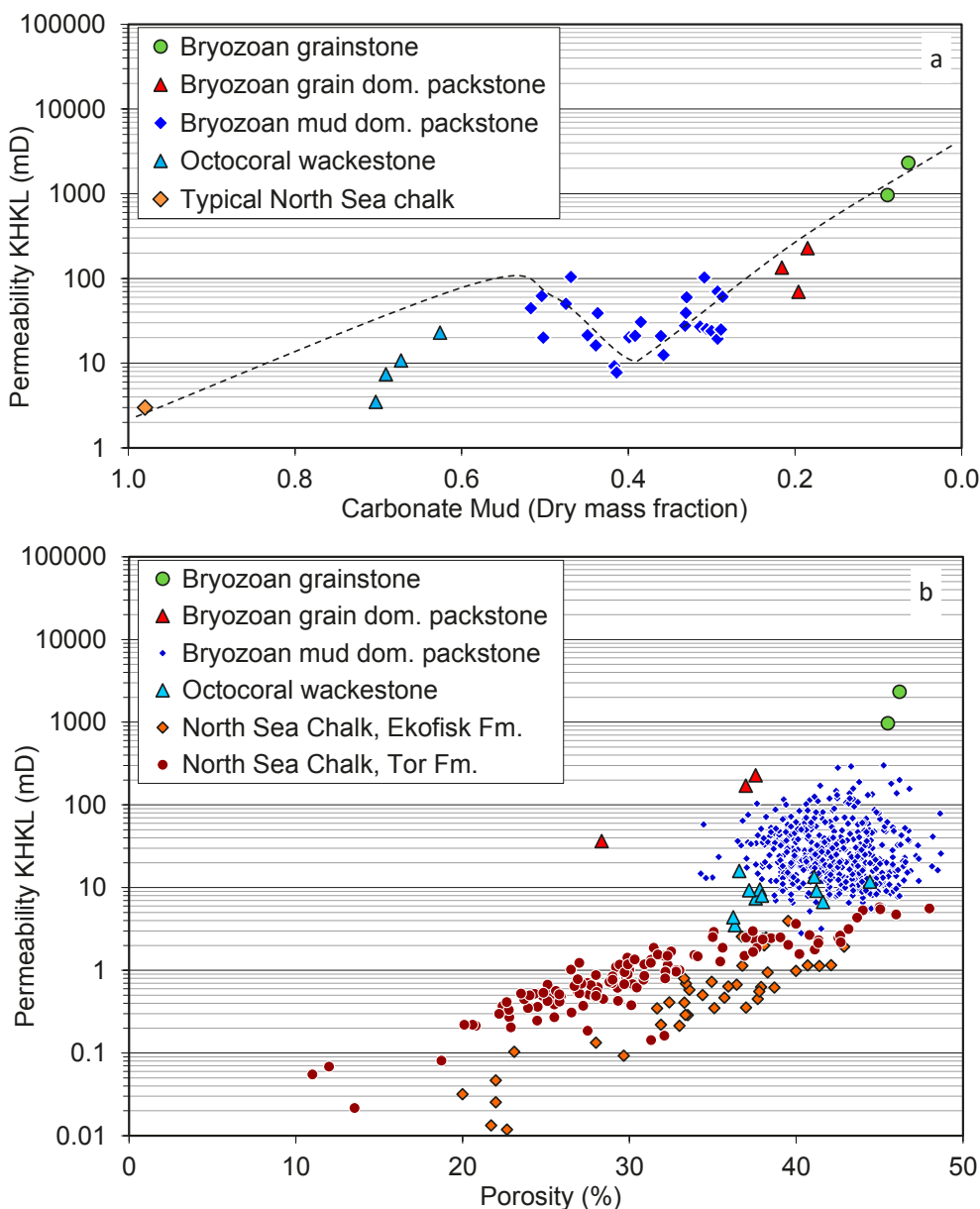

Fig. 14. a: Horizontal Klinkenberg corrected permeability versus amount of carbonate mud. Typical chalk from North Sea reservoirs is shown for comparison. The dashed trendline shows permeability of a binary grain mixture with a local minimum at 0.4 for mud-dominated lithology (Glover & Luo 2020, fig. 1). **b:** Horizontal Klinkenberg corrected permeability versus He-porosity for Faxe quarry limestones of different depositional origins compared with North Sea chalk from the Ekofisk and Tor Formations (Røgen & Fabricius 2002). A high permeability trend is seen for samples with relatively low amounts of carbonate mud. The data cloud for bryozoan mud dominated packstone represents variable amounts of fine particles. Porosity-permeability data for the octocoral limestone falls close to the trend for Tor Formation chalk.

spread and steeper profile than for typical North Sea chalks (Andersen 1995, fig. 3.11), indicating more variable pore size and pore size distribution for the Faxe limestones (Fig. 15a). The entry pressure for bryozoan limestone is *c.* one order of magnitude lower than for chalk because fragmented bryozoans are associated with large interparticle pores (Fig. 15b).
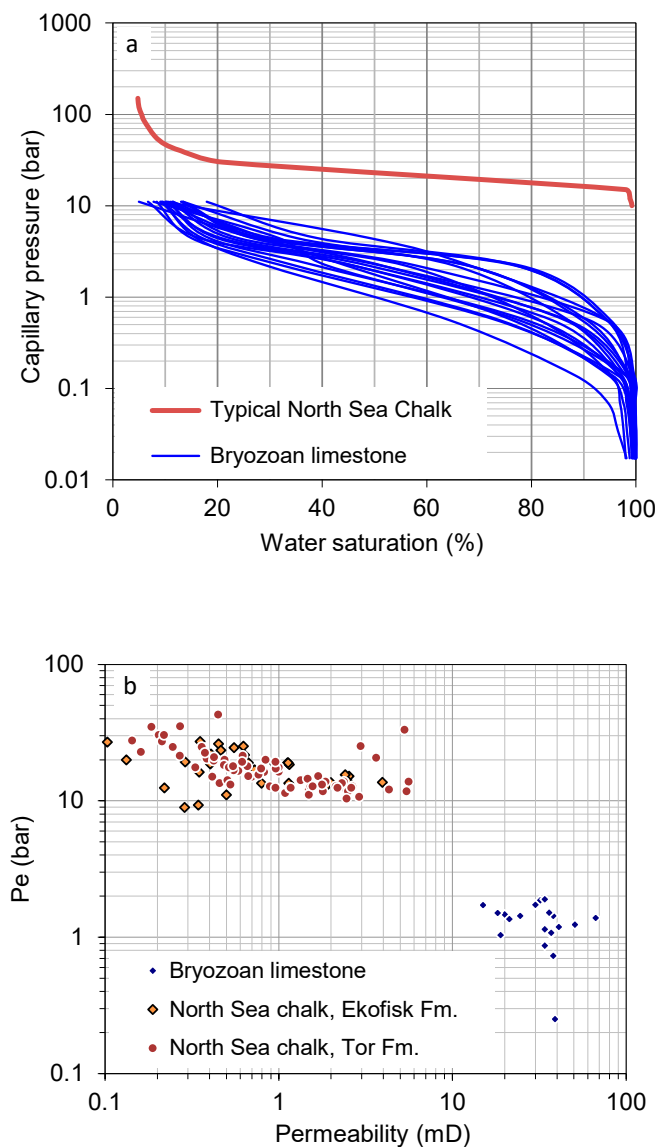

Fig. 15. a: Capillary pressure (Pc) versus water saturation of bryozoan limestone from Faxe quarry as measured by the porous plate method (Lin *et al.* 2017) compared with a typical capillary pressure curve for North Sea chalk (Andersen 1995). The entry pressure of North Sea chalk is 1–2 orders of magnitude higher than for bryozoan limestone and the horizontal Pc curve of the chalk indicates a more homogeneous pore size distribution. **b:** Entry pressure (Pe) versus horizontal permeability illustrates the difference in pore space characteristics between bryozoan limestone and North Sea chalk.

Conclusions

At Faxe quarry, Sjælland, a mound complex of bryozoan limestone and coral limestone that was up to 100 m thick before excavations, was studied using outcrops, well and GPR data. The age of the limestones ranges from the early Danian to the latest middle Danian, including a complete middle Danian section dated as NNTp2F – NNTp4C (Varol 1998), NP3 (Martini 1971). A few kilometres from Faxe quarry, Danian strata are eroded to around 20–50 m in thickness and consist of bryozoan limestone. Bryozoan limestone thicknesses of over 40 m span an area of approximately 12 km² whereas coral limestone is only proven in an area of 2 × 2 km. However, it is likely that coral limestone near Faxe covered a larger area before Neogene and Quaternary erosion.

The internal geometry of the mound complex at Faxe is characterised by three parallel northwest–southeast-striking ridges of middle Danian bryozoan limestone. Each ridge measures 700–1100 m by 200–300 m, with a relief of about 15 m. Bryozoan limestone strata have an overall dip towards the northeast (Fig. 5b). A vertical section along the long axis of the southern bryozoan ridge is exposed in the southern quarry wall where seven typical bryozoan mounds characterise the upper part of the ridge. The dominant deposits above and between the bryozoan ridges are two hexacoral limestone bodies that formed mounds with a vertical thickness of up to 40 m by filling lows between ridges. Boreholes reveal one as an extension to the northeast of the thick northern hexacoral body (Fig. 5b) and another hexacoral limestone body 30 m below the major bodies within middle Danian bryozoan limestone in the southern part of the quarry (Fig. 8). A previously unrecognised occurrence of highly permeable bryozoan grainstone, without flint was observed in a 100 m wide and up to 10 m high section (Fig. 7).

The early and middle Danian deposits at Faxe have been placed into a geochronologic time frame using eccentricity solution La2010a to construct a cyclostratigraphic calibration of middle Danian strata. However, we cannot exclude alternative eccentricity solutions. Cyclicity observed in core porosity and permeability data and supported by nannofossil data is important for our cyclostratigraphic calibration, which indicates an age for the NP2\NP3 nannofossil boundary of around 65.1 Ma. Long permeability cycles modulate shorter cycles in porosity, which are divided by thin decimetre scale zones of indurated, mud poor limestone with high permeability and relatively low porosity. Orbital cycle durations of around 400 ka observed in permeability data may have caused minor sea-level variations in the middle Danian (NP3). We

mapped the surface (Fig. 4d) on which fast growing hexacoral limestone accumulated at a rate of 19 cm/ka compared with middle Danian bryozoan limestone that accumulated at a rate of only 3.1 cm/ka. An age of around 63.3 Ma within nannofossil subzone NNTp4C is assigned to the regional sequence boundary S3–S4 separating older and younger coral limestone.

The proportions of bryozoan limestones and coral limestones before excavation is estimated to approximately 2/3 and 1/3 respectively. The common flint bearing bryozoan limestone is dominated by a mud-dominated packstone texture with bimodal grainsize distribution and closest grain packing for a mud content of 40%. The flint-bearing bryozoan limestone shows a wide range of porosity and permeability with typical values of 42% and 30 mD respectively. Capillary entry pressure is found to be one order of magnitude lower for bryozoan limestone than for chalk with carbonate mudstone texture. For bryozoan limestone with or without flint we find that the more strongly indurated zones have grainstone or grain-dominated textures, low mud content and high permeability. The hexacoral limestone is dominated by a lithified mud matrix and poor reservoir properties.

Acknowledgements

References

Agnini, C., Fornaciari, E., Raffi, I., Catanzariti, R. Pälike, H., Backman, J. & Rio, D. 2014: Biozonation and biochronology of Paleogene calcareous nannofossils from low and middle latitudes. Newsletters on Stratigraphy 47, 131–181. https://doi.org/10.1127/0078-0421/2014/0042

Allen, P.A. & Underhill, J.R. 1989: Swaley cross-stratification produced by unidirectional flows, Bencliff Gritt (Upper Jurassic), Dorset, UK. Journal of the Geological Society, London 146, 241–252. https://doi.org/10.1144/gsjgs.146.2.0241

Andersen, M.A. 1995: Petroleum research in North Sea chalk, 179 pp. Stavanger: RF Rogaland Research.

Bernecker, M. & Weidlich, O. 1990: The Danian (Palaeocene) coral limestone of Fakse, Denmark: A model for ancient aphotic, azooxanthellate coral mounds. Facies 22, 103–138. https://doi.org/10.1007/BF02536947

Bernecker, M. & Weidlich, O. 2005: Azooxanthellate corals in the Late Maastrichtian – Early Paleocene of the Danish basin: bryozoan and coral mounds in a boreal shelf setting. In: Freiwald, A. & Roberts, J.M. (eds): Cold-water corals and ecosystems, 3–25. Berlin: Springer. https://doi.org/10.1007/3-540-27673-4_1

Bjerager, M. & Surlyk, F. 2007a: Danian cool-water bryozoan mounds at Stevns Klint, Denmark – A new class of non-cemented skeletal mounds. Journal of Sedimentary Research 77, 634–660. https://doi.org/10.2110/jsr.2007.064

Bjerager, M. & Surlyk, F. 2007b: Benthic palaeoecology of Danian deep-shelf bryozoan mounds in the Danish Basin. Palaeogeography, Palaeoclimatology, Palaeoecology 250, 184–215. https://doi.org/10.1016/j.palaeo.2007.03.008

Bjerager, M., Surlyk, F., Lykke-Andersen, H., Thibault, N. & Stemmerik, L. 2010: Danian cool-water coral reefs in southern Scandinavia localised over seafloor highs. Marine and Petroleum Geology 27, 455–466. https://doi.org/10.1016/j.marpetgeo.2009.09.008

Bjerager, M., Sheldon, E. & Lauridsen, B.W. 2017: Mound-forming cold-water corals and bryozoans in the Early Paleocene of Denmark. Sedimentology 65, 1331–1353. https://doi.org/10.1111/sed.12424

Bristow, C.S. & Jol, H.M. 2003: An introduction to ground penetrating radar (GPR) in sediments. In: Bristow, C.S. & Jol, H.M. (eds): Ground penetrating radar in sediments. Geological Society, London, Special Publications 211, 167–179. http://dx.doi.org/10.1144/GSL.SP.2001.211.01.01

Bromley, R.G. 1967: Some observations on burrows of thalassinidean crustacean in chalk hardgrounds. Quarterly Journal of the Geological Society 123, 157–182. https://doi.org/10.1144/gsjgs.123.1.0157

Brotzen, F. 1959: On *Tylocidaris* species (Echinodea) and the stratigraphy of the Danian of Sweden. Sveriges Geolologiska Undersökning Ser. C, 571, 1–81.

Buhl-Mortensen, L., Hodnesdal, H. & Thorsnes, T. 2015: The Norwegian sea floor – new knowledge from MAREANO for Ecosystem-Based Management, 192 pp. Trondheim: Geological Survey of Norway. https://www.mareano.no/resultater/the-norwegian-sea-floor

Burnett, J.A., Young, J.R. & Bown, P.R. 2000: Calcareous nannoplankton and global climate change. In: Culver, S.J. & Rawson, P.F. (eds): Biotic response to global change the last 145 million years, 35–50. Cambridge University Press. https://doi.org/10.1017/CBO9780511535505

Cande, S.C. & Kent, D.V. 1995: Revised calibration of the geo-

magnetic polarity timescale for the Late Cretaceous and Cenozoic. Journal of Geophysical Research 100 (B4), 6093–6095. https://doi.org/10.1029/94JB03098

Day, P.I. 1997: The Fischer diagram in the depth domain: A tool for sequence stratigraphy. Journal of sedimentary petrology 67, 982–984. https://doi.org/10.2110/jsr.67.982

Desor, É. 1846: Sur le terrain Danien, nouvel étage de la Craie. Bulletin Societe Géologi France 2(4), 179–181.

Dunham, R.J. 1962: Classification of carbonate rocks according to depositional texture. In: Ham, W.E. (ed.): Classification of carbonate rocks. American Association of Petroleum Geologists Memoir 1, 108–121.

Floris, S. 1979: Guide to Fakse limestone quarry. In: Birkelund, T. & Bromley, R.G. (eds): Cretaceous–Tertiary Boundary Events, Symposium, The Maastrichtian and Danian of Denmark, 152–163. University of Copenhagen.

Floris, S. 1980: The coral banks of the Danian of Denmark. Acta Palaeontological Polonica 25, 531–540.

Freiwald, A., Fosså, J.H., Grehan, A., Koslow, T. & Roberts, J.M. 2004: Cold-water coral reefs, 84 pp. Cambridge: UNEP-WCMC. http://www.unep-wcmc.org/resources/publications/UNEP_WCMC_bio_series/22.htm

Gale, A. 2002: Late Cretaceous to Early Tertiary pelagic deposits: deposition on greenhouse Earth. In: Woodcock, N.H. & Strachan, R.A. (eds): Geological history of Britain and Ireland, 356–373. New York: Wiley. https://doi.org/10.1017/S0016756801255381

Gale, A., Young, J., Shackleton, N.J, Crowhurst, S. & Wray, D. 1999: Orbital tuning of Cenomanian marly chalk successions: Towards a Milankovitch time-scale for the Late Cretaceous. Philosophical Transactions of The Royal Society A: Mathematical, Physical and Engineering Sciences 357, 1815–1829. https://doi.org/10.1098/rsta.1999.0402

Glover, P.W.J. & Luo, M. 2020: The porosity and permeability of binary grain mixtures. Transport in Porous Media 132, 1–37. https://doi.org/10.1007/s11242-020-01378-0.

Gravesen, P. 2001: Den geologiske udforskning af Fakse Kalkbrud fra midten af 1700-tallet til nu. Geologisk Tidsskrift 2001(2), 40 pp.

Hart, M.B. 1987: Orbitally induced cycles in the chalk facies of the United Kingdom. Cretaceous Research 8, 335–348. https://doi.org/10.1016/0195-6671(87)90003-6

Houmark-Nielsen, M. 1988: Pleistocene stratigraphy and glacial history of the central part of Denmark. Bulletin of the Geological Society of Denmark 36, 1–189.

Hovland, M. & Mortensen, P.B. 1999: Norske korallrev og prosesser i havbunnen, 155 pp. Bergen: John Grieg Forlag.

Jakobsen, P.R. 1996: Distribution and intensity of glaciotectonic deformation in Denmark. Bulletin of the Geological Society of Denmark 42, 175–185. https://doi.org/10.2166/nh.1993.0007

Jakobsen, R., Jensen, K.H. & Brettmann, K.L. 1993: Tracer test in fractured chalk, 1. Experimental design and results. Nordic Hydrology 24, 263–274.

Japsen, P. & Bidstrup, T. 1999: Quantification of late Cenozoic erosion in Denmark based on sonic data and basin modeling. Bulletin of the Geological Society of Denmark 46, 79–99.

Johnson, H. & Lott, G.K. 1993: Cretaceous of the central and northern North Sea. In: Knox, R.W.O'B. & Cordey, W.G. (eds): Lithostratigraphic nomenclature of the UK North Sea 2, 169 pp. Nottingham: British Geological Survey.

Johnstrup, F. 1864: Faxekalkens dannelse og senere undergåede forandringer. Det Kongelige Danske Videnskabernes Selskab Skrifter, naturvidenskabelig og matematisk afdeling, 5. Række, Vol. 7, 1–46.

Jørgensen, N.O. 1988: Dolomite and dolomitization in Danian bryozoan limestone from Fakse, Denmark. Bulletin of the Geological Society of Denmark 37, 63–77.

Knox, R.W.O'B. & Holloway, S. 1992: Paleogene of the central and northern North Sea. In: Knox, R.W.O'B. & Cordey, W.G. (eds): Lithostratigraphic nomenclature of the UK North Sea, 31–55, 63–77. Nottingham: British Geological Survey.

Larsen, G. 1961: Kvantitativ petrografisk undersøgelse af nogle sjællandske Danienkalksten. Danmarks Geologiske Undersøgelse 4. Række, Vol. 4(7), 25 pp.

Laskar, J., Fienga, A., Gastineau, M. & Manche, H. 2011: La2010: A new orbital solution for the long-term motion of the Earth. Astronomy and Astrophysics 532, A89, 1–15. https://doi.org/10.1051/0004-6361/201116836

Lauridsen, B.W., Bjerager, M. & Surlyk, F. 2012: The middle Danian Faxe Formation – new lithostratigraphic unit and a rare taphonomic window into the Danian of Denmark. Bulletin of the Geological Society of Denmark 60, 47–60. https://doi.org/10.37570/bgsd-2012-60-04

Lin, Q., Bijeljic, B., Rieke, H. & Blunt, M.J. 2017: Visualization and quantification of capillary drainage in the pore space of laminated sandstone by a porous plate method using differential imaging X-ray microtomography. Water Resources Research 53, 7457–7468. https://doi:10.1002/ 2017WR021083

Lucia, J.F. 1995: Rock-fabric/petrophysical classification of carbonate pore space for reservoir characterization. American Association of Petroleum Geologists Bulletin 79, 1275–1300. https://doi.org/10.1306/7834D4A4-1721-11D7-8645000102C1865D

Lykke-Andersen, H. & Surlyk, F. 2004: The Cretaceous-Palaeogene boundary at Stevns Klint, Denmark: inversion tectonics or sea-floor topography? Journal of the Geological Society, London 161, 343–352. https://doi.org/10.1144/0016-764903-021

Martini, E. 1971: Standard Tertiary and Quaternary Calcareous Nannoplankton Zonation. In: Farinacci, E. (ed.): Proceedings of the 2nd Planktonic Conference, Roma, 1970, 739–785.

Nielsen, L., Schack von Brockdorff, A, Bjerager, M. & Surlyk, F. 2009: Three-dimensional architecture and development of Danian bryozoan mounds at Limhamn, south-west Sweden, using ground-penetrating radar. Sedimentology 56, 695–708. https://doi.org/10.1111/j.1365-3091.2008.00993.x

Ødum, H. 1937: To boringer på Herlufsholm. Herlufsholms Skoles Aarsskrift 1937, 19 pp.

Perdiou, A., Thibault, N., Anderskouv, K., van Buchem, F.S.P.,

Buijs, G.J.A. & Bjerrum, C. J. 2016: Orbital calibration of the late Campanian carbon isotope event in the North Sea. Journal of the Geological Society, London 173, 504–517. https://doi.org/10.1144/jgs2015-120

Rasmussen, J.A., Heinberg, C. & Håkansson, E. 2005: Planktonic foraminifers, biostratigraphy and the diachronous nature of the lowermost Danian Cerithium Limestone at Stevns Klint, Denmark. Bulletin of the Geological Society of Demark, 52, 113–131.

Rebesco, M., Hernández-Molina, F.J., Van Rooij, D. & Wåhlin, A. 2014: Contourites and associated sediments controlled by deep-water circulation processes: state of the art and future considerations. Marine Geology 352, 111–154. https://doi.org/10.1016/j.margeo.2014.03.011

Renne, P.R., Deino, A.L., Hilgen, F.J., Kuiper, K.F., Mitchell, W.S., Morgan, L.E., Mundil, R. & Smit, J. 2013: Timescales of critical events around the Cretaceous-Paleogene boundary. Science 339, 684–687. https://doi.org/10.1126/science.1230492

Røgen, B. & Fabricius, I.L. 2002: Influence of clay and silica on permeability and capillary entry pressure of chalk reservoirs in the North Sea. Petroleum Geoscience 8, 287–293. https://doi.org/10.1144/petgeo.8.3.287

Rosenkrantz, A.P. 1937: Bemærkninger om det østsjællandske Daniens stratigrafi og tektonik. Meddelelser fra Dansk Geologisk Forening 9, 199–212.

Schnetler, K.I. & Milàn, J. 2017: A new Cenozoic record of spinilomatine aporrhaids (Stromboidea, Caenogastropoda) in the early Paleocene of Faxe, Denmark. Bulletin of the Geological Society of Denmark 65, 37–45. https://doi.org/10.37570/bgsd-2017-65-03

Schrøder, A.E. & Surlyk, F. 2019: Adaptive morphologies of the brachiopod fauna from Danian coral mounds at Faxe, Denmark. Palaeogeography, Palaeoclimatology, Palaeoecology 534, 109332. https://doi.org/10.1016/j.palaeo.2019.109332

Sigurdsson, T. & Overgaard, T. 1998: Application of GPR for 3-D visualization of geological and structural variation in a limestone formation. Journal of Applied Geophysics 40, 29–36. https://doi.org/10.1016/S0926-9851(98)00015-9

Stenestad, E. 1976: Geology of the Copenhagen area predominately based on investigations for an urban underground railway. Danmarks Geologiske Undersøgelse III. Række, Vol. 45, 149 pp.

Strasser, A., Hilgen, F.J. & Heckel, P.H. 2006: Cyclostratigraphy – Concepts, definitions and applications. Newsletters on Stratigraphy 42, 75–114. https://doi: 10.1127/0078-0421/2006/0042-0075

Surlyk, F. 1997: A cool-water carbonate ramp with bryozoan mounds: Late Cretaceous-Danian of the Danish basin. In: N.P. James & J.A.D. Clarke (eds): Cool-water carbonates. SEPM Special Publication 56, 293–307.

Surlyk, F. & Håkansson, E. 1999: Maastrichtian and Danian strata in the southeastern part of the Danish Basin. In: Ped-

ersen, G.K. & Clemmensen, L.B. (eds): Field trip guidebook, 29–58. Contributions to Geology (Copenhagen). Geological Museum of the University of Copenhagen, Denmark. 19th Regional European meeting of sedimentology.

Surlyk, F., Dons, T., Clausen, C.K. & Higham, J. 2003: Upper Cretaceous. In: Evans, D. et al. (eds): The Millennium Atlas: Petroleum geology of the central and northern North Sea, 213–233. London: The Geological Society. https://doi.org/10.1017/S0016756803218124

Surlyk, F., Damholt, T. & Bjerager, M. 2006: Stevns Klint, Denmark: Uppermost Maastrichtian chalk, Cretaceous–Tertiary boundary, and lower Danian bryozoan mound complex. Bulletin of the Geological Society of Denmark 54, 1–48. https://doi.org/10.37570/bgsd-2006-54-01

Thomsen, E. 1976: Depositional environment and development of Danian bryozoan biomicrite mounds (Karlby Klint, Denmark). Sedimentology 23, 485–509. https://doi.org/10.1111/j.1365-3091.1976.tb00064.x

Thomsen, E. 1983: Relationships between currents and the growth of Paleocene reef-mounds. Lethaia 16, 165–184. https://doi.org/10.1111/j.1502-3931.1983.tb00651.x

Thomsen, E. 1995: Kridt og kalk i den danske undergrund. In: Nielsen, O.B. (ed.): Aarhus Geokompendier 1, 31–67.

van Buchem, F.S.P., Smit, F.W.H., Buijs, G.J.A. Trudgill, B. & Larsen, P.-H. 2018: Tectonostratigraphic framework and depositional history of the Cretaceous–Danian succession of the Danish Central Graben (North Sea) – new light on a mature area. Geological Society, London, Petroleum Geology Conference series 8, 9–46. https://doi.org/10.1144/PGC8.24

Varol, O. 1998: Palaeogene. In: Bown, P.R. (ed.): Calcareous nannofossil biostratigraphy, 200–224. London: Chapman & Hall.

Wang, P. X., Wang B., Cheng, H., Fasullo, J., Guo, Z., Kiefer, T. & Liu, Z. 2017: The global monsoon across time scales: Mechanisms and outstanding issues. Earth-Science Reviews 174, 84–121. http://dx.doi.org/10.1016/j.earscirev.2017.07.006

Weidlich, O. & Bernecker, M. 1991: Comparative analyses of cementation in brachiopods and corals (Paleocene coral limestone, Fakse, Denmark). Neues Jahrbuch für Geologie und Paläontologie Monatshefte 10, 615–628.

Westerhold, T., Röhl, U., Donner, B., McCarren, H.K. & Zachos, J.C. 2011: A complete high-resolution Paleocene benthic stable isotope record for the central Pacific (ODP Site 1209). Paleoceanography 26, PA2216. https://doi:10.1029/2010PA002092.

Willumsen, M.E. 1995: Early lithification in Danian azooxanthellate scleractinian lithoherms, Faxe quarry, Denmark. Beiträge zur Paläontologie 20, 123–131.

Wright, V.P. 1992: A revised classification of limestones. Sedimentary geology 76, 117–185. https://doi.org/10.1016/0037-0738(92)90082-3

Zijlstra, J.J.P. 1994: Sedimentology of the Late Cretaceous and Early Tertiary (Tuffaceous) chalk of northwest Europe. Geologica Ultraiectina 119, 192 pp.

Furongian (upper Cambrian) trilobites and agnostoids from the Alum Shale Formation of Bornholm, Denmark: revised taxonomy and biostratigraphy

ARNE THORSHØJ NIELSEN & LINE FRIGAARD ANDERSEN

The Furongian (upper Cambrian) trilobite-agnostoid fauna from the Alum Shale Formation of Bornholm, Denmark, is reviewed and revised. The study is based on the museum material stored at the Natural History Museum of Denmark, including the material originally monographed by C. Poulsen (1923) [Bornholms Olenuslag og deres fauna. Danmarks Geologiske Undersøgelse II. Række, Vol. 40, 83 pp]. A total of 8502 specimens, mostly disarticulated sclerites, have been registered. The taxonomy of all species is updated and the best preserved specimens are illustrated. A total of 39 olenid and 5 agnostoid taxa (incl. the Miaolingian *Agnostus pisiformis*) are recorded including one new species, *Ctenopyge magna* n. sp. Two specimens of *Ctenopyge*, treated in open nomenclature as *Ctenopyge* sp. 1 and sp. 2, may also represent new species. 14 taxa have not been previously reported from Bornholm, viz. *Ctenopyge ahlbergi, Ctenopyge tumidoides, Eurycare brevicauda, Leptoplastus abnormis, Leptoplastus crassicornis, Olenus transversus, Parabolina lobata praecurrens, Peltura acutidens, Peltura minor, Peltura westergaardi, Protopeltura planicauda, Protopeltura praecursor, Pseudagnostus leptoplastorum?* and *Sphaerophthalmus drytonensis. Ctenopyge pecten* and *Ctenopyge affinis* are also new to Bornholm as the material formerly described under these names represent *Ctenopyge tenuis* and *C. magna* n. sp., respectively. *Lotagnostus americanus, Ctenopyge fletcheri, Sphaerophthalmus alatus* and *Triangulopyge humilis* were described under different names by C. Poulsen (1923). *Peltura westergaardi* and *Ctenopyge tenuis* are elevated from subspecies to species rank. A redescription of *Leptoplastus bornholmensis* is presented; the species is transferred to *Eurycare*. The identification of isolated skeletal parts of *L. abnormis* and *Leptoplastus ovatus* and *Sphaerophthalmus flagellifer* and *S. drytonensis* are remarked on.

The presence of three agnostoid and 14 trilobite zones is confirmed by fossils and all six Furongian superzones are developed on Bornholm. At least the *Leptoplastus paucisegmentatus* and *Leptoplastus raphidophorus* zones seem to be absent. Other undocumented zones may be unfossiliferous, not exposed or truly absent. Three different trilobite assemblages (potential subzones) are discerned in the *Peltura acutidens–Ctenopyge tumida* Zone; *Ctenopyge tumidoides* and *Sphaerophthalmus angustus* range into the basal part of this zone. All exposures of the Furongian Alum Shale Formation along the Læså and Øleå streams on southern Bornholm are briefly described including GPS coordinates.

Keywords: Furongian, biostratigraphy, taxonomy, trilobites, olenids, Alum Shale, Bornholm, Denmark.

Arne Thorshøj Nielsen [arnet@ign.ku.dk], Department of Geosciences and Natural Resource Management, University of Copenhagen, Øster Voldgade 10, DK-1350 Copenhagen K, Denmark. Line Frigaard Andersen [line.frigaard@gmail.com], Tølløsevej 2, 1. TH, DK-2700 Brønshøj, Denmark.

The Cambro–Ordovician Alum Shale Formation has long been known from discontinuous exposures along the Læså and Øleå streams on southern Bornholm, Denmark (e.g. Grönwall 1902, 1916; C. Poulsen 1922, 1923; Hansen 1945; Berg-Madsen 1985a, b, 1986); for location of outcrops, see Figs 1–2. The shale has also been penetrated by several wells, both cored and uncored, showing that the total thickness of the unit varies between 27 and 39 m on the island (Nielsen *et al.* 2018). The present paper reviews the trilobites found in the Furongian interval, which is 17–23 m thick (Nielsen *et al.* 2018). Regarding stratigraphic terminology, the traditional designations 'Lower', 'Middle' and 'Upper'

Cambrian are now discarded (e.g. Babcock *et al.* 2005; Peng *et al.* 2012) and henceforth, the new terms Miaolingian and Furongian replace the former 'Middle' and 'Upper' Cambrian series, respectively. However, the new and old series are not corresponding precisely as the *Agnostus pisiformis* Zone previously was classified as 'Upper' Cambrian in Scandinavia (e.g. Westergård 1922; C. Poulsen 1923), but now is assigned to the Miaolingian (e.g. Terfelt *et al.* 2008; Nielsen & Ahlberg 2019). The revised classification is readily applicable in Scandinavia as a major faunal turnover marks the Miaolinigian–Furongian boundary with the introduction of olenid trilobites coinciding with the near disappearance of agnostoids.

Parts of the Furongian are highly fossiliferous, and the local trilobite fauna on Bornholm was monographed by C. Poulsen (1923), who described four agnostoid (incl. the Miaolingian *A. pisiformis*) and 24 trilobite taxa. A few additional trilobites have been described subsequently by Kaufmann (1933a), Whittington (1958), V. Poulsen (1963), Rasmussen *et al.* (2015), Schoenemann & Clarkson (2015) and Månsson & Clarkson (2016). C. Poulsen (1923) correlated the succession with the zonation established by Westergård (1922). The chronostratigraphy was later summarized by V. Poulsen (1966) who introduced the revised zonal scheme published by Henningsmoen (1957), but without discussing subzones. This is relevant as the many subzones defined by Henningsmoen (1957) with minor changes were elevated to zonal rank by Terfelt *et al.* (2008). The Furongian zonation for Scandinavia was further revised by Nielsen *et al.* (2014, 2020) and that
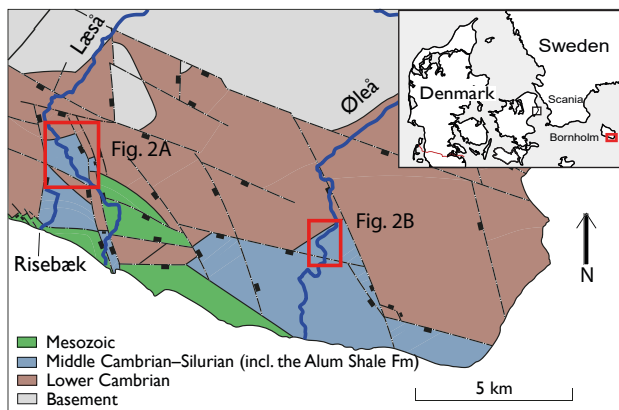
Fig. 1. Simplified geological map of southeastern Bornholm showing location of the Læså, Øleå and Risebæk streams. For locality details, see Fig. 2. Small insert shows location of the island of Bornholm in eastern Denmark.
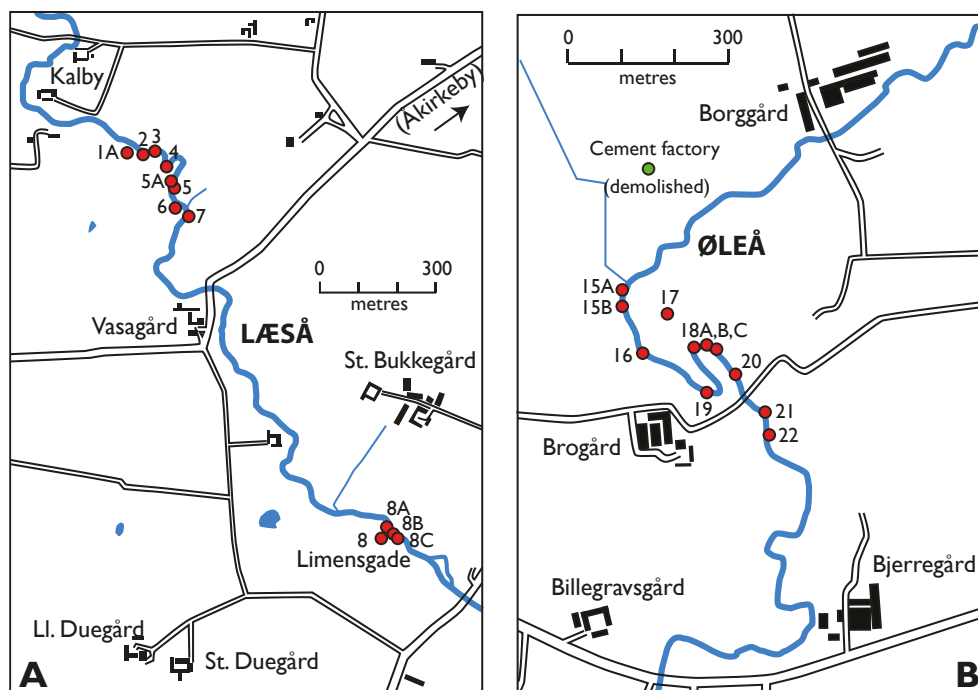
Fig. 2. Maps showing location of the Furongian Alum Shale exposures on Bornholm; see text for details. **A:** Detailed map of the Læså stream between Kalby and Limensgade SW of the town of Åkirkeby, showing location of exposures. **B:** Detailed map of the Øleå stream between Borggård and Sdr. Landevej east of the village of Pedersker, showing location of exposures.

scheme, comprising 23 zones allocated to six super-zones, is adopted here (Fig. 3).

The aim of the present study is to document the Furongian trilobites and agnostoids recovered from Bornholm and to present an updated review of the local biostratigraphy. The recorded total of 43 species and subspecies (incl. agnostoids) are characteristic of 14 trilobite zones representing all six Furongian superzones. Overall, the study confirms the biostratigraphy established by C. Poulsen (1923) with only minor corrections.

Material and methods

The study is based on the fossil material from the Alum Shale Formation on Bornholm stored at the Natural History Museum of Denmark (SNM), includ-

ing the specimens originally described by C. Poulsen (1923), as well as extensive new material collected by ATN in the 1970s. The studied material comprises 8502 counted and identified specimens, mostly disarticulated sclerites of trilobites plus a few agnostoids, but many more uncounted specimens are present in the samples at hand. They have been left out as they require preparation to be safely identified. The majority of the fossils are preserved in so-called anthraconite (early diagenetic bituminous carbonate), and only a few hundreds of specimens have been collected from the shale itself. The older anthraconite samples in the SNM collection are typically penetrated by numerous cracks, due to desiccation of the organic matter and/or pyrite oxidation. The newer material collected by ATN derives from loose limestone nodules found in the Læså stream near Vasagård and Limensgade (Fig. 2A). The nodules were numbered so that the material from each nodule is kept together, which is relevant for its use in biostratigraphic context.

The best preserved specimens of each taxon are illustrated. After preparation, the specimens were coated with ammonium chloride and photographed with a full-frame Canon EOS 5D Mark III camera. A series of 3–30 photos were taken of each specimen and subsequently stacked using the program Helicon Focus. The photographic illustrations were processed using Adope Photoshop software.

Illustrated specimens are numbered individually with the prefix MGUH. Samples in the so-called main collection at the Natural History Museum of Denmark are numbered with the prefix GM; nearly all of this material was collected in the early 1920s or earlier. The samples collected by ATN in the 1970s are numbered using the prefixes ATN and L. Please note that the fossiliferous samples labelled GM, ATN and L typically contain several specimens which therefore are referred to by the same sample number.

Localities

All exposures of Furongian Alum Shale along the Læså and Øleå streams, existing at that time, were described by C. Poulsen (1923) and Hansen (1945). We here briefly describe the localities and provide GPS coordinates (using World Geodetic System 1984, WGS84) measured with a handheld Garmin eTrex model 30. The uncertainty in positioning is typically <3 m. The locality number system introduced by C. Poulsen (1923) is maintained and emended to include new exposures (Figs 2A–B). Miaolingian exposures are not discussed and for this reason some of Poulsen's upper Cambrian localities with the *Agnostus pisiformis* Zone are omitted.

Chrono-stratigraphy			Super-zones	Scandinavian zonation	
				Trilobites	Graptolites/Agnostoids
Ordov. / Lower		Tremad.	(not defined)	(Boeckaspis hirsuta)	R. f. socialis & R. f. parabola
					R. parabola
					(not defined)
Cambrian / Furongian	Stage 10		Acerocarina	Acerocare ecorne	Trilobagnostus holmi
				Westergaardia scanica	
				Acerocarina granulata–Peltura costata	
			Peltura	Parabolina megalops	
				Parabolina lobata	Lotagnostus americanus
				Peltura scarabaeoides	
				Peltura acutidens–Ctenopyge tumida	
	Jiangshanian		Protopeltura	Sphaerophthalmus modestus–Sphaerophthalmus angustus	
				Sphaerophthalmus flagellifer	
				Sphaerophthalmus postcurrens	
				Leptoplastus neglectus	Pseudagnostus cyclopyge
			Leptoplastus	Leptoplastus stenotus	
				Leptoplastus crassicornis–Leptoplastus angustatus	
				Leptoplastus raphidophorus	
				Leptoplastus paucisegmentatus	
			Parabolina	Parabolina spinulosa	
				Parabolina brevispina	
	Paibian	u	Olenus	O. scanicus–O. rotundatus	Glyptagnostus reticulatus
				Olenus dentatus	
				Olenus attenuatus	
		l		Olenus wahlenbergi	
				Olenus truncatus	
				Olenus gibbosus	
	Mia.	Guz.	Paradoxides forchhammeri	Proceratopyge nathorsti–Simulolenus alpha	Agnostus pisiformis

Fig. 3. Current biozonation scheme for the Furongian of Scandinavia (from Nielsen *et al.* 2020; slightly modified with regard to agnostoid zonation, see text). Abbreviations: Mia.: Miaolingian; Guz.: Guzhangian; u: upper; l: lower; Ordov.: Ordovician; Tremad.: Tremadocian; *R.f.*: *Rhabdinopora flabelliformis*.
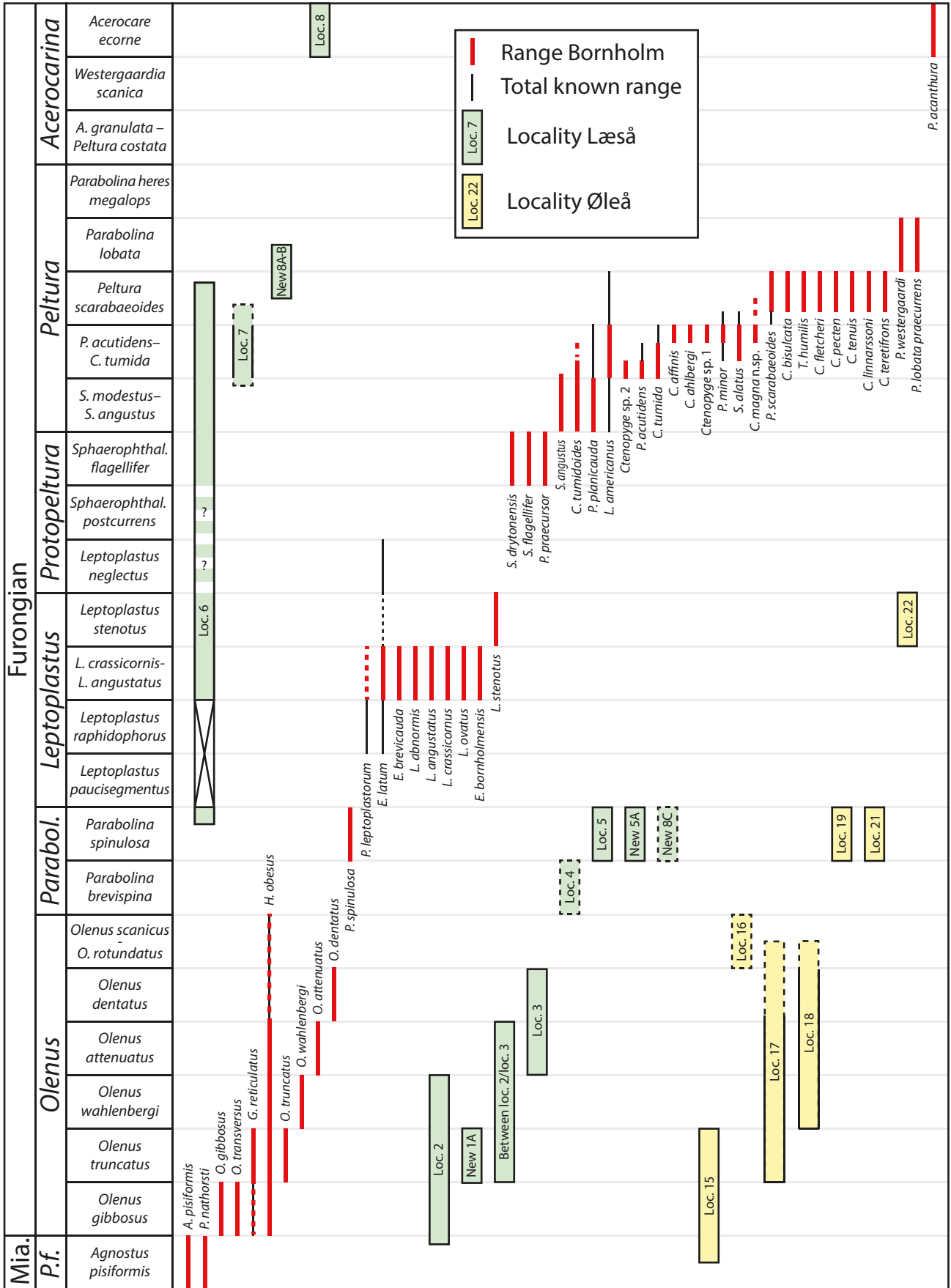
The outcrops in the Læså stream between Kalby and Vasagård (Fig. 2A) intermittently expose the *Olenus*, *Parabolina*, *Leptoplastus*, *Protopeltura* and lower part of the *Peltura* superzones, whereas at Limensgade only the uppermost part of the Furongian is accessible (sporadic exposures of the *Peltura* Superzone plus the very top of the *Acerocarina* Superzone). In the Øleå stream, parts of the *Olenus*, *Parabolina* and *Leptoplastus* superzones are exposed. Figure 4 outlines the zones present (or assumed present) in the different outcrops.

Furongian Alum Shale is also exposed in the Risebæk stream north of Sdr. Landevej (the road from Rønne to Nexø); for location of Risebæk, see Fig. 1. Where the Risebæk stream turns sharply west-north-westwards some 460 m north of the road, the Alum Shale contains *Orusia lenticularis* and represents the *Parabolina* Superzone (ATN, unpublished). The strata tilt *c.* 4–5° southwards and are overlain by Tremadocian Alum Shale and the Dapingian Komstad Limestone Formation immediately north of Sdr. Landevej (Nielsen 1995). Hence, the *Leptoplastus*, *Protopeltura*, *Peltura* and *Acerocarina* superzones are theoretically exposed in the Risebæk stream, at least intermittently, between the sharp turn of the creek and the road, but these exposures have never been investigated.

Læså

For location of exposures, see Fig. 2A.

New locality 1A
55°3'30.25"N, 14°53'6.44"E

A section of highly weathered Alum Shale can be seen along a tractor track in the field some 20 m west of the Læså creek, adjacent to the classical 'Kalby section' through the Miaolingian lower part of the Alum Shale Formation (locality II *sensu* Hansen 1945). The exposed succession, here referred to as new locality 1A, is normally *c.* 0.2 m high and *c.* 3 m long but trenching in 2020 exposed 1.15 m of strongly disturbed shale in a 9 m long section, including one large anthraconite lens in the middle of the exposure. The shale contains common *Olenus truncatus* and some *Homagnostus obesus* [this newly sampled fossil material is not included in the present study] showing that the section represents the basal Furongian. The bedding was measured at 52°/16° SE (n=3) in the northern part of the section and at 155°/14° E (n=2) in the southern part of the section. However, the shale is strongly disturbed due to glacio-tectonics.

Locality 2 (Hansen 1945, locality IV)
55°3'29.97"N, 14°53'8.67"E

Ca. 2.5 m long exposure in the southern bank and creek bed, including a limestone bed some 35 cm thick outcropping in the western part. This bed is a proxy for the Miaolingian/Furongian boundary in most wells on Bornholm penetrating this level (Nielsen *et al.* 2018). The dark grey limestone is fine-grained, compact and splintery, and contains sporadic phosphatic shells of bradoriid arthropods but no trilobites. The orientation of the limestone is 10°/5°E. *Olenus* occurs in the upper part of the section (downstream) according to C. Poulsen (1923), whereas Hansen (1945) reported *Olenus* from the entire section.

The studied material from this locality includes *Agnostus pisiformis, Homagnostus obesus, Glyptagnostus reticulatus, Olenus attenuatus, O. gibbosus, O. transversus, O. truncatus* and *O. wahlenbergi.* This assemblage is indicative of the *A. pisiformis* Zone and various zones in the lower part of the *Olenus* Superzone.

Locality 3 (Hansen 1945, locality V)
West end: 55°3'30.07"N, 14°53'9.97"E; east end: 55°3'29.98"N, 14°53'10.55"E

This locality is a *c.* 12 m long outcrop of shale in the northern bank of the creek with a height of up to 0.8 m. Shale is also exposed in the adjacent creek bed but is usually below the water table. The bedding orientation is 20°/10° SE (n = 2). C. Poulsen (1923) found common *H. obesus* at this locality and Kaufmann (1933a) described *O. dentatus* from a 1 cm thick horizon. Hansen (1945) noted that the shale in some places exhibits undulations, suggesting that hidden limestone concretions are present.

The studied material from this locality includes only *H. obesus* and *O. attenuatus,* showing that the exposed strata represent the *Olenus* Superzone. A shale sample 'from the Læså' without proper label contains a fragmentary cranidium that resembles *O. dentatus* (Fig. 7K) and may derive from this locality.

Locality 4 (Hansen 1945, locality VI)
West end: 55°3'28.77"N, 14°53'11.35"E; east end: 55°3'28.84"N, 14°53'12.11"E

A *c.* 14 m long and up to 1.3 m high exposure in the southern bank and adjacent creek bed continuing almost all the way to the opposite bank. 1.55 m of shale are exposed in total, some below the water table most of the year. An anthraconite lens, *c.* 100 × 14 cm in size, is seen in the upper part of the bank. Three smaller

▲ **Fig. 4.** Ranges of trilobites recorded from Bornholm; standard zonation adopted from Nielsen *et al.* (2020). Inferred stratigraphic ranges of exposures are also shown. For location of exposures, see Fig. 2. Dashed locality boxes: Uncertain age of exposed strata.

lenses, *c.* 45 × 15 cm in size, are exposed near the top in the western end of the section, but they are partially hidden by vegetation. Small barite lenses up to *c.* 15 × 10 cm in size, often smaller ('fist size', Hansen 1945), are common in the shale exposed in the creek bed, i.e. in the lower part of the succession. The bedding orientation is 85°/7° S (n=4). C. Poulsen (1923) found a few poorly preserved *Orusia lenticularis* at this locality suggesting a correlation with the *Parabolina* Superzone.

Locality 5 (Hansen 1945, locality VII)
55°3′26.64″N, 14°53′11.82″E

Exposure in the creek bed adjacent to the eastern bank. Only the top of two anthraconite lenses are now exposed, measuring *c.* 1 × 1 m and *c.* 0.5 × 0.5 m, respectively. No shale is exposed, and it is impossible to measure the orientation of strata. C. Poulsen (1923) found *Orusia lenticularis* at this locality together with a few *Parabolina spinulosa*, which is confirmed by the present study. From this site, Hansen (1945) described four anthraconite lenses, up to 1 m in diameter, and a limestone bed, partly coqinoid, with *Orusia*. The exposed strata represent the *Parabolina* Superzone.

New locality 5A
West end: 55°3′27.12″N, 14°53′12.13″E; east end: 55°3′27.17″N, 14°53′12.48″E

Slightly tilting shale beds are exposed in the creek bed along the western bank on the opposite side of locality 5. The exposure is *c.* 12 m long, but only up to 15 cm high; in total *c.* 0.5 m of shale is exposed. Five anthraconite lenses were observed *in situ*; the lenses are up to *c.* 40 × 30 cm in size. The bedding orientation was measured at 19°/9° E and 42°/6° SE; the scatter is likely due to the presence of limestone nodules.

Locality 6 (Hansen 1945, locality VIII)
Northwest end: 55°3′26.22″N, 14°53′12.00″E; southeast end: 55°3′25.20″N, 14°53′13.07″E

This is the best known Alum Shale section in the Læså stream, originally described by Grönwall (1916) and C. Poulsen (1923). It is *c.* 40 m long and *c.* 6 m high and is located in the southern bank of the creek. Grönwall (1916) reported 25 limestone nodules from this exposure; note that not all concretion levels are shown in the synoptic profile published by C. Poulsen (1923, fig. 2). Fifteen anthraconite lenses, up to 63 × 155 cm in size, can still be seen in the section. The bedding orientation was measured at 112°/9° S (n=6) but is a little irregular due to the common presence of limestone nodules. In the western end of the section, the creek bank is overgrown, but anthraconite lenses and a little shale are exposed here and there, notably in the upper part; this rather covered part is not included in the stated total length of the section.

Several trilobite zones are exposed (C. Poulsen 1923, fig. 2); all stated thicknesses are cited from that publication. *Orusia lenticularis* is common at the base of the section and this basal interval represents the upper 2 m of the *Parabolina* Superzone. Then follows a limestone-dominated horizon, *c.* 0.5 m thick, consisting of more or less amalgamated limestone nodules representing the *Leptoplastus* Superzone. This level is overlain by *c.* 1.1 m of shale with several large anthraconite lenses, representing the *Protopeltura* Superzone. Then follows shale with scattered anthraconite lenses representing the *Peltura* Superzone, where the *Peltura acutidens–Ctenopyge tumida* Zone, 2.10 m, and the *Peltura scarabaeoides* Zone (>1.8 m) are confirmed to be present. Nielsen *et al.* (2018) inferred that the former zone is up to 1.7 m thick in the Læså area based on correlation of gamma logs in wells. C. Poulsen (1923, fig. 2) assigned the uppermost part of the section, exposed high in the rather overgrown western end, to the *Parabolina 'longicornis'* Subzone [now *P. lobata* Zone], but this is incorrect. The sparse material labelled as *Parabolina 'longicornis'* in the museum collection (a couple of free cheeks only) represents *Ctenopyge tenuis* and derives from the *Peltura scarabaeoides* Zone and no specimens of *P. lobata* have been found at localities 6 or 7. Loose slabs of limestone sampled from the scree high in the western part of the section (i.e. immediately below the level suggested to represent the *P. lobata* Zone by C. Poulsen 1923) contain only *P. scarabaeoides* and *T. humilis*, suggesting that the *P. scarabaeoides* Zone extends to the very top of the succession. This is also in better accordance with the thickness of this zone indicated by Nielsen *et al.* 2018 (4.5 m in a nearby well).

The studied material from this locality includes *Ctenopyge affinis*, *C. bisulcata*, *C. fletcheri*, *C. linnarssoni*, *C. magna* n. sp., *C. pecten*, *C. tenuis*, *C. teretifrons*, *C. tumida*, *C. tumidoides*, *Eurycare bornholmensis*, *E. brevicauda*, *E. latum*, *Leptoplastus abnormis*, *L. angustatus*, *L. crassicornis*, *L. ovatus*, *L. stenotus*, *Lotagnostus americanus*, *Parabolina spinulosa*, *Peltura acutidens*, *P. minor*, *P. scarabaeoides*, *Protopeltura planicauda*, *P. praecursor*, *Pseudagnostus leptoplastorum*?, *Sphaerophthalmus alatus*, *S. angustus*, *S. drytonensis*, *S. flagellifer* and *Triangulopyge humilis*. This assemblage confirms the biozonation outlined by C. Poulsen (1923) except for the lack of the *P. lobata* Zone.

Locality 7 (Hansen 1945, locality IX)
55°3′24.57″N, 14°53′14.32″E

This outcrop, *c.* 8 m long and up to 1.3 m high, is located in the eastern bank, where the creek bends south-westwards shortly downstream of locality 6. The bedding orientation is 104°/7° S. Please note that this exposure is incorrectly located on the map shown by C. Poulsen (1923, fig. 1); the exposure far-

ther downstream labelled as 7 on his map represents Tremadocian Alum Shale. However, it is obvious from the adjoining description that locality 7 in fact is positioned as indicated on Fig. 2A (see also Hansen 1945, fig. 8). The studied material from this locality includes *Ctenopyge ahlbergi*, *C. affinis*, *C. bisulcata*, *C. fletcheri*, *C. magna* n. sp., *C. tenuis*, *C. tumida*, *C. tumidoides*, *Sphaerophthalmus alatus* and *S. angustus*, showing that the exposed strata represent the lower part of the *Peltura* Superzone and probably also the *S. modestus–S. angustus* Zone. C. Poulsen (1923) reported also *Ctenopyge teretifrons*, *Peltura scarabaeoides* and *Triangulopyge humilis* (under the name *S. alatus*) from locality 7, but no museum material of these taxa is preserved from the locality. The presence of *C. bisulcata* indicates, however, that the top of the section represents the *P. scarabaeoides* Zone.

The tops of several large anthraconite lenses are exposed in the creek bed downstream of locality 7. C. Poulsen (1923) did not find fossils in these nodules but as the stream here is oriented along strike, they most probably represent the lower part of the *Peltura* Superzone.

Locality 8 (Hansen 1945, locality X)
North-western end: 55°2′55.86″N, 14°53′38.96″E; south-eastern end: 55°2′54.92″N, 14°53′39.21″E

This locality is the abandoned limestone-shale quarry at Limensgade. The quarry was thoroughly cleaned in 2017, providing extensive and excellent exposures – probably the best since the quarry was active in the 1840s. The upper 4.5 m of the Alum Shale Formation is exposed on the lower terrace and the lower 2.3 m of the overlying Middle Ordovician Komstad Limestone is exposed on the upper terrace. The shale succession on the lower terrace is *c.* 30 m long and exposes mainly the Tremadocian Alum Shale but with Furongian Alum Shale near the base (lower 0.5 m). No anthraconite lenses were seen in the basal part in 2017–18 despite intensive search and these concretions seem to be rare (lenses were apparently still visible when Hansen 1945 investigated the site). The bedding orientation is 3°/4° W (n=6) but is rather variable due to the small dip.

In anthraconite lenses in the lowermost part of the section, C. Poulsen (1923) found sparse *Parabolina acanthura*, indicative of the *Acerocarina* Superzone. This level is in turn overlain by 0.1 m of unfossiliferous shale, followed by graptolitic Tremadocian Alum Shale, 4.0 m thick (von Jansson 1979). The smaller thickness of the Tremadocian stated by C. Poulsen (1922, 1923) reflects that he failed to find graptolites lower down.

New exposures in the Læså stream near the Limensgade quarry

For location, see Fig. 2A.

New locality 8A
55°2′56.53″N, 14°53′40.04″E
Low outcrop of highly weathered shale in the south-western bank of the creek. The exposure is *c.* 0.35 m high and *c.* 4 m long. The shale contains a few limestone lenses, and several nodules can be seen lying loose in the creek. Loose material of this kind was sampled by ATN in the late 1970s and has been investigated here (including several anthraconite nodules that were collected downstream of this exposure). The material contains *Ctenopyge linnarssoni*, *C. tenuis*, *Parabolina lobata praecurrens*, *Peltura scarabaeoides*, *P. westergaardi* and *Triangulopyge humilis*, indicating the presence of the *Peltura scarabaeoides* and the *Parabolina lobata* zones (*Peltura* Superzone).

New locality 8B
55°2′55.88″N, 14°53′41.18″E
Shale with some limestone lenses is exposed in the south-western bank of the creek just north of the wooden pedestrian bridge. The section is *c.* 10 m long, and the exposed succession is *c.* 0.7 m thick. The bedding orientation is 4°/12° W. Regarding fossil content, see locality 8A. No fossils have been sampled *in situ*.

New locality 8C
55°2′55.28″N, 14°53′42.04″E
A small outcrop of coarse anthraconite (concretion) and a little shale can be seen in the creek bed near the north-eastern bank, about 20 m downstream of the wooden pedestrian bridge. The total exposed thickness is *c.* 0.4 m. The shale bedding is affected by the concretion, but the general bedding orientation is about 1°–10°/up to 28°W. The rather strong dip suggests proximity of a fault. An articulate brachiopod, *Orusia*?, was found in the anthraconite and the exposed strata likely represent the *Parabolina* Superzone.

Øleå

For location of exposures, see Fig. 2B. Several Furongian trilobites in the SNM collection are labelled 'Cementen' or 'Cementfabrikken, Ølenå' [Cement factory, Øleå], which refer to a former cement factory at Borggård east of Pedersker, which was in operation 1846–1915 (for location, see Fig. 2B). The fossils are said to have been collected from the limestone that was intended to be crushed for cement fabrication. These Furongian fossils must derive from local ice-rafted limestone that apparently also was used for

manufacturing cement in addition to the quarried Miaolingian limestone.

Locality 15A (Hansen 1945, locality 8, upstream part)
North end: 55°1′34.95″N, 15°0′20.82″E; south end: 55°1′34.68″N, 15°0′20.68″E

C. Poulsen's (1923) locality 15, which is located in the western bank of the creek, is subdivided here into 15A and 15B. Site 15A is 12 m long and exposes 1.5 m of shale, of which 0.4 m is below the water table (even in 2018 when the water level was exceptionally low). The bedding orientation is 86°/4° S (n=3).

The material studied from locality 15 (undivided) contains only *Olenus truncatus*. Investigations of locality 15B in 2020 suggested that the shale at locality 15A probably represents the Miaolingian *Agnostus pisiformis* Zone.

Locality 15B (Hansen 1945, locality 8, downstream part)
North end: 55°1′34.43″N, 15°0′20.53″E; south end: 55°1′33.86″N, 15°0′20.75″E

This exposure starts 10 m downstream of site 15A and is 1.3 m high and 18 m long. The section is shale dominated, but a large limestone lens, 150 × 23 cm in size, is seen in the southern end of the outcrop. It contains bradoriid arthropods and the horizon may correspond to the limestone bed seen at locality 2 in the Læså stream. Investigations in 2020 showed that *Olenus* representatives turn up immediately below this limestone and not 0.5 m above it, as stated by C. Poulsen (1923). A pygidium of *Proceratopyge nathorsti* (indicative of the Miaolingian *Proceratopyge nathorsti–Simulolenus alpha* Zone) was found 10 cm below the first occurrence of *Olenus*. The bedding orientation is 54°/5° S (n=2).

Locality 16 (Hansen 1945, locality 9)
West end: 55°1′31.41″N, 15°0′21.67″E; east end: 55°1′30.40″N, 15°0′24.56″E

This is the most extensive exposure of Alum Shale in the Øleå stream. The section in the southern creek bank is 4 m high and 60 m long, although it is partially overgrown and covered by soil. The bedding orientation is 110°/3° S (n=13).

In the eastern end of the section the shale contains five anthraconite lenses, of which the largest measures 55 × 190 cm. The shale contains also common small limestone concretions (c. 10 cm in diameter); the limestone is greyish, very fine-grained, splintery and unfossiliferous except for bradoriid arthropods. At this locality, C. Poulsen (1923) found poorly preserved *Homagnostus obesus* at about 1.25 m above the creek level, showing that the exposed succession represents the *Olenus* Superzone, presumably its upper part. The

studied material from this locality includes only *H. obesus*.

Locality 17 (obliterated)
This small pit, from which shale had been excavated for road material, was located in the field east of the Øleå stream, but is now infilled. C. Poulsen (1923) reported *Glyptagnostus reticulatus*, *Homagnostus obesus* and *Olenus truncatus* from this site; the studied material from the locality includes also *Olenus attenuatus* and *Olenus wahlenbergi*.

Locality 18 (Hansen 1945, locality 10)
Western end: 55°1′31.09″N, 15°0′27.80″E; eastern end: 55°1′31.22″N, 15°0′27.96″E

This shale exposure, 7 m long and up to 0.35 m high, is located in the northern bank of the creek. The bedding orientation is 21°/2° E (n=3). C. Poulsen (1923) found common *Homagnostus obesus* at this site. The studied material from this locality includes also *Glyptagnostus reticulatus, Olenus wahlenbergi* and *O. dentatus*, showing that the shale represents the *Olenus* Superzone.

More Alum Shale has been exposed downstream of this site since C. Poulsen's (1923) investigations. Approximately 10 m downstream of site 18 (GPS coordinates north end: 55°1′31.26″N, 15°0′28.29″E; south end: 55°1′30.97″N, 15°0′28.87″E), a shale exposure, 14 m long and up to 0.5 m high, is present in the northeastern bank of the creek. The bedding orientation is 20°/5° E (n=3). Slightly farther downstream (GPS coordinates 55°1′30.60″N, 15°0′29.09″E) occurs a small exposure of shale in the north-eastern creek bank, up to 0.35 m high and extending for 3.5 m. The bedding orientation is 39°/3°E (n=3).

The three exposures constitute almost one long outcrop, separated by small areas covered by vegetation, mainly tree roots.

Locality 19 (Hansen 1945, locality 11)
Eastern end: 55°1′28.42″N, 15°0′29.60″E; western end: 55°1′28.66″N, 15°0′28.39″E

This shale exposure, 24 m long and up to 1.4 m high, is located in the southern creek bank. Much vegetation is present with tree roots growing in between the shale. The shale can be seen also in the northern creek bank and in the creek bed itself. The bedding orientation is 106°/4° S (n=6) in the southern end of the exposure. At this locality both C. Poulsen (1923) and Hansen (1945) found common *Orusia lenticularis*, indicative of the *Parabolina* Superzone.

Locality 20 (Hansen 1945, locality 12)
Northern end: 55°1′30.13″N, 15°0′30.88″E; southern end: 55°1′29.85″N, 15°0′31.11″E

Highly weathered unfossiliferous shale is exposed here in the north-eastern creek bank for a stretch of *c.* 14 m; *c.* 0.9 m of shale is exposed (some below the water table under normal circumstances). The bedding orientation is 40°/3° E (n=7).

On the map shown by C. Poulsen (1923, fig. 1) this locality is placed a little too far south.

Locality 21 (Hansen 1945, locality 13)

Northern end: 55°1′27.08″N, 15°0′33.92″E; southern end: 55°1′26.89″N, 15°0′34.09″E

About half of this exposure was below the water table even in August 2018 when the water level in the stream was unusually low. Shale, *c.* 0.65 m thick, is exposed in the north-eastern bank and can be followed for *c.* 7.5 m. A (?loose) lens is exposed in the southern end of the exposure immediately below the Quaternary strata. The exposure yields *Orusia lenticularis* as described also by C. Poulsen (1923), indicative of the *Parabolina* Superzone. The bedding orientation is 143°/11° E (n=5).

Locality 22A (Hansen 1945, locality 14)

55°1′26.16″N, 15°0′34.5″E

C. Poulsen (1923) reported findings of a few anthraconite lenses containing *Leptoplastus stenotus* within the creek bed at this site and his species identification is confirmed by the present study. A shale exposure, *c.* 5 m long, was seen in May 2019 in the creek bed (below the water table).

Locality 22B

55°1′25.8″N, 15°0′34.2″E

An anthraconite lens, *c.* 0.8 m in diameter, is exposed here in the creek bed adjacent to the eastern bank. Since no shale is visible, the bedding orientation could not be measured.

Hansen 1945, locality 16

Hansen (1945, p. 20) reported an anthraconite lens and almost horizontally lying Alum Shale from this site, which was not mentioned by C. Poulsen (1923). Reconnaissance field work in May 2019 failed to locate the exposure and it may have referred to a loose raft of Alum Shale embedded in Quaternary till.

Furongian zones on Bornholm

Olenid trilobites are typically extremely abundant in the Furongian part of the Scandinavian Alum Shale Formation and a detailed biostratigraphy was established by Westergård (1922, 1947) and Henningsmoen (1957), with subsequent revisions introduced by Ahl-berg (2003), Terfelt *et al.* (2008), Høyberget & Bruton (2012), Nielsen *et al.* (2014), and Rasmussen *et al.* (2015, 2016). In the present study we use the modified zonation recently introduced by Nielsen *et al.* (2020), and we refer to that paper for further comments on the Scandinavian zonal scheme. The zonation used in the current study is shown in Fig. 3. Agnostoids are generally rare (except for *Homagnostus obesus*) and of very low diversity in the Furongian of Scandinavia. Terfelt et al. (2008) outlined four agnostoid zones (see Fig. 3), which primarily are of relevance for correlation out of Baltica.

The Furongian trilobite zones on Bornholm were remarked on by Johnstrup (1874, 1891) and Grönwall (1916), but C. Poulsen (1923) is the only detailed study published so far. He investigated eight localities along or near the Læså stream, 12 localities along or near the Øleå stream and two localities in the vicinity of Risebæk (for location of these watercourses, see Fig. 1). C. Poulsen (1923) recorded altogether 24 different species and 'variants' of olenids and four agnostoids and he recognized six zones and 11 subzones (including the *A. pisiformis* Zone), following the stratigraphy introduced by Westergård (1922). In the present study, 43 different taxa are reported from the Furongian of Bornholm and they are characteristic of 14 trilobite and three agnostoid zones (Fig. 4).

Some of the material stored at the Natural History Musem of Denmark must have been collected *in situ* (see C. Poulsen 1923, fig. 6) but no records of sampling levels are preserved. Hence, the precise collecting levels of the studied material are essentially unknown. In terms of biostratigraphy, this obviously is not ideal but since most olenid trilobites range through only one or two zones (see summary of ranges in Nielsen *et al.* 2020, fig. 1), it is possible to establish which fossiliferous Furongian zones are exposed on Bornholm with a high degree of confidence.

Agnostoid zonation

The uppermost Miaolingian *Agnostus pisiformis* Zone is characterized by the eponymous index fossil, which is common on Bornholm (recorded at localities 1, 2, 11, 13 and 14 as well as downstream of locality 8C, see taxonomic section). It co-occurs with common phosphatocopines, but no other agnostoids have been collected from the zone. A single pygidium of *Proceratopyge nathorsti* has recently been collected from the very top of the *A. pisiformis* Zone at locality 15B (not illustrated, sample GM 2019-100). The overlying *Glyptagnostus reticulatus* Zone, straddling the entire *Olenus* Superzone (Fig. 3), is defined by the FAD of *G. reticulatus*, which is infrequent on Bornholm, whereas *Homagnostus obesus* is common. Both species have been recorded from the lower part of the *Olenus* Superzone (localities 2–3

and 16–18). Only one agnostoid cephalon, assigned to *Pseudagnostus leptoplastorum*?, have been found at locality 6 in the overlying *Pseudagnostus cyclopyge* Zone, in which agnostoids are exceedingly rare on Bornholm as elsewhere in Scandinavia. The index fossil itself, *P. cyclopyge,* has not been found and identification of the zone remains open to interpretation. The only agnostoid reported from the overlying *Lotagnostus americanus* agnostoid Zone is the eponymous species, of which just one specimen is preserved in the studied collection. According to C. Poulsen (1923) it derives from the *Ctenopyge tumida–Peltura acutidens* olenid Zone at locality 6. This seems to be the level where *L. americanus* turns up in Scandinavia (Westergård 1922, 1947); there are no documented reports from the *Sphaerophthalmus modestus–Sphaerophthalmus angustus* Zone (cf. Ahlberg & Terfelt 2012). No agnostoids from the *T. holmi* Zone have been recorded on Bornholm. In previous literature the zone was inferred starting from about the base of the *P. scarabaeoides* olenid Zone, based on the record of a single pygidium from the conglomerate at the top of the Alum Shale Formation at Uddagården, Falbygden, Sweden (Westergård 1922, p. 69). However, everywhere else in Scandinavia is *T. holmi* known exclusively from the *P. lobata* Zone and we envisage that the conglomerate at Uddagården, which marks an extensive hiatus, in part formed during the *P. lobata* Zone.

Olenid zonation

Olenus Superzone

The *Olenus* Superzone comprises six zones (Fig. 3), and index fossils from five of these are present in the studied material, viz. *O. gibbosus, O. truncatus, O. wahlenbergi, O. attenuatus* and *O. dentatus*. The material derives from localities 2–3, 15, 17 and 18. The base of the superzone is defined by the FAD of *O. gibbosus.* Only a few specimens of that species are at hand, all from locality 2, and apparently *O. gibbosus* is rare or perhaps the eponymous zone is thin and/or not well-exposed. Kaufmann (1933a) did not observe *O. gibbosus* in the Læså sections (localities 2–3) and in a recent unpublished study of the Miaolingian/Furongian boundary beds at locality 15B in the Øleå no specimens were found. Here the base of the Furongian is marked by the FAD of *O. transversus* and maybe this is the general pattern in the Øleå area. The latter species has been found at locality 2, in the creek bed between localities 2 and 3 and at locality 15B. It is conceivable that it characterizes a thin separate interval like in Scania (see Kaufmann 1933b; Westergård 1942, 1944); elsewhere in Scandinavia it co-occurs with *O. gibbosus* (Westergård 1922; Henningsmoen 1957). *Olenus truncatus* and *O. wahlenbergi* are common on Bornholm. The former

has been found at locality 2, in the riverbed between localities 2 and 3, and at locality 15. The latter occurs commonly at localities 17 and 18 and one free cheek is from locality 2. Kaufmann (1933a) described *O. dentatus* from a 1 cm thick horizon in the Læså stream (locality 3). None of that material is kept in the SNM collection, but given Kaufmann's extensive knowledge on *Olenus*, his determination is regarded reliable. A fragmentary cranidium in the SNM collection, likely deriving from locality 3, is tentatively assigned to *O. dentatus* (Fig. 7K). Another safely assigned specimen of *O. dentatus* (external mould of complete specimen) derives from locality 18 (Fig. 7J). Hence, all zones of the *Olenus* Superzone except for the *O. scanicus–O. rotundatus* Zone are proven present by fossils. Nielsen *et al.* (2018) concluded, based on correlation of gamma logs in wells, that also the *O. scanicus–O. rotundatus* Zone is developed on Bornholm. The shale at locality 16, where only *H. obesus* has been recorded, is a likely candidate for this horizon. The lower richly fossiliferous part of the *Olenus* Superzone (*O. gibbosus* Zone to the Last Appearance Datum of *O. dentatus*) is 1.8–2.9 m thick in wells in the Læså area according to gamma log stratigraphy (Nielsen *et al.* 2018, table 5). Kaufmann (1933a, text-fig. 1) measured this interval at close to 2 m in the Læså stream (localities 2–3).

Parabolina Superzone

This superzone comprises two zones (Fig. 3), of which the *Parabolina spinulosa* Zone is confirmed present on Bornholm through findings of the eponymous species at localities 5–6. Nielsen *et al.* (2018) inferred, based on correlation of gamma logs in wells, that also the *Parabolina brevispina* Zone is developed, although perhaps only in the Læså area, but the index fossil has not been found so far. The zone may be non-trilobitic or is not exposed. The shale at locality 4 is a potential candidate; here only sparse *Orusia lenticularis* has been found (C. Poulsen 1923). This brachiopod is very common in both zones of the *Parabolina* Superzone (recorded at localities 4–6, 19, 21).

Leptoplastus Superzone

This superzone is characterized by representatives of *Leptoplastus* and *Eurycare* and comprises four zones (Figs 3–4). The superzone is thin, just *c.* 0.5 m at locality 6 (see C. Poulsen 1923, fig. 2), which is the general trend in wells on Bornholm (Nielsen *et al.* 2018). Only the *Leptoplastus crassicornis–Leptoplastus angustatus* and *Leptoplastus stenotus* zones are developed (localities 6 and 22) and the *Leptoplastus paucisegmentatus* and *L. raphidophorus* zones appear to be absent on Bornholm. In the limestone lenses at locality 6, *Eurycare latum* is very common in a *c.* 5 cm thick basal horizon, but rare specimens of *E. brevicauda*, *L. crassicornis* and *L. ovatus*

have also been found in this interval. Then follows *c.* 5 cm of coarse-grained unfossiliferous anthraconite, in turn overlain by limestone containing *Eurycare bornholmensis, Leptoplastus abnormis, L. angustatus, L. crassicornis, L. ovatus* and *Pseudagnostus leptoplastorum*?, indicative of the *L. crassicornis–L. angustatus* Zone. This zone is presumably about 0.3 m thick (+/- 5 cm). *Leptoplastus angustatus, L. crassicornis* and *L. ovatus* co-occur in the same samples supporting the abandonement of three individual zones (see Rasmussen *et al.* 2015). We note, however, that in 25% of the 85 samples containing *L. angustatus,* the species occurs alone, typically in profusion, showing that at least one horizon (a single bedding plane?) is characterized by this species occurring alone, probably for ecological reasons. The upper part of the superzone contains only *L. stenotus*; it is characteristic of the eponymous zone (?10–20 cm thick). *Leptoplastus stenotus* has been recorded also at locality 22.

Protopeltura Superzone

In the revised zonal scheme for Scandinavia, this superzone is subdivided into four zones (Fig. 3). *Leptoplastus neglectus* has not been found on Bornholm, but correlation of gamma logs in wells suggests that the eponymous zone is developed (Nielsen *et al.* 2018). It is thin, 0.2–0.5 m (maybe even including the overlying *Sphaerophthalmus postcurrens* Zone) and requires detailed sampling to be located. A resampling of the section exposed at locality 6 should be made in order to verify its assumed presence. The absence of samples with *L. neglectus* in the museum collection indicates that the interval contains no limestone. *Sphaerophthalmus postcurrens*, characterizing the overlying zone, likewise has not been encountered on Bornholm, but considering that the zone is very thin in Scania (Westergård 1942, 1944) it may be only a few centimetres thick if developed at all.

Sphaerophthalmus flagellifer, the index species of the overlying zone, is common in the studied museum collection. It co-occurs with common *Sphaerophthalmus drytonensis* and one pygidium of *Protopeltura praecursor* has also been found. This is the first record of the latter two species on Bornholm. *Protopeltura praecursor* is known from the lower three zones of the *Protopeltura* Superzone in Scandinavia (Nielsen *et al.* 2020, fig. 1). *Sphaerophthalmus drytonensis* has been described from the *S. postcurrens* and *S. flagellifer* zones in the Oslo Region and from the latter zone in Sweden (Henningsmoen 1957, Høyberget & Bruton 2012, Rasmussen *et al.* 2016). The *S. flagellifer* Zone is exposed at locality 6 and was stated to be 1.1 m thick by C. Poulsen (1923), but this figure probably includes the *S. modestus–S. angustus* Zone (see below). Nielsen *et al.* (2018, table 5) indicated that the *S. flagellifer* Zone is only *c.* 0.5

m thick in the Læså area. *Sphaerophthalmus flagellifer* or *S. drytonensis* (the material is preserved in shale and cannot be differentiated) have been found also at 106.0 m in the Billegrav-2 core (erroneously recorded as *Leptoplastus* resembling *L. neglectus* by Nielsen *et al.* 2018, p. 250). *Sphaerophthalmus angustus* was reported as *Ctenopyge flagellifera* var. *angusta* by C. Poulsen (1923) from "the upper part of the *S. flagellifer* Zone" at locality 6, indicating the presence of the *Sphaerophthalmus modestus–Sphaerophthalmus angustus* Zone. Nielsen *et al.* (2018) also inferred that this zone is developed on Bornholm, based on correlation of gamma logs in wells. *Sphaerophthalmus angustus* and *Ctenopyge tumidoides*, generally considered indicative of the *S. modestus–S. angustus* Zone (Henningsmoen 1957; Nielsen *et al.* 2020), have been found in many limestone samples; the latter species is new to Bornholm. One specimen of *Protopeltura planicauda* has also been found; this is its first report from Bornholm. Elsewhere in Scandinavia, this species is known also from the overlying *Peltura acutidens–Ctenopyge tumida* Zone, but the one specimens at hand co-occurs with *S. angustus* and *C. tumidoides,* showing a probable derivation from the *S. modestus–S. angustus* Zone. However, several cranidia of *Ctenopyge tumida* (e.g. Fig. 29J, K, Q) and a few specimens of *Peltura acutidens* have been found in 25% of the samples containing *C. tumidoides* and *S. angustus*, showing that these species range into the *Peltura* Superzone. This raises the question whether the *S. angustus–C. tumidoides* assemblage without *C. tumida* and/or *P. acutidens* represent the *S. modestus–S. angustus* Zone or whether the two younger species (of which *P. acutidens* is very rare) fortuitously are missing in 75% of the samples. In order to examine this question, we looked into the derivation and frequency of the trilobites in the different limestone nodules sampled *ex situ* by ATN in the 1970s (which was numbered and kept apart during sampling):

- The *S. angustus–C. tumidoides* assemblage is recorded in 12 individual limestone lenses
- The same 12 lenses also yielded assemblages typical of the *P. acutidens–C.tumida* Zone (see below)
- The mixed *S. angustus–C. tumidoides* assemblage including *C. tumida* and/or *P. acutidens* was recorded in only two of these lenses (four out of 27 samples collected by ATN)
- The mixed assemblage including *C. tumida* and/ or *P. acutidens* is observed in a total of 11 out of the 41 samples at hand containing *S. angustus* and *C. tumidoides* (including older museum material not deriving from the discussed 12 lenses)
- The faunal mixing is real and not due to occurrence of the discussed species in different parts of the samples

Based on these figures and given that *C. tumida* is fairly common in the mixed assemblage, we conclude that a majority of the samples containing the *S. angustus–C. tumidoides* assemblage without younger faunal elements probably derives from the *Protopeltura* Superzone. The fact that the transitional mixed assemblage is seen in only two lenses indicates that the horizon is thin or discontinuous. For further remarks, se discussion on the *Peltura* Superzone below.

Peltura Superzone

The base of this superzone is defined by the FAD of *Peltura acutidens* (Nielsen *et al.* 2014) and it is subdivided into four zones, see Fig. 3. The *Peltura* Superzone is exposed at localities 6–7 and poorly so at Limensgade (localities 8A–B).

The *Peltura acutidens–Ctenopyge tumida* Zone is represented by three different trilobite assemblages that potentially may serve to recognize local subzones on Bornholm. The oldest assemblage contains very common *S. angustus* co-occurring with fairly common *C. tumidoides* and *C. tumida* as well as very rare *P. acutidens*. This transitional assemblage, discussed above, shows that *S. angustus* and *C. tumidoides* range into the basal part of the *Peltura* Superzone. In fact, very rare specimens of *C. tumidoides* have been found associated with *S. alatus*, demonstrating an even longer upwards range of this species. The two younger assemblages from the *P. acutidens–C. tumida* Zone are both characterized by *S. alatus*, which is overwhelmingly common in nearly all samples. In addition to the omnipresent *S. alatus*, one set of samples is characterized by common *C. tumida* co-occuring with very rare *C. tumidoides* and pelturids which could not be assigned to species. The other set of samples contains *S. alatus*, which is predominant, co-occurring with common *Ctenopyge affinis,* moderately common *C. ahlbergi* and *C. magna* n. sp. and infrequent *Peltura minor*. This latter assemblage seemingly corresponds to the abandoned *C. affinis* (Sub)Zone (see Høyberget & Bruton 2012; Nielsen *et al.* 2020); no *C. tumida* has been found in these samples. The stratigraphically important *P. acutidens* and *P. minor* have not been previously reported from Bornholm and *C. ahlbergi* is also new to the local fauna.

All three assemblages of the *P. acutidens–C. tumida* Zone have been recorded from the same 12 anthraconite nodules that also yielded samples with a *S. angustus–C. tumidoides* assemblage as discussed above. Even the largest nodules in the Alum Shale Fm are ≤1 m thick, implying that the two older assemblages of the *P. acutidens–C. tumida* Zone as well as the *S. angustus–C. tumidoides* assemblage must derive from rather thin intervals each measuring a few decimetres at most. This also entails that the main upper part of the *P. acutidens–C. tumida* Zone, which is 1.5–1.7 m thick in the Læså area (Nielsen *et al.* 2018), likely is characterized by the *C. affinis* assemblage, but no individual nodules containing exclusively this fauna were found by ATN in the 1970s. This suggests that the upper part of the zone is devoid of limestone concretions, or that they are rare. Judging from C. Poulsen (1923, fig. 2), *C. tumida* may have a longer range upwards than indicated by the sampled anthraconite nodules from the *Protopeltura/Peltura* boundary interval.

The overlying horizon is now referred to as the *Peltura scarabaeoides* Zone (Fig. 3). It broadly corresponds to the *Ctenopyge bisulcata* and *Ctenopyge linnarssoni* (sub)zones in the schemes published by Henningsmoen (1957) and Terfelt *et al.* (2008), but *P. scarabaeoides* appears before *C. bisulcata*. Both of these former index species are present in the studied material, but *C. bisulcata* is rare. C. Poulsen (1923) reported the latter species from the upper part of the *P. scarabaeoides* Zone at locality 6, but it should be observed that the exposed section represents only the lower half of that zone (cf. Nielsen *et al.* 2018). We also note that *C. bisulcata* has been found at locality 7, indicating a range from near the base of the *P. scarabaeoides* Zone as that section represents mainly the *P. acutidens–C. tumida* Zone.

Ctenopyge linnarssoni is common at locality 6 according to C. Poulsen (1923); new material collected by ATN demonstrates that it is present also at Limensgade (localities 8A–B), where it co-occurs with common *C. tenuis, C. teretifrons, P. scarabaeoides* and *T. humilis*. These taxa are all characteristic of the *P. scarabaeoides* Zone (Nielsen *et al.* 2020). *Ctenopyge pecten* also occurs sparsely in the zone and has been found mainly at locality 6; it is new to Bornholm as *C. pecten sensu* C. Poulsen (1923) represents *C. tenuis*. No samples contain *P. scarabaeoides* co-occurring with *S. alatus* as seen in the basal part of the *P. scarabaeoides* Zone in the Oslo Region (Høyberget & Bruton 2012). This level may not be developed on Bornholm or it is devoid of limestone concretions.

A presence of the *Parabolina lobata* Zone on Bornholm was indicated by C. Poulsen (1923) [in his terminology: Subzone with *Parabolina longicornis* and *Peltura scarabaeoides*], but the free cheeks he assigned to *P. longicornis* are here identified as *C. tenuis* (see taxonomic section). The one sample with these free cheeks also contains various other taxa, erroneously listed from the *P. 'longicornis'* Subzone by C. Poulsen (1923) (see 'Discussion and conclusions' below). Scree samples collected from just below the uppermost anthraconite horizon in the western end of locality 6 (level G in C. Poulsen 1923, fig. 2) yielded a meagre *P. scarabaeoides* Zone assemblage dominated by *T. humilis*. Since no material of *P. lobata* has been found in the numerous

limestone samples available from locality 6, we conclude that the *P. lobata* Zone is not developed at this locality, which is in accordance with the thicknesses of the *P. scarabaeoides* Zone in the Læså area indicated by Nielsen *et al.* (2018). However, *Parabolina lobata praecurrens* is actually recorded in several samples collected by ATN in the 1970s at Limensgade (localities 8A–B); this subspecies is characteristic of the *P. lobata* Zone in Scania and the Oslo Region (Henningsmoen 1957; Terfelt *et al.* 2011; Nielsen *et al.* 2020).

Peltura westergaardi also occurs in the *P. lobata* Zone on Bornholm; it is characteristic of the same stratigraphic level in Sweden and Norway (Henningsmoen 1957; Terfelt *et al.* 2011), although it has its FAD in the very top of the underlying *P. scarabaeoides* Zone in the Oslo Region (Nielsen *et al.* 2020). This taxon has not been previously reported from Bornholm and very little of the material labelled as *P. scarabaeoides* in the original museum collection studied by C. Poulsen (1923) represents this species. A few orthid brachiopods have also been found in the *P. lobata* Zone on Bornholm.

Parabolina megalops, characteristic of the uppermost zone in the *Peltura* Superzone (Fig. 3), has not been recorded from Bornholm and Nielsen *et al.* (2018) inferred that this zone is probably absent, based on correlation of gamma logs in wells. However, the *Peltura*/*Acerocarina* superzone boundary interval is not exposed and it is thus inaccessible for sampling.

Acerocarina Superzone

This superzone comprises three zones (Fig. 3), but only the uppermost part is exposed at locality 8 (C. Poulsen 1922, 1923). Findings of rare *Parabolina acanthura* at the base of the section exposed in the Limensgade shale/limestone quarry (C. Poulsen 1923) is taken as indicative of the *Acerocare ecorne* Zone (see e.g. Terfelt 2006), although this species locally ranges into the basal Ordovician in the Oslo area (Bruton *et al.* 1988; see also Nielsen *et al.* 2020).

Nielsen *et al.* (2018) inferred that also the lower parts of the *Acerocarina* Superzone are developed on Bornholm, but the biozones are too thin to be tracked individually on the basis of gamma log correlation. This interval may theoretically be exposed in the Risebæk creek but those outcrops have never been examined.

Discussion and conclusions

The studied museum material of Furongian olenids and agnostoids from Bornholm represents 43 taxa. Fourteen of these have not been reported from the island previously, viz. *Ctenopyge ahlbergi*, *C. tumidoides*, *Eurycare brevicauda*, *Leptoplastus abnormis*, *L. crassicornis*, *Olenus transversus*, *Parabolina lobata praecurrens*, *Peltura acutidens*, *P. minor*, *P. westergaardi*, *Protopeltura planicauda*, *P. praecursor*, *Pseudagnostus leptoplastorum?* and *Sphaerophthalmus drytonensis*. Five species described by C. Poulsen (1923) are here transferred to other taxa that technically speaking also are new to Bornholm, viz. *Lotagnostus americanus* ('*Agnostus trisectus*'), *Ctenopyge magna* n. sp. ('*Ctenopyge affinis*'), *Ctenopyge fletcheri* ('*Ctenopyge directa*'), *Sphaerophthalmus alatus* ('*Sphaerophthalmus major*') and *Triangulopyge humilis* ('*Sphaerophthalmus alatus*') (names in brackets are those used by C. Poulsen 1923). The material treated as *Ctenopyge pecten* by C. Poulsen (1923) represents *C. tenuis* (see also V. Poulsen 1963), which is common on Bornholm. However, *C. pecten s.str.* is actually present as well but it is comparatively infrequent. The sparse museum material assigned to *Parabolina longicornis* [now *P. lobata*] by C. Poulsen (1923) is here identified as *C. tenuis*. The cranidia assigned to *C. affinis* by C. Poulsen (1923) are separated as *C. magna* n. sp. and a different group of *Ctenopyge* is identified as *C. affinis*, which is quite common on Bornholm. Strangely, this morph was not dealth with by C. Poulsen (1923).

Eurycare bornholmensis is common in the material at hand. Findings of nearly complete specimens with 16 thoracic segments suggest an affiliation with *Eurycare* rather than *Leptoplastus*, although the interocular cheeks are slightly narrower than typical for representatives of *Eurycare*. The free cheek with a robust long spine is also of *Eurycare* type. *Eurycare bornholmensis* has a well-defined preglabellar area, a trait shared with several species of *Leptoplastus*. *Eurycare bornholmensis* is endemic to Bornholm, but it strongly resembles the Norwegian *E. explanatum* and a separation only at subspecies level may be contemplated.

Leptoplastus abnormis is overall quite similar to *L. ovatus*. The former may possibly have slightly longer genal spines (Westergård 1944; Ahlberg *et al.* 2006) and perhaps a more elongate, usually slightly tapering glabella (this study), but the long pleural spines in the rear part of the thorax are the salient distinguishing feature. However, cranidia and pygidia of the two species - and probably also the free cheeks, as the genal spine often is broken - are very difficult to distinguish, and complete specimens seem to be required for safe differentiation of these taxa. In the material at hand no complete specimens of *L. ovatus* are available and we strongly suspect that the extensive material of disarticulated skeletal parts is mixed with *L. abnormis*. This suspicion also concerns Scandinavian material in general assigned to *L. ovatus* by various authors.

Our study shows that *S. angustus* and *C. tumidoides* range into the basal part of the *Peltura* Superzone,

which has not been reported previously from Scandinavia. However, Høyberget & Bruton (2012, p. 440; fig. 5i) mentioned that a morph of *S. angustus* approaching *S. alatus* occurs together with *C. tumida* and *P. acutidens* in the lowermost part of the *C. tumida* Zone, but no further details were provided, and this occurrence was not shown on their range chart (*ibid*. fig. 2). Terfelt & Ahlgren (2009, fig. 3) reported a co-occurrence of *Ctenopyge* (*Eoctenopyge*) *angusta* with *C. tumida* and *P. minor* in a section on eastern Kinnekulle, but no material was illustrated, and the identification remains uncertain. The absence of *S. alatus* in the section is a concern. *Ctenopyge tumidoides,* reported as *C. tumida* by Clarkson *et al.* (2004), seems to range into the *C. tumida* Zone also in Västergötland; for details, see the taxonomic section.

In general, no information on sampling levels is available for the studied museum material and identification of biozones is based on comparison with ranges recorded elsewhere in Scandinavia (see summary in Nielsen *et al.* 2020, fig. 1). This approach is fairly straightforward given that the majority of trilobites known from the Alum Shale have short ranges, typically only through one zone and very rarely through more than two zones. The taxa found on Bornholm indicate that all six Furongian superzones established by Nielsen *et al.* (2014) are developed. Of the 23 trilobite zones, recognized by Nielsen *et al.* (2020) (see Fig. 3), 14 fossiliferous zones are confirmed present on Bornholm (Fig. 4). Correlations based on gamma log stratigraphy in wells suggest that also the *Olenus scanicus–O. rotundatus*, *Parabolina brevispina*, *Leptoplastus neglectus* and at least one and more likely both of the basal zones in the *Acerocarina* Superzone are developed on Bornholm (Nielsen *et al.* 2018). The *S. postcurrens* Zone may be very thin or absent; theoretically it may be accessible for sampling at locality 6. The *Leptoplastus paucisegmentatus* and *L. raphidophorus* zones in the basal *Leptoplastus* Superzone seem to be absent. The *Parabolina megalops* Zone in the upper *Peltura* Superzone was inferred absent (or thin) by Nielsen *et al.* (2018), but the *Peltura/Acerocarina* superzone boundary interval is not exposed and, thus, the faunal succession across the boundary cannot be sampled.

Overall, the present revision of Furongian trilobites from Bornholm corroborates the zonation outlined by C. Poulsen (1923) and essentially all additions to the faunal list support his original conclusions.

The present study calls for reinvestigation of the exposure at locality 6 in the Læså stream, which should be sampled in order to ascertain whether or not the *Leptoplastus neglectus* and *Sphaerophthalmus postcurrens* zones are developed.

We note that some details regarding specific occurrences reported by C. Poulsen (1923) are inaccurate, which in ascending order concern:

- *Ctenopyge neglecta* var. *bornholmensis* [here *Eurycare bornholmensis*] was reported to occur in the uppermost part of the horizon with *Eurycare angustatum* [here *L. crassicornis–L. angustatus* Zone]. However, *E. bornholmensis* seems to be common throughout the *L. crassicornis–L. angustatus* Zone above the basal *E. latum* dominated interval

- *Ctenopyge magna* n. sp. was reported (as *C. affinis*) from the *P. scarabaeoides* Subzone [here Zone] based on alleged co-occurrence with *T. humilis* [reported as *S. alatus*] and *C. pecten* (?). A reinvestigation of the museum samples in question shows that they contain *C. magna* n. sp., *S. alatus* [*s.str.*], *C. ahlbergi* and *C. affinis s.str.* and must derive from the upper part of the *P. acutidens–C. tumida* Zone

- *Ctenopyge fletcheri* – under the name *C. directa* – was reported from the *C. tumida* subzone [here *P. acutidens–C. tumida* Zone]. However, no material of *C. fletcheri* associated with trilobites characteristic of that zone is preserved in the museum collection. It remains speculative, but maybe the report was based on misidentification of detached thoracic segments of *C. ahlbergi* that superficially resemble the broad, flat genal spines of *C. fletcheri*

- *Ctenopyge bisulcata* was reported from the upper part of the *P. scarabaeoides* Zone, but it should be observed that the section exposed at locality 6 in fact represents only the lower half of that zone (cf. Nielsen *et al.* 2018). The record of *C. bisulcata* from locality 7 demonstrates that this species occurs from near the base of the *P. scarabaeoides* Zone also on Bornholm

- *Ctenopyge pecten* [here *C. tenuis*], *C. teretifrons*, *C. linnarssoni* and *Sphaerophthalmus alatus* [here *T. humilis*] were all reported to range into the *Parabolina longicornis* Subzone [here: *P. lobata* Zone]; a statement repeated for *C. tenuis* by V. Poulsen (1963). However, the free cheeks identified as *P. longicornis* by C. Poulsen (1923) represent *C. tenuis* and derive from the *P. scarabaeoides* Zone. Hence, the four species listed do not range into the *P. lobata* Zone

- No *P. lobata* Zone is developed at locality 6 as indicated by C. Poulsen (1923, fig. 2)

In general, the thickness of the individual zones cannot be established, partly due to the fact that the fossils are sampled *ex situ* and partly due to discontinuous exposure. The reader is instead referred to the study based on well log correlation published by Nielsen *et al.* (2018). A few details on thicknesses were provided by C. Poulsen (1923; see in particular his description of locality 6), and Kaufmann (1933a, text-fig. 1).

Taxonomy

Most olenid taxa are described in detail by Westergård (1922) and/or Henningsmoen (1957) and the reader is referred to these authoritative monographs for details. The latter author also provided a brief summary of diagnostic characters for each taxon. The descriptive terminology used by Henningsmoen (1957) is adopted here. The studied material is stored at the Natural History Museum of Denmark. Regarding specimen and samples numbers, see section on 'Material and methods'.

Trilobites are exceedingly abundant in many of the limestone samples and the common species (e.g. *L. ovatus*, *S. alatus* and *T. humilis*) are each represented by many more specimens than counted here (>>1000), registering only relatively well preserved and/or easily observable skeletal parts.

Class Trilobita Walch, 1771

Order Agnostida Salter, 1864

Family Agnostidae M'Coy, 1849

Genus *Agnostus* Brongniart, 1822
Type species: *Entomostracites pisiformis* Wahlenberg, 1818, designated by Jaekel (1909).

Agnostus pisiformis (Wahlenberg, 1818)
Fig. 5
1922   *Agnostus pisiformis* (L.) – Westergård, pp. 115–116, pl. 1, figs 1–3.
v 1923   *Agnostus pisiformis* Linné – C. Poulsen, pp. 21–22, pl. 1, fig. 1.
1958a   *Agnostus (Agnostus) pisiformis* Linnæus 1757 – Henningsmoen, pp. 181–182, pl. 5, figs 1–12.
1996   *Agnostus pisiformis* (Wahlenberg, 1818) – Ahlberg & Ahlgren, pp. 130–131.
2003   *Agnostus pisiformis* (Wahlenberg, 1818) – Terfelt, p. 411; fig. 4A.
2017   *Agnostus pisiformis* (Wahlenberg, 1818) – Rasmussen *et al.*, pp. 8–9.
2017   *Agnostus pisiformis* (Wahlenberg 1818) – Jackson & Budd, pp. 467–484.
See Ahlberg & Ahlgren (1996) and Rasmussen *et al.* (2017) for additional synonymy.

Lectotype. Cephalon Vg. 819 from Hönsäter, Kinnekulle, Sweden. Originally figured by Wahlenberg (1818, pl. 1, fig. 5) and refigured by Reyment (1976, fig. 3a–b). Designated by Shergold *et al.* (1990).

Material. Four complete specimens, 173 cephala (see remarks) and 148 pygidia. The species occurs alone and has been found at localities 1, 2, 11, 13 and 14 as well as downstream of locality 8C in the Læså riverbed (exposure not numbered, GPS coordinates 55°2′54.81″N, 14°53′43.04″E).

Occurrence. Very common in the eponymous upper Miaolingian zone throughout Scandinavia with a lower range from the uppermost part of the *Lejopyge laevigata* Zone (Ahlberg & Ahlgren 1996; Rasmussen *et al.* 2017 and references therein). Within south-central Sweden, it is often reworked into the basal *Olenus* Superzone. *Agnostus pisiformis* is reported also from Poland, Great Britain, Canada (Newfoundland) and Russia (Bennett Island) (Lendzion & Orlowski 1991, Ahlberg 2003, Danukalova *et al.* 2014). On Bornholm, it is common in the eponymous zone which prior to ratification of the Furongian (Peng & Babcock 2003) was classified as 'Upper' Cambrian.

Comparison. Agnostus pisiformis is a larger species than *H. obesus* (maximum length of cephala/pygidia *c.* 6 mm vs. *c.* 3.5 mm in *H. obesus*). The cephala of these species are identical (see remarks by Westergård 1947, p. 4) and pygidia are required for safe identification. In *H. obesus,* the pygidial axis is wider, strongly inflated and has a rounded terminal piece. *Agnostus pisiformis* has a more slender axis with a pointed terminal piece.

Remarks. The cephala assigned to *A. pisiformis* are identified by co-occurring with safely identified pygidia. The length of marginal spines in the pygidium varies and cephala may exhibit weak scrobiculation (see Fig. 5). The many species and subspecies recognized by Mischnik (2006a, 2006b) and Buchholz (1991, 1999, 2000, 2016) including *A.? confusus, A. distinctus, A. procerus, A. pisiformis dissimilis,* and *A. pisiformis vastificus,* all based on material from ice-rafted boulders collected in Germany, are here regarded as within the variation range of *A. pisiformis.*

Genus *Homagnostus* Howell, 1935
Type species: *Agnostus pisiformis* var. *obesus* Belt, 1867, by original designation.

Homagnostus obesus (Belt, 1867)
Fig. 6D–E
1922   *Agnostus pisiformis obesus* Belt [*partim*] – Westergård, p. 116, pl. 1, figs 4a–b; non pl. 1, figs 5–6 [= *H. ultraobesus?* Lermontova, 1940].
v 1923   *Agnostus pisiformis* Linné var. *obesus* Belt – C. Poulsen, pp. 22–23, pl. I, fig. 2.
1958a   *Agnostus (Homagnostus) obesus* BELT 1867 – Henningsmoen, pp. 182–184, pl. 5, figs 13–16.

1996   *Homagnostus obesus* (Belt, 1867) – Ahlberg & Ahlgren, p. 131, figs 3A–G.

2003   *Homagnostus obesus* (Belt, 1867) – Terfelt, p. 411; fig. 4B.

2016   *Homagnostus obesus* – Ahlberg *et al.,* p. 496, figs 4; 6I, J.

2017   *Homagnostus obesus* (Belt, 1867) – Rasmussen *et al.,* p. 9.

For further synonymy, see Ahlberg & Ahlgren (1996) and Rasmussen *et al.* (2017).
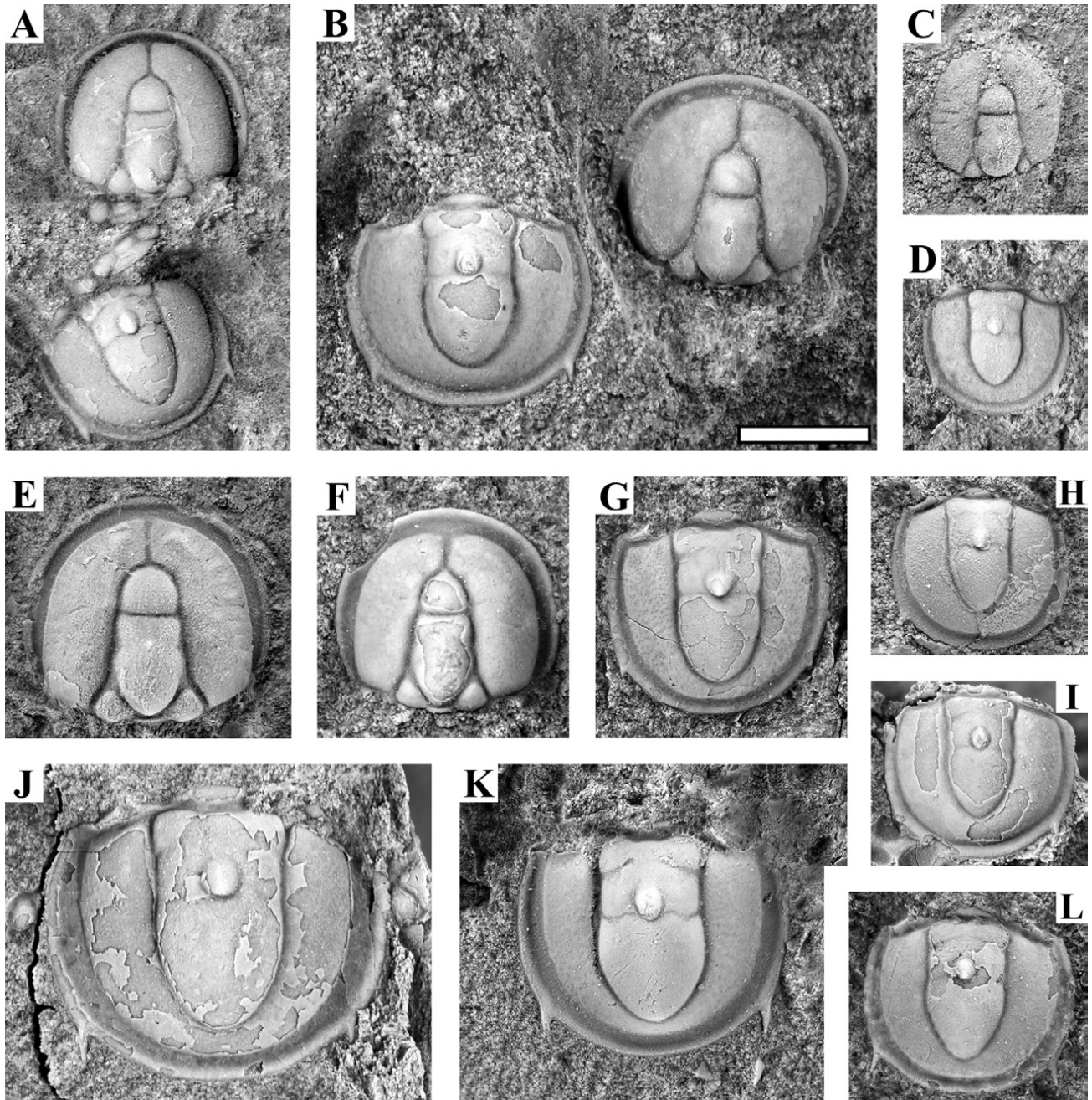
Lectotype. Nearly complete specimen BM I7646, fig-

Fig. 5. *Agnostus pisiformis*, all preserved in anthraconite. White scale bar: 2 mm. **A:** Complete specimen, loc. 2, sample L2 (MGUH 33536). **B:** Cephalon and pygidium, loc. 14, sample GM 2019-91 (MGUH 33537). **C:** Slightly scrobiculate cephalon, loc. 2, sample L1 (MGUH 33539). **D:** Pygidium, loc. 1, sample GM 1877-2002 (MGUH 33543). **E:** Cephalon showing very indistinct scrobiculation, loc. 2, sample L1 (MGUH 33540). **F:** Cephalon, loc. 14, sample GM 2019-91 (MGUH 33538). **G:** Pygidium, loc. 1, sample GM 1877-2002 (MGUH 33544). **H:** Pygidium, loc. 2, sample L1 (MGUH 33541). **I:** Pygidium, loc. 1, sample 1877-2002 (MGUH 33545). **J:** Pygidium with relatively long marginal spines, loc. 1, sample GM 1922-132B (MGUH 33547). **K:** Pygidium with relatively long marginal spines, loc. 2, sample L1. (MGUH 33542). **L:** Pygidium with relatively long marginal spines, loc. 1, sample GM 1877-2002 (MGUH 33546).

ured by Belt (1867, pl. 12, fig. 4a) from the Maentwrog Formation of North Wales, *Olenus* Superzone, United Kingdom, designated and refigured by Rushton in Allen *et al.* (1981, pl. 16, fig. 2).

Material. Ten complete specimens and 82 pygidia. 70 associated cephala are tentatively assigned (see comments on *A. pisiformis*). *Homagnostus obesus* co-occurs with *Olenus truncatus* and *O. wahlenbergi* in the material at hand, which derives from localities 2, 3, 16, 17 and 18.

Occurrence. *Olenus* Superzone (all zones) in all districts of Scandinavia including Bornholm; *H. obesus* is reported also from Great Britain, Newfoundland, Siberia, Kazakhstan, Korea and North America (Ahlberg & Ahlgren 1996; Ahlberg & Terfelt 2012).

Comparison. See *A. pisiformis*.

Genus *Glyptagnostus* Whitehouse, 1936
Type species: *Glyptagnostus toreuma* Whitehouse, 1936 [= *Agnostus reticulatus* Angelin, 1851], by original designation.

Glyptagnostus reticulatus (Angelin, 1851)
Fig. 6A–C

1922   *Agnostus reticulatus* Angelin – Westergård, p. 117, pl. 1, figs 9–10.
v 1923   *Agnostus reticulatus* Angelin – C. Poulsen, p. 23, pl. 1, fig. 3.
1947   *Glyptagnostus reticulatus nodulosus* subsp. n. – Westergård, p. 7, pl. 1, fig. 7–9.
1958a   *Glyptagnostus reticulatus reticulatus* Angelin 1851 – Henningsmoen, pp. 184–185, pl. 5, fig. 17.
1996   *Glyptagnostus reticulatus reticulatus* (Angelin, 1851) – Ahlberg & Ahlgren, pp. 135–136, figs 4I–P.
2012   *Glyptagnostus reticulatus* (Angelin, 1851) – Ahlberg & Terfelt, pp. 1004–1006, figs 3a–b.

See Ahlberg & Ahlgren (1996) for additional synonymy.

Lectotype. Cephalon SGU 120, figured by Westergård (1922, pl. 1, fig. 2), one of Angelin's cotypes from Andrarum, southern Sweden, designated by Henningsmoen (1958a).
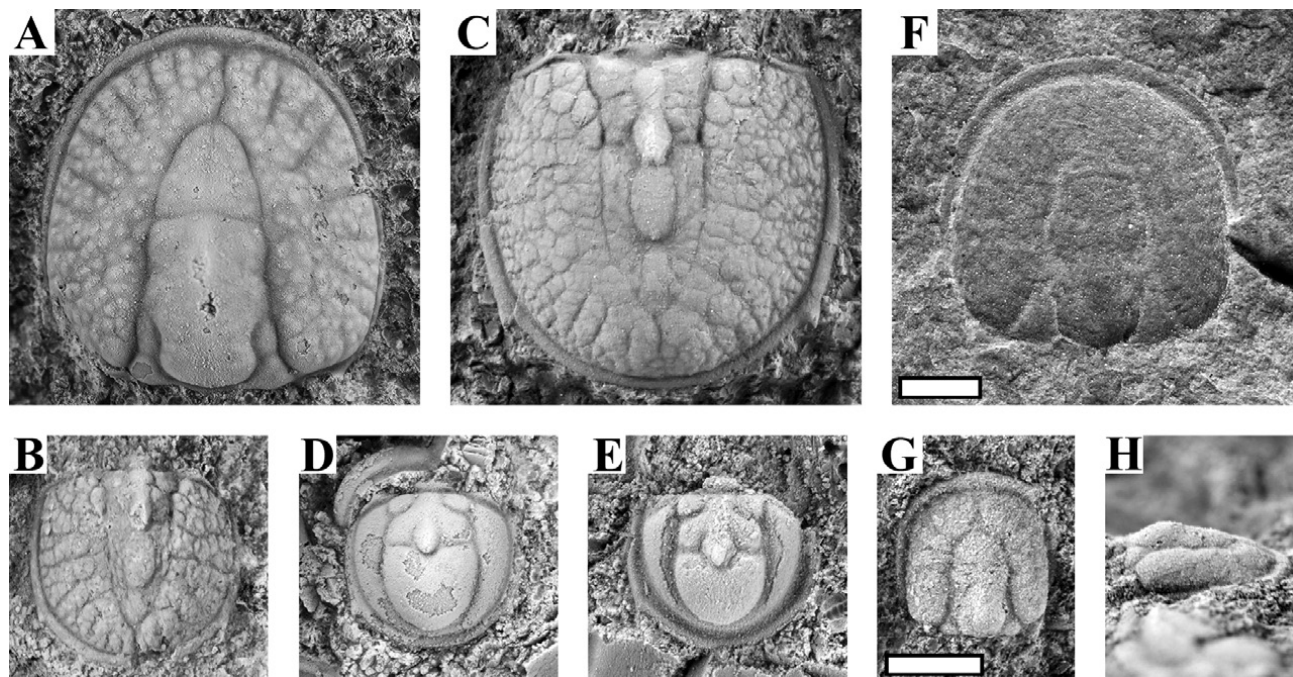

Fig. 6. Various agnostoids, all preserved in anthraconite except F. White scale bars: 1 mm; please note that G–H are shown at larger magnification. **A:** *Glyptagnostus reticulatus,* cephalon, sample GM 1871-602, 'Cement factory', Øleå (MGUH 33548). **B:** *Glyptagnostus reticulatus*, pygidium, loc. 17, sample GM 2019-36 (MGUH 33549). **C:** *Glyptagnostus reticulatus*, pygidium, loc. 17, specimen MGUH 1956 (previously illustrated by C. Poulsen 1923, pl. I, fig. 3). **D:** *Homagnostus obesus*, pygidium, sample GM 2019-51, loc. 17 (MGUH 33550). **E:** *Homagnostus obesus*, pygidium, sample GM 2019-74, loc. 17 (MGUH 33551). **F:** *Lotagnostus americanus*, external mould of cephalon preserved in shale (the corresponding positive is fragmentary), loc. 6, sample GM 1922-141O (MGUH 33552). **G–H:** *Pseudagnostus leptoplastorum*?, dorsal and side view of small cephalon, loc. 6, sample ATN-123 (MGUH 33553).

Material. Four complete specimens, four cephala and six pygidia, occurring alone. The material derives from localities 2, 17 and 18. The complete specimens at hand (all preserved in shale) are poorly preserved and not suitable for illustration.

Occurrence. In Scandinavia, this species occurs sparsely in the *O. gibbosus* and *O. truncatus* trilobite zones (Ahlberg & Terfelt 2012). *Glyptagnostus reticulatus* has a nearly cosmopolitan distribution (Terfelt *et al.* 2008) and is the primary marker for the base of the Furongian (Peng & Babcock 2003).

Comparison. Glyptagnostus reticulatus is readily distinguished from the associated *H. obesus* by its scrobiculate cephalon and pygidium and comparatively narrow glabella and pygidial axis.

Remarks. Glyptagnostus reticulatus nodulosus, characterized by a finer scrobiculation, is here regarded as within the variation range of the main form.

Genus *Lotagnostus* Whitehouse, 1936
Type species: *Agnostus trisectus* Salter, 1864, by original designation.

Lotagnostus americanus (Billings, 1860)
Fig. 6F
1922   *Agnostus trisectus* Salter – Westergård, p. 117, pl. 1, figs 11–12.
v 1923   *Agnostus trisectus* Salter – C. Poulsen, pp. 24–25, textfig. 5.
1996   *Lotagnostus trisectus* (Salter, 1864) – Ahlberg & Ahlgren, pp. 133–135, figs 4A–B.
2005   *Lotagnostus americanus* (Billings, 1860) – Peng & Babcock, pp. 110–113, fig. 2.
2012   *Lotagnostus americanus* (Billings, 1860) – Ahlberg & Terfelt, pp. 1004–1006, figs 4a–f.
2015   *Lotagnostus americanus* (Billings, 1860) – Peng *et al.*, pp. 281–303, figs 1–11.
For further synonymy, see Ahlberg & Ahlgren (1996), Peng & Babcock (2005) and Peng *et al.* (2015).

Holotype. Pygidium GSC 859 from the Lévis Formation, North Ridge, Lévis, Quebec, by monotypy (see Rushton 2009, p. 276). Figured by Westrop *et al.* (2011, fig. 5A–C).

Material. A single cephalon from locality 6, preserved in shale. No associated fauna.

Occurrence. Lotagnostus americanus ranges through the eponymous agnostoid zone in Scandinavia, corresponding to the *P. acutidens–C. tumida* and *P. scarabaeoides* olenid zones (cf. Westergård 1922; Ahl-

berg & Terfelt 2012). There are no confirmed reports of an occurrence in the upper part of the *Protopeltura* Superzone. It has a near global distribution (Peng *et al.* 2015) but is rare in Scandinavia. The specimen at hand derives from the *P. acutidens–C. tumida* Zone according to C. Poulsen (1923).

Remarks. The variability of this species and whether or not it is a senior synonym of various younger names (e.g. *Trilobagnostus trisectus*) is a contentious issue (e.g. Westrop *et al.* 2011; Peng *et al.* 2015). *Lotagnostus americanus* is a potential index species for the as yet unnamed Cambrian Stage 10. We here follow the majority of trilobite specialists, accepting *Lotagnostus americanus* as a rather variable species including forms described under different names; for discussion, see Peng *et al.* (2015). At any rate, the very sparse material from Bornholm does not contribute to this ongoing discussion.

Genus *Pseudagnostus* Jaekel, 1909
Type species: *Agnostus cyclopyge* Tullberg, 1880, by original designation.

Pseudagnostus leptoplastorum Westergård, 1944?
Fig. 6G–H
? 1944   *Pseudagnostus leptoplastorum* sp. n. – Westergård, p. 39, pl. 1, fig. 1.
? 1962   *Pseudagnostus leptoplastorum* Westergard, 1944 – Ivshin, pp. 16–18, textfig. 3; pl. 1, figs 8–18.
? 1971   *Pseudagnostus* cf. *leptoplastorum* Westergaard – Taylor & Rushton, p. 28.

Holotype. By monotypy, flattened pygidium SGU 4214, preserved in shale from the *Leptoplastus raphidophorus* Zone, Andrarum, southern Sweden, illustrated by Westergård (1944, pl. 1, fig. 1).

Material. One cephalon from locality 6. It is associated with *Eurycare bornholmensis*.

Occurrence. Westergård (1944) reported this extremely rare species (based on a single pygidium) from the *L. raphidophorus* Zone at Andrarum, Sweden, while Taylor & Rushton (1971) reported a cephalon referred to as *Pseudagnostus* cf. *leptoplastorum* from the *L. crassicornis* Zone in England. The single specimen from Bornholm derives from the *L. crassicornis–L. angustatus* Zone. No additional material has been described from Scandinavia (cf. Ahlberg & Terfelt 2012) whereas extensive material was described by Ivshin (1962) from the *Irvingella* Zone in central Kazakhstan (see remarks).

Remarks. The specimen presumably represents *P. leptoplastorum* and is the first cephalon of this taxon

recorded from Scandinavia. Ivshin (1962) described *P. leptoplastorum* from Kazakhstan, including illustrations and description of cephala. In comparison, the specimen at hand has a parallel-sided non-tapering glabella and there seems to be a minute mesial tubercle in the transglabellar furrow as well as barely perceptible scrobiculation, not seen in the Kazakhstan material (cf. Ivshin 1962, text-fig. 3). Hence identification remains uncertain – but it is obviously also questionable whether the Kazakhstanian material represents *P. leptoplastorum s. str.* considering how poorly known this taxon is. The cephalon referred to by Taylor & Rushton (1971) was neither illustrated nor described. Attempts to obtain photos of that specimen were unsuccessful.

Order Ptychopariida Swinnerton, 1915

Family Olenidae Burmeister, 1843

Genus *Olenus* Dalman, 1827
Type species: *Entomostracites gibbosus* Wahlenberg, 1818, designated by Salter (1864).

Olenus attenuatus (Boeck, 1838)
Fig. 7A–C
1922   *Olenus attenuatus* (Boeck) – Westergård, pp. 128–130, pl. IV, figs 15–19, pl. V, figs 1–9.
v 1923   *Olenus attenuatus* Boeck – C. Poulsen, pp. 27–28, pl. I, fig. 7.
1957   *Olenus attenuatus* (Boeck, 1838) – Henningsmoen, pp. 102–104, textfig. 16; pl. 3.
2017   *Olenus attenuatus* (Boeck, 1838) – Rasmussen *et al.*, pp. 14–15, fig. 8H.
For further synonymy, see Rasmussen *et al.* (2017).

Neotype. Complete specimen Ar 1640 (Naturhistoriska Riksmuseet, Stockholm) from Andrarum, southern Sweden, probably Angelin's original, figured by Westergård (1922, pl. V, fig. 2) and designated by Henningsmoen (1957).

Material. Nine cranidia with up to eight contiguous thoracic segments, two pygidia and one free cheek (tentatively assigned, but associated with thoracic segments showing imprints of axial nodes). The material derives from localities 2, 3 and 17. *Olenus attenuatus* occurs alone in the material at hand.

Occurrence. Index fossil for the eponymous zone in Scandinavia incl. Bornholm (Westergård 1922, 1947; Henningsmoen 1957; Terfelt *et al.* 2008; Nielsen *et al.* 2020).

Comparison. The salient distinguishing feature of this species is the presence of small axial spines on the thoracic segments, but the cranidium is also fairly easily identified due to the relatively wide postocular cheeks, so it is 2.1–2.4 times as wide as long. The pygidium can be confused with *O. gibbosus*, but *O. attenuatus* has only 1 pair of marginal spines, 4–7 axial rings, a pleural field that is narrower than the axis and the overall pygidial outline is subtriangular. The free cheeks of *O. attenuatus*, *O. dentatus* and *O. truncatus* are essentially identical.

Olenus dentatus Westergård, 1922
Fig. 7J, K?
1922   *Olenus dentatus* n. sp. – Westergård, p. 130, pl. V, figs 10–15.
1933a   *Olenus dentatus* (Westergård) – Kaufmann, pp. 58–62.
1957   *Olenus dentatus* Westergård, 1922 – Henningsmoen, pp. 104–105, pl. 3.
2005   *Olenus dentatus* (Westergård, 1922) – Lauridsen & Nielsen, pp. 1043, 1044, 1051, 1053, textfig. 5, pl. 1, figs 2, 13, 14.
For further synonymy, see Henningsmoen (1957).

Lectotype. Cranidium SGU 208 from Andrarum, southern Sweden, figured by Westergård (1922, pl. V, fig. 10) and designated by Henningsmoen (1957).

Material. One external mould of a complete specimen from locality 18 and one fragmentary cranidium (tentatively assigned) from the Læså (probably locality 3). Both specimens are preserved in shale and occur alone. The complete specimen is the first articulated specimen recorded of this species (cf. Westergård 1922, Henningsmoen 1957).

Occurrence. Index fossil for the eponymous zone in Scania and Bornholm; the species possibly occurs also in Great Britain (Henningsmoen 1957; Terfelt *et al.* 2008; Nielsen *et al.* 2020). It has previously been reported from Bornholm by Kaufmann (1933a).

Comparison. Olenus dentatus is characterized by having a wide and long glabella, a rather narrow thorax with 15 segments, tapering rearwards, and a comparatively wide axis, and a relatively short pygidium with one pair of marginal spines and a conical axis consisting of only 3–4 axial rings. It is readily separated from the other species of *Olenus*.

Remarks. Kaufmann (1933a) reported 15 cranidia and two pygidia of *O. dentatus* from the Læså stream, probably locality 3, collected from a 1 cm thick horizon at 7 cm above the *O. attenuatus* Zone. No specimens were illustrated, and no material was deposited in
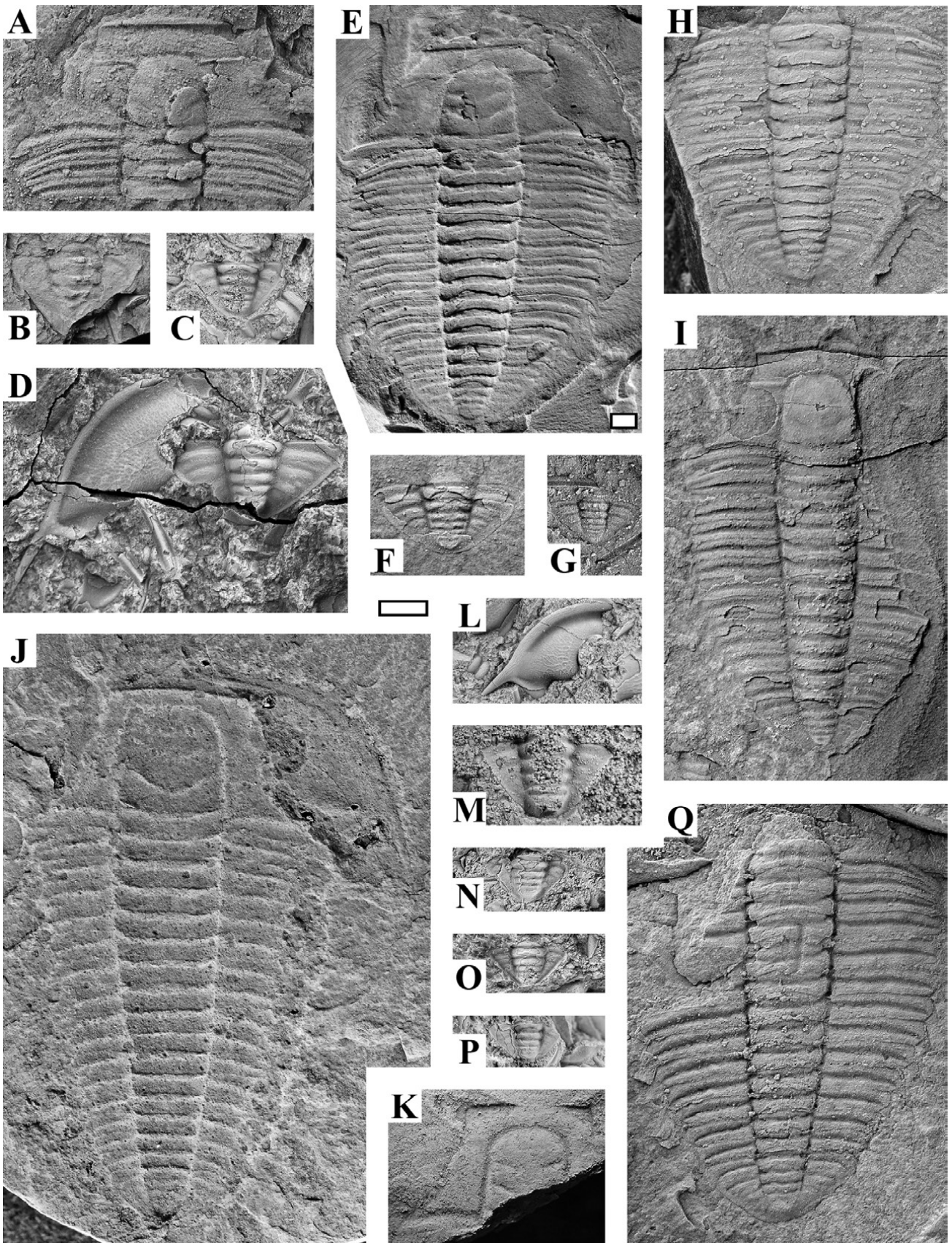
the Geological Museum collection in Copenhagen but given Kaufmann's detailed knowledge on *Olenus* his identification is presumably correct.

Olenus gibbosus (Wahlenberg, 1818)
Fig. 7D

1922   *Olenus gibbosus* (Wahlenberg) – Westergård, pp. 124–125, pl. III, figs 1–10.
v 1923   *Olenus gibbosus* Wahlenberg – C. Poulsen, pp. 26–27, pl. 1, figs 4, 5?
1957   *Olenus gibbosus* (Wahlenberg, 1821) – Henningsmoen, pp. 105–106, pl. 1, fig. 1, pl. 3, pl. 9, fig. 7.
2003   *Olenus gibbosus* (Wahlenberg, 1821) – Terfelt, p. 411, fig. 4E, F.
2016   *Olenus gibbosus* – Ahlberg *et al.*, p. 496, figs 4; 6E–G, M, N.
2017   *Olenus gibbosus* (Wahlenberg, 1818) – Rasmussen *et al.*, p. 15, figs 8A–B.

For further synonymy, see Henningsmoen (1957) and Rasmussen *et al.* (2017).

Type material. Not designated, see Henningsmoen (1957).

Material. One cephalon with three thoracic segments, two free cheeks and four pygidia; all from locality 2.

Occurrence. Index fossil for the eponymous zone in Scandinavia and England (Westergård 1922; Henningsmoen 1957; Terfelt *et al.* 2008).

Comparison. Olenus gibbosus can be distinguished from almost all other *Olenus* species by its free cheek with an obtuse inner spine angle, the only exception being *O. transversus*. However, it is most easily identified by its pygidium having one or two pairs of marginal spines and relatively wide pleural fields. For comparison with *O. attenuatus*, see that species.

Remarks. Olenus gibbosus appears to be rare on Bornholm and/or maybe the zone in question is very thin and perhaps developed only in the Læså area. In a recent study of locality 15B (unpublished), this species was not recorded and the base of the Furongian is here marked by the FAD of *O. transversus*.

Olenus transversus Westergård, 1922
Fig. 7Q

1922   *Olenus transversus* Linnarsson in museo – Westergård, pp. 125–126, pl. III, figs 11–17, pl. 5, figs 16–17?.
1957   *Olenus transversus* Westergård, 1922 – Henningsmoen, p. 108, pl. 3.
2017   *Olenus transversus* Westergård, 1922 – Rasmussen *et al.*, p. 16, fig. 8C–D.

For further synonymy, see these references.

Lectotype. An almost complete specimen (SGU 173) preserved in shale from Andrarum, southern Sweden, figured by Westergård (1922, pl. III, fig. 11) and designated by Henningsmoen (1957).

Material. One almost complete specimen, two free cheeks and four pygidia with up to 13 contiguous thoracic segments attached. Another two pygidia with up to six thoracic segments are tentatively assigned. The almost complete specimen derives from the Læså riverbed between localities 2 and 3, while the other material derives from locality 2. In early March 2020, *O. transversus* was found also at locality 15B (material not included in the present study). This species occurs alone in the samples at hand. Neither C. Poulsen (1923) nor Kaufmann (1933a) recorded this species from Bornholm.

Occurrence. Olenus transversus occurs in the *O. gibbosus* Zone in Scandinavia (Westergård 1922, 1947; Henningsmoen 1957). In SE Scania, the species occurs alone in a thin horizon in between the intervals with

▲ **Fig. 7.** Species of *Olenus*. White scale bars: 2 mm; D is shown at lower magnification. **A–C:** *Olenus attenuatus.* **A:** Cranidium with two thoracic segments, preserved in shale, loc. 2, sample L104 (MGUH 33555). **B:** Pygidium, preserved in shale, loc. 3, sample GM 1897-1300 (MGUH 33556). **C:** Pygidium, preserved in anthraconite, loc. 17, sample GM 2019-63 (MGUH 33557). **D:** Free cheek and pygidium of *Olenus gibbosus*, preserved in anthraconite, loc. 2, MGUH 1957 (previously illustrated by C. Poulsen 1923, pl. I, fig. 4). **E–I:** *Olenus truncatus*, loc. 2, all preserved in shale. **E:** External mould of almost complete specimen, sample GM 1870-876 (MGUH 33558). **F:** Pygidium, sample GM 1922-133B (MGUH 33559). **G:** Pygidium, sample L112 (MGUH 33561). **H:** Pygidium with ten thoracic segments, sample GM 1922-133B (MGUH 33560). **I:** Almost complete specimen, sample GM 1922-133D (MGUH 33562). **J:** *Olenus dentatus,* external mould of almost complete specimen preserved in shale, sample GM 2019-102, loc. 18 (MGUH 33563). **K:** *Olenus dentatus?,* fragmentary cranidium preserved in shale, Læså, probably loc. 3, sample GM 2019-98 (MGUH 33564). **L–P:** *Olenus wahlenbergi,* all preserved in anthraconite, loc. 17. **L:** Free cheek, sample GM 2019-62 (MGUH 33565). **M:** Pygidium, sample GM 2019-59 (MGUH 33566). **N:** Pygidium, sample GM 2019-55 (MGUH 33567). **O:** Pygidium, sample GM 2019-68 (MGUH 33569). **P:** Pygidium, sample GM 2019-55 (MGUH 33568). **Q:** Thorax and pygidium of *Olenus transversus,* preserved in shale, loc. 2, sample L111 (MGUH 33570).

O. gibbosus and *O. truncatus* (Westergård 1922, 1944). Presumably a similar separate *O. transversus* level is developed on Bornholm considering that the species occurs alone in all samples at hand.

Comparison. Olenus transversus can be distinguished from the other *Olenus* species, except *O. gibbosus*, by its free cheek with an obtuse inner spine angle. In most other *Olenus* species the inner spine angle is 90°. *Olenus transversus* is, however, most readily identified by its pygidium. It has no marginal spines, and the pleural fields are markedly wider than the axis; the more rounded overall pygidial outline is also characteristic. *Olenus truncatus* has a subtriangular pygidium where each pleural field is as wide as the axis, while in *O. wahlenbergi* the pygidium is triangular in outline and the pleural fields are markedly narrower than the axis.

Olenus truncatus (Brünnich, 1781)
Fig. 7E–I
1922   *Olenus truncatus* (Brünnich) – Westergård, pp. 126–127, pl. III, figs 18–19, pl. IV, figs 1–4.
v 1923   *Olenus truncatus* Brünnich – C. Poulsen, pp. 25–26, textfig. 6; pl. I, fig. 6.
1957   *Olenus truncatus* (Brünnich 1781) – Henningsmoen, pp. 109–110, pl. 3.
2017   *Olenus truncatus* (Brünnich, 1781) – Rasmussen *et al.*, pp. 16–17, fig. 8E–F.
For further synonymy, see Rasmussen *et al.* (2017).

Type material. Not designated, see Henningsmoen (1957).

Material. Six almost complete specimens and 19 pygidia, including one with ten contiguous thoracic segments. Additionally, one cephalon, ten cranidia and eight free cheeks are tentatively assigned, these specimens derive from samples containing safely identified pygidia. The material derives from locality 2 and the riverbed between localities 2 and 3; one sample (GM 1922-147) is from locality 15. C. Poulsen (1923) reported the species also from locality 17 and one shale sample (GM 1922-147B) from this site is in fact labelled *O. truncatus*. However, only cranidia are present and given the high similarity between cranidia of various species of *Olenus* they cannot be identified with certainty. *Olenus truncatus* co-occurs with *H. obesus* and *O. wahlenbergi* in the samples at hand (see remarks).

Occurrence. Index fossil for the eponymous zone in Scandinavia. *Olenus truncatus* has been reported also from Great Britain and Texas (Westergård 1922, 1947; Henningsmoen 1957; Terfelt *et al.* 2008; Rasmussen *et al.* 2017; Nielsen *et al.* 2020).

Comparison. For comparison with *O. transversus* and *O. wahlenbergi,* see *O. transversus.*

Remarks. Olenus truncatus and *O. wahlenbergi* are both present in sample L103. However, the two species occur on separate bedding planes, and the sample apparently straddles the boundary between the two zones. According to Kaufmann (1933a p. 59), the *O. truncatus* Zone is only 12 cm thick in the Læså stream.

Olenus wahlenbergi Westergård, 1922
Fig. 7L–P
1922   *Olenus wahlenbergi* n. sp. – Westergård, p. 128, pl. IV, figs 5–14.
v 1923   *Olenus wahlenbergi* Wgd. – C. Poulsen, pp. 29–29, textfig. 7.
1957   *Olenus wahlenbergi* Westergård 1922 – Henningsmoen, pp. 110–111, pl. 3.
1995   *Olenus wahlenbergi* Westergård, 1922 – Clarkson & Taylor, pp. 13–34, figs 1–16.
2003   *Olenus wahlenbergi* Westergård, 1922 – Terfelt, p. 411, fig. 4C, D.
2005   *Olenus wahlenbergi* (Wahlenberg, 1821) [*sic*] – Lauridsen & Nielsen, pp. 1041–1056; pl. 1, figs 8–10.
For further synonymy, see Henningsmoen (1957).

Lectotype. Almost complete specimen (SGU 186) from Andrarum, southern Sweden, figured by Westergård (1922, pl. IV, fig. 5) and designated by Henningsmoen (1957).

Material. 26 free cheeks and 11 pygidia. 176 tentatively assigned cranidia derive from samples containing safely identified pygidia and/or free cheeks. The majority of the material derives from locality 17, with a few samples from locality 18 and one free cheek from locality 2. In the latter sample, *Olenus truncatus* has also been found (see remarks on that species). Kaufmann (1933a) also recorded *O. wahlenbergi* from the Læså stream (probably locality 2) but no material was illustrated. *Olenus wahlenbergi* is often associated with *H. obesus* in the samples at hand.

Occurrence. Index fossil for the eponymous zone in Scandinavia and Great Britain (Henningsmoen 1957; Terfelt *et al.* 2008; Nielsen *et al.* 2020).

Comparison. For comparison with *O. transversus* and *O. truncatus,* see the former. *Olenus wahlenbergi* is characterized by its free cheek having a large eye aperture and the course of the spine deviating slightly outwards from the direction of the lateral margin.

Genus *Parabolina* Salter, 1849
Type species: Entomostracites spinulosus Wahlenberg, 1818 by monotypy.

SubGenus *Parabolina* (*Parabolina*) Salter, 1849
Type species: As for genus.

***Parabolina* (*Parabolina*) *acanthura* (Angelin, 1854)**
Fig. 8A–B
v 1923   *Parabolina acanthura* Angelin – C. Poulsen, pp. 31–32, textfigs 10–11.
1957   *Parabolina acanthura* (Angelin 1854) – Henningsmoen, p. 116, pl. 7, pl. 10, figs 1–6.
2006   *Parabolina (Parabolina) acanthura* (Angelin, 1854) – Terfelt, pp. 1341–1342, pl. 1, figs 1–7.
For further synonymy, see Terfelt (2006).

Lectotype. Cranidium (RM 1655a) selected from Angelin's (1854) syntypes, designated and figured by Terfelt (2006, pl. 1, fig. 4).

Material. One cephalon, three cranidia and two free cheeks. A hypostome and an isolated thoracic pleura from the same horizon are also labelled as *P. acanthura*, but their identification remains tentative. All material is from locality 8. C. Poulsen (1923) described the species as very rare.

Occurrence. Upper part of the *Acerocare ecorne* Zone in Scandinavia and Great Britain (Westergård 1922; Henningsmoen 1957; Terfelt 2006). In Norway, *P. acanthura* ranges into the basal part of the Tremadocian (Henningsmoen 1957; Bruton *et al.* 1988).

Comparison. Parabolina acanthura is distinguished from *Parabolina heres heres* by having a shorter preglabellar field, an acute inner spine angle (right angled in *P. h. heres*), and a pygidium with only 3 pairs of marginal spines (4–5 pairs in *P. h. heres*). The pygidium of *P. heres hexacantha* [= *P. lata sensu* Heningsmoen 1957, see Nielsen *et al.* 2020] has three pairs of marginal spines that are longer than in *P. acanthura*.

***Parabolina* (*Parabolina*) *spinulosa* (Wahlenberg, 1818)**
Fig. 8E–H
1818   *Entomostracites spinulosus* – Wahlenberg, pp. 38–39, pl. I, fig. 3.
1922   *Parabolina spinulosa* (Wahlenberg) – Westergård, pp. 134–135, pl. VI, figs 14–20.
v 1923   *Parabolina spinulosa* Wahlenberg – C. Poulsen, pp. 29–31, textfig. 8.
1957   *Parabolina spinulosa* (Wahlenberg 1821) – Henningsmoen, pp. 126–128, pl. 1, fig. 2, pl. 3, textfig. 12.

1973   *Parabolina spinulosa* (Wahlenberg, 1821) – Schrank, p. 814, pl. I, figs 1–12, pl. II, figs 1–2.
1976   *Parabolina spinulosa* (Wahlenberg) – Reyment, fig. 1a–b.
2003   *Parabolina spinulosa* (Wahlenberg, 1818) – Terfelt, p. 411, fig. 4G, H.
2017   *Parabolina spinulosa* (Wahlenberg, 1818) – Rasmussen *et al.*, pp. 17–18.
For further synonymy, see Rasmussen *et al.* (2017).

Lectotype (designated here). Complete specimen PMU Sk-1 from Andrarum, Scania, originally illustrated by a drawing (Wahlenberg 1818, pl. 1, fig. 3); refigured by Reyment (1976, fig. 1a).

Material. 20 cranidia, seven free cheeks and eight pygidia. Most of the material derives from locality 6, but the species has been found also at locality 5. *Parabolina spinulosa* is associated with extremely common articulate brachiopods (*Orusia lenticularis*) in the samples at hand.

Occurrence. Index fossil for the eponymous zone. *Parabolina spinulosa* occurs widespread in Scandinavia, England and Canada (Westergård 1922; Henningsmoen 1957; Taylor & Rushton 1971; Rasmussen *et al.* 2015; Nielsen *et al.* 2020). It has also been reported from the overlying *Leptoplastus paucisegmentatus* Zone (Westergård 1947), based on co-occurrence with *Leptoplastus minor*, synonymized with *L. paucisegmentatus* by Westergård (1944, 1947). However, this interpretation is questioned by Nielsen *et al.* (2020), inferring reworking.

Comparison. The cranidium of *Parabolina spinulosa* can be distinguished from that of *P. brevispina* e.g. by its wider postocular cheek. Pygidia of *P. spinulosa* have 5–6 axial rings and 3–5 pairs of long marginal spines, while *P. brevispina* pygidia only have three axial rings and 3–4 pairs of short marginal spines.

Subgenus *Parabolina* (*Neoparabolina*) Nikolaisen & Henningsmoen, 1985
Type species: *Parabolina frequens* (Barrande, 1868), by original designation.

***Parabolina* (*Neoparabolina*) *lobata praecurrens* Westergård, 1944**
Fig. 8C–D
1944   *Parabolina longicornis praecurrens* var. n. – Westergård, p. 39, pl. 1, figs 9–11.
1957   *Parabolina lobata praecurrens* Westergård 1944 – Henningsmoen, pp. 123–124.
1973   *Parabolina lobata praecurrens* Westergård, 1944 – Schrank, p. 814–815, pl. II, figs 3–5, ?6.

2004 *Parabolina (Neoparabolina) praecurrens* Westergård 1944 – Buchholz, pp. 17–18, pl. 6, figs 7–10, pl. 7, figs 1–8.
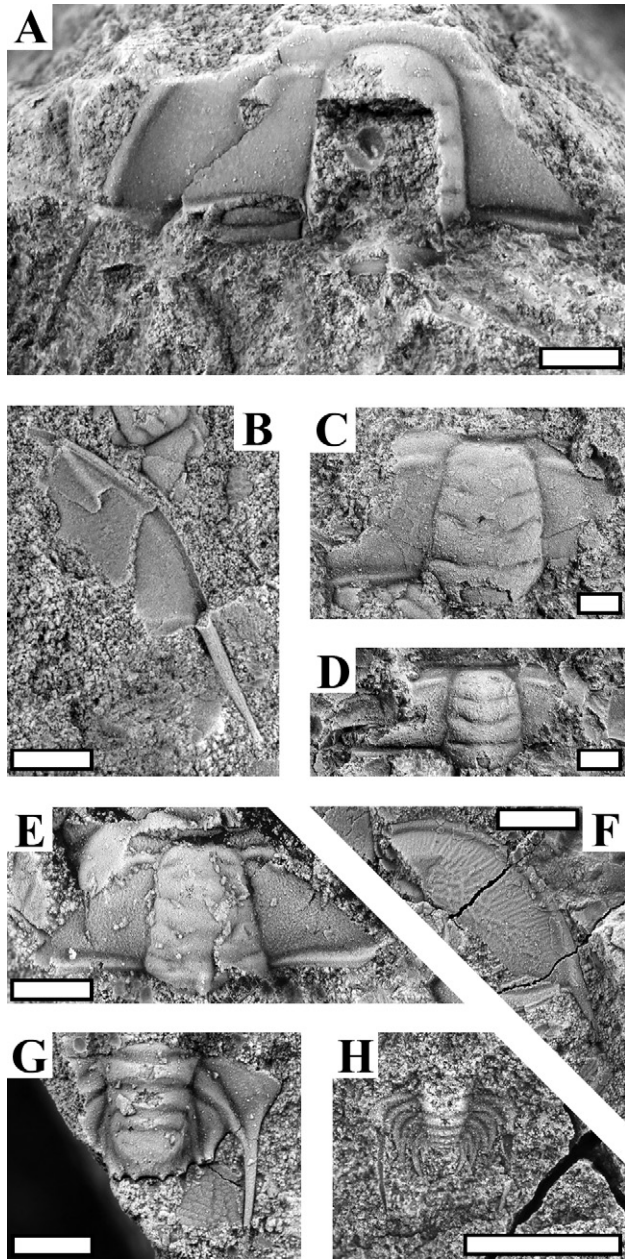
Fig. 8. Various species of *Parabolina*, all preserved in anthraconite. White scale bars: 1 mm. **A–B:** *Parabolina acanthura*, loc. 8. **A:** Fragmentary cephalon, sample GM 1924-1A (MGUH 33571). **B:** Free cheek seen from ventral side (partial external mould), loc. 8, MGUH 1980 (previously illustrated by C. Poulsen 1923, textfig. 11b). **C–D:** *Parabolina lobata praecurrens*, loc. 8B. **C.** Cranidium, sample L16 (MGUH 33572). **D:** Cranidium, sample L12 (MGUH 33574). **E–H:** *Parabolina spinulosa*, loc. 6. **E:** Cranidium, sample GM 1922-137B (MGUH 33575). **F:** Free cheek, sample GM 1922-137B (MGUH 33576). **G:** Pygidium, sample GM 1922-137B (MGUH 33577). **H:** Juvenile pygidium, sample GM 1922-137B (MGUH 33578).

2005 *Parabolina (Neoparabolina) lobata praecurrens* Westergård, 1944 – Terfelt *et al.*, pp. 197–200, fig. 4G–H.

For complete synonymy, see Henningsmoen (1957) and Terfelt *et al.* (2005).

Holotype. Cranidium SGU 4222 from the Gislövhammar-1 drill core, Sweden, figured by Westergård (1944, pl. 1, fig. 9).

Material. 21 cranidia, all rather poorly preserved and more or less fragmentary. The material derives from loose limestone boulders in the Læså creek bed at Limensgade (localities 8A–B). *Parabolina lobata praecurrens* co-occurs with *Peltura westergaardi* and rare articulate brachiopods.

Occurrence. Parabolina lobata Zone in Scania and the Oslo Region (Westergård 1944, 1947; Henningsmoen 1957). According to Westergård (1944) and Terfelt *et al.* (2005), *P. lobata praecurrens* is characteristic for the lower part of this zone.

Comparison. In comparison with *P. lobata lobata, P. lobata praecurrens* lacks a preglabellar field and also tends to have narrower fixed cheeks (see remarks). For description of pygidia, see Buchholz (1999, 2004).

Remarks. This is the first report of this subspecies from Bornholm. The free cheeks that C. Poulsen (1923) assigned to *Parabolina longicornis* [= *P. lobata*] are here allocated to *Ctenopyge tenuis* (*q.v.*) and thus no original museum material represents *P. lobata*. Henningsmoen (1957) and Terfelt *et al.* (2005) mentioned that *P. lobata praecurrens* has narrower fixed cheeks than *P. lobata lobata*, but Terfelt *et al.* (2005) remarked on the presence of intermediate forms with narrower fixed cheeks and a shorter preglabellar field than typical for *P. lobata lobata*. Terfelt *et al.* (2005) assigned cranidia with a pronounced preglabellar field to *P. lobata lobata* and cranidia lacking or having a very short preglabellar field to *P. lobata praecurrens*. The cranidia from Bornholm have a very short or no preglabellar field.

Genus *Leptoplastus* Angelin, 1854
Type species: Leptoplastus stenotus Angelin, 1854, designated by Vogdes (1890).

***Leptoplastus abnormis* Westergård, 1944**
Figs 9–10.

v 1923 *Leptoplastus ovatus* Angelin [*partim*] – C. Poulsen, pp. 35–36.
v 1923 *Leptoplastus stenotus* Angelin [*partim*]– C. Poulsen, pp. 36–37.

1944   *Leptoplastus abnormis* sp. n. – Westergård, p. 41, pl. 1 fig. 23; pl. 2, fig. 1.

1973   *Leptoplastus ovatus* Angelin, 1854 [*partim*] – Schrank, p. 817, pl. III, fig. 13.

2006   *Leptoplastus abnormis* Westergård, 1944 – Ahlberg *et al.*, pp. 105–106, figs 6G, 7B.

2015   *Leptoplastus ovatus* (Angelin, 1854) [*partim*] – Rasmussen *et al.*, pp. 14–15, fig. 6C–D.

2017   *Leptoplastus abnormis* Westergård, 1944 – Rasmussen *et al.*, p. 13, fig. 5A.

For further synonymy, see Rasmussen *et al.* (2017).

Holotype. Almost complete specimen SGU 4235 from Andrarum, southern Sweden, figured by Westergård (1944, pl. 1, fig. 23).

Material. The highly characteristic thorax of *L. abnormis* with long spines in the rear part has been found in ten samples including a nearly complete specimen and external moulds of three nearly complete specimens, all without free cheeks (e.g. Figs 9A–D). The remaining skeletal parts are exceedingly alike *L. ovatus* but one cephalon, 352 cranidia and nine free cheeks, all from locality 6, are tentatively assigned to *L. abnormis* (see remarks). Please note that the extensive material listed as *L. ovatus* in Appendix 1 rather likely still contains some *L. abnormis* and no differentiation of pygidia has been attempted. *Leptoplastus abnormis,* as interpreted here, co-occurs with *Eurycare bornholmensis, Leptoplastus angustatus, L. crassicornis* and *L. ovatus.*

Occurrence. Leptoplastus crassicornis–L. angustatus Zone in Scania and Öland, Sweden, perhaps Slemmestad in the Oslo Region, Norway (see remarks), and Bornholm (Westergård 1944, 1947; Ahlberg *et al.* 2006; Rasmussen *et al.* 2017; this study).

Comparison. In comparison with *L. angustatus* and *L. crassicornis*, the cranidium of *L. abnormis* has a more bulbous and short glabella, the interocular area is significantly narrower (tr.) and the postocular cheeks are shorter (exsag.); the free cheek has a much shorter spine and shorter posterior margin. For comparison with *L. ovatus*, see remarks.

Remarks. Nearly all identifiable thoraxes of *Leptoplastus* in the material at hand represent *L. abnormis* whereas no contiguous thoracic segments assignable to *L. ovatus* have been recorded. Initially all detached skeletal parts of *ovatus*-type (i.e. cranidia with relatively short, wide glabella, narrow interocular cheeks and short (exsag.) postocular cheeks; free cheeks with short almost straight spine) were identified as *L. ovatus* and none as *L. abnormis*, making it obvious that the disarticulated slerites of these species were mixed up.

According to Henningsmoen (1957), *L. abnormis* has an elongate glabella, interocular cheeks that are ½ as wide as glabella at eye-line and postocular cheeks that are ¾ as wide (tr.) as the occipital ring, whereas *L. ovatus* was diagnosed as having a glabella that is approximately as wide as long, interocular cheeks that are ¼ as wide as the adjacent glabella and postocular cheeks that are somewhat narrower (tr.) than the occipital ring. Ahlberg *et al.* (2006, fig. 7B) indicated that *L. abnormis* has its palpebral lobes situated relatively far forwards opposite L2, while the lobes are located opposite L1–S1 in *L. ovatus.* The free cheek of *L. abnormis* may have a slightly longer genal spine than *L. ovatus* (Westergård 1944; Ahlberg *et al.* 2006). No separating characters for pygidia have been published.

All material studied here is preserved in limestone, whereas the few semi-complete specimens of *L. abnormis* from Scania described by Westergård (1944) and Ahlberg *et al.* (2006) are preserved in shale. This is relevant as compaction may have distorted the outline of the material hitherto described, and also influenced the drawn reconstruction published by Ahlberg *et al.* (2006, fig. 7B).

A closer examination of the *ovatus*-type cranidia was based on photos of 101 fairly preserved specimens of different sizes. The pilot study revealed that three morphs can be distinguished based on visual appearance: i) one with a short glabella+occipital ring that essentially does not taper (Fig. 14), ii) one with a slightly to clearly elongate glabella+occipital ring that essentially does not taper (Figs 9J, 10E–L) and iii) one where the elongate glabella+occipital ring tapers (Figs 9E–I, 10C–D, M). In order to characterize these morphs further, several cranidial features were measured; the results are summarized in Table 1 and illustrated in Fig. 11. In the non-tapering morph with short glabella, tentatively treated as *L. ovatus*, the width of the occipital ring corresponds on average to 0.83 of the combined length of glabella+occipital ring, whereas this ratio averages 0.86 in the two other morphs that both are assumed to represent *L. abnormis* (Table 1 and Fig. 11, ratio A).

The key difference between the two taxa, based on visual examination, is the relative length of the glabella. Most unexpectedly, the measured length/width ratio of the glabella itself (i.e. without the occipital ring) is identical in the two groupings (Table 1 and Fig. 11, ratio D). Hence, one of the few measurable differences is the laterally expanded occipital ring seen in most (but not all) medium-sized and larger cranidia of *L. abnormis* (Table 1 and Fig. 11, ratio A). Increased tapering of the glabella+occipital ring during growth is a phenomenon seen also in other olenids, e.g. *C. affinis* (Fig. 20) and *S. alatus* (Fig. 32) and which justifies the assignment of small cranidia with non-tapering,
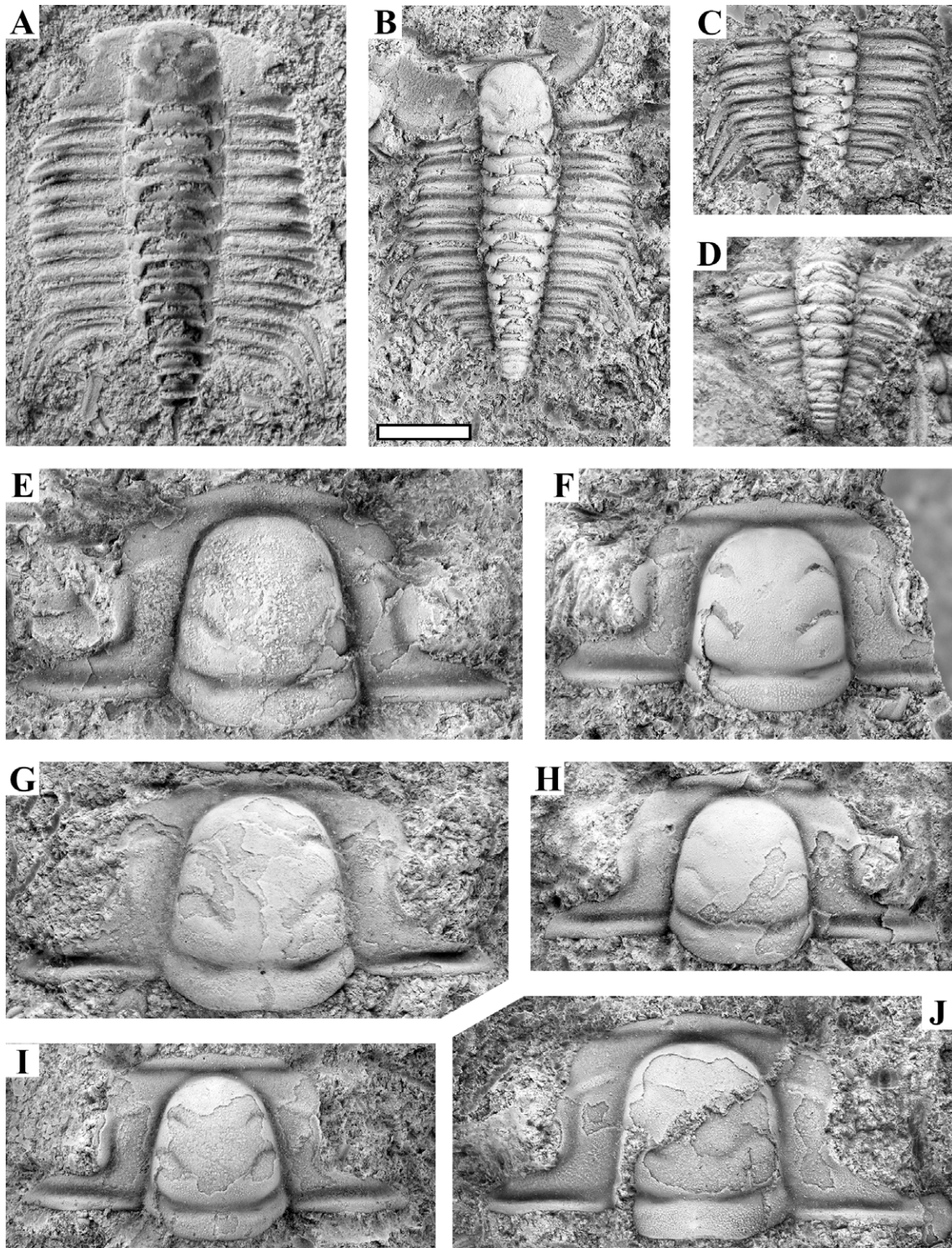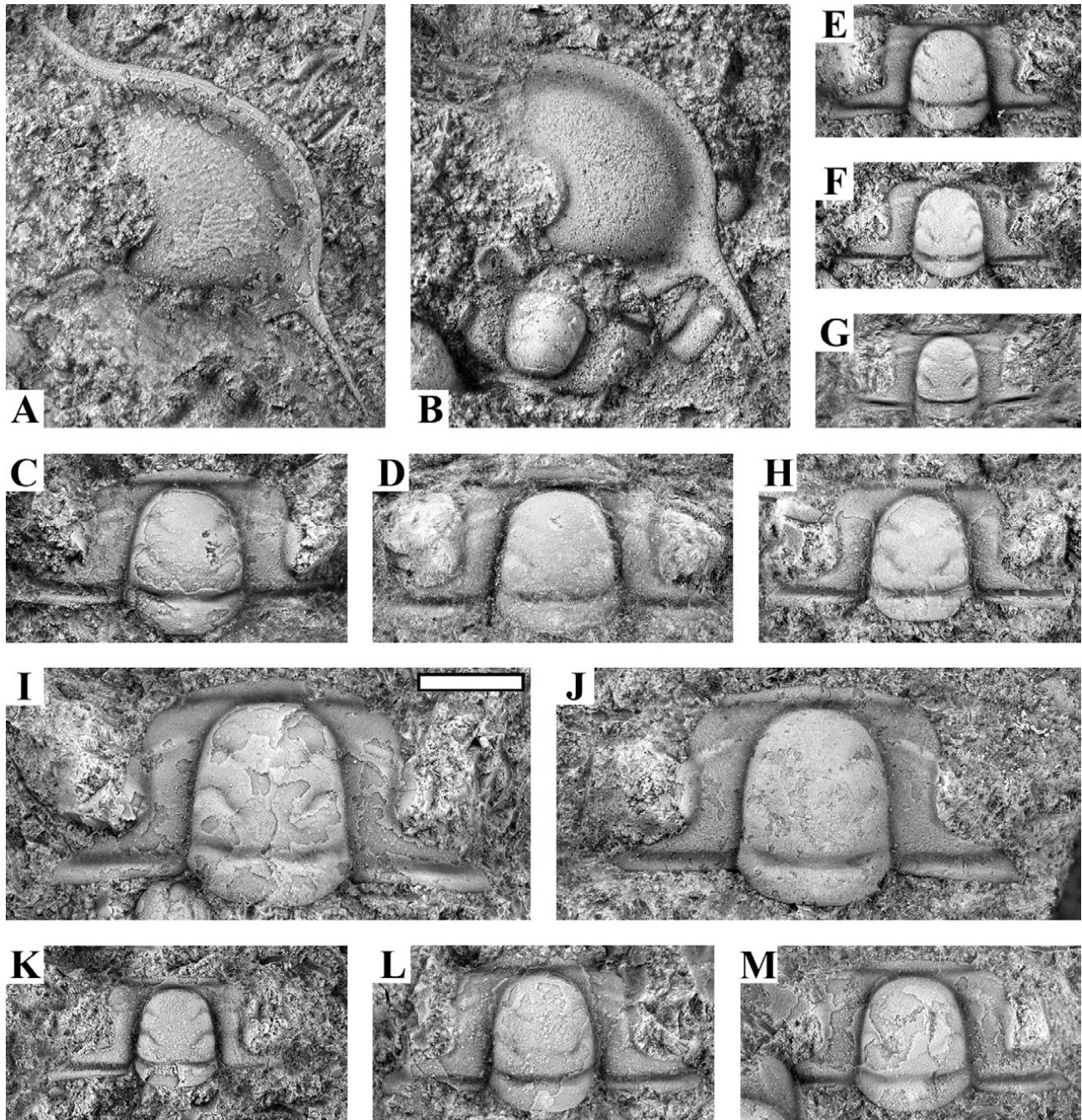
Fig. 9. *Leptoplastus abnormis*, all preserved in anthraconite from locality 6; regarding assignment of cranidia, see text. White scale bar: 2 mm. **A:** External mould of almost complete specimen, sample ATN-304 (MGUH 33579). **B:** Small, almost complete specimen (somewhat damaged), sample ATN-260 (MGUH 33582). **C:** Part of thorax, sample ATN-301 (MGUH 33583). **D:** Small thorax with attached pygidium; the pleural spines are broken and the specimen is tentatively assigned, sample ATN-265 (MGUH 33585). **E:** Cranidium, sample ATN-261 (MGUH 33588). **F:** Cranidium, sample ATN-331 (MGUH 33589). **G:** Cranidium, sample ATN-288 (MGUH 33592). **H:** Cranidium, sample ATN-262 (MGUH 33597). **I:** Cranidium, sample ATN-276 (MGUH 33599). **J:** Cranidium with non-tapering glabella, tentatively assigned, sample ATN-288 (MGUH 33593) (see also Fig. 10I–L).

barely elongate glabella to *L. abnormis* (Fig. 10E–G). Otherwise, the cranidial ratios of *L. ovatus* and *L. abnormis* are quite similar (Table 1, Fig. 11) except that the postocular cheek in large cranidia is relatively wider in *L. ovatus* than in *L. abnormis*, and which is also reflected in the cranidial W/L ratio in adults (ratio B2). The relative width of the occipital ring (ratio C, Table 1 and Fig. 11) increases hardly at all during growth and

Fig. 10. *Leptoplastus abnormis* (*s.l.*), all preserved in anthraconite from locality 6; regarding assignment of cranidia and free cheeks, see text. White scale bar: 2 mm. **A–B:** Free cheeks, tentatively assigned to *Leptoplastus abnormis*, samples ATN-119 and ATN-288 (MGUH 33601, 33594). **C–H:** Medium sized cranidia. **C:** Sample L126 (MGUH 33603). **D:** Sample ATN-332 (MGUH 33607). **E:** Sample ATN-301 (MGUH 33584). **F:** Sample ATN-265 (MGUH 33586). **G:** Sample ATN-335 (MGUH 33609). **H:** Sample ATN-265 (MGUH 33587). **I–L.** Cranidia with essentially non-tapering, slightly elongate glabella, identified as *Leptoplastus* cf. *abnormis*. **I:** Sample ATN-347 (MGUH 33611). **J:** Sample ATN-331 (MGUH 33590). **K:** Cranidium, sample ATN-241 (MGUH 33612). **L:** Sample ATN-293 (MGUH 33613). **M:** Cranidium, sample ATN-346 (MGUH 33614).
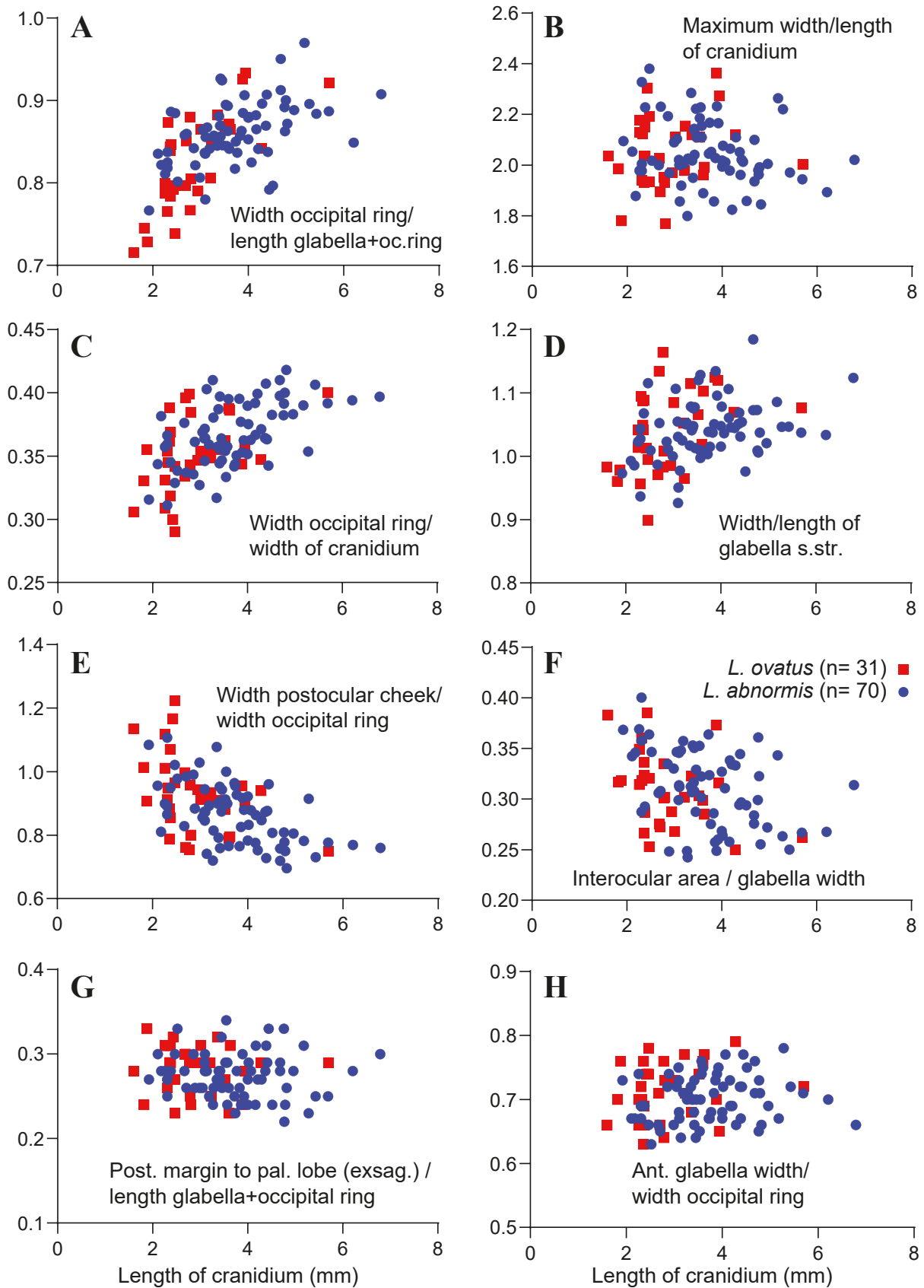
Fig. 11. Scatter plots of various cranidial features of *Leptoplastus abnormis* and *Leptoplastus ovatus*. See text for discussion; average values and variation ranges are listed in Table 1. All x-axes are length of cranidium (mm). Legend in F.

is surprisingly similar in the two taxa. The distance (exsag.) between the posterior cranidial margin and posterior corner of the palpebral lobe is also identical in both taxa (ratio G, Table 1). The eyes are thus not located more forwards in the specimens assigned to *L. abnormis* (cf. Ahlberg *et al.* 2006), and midpoint of the palpebral lobes is located opposite S1 to L1 (Figs 9–10). Also, the width of the interocular cheek at eye-line (tr.) is identical in the two taxa (ratio F, Table 1).

As it appears, the only measurable differences between the discussed species are the slightly wider postocular cheeks in adult *L. ovatus* cranidia and the wider occipital ring of the medium-sized and larger cranidia assigned to *L. abnormis,* which engenders a tapering appearance of the glabella+occipital ring.

In this connection, please note that the complete specimen of *L. abnormis* illustrated in Fig. 9B has a cranidium only 2.4 mm long. The two specimens of *L. abnormis* originally illustrated by Westergård (1944) both have cranidia *c.* 3.5 mm long. One of them shows a tapering glabella (*ibid*. pl. 2, fig. 1) whereas the other (the holotype) does not (*ibid*. pl. 1, fig. 23).

A biometric study, including complete specimens of *L. ovatus* as well as disarticulated *ovatus*-type material from across Scandinavia, should be undertaken. For instance, the cranidium and free cheek from Slemmestad assigned to *L. ovatus* by Rasmussen *et al.* (2015) in our opinion resemble the morph identified here as *L. abnormis* as the glabella is tapering and the genal spine is comparatively sturdy.

Table 1. Cranidial ratios of *Leptoplastus ovatus* (morph with short, essentially non-tapering glabella) and *Leptoplastus abnormis* (morphs with relatively longer glabella, tapering or non-tapering) based on measurements of 101 well-preserved cranidia

	L. ovatus (n=31)	*L. abnormis* (n=70)
A. Width occipital ring (tr.) / length of glabella+occipital ring	avg. 0.83 (0.72–0.93)	avg. 0.86 (0.77–0.97)
A1. Cranidia < 3 mm long (n=20 and 15, respectively)	avg. 0.79 (0.72–0.88)	avg. 0.83 (0.78–0.89)
A2. Cranidia ≥3 mm long (n=11 and 55, respectively)	avg. 0.88 (0.81–0.93)	avg. 0.87 (0.78–0.99)
B. Cranidial maximum width/maximum length	avg, 2.05 (1.77–2.36)	avg. 2.05 (1.80–2.38)
B1. Cranidia < 3 mm long (n=20 and 15, respectively)	avg. 2.01 (1.77–2.30)	avg. 2.09 (1.88–2.38)
B2. Cranidia ≥3 mm long (n=11 and 55, respectively)	avg. 2.11 (1.96–2.36)	avg. 2.03 (1.80–2.28)
C. Width occipital ring (tr.) / width of cranidium	avg. 0.35 (0.29–0.40)	avg. 0.37 (0.31–0.42)
Ca. Cranidia < 3 mm long (n=20 and 15, respectively)	avg. 0.35 (0.29–0.40)	avg. 0.35 (0.31–0.38)
Cb. Cranidia ≥3 mm long (n=11 and 55, respectively)	avg. 0.36 (0.34–0.40)	avg. 0.37 (0.32–0.42)
D. Max. width/length ratio of glabella s.str.	avg. 1.04 (0.90–1.16)	avg. 1.04 (0.93–1.18)
Da. Cranidia < 3 mm long (n=20 and 15, respectively)	avg. 1.02 (0.90–1.16)	avg. 1.02 (0.94–1.12)
Db. Cranidia ≥3 mm long (n=11 and 55, respectively)	avg. 1.07 (0.96–1.12)	avg. 1.05 (0.93–1.18)
E. Width (tr.) of postocular cheek / width occipital ring	avg. 0.93 (0.75–1.22)	avg. 0.87 (0.70–1.11)
E1. Cranidia < 3 mm long (n=20 and 15, respectively)	avg. 0.96 (0.75–1.22)	avg. 0.95 (0.81–1.11)
E2. Cranidia ≥3 mm long (n=11 and 55, respectively)	avg. 0.88 (0.75–0.96)	avg. 0.84 (0.70–1.08)
F. Width (tr.) of interocular cheek /width of adjacent glabella at eye-line (n= 30 and 67, respectively)	avg. 0.31 (0.25–0.39)	avg. 0.31 (0.24–0.40)
F1. Cranidia < 3 mm long (n=20 and 15, respectively)	avg. 0.32 (0.25–0.39)	avg. 0.33 (0.25–0.40)
F2. Cranidia ≥3 mm long (n=10 and 52, respectively)	avg. 0.30 (0.25–0.37)	avg. 0.30 (0.24–0.37)
G. Distance (exsag.) post. cranidial margin to post. corner of palpebral lobe / length of glabella+occipital ring	avg. 0.28 (0.23–0.33)	avg. 0.27 (0.22–0.34)
G1. Cranidia < 3 mm long (n=20 and 15, respectively)	avg. 0.28 (0.23–0.33)	avg. 0.28 (0.25–0.33)
G2. Cranidia ≥3 mm long (n=11 and 55, respectively)	avg. 0.28 (0.23–0.32)	avg. 0.27 (0.22–0.34)
H. Width of glabella (tr.) at eye ridge/width of occipital ring	avg. 0.71 (0.63–0.79)	avg. 0.70 (0.63–0.78)
H1. Cranidia < 3 mm long (n=20 and 15, respectively)	avg. 0.71 (0.63–0.78)	avg. 0.69 (0.63–0.74)
H2. Cranidia ≥3 mm long (n=11 and 55, respectively)	avg. 0.73 (0.65–0.79)	avg. 0.70 (0.64–0.78)
I. Width of glabella (tr.) at eye ridges/max. width of glabella immediately in front of occipital ring	avg. 0.74 (0.64–0.81)	avg. 0.75 (0.66–0.84)
I1. Cranidia < 3 mm long (n=20 and 15, respectively)	avg. 0.73 (0.64–0.79)	avg. 0.73 (0.66–0.81)
I2. Cranidia ≥3 mm long (n=11 and 55, respectively)	avg. 0.77 (0.69–0.81)	avg. 0.76 (0.71–0.84)

See also Fig. 11, where the ratios are plotted vs. cranidial length.
Much of the dataset is obtained from an unpublished student project (Holm 2020).
For remarks on identification of *L. ovatus* and *L. abnormis*, see text.

Findings of the characteristic thorax shows that *L. abnormis* unquestionably occurs in the *Leptoplastus* Superzone on Bornholm. A few *ovatus*-type free cheeks with comparatively long spines have also been tentatively assigned (Fig. 10A–B), following Westergård (1944). We presume, but cannot prove beyond doubt, that also *L. ovatus* is present and it is stressed that the indicated identification of disarticulated sclerites remains preliminary.

Leptoplastus angustatus (Angelin, 1854)
Fig. 12.

1904   *Eurycare angustatum* Ang. [*partim*] – Persson, pp. 517–520, pl. 9, figs 11–13; non pl. 9, figs 9–10 [= *Eurycare*? sp.].

1922   *Eurycare angustatum* Angelin – Westergård, p. 150, pl. X, figs 4–9.

v 1923   *Eurycare angustatum* Angelin [*partim*] – C. Poulsen, pp. 34–35, pl. 1, fig. 10; non pl. 1, fig. 9 [= *L. crassicornis*, see Fig. 13D]. [The museum material labelled as *Eurycare angustatum* includes *L. crassicornis* and *L. ovatus*].

v 1923   *Leptoplastus stenotus* Angelin [*partim*] – C. Poulsen, pp. 36–37.

1957   *Leptoplastus angustatus* (Angelin 1854) – Henningsmoen, pp. 164–165, pl. 4; pl. 16, figs 10–13.

1973   *Leptoplastus angustatus* (Angelin, 1854) – Schrank, pp. 818–819, pl. IV, fig. 13–22; pl. V, fig. 1–4.

2004   *Leptoplastus angustatus* (Angelin 1854) – Mischnik, pp. 109–110, pl. 3, fig. 2.

2006   *Leptoplastus angustatus* (Angelin, 1854) [*partim*] – Ahlberg *et al.*, pp. 102, 105, figs 4B–C, 6B–C, 7D; non fig. 6A [= *L. crassicornis*].

2016   *Leptoplastus angustatus* (Angelin, 1854) – Rasmussen *et al.*, p. 13.

For further synonymy, see Rasmussen *et al.* (2016).

Type material. Not designated, see Henningsmoen (1957).

Material. 457 cranidia, 203 free cheeks and 28 pygidia; all from locality 6 (a few older museum specimens just labelled 'Læså' must also derive from this locality). Four additional pygidia may belong to the species but are too poorly preserved to be safely assigned. *Leptoplastus angustatus* co-occurs with *E. bornholmensis, L. abnormis, L. crassicornis* and *L. ovatus* in the samples at hand.

Occurrence. Characteristic for the *L. crassicornis–L. angustatus* Zone in Scandinavia (Rasmussen *et al.* 2015; Nielsen *et al.* 2020 and references therein).

Comparison. Leptoplastus crassicornis is distinguished from *L. angustatus* by having a more elongate glabella. These species have rather similar looking free cheeks with a very long curved spine, but in *L. crassicornis,* the spine is wider, somewhat flattened and provided with a central keel (Fig. 13H–J), whereas in *L. angustatus* the spine is more slender and rounded in cross-section (Fig. 12M–P). For comparison with free cheeks of *E. bornholmensis*, see that species. In comparison with *L. angustatus*, the crania of *L. ovatus* and *L. abnormis* have a less elongate, more bulbous glabella, the interocular cheeks are narrower and the postocular cheeks are shorter (exsag.). Due to the longer (exsag.) postocular cheeks of *L. angustatus*, the eyes are positioned more anteriorly than in *L. ovatus* and *L. abnormis*.

Remarks. The fact that *L. angustatus* co-occurs with *L. ovatus* and *L. crassicornis* on Bornholm corroborates the zonal revision proposed by Rasmussen *et al.* (2015), abandoning separate *L. crassicornis, L. ovatus* and *L. angustatus* zones. The latter taxon seems, though, to predominantly occur towards the top of the zone at several Scandinavian localities (e.g. Westergård 1944, 1947; Henningsmoen 1957; Rasmussen *et al.* 2015). Its distribution within the zone on Bornholm cannot be unravelled based on the material at hand, but it co-occurs with all the other nominate zonal index species (see above). However, in 25% of the samples containing *L. angustatus*, the species occurs alone, usually in profusion and with many juveniles. Hence, at least

▼ **Fig. 12.** *Leptoplastus angustatus*, all preserved in anthraconite from locality 6. White scale bars: 1 mm; please note that juvenile cranidia J–L and pygidia R–U are shown at a greater magnification (scale bar in Q). **A:** Cranidium, sample ATN-110 (MGUH 33615). **B:** Cranidium, sample ATN-223 (MGUH 33622). **C:** Cranidium, sample ATN-252 (MGUH 33624). **D:** Cranidium, sample ATN-153 (MGUH 33626). **E:** Cranidium, sample ATN-110 (MGUH 33616). **F:** Cranidium, sample ATN-288 (MGUH 33595). **G:** Cranidium, sample ATN-153 (MGUH 33627). **H:** Cranidium, sample ATN-335 (MGUH 33610). **I:** Small cranidium, sample ATN-304 (MGUH 33580). **J:** Juvenile cranidium, sample GM 1888-289A (MGUH 33628). **K:** Juvenile cranidium, sample ATN-334 (MGUH 33630) **L:** Juvenile cranidium, sample GM 1888-289A (MGUH 33629). **M:** Free cheek, sample ATN-110 (MGUH 33617). **N:** Free cheek, sample ATN-224 (MGUH 33631). **O:** Free cheek, sample ATN-223 (MGUH 33623). **P:** Free cheek, sample ATN-278 (MGUH 33633). **Q:** Pygidium, sample ATN-332 (MGUH 33608). **R:** Pygidium, tentatively assigned, sample ATN-224 (MGUH 33632). **S:** Pygidium, sample L32 (MGUH 33636). **T:** Pygidium, sample GM 1888-289C (MGUH 33637) (same sample as MGUH 1962). **U:** Pygidium, sample ATN-110 (MGUH 33618).
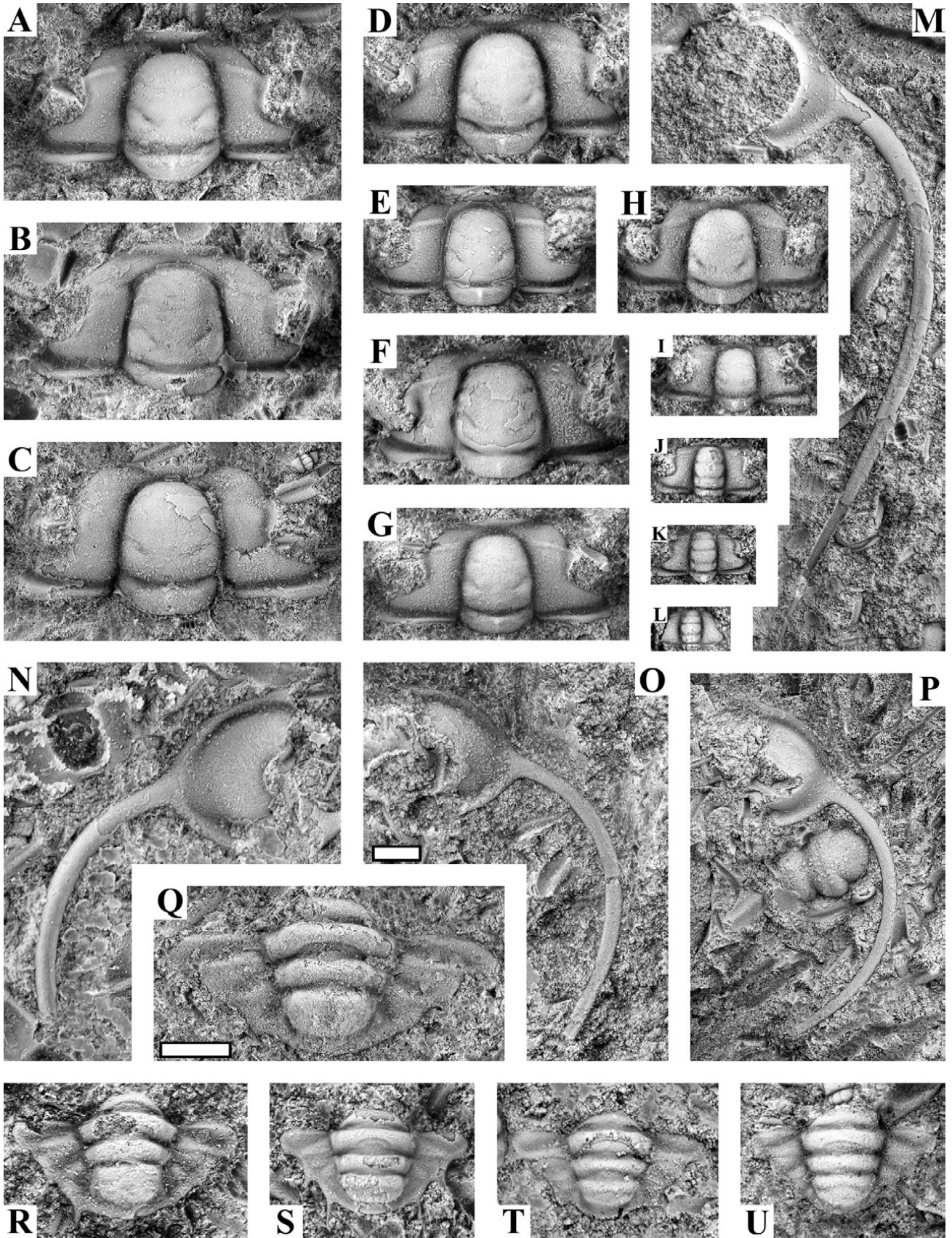
one level within the *L. crassicornis–L. angustatus* Zone on Bornholm is characterized by sole occurrence of *L. angustatus*, but it may just be a single bedding plane.

Leptoplastus crassicornis (Westergård, 1944)
Fig. 13.

v 1923   *Eurycare angustatum* Angelin [*partim*] – C. Poulsen, pp. 34–35, pl. I, fig. 9. [The specimen is here re-illustrated in Fig. 13D].
v 1923   *Leptoplastus stenotus* Angelin [*partim*] – C. Poulsen, pp. 36–37.
1944   *Eurycare angustatum crassicorne* var. n. – Westergård, pp. 41–42, pl. 2, figs 2–4.
1957   *Leptoplastus crassicorne* (Westergård 1944) – Henningsmoen, p. 167, pl. 4; pl. 14, figs 1–13.
1958a   *Leptoplastus crassicornis* – Henningsmoen, p. 187.
1973   *Leptoplastus crassicorne* (Westergård, 1944) – Schrank, pp. 816–817, pl. III, figs 5?, 6, 7?, 8–11.
2004   *Leptoplastus crassicornis* (Westergård 1944) – Mischnik, p. 108, pl. 2, fig. 7.
2006   *Leptoplastus crassicornis* (Westergård 1944) – Ahlberg *et al.*, p. 102, figs 5H–I, 7E.
2006   *Leptoplastus angustatus* (Angelin, 1854) [*partim*] – Ahlberg *et al.*, fig. 6A.
2017   *Leptoplastus crassicornis* (Westergård, 1944) – Rasmussen *et al.*, pp. 13–14.

For further synonymy, see Rasmussen *et al.* (2017).

Holotype. Complete specimen SGU 4237 from Andrarum, southern Sweden, figured by Westergård (1944, pl. 2, fig. 2).

Material. 37 cranidia, 12 free cheeks and six pygidia; all from locality 6. *Leptoplastus crassicornis* co-occurs with *Eurycare bornholmensis, E. latum, Leptoplastus angustatus, L. abnormis* and *L. ovatus* in the material at hand.

Occurrence. Index fossil for the *L. crassicornis–L. angustatus* Zone in Scandinavia (Rasmussen *et al.* 2015; Nielsen *et al.* 2020). *Leptoplastus crassicornis* has been reported also from England (Taylor & Rushton 1971).

Comparison. The free cheek of *L. crassicornis* with a long, robust, somewhat flattened genal spine is distinctive and safely confirms the presence of this species on Bornholm. The cranidium reminds of *L. angustatus*, for comparison, see that species. The free cheek somewhat resembles that of *E. latum*, but the spine curves stronger and the genal field of *E. latum* is more vaulted.

Remarks. This species was mentioned from Bornholm by Henningsmoen (1957, p. 167) but its presence has never been documented. Only sparse material has been found and *L. crassicornis* appears to be comparatively infrequent. This should be evaluated in light of the fact that a very extensive sample material from the *Leptoplastus* Superzone is at hand.

Leptoplastus ovatus Angelin, 1854
Fig. 14

1904   *Leptoplastus ovatus* Ang. – Persson, pp. 520–522, pl. 9, figs 17–23.
1922   *Leptoplastus ovatus* Angelin – Westergård, pp. 145–146, pl. VIII, figs 18–21.
v 1923   *Leptoplastus ovatus* Angelin [*partim*] – C. Poulsen, pp. 35–36, textfig. 12. [The material includes *L. abnormis*].
v 1923   *Leptoplastus stenotus* Angelin [*partim*] – C. Poulsen, pp. 36–37.
v 1923   *Eurycare angustatum* Angelin [*partim*] – C. Poulsen, pp. 34–35.
1957   *Leptoplastus ovatus* Angelin 1854 – Henningsmoen, pp. 173–174, pl. 4; pl. 13, figs 8–10.
1973   *Leptoplastus ovatus* Angelin, 1854 [*partim*] – Schrank, p. 817, pl. III, fig. 12, 14–16; non pl. III, fig. 13 [= *L. abnormis*].
2004   *Leptoplastus ovatus* Angelin 1854 – Mischnik, p. 108, pl. 2, fig. 6.
2015   *Leptoplastus ovatus* (Angelin, 1854) [*partim*] – Rasmussen *et al.,* pp. 14–15, non fig. 6C–D [= *L. abnormis*].
2017   *Leptoplastus ovatus* (Angelin, 1854) – Rasmussen *et al.*, p. 14, fig. 7C, E, F.

For further synonymy, see Rasmussen *et al.* (2017).

Lectotype. Complete specimen Ar 1721 (Naturhistoriska Riksmuseet, Stockholm) from Andrarum, southern Sweden, figured by Westergård (1922, pl. VIII, fig. 18), and supposed to be Angelin's type specimen. Designated by Henningsmoen (1957).

Material. 401 cranidia, 429 free cheeks, one hypostome? and 35 pygidia (free cheeks, hypostome and pygidia are tentatively assigned and probably include specimens of *L. abnormis*); all from locality 6. *Leptoplastus ovatus* co-occurs with *Eurycare bornholmensis, E. latum, L. abnormis, L. angustatus* and *L. crassicornis.*

Occurrence. Leptoplastus crassicornis–L. angustatus Zone in Scandinavia (Westergård 1944; Ahlberg *et al.* 2006; Rasmussen *et al.* 2015; Nielsen *et al.* 2020). *Leptoplastus ovatus* is reported also from England (Taylor & Rushton 1971) and possibly maritime Canada (Henningsmoen 1957).

Comparison. For comparison with *L. angustatus* and *L. abnormis,* see those taxa. Disarticulated skeletal parts of *L. ovatus* and *L. abnormis* are almost indistinguishable and despite detailed study the may still be mixed to some extent.

Remarks. Measurements of cranidia of the morph we here identify as *L. ovatus* (see remarks on *L. abnormis*) show that width of the interocular cheeks at eye-line (tr.) corresponds to 0.25–0.4 of the adjacent glabella width (Table 1), a range slightly wider than indicated for this species by Henningsmoen (1957).
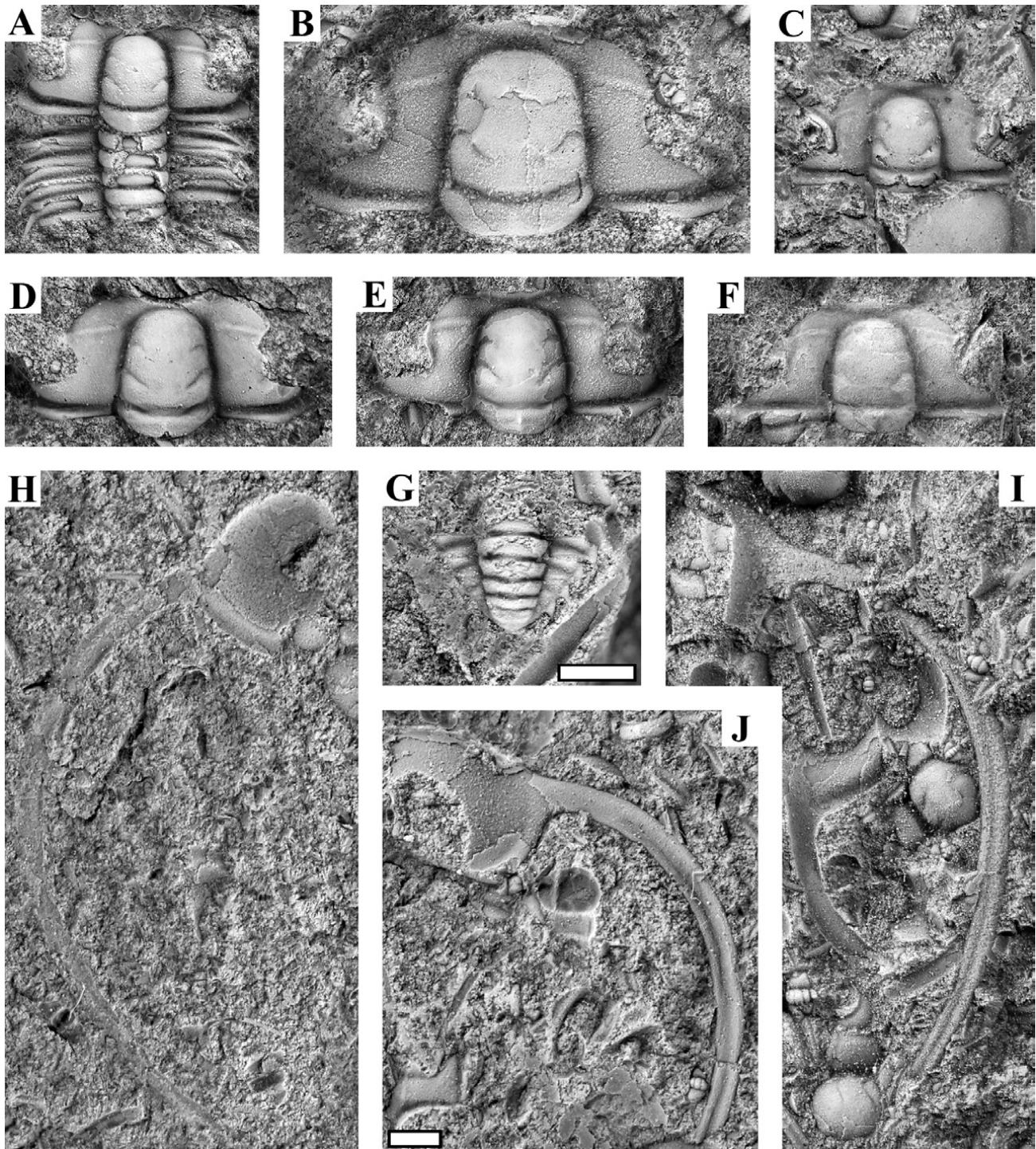

Fig. 13. *Leptoplastus crassicornis*, all preserved in anthraconite from locality 6. White scale bars: 1 mm; pygidium (G) is shown at greater magnification. **A:** Cranidium with four thoracic segments, sample ATN-110 (MGUH 33619). **B:** Large cranidium, sample ATN-216 (MGUH 33638). **C:** Small cranidium, sample GM 1888-289D (MGUH 33639). **D:** Cranidium illustrated as *Eurycare angustatum* by C. Poulsen (1923, pl. I, fig. 9) (MGUH 1962). **E:** Cranidium, sample ATN-278 (MGUH 33634). **F:** Cranidium, sample ATN-110 (MGUH 33620). **G:** Pygidium, sample ATN-278 (MGUH 33635). **H:** External mould of free cheek, sample ATN-220 (MGUH 33640). **I:** Free cheek, sample ATN-178 (MGUH 33641). **J:** Free cheek, sample ATN-252 (MGUH 33625).

Leptoplastus stenotus Angelin, 1854
Fig. 15

1904   *Leptoplastus stenotus* Ang. – Persson, pp. 522–523, pl. 9, figs 14–16.

1922   *Leptoplastus stenotus* Angelin – Westergård, pp. 146–147, pl. IX, figs 1–6.

v 1923   *Leptoplastus stenotus* Angelin [*partim*] – C. Poulsen, pp. 36–37, textfigs 13–14, 21. [The material also contains *L. abnormis*, *L. angustatus*, *L. crassicornis* and *L. ovatus*, see remarks].

1957   *Leptoplastus stenotus* Angelin 1854 – Henningsmoen, pp. 177–178, pl. 2, fig. 16; pl. 4.
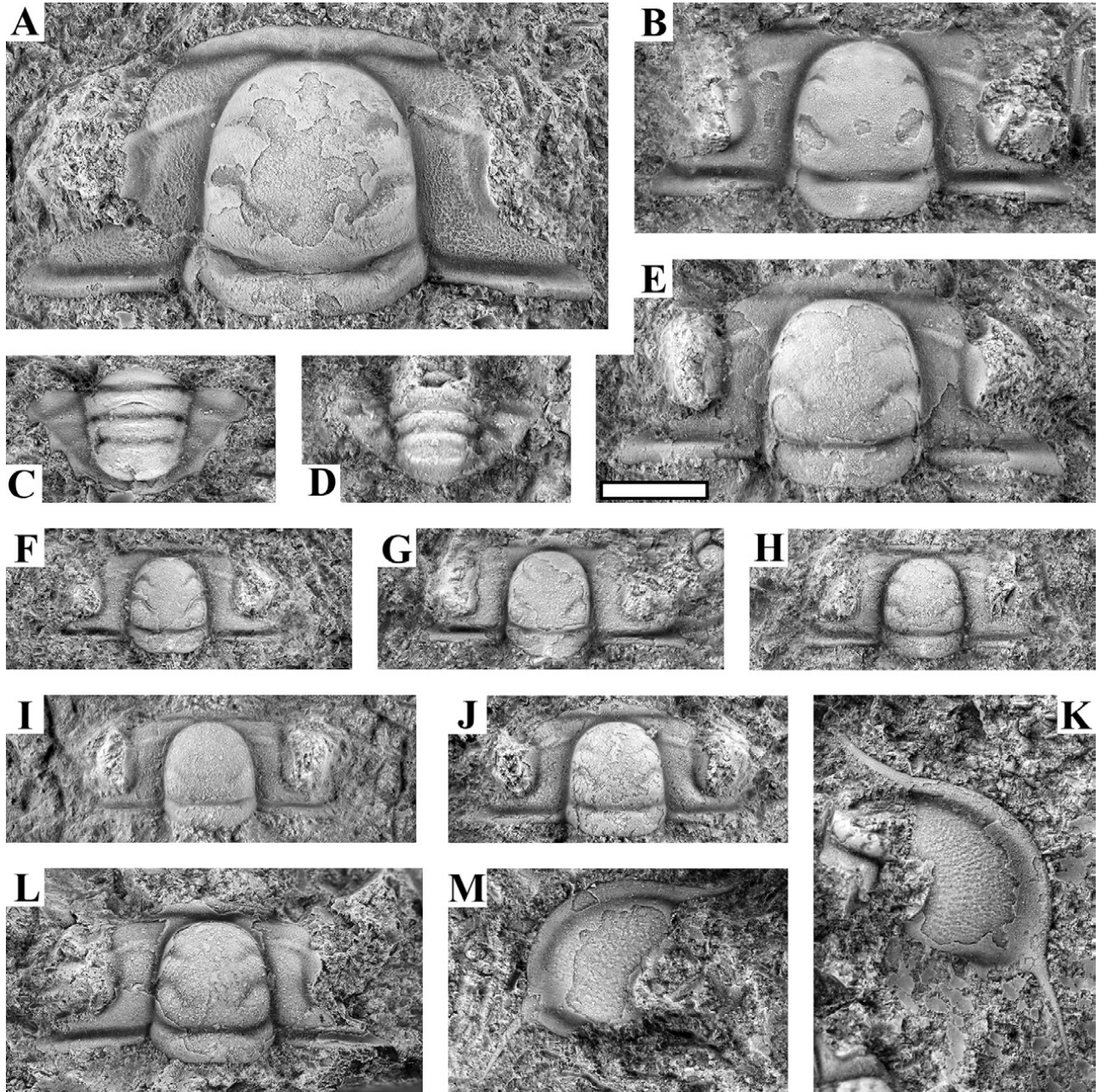
Fig. 14. *Leptoplastus ovatus*, all preserved in anthraconite from locality 6. Regarding assignment of disarticulated sclerites, see text. Free cheecks and pygidia (O–S) may alternatively belong to *L. abnormis*. White scale bar: 2 mm. **A:** Large cranidium, sample ATN-270 (MGUH 33642). **B:** Cranidium, sample ATN-276 (MGUH 33600). **C:** Pygidium, sample ATN-110 (MGUH 33621). **D:** Pygidium, sample ATN-119 (MGUH 33602). **E:** Cranidium, sample ATN-263 (MGUH 33643). **F:** Cranidium, sample ATN-306 (MGUH 33645). **G:** Cranidium, sample L126 (MGUH 33604). **H:** Cranidium, sample ATN-108 (MGUH 33649). **I:** Cranidium, sample ATN-288 (MGUH 33596). **J:** Cranidium, sample ATN-331 (MGUH 33591). **K:** Free cheek, sample ATN-263 (MGUH 33644). **L:** Cranidium, sample ATN-251 (MGUH 33650). **M:** Free cheek, sample ATN-156 (MGUH 33652).

1973 *Leptoplastus stenotus* Angelin, 1854 – Schrank, pp. 819, pl. V, fig. 5–11.
2015 *Leptoplastus stenotus* (Angelin, 1854) – Rasmussen *et al.*, p. 16, fig. 12.
For further synonymy, see Rasmussen *et al.* (2015).

Neotype. Designated here, complete specimen LO 3073, from Andrarum, southern Sweden, illustrated by Westergård (1922, pl. IX, fig. 4).

Material. 142 cranidia, 12 free cheeks and 5 pygidia. Six specimens are from locality 22 and the remaining material is from locality 6. *Leptoplastus stenotus* occurs alone.

Occurrence. Index fossil for the eponymous zone in Scandinavia (Henningsmoen 1957; Terfelt *et al.* 2008; Rasmussen *et al.* 2015; Nielsen *et al.* 2020).

Comparison. The cranidium of *L. stenotus* is distinguished from the cranidia of *L. angustatus* and *L. crassicornis* by its preglabellar field. The free cheek differs from that of *L. ovatus* by having a longer genal spine, which, however, often is broken.

Remarks. Two museum samples, both numbered GM 1922-139E, are labelled as *L. stenotus* but contain several cranidia, free cheeks, and two pygidia here identified as *L. abnormis*, *L. ovatus*, *L. crassicornis* and *L. angustatus*. The samples also contain an *E. bornholmensis* cranidium and some *L. abnormis* thoracic segments, but no *L. stenotus*.

Genus *Eurycare* Angelin, 1854
Type species: *Eurycare brevicauda* Angelin, 1854, designated by Vogdes (1925).

Eurycare bornholmensis (Poulsen, 1923)
Figs 16–18

v 1923 *Ctenopyge neglecta*, Westergård var. *bornholmensis* n. var. – C. Poulsen, pp. 37–38, pl. I, fig. 11.
1957 *Leptoplastus bornholmensis* (Poulsen, 1923) – Henningsmoen, p. 165.
1973 *Leptoplastus bornholmensis* (Poulsen, 1923) – Schrank, pp. 817–818, pl. IV, figs 10–12.
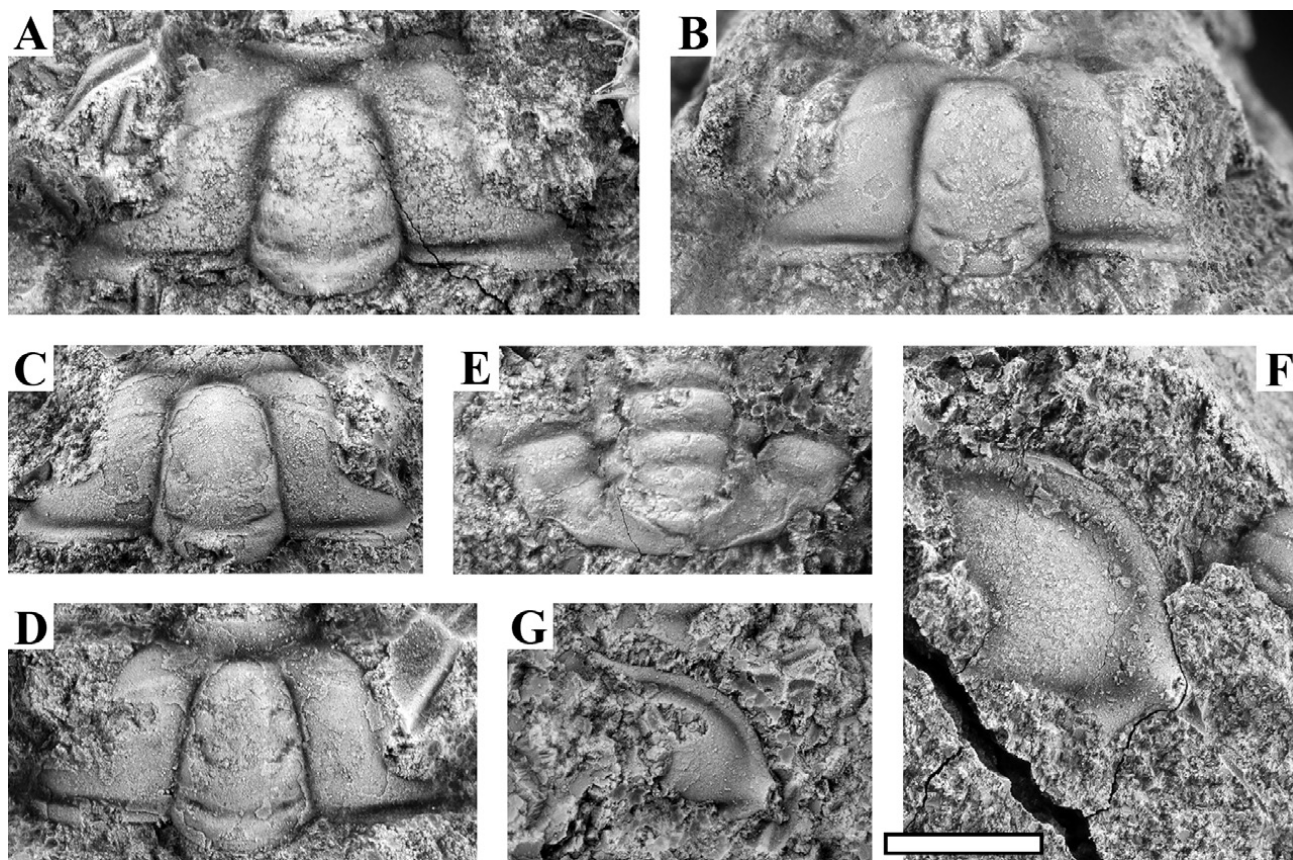
Fig. 15. *Leptoplastus stenotus*, all preserved in anthraconite. White scale bar: 2 mm. **A:** Cranidium, sample L125, loc. 6 (MGUH 33655). **B:** Cranidium, sample ATN-266, loc. 6 (MGUH 33657). **C:** Cranidium, sample ATN-266, loc. 6 (MGUH 33658). **D:** Cranidium, sample L125, loc. 6 (MGUH 33656). **E:** Pygidium, sample GM 1922-152, loc. 22 (MGUH 33659). **F:** Free cheek, sample GM 1922-152, loc. 22 (MGUH 33660). **G:** Free cheek, sample GM 1922-152, loc. 22 (MGUH 33661).

v 2015 *Leptoplastus bornholmensis* (Poulsen, 1923) – Rasmussen *et al.,* pp. 11–12, fig. 8.

Lectotype. External mould of cranidium MGUH 1964, originally illustrated by C. Poulsen (1923, pl. 1 fig. 11) and designated by Henningsmoen (1957). The lectotype was re-illustrated by Rasmussen *et al.* (2015, fig. 8).

Diagnosis (emended Henningsmoen 1957): Glabella elongate, parallel-sided and moderately vaulted. Well-developed preglabellar field. Very slightly oblique eye ridges, almost transverse. Midpoint of palpebral lobes opposite L2. Interocular cheeks from ¾ to as wide as glabella at eye-line and postocular cheeks from 1.6 to 1.8 times as wide as the occipital ring. Thorax with 16 thoracic segments having short pleural spines. Pygidium triangular, with four axial rings and at least three pairs of marginal spines.

Material. Two semi-complete specimens, 123 cranidia (including one with 13 and one with 14 contiguous thoracic segments), eight free cheeks, one hypostome (tentatively assigned) and seven pygidia. All material derives from locality 6. *Eurycare bornholmensis* co-occurs with *L. abnormis, L. angustatus, L. crassicornis, L. ovatus* and *P. leptoplastorum?*.

Occurrence. Known only from the *L. crassicornis–L. angustatus* Zone on Bornholm (C. Poulsen 1923; this study), but see comparison with *E. explanatum* below.

Description: Cranidium 2 ½ times as wide as long, trapezoidal in overall outline. Glabella about 1.2 times as long as wide, parallel-sided, moderately vaulted, with up to three pairs of lateral glabellar furrows directed obliquely backwards-inwards (Figs 17D, G, I), but usually only two pairs are visible. Well-developed preglabellar field; anterior border form a swollen ridge along the anterior margin, being widest mesially. Mesial arc visible in frontal view. Eye ridges very slightly oblique, almost transverse. Midpoint of palpebral lobes situated opposite L2. Palpebral lobes slightly less than 1/3 as long (exsag.) as glabella (incl. occipital ring). Interocular cheeks from ¾ to as wide as glabella at eye-line (tr.). Postocular facial suture divergent sinuous. Postocular cheeks 1.6 to 1.8 times as wide as occipital ring; gently curving border furrow present, most deeply impressed centrally. Distinct occipital furrow. Elongate mesial tubercle on occipital ring seen in well preserved specimens (Fig. 17B). Fragmentary hypostome (tentatively assigned) oval in outline with entire posterior margin and strongly swollen median body overhanging posterior margin (median body lost during preparation; specimen not suited for illustration). Free cheek with rounded lateral margin showing flattened, moderately

narrow border; posterior margin short. Stout genal spine situated far back, curving gently backwards and inwards (Fig. 16). The genal spine reminds of the one in *L. angustatus* but it is more sturdy, oval in cross-section and the spine base is broader and raised a little (Figs 16, 17E–F). Thorax with 16 segments, each provided with short pleural spines. The anterior 5 segments increase gently in width, the following segments taper rearwards. Pleural regions twice as wide as axis where the thorax is widest (excluding the short pleural spines). Pygidium triangular in outline and almost twice as wide as long. Axis consists of four rings in addition to anterior half ring and terminal piece; it occupies 0.3 or a little more of the total pygidial width at the anterior margin. At least three pairs of marginal spines (broken in all specimens).

Comparison. The cranidium of *E. bornholmensis* somewhat resembles the cranidium of *E. brevicauda* but has a more distinct preglabellar field and significantly wider (tr.) postocular cheeks. The pygidium of *E. bornholmensis* is more distinctly triangular in shape compared to the sub-semicircular and relatively broader pygidium in *E. brevicauda*. *Eurycare bornholmensis* differs from *L. neglectus* and *L. norvegicus* by having wider interocular and postocular cheeks and 16 thoracic segments. The long, curved genal spine of *E. bornholmensis* reminds of that in *L. angustatus*, but the free cheek of the latter has a much longer posterior margin and the spine and spine base are less sturdy.
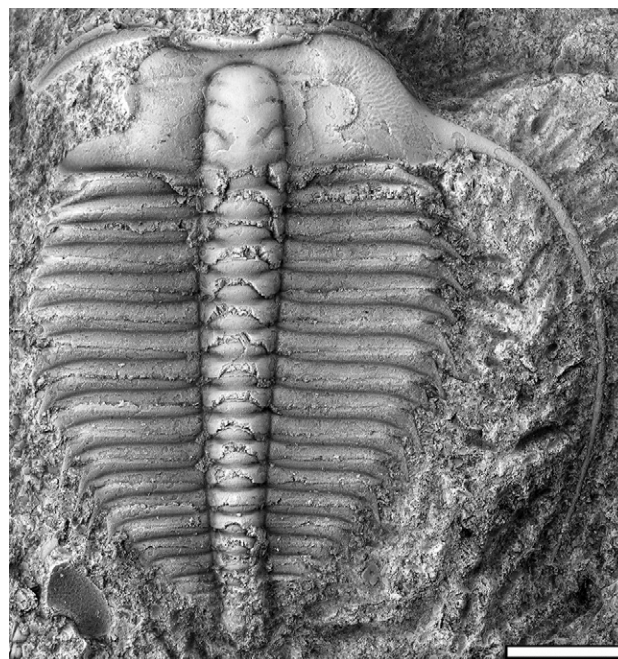

Fig. 16. *Eurycare bornholmensis*, almost complete specimen preserved in anthraconite from locality 6, sample ATN-329 (MGUH 33662). White scale bar: 3 mm. See also Fig. 17F.
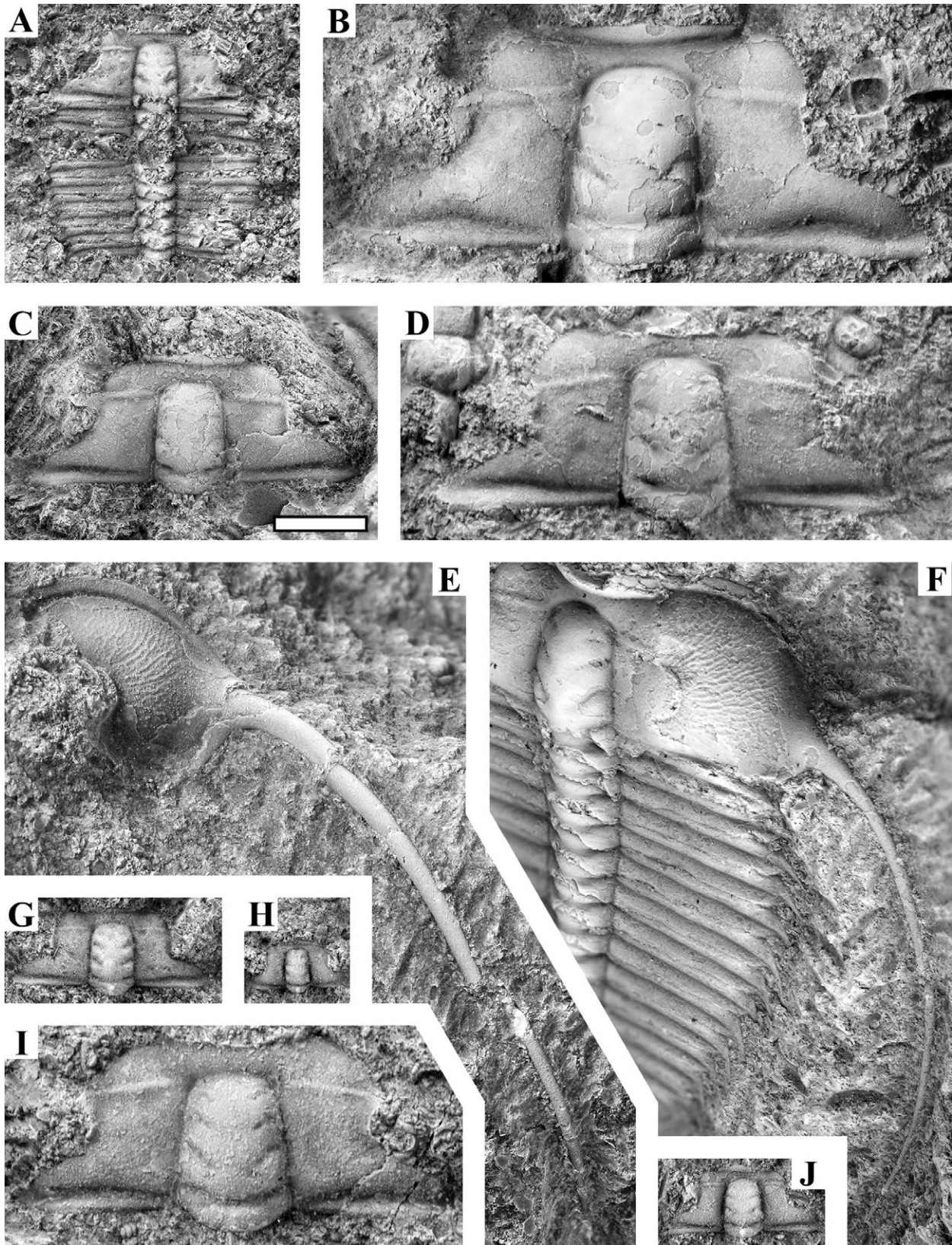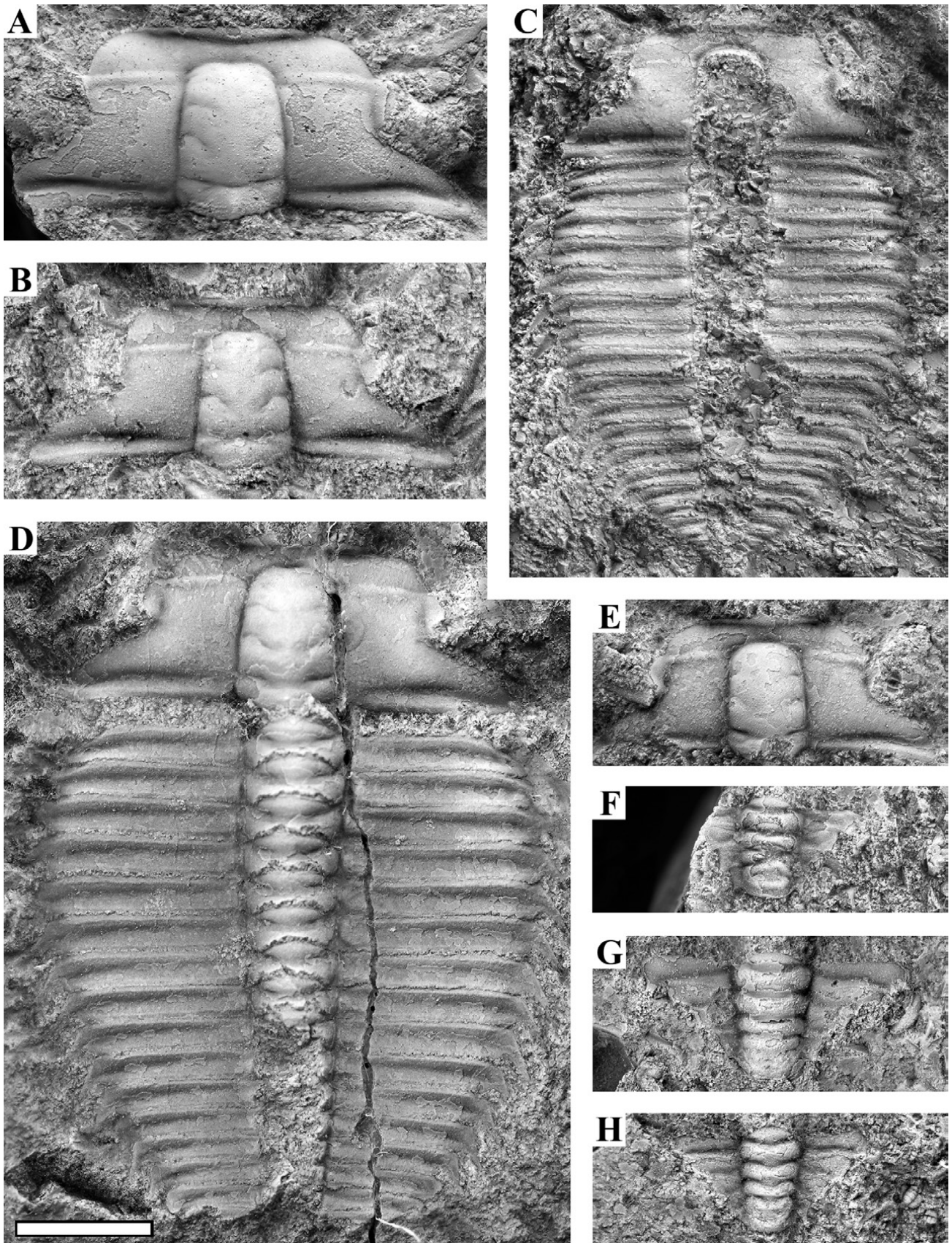
Fig. 17. *Eurycare bornholmensis*, all preserved in anthraconite from locality 6. White scale bar: 2 mm. **A:** Cranidium with eight thoracic segments, sample ATN-136 (MGUH 33663). **B:** Cranidium, sample L126 (MGUH 33605). **C:** Cranidium, sample L126 (MGUH 33606). **D:** Cranidium, sample ATN-157 (MGUH 33665). **E:** Free cheek, sample ATN-251 (MGUH 33651). **F:** Free cheek, sideview, sample ATN-329 (MGUH 33662), the complete specimen is shown in Fig. 16. **G:** Small cranidium, sample ATN-154 (MGUH 33666). **H:** Juvenile cranidium, sample ATN-156 (MGUH 33653). **I:** Cranidium, sample ATN-156 (MGUH 33654). **J:** Small cranidium, sample ATN-306 (MGUH 33646).

Fig. 18. *Eurycare bornholmensis*, all preserved in anthraconite from locality 6. White scale bar: 2 mm. **A:** Cranidium, sample ATN-306 (MGUH 33647). **B:** Cranidium, sample ATN-248 (MGUH 33667). **C:** Almost complete specimen, sample ATN-136 (MGUH 33664). **D:** Almost complete specimen, sample ATN-120 (MGUH 33668). **E:** Cranidium, sample ATN-262 (MGUH 33598). **F:** Pygidium, sample ATN-306 (MGUH 33648). **G:** Pygidium, sample ATN-123 (MGUH 33554). **H:** Pygidium, sample ATN-304 (MGUH 33581).

The cranidium of *Eurycare intermedium* (regarding generic assignment, see Ahlberg *et al.* 2006) is quite similar to that of *E. bornholmensis*, but the glabella appears slightly wider and the postocular cheeks are narrower (tr.). In *E. intermedium,* the postocular cheek is thus *c.* 1.4 times as wide as the occipital ring (see Westergård 1944 and Ahlberg *et al.* 2006, fig. 6D) vs. 1.6 – 1.8 times as wide as the occipital ring in *E. bornholmensis*. The outline of the genal spine base also differs, being much broader in *E. bornholmensis,* and *E. intermedium* has >9, probably 12, thoracic segments (Westergård 1944), whereas *E. bornholmensis* has 16 thoracic segments.

The cranidium of *E. explanatum* is almost indistinguishable from that of *E. bornholmensis* but again appears to have slightly narrower (tr.) postocular cheeks (however, up to 1.63 times as wide as the occipital ring, see Henningsmoen 1957, pl. 16, fig. 5); they also seem to be marginally longer (exsag.), reflecting that the eyes are located slightly more forwards in the Norwegian form (centre of palpebral lobes opposite S2 vs. L2 in *E. bornholmensis*). Nonetheless, the differences are subtle and maybe these taxa should be separated only as subspecies. The number of thoracic segments in *E. explanatum* is unknown. The pygidium of a suspected *E. explanatum* illustrated by Henningsmoen (1957, pl. 16, fig. 4) has wider pleural fields than the pygidia of *E. bornholmensis* (Fig. 18F–H).

Remarks. C. Poulsen (1923) erected this species as a variant of '*C.*' *neglecta* and described it as fairly common in the upper part of the '*Eurycare angustatum* Subzone'. It was transferred to *Leptoplastus* by Henningsmoen (1957). A large material is at hand, including a few almost complete specimens with 16 thoracic segments, suggesting a closer affinity with *Eurycare* as representatives of *Leptoplastus* have only up to 12 thoracic segments (Henningsmoen 1957). The many new cranidia also demonstrate that *E. bornholmensis* has wider postocular cheeks than most representatives of *Leptoplastus*, whereas the width of the interocular cheeks is intermediate between the two genera. The genal spine is stout like in other species of *Eurycare*. The presence of a well-developed preglabellar field is a trait shared with some species of *Leptoplastus*.

Eurycare brevicauda **Angelin, 1854**
Fig. 19A
1922   *Eurycare brevicauda* Angelin – Westergård, pp. 148–149, pl. IX, figs 11–12.
1957   *Eurycare brevicauda* Angelin 1854 – Henningsmoen, p. 179, pl. 2, fig. 19; pl. 4.
2006   *Eurycare brevicauda* Angelin – Ahlberg *et al.*, fig. 5.
2015   *Eurycare brevicauda* Angelin 1854 – Rasmussen *et al.*, p. 9, fig. 6G.

2017   *Eurycare brevicauda* Angelin 1854 – Rasmussen *et al.*, p. 12, fig. 7A.

Lectotype. Not designated, but see remarks by Westergård (1922, p. 149) and Henningsmoen (1957).

Material. One small cranidium from locality 6. It is associated with common *E. latum*.

Occurrence. Known only from the *L. crassicornis–L. angustatus* Zone in Scandinavia (Henningsmoen 1957; Rasmussen *et al.* 2015). This is the first report from Bornholm.

Comparison. For comparison with *E. latum*, see that species. *Eurycare brevicauda* and *E. spinigerum* have identical cranidia and almost identical pygidia and are separated primarily by having different numbers of thoracic segments (14 in *E. brevicauda* vs. 12–13 segments in *E. spinigerum*). For this reason, the assignment of the single detached cranidium from Bornholm may be taken as tentative.

Eurycare latum **(Boeck, 1838)**
Fig. 19B–J
1904   *Eurycare latum* Boeck – Persson, pp. 513–517, pl. 8, figs 1–7.
1922   *Eurycare latum* (Boeck) – Westergård, p. 148, pl. IX, figs 7–10.
v 1923   *Eurycare latum* Boeck – C. Poulsen, pp. 32–33, pl. I, fig. 8.
1957   *Eurycare latum* (Boeck 1838) – Henningsmoen, pp. 181–182, pl. 4; pl. 16, figs 6–9.
1973   *Eurycare latum* (Boeck, 1838) – Schrank, pp. 819–820, pl. IV, figs 1–5.
2004   *Eurycare latum* (Boeck 1838) – Mischnik, pp. 110–111, pl. 2, fig. 8.
2017   *Eurycare latum* (Boeck, 1838) – Rasmussen *et al.*, p. 12, fig. 7B.
For further synonymy, see Rasmussen *et al.* (2017).

Lectotype. Small cranidium PMO 56383a from Gamlebyen, Oslo, Norway; designated and illustrated by Henningsmoen (1957, pl. 16, fig. 9).

Material. 156 cranidia including one with six contiguous thoracic segments, 23 free cheeks and 18 pygidia; all from locality 6. The species mostly occurs alone (in profusion), but in a few samples it is associated with rare specimens of *E. brevicauda*, *L. crassicornis* and *L. ovatus*.

Occurrence. Common in the *L. crassicornis–L. angustatus* Zone in Norway and Sweden (Westergård 1947; Ahlberg *et al.* 2006; Rasmussen *et al.* 2015, 2016, 2017),
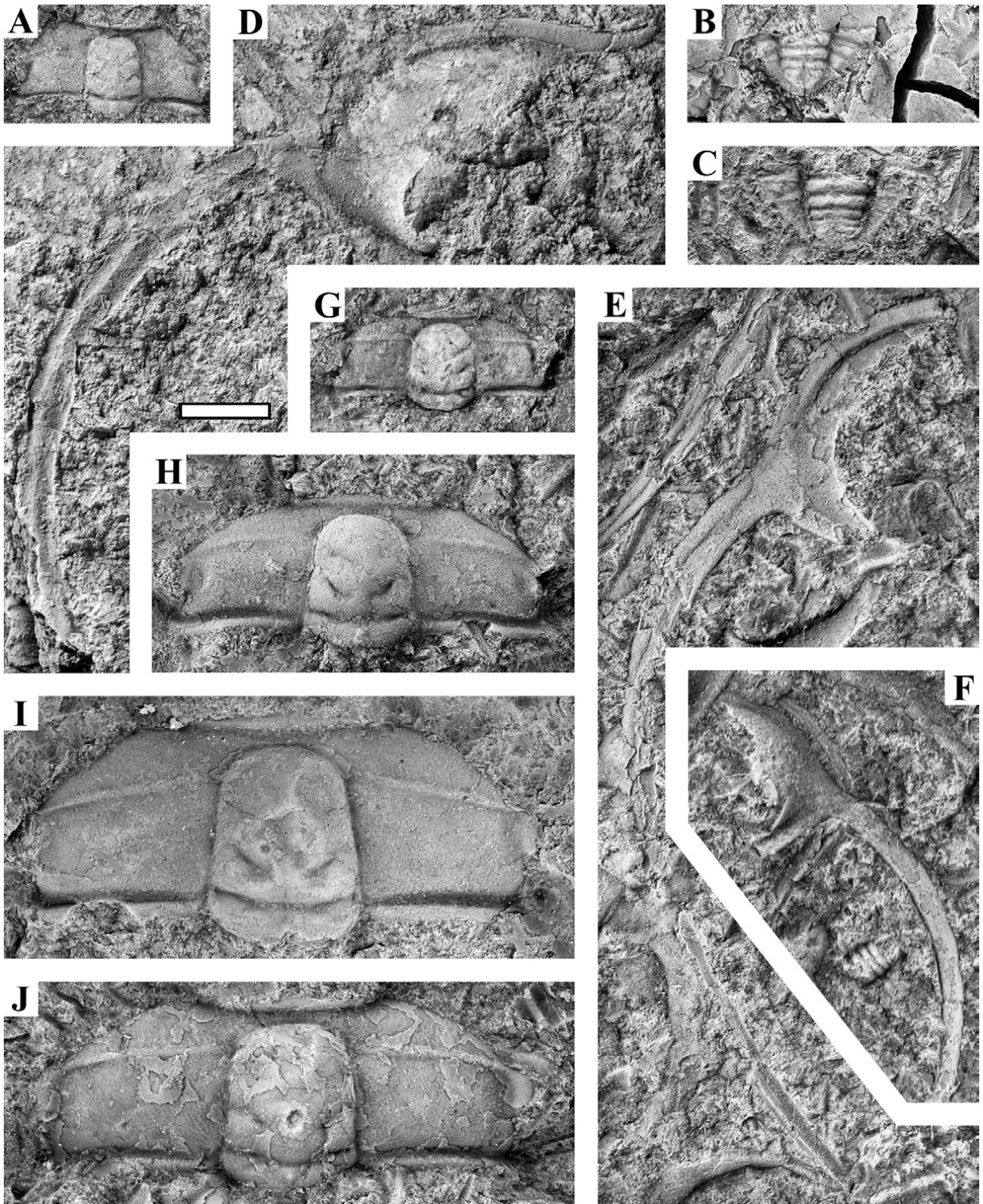
Fig. 19. *Eurycare brevicauda* (**A**) and *Eurycare latum* (**B–I**), all preserved in anthraconite from locality 6. White scale bar: 3 mm; please note that these specimens are shown at a lower magnification than used for most of the illustrations. **A:** Small cranidium, sample ATN-282 (MGUH 33669). **B:** Pygidium, sample GM 1922-138B (MGUH 33670). **C:** Pygidium, sample ATN-114 (MGUH 33671). **D:** Free cheek, sample ATN-272 (MGUH 33373). **E:** Free cheek, sample ATN-114 (MGUH 33672). **F:** Free cheek, sample ATN-159 (MGUH 33675). **G:** Cranidium, sample ATN-280 (MGUH 33677). **H:** Cranidium, sample ATN-272 (MGUH 33674). **I:** Cranidium, sample ATN-279 (MGUH 33678). **J:** Cranidium, sample ATN-159 (MGUH 33676).

and also mentioned from England (Taylor & Rushton 1971). Rasmussen *et al.* (2015) recorded it also from the *L. raphidophorus* and *L. neglectus* zones at Slemmestad, Norway. On Bornholm, *E. latum* occurs only in the basal part of the *Leptoplastus* Superzone, distinguished as the *E. latum* Subzone by C. Poulsen (1923). The co-occurrence with rare *L. crassicornis* and *L. ovatus* is suggestive of the *L. crassicornis–L. angustatus* Zone. At locality 6, *E. latum* is very common in a lower horizon, *c.* 5 cm thick, separated by coarse-grained unfossiliferous anthraconite, also *c.* 5 cm thick, from an overlying fine-grained limestone containing a more diverse *L. crassicornis–L. angustatus* Zone fauna without *E. latum*.

Comparison. Eurycare latum is readily distinguished by its unusually wide fixed cheeks. However, the cranidium can resemble that of *E. brevicauda* and *E. spinigerum*, but the interocular cheeks of those species are only as wide as glabella at eye-line, while *E. latum* has interocular cheeks that are 1 ⅕ to 1 ⅖ times as wide as the adjacent glabella. The free cheek of *E. latum* resembles that of *L. crassicornis;* for comparison, see the latter species.

Genus *Ctenopyge* Linnarsson, 1880
Type species: *Olenus (Sphaerophthalmus) pecten* Salter, 1864, designated by Vogdes (1890).

Subgenus *Ctenopyge* (*Ctenopyge*) Linnarsson, 1880
Type species: As for genus.

***Ctenopyge (Ctenopyge) affinis* Westergård, 1922**
Fig. 20
1922   *Ctenopyge affinis* n. sp. [*partim*] – Westergård, pp. 157–158, pl. XII, figs 1–6, 14; non pl. XII, figs 7–13 [= *Ctenopyge gracilis*]; non pl. XII, fig. 15 [= *C. pecten*?].
v non 1923 *Ctenopyge affinis* Westergård – C. Poulsen, pp. 41–42, pl. 2, fig. 5 [= *C. magna* n. sp.].
1957   *Ctenopyge affinis affinis* Westergård 1922 – Henningsmoen, pp. 200–201, pl. 5; pl. 19, fig. 22.

Lectotype. Cranidium SGU 327 from Andrarum, southern Sweden, figured by Westergård (1922, pl. XII, fig. 1) and designated by C. Poulsen (1923).

Material. 222 cranidia and 15 free cheeks. The far majority of the material is from locality 6, but a few specimens derive from locality 7. *Ctenopyge affinis* co-occurs with *C. magna* n. sp., *C. ahlbergi, Ctenopyge* sp. 1, *P. minor* and *S. alatus.*

Occurrence. Upper part of the *Peltura acutidens–Ctenopyge tumida* Zone, Scandinavia (Henningsmoen 1957;

Høyberget & Bruton 2012). The report from the lower part of the *Peltura scarabaeoides* Zone (Westergård 1947) probably refers to *C. gracilis*. On Bornholm, the species has been found only in the upper part of the *P. acutidens–C. tumida* Zone.

The *C. affinis* Zone *sensu* Terfelt *et al.* (2008) was amalgamated with the *C. tumida* Zone by Høyberget & Bruton (2012) since *C. affinis* is rare in most regions of Scandinavia and, hence, not suitable as an index fossil. This approach is followed here, but on Bornholm a subzone characterized by *C. affinis, C. ahlbergi* and *C. magna* n. sp. actually seems to be developed in the upper part of the *P. acutidens–C. tumida* Zone (see section on 'Olenid zonation').

Comparison. Ctenopyge affinis is separated from *C. gracilis* by having a broader, tapering glabella, most distinctly so in larger specimens, with a less inflated anteroglabella. *Ctenopyge affinis* also reaches larger maximum sizes. The free cheek of *C. affinis* has a less curving spine that follows the general course of the cheek margin and the posterior cheek margin is very short in comparison with the free cheeks of *C. gracilis*.

For comparison with *C. magna* n. sp., see that species. The cranidium of the co-occurring *C. ahlbergi* has a much more inflated anteroglabella, the front of the cranidium is therefore significantly higher and the rear part of glabella also shows a characteristic distinct constriction in front of the occipital furrow and deep lateral pits accentuate the occipital furrow, so well-preserved specimens are readily separated from *C. affinis*.

Ctenopyge oelandica is based on a single juvenile cranidium from the *P. acutidens–C. tumida* Zone at Degerhamn, Öland (Westergård 1922). The tiny cranidium is characterized by a parallel-sided glabella and unusually strongly curving eye ridges, reflecting that the eyes are situated far back. Buchholz (2000) illustrated a larger cranidium from erratics in Germany, also assigned to *C. oelandica*. The latter cranidium overall looks like the holotype, but it is relatively slightly less wide (ontogenetic change?), and therefore the eye ridges are shorter. The German cranidium resembles several of the smaller to medium-sized cranidia here assigned to *C. affinis* (e.g. Fig. 20Ø), but in all specimens from Bornholm the eyes are situated more anteriorly and thus the eye ridges curve less strongly rearwards. However, this feature exhibits some variation (e.g. Fig. 20Q vs. Y). Additional material of *C. oelandica* is needed to constrain its variation range.

Without complete specimens at hand it is impossible to discuss *C. rushtoni*, described by Clarkson *et al.* (2004).

Remarks. Henningsmoen (1957) recognized two sub-

species of *C. affinis*, viz. *C. a. affinis* (larger and with a distinctly tapering glabella) and *C. a. gracilis* (smaller and with an almost parallel-sided glabella). *Ctenopyge gracilis* was treated at species level by Clarkson *et al.* (2004) and we also prefer to rank *C. gracilis* and *C. affinis* as separate species.

The sparse material identified as *C. affinis* by C. Poulsen (1923) is here assigned to *C. magna* n. sp. and a smaller form, which is much more common on Bornholm, is identified as *C. affinis*. Strangely, this common species was not treated by C. Poulsen (1923) (15 cranidia of *affinis s.str.* are registered in the 1902-samples containing "*C. affinis*" discussed by C. Poulsen, see Appendix 1). *Ctenopyge affinis* shows ontogenetic changes and juvenile cranidia are rather *C. gracilis*-like having a parallel-sided, slender glabella. However, the anteroglabella is less inflated than in equal-sized *C. gracilis* cranidia, although we note that the anteroglabella exhibits considerable variation in shape and degree of inflation in *C. affinis* (e.g. Fig. 20A, F, I; juvenile condition illustrated in Fig. 20L–O, Ø). Larger cranidia have a clearly tapering glabella, which is the salient distinguishing character of *C. affinis* in comparison with *C. gracilis*. It appears also to be a consistent character of *C. affinis* cranidia to have a weakly impressed pair of S3 indentations situated close to the axial furrows, visible in dorsal view; this feature is not so distinctive in *C. gracilis*, maybe due to the stronger inflation of the anteroglabella, concealing the S3 in dorsal view.

The Scanian holotype of *C. affinis* has a comparatively little inflated antero-glabella (Westergård 1922, pl. XII, fig. 1), whereas the second Scanian specimen illustrated by Westergård (ibid. pl. XII, fig. 2) is very similar to most of the similar-sized cranidia from Bornholm. The free cheeks in the material at hand also comply with the description of *affinis* cheeks provided by Westergård (1922).

Ctenopyge (Ctenopyge) ahlbergi Clarkson, Ahlgren & Taylor, 2004

Fig. 21

? 2003 *Ctenopyge* cf. *affinis* – Terfelt, fig. 4L–N.
2004 *Ctenopyge (Ctenopyge) ahlbergi* n. sp. – Clarkson *et al.*, pp. 125–127, textfigs 11; 12A, B, E, F; 13–14.

Holotype. Complete juvenile specimen LO 8976T from Blomberg, Kinnekulle, Västergötland, illustrated by Clarkson *et al.* (2004, textfig. 11A).

Material. 38 cranidia incl. two external moulds, and seven free cheeks. Most of the specimens are from locality 6, but a few derive from locality 7. Several disarticulated thoracic segments probably also belong to this species. *Ctenopyge ahlbergi* co-occurs with *C. affinis*, *C. magna* n. sp., *Ctenopyge* sp. 1, *S. alatus* and *P. minor*.

Occurrence. Known only from the *P. acutidens*–*C. tumida* Zone in Västergötland and on Bornholm (Clarkson *et al.*, 2004, this study). The cranidia from Västergötland identified as *C. cf. affinis* by Terfelt (2003) resemble *C. ahlbergi* but may alternatively represent *C. gracilis*.

Comparison. The cranidium is very distinctive and cannot be confused with any of the associated species. The deep lateral impressions in the occipital furrow, the outline of the deep S1 and the distinctly inflated anteroglabella creating a high front of the cranidium are distinctive traits. The closest relative may be *C. gracilis* that also has a rather inflated anteroglabella, but this species has only a shallow or no indentation of the rear part of glabella. The pleural spines on the thoracic segments also have a different outline in these species, being flattened in *C. ahlbergi* (for details, see Clarkson *et al.* 2004).

Remarks. This is the first report of this species outside Västergötland; regarding identification, see especially

▼ **Fig. 20.** *Ctenopyge affinis*, all preserved in anthraconite from locality 6; the free cheeks may alternatively belong to *C. magna* n. sp. In order to save space the cheeks are rotated clockwise relative to life position. Note the non-tapering glabella in juveniles and smaller cranidia. White scale bar: 2 mm. **A–C:** Large cranidium, dorsal, frontal and side views, sample ATN-117 (MGUH 33679). **D:** Cranidium, sample ATN-117 (MGUH 33680). **E:** Cranidium, sample ATN-130 (MGUH 33688). **F–G:** Large cranidium, dorsal and side view, sample ATN-134 (MGUH 33690). **H–J:** Cranidium with unusually inflated anteroglabella, dorsal, frontal and side views, sample ATN-130 (MGUH 33689). **K:** Large cranidium, sample ATN-222 (MGUH 33703). **L–N:** Small cranidium, dorsal, frontal and side views, sample ATN-116 (MGUH 33706). **O:** Small cranidium, sample ATN-117 (MGUH 33681). **P:** Large cranidium, sample ATN-113 (MGUH 33711). **Q:** Cranidium, sample ATN-103 (MGUH 33719). **R:** Cranidium, sample ATN-134 (MGUH 33691). **S:** Cranidium, sample ATN-147 (MGUH 33723). **T:** Cranidium, sample ATN-146 (MGUH 33725). **U:** Large cranidium, sample ATN-222 (MGUH 33704). **V:** Cranidium, sample ATN-113 (MGUH 33712). **W:** Large cranidium, sample ATN-113 (MGUH 33713). **X:** Large cranidium, ATN-146 (MGUH 33726). **Y:** Cranidium, sample ATN-117 (MGUH 33682). **Z:** Cranidium, sample ATN-113 (MGUH 33714). **Æ:** Cranidium, sample ATN-134 (MGUH 33692). **Ø:** Juvenile cranidium, note the occipital spine, sample ATN-134 (MGUH 33693). **1:** Free cheek, sample ATN-146 (MGUH 33727). **2:** Free cheek, sample ATN-103 (MGUH 33720). **3:** Free cheek, sample ATN-116 (MGUH 33707). **4:** Free cheek, sample ATN-132 (MGUH 33730).
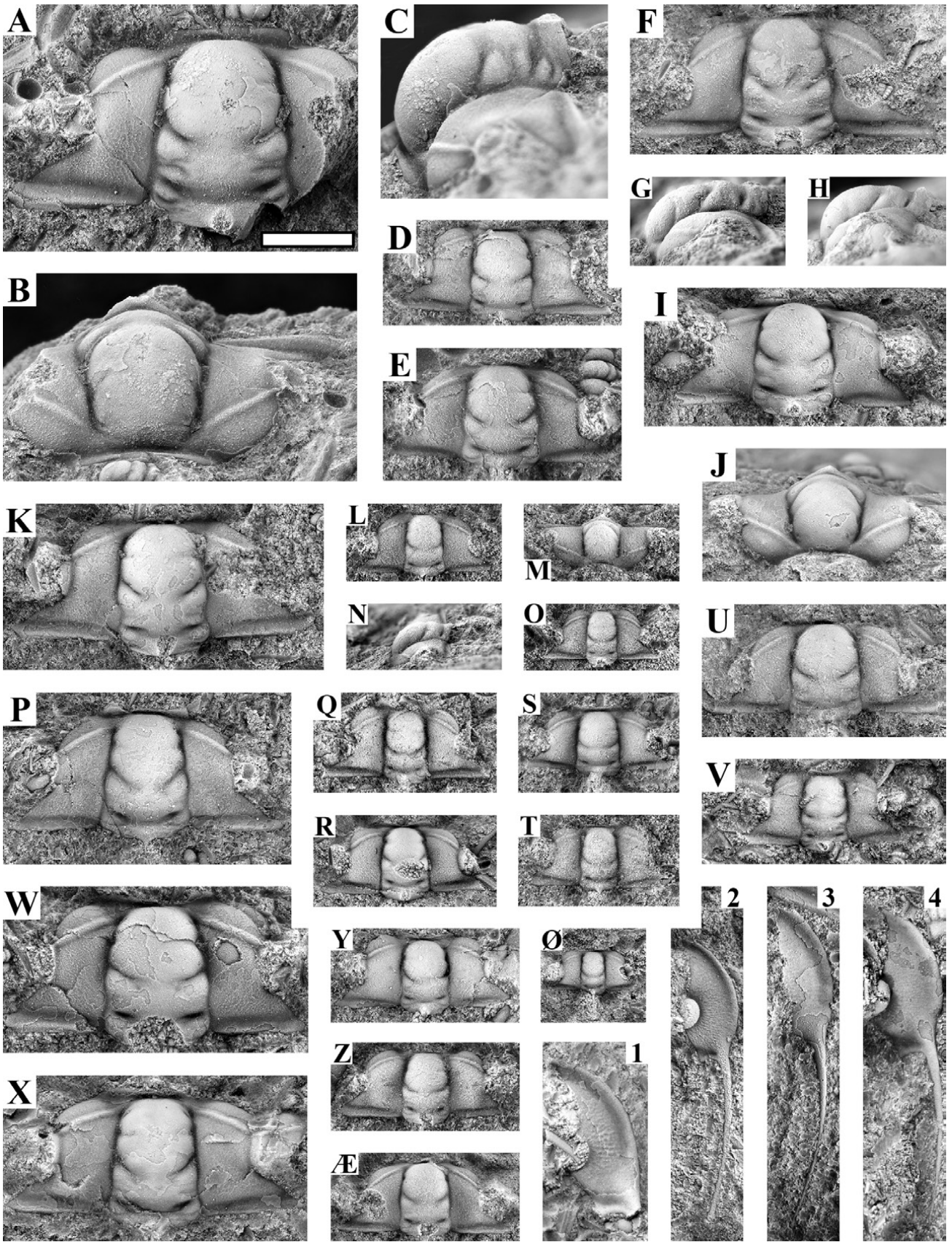
the largest Swedish specimen illustrated by Clarkson *et al.* (2004, fig. 11C–D), clearly showing the characteristic cranidium albeit in a slightly oblique view. The cranidia at hand are significantly larger than the material originally described from Västergötland.

Ctenopyge (Ctenopyge) bisulcata (Phillips, 1848)
Fig. 22A–B

1922	*Ctenopyge bisulcata* (Phillips) [*partim*] – Westergård, pp. 159–160, pl. XII, figs 19–20, 22–25, non fig. 21 [= *C. tumida*].
v 1923	*Ctenopyge bisulcata* Phillips – C. Poulsen, pp. 46–47, pl. 2, fig. 4.
1957	*Ctenopyge (Ctenopyge) bisulcata* (Phillips 1848) – Henningsmoen, pp. 203–204, pl. 5.
1973	*Ctenopyge (Ctenopyge) bisulcata* (Phillips, 1848) – Schrank, pp. 827–828, pl. VIII, fig. 9–16, 17?, 18; pl. IX, figs 1–2.
2016	*Ctenopyge (Ctenopyge) bisulcata* (Phillips 1848) – Rasmussen *et al*. pp. 10–11, fig. 5.

For a more comprehensive list of synonymy, see Rasmussen *et al.* (2016).

Lectotype. Original of Phillips (1848, fig. 1 on p. 55) from the White-Leaved Oak Shales (Merioneth Series) of the Malvern Hills, United Kingdom, was selected as 'holotype' by Stubblefield (1938). The whereabouts of the type specimen is currently unknown (Morris 1988).

Material. Six cranidia preserved in shale from locality 6 (no associated fauna) and locality 7 (co-occurring with common *C. fletcheri*).

Occurrence. Ctenopyge bisulcata was coined as index fossil for a lower subzone of the *P. scarabaeoides* Zone by Henningsmoen (1957), later elevated to zonal rank by Terfelt *et al.* (2008). This interval is assigned here to the *P. scarabaeoides* Zone following Nielsen *et al.* (2020). The sparse material of *C. bisulcata* from Bornholm derives from the "upper part of the *P. scarabaeoides* (Sub)Zone" according to C. Poulsen (1923). However, the species occurs near the base of the zone at locality 7 and the section exposed at locality 6 only represents the lower half of the *P. scarabaeoides* Zone (cf. Nielsen *et al.* 2018). Hence, *C. bisulcata* is characteristic of the lower part of the *P. scarabaeoides* Zone on Bornholm as elsewhere in Scandinavia. The species is known also from Great Britain and Canada (Nova Scotia) (Henningsmoen 1957).

Comparison. The cranidium resembles that of *C. fletcheri* but is wider. In *C. bisulcata,* the postocular cheeks are thus about 1.5 times as wide as the occipital ring vs. about as wide as the occipital ring in *C. fletcheri*. The cranidium of *C. linnarssoni* is also rather wide, but in *C. bisulcata* the eye ridges are oblique and not transverse

as in *C. linnarssoni.* Furthermore, in *C. bisulcata,* the postocular cheeks are divergent sinuous while they are divergent convex in *C. linnarssoni* (terminology according to Henningsmoen 1957, fig. 2).

Remarks. Peltura scarabaeoides appears earlier than *C. bisulcata* and correlation of the lower boundary of the now abandoned *C. bisulcata* Subzone with the base of the *P. scarabaeoides* Zone (Henningsmoen 1957) was an inaccurate approximation (for details, see Nielsen *et al.* 2020).

Ctenopyge (Ctenopyge) fletcheri (Matthew, 1901)
Fig. 22C–G

1922	*Ctenopyge directa* Lake [*partim*] – Westergård, pp. 158–159, pl. 12, fig. 17.
v 1923	*Ctenopyge directa* Lake – C. Poulsen, pp. 45–46, pl. III.
1957	*Ctenopyge (Ctenopyge) fletcheri* (Matthew 1901) – Henningsmoen, pp. 205–207, pl. 5; pl. 22, figs 1–6.
1973	*Ctenopyge (Ctenopyge) fletcheri* (Matthew, 1901) – Schrank, p. 833, pl. X, figs 16–20.
2017	*Ctenopyge (Ctenopyge) fletcheri* (Matthew, 1901) – Rasmussen *et al.,* pp. 10–11, figs 6A–B.

For further synonymy, see Rasmussen *et al.* (2017).

Lectotype. Free cheek figured by Matthew (1901, pl. IV, fig. 7d and 1903, pl. XVII, fig. 7d) from Band C3b, Escasonie Shore, East Bay, Nova Scotia, designated by Henningsmoen (1957).

Material. 41 cranidia and 15 free cheeks from localities 6 and 7. The species is associated with cranidia of *Peltura* sp. (probably *P. scarabaeoides*), *C. bisulcata* and *T. humilis*.

Occurrence. Peltura scarabaeoides Zone in Scandinavia, Great Britain, Poland and Canada (Henningsmoen 1957; Żylińska 2001, 2002). *Ctenopyge fletcheri* – under the name *C. directa* – was recorded from the *C. tumida* and *P. scarabaeoides* subzones at localities 6 and 7 by C. Poulsen (1923). However, the report from the *P. acutidens–C. tumida* Zone seems to be an error; no museum material derives from that level.

Comparison. See *C. linnarssoni* and *C. bisulcata*.

Remarks. The discussed material was assigned to *C. directa* by C. Poulsen (1923). However, that species has interocular cheeks that are as wide as or just slightly wider than the glabella at eye-line (Henningsmoen 1957; see also Westergård 1922, pl. XII, fig. 16). The material at hand has interocular cheeks that are about ¾ as wide (tr.) as the glabella at eye-line and which fits with the description of *C. fletcheri* (see Henningsmoen
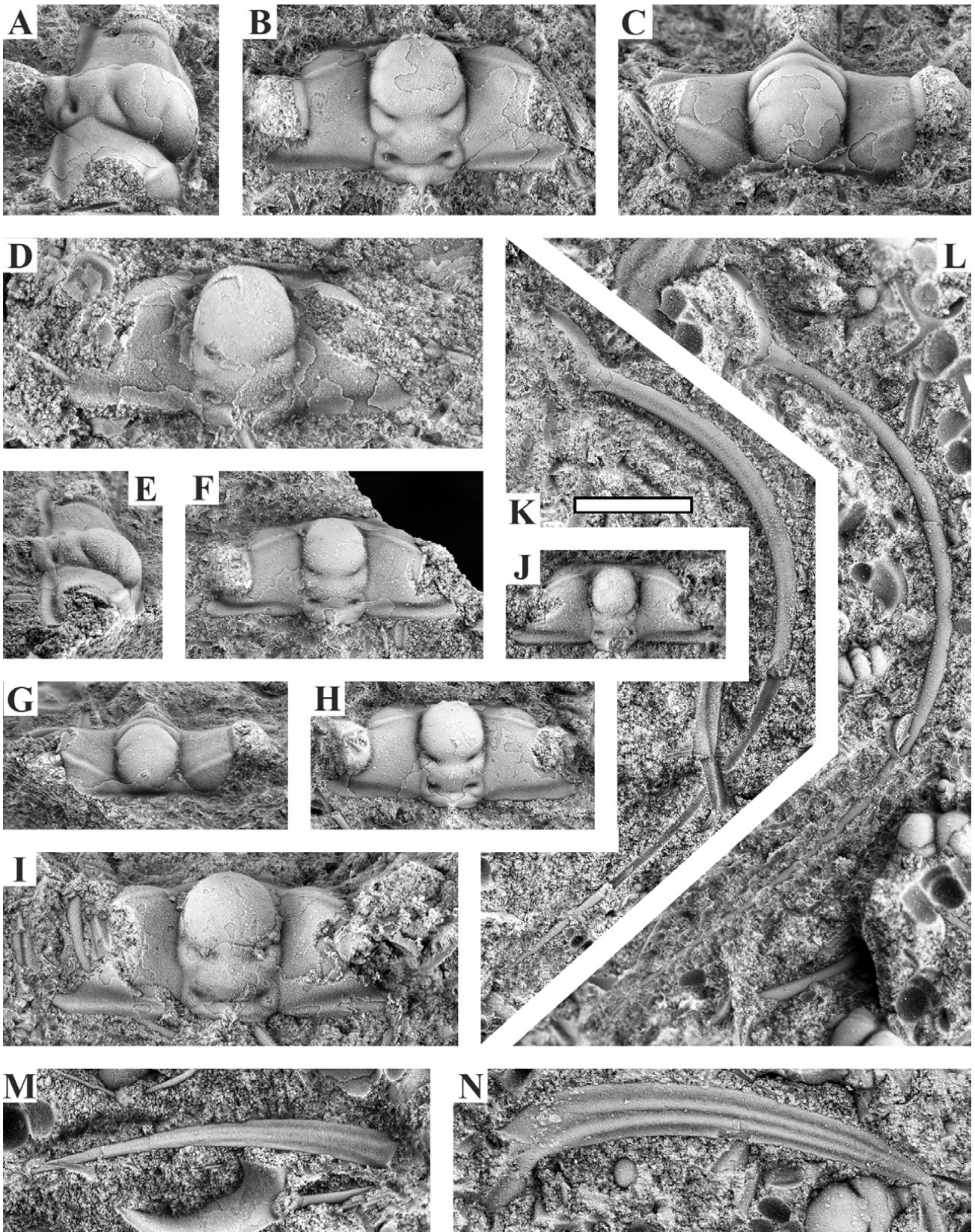
Fig. 21. *Ctenopyge ahlbergi,* all preserved in anthraconite from locality 6. White scale bar: 2 mm. **A–C:** Cranidium, different views, sample ATN-117. (MGUH 33683). **D:** Largest cranidium found, sample ATN-205. (MGUH 33733). **E–G:** Cranidium, different views, sample ATN-117. (MGUH 33684). **H:** Cranidium, sample ATN-134. (MGUH 33694). **I:** Cranidium, sample ATN-132. (MGUH 33731). **J:** Cranidium, sample ATN-134. (MGUH ¤33695). **K:** Free cheek, sample ATN-117. (MGUH 33685). **L:** Free cheek, sample ATN-134. (MGUH 33696). **M:** Pleural spine of thoracic segment, sample ATN-134. (MGUH 33697). **N.** Pleural spine of thoracic segment, sample ATN-113. (MGUH 33715).

1957). The characteristic free cheeks with long, flattened spines also match *C. fletcheri* as described and illustrated by Henningsmoen (1957).

Ctenopyge (Ctenopyge) linnarssoni Westergård, 1922
Fig. 23

1922   *Ctenopyge Linnarssoni* n. sp. – Westergård, pp. 162–163, pl. XIII, figs 2–5.

v 1923   *Ctenopyge Linnarssoni* Westergård – C. Poulsen, p. 45, pl. 1, fig. 17.

1957   *Ctenopyge (Ctenopyge) linnarssoni* Westergård 1922 – Henningsmoen, p. 207, pl. 5; pl. 22, fig. 8.

1973   *Ctenopyge (Ctenopyge) linnarssoni* Westergård, 1922 – Schrank, pp. 830–831, pl. IX, figs 13–17.

?2003   *Ctenopyge (Ctenopyge) linnarssoni* Westergård, 1922 – Terfelt, p. 413, fig. 4O.

2016   *Ctenopyge linnarssoni* – Ahlberg *et al.*, p. 498, figs 4, 6C.

2017   *Ctenopyge (Ctenopyge) linnarssoni* Westergård, 1922 – Rasmussen *et al.*, p. 11, fig. 6C.
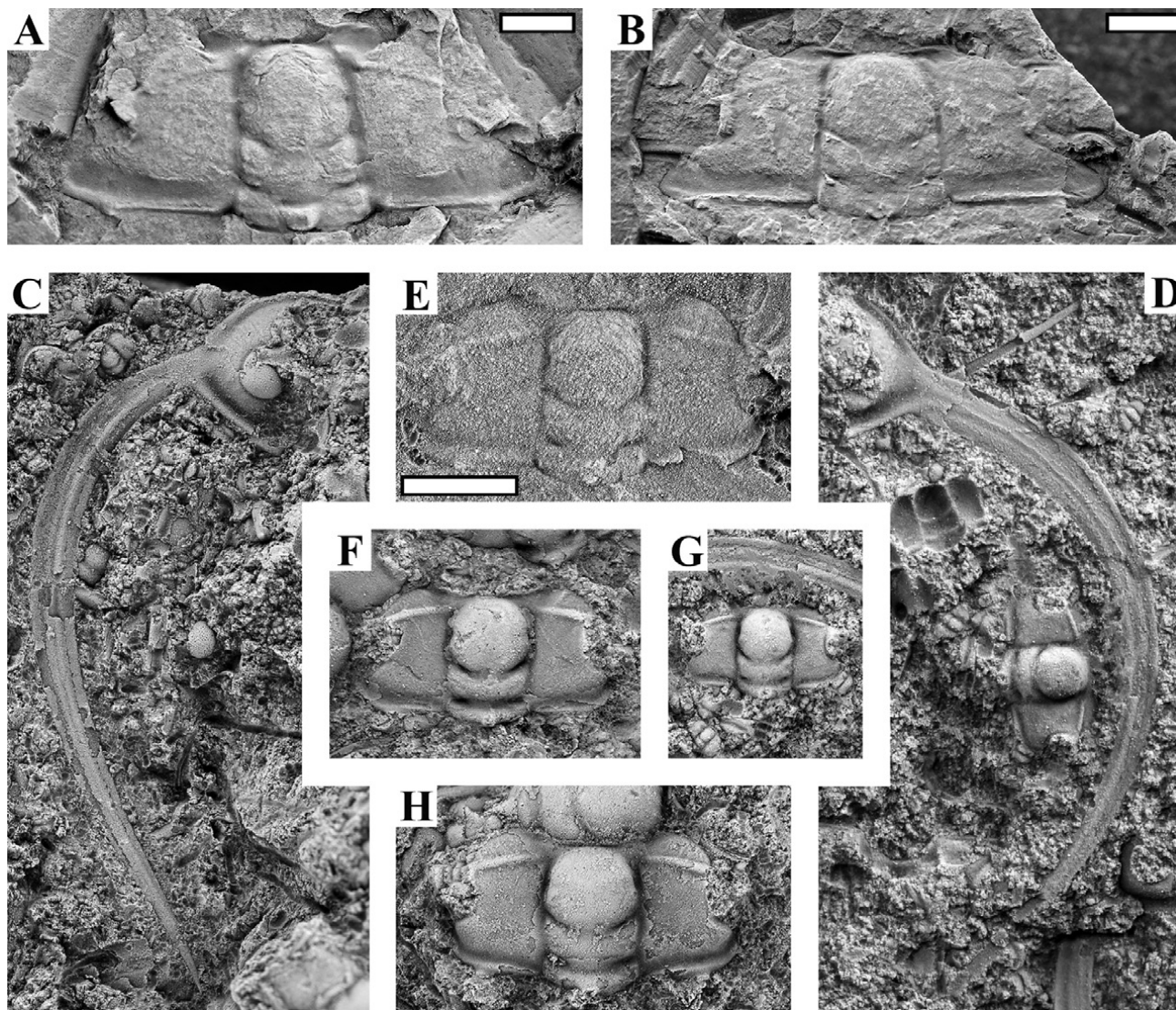
Fig. 22. *Ctenopyge bisulcata* (**A–B**) and *Ctenopyge fletcheri* (**C–H**). White scale bars: 2 mm; please note that the cranidia of *C. bisulcata* are shown at a smaller magnification. **A:** Cranidium preserved in shale from loc. 6, sample GM 1922-142R (MGUH 33735). **B:** Cranidium preserved in shale from loc. 6, specimen MGUH 1974 (previously illustrated by C. Poulsen 1923, pl. II, fig. 4). **C:** Free cheek preserved in anthraconite, loc. 6, sample GM 1881-337A (MGUH 33736). **D:** Free cheek preserved in anthraconite, loc. 6, specimen MGUH 1978a. The specimen is located on a bedding surface in sample GM 1881-337B illustrated by C. Poulsen (1923, pl. III). This surface also includes the specimens illustrated here as F and G. **E:** Cranidium preserved in shale, loc. 7, sample GM 1922-143 (MGUH 33738). **F–G:** Two cranidia preserved in anthraconite, loc. 6, specimens MGUH 1978b–c. **H:** Cranidium preserved in anthraconite, loc. 6, sample GM 1881-337A (MGUH 33737).

For further synonymy, see Rasmussen *et al.* (2017).

Lectotype. Cranidium SGU 356 from Andrarum, southern Sweden, figured by Westergård (1922, pl. XIII, fig. 2) and designated by Henningsmoen (1957).

Material. 38 cranidia and two free cheeks. Twelve of these cranidia derive from sample L17, found in the Læså stream at Limensgade (localities 8A–8B). Two cranidia and one free cheek are labelled "between Hjulmagergård and Vasagård" and another two cranidia are labelled "from the Læså area" (unspecified). These specimens are probably from locality 6 like most of the remaining material. *Ctenopyge linnarssoni* co-occurs with *C. pecten*, *C. tenuis*, *C. teretifrons*, *P. scarabaeoides* and *T. humilis* in the studied samples.

Occurrence. Ctenopyge linnarssoni is characteristic for the upper part of the *P. scarabaeoides* Zone and has been reported from Scandinavia, Poland, Great Britain and Canada (Westergård 1922; Henningsmoen 1957; Żylińska 2001; Terfelt *et al.* 2008; Rasmussen *et al.* 2017). The report from the *P. lobata* ['*longicornis*'] Zone on Bornholm (C. Poulsen 1923) is an error, see 'Discussion and conclusions'.

Comparison. The cranidium of *C. linnarssoni* reminds of that of *C. fletcheri,* but the latter has oblique eye ridges, whereas they are transverse or only slightly oblique in *C. linnarssoni. Ctenopyge fletcheri* also has narrower fixed cheeks, the interocular cheek is only ¾ as wide as the glabella at eye-line, while the postocular cheeks are about as wide as the occipital ring. *Ctenopyge linnarssoni* has interocular cheeks as wide as the glabella at eye-line, and the postocular cheeks are almost 1½ times as wide as the occipital ring. For comparison with *C. bisulcata*, see that species.

Ctenopyge (Ctenopyge) magna n. sp.
Fig. 24
v 1923 *Ctenopyge affinis* Westergård – C. Poulsen, pp. 41–42, pl. 2, fig. 5.

Derivation of name: Latin *magna*, meaning great or large, alluding to the extraordinary size of this *Ctenopyge* species.

Holotype. Cranidium MGUH 1975 from locality 6, Læså, Bornholm, originally illustrated as *C. affinis* by C. Poulsen (1923, pl. 2, fig. 5); here re-illustrated in Fig. 24A–C.

Diagnosis: Large *Ctenopyge* species. Glabella unusually broad, tapering, most pronouncedly so in the largest specimens; occipital furrow deeply impressed laterally with low swellings on the occipital ring behind the impressions; S1 deeply impressed laterally, oblique, not transglabellar; glabellar front truncate; eye ridges oblique; midline of eye situated opposite S1; moderately long spine on occipital ring; interocular cheek *c.* half as wide as the adjacent glabella at eye line (slightly narrower in large specimens, slightly wider in small specimens); postocular cheek triangular and ¾ as wide (tr.) as the occipital ring in large specimens; free cheek assumed belonging to this species of *affinis*-type with long, only gently curving spine almost forming a contuinuation of the course of the lateral margin; posterior margin short, straight.

Material. 41 cranidia, two free cheeks (tentatively assigned) and one hypostome. Most of the material is from locality 6, but a few specimens derive from locality 7. *Ctenopyge magna* n. sp. co-occurs with *C. affinis*, *C. ahlbergi*, and *S. alatus*. A single sample contains a cranidium of *C. magna* n. sp. in association with *T. humilis, C. tenuis* and *P. scarabaeoides*.

Occurrence. The material at hand derives almost exclusively from the upper part of the *P. acutidens–C. tumida* Zone; one specimen (Fig. 24I) is from the *P. scarabaeoides* Zone. The new species is currently known only from Bornholm.

Description: Large olenid, the holotype cranidium is 20 mm wide across the postocular cheeks and the largest cranidium found must originally have been ≈25 mm wide, judging from the with of the occipital ring (Fig. 24E). The cranidium is subtrapezoidal in overall outline. Glabella occupies a large proportion of the cranidium; it tapers fairly strongly, most pronouncedly so in the largest specimens. Glabellar front truncate; anteroglabella not as strongly inflated as in *C. ahlbergi* and *C. gracilis* and in sagittal profile descends evenly to the preglabellar furrow (Fig. 24C, O); glabella also moderately convex transversely; highest point behind S1. Three pairs of lateral glabellar furrows of which S1 is developed as elongate deep lateral impressions, directed obliquely inwards-backwards, reaching the axial furrows abaxially, but not united across the glabella. S2 and S3 are much shallower, but always visible; they are both directed inwards at an almost right angle to the axial furrows. Occipital ring wider than the rear part of glabella; it carries a fairly long spine (preserved in only two specimens, Fig. 24F) and a small mesial node is located immediately in front of the raised spine base (Figs 24E–F). The occipital furrow is laterally strongly accentuated by a pair of oblong deep pits; the furrow is shallow mesially, so the occipital ring appears as an integrated continuation of the glabella. A pair of elongate low swellings are seen on the occipital ring
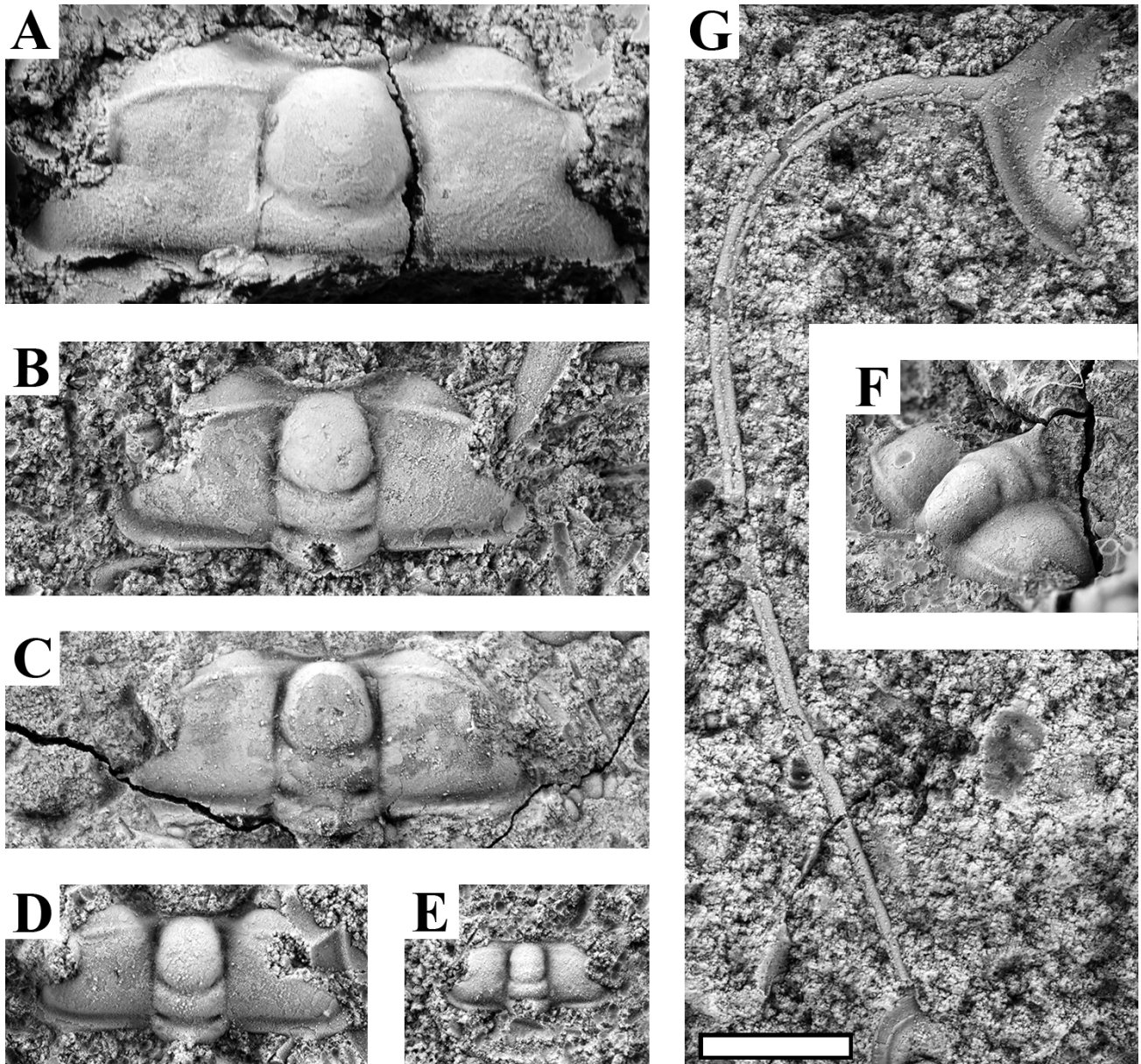
Fig. 23. *Ctenopyge linnarssoni*, all preserved in anthraconite. White scale bar: 2 mm. **A:** Cranidium, locs 8A–B, sample L17 (MGUH 33739). **B:** Cranidium, loc. 8A–B, sample L17 (MGUH 33740). **C:** Cranidium MGUH 1970, loc. 6; previously illustrated by C. Poulsen (1923 pl. 1, fig. 17). **D:** Cranidium, locs 8A–B, sample L17 (MGUH 33741). **E:** Juvenile cranidium, Læså area unspecified [probably loc. 6], sample GM 1877-2000 (MGUH 33745). **F:** Cranidium with occipital spine partially preserved, loc. 6, sample GM 1922-142I (MGUH 33746). **G:** Free cheek, Læså area between Hjulmagergård and Vasagård [probably loc. 6], sample GM 1871-666 (MGUH 33758).

▼ **Fig. 24.** *Ctenopyge magna* n. sp., all preserved in anthraconite from locality 6. Note the less pronounced tapering of the glabella in the smaller cranidia. White scale bar: 2 mm; please observe that the specimens are shown at a lower magnification than used for most of the illustrations in this paper. **A–C:** Different views of large cranidium, MGUH 1975, previously illustrated by C. Poulsen (1923, pl. II, fig. 5). **D:** Dislocated free cheek, assumed belonging to this species, and cranidium, sample ATN-116 (MGUH 33709). **E:** Fragmentary cranidium, sample ATN-147, the largest specimen at hand. A small cranidium of *C. affinis* in the axial furrow is kept as curiosum (MGUH 33724). **F:** Fragmentary cranidium with intact occipital spine. Note the small occipital node in front of the spine. Sample ATN-137 (MGUH 33759). **G:** Medium sized cranidium, sample GM 1902-1212 (MGUH 33760). **H:** Small cranidium, sample GM 1902-1209 (MGUH 33761). **I:** Small cranidium, the only one found in the *P. scarabaeoides* Zone, sample GM 1922-142S (MGUH 33764). **J:** Small cranidium, sample GM 1902-1209 (MGUH 33762). **K:** Medium sized cranidium, sample ATN-113 (MGUH 33716). **L.** Small cranidium, sample ATN-103 (MGUH 33721). **M:** Small cranidium, tentatively assigned, sample ATN-117 (MGUH 33686). **N–O:** Different views of small cranidium, tentatively assigned, sample ATN-116 (MGUH 33709). **P:** Hypostome, sample ATN-134 (MGUH 33698).
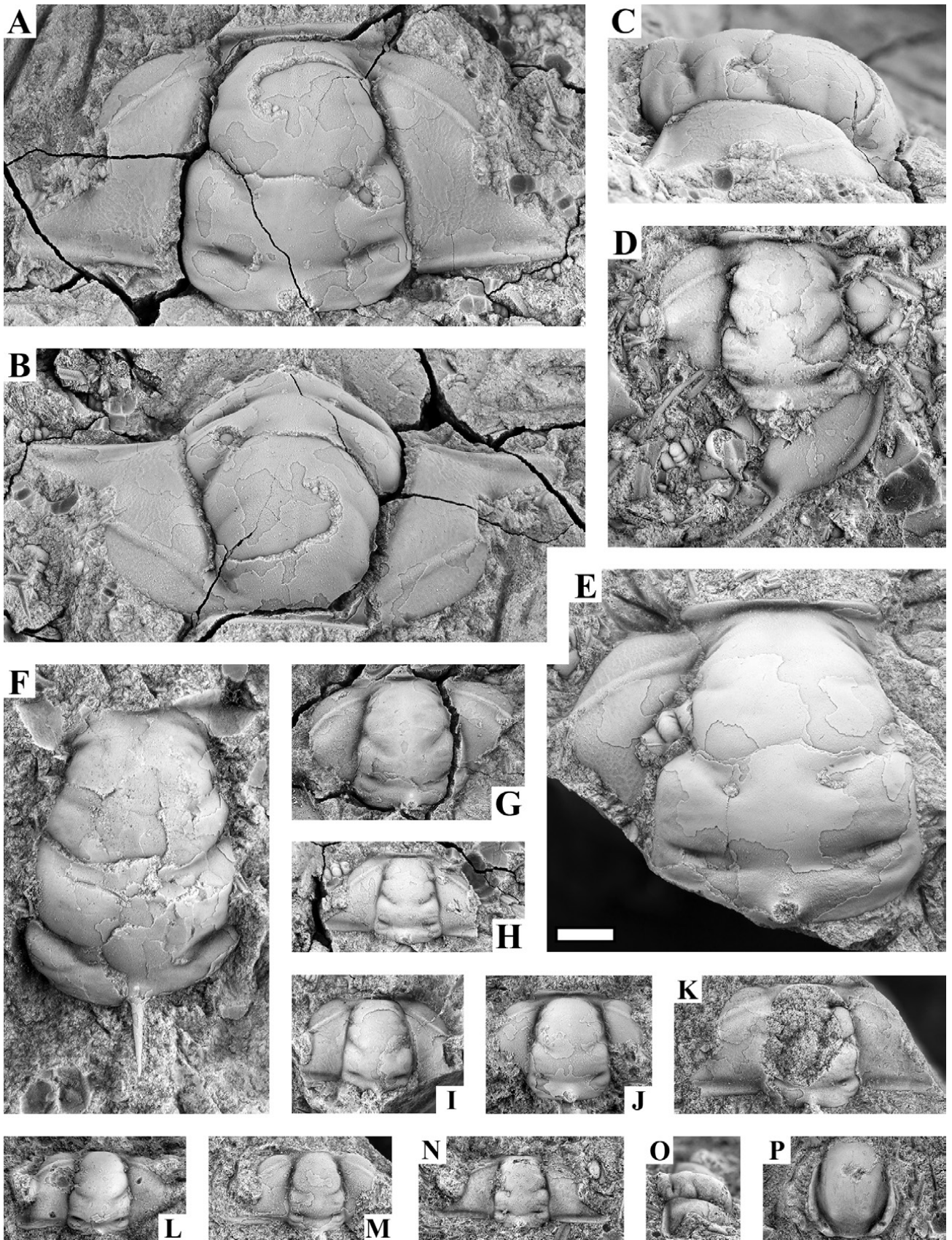
posterolaterally of the oblong deep pits in the occipital furrow; these swellings are separated by shallow furrows from the remainder of the occipital ring. Similar very shallow furrows with the same orientation are sometimes visible also on the rear part of glabella in front of the deep occipital pits, i.e. between the occipital furrow and S1 (see e.g. Fig. 24A, C). Axial furrows deep, gently undulating with indentations at the occipital furrow and each of the lateral glabellar furrows. Glabella is delimited anteriorly by a deep preglabellar furrow coincident with the anterior border furrow; no preglabellar area. Frontal area extremely narrow, consisting only of the narrow, upturned anterior border. Anterior margin of cranidium is gently concave in anterior view, truncate in dorsal view. Midline of palpebral lobes situated opposite S1; interocular cheek only *c.* half as wide as glabella at eye line (slightly narrower in large specimens and a little wider in small specimens); it is very slightly convex, sloping gently towards the palpebral lobes. The palpebral lobes are broken in most specimens, but apper to be rather narrow (tr.); they are delimited by wide and shallow but clearly defined palpebral furrows. Eye ridges distinct, directed obliquely backwards-outwards from the axial furrows and usually appear slightly curved in dorsal view. Postocular cheeks triangular in overall outline, comparatively long (exsag,) and short (tr.), gently down-sloping outwards. Posterior border furrow wide, rather shallow, running parallel with the posterior cranidial margin, but terminating adaxially a little short of the axial furrows. Posterior border moderately convex (exsag.), almost straight (tr.), widening slightly and getting less convex abaxially. Anterior sections of the facial suture are directed outwards-forwards for a short stretch in front of the eyes, then turn inwards, curving gently forwards-inwards and intersect the anterior cranidial margin level with maximum glabellar width (excl. of the occipital ring); the posterior sections of the facial suture are straight, diverging backward at an angle of *c.* 60° to the sagittal line. In some cranidia the surface of the cheeks exhibits a reticulate pattern (e.g. 24A, E). Nearly all cranidia are more or less fragmentary and compacted, suggesting that the test is thin and fragile.

Free cheek associated with cranidium (Fig. 24D) is assumed belonging to this species. It appears very similar to the free cheeks attributed to *C. affinis* (Fig. 20:1–4) having a presumably rather straight spine almost continuing the course of the lateral margin, a narrow border petering out close to the spine base and a short, straight posterior margin.

An unusually large hypostome (Fig. 24P) likely belongs to the new species.

Pygidium unknown.

Comparison. The cranidium of *C. magna* n. sp. some-what resembles that of the co-occurring *C. affinis* but the glabella is significantly more 'bulbous' and tapers more in similar-sized specimens. *Ctenopyge magna* n. sp. also attains considerably larger maximum size. It is, however, difficult to separate small cranidia of *C. magna* n. sp. with a less tapering and narrower glabella (Fig. 24L–O) from those of *C. affinis* and identification remains tentative, based on the degree of glabella inflation.

Remarks. Several free cheeks (e.g. Fig. 20:1–4) have been assigned to *C. affinis* but may alternatively represent small *C. magna* n. sp.; compare with Fig. 24B.

C. Poulsen (1923) described ten large cranidia identified as *C. affinis* from five museum samples collected in 1902, which according to him also contain *S. alatus* [in C. Poulsen's terminology a mislabel for *T. humilis*] and fragments of *C. pecten* (?). The samples, numbered GM 1902-1208 to GM 1902-1212, are now intensively cracked, but a total of six cranidia and five external moulds of cranidia of *C. magna* n. sp. were recorded. Sample GM 1902-1208 has been impregnated with epoxy and the fossil content can no longer be observed. The samples also contain *S. alatus* [*s.str.*], *C. ahlbergi* and *C. affinis* [*s.str.*] and it is probably the latter that was misidentified as *C. pecten* (?) by C. Poulsen. In any case, these samples are not from the *P. scarabaeoides* Zone.

Ctenopyge (Ctenopyge) pecten (Salter, 1864)
Fig. 25A–F

1922   *Ctenopyge pecten* (Salter) [*partim*] – Westergård, pp. 160–161, pl. XII, figs 26?, 27–28, 30–33; pl. XIII, fig. 1; non pl. XII, fig. 29 [= *C. tenuis*].
? 1922   *Ctenopyge affinis* n. sp. [*partim*] – Westergård, pp. 157–158, pl. XII, fig. 15.
Non 1923   *Ctenopyge pecten* Salter – C. Poulsen, pp. 42–44, pl. II, figs 1–3 [= *C. tenuis*].
1947   *Ctenopyge pecten* (Salter) – Westergård, pl. 3, fig. 12.
1957   *Ctenopyge (Ctenopyge) pecten* (Salter 1864) – Henningsmoen, pp. 208–209; pl. 2, fig. 18?; pl. 5; pl. 22, figs 9–10.
1959   *Ctenopyge (Ctenopyge) pecten* (Salter, 1864) – C. Poulsen, p. O264, fig. 195:7.
1973   *Ctenopyge (Ctenopyge) pecten pecten* (Salter, 1864) – Schrank, pp. 828–829, pl. IX, figs 3–6.
2004   *Ctenopyge (Ctenopyge) pecten pecten* (Salter 1864) – Mischnik, p. 116, pl. 4, figs 6, ?7–8.
For further synonymy, see Henningsmoen (1957).

Type material. Not designated. Syntypes BGS GSM 8960, 8981, ?8914-19 are from the White-Leaved Oak Shales, Malvern, United Kingdom (Morris 1988).

Material. 21 cranidia. Three cranidia are labelled

'between Hjulmagergård and Vasagård' (locality 6?), one is from 'the Læså area' (also most likely locality 6), two are from 'Cementen' (i.e. ice-rafted material, Øleå), while the remaining cranidia are from locality 6. *Ctenopyge pecten* co-occurs with *C. linnarssoni*, *C. tenuis*, *C. teretifrons*, *P. scarabaeoides* and *T. humilis* in the studied samples.

Occurrence. Ctenopyge pecten occurs comparatively infrequently in the *P. scarabaeoides* Zone and has been reported from Scandinavia, Great Britain and Canada (Westergård 1922; Henningsmoen 1957; Terfelt *et al.* 2008; Høyberget & Bruton 2012). It occurs at the same stratigraphic level on Bornholm.

Comparison. The cranidium of *C. pecten* reminds of that of *C. tenuis*, but the eyes are situated further back so the postocular cheeks are shorter (exsag.) and typically also longer (tr.). The free cheeks has a more strongly curving and presumably longer genal spine than *C. tenuis* and the location of the eye incision should also differ, but so far this inference has not been verified. See also 'comparison' with *C. tenuis* below.

Remarks. The material assigned to *C. pecten* by C. Poulsen (1923) represents *C. tenuis* (see V. Poulsen 1963) which is common in the *P. scarabaeoides* Zone on Bornholm. However, *C. pecten s.str.* is also present although much more sparsely. Not all cranidia of *C. pecten* have as wide (tr.) and gracile postocular cheeks as those illustrated by Westergård (1922 pl. XII, figs

30–31) and some approaches the additional specimens he illustrated (*ibid.*, pl. XII, figs 26–27) with shorter (tr.) and slightly longer (exsag.) postocular cheeks. The latter two cranidia illustrated by Westergård were synonymized with *C. tenuis* by V. Poulsen (1963), but we consider them as within the range of variation of *C. pecten*, whereas another cranidium illustrated by Westergård (1922, pl. XII, fig, 29) clearly belongs to *C. tenuis*.

Ctenopyge (Ctenopyge) tenuis Poulsen, 1963
Figs 26–27

1922   *Ctenopyge pecten* (Salter) [*partim*] – Westergård, pl. XII, fig. 29.
v 1923   *Parabolina longicornis* Westergård [*partim*] – C. Poulsen, p. 31; non textfig. 9 [= *P. lobata lobata*].
v 1923   *Ctenopyge pecten* Salter – C. Poulsen, pp. 42–44, pl. II, figs 1–3.
v 1963   *Ctenopyge (Ctenopyge) pecten tenuis* n. subsp. – V. Poulsen, pp. 1–9, figs 1a–c.
1973   *Ctenopyge (Ctenopyge) pecten tenuis* V. Poulsen, 1963. – Schrank, pp. 829–830, pl. IX, figs 7–12; pl. X, figs 12, 13?.

Holotype. Incomplete thorax with pygidium (MGUH 1973) and external mould of the same specimen (MGUH 1972), figured by C. Poulsen (1923, pl. 2, figs 2–3) and V. Poulsen (1963, figs 1a–b). The holotype and matching external mould are refigured here in Figs 26N and 27D.
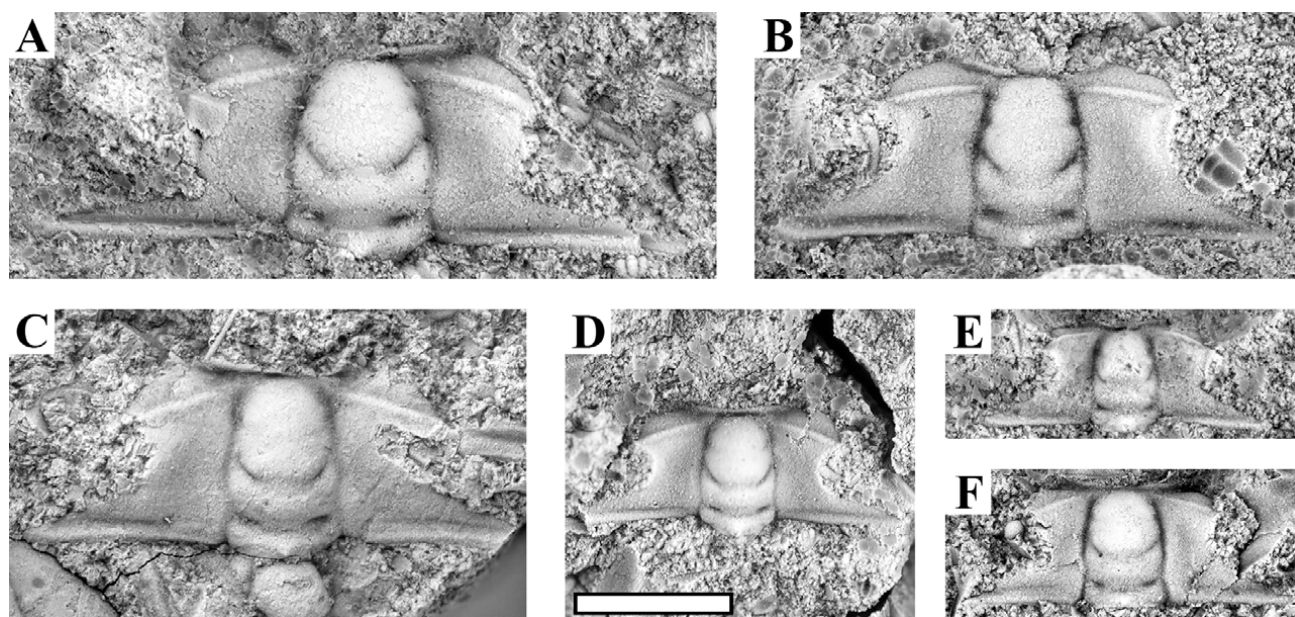

Fig. 25. Cranidia of *Ctenopyge pecten,* all preserved in anthraconite. B and C are labelled 'Cementen, Øleå', the remaining specimens are from locality 6. White scale bar: 2 mm. **A:** Sample L43 (MGUH 33767). **B:** Sample GM 1874-28 (MGUH 33771). **C:** Sample GM 1871-655 (MGUH 33772). **D:** Sample GM 1922-142I (MGUH 33749). **E:** Sample L52 (MGUH 33773). **F:** Sample GM 1874-27 (MGUH 33774).

Material. 327 cranidia, seven free cheeks, one thorax with 4–5 contiguous segments and 24 pygidia with up to nine attached thoracic segments. One cranidium was found in sample L17 at Limensgade (localities 8A–8B), 20 cranidia and one free cheek are labelled 'Cementen' (i.e. ice-rafted material, Øleå), while all other material derives from locality 6. C. Poulsen (1923) listed *C. tenuis* [as *C. pecten*] also from locality 7, but no museum material of the species is at hand from that locality. *Ctenopyge tenuis* co-occurs with *C. linnarssoni, C. pecten, C. teretifrons, P. scarabaeoides* and *T. humilis* in the studied samples.

Occurrence. Peltura scarabaeoides Zone on Bornholm and in Sweden (V. Poulsen 1963; present study). *Ctenopyge tenuis* does not range into the *P. lobata* ['*longicornis*'] Zone as reported by C. Poulsen (1923) (see 'Discussion and conclusions').

Diagnosis (new): A *Ctenopyge pecten*-like species with almost parallel-sided glabella; S1 oblique, distinctly impressed abaxially, shallow mesially; S2 and S3 short, indistinct; eye ridges slightly oblique; centres of palpebral lobes opposite L2; interocular cheeks about three-fourths as wide as glabella at eye line in adult specimens; postocular cheeks on average *c.* 1.4 times as wide as occipital ring; postocular facial suture diverges rearwards-outwards at an angle of 50–60° from sagittal line; free cheeks with long rounded spine, curving gently, short straight posterior lateral margin, and markedly longer, gently convex anterior lateral margin; thorax with long flattened pleural spines; pleural region of thorax (excluding spine) up to two times as wide as the axis; pygidium with 7-8 axial rings in addition to the articulating half ring and terminal piece; long axial spine; pleurae (not united with each other?) with long flattened pleural spines.

Supplementary description: For a general description, see V. Poulsen (1963). Glabella almost parallel-sided with three pairs of lateral glabellar furrows, of which S1 is well-impressed laterally and shallow mesially whereas S2 and S3 are indistinct, short and not transglabellar. The shape of the anteroglabella varies from being slightly trapezoidal, tapering forwards with truncate front in some specimens (e.g. Fig. 26F), to more parallel-sided with rounded front in other specimens (e.g. Fig. 26J). Slightly oblique eye ridges; rear edge of palpebral lobe roughly level with S1, so midline of palpebral lobes level with L2. Interocular cheeks are *c.* ¾ as wide as the glabella at eye-line in adult specimens; the ratio varies between 0.73–0.84, averaging 0.76 (n = 7). The interocular cheeks are relatively narrower in small cranidia less than 1.5 mm long; here the corresponding width varies between 0.55–0.73 and averages 0.65 (n=4). Postocular cheeks rather variable in width (tr.) irrespective of cranidial size; in measured specimens the width varies from 1.24 to 1.66 times the width of the occipital ring, averaging 1.39 (n= 13). Postocular facial suture sinuous, diverging backwards at an angle of 50–60° from sagittal line, which is an important distinguishing feature. Free cheek has a long, moderately curving and slender spine. Thorax consists of >9 segments, widest across the middle segments, tapering backwards in the posterior part, all with long, flattened pleural spines. The axis constitutes about ⅕ of the total width of the thorax (excluding spines) where the thorax is widest. The pygidium is rounded to semi-triangular in outline. At least the anterior six pygidial segments are provided with long marginal spines. The axis is slightly tapering and consists of 7–8 segments in addition to the articulating half ring and terminal piece. Axial rings nos 5–7 provide a base for a long axial spine. For further details, see V. Poulsen (1963).

Comparison. Ctenopyge tenuis is distinguished from *C. pecten* by the angle of the postocular facial suture relative to the sagittal axis. In *C. tenuis*, this angle is between 50–60° vs. 70°–80° in *C. pecten* (with a few specimens showing 65°), so overall the cranidium of *C. pecten* is wider. The genal spine seems to be only gently curving in *C. tenuis* versus strongly curving in *C. pecten*. Besides, in *C. tenuis* the thoracic axis constitutes slightly more than 1/5 of the total thoracic width (where the thorax is widest, excluding spines), while

▼ **Fig. 26.** *Ctenopyge tenuis*, all preserved in anthraconite and from locality 6 unless otherwise stated. White scale bar: 3 mm. **A:** Cranidium MGUH 1971, previously illustrated by C. Poulsen (1923, pl. II, fig.1). **B:** Cranidium, sample GM 1922-142I (MGUH 33747). **C:** Cranidium, sample GM 1922-142I (MGUH 33754). **D:** Small cranidium, sample GM 1922-142A (MGUH 33777). **E:** Small cranidium, sample GM 1881-1804; no information on locality (MGUH 33780). **F:** Cranidium, sample L43 (MGUH 33768). **G:** Cranidium, sample L48 (MGUH 33781). **H:** Small cranidium, sample GM 1922-142B; locality 6 (MGUH 33783). **I:** Small cranidium, sample GM 1874-27, 'Cementen', Øleå (MGUH 33775). **J:** Cranidium, sample GM 1881-1797 (MGUH 33784). **K:** Cranidium, sample GM 1922-142I (MGUH 33755). **L.** Cranidium, sample GM 1922-142I (MGUH 33750). **M:** Cranidium, sample L41 (MGUH 33785). **N:** Holotype, incomplete thorax with pygidium, MGUH 1973 (previously illustrated by C. Poulsen 1923, pl. II, fig. 3 and V. Poulsen 1963, fig. 1a; see also Fig. 27D).
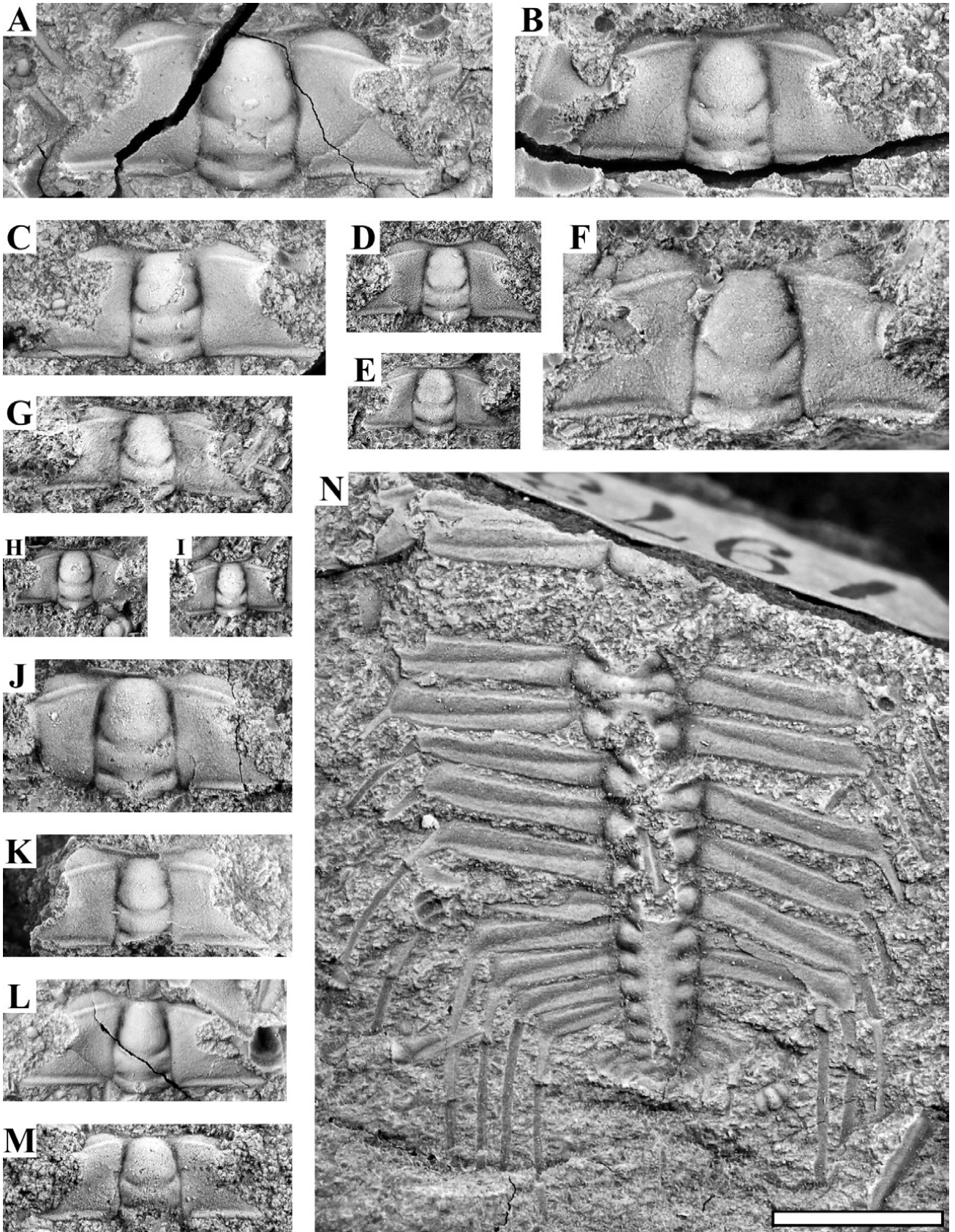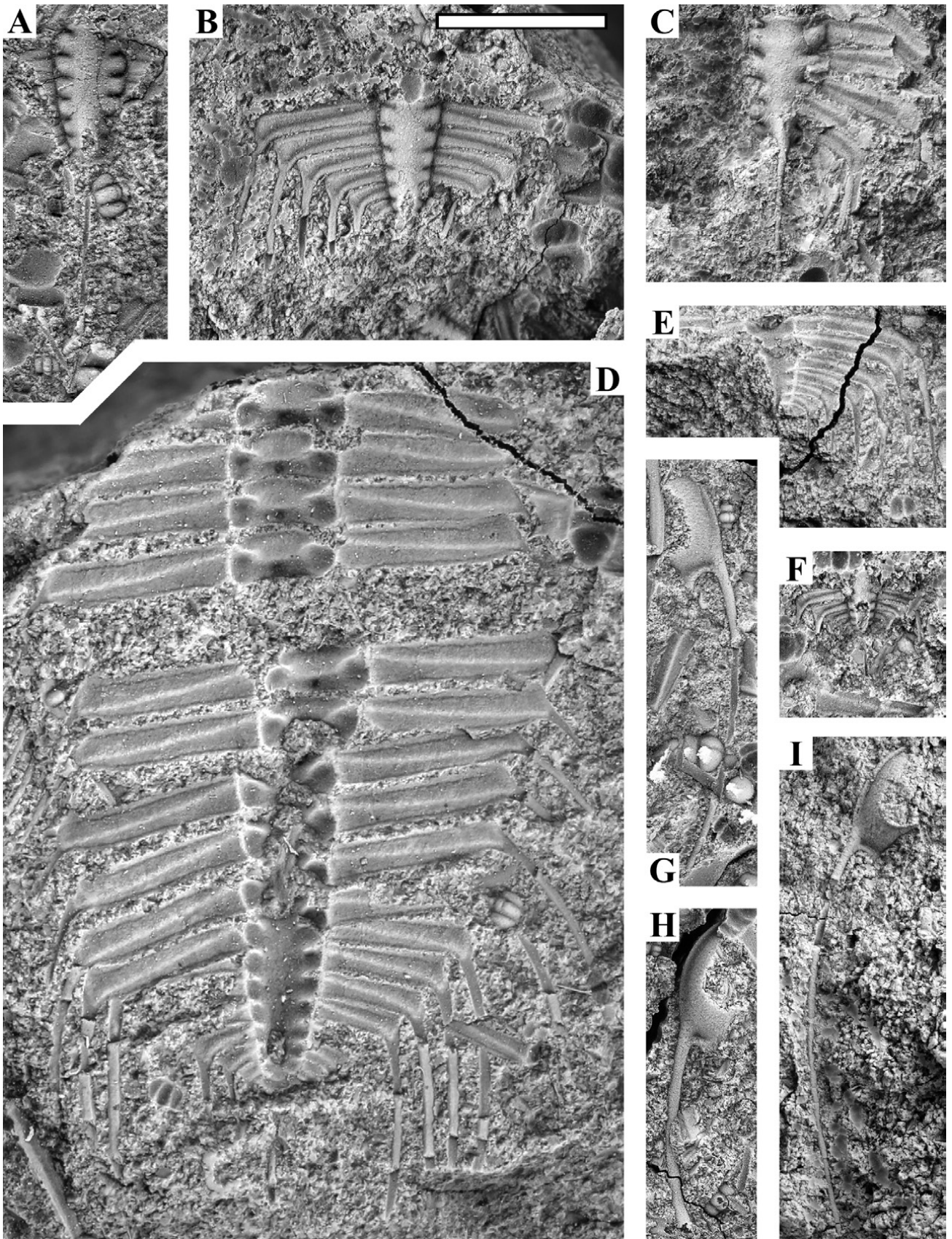
in *C. pecten* the axis occupies only slightly more than 1/10 of the thoracic width. *Ctenopyge pecten* also has a more rapidly tapering posterior part of the thorax. The pygidia of the two species are apparently essentially identical.

Remarks. Westergård (1922) and Henningsmoen (1957) included two different forms under the name *C. pecten*. Westergård (1922) illustrated both, whereas Henningsmoen (1957) only showed the wider form assigned here to *C. pecten*. V. Poulsen (1963) separated *tenuis* as a subspecies of *C. pecten*; we prefer a separation at species level as these taxa co-occur on Bornholm. A diagnosis in the style of Henningsmoen (1957) is provided for *C. tenuis* as no summery of characteristics was given by V. Poulsen (1963).

V. Poulsen (1963) described the thoracic axis of *C. tenuis* as being ⅔ as wide as the pleural regions (excluding spines). However, in the holotype specimen, the axis is less than 0.6 times as wide as the adjacent pleural region (measured where the thorax is widest) and about ⅕ of the total width of the thorax.

Two free cheeks assigned to *P. 'longicornis'* by C. Poulsen (1923) are identified here with *C. tenuis* together with additional free cheeks. The specimens are not well-preserved, but it is obvious that the genal spine is long and slender. The genal field is elongate and the outer lateral margin is convex and much longer than the posterior lateral margin. Although the spine is less curved, these free cheeks (Figs 27G–I) overall resemble those of *C. pecten* figured by Westergård (1947, pl. 3, fig. 12) and Schrank (1973, pl. IX figs 7, 10), and given the otherwise strong resemblance between *C. tenuis* and *C. pecten* we conclude that they belong to *C. tenuis*. Besides, the specimens do not look like any other species of *Ctenopyge* occurring at that level.

Ctenopyge (Ctenopyge) teretifrons (Angelin, 1854)
Fig. 28
1922 *Ctenopyge teretifrons* (Angelin) [*partim*] – Westergård, p. 162, pl. XIII, fig. 6; non pl. XIII, figs 7–8 [= *C. fletcheri*].
v 1923 *Ctenopyge teretifrons* Angelin – C. Poulsen, pp. 44–45, pl. 1, fig. 16.
1957 *Ctenopyge (Ctenopyge) teretifrons* (Angelin 1854) – Henningsmoen, pp. 209–210, pl. 5.

1973 *Ctenopyge (Ctenopyge) teretifrons* (Angelin 1854) – Schrank, pp. 831–832, pl. X, fig. 1–2, ?3.
For further synonymy, see Henningsmoen (1957).

Type material. Not designated (see Henningsmoen 1957).

Material. 71 cranidia, mostly from locality 6. A single specimen is labelled 'Cementen' (i.e. ice-rafted material, Øleå) and there is no locality information on four specimens. C. Poulsen (1923) reported this species also from locality 7, but no museum material is available from that locality. *Ctenopyge teretifrons* co-occurs with *C. linnarssoni*, *C. pecten*, *C. tenuis*, *P. scarabaeoides* and *T. humilis* in the studied samples.

Occurrence. Peltura scarabaeoides Zone, Sweden, England and Wales (Henningsmoen 1957). *Ctenopyge teretifrons* occurs at the same level on Bornholm and the report from the *P. lobata* ['longicornis'] Zone (C. Poulsen 1923) is an error, see 'Discussion and conclusions'.

Comparison. In comparison with *C. linnarssoni*, the cranidium of *C. teretifrons* is wider, with interocular cheeks that are almost 1 ½ times as wide as the glabella at eye-line and postocular cheeks that are about twice as wide as the occipital ring (see remarks), while *C. linnarssoni* has interocular cheeks as wide as the glabella at eye-line and the postocular cheeks are only *c.* 1 ½ times as wide as the occipital ring. *Ctenopyge teretifrons* has also a distinctive, rather inflated 'globular' anteroglabella.

Remarks. In a few measured cranidia, the width of the interocular area at eye line is 1.1–1.7 times the width of the adjacent glabella, averaging 1.4 (n=8). The postocular cheeks are 1.6–2.1 times as wide as the occipital ring, averaging 1.9 (n=8). The narrowest interocular area and postocular cheeks are seen in the smaller cranidia (<1.5 mm long).

Subgenus *Ctenopyge (Mesoctenopyge)* Henningsmoen, 1957
Type species: *Ctenopyge spectabilis* Brøgger, 1882 by original designation.

▲ **Fig. 27.** *Ctenopyge tenuis,* all preserved in anthraconite and from locality 6, unless otherwise stated. White scale bar: 3 mm. **A:** Fragmentary pygidium, sample GM 1922-142M (MGUH 33788). **B:** Pygidium, sample GM 1922-142M (MGUH 33789). **C:** Fragmentary pygidium, sample L38 (MGUH 33790). **D:** Incomplete thorax with pygidium (external mould of holotype MGUH 1973 illustrated in Fig. 26N), specimen MGUH 1972. **E:** External mould of pygidium, sample GM 1871-636, Læså area from between Hjulmagergård and Vasagård [loc. 6 or 7] (MGUH 33793). **F:** Fragmentary small pygidium, sample GM 1874-27, collected at 'Cementen', Øleå (MGUH 33776). **G:** One of two free cheeks, sample GM 1922-142J, labelled as *Parabolina longicornis* by C. Poulsen, see text (MGUH 33794). **H:** Free cheek, sample GM 1922-142I (MGUH 33748). **I:** Free cheek, sample GM 1922-142S (MGUH 33765).

Ctenopyge (Mesoctenopyge) tumida Westergård, 1922

Fig. 29

1922 *Ctenopyge tumida* n. sp. [*partim*] – Westergård, pp. 155–156, pl. XI, figs 15–18; non pl. XI, figs 19–20 [= *Ctenopyge tumidoides*].

1922 *Ctenopyge bisulcata* (Phillips) [*partim*] – Westergård, pl. XII, fig. 21.

v 1923 *Ctenopyge tumida* Westergård [*partim*] – C. Poulsen, pp. 39–41, pl. 1, fig. 14; non textfig. 16 [= *Ctenopyge tumidoides*].

1957 *Ctenopyge (Mesoctenopyge) tumida* Westergård 1922 – Henningsmoen, pp. 198–199, pl. 5, pl. 20, fig. 16.

1973 *Ctenopyge (Mesoctenopyge) tumida* Westergård, 1922 – Schrank, pp. 825–826, pl. VII, figs 13–20, 22–23.

non 2004 *Ctenopyge (Mesoctenopyge) tumida* Westergård, 1922 – Clarkson *et al.*, pp. 129–130, 134, 137, figs 17, 18A–D, 19, 20A–D. [= *C. tumidoides*].

2015 *Ctenopyge (Mesoctenopyge) tumida* Westergård, 1922 – Schoenemann & Clarkson, pp. 133–139, figs 1F–H, 3.

2016 *Ctenopyge (Mesoctenopyge) tumida* Westergård, 1922 – Månsson & Clarkson, pp. 178–182, figs 7–11.

2016 *Ctenopyge tumida* – Ahlberg *et al.*, p. 498, figs 4, 6O.

2017 *Ctenopyge (Mesoctenopyge) tumida* Westergård, 1922 – Rasmussen *et al.*, pp. 11–12, fig. 6E.

For further synonymy, see Månsson & Clarkson (2016) and Rasmussen *et al.* (2017).

Lectotype. Cranidium SGU 315 figured by Westergård (1922, pl. XI, fig. 16) from Andrarum, southern Sweden, designated by Henningsmoen (1957).

Material. 141 cranidia and nine free cheeks. Nearly all of the material is from locality 6; one cranidium and a free cheek were found at locality 7. *Ctenopyge tumida* co-occurs with *C. tumidoides*, *Ctenopyge* sp. 2, *P. acutidens*, *S. alatus* and *S. angustus* in the studied samples.

Occurrence. Ctenopyge tumida is characteristic of the *P. acutidens–C. tumida* Zone (Terfelt *et al.* 2008; Nielsen *et al.* 2020). It has been recorded from Scandinavia (incl. Bornholm), Great Britain and Poland (Henningsmoen 1957; Żylińska 2001, 2002; Terfelt *et al.* 2008).

Comparison. Ctenopyge tumida is quite similar to *C. tumidoides* but has a transverse postocular facial suture whereas it runs obliquely backwards in *C. tumidoides*.
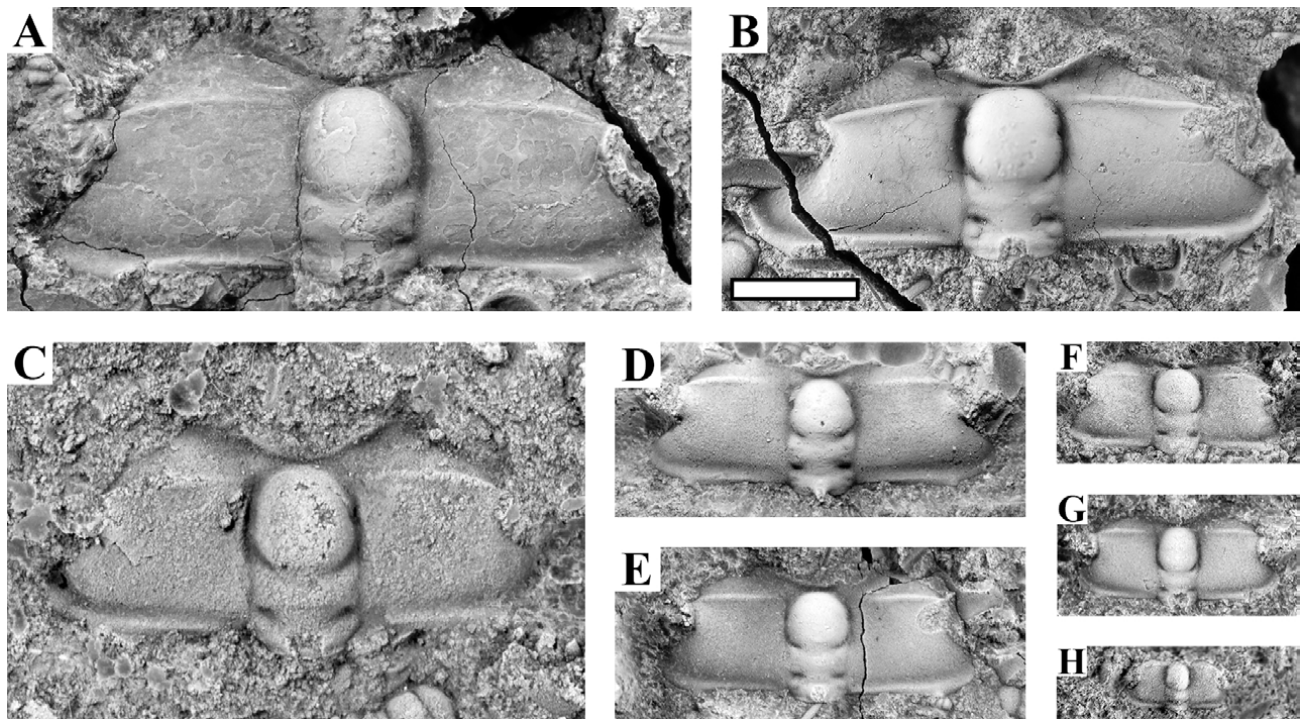
Fig. 28. Cranidia of *Ctenopyge teretifrons,* all preserved in anthraconite from locality 6. White scale bar: 2 mm. **A:** Sample GM 1922-142T (MGUH 33796). **B:** MGUH 1969, previously illustrated by C. Poulsen (1923, pl. 1, fig. 16). **C:** Sample L41 (MGUH 33786). **D:** Sample GM 1922-142D (MGUH 33797). **E:** Sample GM 1922-142I (MGUH 33751). **F:** Sample GM 1922-142S (MGUH 33766). **G:** Sample GM 1922-142B (MGUH 33798). **H:** Sample GM 1881-1796 (MGUH 33800).

Hence, the adaxial parts of the postocular cheeks are shorter (exsag.) in *C. tumida* compared with *C. tumidoides*. *Ctenopyge tumida* also has slightly wider (tr.) postocular cheeks being almost 1 ½ times as wide as the occipital ring, while they are only slightly wider than the occipital ring in *C. tumidoides*. The strong resemblance between *C. tumida* and *C. tumidoides* makes identification difficult if the postocular cheeks are broken or not fully visible.

Remarks. 23 cranidia of *C. tumida* (examples shown in Fig. 29J–K, Q) have been found associated with *C. tumidoides* and *S. angustus*. The latter two species are usually regarded as indicative of the *S. modestus–S. angustus* Zone, but apparently they range into the basal *Peltura* Superzone (see section on 'Olenid zonation').

One of the cranidia illustrated as *C. bisulcata* by Westergård (1922, pl. XII, fig. 21) has a course of the posterior branches of the facial suture entirely similar to that of *C. tumida*.

The cranidia described as *C. tumida* by Clarkson *et al.* (2004) have oblique postocular facial sutures and are here identified as *C. tumidoides*.

Ctenopyge (Mesoctenopyge) tumidoides
Henningsmoen, 1957
Fig. 30
1922	*Ctenopyge tumida* n. sp. [*partim*] – Westergård, pp. 155–156, pl. XI, figs 19–20.
1923	*Ctenopyge tumida* Westergård [*partim*] – C. Poulsen, pp. 39–41, textfig. 16.
1957	*Ctenopyge (Mesoctenopyge) tumidoides* n. sp. – Henningsmoen, pp. 199–200, pl. 5; pl. 20, fig. 15.
2004	*Ctenopyge (Mesoctenopyge) tumida* Westergård, 1922 – Clarkson *et al.*, pp. 129–130, 134, 137, figs 17, 18A–D, 19, 20A–D.

Holotype. Cranidium with five attached thoracic segments (SGU 318) figured by Westergard (1922, pl. XI, fig. 19) from Andrarum, southern Sweden.

Material. 141 cranidia (including 21 external moulds) and 11 free cheeks, co-occurring with common *S. angustus,* very rare *P. planicauda, P. acutidens* and *Ctenopyge* sp. 2, and occasional *C. tumida*, see remarks on the latter species. Most specimens are from locality 6, but a few were found at locality 7.

Occurrence. Sphaerophthalmus modestus–S. angustus Zone in the Oslo Region and Scania (see Henningsmoen 1957). *Ctenopyge tumidoides* has not been reported from Bornholm previously due to mixing with *C. tumida;* it is, in fact, quite common. The majority of the specimens

derive from samples with common *S. angustus*, but a few samples also contain *C. tumida* and/or *P. acutidens*. One sample (ATN-197) even contains several cranidia of *C. tumidoides* associated with *S. alatus* and *C. tumida*. *Ctenopyge tumidoides* thus seems to range into the lowermost part of the *Peltura* Superzone, which apparently also is the case in Västergötland (see remarks).

*Comparison.* For comparison with *C. tumida*, see that species.

Remarks. The small cranidia allocated to *C. tumida* by Clarkson *et al.* (2004) have oblique postocular facial sutures and short (tr.) postocular cheeks and are here assigned to *C. tumidoides*; compare with the smallest cranidia of *C. tumida* (Fig. 29N, R) and *C. tumidoides* (Fig. 30L) illustrated from Bornholm vs. Clarkson *et al.* (2004 fig. 17B). The material from Västergötland described by Clarkson *et al.* (2004) co-occurs with *C. ahlbergi* and apparently derives from the *P. acutidens–C. tumida* Zone. On Bornholm, *C. tumidoides* co-occurs with *C. tumida* and *P. acutidens* in the lower part of the *P. acutidens–C. tumida* Zone but not with *C. ahlbergi* (see section on 'Olenid zonation').

Ctenopyge sp. 1
Fig. 31A

Material. One cranidium from sample L77 found at locality 7. It co-occurs with *C. affinis*, *C. ahlbergi* and *S. alatus* and this assemblage is indicative of the upper part of the *P. acutidens–C. tumida* Zone.

Remarks. The cranidium, which is 3.35 mm wide and *c.* 1.95 mm long (the anterior margin is damaged) has unusually narrow cheeks. The glabella morphology suggests that it is a representative of *Ctenopyge* but it cannot be assigned to any known species. The little-known *C. oelandica* (see Westergård 1922, Buchholz 2000) has strongly curving eye ridges, which clearly sets it apart from *Ctenopyge* sp. 1. *Ctenopyge rushtoni* – of which only juveniles are described (Clarkson *et al.* 2004) – has a cranidium that is quite *C. gracilis*-like with much wider cheeks than *Ctenopyge* sp. 1 and the glabella of *C. rushtoni* and notably the anteroglabella is also significantly more inflated. *Ctenopyge affinis* has posterior indentations in the glabella immediately in front of the occipital furrow and the postocular cheeks are clearly wider than the occipital ring (*c.* 1.2 times as wide in adult specimens). In *Ctenopyge* sp. 1, the glabella has no lateral indentations in the rear part and it tapers evenly and gently forwards; the postocular cheeks are also markedly narrower (tr.) than the occipital ring (*c.* ¾ as wide). Unless it is a pathological specimen, it likely represents a new species.
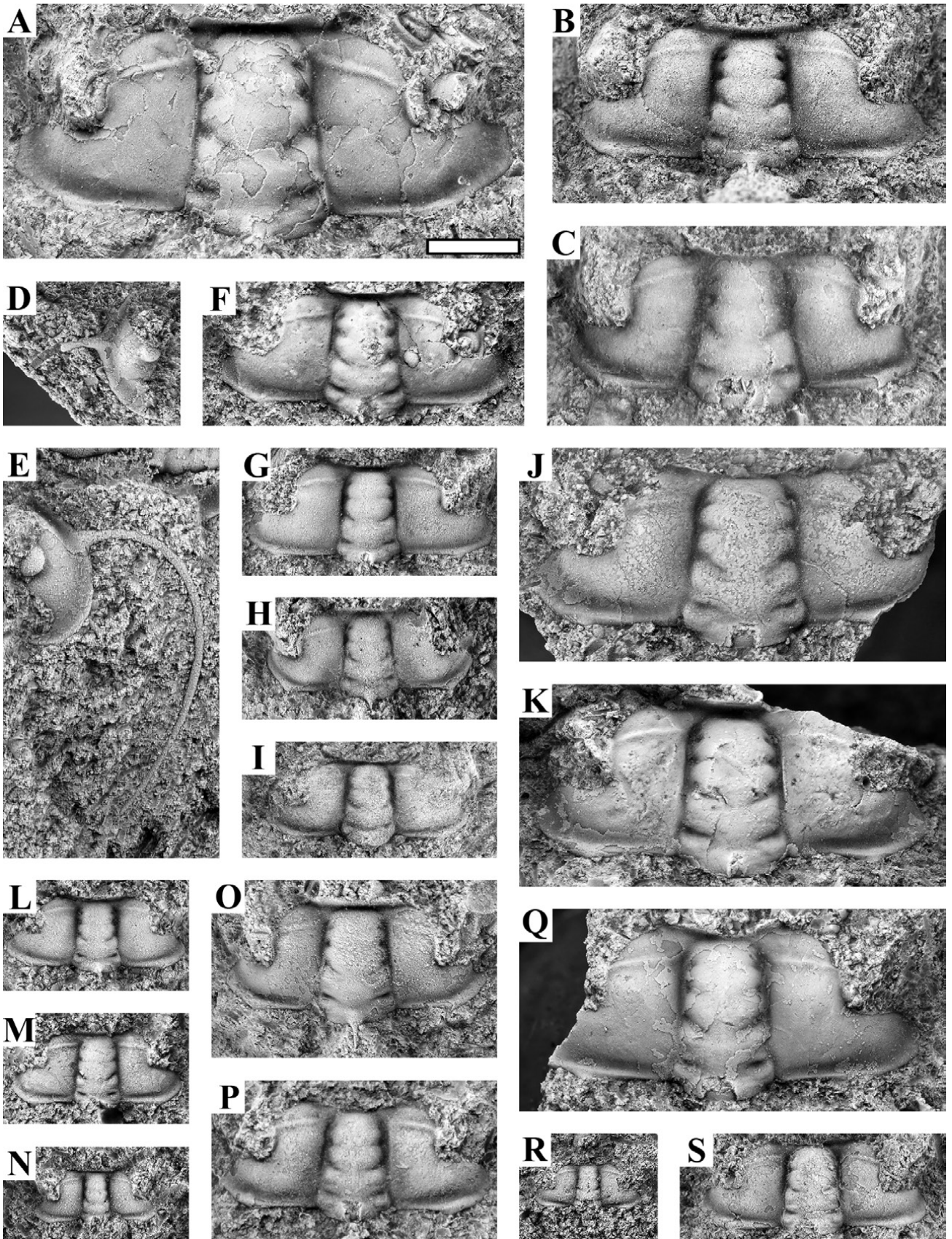
Ctenopyge sp. 2
Fig. 31B

Material. One free cheek from sample GM 1922-141P that also contains *S. angustus*, *C. tumidoides* and *C. tumida*. This assemblage is indicative of the lowermost part of the *P. acutidens–C. tumida* Zone. The sample is from locality 6.

Remarks. The free cheek is 3 mm long excl. spine and *c.* 5.5 mm incl. spine, but which is broken. The spine is rather straight for a *Ctenopyge* and overall, the specimen resembles the free cheeks assigned to *C. affinis* and *C. magna* n. sp. The co-occurring *C. tumida* and *C. tumidoides* have free cheeks with a much different morphology and no other cranidia of *Ctenopyge* have been found at this level. In comparison with the free cheeks assigned to *C. affinis* and *C. magna* n. sp., *Ctenopyge* sp. 2 is relatively wider, and it also has a broader lateral border and a posterior margin that appears to be approximately twice as long. Hence, the discussed free cheek is not likely to be an early representative of *C. affinis* or *C. magna* n. sp., and it may represent a new species.

Genus *Sphaerophthalmus* Angelin, 1854
Type species: *Trilobites alatus* Boeck, 1838, designated by Linnarsson (1880).

Sphaerophthalmus alatus (Boeck, 1838)
Fig. 32
1922   *Sphærophthalmus major* Lake – Westergård, pp. 163–165, pl. XIII, figs 9–19.
Non 1922 *Sphærophthalmus alatus* (Boeck) – Westergård, pp. 165–166, pl. XIII, figs 20–29 [= *Triangulopyge humilis*].
v 1923   *Sphaerophthalmus major* Lake [*partim*] – C. Poulsen, pp. 47–48, pl. 1, fig. 15; non textfig. 17a–b [= *S. angustus*].
v Non 1923 *Sphaerophthalmus alatus* Boeck – C. Poulsen, pp. 49–50 [= *Triangulopyge humilis*].
1957   *Sphaerophthalmus alatus* (Boeck 1838) – Henningsmoen, pp. 212–215, pl. 2, fig. 15; pl. 5; pl. 22, figs 18–26.
1973   *Sphaerophthalmus alatus* (Boeck, 1838) – Schrank, pp. 834–835, pl. X, figs 21–23; pl. XI, figs 1–15.
2012   *Sphaerophthalmus alatus* (Boeck, 1838) [*partim*] – Høyberget & Bruton, pp. 438–439, figs 4A, H, 5A–H, J–K, non fig. 5i [= *S. angustus*].
2015   *Sphaerophthalmus alatus* (Boeck, 1838) – Schoenemann & Clarkson, pp. 133–139, figs 1A–E, 2.
2016   *Sphaerophthalmus alatus* (Boeck, 1838) – Månsson & Clarkson, pp. 173–178, figs 1–6.
2016   *Sphaerophthalmus alatus* – Ahlberg *et al.*, p. 498, figs 4, 6A–B.
2017   *Sphaerophthalmus alatus* (Boeck, 1838) – Rasmussen *et al.*, pp. 21–22, fig. 6F.
For further synonymy, see Høyberget & Bruton (2012) and Rasmussen *et al.* (2017).

Lectotype. Cranidium PMO 56371 from Gamlebyen, Oslo, Norway. Designated by Størmer (1940) and figured by Henningsmoen (1957, pl. 22, figs 23, 24) and Høyberget & Bruton (2012, figs 5A, D).

Material. Extremely abundant cranidia of which *c.* 1011 are registered, whereas only 23 free cheeks and 2 pygidia have been identified. Most of the material derives from locality 6 (a few older museum samples labelled 'Læså between Hjulmagergård and Vasagård' or just 'Læså' probably also originate from this locality), but a few specimens derive from locality 7. In the studied samples, *S. alatus* co-occurs with *C. affinis*, *C. ahlbergi*, *C. magna* n. sp., *C. tumida*, *C. tumidoides*, *Ctenopyge* sp. 1 and *P. minor*.

Occurrence. Very common in the *P. acutidens–C. tumida* Zone in Scandinavia and Poland; *S. alatus* has been recorded also from the lowermost part of the *P. scarabaeoides* Zone (Henningsmoen 1957; Żylińska 2001, 2002; Høyberget & Bruton 2012). From Bornholm, C. Poulsen (1923) reported it (under the name *S. major*) from the *C. tumida* Subzone [= *P. acutidens–C. tumida* Zone], which is confirmed by the present study. No co-occurrence with *P. scarabaeoides* has been observed in the samples at hand.

▲ **Fig. 29.** *Ctenopyge tumida*, all preserved in anthraconite from locality 6. J–K and Q are from samples dominated by *Ctenopyge tumidoides* and *Sphaerophthalmus angustus*, see text. White scale bar: 2 mm. **A:** Large cranidium, sample L61 (MGUH 33801). **B:** Cranidium, sample ATN-197 (MGUH 33802). **C:** Cranidium, sample ATN-238 (MGUH 33809). **D:** Free cheek, sample ATN-175 (MGUH 33811). **E:** Free cheek, sample ATN-197 (MGUH 33803). **F:** Cranidium, specimen MGUH 1967, originally illustrated by C. Poulsen (1923, pl. 1, fig. 14). **G:** Cranidium, sample ATN-171 (MGUH 33813). **H:** Cranidium, sample GM 2019-17 (MGUH 33816). **I:** Cranidium, sample ATN-197 (MGUH 33804). **J:** Cranidium, sample GM 1922-141J (MGUH 33818). **K:** Cranidium, sample GM 1922-141P (MGUH 33819). **L.** Cranidium, sample ATN-197 (MGUH 33805). **M:** Cranidium, sample ATN-197 (MGUH 33806). **N:** Juvenile cranidium, sample ATN-171 (MGUH 33814). **O:** Cranidium, sample GM 2019-17 (MGUH 33817). **P:** Cranidium, sample L53 (MGUH 33828). **Q:** Cranidium, sample GM 1922-141P (MGUH 33824). **R:** Cranidium, sample ATN-197 (MGUH 33807). **S:** Cranidium, sample ATN-175 (MGUH 33812).

Comparison. For comparison with *S. angustus, C. affinis* and *T. humilis,* see these species and remarks below.

Remarks. In general, *S. alatus* and *S. angustus* were not separated by C. Poulsen (1923) and except for GM 1922-141P, all the museum samples with *S. alatus* and *S. angustus* listed in Appendix 1 were labelled as *S. major.*

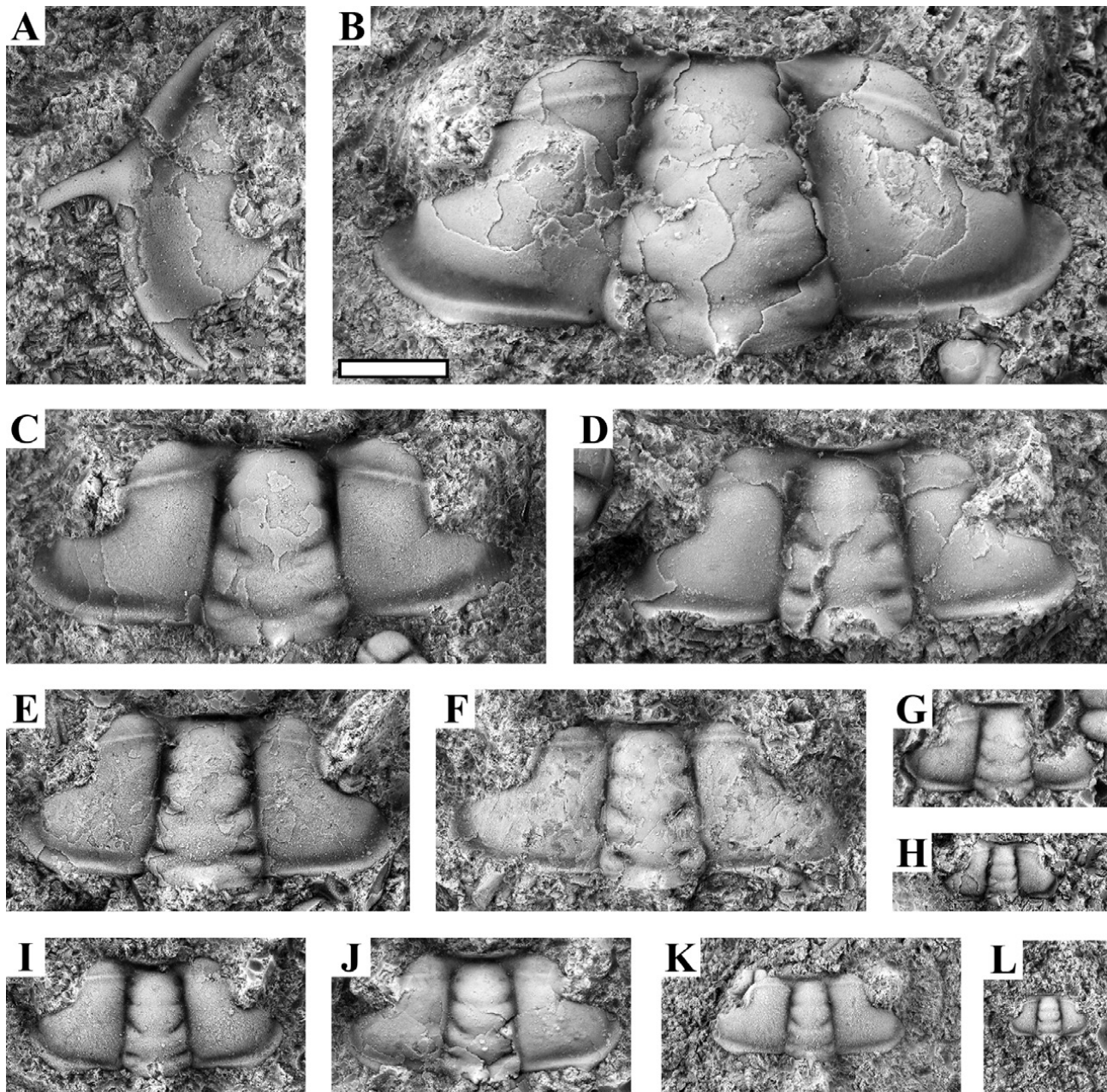Large cranidia of *S. alatus* have a tapering glabella (Fig. 32A–D) whereas the glabella is parallel-sided in smaller specimens (Fig. 32E–O). The distinct S1, which

Fig. 30. A–L. *Ctenopyge tumidoides,* all preserved in anthraconite from locality 6. White scale bar: 2 mm. The specimens shown in B and C are from the *P. acutidens–C. tumida* Zone; the remaining material is assumed to be from the *S. modesta–S. angustus* Zone. **A:** Free cheek, sample L87 (MGUH 22829). **B:** Very large cranidium, sample L57 (MGUH 33832). **C:** Large cranidium, Sample L87 (MGUH 33830). **D:** Large cranidium, Sample L87 (MGUH 33831). **E:** Cranidium, sample L71 (MGUH 33834). **F:** Cranidium, sample L80 (MGUH 33835). **G:** Cranidium from sample ATN-190, which contains many cranidia of *Ctenopyge tumida* and *Sphaerophthalmus alatus* as well as several cranidia of *C. tumidoides* (MGUH 33838). **H:** Juvenile cranidium, sample ATN-145 (MGUH 33839). **I:** Cranidium from sample ATN-197, which contains many cranidia of *Ctenopyge tumida* and *Sphaerophthalmus alautus* as well as *C. tumidoides* (MGUH 33808). **J:** Cranidium from sample GM 1922-141P, which is dominated by *Ctenopyge tumida* and *Sphaerophthalmus alatus* (MGUH 33820). **K:** small cranidium GM 1922-141N (MGUH 33842). **L.** Juvenile cranidium GM 1922-141G (MGUH 33843).
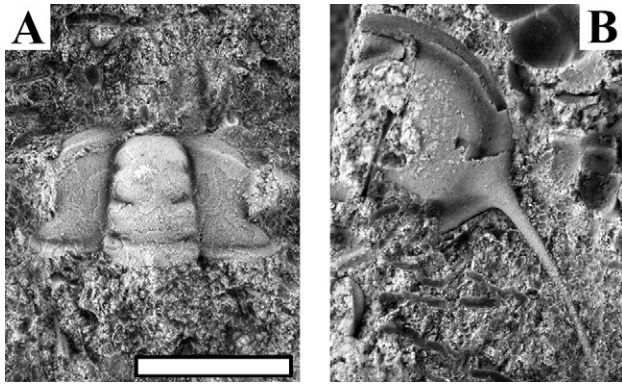
Fig. 31. A: *Ctenopyge* sp. 1, cranidium, sample L77, anthraconite, loc. 7 (MGUH 33844). **B:** *Ctenopyge* sp. 2, free cheek, sample GM 1922-141P, anthraconite, loc. 6 (MGUH 33821). The white scale bar: 2 mm.

is important for identification, is shallower in larger cranidia, especially mesially. Due to these changes, cranidia become increasingly *S. angustus*-like with size and very large cranidia are exceedingly similar (Fig. 32A–B). Still, S1 is marginally more distinct and the postocular cheeks bend down just slightly stronger, but small and medium-sized cranidia are much easier to distinguish. It is emphasized that the illustrated '*angustus*-like' very large *S. alatus* cranidia derive from samples containing numerous, readily identified smaller cranidia of *S. alatus* co-occurring with *C. tumida*.

Pygidia are mostly overlooked, as they are lying sideways in the sediment due to the long caudal spine (cf. Høyberget & Bruton 2012); no attempt has been made to identify isolated spines from free cheeks and pygidia.

Sphaerophthalmus angustus (Westergård, 1922)
Fig. 33
1922	*Ctenopyge flagellifera angusta* n.var. [*partim*] – Westergård, p. 153, pl. 11, figs 2–5, 8.
v 1923	*Ctenopyge flagellifera* Angelin var. *angusta* Westergård [*partim*] – C. Poulsen, p. 39.
v 1923	*Sphaerophthalmus major* Lake [*partim*] – C. Poulsen, pp. 47–48, textfig. 17a–b.
1957	*Ctenopyge (Eoctenopyge) angusta* Westergård – Henningsmoen, p. 187, pl. 5, pl. 19, figs 11–16, 18.
2012	*Sphaerophthalmus angustus* (Westergård, 1922) – Høyberget & Bruton, pp. 439–440, Figs 4B and A–F.
2012	*Sphaerophthalmus alatus* (Boeck, 1838) [*partim*] – Høyberget & Bruton, pp. 438–439, fig. 5i.
2016	*Sphaerophthalmus angustus* (Westergård, 1922) – Rasmussen *et al.*, pp. 19–20, fig. 9A.

For further synonyms, see Henningsmoen (1957) and Høyberget & Bruton 2012.

Lectotype. Cranidium SGU305, figured by Westergard (1922, pl. 11, fig. 3) from Andrarum, southern Sweden, designated by Henningsmoen (1957).

Material. >911 cranidia and at least 23 free cheeks. The far majority of the material is from locality 6, but a few specimens derive from locality 7. On Bornholm, the species co-occurs with *C. tumidoides*, *Ctenopyge* sp. 2, *P. planicauda*, *P. acutidens* and *C. tumida*.

Occurrence. This species has hitherto been considered characteristic of the *S. modestus*–*S. angustus* Zone in Scandinavia (Henningsmoen 1957; Høyberget & Bruton 2012; Nielsen *et al.* 2020). From Bornholm, C. Poulsen (1923) reported "var. *angusta*" as common in the upper part of what he called the *C. flagellifer* Subzone (see remarks). However, the material at hand suggests that *S. angustus* on Bornholm ranges from the *S. modestus*–*S. angustus* Zone, where it is associated with *C. tumidoides*, into the basal part of the *P. acutidens*–*C. tumida* Zone, where it is associated with *C. tumidoides*, *C. tumida* and *P. acutidens* (for details, see section on 'Olenid zonation').

Comparison. This species resembles *S. alatus*, but in the latter the glabellar furrows are deeper and more distinct and confluent with the axial furrows. S1 is particularly distinct in *S. alatus* and there is no shallowing towards the axial furrow. In *S. angustus,* the occipital furrow and S1 are less distinctly impressed and with some shallowing towards the axial furrow. The postocular cheeks of *S. alatus* are more strongly bent downwards than in *S. angustus*, hence the cranidial width across the postocular cheeks (tr.) is larger in the latter. In the free cheeks, the posterior border is straight in *S. angustus* and typically a little curved in *S. alatus,* but atypical specimens with a straight posterior margin occurs also (Fig. 32R).

Remarks. The taxon was described as occurring commonly in the section at locality 6 (C. Poulsen 1923, p. 39), but the few samples labelled as '*Ctenopyge flagellifera* var. *angusta*' (GM 1922-140B) contain only *S. flagellifer* and *S. drytonensis* (examples are shown in Figs 34M, 35E–F, H, J). Sample GM 1922-141P (originally labelled as *S. major* [i.e. *S. alatus*]) was exhibited in the Geological Museum in 1960 as *Ctenopyge angusta*, showing that C. Poulsen realized the misidentification of the cranidia at that stage. Several additional museum samples contain *S. angustus* (listed in Appendix 1), but all were labelled as *S. major*.
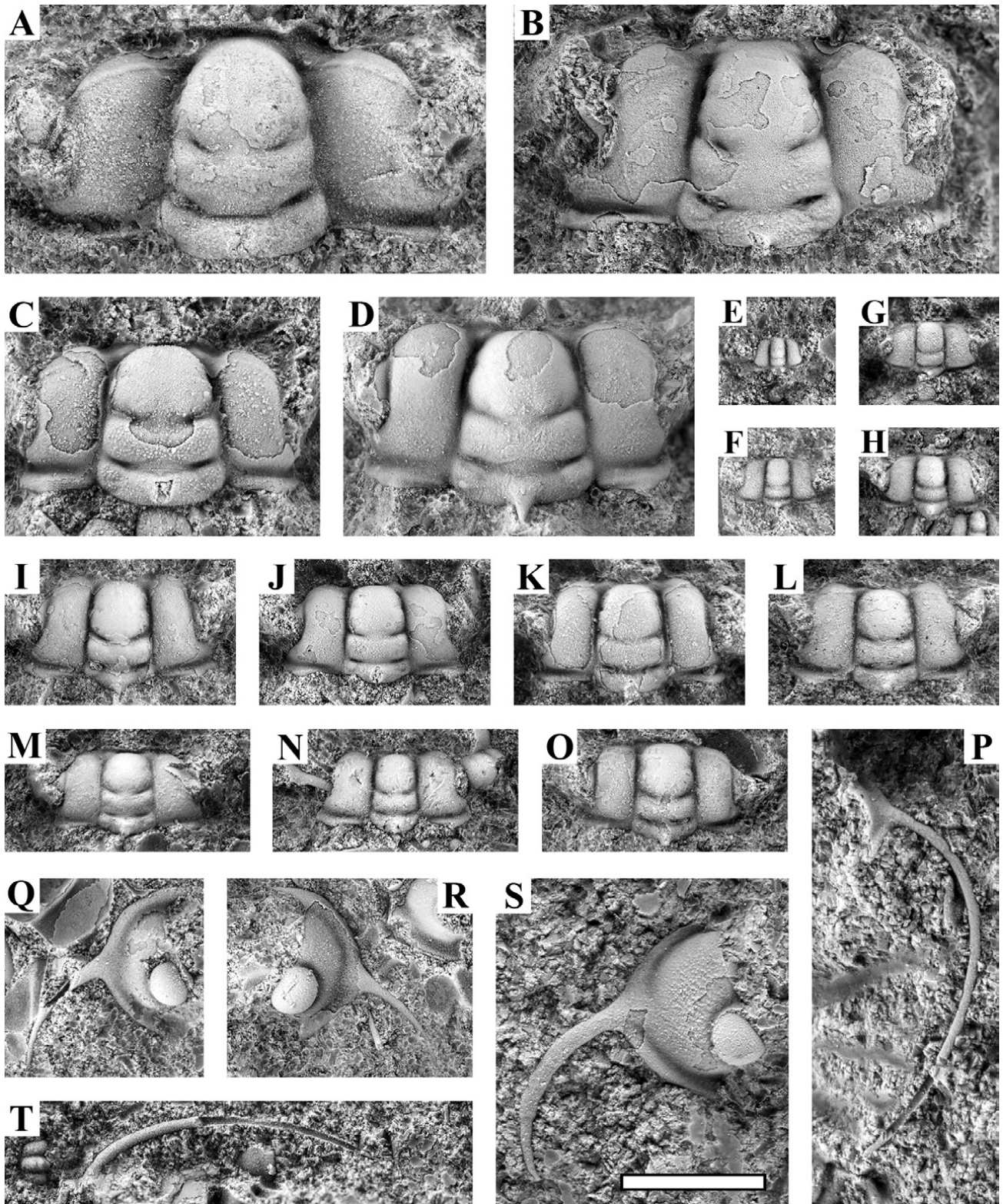
Sphaerophthalmus drytonensis (Cobbold, 1934)
Fig. 34, Fig. 35P–T.
? 1894	*Ctenopyge Acadica,* n. sp. – Matthew, pp. 109–110, pl. XVII, fig. 13a–e.

1922   *Ctenopyge flagellifera* (Angelin) [*partim*] – Westergård, pp. 152–152, pl. X, figs 19, 21a; pl. XI, fig. 1 [see remarks].

v 1923   *Ctenopyge flagellifera* Angelin [*partim*] – C. Poulsen, pp. 38–39, textfig. 15; pl. 1, figs 12?–13.

v 1923   *Ctenopyge flagellifera* Angelin var. *angusta* Westergård [*partim*] – C. Poulsen, p. 39.

1957   *Ctenopyge (Eoctenopyge) drytonensis* Cobbold

1934 [*partim*] – Henningsmoen, pp. 188–189, pl. 5, pl. 18, figs 5–9 and 11–14; non fig. 10 [= *S. flagellifer*].

1957 *Ctenopyge (Eoctenopyge) flagellifera* (Angelin 1854) [*partim*] – Henningsmoen, pp. 189–191, pl. 18, fig. 1.

2012 *Sphaerophthalmus drytonensis* (Cobbold, 1934) – Høyberget & Bruton, pp. 441–442, fig. 8.

2016 *Sphaerophthalmus drytonensis* Cobbold, 1934 – Rasmussen *et al.*, p. 20, fig. 9D,

For further synonymy, see these publications.

Holotype. Cranidium GSM 51776 from Dryton Brook, Rushton area, Shropshire, England. Figured by Cobbold (1934, pl. 45, fig. 9) and Henningsmoen (1957, pl. 18, fig. 8).

Material. External mould of one complete specimen, 486 cranidia and 114 free cheeks from the *C. flagellifer* Zone at locality 6. The species is associated wth common *C. flagellifer;* a single pygidium of *Protopeltura praecursor* has been found in one sample.

Occurrence. In the Oslo Region, the species ranges from the *S. postcurrens* Zone into the *S. flagellifer* Zone (Henningsmoen 1957, Høyberget & Bruton 2012). From Sweden, *S. drytonensis* has been reported only from the *S. flagellifer* Zone at Hunneberg (Rasmussen *et al.* 2016), but it has most likely been mixed with *S. flagellifer* in previous studies. In our interpretation, much of the material described as *S. flagellifer* by Westergård (1922) from Andrarum, Scania, represents *S. drytonensis* (see remarks). This is the first report of *S. drytonensis* from Bornholm, where it occurs commonly in the *S. flagellifer* Zone.

Comparison. The free cheek is distinguished from those of the co-occurring *S. flagellifer* by having a slightly more sturdy, less curving and shorter spine; the posterior lateral margin is rather strongly convex (dorsal view) and shorter than the less convex anterior lateral margin; the posterior border is comparatively wide and clearly wider than the anterior lateral border; the border furrow is indistinct inside the spine base. The most characteristic separating feature is, however, the asymmetry of the lateral margin behind and in front of the spine base: The obtuse inner spine angle is placed more laterally relative to the base of the spine than the outer spine angle. In comparison, the free cheek of *S. flagellifer* has a moderately narrow lateral border of nearly equal width throughout (minor widening posteriorly); the spine is a more gracile, longer and curves more strongly; the border furrow continues without shallowing inside the spine base; there is no asymmetry in the position of the lateral margin behind and in front of the spine base; the posterior margin is longer than the anterior margin so the spine is situated relatively anteriorly and overall, the lateral margin of the free cheek curves evenly throughout. The cranidia of the two species are very alike. The key separating feature is a fairly impressed, elongate, often but not always geniculate S1 in *S. drytonensis* that extends to the axial furrows, as opposed to the pit-like, rather shallow S1 in *S. flagellifer* that does not reach the axial furrows. Other differences like a longer frontal area (sag.) in *S. drytonensis*, a more strongly tapering glabella, a shallowing of the axial furrow at the anterior corners of the glabella, presence of shallow S2 and S3 and convex versus flat gently sloping interocular area (Henningsmoen 1957, Høyberget & Bruton 2012) have proven impossible to apply as consistent separating characters in the material from Bornholm; for further comments, see remarks.

Remarks. Sphaerophthalmus drytonensis is very common on Bornholm and actually more common than the associated *S. flagellifer.* The cranidium illustrated as *C. flagellifera* by C. Poulsen (1923 pl. I, fig. 13) is here assigned to *S. drytonensis* whereas the illustrated second cranidium with attached thoracic segments (*ibid.*, pl. I, fig. 12) has a slightly dissolved test and cannot be identified with certainty, but it may also represent *S. drytonensis.*

▲ **Fig. 32.** *Sphaerophthalmus alatus*, all preserved in anthraconite from locality 6. White scale bar: 2 mm. Note the tapering glabella in large cranidia vs. the parallel-sided glabella in small cranidia; see text for further remarks. **A:** Very large cranidium, sample ATN-112 (MGUH 33845). **B:** Very large cranidium with comparatively narrow occipital ring (sag.), sample L81 (MGUH 33846). **C:** Large cranidium, sample ATN-133 (MGUH 33848). **D:** Large cranidium, sample ATN-205 (MGUH 33734). **E:** Juvenile cranidium, sample ATN-134 (MGUH 33699). **F:** Juvenile cranidium, sample GM 1902-1209 (MGUH 33763). **G:** Juvenile cranidium, sample ATN-134 (MGUH 33700). **H:** Juvenile cranidium, sample ATN-134 (MGUH 33701). **I:** Cranidium, sample ATN-116 (MGUH 33710). **J:** Cranidium, sample ATN-139 (MGUH 33849). **K:** Cranidium, sample ATN-222 (MGUH 33705). **L:** Cranidium, sample ATN-103 (MGUH 33722). **M:** Cranidium, sample ATN-146 (MGUH 33728). **N:** Cranidium, sample ATN-117 (MGUH 33687). **O:** Cranidium, sample ATN-113 (MGUH 33717). **P:** Free cheek, sample ATN-238 (MGUH 33810). **Q:** Free cheek, sample ATN-146 (MGUH 33729). **R:** Free cheek with atypical straight posterior margin (i.e. *S. angustus*-like), sample ATN-134 (MGUH 33702). The associated fauna shows that this free cheek is from the upper part of the *P. acutidens–C. tumida* Zone well above the range of *S. angustus*. **S:** Free cheek, sample L81 (MGUH 33847). **T:** Pygidium with large spine (side view), sample ATN-171 (MGUH 33815).
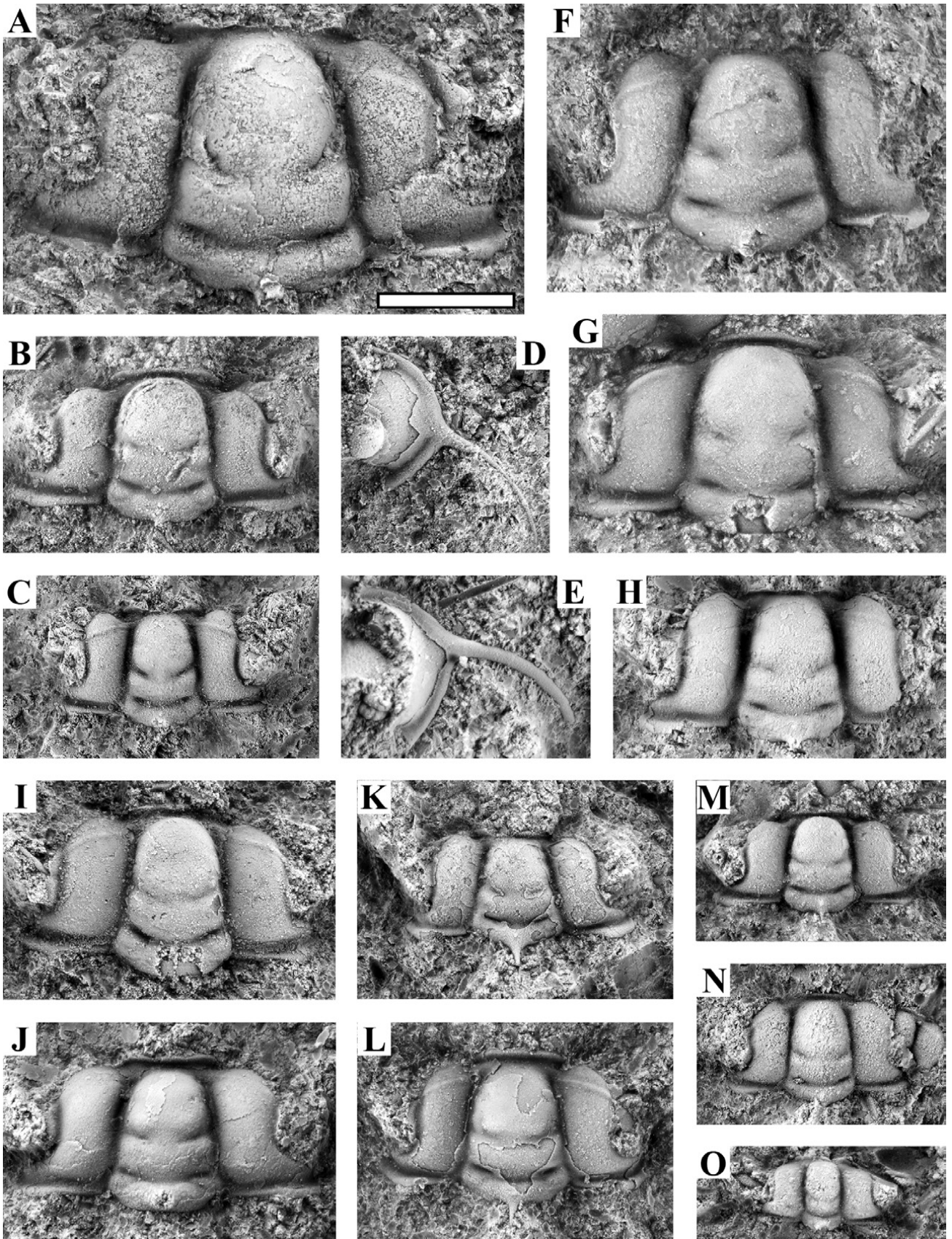
The cranidia of *S. flagellifer* and *S. drytonensis* are exceedingly alike and identification has been based exclusively on the morphology of S1 as stated above. A slight dissolution of the test surface is a problem in several samples (see e.g. Figs 34I, 35L–M) and this obviously does not make it easier to differentiate the cranidia. Flattened cranidia preserved in shale cannot be assigned. In addition to the morphology of S1, there seems to be a trend that S2 and S3 often are visible in *S. drytonensis*, but this is not always the case. S1–S3 seem to be more distinctly impressed in juvenile cranidia, probably including juveniles of *S. flagellifer*, and small specimens appear impossible to assign safely.

The free cheeks are very characteristic and readily separated. We note that the ratio in this study between identified cranidia of *S. flagellifer*/*S. drytonensis* is 0.43 (207 counted specimens vs. 486 specimens) which compares reasonably well with the ratio between the more readily identified free cheeks (0.36), indicating that the chosen approach to identification of cranidia is plausible although some mixing may persist, in part due to the intermittent dissolution of the test surface.

According to the criterion used herein for separation of *S. flagellifer* and *S. drytonensis,* the cranidia of *S. flagellifer* illustrated by Westergård (1922) all represent *S. drytonensis* and the only safely assigned skeletal part of *S. flagellifer* illustrated is the free cheek (*ibid*. pl. X, fig. 20 [neotype]). This indicates that *S. drytonensis* is more widespread in Sweden than currently reported. It is, however, difficult to ascertain whether or not S1 reaches the axial furrows based on illustrations in dorsal view, so the reassignment of Westergårds illustrated material may be taken as tentative.

The semi-complete specimen illustrated by Henningsmoen (1957, pl. 18, fig. 1) as *C. flagellifera* has distinct, elongate S1 and is here allocated to *S. drytonensis*.

Ctenopyge acadica Matthew, 1894 was synonymized with *S. flagellifer* by Henningsmoen (1957). However, the drawn illustration of the *C. acadica* cranidium (Matthew 1894, pl. 17, fig. 13a) shows a transglabellar S1 as well as short S2 and S3 furrows and this pattern was described also in the accompanying text. Hence, it is unlikely that *C. acadica* is a synonym of *S. flagellifer*. The genal spine is also drawn rather short,

drytonensis-like, but there is not indicated an asymmetry of the inner and outer genal angle and the posterior border is not widening. For the time being we prefer an assignment of the Bornholm material to *S. drytonensis*, which in Scandinavia is a well-defined taxon. A restudy of the type material of *C. acadica* and notably its free cheek is needed to unravel whether or not it is a senior synonym of *S. drytonensis*; for the time being we regard *C. acadica* as a *nomen dubium*.

Sphaerophthalmus flagellifer **Angelin, 1854**
Fig. 35A–O.

1922   *Ctenopyge flagellifera* (Angelin) [*partim*] – Westergård, pp. 152–152, pl. X, fig. 20; non figs 19, 21a; pl. XI, fig. 1 [= *S. drytonensis*; see remarks on this species above].

v 1923 *Ctenopyge flagellifera* Angelin [*partim*] – C. Poulsen, pp. 38–39, non textfig. 15; pl. 1, figs 12–13 [= *S. drytonensis*].

v 1923 *Ctenopyge flagellifera* Angelin var. *angusta* Westergård [*partim*] – C. Poulsen, p. 39.

Non 1952 *Ctenopyge flagellifera* (Angelin) – Hutchinson, pp. 87–88, pl. IV, fig. 11.

1957   *Ctenopyge (Eoctenopyge) flagellifera* (Angelin 1854) [*partim*] – Henningsmoen, pp. 189–191, pl. 2, fig. 17; pl. 5; pl. 18, figs 2–4, non fig. 1 [= *S. drytonensis*].

1973   *Ctenopyge (Eoctenopyge) flagellifera* (Angelin 1854) – Schrank, p. 822, pl. VI, figs 13, ?14, ?15.

2012   *Sphaerophthalmus flagellifer* Angelin, 1854 – Høyberget & Bruton, pp. 442–444, figs 4E, 9A–H.

2017   *Sphaerophthalmus flagellifer* Angelin, 1854 – Rasmussen *et al.*, p. 22.

For further synonymy, see Høyberget & Bruton (2012) and Rasmussen *et al.* (2017).

Neotype. Free cheek SGU 5510 from Andrarum, southern Sweden, the same locality as Angelin's lost type specimen derived from, designated by Henningsmoen (1957). Illustrated by Linnarsson (1880, pl. 1, fig. 14) and Westergård (1922, pl. X, fig. 20).

Material. 207 cranidia and 41 free cheeks, all from locality 6. The species is associated with common

---

▲ **Fig. 33.** *Sphaerophthalmus angustus*, all preserved in anthraconite from locality 6. White scale bar: 2 mm. **A:** Large cranidium, sample L60 (MGUH 33851). **B:** Cranidium, sample GM 1922-141P (MGUH 33825). **C:** Cranidium, sample L92 (MGUH 33852). **D:** Free cheek, note the straight posterior margin, sample L80 (MGUH 33836). **E:** Free cheek, note the straight posterior margin, sample ATN-145 (MGUH 33840). **F:** Large cranidium, sample L78 (MGUH 33853). **G:** Large cranidium, sample GM 1922-141P (MGUH 33826). **H:** Cranidium, sample L124 (MGUH 33854). **I:** Cranidium, sample GM 1922-141P (MGUH 33822). **J:** Cranidium, sample L124 (MGUH 33855). **K:** Cranidium with preserved occipital spine and unusually short glabella, sample L80 (MGUH 33837). **L:** Cranidium with preserved occipital spine, sample L57 (MGUH 33833). **M:** Cranidium with preserved occipital spine, sample GM 1922-141P (MGUH 33827). **N.** Cranidium, sample ATN-151 (MGUH 33856). **O:** Juvenile cranidium, sample GM 1922-141P (MGUH 33823).
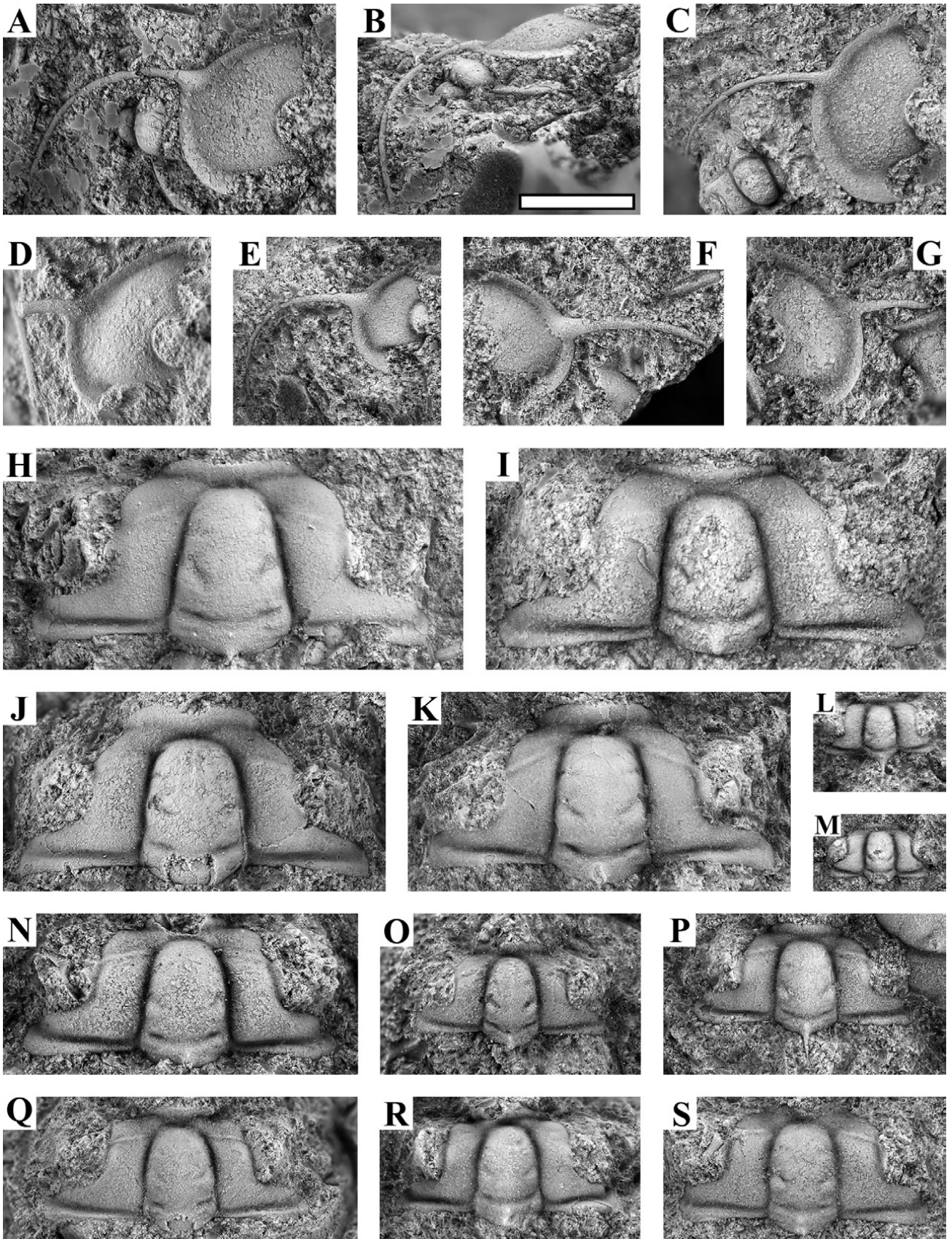
Sphaerophthalmus drytonensis whereas *Protopeltura praecursor* has been found in only one sample.

Occurrence. Common in the eponymous zone in Scandinavia, Great Britain and Canada (Westergård 1922; Henningsmoen 1957; Høyberget & Bruton 2012). In the Oslo Region, the species ranges into the lowermost *S. modestus–S. angustus* Zone (Høyberget & Bruton 2012). C. Poulsen (1923) reported '*Ctenopyge*' *flagellifera* only from the eponymous (sub)zone on Bornholm but the majority of the specimens in the museum collection represents *S. drytonensis.*

Comparison. Sphaerophthalmus flagellifer can be differentiated from *S. modestus* by the presence of an occipital spine, and by having more slender (exsag.) and longer (tr.) postocular cheeks. The genal spine is also located much further forwards in the free cheeks of *S. flagellifer. Sphaerophthalmus flagellifer* has wider (tr.) and longer (exsag.) postocular cheeks than *S. angustus* and midline of the eyes is situated opposite S2 compared to S1 in *S. angustus.* For comparison with *S. drytonensis,* see that species.

Remarks. Høyberget & Bruton (2012) gave a thorough description of *S. flagellifer* including a drawn reconstruction of a complete specimen (*ibid.* fig. 4E). This was, however, based on small specimens, and they stated that the posterior lateral margin of the free cheek becomes longer in larger specimens (and thus displaces the genal spine forwards). For comments on assignment of the cranidia illustrated by Westergård (1922) and C. Poulsen (1923), see remarks on *S. drytonensis.* The thoraxes and pygidia illustrated by Westergård (1922) cannot be assigned to species for the time being, as these skeletal parts of *S. drytonensis* are unknown.

The poorly illustrated *C. flagellifera* from Cape Breton Island, Canada, reported by Hutchinson (1952), has a distinct S1 and is not likely to represent *S. flagellifer.* The illustration does not permit a reassignment.

Westergård (1922) and Henningsmoen (1957) discussed *Ctenopyge falcifera* Lake, 1923 as a possible synonym of *S. flagellifer.* The specimen is preserved in shale and the free cheek is unknown. Lake (1913) described S1 as 'decidedly oblique' which is not bringing the rounded outlined typical for *S. flagellifer* to mind, but further considerations are pointless until better preserved material (including free cheeks) becomes available.

Genus *Triangulopyge* Høyberget & Bruton, 2012
Type species: *Olenus humilis* Phillips, 1848, by original designation.

Triangulopyge humilis **(Phillips, 1848)**
Fig. 36.

1922	*Sphærophthalmus alatus* (Boeck) – Westergård, pp. 165–166, pl. XIII, figs 20–29.
v 1923	*Sphaerophthalmus alatus* Boeck – C. Poulsen, pp. 49–50.
1957	*Sphaerophthalmus humilis* (Phillips 1848) – Henningsmoen, pp. 215–217, pl. 5; pl. 22, figs 7, 11–15.
1973	*Sphaerophthalmus humilis* (Phillips, 1848) – Schrank, pp. 837–838, pl. XII, figs 14–30.
2012	*Triangulopyge humilis* (Phillips, 1848) – Høyberget & Bruton, p. 447, figs 12A, 13A–J.
2017	*Triangulopyge humilis* (Phillips, 1848) – Rasmussen *et al.*, pp. 22–23, fig. 10B.

For further synonymy, see Høyberget & Bruton (2012) and Rasmussen *et al.* (2017).

Lectotype. Cranidium Ox A287a from the Phillips collection, collected from the White Leaved Oak Shale, Malvern, United Kingdom. Figured by Rushton (1968, pl. 78, fig. 13) and designated by Høyberget & Bruton (2012).

Material. 610 cranidia, five free cheeks and eight pygidia, but the far majority of specimens have not been registered as preparation is needed for safe assignment. The material predominantly derives from locality 6, but a few specimens were collected at Limensgade (localities 8A–B), three samples are from 'Cementen' (i.e. ice-rafted material, Øleå) and one is not labelled. C. Poulsen (1923) reported the species (as *S. alatus*) also from locality 7 but no material from that site is

▲ **Fig. 34.** *Sphaerophthalmus drytonensis,* all preserved in anthraconite from locality 6. White scale bar: 2 mm. **A–B:** Free cheek, dorsal and posterior view, sample L23 (MGUH 33857). **C:** Free cheek, sample ATN-105 (MGUH 33858). **D:** Free cheek, sample ATN-256 (MGUH 33869). **E:** Free cheek, small specimen, sample ATN-105 (MGUH 33859). **F:** Free cheek, sample GM 1922-140C (MGUH 33870). **G:** Free cheek, sample L24 (MGUH 33871). **H:** Large cranidium, sample ATN-105 (MGUH 33860). **I:** Large cranidium, previously illustrated by C. Poulsen (1923 pl. I, fig. 13) as *C. flagellifera* (MGUH 1966). **J:** Cranidium, sample ATN-131 (MGUH 33872). **K:** Cranidium, sample ATN-105 (MGUH 33861). **L:** Small cranidium with intact occipital spine, sample L19 (MGUH 33873). **M:** Cranidium, sample GM 1922-140B (MGUH 33875). **N:** Cranidium, sample L29 (MGUH 33880). **O:** Cranidium, sample L29 (MGUH 33881). **P:** Cranidium with intact occipital spine, sample ATN-105 (MGUH 33862). **Q:** Cranidium, sample ATN-181 (MGUH 33883). **R:** Cranidium, sample ATN-105 (MGUH 33863). **S:** Cranidium, sample L27 (MGUH 33884).
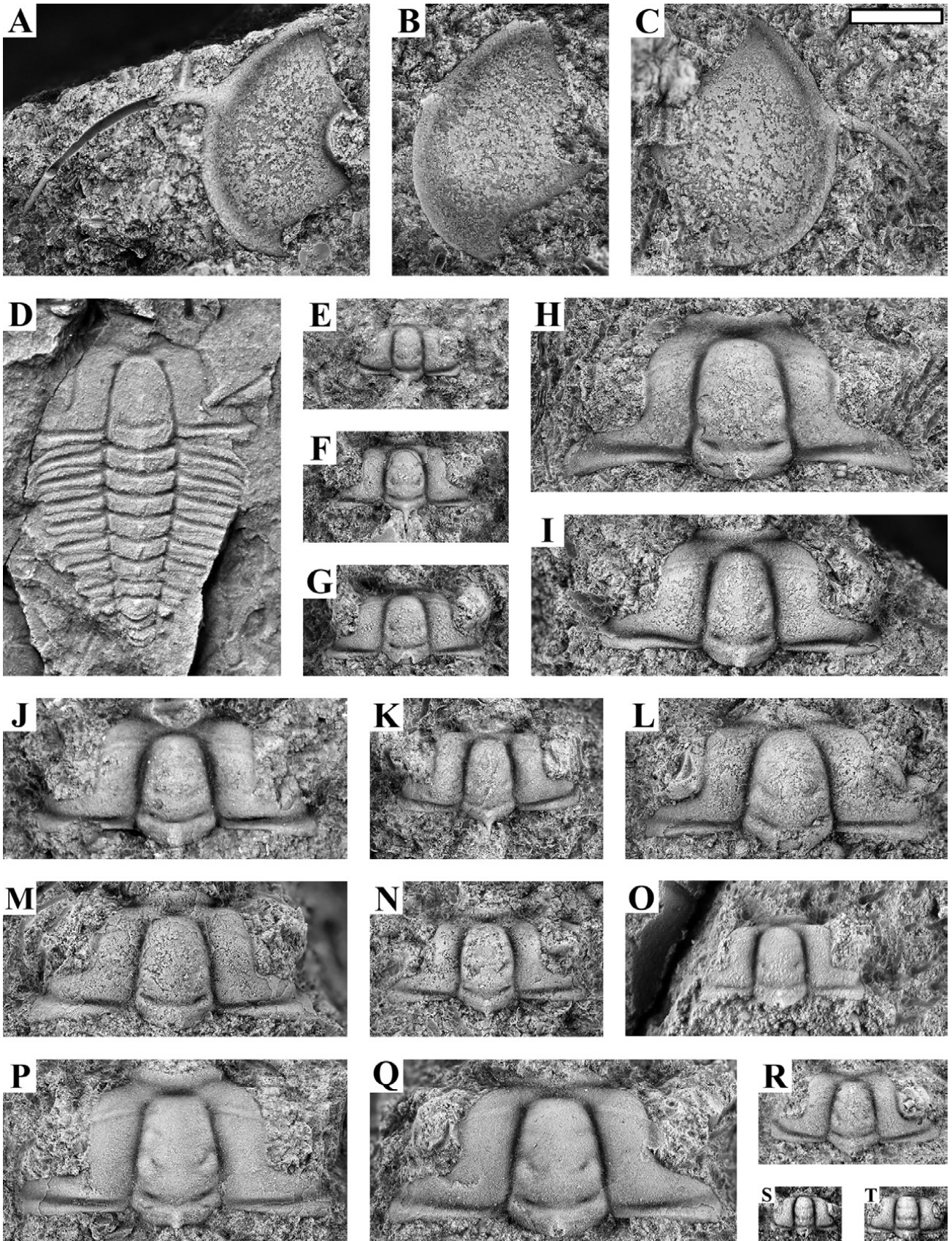
kept in the museum collection. *Triangulopyge humilis* co-occurs with *C. linnarssoni*, *C. pecten*, *C. tenuis*, *C. teretifrons* and *P. scarabaeoides* in the studied samples. The report of this species (under the name *S. alatus*) from the *P. lobata* ['*longicornis*'] Zone (C. Poulsen 1923) is an error, see 'Discussion and conclusions'.

Occurrence. Extremely common in the *P. scarabaeoides* Zone in Scandinavia (Høyberget & Bruton 2012) including Bornholm (this study). *Triangulopyge humilis* was listed also from the *P. lobata* Zone by Terfelt *et al.* (2008), based on Ahlberg *et al.* (1995) who reported phosphatized juvenile specimens from Västergötland. However, that material is considered reworked herein. Outside Scandinavia, *T. humilis* is known from Poland, England, Wales and Canada (Westergård 1922, 1947; Henningsmoen 1957; Żylińska 2001, 2002).

Comparison. In comparison with *T. majusculus*, the cranidium of *T. humilis* is narrower with interocular cheeks that are less than half as wide as glabella at eye-line and postocular cheeks that are about ⅔ as wide (tr.) as the occipital ring, while *T. majusculus* has interocular cheeks that are just slightly narrower than glabella at eye-line and the postocular cheeks are about as wide as the occipital ring. *Triangulopyge humilis* also has an occipital spine, a feature not seen in *T. majusculus* (however, often the spine is not preserved). *Triangulopyge majusculus* has a more rounded and wider pygidium compared to *T. humilis* which has pleural fields markedly narrower than the axis and a more equilateral triangular pygidial outline.

The small cranidia of *T. humilis* and *S. alatus* are superficially somewhat alike, but the palpebral lobes are situated opposite L1 in *T. humilis* and opposite S1 in *S. alatus* and the fixed cheeks are widening (tr.) in front of the palpebral lobes in *T. humilis*, which is very characteristic. Comparing larger cranidia, *S. alatus* has a more distinctly tapering glabella with a rounded front; in *T. humilis* the glabella is less pronouncedly tapering and the antero-glabella is parallel-sided with a more truncate front; S1 is also shallow mesially in *S. alatus*, unlike in *T. humilis*. The two species are readily separated by their pygidia, as *S. alatus* has a long caudal spine, unlike *T. humilis,* but the tiny pygidia are easily overlooked, and registered specimens are rare in the material at hand.

Remarks. We have observed that the occipital spine is longer in small specimens than in large cranidia (Fig. 36).

Genus *Protopeltura* Brøgger, 1882
Type species: *Peltura praecursor* Westergård, 1909, designated by Henningsmoen (1958b).

Protopeltura planicauda (Brøgger, 1882)
Fig. 37E

|	
1922	*Peltura planicauda* Brögger – Westergård, p. 173, pl. XV, fig. 2.
1957	*Protopeltura planicauda* (Brögger 1882) – Henningsmoen, pp. 228–229, pl. 6; pl. 24, figs 11–13.
2017	*Protopeltura planicauda* (Brögger, 1882) – Rasmussen *et al.*, p. 20, figs 9A–B.

For further synonymy, see these references.

Lectotype. Pygidium PMO H2715a from Slemmestad, Norway, originally figured by Brøgger (1882, pl. II, fig. 8). Designated and refigured by Henningsmoen (1957, pl. 24, fig. 13).

Material. One pygidium from locality 6. This is the first record of this species from Bornholm.

Occurrence. Sphaerophthalmus modestus–S. angustus and *P. acutidens–C. tumida* zones in Scandinavia (Westergård 1947; Henningsmoen 1957; Rasmussen *et al.* 2016, 2017). The single specimen at hand co-occurs with *C. tumidoides* and *S. angustus*, suggestive of the *S. modestus–S. angustus* Zone (but see section on 'Olenid zonation').

▲ **Fig. 35.** *Sphaerophthalmus flagellifer* (A–O) and *Sphaerophthalmus drytonensis* (P–T), preserved in anthraconite except D (flattened, preserved in shale). All specimens are from locality 6. White scale bar: 2 mm. *Sphaerophthalmus flagellifer*: **A:** Free cheek, sample L26 (MGUH 33885). **B:** Free cheek, spine is not preserved, sample L26 (MGUH 33886). **C:** Free cheek, sample L28 (MGUH 33889). **D:** Cranidium with thorax, tentatively assigned; this specimen may alternatvely represent *S. drytonensis*, sample GM 1872-1070 (MGUH 33891). **E–F:** Small cranidia with comparaticely distinct S1, sample GM 1922-140B (MGUH 33876 & 33877). **G:** Small cranidium, sample ATN-215 (MGUH 33892). **H:** Large cranidium, sample GM 1922-140B (MGUH 33879). **I:** Cranidium, sample L26 (MGUH 33887). **J:** Cranidium, sample GM 1922-140B (MGUH 33878). **K:** Cranidium, sample L26 (MGUH 33888). **L:** Cranidium with slightly elongate S1, but which do not reach the axial furrows, sample L19 (MGUH 33874). **M:** Cranidium, with slightly elongate but very shallow S1 that do not reach the axial furrows, sample GM 1897 (MGUH 33893). **N:** Cranidium, sample L28 (MGUH 33890). **O:** Cranidium, sample ATN-125 (MGUH 33894). **P:** Large cranidium with comparatively distinct S2 and S3 furrows, sample ATN-105 (MGUH 33864). **Q:** Large cranidium, sample ATN-105 (MGUH 33865). **R:** Cranidium, sample L29 (MGUH 33882). **S:** Juvenile cranidium, tentatively assigned, sample ATN-105 (MGUH 33866). **T:** Juvenile cranidium, tentatively assigned, sample ATN-105 (MGUH 33867).
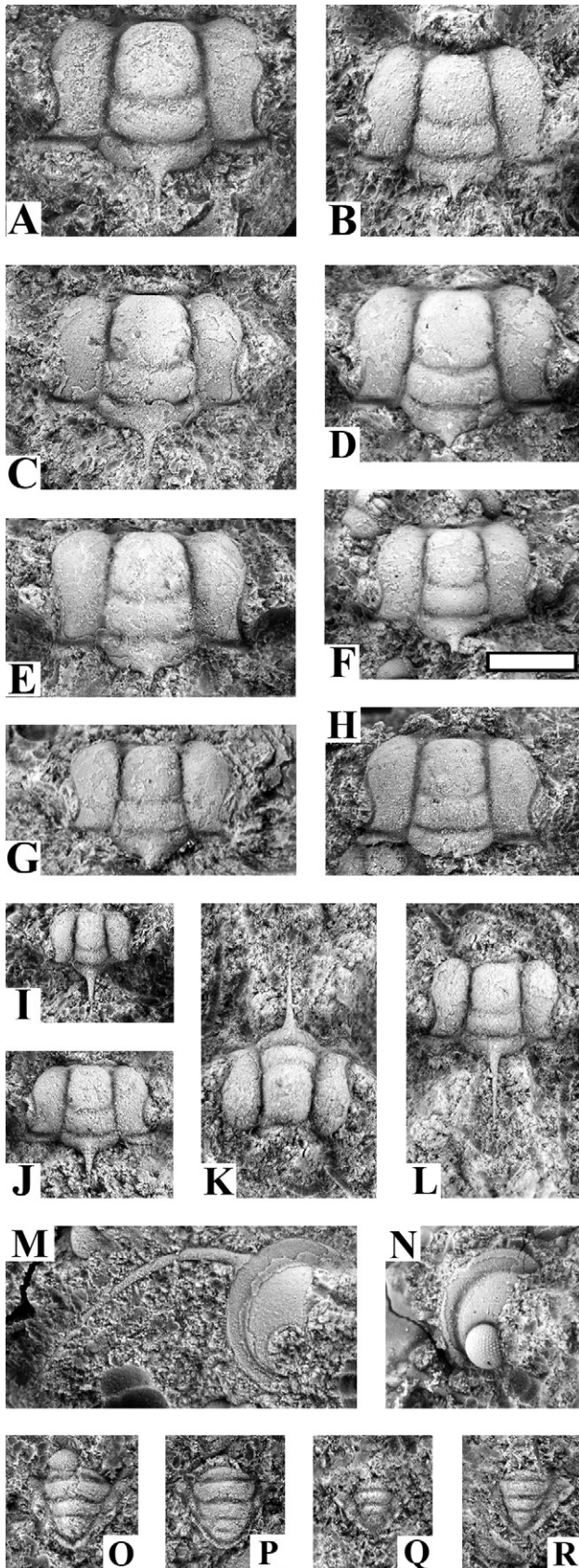
Comparison. In comparison with *P. bidentata*, the pygidium of *P. planicauda* is wider with a rounded outline, while the former has a slightly more triangular overall shape.

Protopeltura praecursor Westergård, 1909
Fig. 37D

1922   *Protopeltura præcursor* (Westergård) – Westergård, p. 171, pl. XIV, figs 23–29, 31; pl. XV, fig. 1.

1957   *Protopeltura praecursor* (Westergård 1909) – Henningsmoen, pp. 229–230, Pl. 2, fig. 2; pl. 6; pl. 24, figs 1-5.

2017   *Protopeltura praecursor* (Westergård, 1909) – Rasmussen *et al.*, p. 21.

For a complete list of synonymy, see Henningsmoen (1957) and Rasmussen *et al.* (2017).

Lectotype. Pygidium PM0 H 2716b [not 2715a as stated by Henningsmoen 1957, p. 229] from Nærsnæs, Norway, originally figured by Brøgger (1882, pl. I, fig. 14c). Designated and refigured by Henningsmoen (1957, pl. 24, fig. 5).

Material. One pygidium, collected at locality 6. It co-occurs with common *S. drytonensis* and *S. flagellifer*.

Occurrence. Comparatively long-ranging species recorded from the *L. neglectus*, *L. postcurrens* and *S. flagellifer* zones in Scandinavia (Nielsen *et al.* 2020). This is the first record of *P. praecursor* from Bornholm.

Comparison. Protopeltura praecursor cannot be confused with any other species occurring in the *S. flagellifer* Zone.

Fig. 36. *Triangulopyge humilis,* all preserved in anthraconite from locality 6. White scale bar is 1 mm. **A**. Large cranidium, sample L41 (MGUH 33787). **B**. Cranidium, sample L45 (MGUH 33895). **C**. Cranidium, sample L39 (MGUH 33896). **D**. Cranidium, sample L38 (MGUH 33791). **E**. Cranidium, sample L39 (MGUH 33897). **F**. Cranidium, sample L43 (MGUH 33769). **G.** Cranidium, sample L42 (MGUH 33898). **H**. Small cranidium with occipital spine, sample GM 1871-671 (MGUH 33899). **I.** Small cranidium with occipital spine, sample GM 1922-142A (MGUH 33779). **J.** Small cranidium with occipital spine, sample GM 1871-671 (MGUH 33900). **K-L.** Small cranidium with occipital spine, frontal and dorsal view, sample GM 1871-675A (MGUH 33901). **M**. Free cheek, sample GM 1922-142I (MGUH 33752). **N**. Free cheek, sample GM 1922-142I (MGUH 33753). **O.** Pygidium, sample L48 (MGUH 33782). **P.** Pygidium, sample L38 (MGUH 33792). **Q.** Pygidium, sample GM 1922-142A (MGUH 33778). **R**. Pygidium, sample GM 1922-142J (MGUH 33795).

Genus *Peltura* Milne Edwards, 1840

Type species: *Entomostracites scarabæoides* Wahlenberg, 1818, designated by Hawle & Corda (1847).

Peltura acutidens Brøgger, 1882
Fig. 37A–C

1922   *Peltura scarabæoides acutidens* Brögger – Westergård, p. 175, pl. XV, figs 14–17.
1957   *Peltura acutidens* Brögger 1882 – Henningsmoen, pp. 233–234, pl. 6; pl. 25, figs 1, 3, 4, 7, 9, 11.
1973   *Peltura acutidens* Brögger, 1882 – Schrank, pp. 940–841, pl. XIV, figs 2–7.
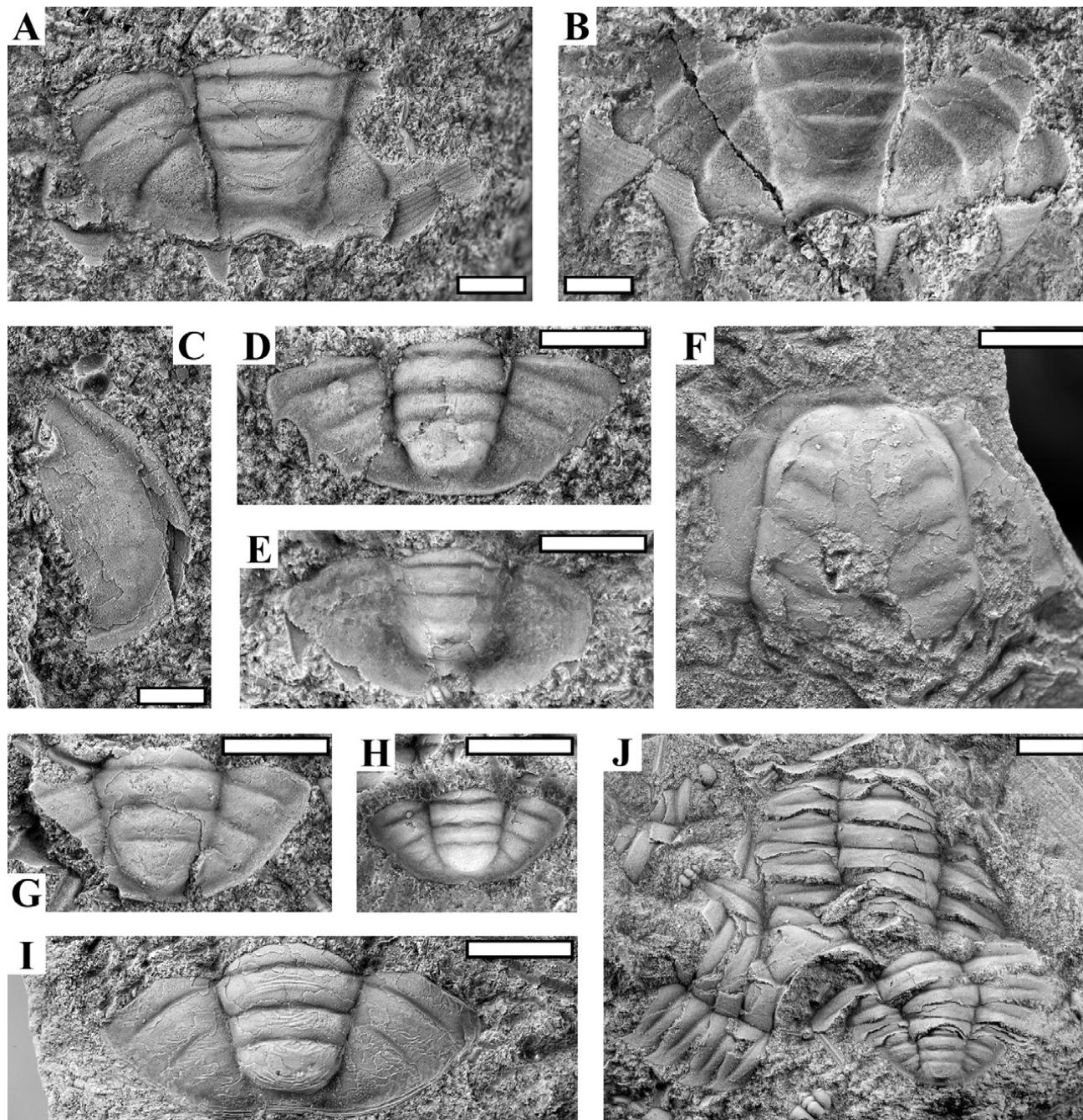
Fig. 37. Pelturids, all preserved in anthraconite from locality 6. White scale bars: 2 mm. **A–C:** *Peltura acutidens.* **A:** Pygidium, sample ATN-327 (MGUH 33902a). **B:** External mould of the specimen illustrated in A showing marginal spines, sample ATN-111 (MGUH 33902b). **C:** Free cheek, sample L82 (MGUH 33903). **D:** *Protopeltura praecursor,* sample ATN-105 (MGUH 33868). **E:** *Protopeltura planicauda,* sample ATN-145 (MGUH 33841). **F–J:** *Peltura minor.* **F:** Cranidium which may belong to one of the thoraxes illustrated in J: Sample ATN-127 (MGUH 33904). **G:** Pygidium, sample ATN-132 (MGUH 33732). **H:** Pygidium, sample ATN-139 (MGUH 33850). **I:** Pygidium, sample ATN-113 (MGUH 33718). **J:** Incomplete thoraxes (two specimens) with pygidium, sample ATN-127 (MGUH 33905).

2017 *Peltura acutidens* Brøgger, 1882 – Rasmussen *et al.*, p. 18.

For further synonymy, see Rasmussen *et al.* (2017).

Lectotype. Pygidium PMO H 2720, collected at Slemmestad, Norway, and originally figured by Brøgger (1882, pl. II, fig. 9). Designated and refigured by Henningsmoen (1957, pl. 25, fig. 11).

Material. One pygidium and one free cheek (?) found at locality 6. *Ctenopyge tumidoides* and *S. angustus* occur in the same samples.

Occurrence. Characteristic for the *P. acutidens–C. tumida* Zone and known from Scandinavia and Poland (Westergård 1922, 1947; Henningsmoen 1957; Rasmussen *et al.* 2016, 2017; Żylińska 2001, 2002). This is the first report of *P. acutidens* from Bornholm, where it seems to be exceedingly rare as many limestone samples are at hand from the *P. acutidens–C. tumida* Zone.

Comparison. Cranidia and free cheeks of *P. acutidens, P. minor, P. scarabaeoides* and *P. westergaardi* are essentially similar and no effort has been made to assign these skeletal parts; pygidia are needed in order to safely identify these species. *Peltura minor* pygidia are readily identified by their lack of marginal spines. In *P. scarabaeoides,* the distance between the inner pair of marginal spines is slightly wider than the anterior half ring; in *P. westergaardi* the distance is equal to or slightly narrower than the anterior half ring and in *P. acutidens* the distance is marginally narrower than the terminal piece. The axis is relatively wide in pygidia of *P. scarabaeoides*, anteriorly occupying >0.4 of the pygidial width, vs. less than 0.4 in the other species discussed. External terrace lines are more extensive on pygidia of *P. scarabaeoides* than seen on *P. westergaardi* pygidia. The border in *P. acutidens* is also more distinct than in *P. scarabaeoides*. *Peltura scarabaeoides* has moderately short marginal spines that typically are bent downwards, while *P. acutidens* and *P. westergaardi* have significantly longer spines and they are typically horizontal. The pygidium of *P. acutidens* is relatively wide with markedly wider pleural fields than in the pygidia of *P. scarabaeoides* and *P. westergaardi*.

Peltura minor (Brøgger, 1882)
Fig. 37F–J
1922 *Peltura minor* (Brögger) – Westergård, p. 175, pl. XV, figs 3–11.
1947 *Peltura minor* (Brögger) – Westergård, pl. 2, fig. 12.
1957 *Peltura minor* (Brögger 1882) – Henningsmoen, pp. 235–236, pl. 6; pl. 25, figs 2, 5.

1973 *Peltura minor* (Brögger, 1882) – Schrank p. 841, pl. XIV, figs 8–9.
2003 *Peltura minor* (Brøgger, 1882) – Terfelt, p. 412, fig. 4K.
2017 *Peltura minor* (Brøgger, 1882) – Rasmussen *et al.*, pp. 18–19.

For further synonymy, see Rasmussen *et al.* (2017).

Lectotype. Pygidium PMO no H 2713a from Slemmestad, Norway, originally figured by Brøgger (1882, pl. II, fig. 10). Designated and refigured by Henningsmoen (1957, pl. 25, fig. 5).

Material. Six pygidia incl. one with nine contiguous thoracic segments, all from locality 6. *Peltura minor* co-occurs with *C. affinis, C. ahlbergi, C. magna* n. sp. and *S. alatus* in the samples at hand.

Occurrence. Characteristic for the *P. acutidens–C. tumida* Zone in Scandinavia (Westergård 1922, 1947; Henningsmoen 1957; Rasmussen *et al.* 2016, 2017), but with an upper range into the very base of the *P. scarabaeoides* Zone (e.g. Westergård 1922, figs 11, 26; Høyberget & Bruton 2012, fig. 2). On Bornholm, it appears to be typical of the upper part of the *P. acutidens–C. tumida* Zone. It is a general trait that *P. minor* appears slightly above the base of the *P. acutidens–C. tumida* Zone in Scandinavia (cf. Westergård 1922).

Comparison. For comparison with *P. acutidens* and *P. scarabaeoides,* see the former.

Remarks. This species has not been reported from Bornholm previously and it seems to be infrequent, as many samples are at hand from the *P. acutidens–C. tumida* Zone. Henningsmoen (1957) defined a *P. minor* Zone, subdivided into four subzones. However, *P. minor* has its FAD in the *P. acutidens–C. tumida* Zone and does not occur in the lower two subzones defined for the zone by Henningsmoen. The reported presence in older strata appears to be a *lapsus calami* (Nielsen *et al.* 2020).

Peltura scarabaeoides (Wahlenberg, 1818)
Fig. 38
1922 *Peltura scarabæoides* (Wahlenberg) [*partim*] – Westergård, pp. 173–174, pl. XV, fig. 18; non pl. XV, figs 12–13 [= *Peltura westergaardi*, see remarks].
v 1923 *Peltura scarabaeoides* Wahlenberg [*partim*] – C. Poulsen, pp. 50–52, textfig. 18; pl. II, figs 6–7; non pp. 58–59, textfig. 22 [= *P. westergaardi*].
1957 *Peltura scarabaeoides scarabaeoides* (Wahlenberg 1821) – Henningsmoen, pp. 237–239, pl. 2, fig. 1; pl. 6; pl. 25, figs 6, 13–14; pl. 26, figs 1–2.
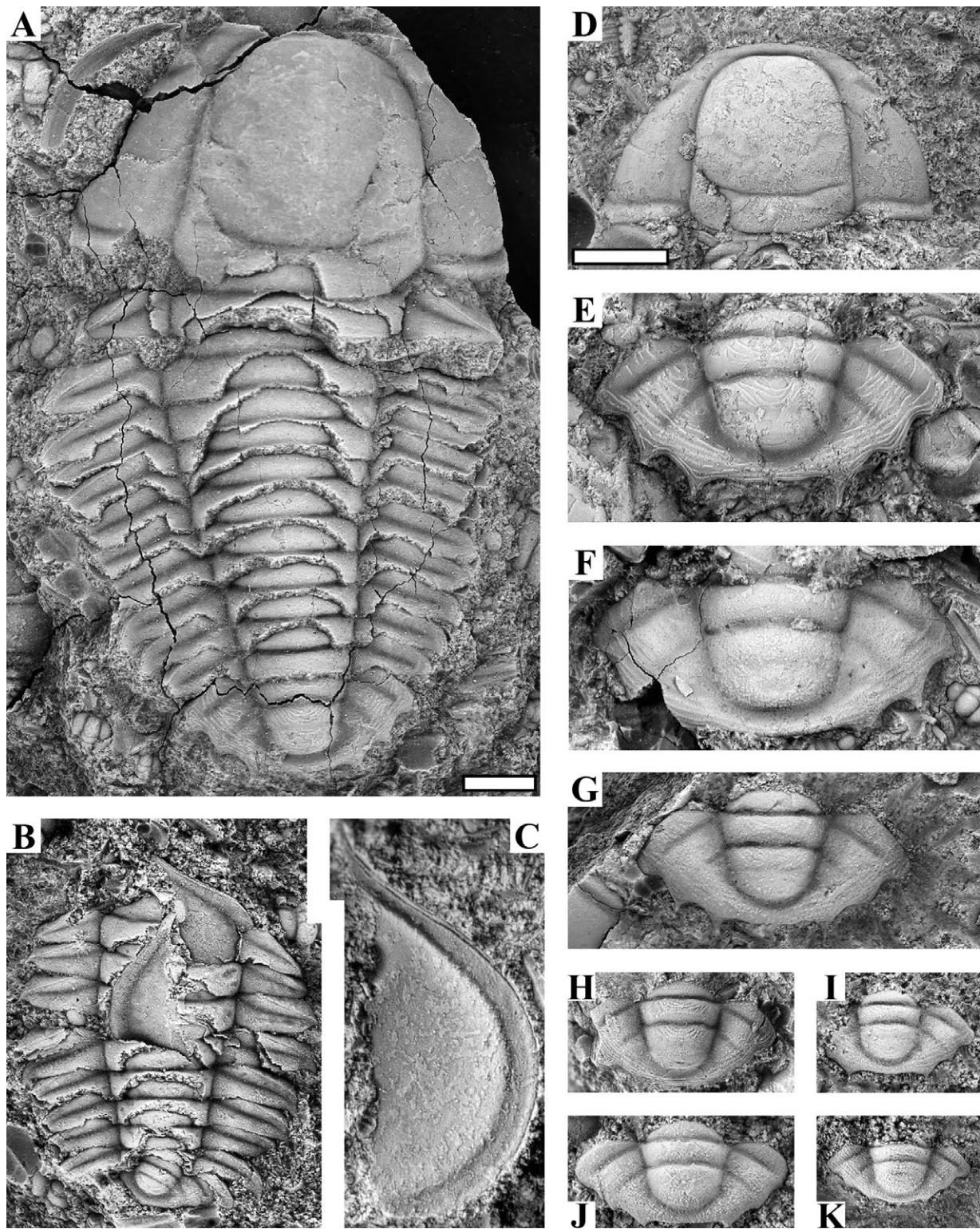
Fig. 38. *Peltura scarabaeoides,* all preserved in anthraconite. White scale bars: 2 mm; note that A is shown at smaller magnification. **A:** Almost complete specimen, found in the Læså stream near Vasagård [probably loc. 6], sample GM 1881-1805 (MGUH 33906). **B:** Pygidium with seven thoracic segments and two partly visible free cheeks, probably exuvium, 'Cementen', Øleå, sample GM 1874-30 (MGUH 33907). **C:** External mould of free cheek, loc. 6, sample L43 (MGUH 33770). **D:** Cranidium possibly belonging to this species, loc. 6, sample GM 1922-142B (MGUH 33799). **E:** Pygidium, found in the Læså area between Hjulmagergård and Vasagård [probably loc. 6], sample GM 1871-626 (MGUH 33908). **F:** Pygidium, loc. 6, sample GM 1922-142C (MGUH 33909). **G:** Pygidium, loc. 6, sample GM 1922-142I (MGUH 33756). **H:** Pygidium, loc. 6, sample GM 1922-142I (MGUH 33757). The broad-based marginal spines point downwards in this small specimen and are difficult to see in dorsal view. **I–K:** Three pygidia, locs 8A–B, sample L17 (MGUH 33742, 33743, 33744).

Non 1958 *Peltura scarabaeoides* (Wahlenberg 1821) – Whittington, pp. 200–206, pl. 38. [= *P. westergaardi*].

1973 *Peltura scarabaeoides scarabaeoides* (Wahlenberg, 1821) [*partim*] – Schrank, pp. 841–842; pl. XIV, fig. 10–15,17–23; non pl. XIV, fig. 16 [= *P. westergaardi*].

2003 *Peltura scarabaeoides* (Wahlenberg 1821) – Terfelt, p. 412, fig. 4I.

2016 *Peltura scarabaeoides scarabaeoides* – Ahlberg *et al.*, p. 498, figs 4, 6H.

2017 *Peltura scarabaeoides scarabaeoides* (Wahlenberg, 1818) – Rasmussen *et al.*, pp. 19–20.

For further synonymy, see Rasmussen *et al.* (2017).

Type material. Not designated, see Henningsmoen (1957).

Material. One almost complete specimen (Fig. 38A) and 84 pygidia, incl. one with eight contiguous thoracic segments. The majority of the material derives from locality 6, with additional material collected at 'Cementen' (Øleå) and Limensgade (localities 8A–B). C. Poulsen (1923) reported the species also from locality 7 but no material from that site is kept in the museum collection. 160 cranidia, including one with ten attached thoracic segments, and 112 free cheeks from samples with safely assigned pygidia are tentatively assigned. *Peltura scarabaeoides* co-occurs with *C. linnarssoni, C. pecten, C. tenuis, C. teretifrons,* and *T. humilis* in the samples at hand.

Occurrence. Characteristic for the eponymous zone in Scandinavia, Poland, Great Britain and Canada (Westergård 1922, 1947; Henningsmoen 1957; Żylińska 2001, 2002). *Peltura scarabaeoides* occurs at the same stratigraphic level on Bornholm.

Comparison. See *P. acutidens.*

Remarks. Three samples from a well south of Lille Duegård (GM 2019-93, GM 2019-94, GM 2019-95), collected by Grönwall, and labelled as *P. scarabaeoides*, contain numerous *P. westergaardi* occurring alone
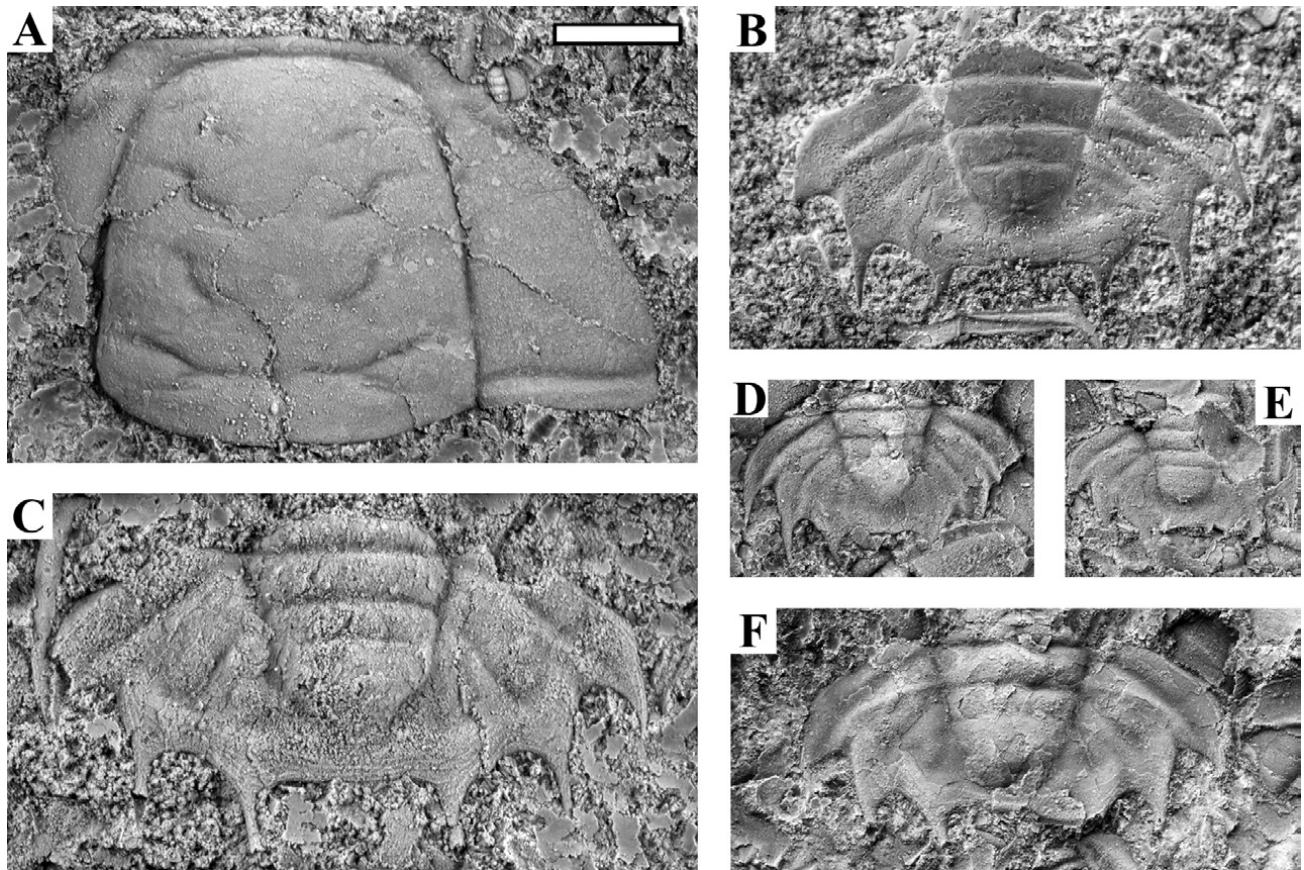
Fig. 39. *Peltura westergaardi*, all preserved in anthraconite from localities 8A–B: White scale bar: 2 mm. **A:** Cranidium presumably belonging to this species, sample L16 (MGUH 33573). **B:** External mould of pygidium, sample L10 (MGUH 33910). **C:** Pygidium, sample L11 (MGUH 33911). **D:** Pygidium, sample L13 (MGUH 33912). **E:** Pygidium, sample L14 (MGUH 33913). **F:** Pygidium, sample L15 (MGUH 33914).

including many juveniles treated by C. Poulsen (1923) and Whittington (1958).

Two complete specimens figured by Westergård (1922, pl. XV, figs 12–13) have pygidia with rather long horizontal marginal spines, relatively narrow axis and the distance between the inner spine pair is smaller than the anterior axial width. Westergård (*ibid.* p. 174) considered these as transitional to *acutidens*, and described that such forms with marginal spines co-occur with *scarabaeoides* in Närke and on Kinnekulle. Unpublished material from the latter locality shows extensive stratigraphical overlap between *P. scarabaeoides* (partly reworked?) and *P. westergaardi*. We identify the discussed specimens illustrated by Westergård as *P. westergaardi*.

Peltura westergaardi Henningsmoen, 1957
Fig. 39

1922		*Peltura scarabæoides* (Wahlenberg) [*partim*] – Westergård, pp. 173–174, pl. XV, figs 12–13. [See remarks on *P. scarabaeoides* above].
v 1923		*Peltura scarabaeoides* Wahlenberg [*partim*] – C. Poulsen, pp. 58–59, textfigs 18, 22.
1957		*Peltura scarabaeoides westergaardi* n. subsp. – Henningsmoen, pp. 239–240, pl. 7; pl. 25, figs 8, 10, 12, 15–17.
v 1958		*Peltura scarabaeoides* (Wahlenberg 1821) – Whittington, pp. 200–206, pl. 38.
1973		*Peltura scarabaeoides scarabaeoides* (Wahlenberg, 1821) [*partim*] – Schrank, pl. XIV, fig. 16.
1973		*Peltura scarabaeoides westergaardi* Henningsmoen, 1957 – Schrank, p. 843; pl. XV, figs 1–6.
2017		*Peltura scarabaeoides westergaardi* (Henningsmoen, 1957) – Rasmussen *et al.*, p. 20, fig. 9D.

For further synonymy, see Rasmussen *et al.* (2017).

Holotype. Cranidium SGU 4255 from Åkarpsmölle, Sweden, figured by Westergård (1944, pl. 3, fig. 3).

Material. 25 pygidia. In addition, one cephalon, 116 cranidia, 2 hypostomes and 12 free cheeks from samples with safely identified pygidia are tentatively assigned. The majority of the material derives from Limensgade (localities 8A–B), where *P. westergaardi* co-occurs with *P. (N.) lobata praecurrens* and rare orthid brachiopods. A few samples are from a well south of Ll. Duegård, see remarks.

Occurrence. Parabolina lobata Zone in Scandinavia and possibly Poland (Westergård 1947; Henningsmoen 1957; Żylińska 2001, 2002; Rasmussen *et al.* 2017). This is the first record from Bornholm where *P. westergaardi* occurs at the same stratigraphic level. In the Oslo Region, *P. westergaardi* has its FAD in the uppermost part of the *P. scarabaeoides* Zone (Nielsen *et al.* 2020) and this also seems to be the case on Kinnekulle, Västergötland (unpublished).

Comparison. See *Peltura acutidens.*

Remarks. We prefer to treat this taxon at species rather than subspecies level. Samples GM 2019-93 to -95 collected from a well south of Ll. Duegård (for location, se Fig. 2A) contains many juveniles as well as several adult *P. westergaardi*, occurring alone. The well-preserved juveniles were treated by C. Poulsen (1923) and Whittington (1958) (as *P. scarabaeoides*) (their illustrated specimens are numbered MGUH 1987, 1988, 1989).

Acknowledgements

References

Ahlberg, P. 2003: Trilobites and intercontinental tie points in the Upper Cambrian of Scandinavia. Geologica Acta 1, 127–134.

Ahlberg, P. & Ahlgren, J. 1996: Agnostids from the Upper Cambrian of Västergötland, Sweden. GFF 118, 129–140. https://doi.org/10.1080/11035899609546247

Ahlberg P., Szaniawski, Clarkson, E.N.K. & Bengtson, S. 1995: Phosphatised olenid trilobites and associated fauna from the Upper Cambrian of Västergötland, Sweden. Acta Palaeontologica Polonica 50, 429–440.

Ahlberg, P., Månsson, K., Clarkson, E. & Taylor, C. 2006: Faunal

turnovers and trilobite morphologies in the upper Cambrian *Leptoplastus* Zone at Andrarum, southern Sweden. Lethaia 39, 97–110. https://doi.org/10.1080/00241160600623731

Ahlberg, P. & Terfelt, F. 2012: Furongian (Cambrian) agnostoids of Scandinavia and their implications for intercontinental correlation. Geological Magazine 149, 1001–1012. https://doi.org/10.1017/s0016756812000167

Ahlberg, P., Eriksson, M.E., Lundberg F. & Lindskog A. 2016: Cambrian stratigraphy of the Tomten-1 drill core, Västergötland, Sweden, GFF 138, 490–501. https://doi.org/10.1080/11035897.2016.1190545

Allen, P.M., Jackson, A.A. & Rushton, A.W.A. 1981: The stratigraphy of the Mawddach Group in the Cambrian succession of North Wales. Proceedings of the Yorkshire Geological Society 43, 295–329. https://doi.org/10.1144/pygs.43.3.295

Angelin, N.P. 1854: Palæontologia Scandinavica 2, 21–92. Lund. [In Latin].

Babcock, L. E., Peng, S. C., Geyer, G. & Shergold, J. H. 2005: Changing perspectives on Cambrian chronostratigraphy and progress toward subdivision of the Cambrian System. Geosciences Journal 9, 101–106. https://doi.org/10.1007/bf02910572

Belt, T. 1867: On some new trilobites from the Upper Cambrian rocks of North Wales. Geological Magazine 4, 294–295. https://doi.org/10.1017/s0016756800205748

Berg-Madsen, V. 1985a: The Middle Cambrian of Bornholm, Denmark. A stratigraphical revision of the lower alumshale and associated anthraconites. Geologiska Föreningens i Stockholm Förhandlingar 106, 357–376. https://doi.org/10.1080/11035898509454664

Berg-Madsen, V. 1985b: A review of the Andrarum Limestone and the upper alum shale (Middle Cambrian) of Bornholm, Denmark. Bulletin of the geological Society of Denmark 34, 133–143.

Berg-Madsen, V. 1986: Oversigt over det reviderede Mellem Kambrium på Bornholm. Dansk geologisk forening Årsskrift for 1985, 1–13. [In Danish].

Brøgger, W.C. 1882: Die Silurischen Etagen 2 und 3 im Kristianiagebiet und auf Eker. Universitetsprogramm für 2. Sem. 1882, 376 pp. Kristiania (Oslo). [In German]. https://doi.org/10.1017/s0016756800166555

Bruton, D.L., Koch, L. & Repetski, J.E. 1988: The Nærsnes section, Oslo Region, Norway: trilobite, graptolite and conodont fossils reviewed. Geological Magazine 125, 451–455. https://doi.org/10.1017/s0016756800013078

Buchholz, A. 1991: Trilobiten aus Geschieben der oberkambrischen Stufe 1. Archiv für Geschiebekunde 1, 105–116. [In German].

Buchholz, A. 1999: Granitzia n. gen., ein neues Element der Trilobitenfauna aus Geschieben der oberkambrischen Stufe 5 Vorpommerns (Norddeutschland). Archiv für Geschiebekunde 2, 449–458. [In German].

Buchholz, A. 2000: Für und wider Ctenopyge oelandica Westergård, 1922 - Bemerkungen an Hand eines Geschiebefundes aus Vorpommern (Norddeutschland). Archiv für Geschie-

bekunde 2, 805–808. [In German].

Buchholz, A. 2004: Die Gattung Parabolina Salter 1849 (Trilobita) in oberkambrischen Geschieben Mecklenburg-Vorpommerns (Norddeutschland). Der Geschiebesammler 37, 3–34. [In German].

Buchholz, A. 2016: Bio- und Lithofazies in Geschieben der mittelkambrischen Agnostus pisiformis-Zone Skandinaviens aus Mecklenburg-Vorpommern Nordostdeutschland). Archiv für Geschiebekunde 7, 325–368. [In German].

Clarkson, E.N.K. & Taylor, C.M. 1995: The lost world of the olenid trilobites. Geology Today 11, 147–154. https://doi.org/10.1111/j.1365-2451.1995.tb00944.x

Clarkson, E.N.K., Ahlgren, J. & Taylor, C.M. 2004: Ontogeny, structure and functional morphology of some spiny *Ctenopyge* species (Trilobita) from the Upper Cambrian of Västergötland, Sweden. Transactions of the Royal Society of Edinburgh: Earth Sciences 94, 115–143. https://doi.org/10.1017/s0263593300000559

Danukalova, M.K., Kuzmichev, A.B. & Korovnikov, I.V. 2014: The Cambrian of Bennett Island (New Siberian Islands). Stratigraphy and Geological Correlation 22, 347–369. https://doi.org/10.1134/s0869593814040042

Grönwall, K.A. 1902: Bornholms Paradoxideslag og deres Fauna. Danmarks Geologiske Undersøgelse II. Række, Vol. 13, 230 pp. [In Danish]. https://doi.org/10.34194/raekke2.v13.6795

Grönwall, K.A. 1916: Palæozoiske Dannelser. In: Grönwall, K.A. & Milthers, V.: Beskrivelse til Geologisk Kort over Danmark. Kortbladet Bornholm. Danmarks Geologiske Undersøgelse I. Række, Vol. 13, 43–86. [In Danish]. https://doi.org/10.34194/raekke1.v13.6766

Hansen, K. 1945: The Middle and Upper Cambrian sedimentary rocks of Bornholm. Danmarks Geologiske Undersøgelse II. Række, Vol. 72, 81 pp. https://doi.org/10.34194/raekke2.v72.6861

Hawle, I. & Corda A.J.C. 1847: Prodom einer Monographie der böhmischen Trilobiten. Abhandlungen der Königliche böhmischen Gesellschaft der Wissenschaften, Abhandlung 5, 176 pp. Prague. [In German].

Henningsmoen, G. 1957: The trilobite family Olenidae, with description of Norwegian material and remarks on the Olenid and Tremadocian Series. Norsk Videnskaps-Akademi i Oslo 1, 303 pp.

Henningsmoen, G. 1958a: The Upper Cambrian faunas of Norway with descriptions of non-Olenid invertebrate fossils. Norsk Geologisk Tidsskrift 38, 179–196.

Henningsmoen, G. 1958b: Proposed use of the plenary powers to designate a type species in harmony with accustomed usage for the genus "*Protopeltura*" Brögger, 1882 (class Trilobita), a genus based upon a misidentified type species. Bulletin of Zoological Nomenclature 12, 31–32. https://doi.org/10.5962/bhl.part.2854

Holm, T.B. 2020: Distinguishing between *Leptoplastus abnormis* and *Leptoplastus ovatus*. A biometrical analysis of cranidium-shape. Project course in Geology-Geoscience, University of

Copenhagen, 15 pp. [Unpublished student report].

Hutchinson, R.D., 1952: The stratigraphy and trilobite faunas of the Cambrian sedimentary rocks of Cape Breton Island, Nova Scotia. Geological Survey of Canada Memoir 263, 124 pp. https://doi.org/10.4095/101599

Høyberget, M. & Bruton, D.L. 2012: Revision of the trilobite genus *Sphaerophthalmus* and relatives from the Furongian (Cambrian) Alum Shale Formation, Oslo Region, Norway. Norwegian Journal of Geology 92, 433–450. https://doi.org/10.17850/njg98-1-04

Ivshin, N.K. 1962: Upper Cambrian Trilobites of Kazakhstan, Part 2, 412 pp. Alma-Ata: Institute of Geological Sciences, Publishing House of the Academy of Sciences of the Kazakh SSR. [In Russian].

Jackson, I.S.C. & Budd, G.E. 2017: Intraspecific morphological variation of *Agnostus pisiformis*, a Cambrian Series 3 trilobite-like arthropod. Lethaia 50, 467–485. https://doi.org/10.1111/let.12201

Jaekel, O. 1909: Über die Agnostiden. Zeitschrift der Deutschen Geologischen Gesellschaft 61, 380–401. [In German].

Johnstrup, F. 1874: Oversigt over de palæozoiske Dannelser paa Bornholm. Beretning 11'te skandinaviske Naturforskermøde i Kjøbenhavn 1873, 1–10. København. [In Danish].

Johnstrup, F. 1891: Abriss der Geologie von Bornholm, als Führer zu der Exkursion der Deutschen Geologischen Gesellschaft nach der Insel Bornholm in Anschluss an die Allgemeine Versammlung in Greifswald 1889. Deutsche geologische Gesellschaft, 1–33. Greifswald. [In German].

Kaufmann, R. 1933a: Die Einstufung der Olenus-Arten von Bornholm. Paläontologische Zeitschrift 15, 57–63. [In German]. https://doi.org/10.1007/bf03041640

Kaufmann, R. 1933b: Variationsstatistische Untersuchungen über die "Artabwandlung" und "Artumbildung" an der Oberkambrischen Trilobitengattung Olenus Dalm. Abhandlungen aus dem Geologische-Palaeontologischen Institut der Ernst-Moritz-Arndt-Universität Greifswald X, 1–54. [In German].

Lake, M.A.P. 1913: A Monograph of the British Cambrian Trilobites, part IV. Monograph of the Palaeontographical Society 66, 65–88. https://doi.org/10.1080/02693445.1913.12035562

Lauridsen, B.W. & Nielsen, A.T. 2005: The upper Cambrian trilobite *Olenus* at Andrarum, Sweden: A case of iterative evolution? Palaeontology 48, 1041–1056. https://doi.org/10.1111/j.1475-4983.2005.00499.x

Lendzion, K. & Orłowski, S. 1991: Agnostidae McCoy, 1849. In S. Sokołowski (ed.): Geology of Poland: Atlas guide and characteristics fossils. Volume 3. Part 1a. Paleozoic (including Upper Proterozoic), 44–45. Warsaw: Publishing House Wydawnictwa Geologiczne.

Linnarsson, J.G.O. 1880: Om försteningarne i de svenska lagren med Peltura och Sphaerophthalmus. Sveriges Geologiska Undersokning, serie C43, 31 pp. [In Swedish]. https://doi.org/10.1080/11035898009446311

Månsson, K. & Clarkson, E.N.K. 2016: Early ontogeny of the Furongian (Cambrian) olenid trilobites *Sphaerophthalmus*

alatus (Boeck, 1838) and *Ctenopyge (Mesoctenopyge) tumida* Westergård, 1922 from Bornholm, Denmark. Earth and Environmental Science Transactions of the Royal Society of Edinburgh 106, 171–183. https://doi.org/10.1017/s1755691016000086

Matthew, G.F. 1894: Illustrations of the fauna of the St. John Group, No. VIII. Transactions of the Royal Society of Canada, section 4, 12 (for 1893), pp. 85–129.

Matthew, G.F. 1901: New species of Cambrian fossils from Cape Breton. Bulletin of the Natural History Society, New Brunswick, 4, 269–286.

Matthew, G.F. 1903: Report on the Cambrian rocks of Cape Breton, 246 pp. Ottawa: Geological Survey of Canada. https://doi.org/10.5962/bhl.title.22934

Mischnik, W. 2004: Seltene Trilobitenarten und Faunengemeinschaften oberkambrischer Geschiebe aus Ost-Holstein und West-Mecklenburg (Norddeutschland). Der Geschiebesammler 37, 95–136. [In German].

Mischnik, W. 2006a: *Agnostus (Agnostus?) confusus* n. sp. aus einem Geschiebe der oberkambrischen Stufe 1 (*Agnostus pisiformis*-Stufe) von West-Mecklenburg (Norddeutschland). Geschiebekunde aktuell 20, 1–4. [In German].

Mischnik, W. 2006b: *Agnostus (Agnostus) distinctus* n. sp. aus oberkambrischen Geschieben der Stufe 1 des südöstlichen Schleswig-Holsteins und West-Mecklenburgs (Norddeutschland). Der Geschiebesammler 39, 3–13. [In German].

Morris, S.F., 1988: A review of British trilobites, including a synoptic revision of Salter's monograph. Palaeontographical Society Monograph 574, 316 pp.

Nielsen, A.T., 1995: Trilobite systematics, biostratigraphy and palaeoecology of the Lower Ordovician Komstad Limestone and Huk Formations, southern Scandinavia. Fossils & Strata 38, 374 pp. https://doi.org/10.1016/s0031-0182(97)81135-2

Nielsen, A.T., Weidner, T., Terfelt, F. & Høyberget, M. 2014: Upper Cambrian (Furongian) biostratigraphy in Scandinavia revisited: definition of superzones. GFF 136, 193–197. https://doi.org/10.1080/11035897.2013.878748

Nielsen, A. T., Schovsbo, N.H., Klitten, K., Woolhead, D. & Rasmussen, C.M.Ø. 2018: Gamma-ray log correlation and stratigraphic architecture of the Cambro-Ordovician Alum Shale Formation on Bornholm, Denmark: Evidence for differential syndepositional isostasy. Bulletin of the Geological Society of Denmark 66, 237–273. https://doi.org/10.37570/bgsd-2018-66-15

Nielsen, A.T. & Ahlberg, P., 2019: The Miaolingian, a new name for the 'Middle' Cambrian (Cambrian Series 3): identification of lower and upper boundaries in Baltoscandia. GFF 141, 162–173. https://doi.org/10.1080/11035897.2019.1621374

Nielsen, A.T., Høyberget, M. & Ahlberg, P. 2020: The Furongian (upper Cambrian) Alum Shale of Scandinavia: Revision of zonation. Lethaia 53, 462–485. https://doi.org/10.1111/let.12370

Peng, S. & Babcock, L.E. 2003: The first "Golden Spike" within Cambrian. Episodes 26, 326.

Peng, S. & Babcock, L.E. 2005: Two Cambrian agnostoid

trilobites, *Agnostotes orientalis* (Kobayashi, 1935) and *Lotagnostus americanus* (Billings, 1860): Key species for defining global stages of the Cambrian System. Geosciences Journal 9, 107–115. https://doi.org/10.1007/bf02910573

Peng, S.C., Babcock, L.E., & Cooper, R.A. 2012: The Cambrian period. In: Gradstein, F.M., Ogg, J.G. Schmitz, M.D. & Ogg, G.M. (eds.): The Geologic Time Scale 2012, 437–488. Amsterdam: Elsevier. https://doi.org/10.1016/b978-0-444-59425-9.00019-6

Peng, S.C., Babcock, L.E., Zhu, X.J., Ahlberg, P., Terfelt, F. & Dai, T. 2015: Intraspecific variation and taphonomic alteration in the Cambrian (Furongian) agnostoid *Lotagnostus americanus*: new information from China. Bulletin of Geosciences 90, 281–306. https://doi.org/10.3140/bull.geosci.1500

Person, E. 1904: Till kännedomen om oleniderna i "zonen med Eurycare och Leptoplastus" vid Andrarum. Geologiska Föreningens i Stockholm Förhandlingar 26, 507–528. [In Swedish]. https://doi.org/10.1080/11035890409445492

Phillips, J. 1848: The Malvern Hills compared with the Palaeozoic Districts of Abberley, Woolhope, May, Hill, Torthworth, and Usk. With Palaeontological Appendix. Memoirs of the Geological Survey of Great Britain 2, 1–386.

Poulsen, C. 1922: Om Dictyograptusskiferen på Bornholm, Danmarks Geologiske Undersøgelse Række IV, Vol. 1(l6), 28 pp. (Also printed in Meddelelser fra Dansk Geologisk Forening 6). [In Danish]. https://doi.org/10.34194/raekke4.v1.6966

Poulsen, C. 1923: Bornholms Olenuslag og deres fauna. Danmarks Geologiske Undersøgelse II. Række, Vol. 40, 83 pp. [In Danish]. https://doi.org/10.34194/raekke2.v40.6826

Poulsen, C. 1959: Familiy Olenidae Burmeister, 1843. In Moore, R.C. (ed.): Treatise on Invertebrate Paleontology, part 0, Arthropoda 1, pp. O262–267. Lawrence: University of Kansas Press.

Poulsen, V. 1963: *Ctenopyge (Ctenopyge) pecten tenuis* n. subsp. from the Upper Cambrian of Bornholm. Det Kongelige Danske Videnskabernes Selskab, Biologiske Meddelelser 23(13), 1–9.

Poulsen, V. 1966: Cambro-Silurian Stratigraphy of Bornholm. Meddelelser fra Dansk Geologisk Forening 16, 117–137.

Rasmussen, B.W., Nielsen, A.T. & Schovsbo, N.H. 2015: Faunal succession in the upper Cambrian (Furongian) *Leptoplastus* Superzone at Slemmestad, southern Norway. Norwegian Journal of Geology 95, 1–22. https://doi.org/10.17850/njg95-1-01

Rasmussen, B.W., Rasmussen, J.A. & Nielsen, A.T. 2016: Biozonation of the Furongian (upper Cambrian) Alum Shale Formation at Hunneberg, Sweden. GFF 138, 467–489. https://doi.org/10.1080/11035897.2016.1168866

Rasmussen, B.W., Rasmussen, J.A. & Nielsen, A.T. 2017: Biostratigraphy of the Furongian (upper Cambrian) Alum Shale Formation at Degerhamn, Öland, Sweden. GFF 139, 92–118. https://doi.org/10.1080/11035897.2016.1276099

Reyment, R.A. 1976: Göran (Georg) Wahlenberg's collection. De Rebus 3, 2–11. Uppsala: Paleontologiska Museet.

Rushton, A.W.A. 1968: Revision of two Upper Cambrian trilobites. Palaeontology 11, 410–420.

Rushton, A.W.A. 2009: Revision of the Furongian agnostoid *Lotagnostus trisectus* (Salter). Memoirs of the Association of Australasian Palaeontologists 37, 273–279.

Salter, J.W. 1864: Trilobites (chiefly Silurian). Figures and descriptions illustrative of British organic remains. Decade 11. Memoirs of the Geological Survey of the United Kingdom, 1–60. https://doi.org/10.5962/bhl.title.61418

Schoenemann, B. & Clarkson, E.N.K. 2015: Eyes and vision in the coeval Furongian trilobites *Sphaerophthalmus alatus* (Boeck, 1838) and *Ctenopyge (Mesoctenopyge) tumida* Westergård, 1922, from Bornholm, Denmark. Palaeontology 58, 133–140. https://doi.org/10.1111/pala.12128

Schrank, E. 1973: Trilobiten aus Geschieben der oberkambrischen Stufen 3–5. Paläontologische Abhandlungen 4, 805-891. [In German].

Shergold, J.H., Laurie, J.R. & Xiaowen, S. 1990: Classification and review of the trilobite order Agnostida Salter, 1864: an Australian perspective. Bureau of Mineral Resources, Geology and Geophysics Report 296, 1–93.

Stubblefield, C.J. 1938: The types and figured specimens in Phillips and Salter's palaeontological appendix to John Phillips' memoir on 'The Malvern Hills Compared With The Palaeozoic Districts of Abberley, etc.' (Mem. Geol. Surv., Volume II, Part I, June 1848). Summary of Progress of the Geological Survey of Great Britain and the Museum of Practical Geology for the year 1936, Part II, 27–51.

Størmer, L. 1940: Early descriptions of Norwegian trilobites. The type specimens of C. Boeck, M. Sars and M. Esmark. Norsk Geologisk Tidsskrift 20, 113–151.

Taylor, K. & Rushton, A.W.A. 1971: The pre-Westphalian geology of the Warwickshire Coalfield. Bulletin of the Geological Survey of Great Britain 35, 1–152.

Terfelt, F. 2003: Upper Cambrian trilobite biostratigraphy and taphonomy at Kakeled on Kinnekulle, Västergötland, Sweden. Acta Palaeontologica Polonica 48, 409–416.

Terfelt, F. 2006: Review of uppermost Furongian trilobites from Scania, southern Sweden, based on type material. Palaeontology 96, 1339–1355. https://doi.org/10.1111/j.1475-4983.2006.00600.x

Terfelt, F., Ahlberg, P., Eriksson, M.E. & Clarkson, E.N.K. 2005: Furongian (upper Cambrian) biostratigraphy and trilobites of the Håslöv-1 drill core, Scania, S. Sweden. GFF 127, 195–203. https://doi.org/10.1080/11035890501273195

Terfelt, F., Eriksson, M.E., Ahlberg, P. & Babcock, L.E. 2008: Furongian Series (Cambrian) biostratigraphy of Scandinavia – a revision. Norwegian Journal of Geology 88, 73–87.

Terfelt, F., Ahlberg, P. & Eriksson, M.E. 2011: Complete record of Furongian polymerid trilobites and agnostoids of Scandinavia - a biostratigraphical scheme. Lethaia 44, 8–14. https://doi.org/10.1111/j.1502-3931.2009.00211.x

Tullberg, S.A. 1880: Om Agnostus-arterna i de kambriska aflagringarne vid Andrarum. Sveriges geologiska undersökning C42, 1–37. [In Swedish]. https://doi.org/10.1080/11035898009446304

Vogdes, A.W. 1890: A bibliography of Paleozoic Crustacea from 1698 to 1889 including a list of North American species and a systematic arrangement of genera. Bulletin of the United States Geological Survey 63, 1–177. https://doi.org/10.3133/b63

Vogdes, A.W. 1925: Paleozoic Crustacea. Parts I–III. Transactions of the San Diego Society of Natural History IV, 1–154.

von Jansson, C. 1979: Zur biostratigraphie des Tremadociums auf Bornholm, Dänemark. Unpublished diplom thesis, 51 pp. University of Hannover. [In German].

Wahlenberg, G. 1818 (and 1821): Petrificata Telluris Svecanae. Nova Acta Regiae Societatis Scientiatum Upsaliensis 8, 116 pp. Uppsala. [In Latin].

Westergård, A.H. 1922: Sveriges olenidskiffer. Sveriges geologiska undersökning Ca 18, 205 pp. [In Swedish].

Westergård, A.H. 1942: Stratigraphic results of the borings through the Alum Shales of Scania made in 1941–1942. Lunds Geologiska Fältklubb 185, 20 pp.

Westergård, A.H. 1944: Borrningar genom Skånes alunskiffer 1941–42. Sveriges geologiska undersökning C 459, 45 pp. [In Swedish].

Westergård, A.H. 1947: Supplementary Notes on the Upper Cambrian Trilobites of Sweden. Sveriges geologiska undersökning C 489, 34 pp.

Westrop, S.R., Adrain, J.M. & Landing, E. 2011: The Cambrian (Sunwaptan, Furongian) agnostoid arthropod *Lotagnostus* Whitehouse, 1936, in Laurentian and Avalonian North America: systematics and biostratigraphic significance. Bulletin of Geosciences 86, 569–594. https://doi.org/10.3140/bull.geosci.1256

Whittington, H.B. 1958: Ontogeny of the trilobite *Peltura scarabaeoides* from the Upper Cambrian, Denmark. Palaeontology 1, 200–206.

Żylińska, A. 2001: Late Cambrian trilobites from the Holy Cross Mountains, central Poland. Acta Geologica Polonica 51, 333–383. https://doi.org/10.2478/agp-2013-0002

Żylińska, A. 2002: Stratigraphic and biogeographic significance of Late Cambrian trilobites from Łysogóry (Holy Cross Mountains, central Poland). Acta Geologica Polonica 52, 217–238. https://doi.org/10.2478/agp-2013-0002

Appendix 1: List of material

The fossils are preserved in anthraconite (bituminous limestone) unless otherwise stated.

Agnostus pisiformis **(Wahlenberg, 1818).** *4 complete specimens, 173 cephala and 148 pygidia.* Samples L1 (5 cephala, 6 pygidia), L2 (13 cephala, 10 pygidia, 1 complete specimens), GM 864 (11 cephala, 6 pygidia), GM 1870-538 (8 cephala, 10 pygidia), GM 1870-832 (2 cephala, 1 pygidium), GM 1870-834 (3 cephala, 3 pygidia), GM 1870-835 (14 cephala, 8 pygidia), GM 1870-836 (11 cephala, 9 pygidia), GM 1870-837 (9 cephala, 5 pygidia), GM 1877-2002 (25 cephala, 26 pygidia), GM 1883-340 (12 cephala, 11 pygidia), GM 1922-132A (16 cephala, 11 pygidia), GM 1922-132C (19 cephala, 17 pygidia), GM 1922-132B (4 cephala, 3 pygidia), GM 1922-144 (complete specimen), GM 1922-145 (pygidium), GM 1922-146A (5 cephala, 12 pygidia), GM 1922-146B (cephalon, 2 pygidia, 1 complete specimen), GM 2019-29 (2 cephala), GM 2019-30 (cephalon), GM 2019-31 (4 cephala, 3 pygidia), GM 2019-32 (cephalon), GM 2019-33 (2 cephala, 3 pygidia), GM 2019-91 (2 cephala, 1 pygidium), unnumbered sample incl. MGUH 1954 (3 cephala, 1 complete specimen).

Homagnostus obesus **(Belt, 1867)**. *10 complete specimens, 70 cephala and 82 pygidia.* Samples (all shale): ATN-323 (4 pygidia) (with *O. truncatus*), ATN-325 (3 cephala, 1 pygidium) (with *O. truncatus*), ATN-326 (3 cephala, 5 pygidia), GM 1871-692 (cephalon, 2 pygidia), GM 1871-811 (pygidium), GM 1892-1300 (cephalon, 2 pygidia) (with *O. wahlenbergi*), GM 1922-134 (cephalon, 3 pygidia), GM 1922-148 (cephalon, 5 pygidia), GM 1922-149A (3 cephala, 4 pygidia), GM 1922-150B (11 cephala, 7 pygidia, 7 complete specimens), GM 1922-150C (7 cephala, 6 pygidia, 1 complete specimen), GM 1935-54 (9 cephala, 15 pygidia, 1 complete specimen), GM 2019-37 (pygidium), GM 2019-38 (complete specimen), GM 2019-39 (2 cephala), GM 2019-40 (2 cephala, 2 pygidia) (with *O. wahlenbergi*), GM 2019-45 (cephalon, 1 pygidium) (with *O. wahlenbergi*), GM 2019-51 (2 cephala, 4 pygidia) (with *O. wahlenbergi*), GM 2019-55 (8 cephala, 4 pygidia) (with *O. wahlenbergi*), GM 2019-58 (2 cephala), GM 2019-59 (2 cephala, 1 pygidium) (with *O. wahlenbergi*), GM 2019-61 (cephalon), GM 2019-62 (2 cephala, pygidium) (with *O. wahlenbergi*), GM 2019-64 (3 pygidia) (with *O. wahlenbergi*), GM 2019-67 (3 cephala) (with *O. wahlenbergi*), GM 2019-69 (pygidium) (with *O. wahlenbergi*), GM 2019-70 (cephalon, 3 pygidia) (with *O. wahlenbergi*), GM 2019-74 (pygidium) (with *O. wahlenbergi*), GM 2019-80 (cephalon) (with *O. wahlenbergi*), GM 2019-81 (cephalon) (with *O. wahlenbergi*), GM 2019-83 (pygidium) (with *O. wahlenbergi*), GM 2019-85 (2 cephala) (with *O. wahlenbergi*), GM 2019-86 (cephalon) (with *O. wahlenbergi*), GM 2019-87 (3 pygidia) (with *O. wahlenbergi*), MGUH 1955 (pygidium).

Glyptagnostus reticulatus **(Angelin, 1851)**. *Four complete specimens, 4 cephala and 6 pygidia.* Samples GM 1871-602 (cephalon, 1 pygidium), GM 1902-1196 (pygidium), GM 1922-133 (pygidium) (shale), GM 1922-150A (cephalon), GM 1938-43 (cephalon, 2 complete specimens), GM 1939-22 (cephalon, 2 complete specimens), GM 2019-34 (pygidium), GM 2019-35 (external mould of pygidium) (counter piece to GM 2019-36), GM 2019-36 (pygidium) (positive counter piece to GM 2019-35), MGUH 1956 (pygidium).

Lotagnostus americanus **(Billings, 1860)**. *One cephalon*, sample GM 1922-141O.

Pseudagnostus leptoplastorum **Westergård, 1944?** *One cephalon*, sample ATN-123 (with *E. bornholmensis*).

Olenus attenuatus **(Boeck, 1838)**. *9 cranidia with up to 8 contiguous thoracic segments, 1 free cheek(?) and 2 pygidia.* Samples L104 (cranidium with two thoracic segments), L105 (cranidium), L115 (cranidium), L118 (possible free cheek), GM 1897-1300 (5 cranidia incl. 2 with up to 8 thoracic segments, 1 pygidium), GM 2019-63 (3 cranidia?, pygidium), MGUH 1960 (cranidium with 4 thoracic segments).

Olenus dentatus **Westergård, 1922**. *External mould of one almost complete specimen and 1 tentatively assigned cranidium.* Samples GM 2019-98, GM 2019-102.

Olenus gibbosus **(Wahlenberg, 1818)**. *One cephalon with three thoracic segments attached, 2 free cheeks and 4 pygidia.* Samples MGUH 1958 (cephalon with 3 thoracic segments), GM 2019-41 (pygidium), GM 2019-42 (free cheek), GM 2019-43 (2 pygidia), unnumbered sample (incl. MGUH 1957) (free cheek, pygidium).

Olenus transversus **Westergård, 1922**. *One almost complete specimen, 2 free cheeks and 4 pygidia with up to 13 thoracic segments attached. Additionally, 2 pygidia with up to 6 thoracic segments have been tentatively assigned.* Samples ATN-320 (almost complete specimen), ATN-322 (pygidium), L99? (pygidium), L100 (pygidium), L101? (pygidium with 6 thoracic segments), L108 (pygidium), L111 (pygidium with 13 thoracic segments), L119 (2 free cheeks).

***Olenus truncatus* (Brünnich, 1781)**. *11 almost complete specimens and 21 pygidia, including one with 10 contiguous thoracic segments. Additionally, 1 cephalon, 7 cranidia and 9 free cheeks have been tentatively assigned*. Samples ATN-323 (pygidium) (with *H. obesus*), ATN-324 (cephalon, 3 pygidia), ATN-325 (3 pygidia) (with *H. obesus*), L95 (free cheek, pygidium), L98 (pygidium), L103 (3 pygidia) (with *O. wahlenbergi*), L112 (2 pygidia), GM 1870-876 (3 external moulds of complete specimens, cranidium?, 2 pygidia), GM 1914 (1 almost complete specimen, 3 pygidia), GM 1922-133B (cranidium with 10 thoracic segments, 2 free cheeks, 2 pygidia incl. one with 10 thoracic segments), GM 1922-133C (2 almost complete specimens, 5 free cheeks), GM 1922-133D (complete specimen), GM 1922-136 (almost complete specimen), GM 1922-138 (almost complete specimen), GM 1922-147 (5 cranidia, 1 free cheek), GM 2019-46 (almost complete specimen), MGUH 1959 (almost complete specimen).

***Olenus wahlenbergi* Westergård, 1922**. *26 free cheeks and 11 pygidia. 176 cranidia have been tentatively assigned*. Sample L103 (free cheek) (with *O. truncatus*), GM 1892-1300 (pygidium) (with *H. obesus*), GM 1938-42 (pygidium), GM 2019-40 (2 free cheeks, 3 cranidia) (with *H. obesus*), GM 2019-44 (5 cranidia, 2 free cheeks), GM 2019-45 (14 cranidia, 3 free cheeks) (with *H. obesus*), GM 2019-47 (cranidium), GM 2019-48 (cranidium?, free cheek?), GM 2019-49 (5 cranidia, 1 free cheek), GM 2019-50 (15 cranidia, 1 free cheek), GM 2019-51 (5 cranidia) (with *H. obesus*), GM 2019-52 (cranidium, 2 free cheeks), GM 2019-53 (3 cranidia, 1 free cheek), GM 2019-54 (free cheek), GM 2019-55 (10 cranidia, 1 free cheek, 2 pygidia) (with *H. obesus*), GM 2019-56 (6 cranidia), GM 2019-57 (cranidium), GM 2019-59 (4 cranidia, 1 free cheek, 1 pygidium) (with *H. obesus*), GM 2019-60 (4 cranidia), GM 2019-62 (2 cranidia, 2 free cheeks) (with *H. obesus*), GM 2019-64 (5 cranidia) (with *H. obesus*), GM 2019-65 (3 cranidia, 2 pygidia), GM 2019-66 (2 cranidia), GM 2019-67 (3 cranidia) (with *H. obesus*), GM 2019-68 (6 cranidia, 1 pygidium), GM 2019-69 (5 cranidia, 1 free cheek, 1 pygidium) (with *H. obesus*), GM 2019-70 (10 cranidia, 1 free cheek) (with *H. obesus*), GM 2019-71 (3 cranidia), GM 2019-72 (3 cranidia, 3 free cheeks), GM 2019-73 (3 cranidia, 2 free cheeks), GM 2019-74 (4 cranidia) (with *H. obesus*), GM 2019-75 (2 cranidia), GM 2019-76 (cranidium), GM 2019-77 (10 cranidia), GM 2019-78 (3 cranidia), GM 2019-79 (2 cranidia), GM 2019-80 (3 cranidia) (with *H. obesus*), GM 2019-81 (cranidium) (with *H. obesus*), GM 2019-82 (4 cranidia), GM 2019-83 (4 cranidia, 1 pygidium) (with *H. obesus*), GM 2019-84 (3 cranidia), GM 2019-85 (3 cranidia), GM 2019-86 (5 cranidia), GM 2019-87 (8 cranidia, 1 pygidium).

***Parabolina acanthura* (Angelin, 1854)**. *One cephalon, 3 cranidia and 2 free cheeks. One hypostome and isolated pleura are tentatively assigned*. Samples GM 1924-1A (cephalon), GM 1924-1B (cranidium), GM 1924-1C (cranidium), GM 1924-1D (cranidium, 3 free cheeks – all specimens fragmentary), MGUH 1979 (hypostome), GM 1924.1E incl. MGUH 1980 (cranidium, free cheek), MGUH 1981 (pleura).

***Parabolina spinulosa* (Wahlenberg, 1818)**. *20 cranidia, 7 free cheeks and 8 pygidia*. Samples GM 1870-861 (cranidium) (with *Orusia lenticularis*), GM 1879-861 (cranidium) (with *Orusia lenticularis*), GM 1887-399 (3 cranidia) (with *Orusia lenticularis*), GM 1897-399 (cranidium) (with *Orusia lenticularis*), GM 1922-137A (2 cranidia, 2 free cheeks) (with Orusia lenticularis), GM 1922-137B (6 cranidia, 2 free cheeks, 5 pygidia), GM 1922-137C (2 pygidia), GM 1922-137D (cranidium), GM 1922.137E (cranidium, 1 juvenile cranidium, 1 free cheek, 1 pygidium incl. MGUH 1985), GM 1946-4 (2 free cheeks), GM 2019-92 (3 fragmentary cranidia) (with *O. lenticularis*).

***Parabolina lobata praecurrens* Westergård, 1944**. *21 cranidia*. Samples L3 (cranidium), L10 (cranidium) (with *P. westergaardi*), L11 (9 cranidia) (with *P. westergaardi*), L12 (5 cranidia) (with *P. westergaardi, Peltura* sp.), L14 (cranidium) (with *P. westergaardi, Peltura* sp.), L16 (2 cranidia) (with *P. westergaardi, Peltura* sp., orthid brachiopod), L18 (2 cranidia) (with orthid brachiopod).

***Leptoplastus abnormis* Westergård, 1944**. *4 almost complete specimens, 1 cephalon, 352 cranidia, external mould of one cranidium with ~10 thoracic segments, 3 specimens with continuous thoracic segments and 9 free cheeks*. Samples ATN-108 (2 cranidia) (with *E. bornholmensis, L. angustatus, L. ovatus*), ATN-119 (2 possible free cheeks) (with *E. bornholmensis, L. ovatus*), ATN-122 (11 cranidia) (with *E. bornholmensis, L. ovatus*), ATN-124 (15 cranidia) (with *E. bornholmensis, L. angustatus, L. ovatus*), ATN-129 (cranidium) (with *E. bornholmensis, L. angustatus, L. ovatus*), ATN-149 (external mould of complete specimen) (with *L. angustatus*), ATN-154 (3 cranidia) (with *E. bornholmensis, L. ovatus*), ATN-155 (cranidium) (with *L. angustatus*), ATN-156 (15 cranidia) (with *E. bornholmensis, L. angustatus, L. ovatus*), ATN-157 (6 cranidia) (with *E. bornholmensis, L. angustatus, L. ovatus*), ATN-170 (cranidium, 1 thoracic segment) (with *E. bornholmensis, L. angustatus, L. ovatus*), ATN-176 (3 cranidia) (with *E. bornholmensis, L. angustatus, L. ovatus*), ATN-217 (12 cranidia) (with *E. bornholmensis, L. ovatus*), ATN-219 (4 external moulds of cranidia), ATN-228 (cranidium) (with *L. angustatus*), ATN-232 (3 cranidia) (with *L. ovatus*), ATN-241 (4 cranidia) (with *L. ovatus*), ATN-243 (8 cranidia) (with *L. ovatus*), ATN-251 (cranidium) (with *E. bornholmensis, L. angustatus, L. ovatus*), ATN-252 (cranidium) (with *L. angustatus, L. crassicornis, L. ovatus*), ATN-254 (cranidium) (with *L. angustatus?, L. ovatus*), ATN-260 (complete specimen) (with *L. angustatus, L.ovatus, E. bornholmensis*), ATN-261 (4 cranidia, 2 free cheeks) (with *L. angustatus, L. ovatus*), ATN-262 (2 cranidia) (with *E. bornholmensis, L. ovatus*), ATN-263 (5 cranidia, 1 thoracic segment) (with *L. angustatus, L. crassicornis, L. ovatus*), ATN-264 (cranidium), ATN-265 (4 cranidia, 1 thorax with pygidium) (with *E. bornholmensis, L. angustatus, L. crassicornis, L. ovatus*), ATN-270 (7 cranidia) (with *L. ovatus*), ATN-271 (cranidium, 1 free cheek) (with *E. bornholmensis, L. ovatus*), ATN-275 (cranidium) (with *E. bornholmensis, L. angustatus*), ATN-276 (14 cranidia) (with *E. bornholmensis, L. angustatus, L. crassicornis, L. ovatus*), ATN-277 (external mould of cranidium) (with *E. bornholmensis, L. angustatus, L.*

ovatus), ATN-278 (2 cranidia) (with *E. bornholmensis, L. angustatus, L. crassicornis, L. ovatus*), ATN-283 (cranidium) (with *L. ovatus*), ATN-288 (11 cranidia, 1 free cheek) (with *L. angustatus, L. ovatus*), ATN-293 (2 cranidia, thorax) (with *L. angustatus, L. crassicornis?, L. ovatus*), ATN-301 (2 cranidia, 6 contiguous thoracic segments) (with *L. angustatus, L. ovatus*), ATN-302 (cranidium) (with *L. ovatus*), ATN-304 (8 cranidia, 2 external moulds of complete specimens, contiguous thoracic segment, 1 free cheek) (with *E. bornholmensis, L. angustatus, L. crassicornis, L. ovatus*), ATN-306 (3 cranidia) (with *E. bornholmensis, L. ovatus*), ATN-307 (5 cranidia) (with *E. bornholmensis, L. ovatus*), ATN-328 (8 cranidia) (with *E. bornholmensis, L. angustatus, L. crassicornis, L. ovatus*), ATN-331 (6 cranidia) (with *L. angustatus, L. ovatus*), ATN-332 (3 cranidia) (with *L. angustatus, L. ovatus*), ATN-335 (2 cranidia) (with *L. angustatus, L. ovatus*), ATN-336 (cranidium) (with *E. bornholmensis, L. angustatus, L. ovatus*), ATN-337 (3 cranidia), ATN-338 (cephalon, 1 cranidium with 4 thoracic segments attached) (with *L. ovatus*), ATN-339 (7 cranidia) (with *E. bornholmensis, L. ovatus*), ATN-340 (cranidium) (with *E. bornholmensis, L. angustatus, L. ovatus*), ATN-341 (5 cranidia) (with *L. angustatus, L. ovatus*), ATN-342 (11 cranidia) (with *E. bornholmensis, L. ovatus*), ATN-343 (2 cranidia) (with *E. bornholmensis, L. angustatus, L. ovatus*), ATN-346 (15 cranidia) (with *E. bornholmensis, L. angustatus, L. ovatus*), ATN-347 (3 cranidia) (with *L. angustatus, L. ovatus*), ATN-348 (11 cranidia) (with *L. crassicornis, L. ovatus*), L126 (4 cranidia) (with *E. bornholmensis, L. ovatus*), GM 1902-1201 (external mould of cranidium) (with *L. ovatus*), GM 1922-138D (2 cranidia) (with *L. crassicornis, L. ovatus, E. bornholmensis*), GM 1922-139E (2 cranidia, 2 thoracic segments) (with *E. bornholmensis, L. angustatus, L. crassicornis, L. ovatus*), GM 2019-88 (2 cranidia) (with *L. ovatus*), GM 2019-89 (4 cranidia) (with *L. ovatus*), GM 2019-90 (18 cranidia, 2 thoracic segments, 2 possible free cheeks) (with *E. bornholmensis, L. angustatus, L. ovatus*).

Leptoplastus angustatus **(Angelin, 1854)**. *457 cranidia incl. two with up to 9 thoracic segments, 203 free cheeks and 28 pygidia*. Samples ATN-108 (cranidium) (with *E. bornholmensis, L. abnormis, L. ovatus*), ATN-109 (free cheek) (with *L. ovatus*), ATN-110 (19 cranidia, 2 free cheeks, 2 pygidia) (with *E. bornholmensis, L. crassicornis*), ATN-118 (2 free cheeks) (with *E. bornholmensis, L. ovatus*), ATN-124 (2 free cheeks) (with *E. bornholmensis, L. abnormis, L. angustatus, L. ovatus*), ATN-129 (free cheek) (with *E. bornholmensis, L. abnormis, L. ovatus*), ATN-136 (free cheek) (with *E. bornholmensis*), ATN-142 (>20 cranidia, >3 free cheeks, 1 pygidium), ATN-149 (cranidium with 9 thoracic segments, 1 free cheek) (with *L. abnormis*), ATN-152 (cranidium, free cheek) (with *L. ovatus*), ATN-153 (11 cranidia, 14 free cheeks, 3 pygidia) (with *L. crassicornis*), ATN-155 (10 cranidia, >10 free cheeks) (with *L. abnormis*), ATN-156 (3 cranidia, 1 free cheek) (with *E. bornholmensis, L. abnormis, L. ovatus*), ATN-157 (cranidium) (with *E. bornholmensis, L. abnormis, L. ovatus*), ATN-158 (19 cranidia, >2 free cheeks) (with *L. crassicornis, L. ovatus*), ATN-162 (pygidium) (with *L. ovatus*), ATN-163 (cranidium), ATN-170 (cranidium) (with *E. bornholmensis, L. abnormis, L. ovatus*), ATN-176 (5 cranidia, 1 free cheek) (with *E. bornholmensis, L. abnormis, L. ovatus*), ATN-177 (2 free cheeks) (with *L. ovatus*), ATN-216 (>25 cranidia, 7 free cheeks) (with *E. bornholmensis, L. crassicornis*), ATN-223 (>39 cranidia, >10 free cheeks, 2 pygidia), ATN-224 (3 free cheeks, 1 pygidium?) (with *E. bornholmensis*), ATN-228 (3 cranidia, 1 free cheek) (with *L. abnormis*), ATN-233 (3 cranidia, 3 free cheeks) (with *L. ovatus*), ATN-234 (cranidium), ATN-247 (5 cranidia, 2 free cheeks, 1 pygidium), ATN-251 (free cheek) (with *E. bornholmensis, L. abnormis, L. ovatus*), ATN-252 (10 cranidia, 1 free cheek, >3 pygidia) (with *L. abnormis, L. crassicornis, L. ovatus*), ATN-253 (6 cranidia, 2 free cheeks) (with *L. ovatus*), ATN-254 (free cheek?) (with *L. abnormis, L. ovatus*), ATN-259 (cranidium) (with *L. crassicornis*), ATN-260 (pygidium) (with *L. ovatus, L. abnormis, E. bornholmensis*), ATN-261 (cranidium) (with *L. abnormis, L. ovatus*), ATN-263 (pygidium) (with *L. abnormis, L. crassicornis, L. ovatus*), ATN-265 (3 cranidia, 1 free cheek) (with *E. bornholmensis, L. abnormis, L. crassicornis, L. ovatus*), ATN-269 (free cheek) (with *L. ovatus*), ATN-274 (16 cranidia, 6 free cheeks), ATN-275 (cranidium, 1 free cheek) (with *E. bornholmensis, L. abnormis*), ATN-276 (free cheek) (with *E. bornholmensis, L. abnormis, L. crassicornis, L. ovatus*), ATN-277 (2 cranidia, 1 free cheek) (with *E. bornholmensis, L. abnormis, L. ovatus*), ATN-278 (7 cranidia, 4 free cheeks, 1 pygidium) (with *E. bornholmensis, L. abnormis, L. crassicornis, L. ovatus*), ATN-281 (6 cranidia, 1 free cheek) (with *L. crassicornis*), ATN-285 (7 cranidia, >4 free cheeks), ATN-288 (cranidium) (with *L. abnormis, L. ovatus*), ATN-289 (14 cranidia, 1 pygidium), ATN-292 (14 cranidia, 4 free cheeks) (with *E. bornholmensis, L. ovatus*), ATN-293 (cranidium) (with *L. abnormis, L. crassicornis?, L. ovatus*), ATN-295 (cranidium), ATN-297 (>16 cranidia, 2 free cheeks), ATN-298 (>7 cranidia, 2 free cheeks), ATN-299 (free cheek, 2 pygidia) (with *E. bornholmensis, L. ovatus*), ATN-301 (free cheek) (with *L. abnormis, L. ovatus*), ATN-303 (12 cranidia, 4 free cheeks, 1 pygidium), ATN-304 (7 cranidia, >18 free cheek) (with *E. bornholmensis, L. abnormis, L. crassicornis, L. ovatus*), ATN-305 (25 cranidia, 9 free cheeks, 1 pygidium) (with *L. crassicornis*), ATN-328 (cranidium, 1 free cheek) (with *E. bornholmensis, L. abnormis, L. crassicornis, L. ovatus*), ATN-331 (free cheek) (with *L. abnormis, L. ovatus*), ATN-332 (free cheek) (with *L. abnormis, L. ovatus*), ATN-334 (3 cranidia, 16 very small juvenile cranidia, 5 free cheeks), ATN-335 (5 free cheeks) (with *L. abnormis, L. ovatus*), ATN-336 (cranidium) (with *E. bornholmensis, L. abnormis, L. ovatus*), ATN-340 (4 free cheeks) (with *E. bornholmensis, L. abnormis, L. ovatus*), ATN-341 (cranidium, 1 free cheek) (with *L. abnormis, L. ovatus*), ATN-343 (cranidium) (with *E. bornholmensis, L. abnormis, L. ovatus*), ATN-344 (4 cranidia, 1 free cheek), ATN-346 (2 cranidia, 2 free cheeks) (with *E. bornholmensis, L. abnormis, L. ovatus*), ATN-347 (free cheek) (with *L. abnormis, L. ovatus*), L31 (3 cranidia, 1 free cheek), L32 (2 free cheeks, pygidium), L33 (3 cranidia, 3 free cheeks, 1 pygidium), L54 (>12 cranidia, >4 free cheeks, 1 pygidium), GM 1870-847 (cranidium) (with *L. ovatus*), GM 1870-848 (cranidium) (with *L. crassicornis, L. ovatus*), GM 1871-607 (3 cranidia) (with *E. bornholmensis, L. ovatus*), GM 1888-289A (8 cranidia, 7 free cheeks) (with *L. crassicornis, L. ovatus*), GM 1888-289B (cranidium, 4 free cheeks), GM 1888-289C (13 cranidia, 5 free cheeks, 1 pygidium) (with *L. crassicornis*), GM 1888-289D (4 cranidia), (with *L. crassicornis, L. ovatus*), GM 1922-139A (2 cranidia, 2 free cheeks) (with *E. bornholmensis*), GM 1922-139B (4 cranidia, 8 free cheeks) (with *L. crassicornis, L. ovatus*), GM 1922-139C (3 cranidia,

2 free cheeks), GM 1922-139D (pygidium), GM 1922-139E (cranidium) (with *E. bornholmensis, L. abnormis, L. crassicornis, L. ovatus*), GM 1922-139G (2 cranidia) (with *E. bornholmensis, L. ovatus*), GM 1930-99/100 (2 cranidia, 2 free cheeks) (with *E. bornholmensis, L. ovatus*), GM 2019-28 (2 cranidia), GM 2019-90 (6 cranidia) (with *E. bornholmensis, L. abnormis, L. ovatus*), MGUH 1963 (free cheek).

Leptoplastus crassicornis (Westergård, 1944*). 37 cranidia, 12 free cheeks and 6 pygidia*. Samples ATN-110 (2 cranidia incl. one with 4 thoracic segments) (with *E. bornholmensis, L. angustatus*), ATN-153 (cranidium) (with *L. angustatus*), ATN-158 (2 cranidia) (with *L. angustatus, L. ovatus*), ATN-178 (free cheek) (with juvenile *Eurycare* sp.), ATN-216 (cranidium, 2 free cheeks, 2 pygidia) (with *E. bornholmensis, L. angustatus*), ATN-220 (external mould of free cheek), ATN-252 (4 cranidia, 1 free cheek) (with *L. abnormis, L. angustatus, L. ovatus*), ATN-259 (cranidium) (with *L. angustatus*), ATN-263 (cranidium) (with *L. abnormis, L. angustatus, L. ovatus*), ATN-265 (pygidium with attached thoracic segments) (with *E. bornholmensis, L. abnormis, L. angustatus, L. ovatus*), ATN-273 (2 cranidia) (with *E. latum*), ATN-276 (2 cranidia incl. one with a few thoracic segments attached) (with *E. bornholmensis, L. abnormis, L. angustatus, L. ovatus*), ATN-278 (cranidium, 1 pygidium) (with *E. bornholmensis, L. abnormis, L. angustatus, L. ovatus*), ATN-281 (cranidium) (with *L. angustatus*), ATN-284 (cranidium) (with *E. latum*), ATN-293 (cranidium?) (with *L. abnormis, L. angustatus, L. ovatus*), ATN-304 (cranidium) (with *E. bornholmensis, L. abnormis, L. angustatus, L. ovatus*), ATN-305 (cranidium with contiguous thoracic segments) (with *L. angustatus*), ATN-328 (cranidium) (with *E. bornholmensis, L. abnormis, L. angustatus, L. ovatus*), ATN-348 (free cheek) (with *L. abnormis, L. ovatus*), GM 1870-848 (2 cranidia) (with *L. angustatus, L. ovatus*), GM 1888-289A (cranidium, 1 free cheek) (with *L. angustatus, L. ovatus*), GM 1888-289C (cranidium, 3 free cheeks, 2 pygidia) (with *L. angustatus, L. ovatus*), GM 1888-289D (4 cranidia) (with *L. angustatus, L. ovatus*), GM 1922-138D (2 cranidia) (with *L. abnormis, L. ovatus, E. bornholmensis*), GM 1922-139B (cranidium, 2 free cheeks) (with *L. angustatus, L. ovatus*), GM 1922-139E (cranidium) (with *L. abnormis, L. angustatus, L. ovatus*), GM 1922-850 (cranidium) (with *L. ovatus*), MGUH 1962 (cranidium).

Leptoplastus ovatus Angelin, 1854*. OBS: Some of the listed cranidia and in particular free cheeks and pygidia probably represent* L. abnormis*. 401 cranidia, 429 free cheeks, 1 hypostome? and 35 pygidia*. Samples ATN-106 (2 cranidia) (with *E. bornholmensis*), ATN-108 (2 cranidia, 12 free cheeks) (with *E. bornholmensis, L. abnormis, L. angustatus*), ATN-109 (cranidium) (with *L. angustatus*), ATN-118 (2 cranidia) (with *E. bornholmensis, L. angustatus*), ATN-119 (10 cranidia, 5 free cheeks, 1 pygidium) (with *E. bornholmensis, L. abnormis*), ATN-120 (3 cranidia, 1 free cheek) (with *E. bornholmensis*), ATN-122 (10 cranidia, >15 free cheeks) (with *E. bornholmensis, L. abnormis*), ATN-124 (21 cranidia, >20 free cheeks, 1 pygidium) (with *E. bornholmensis, L. abnormis, L. angustatus*), ATN-129 (6 cranidia, 5 free cheeks) (with *E. bornholmensis, L. abnormis, L. angustatus*), ATN-152 (4 cranidia, 5 free cheeks) (with *L. angustatus*), ATN-154 (11 cranidia, 24 free cheeks, 1 pygidium) (with *E. bornholmensis, L. abnormis*), ATN-156 (6 cranidia, 20 free cheeks) (with *E. bornholmensis, L. abnormis, L. angustatus*), ATN-157 (8 cranidia, 4 free cheeks, 1 pygidium) (with *E. bornholmensis, L. abnormis, L. angustatus*), ATN-158 (2 cranidia) (with *L. angustatus, L. crassicornis*), ATN-160 (cranidium), ATN-162 (2 cranidia, 1 free cheek) (with *L. angustatus*), ATN-167 (2 free cheeks), ATN-170 (5 cranidia. 3 free cheeks) (with *E. bornholmensis, L. abnormis, L. angustatus*), ATN-172 (4 cranidia, 1 free cheek), ATN-174 (cranidium), ATN-176 (18 cranidia, >28 free cheeks, 1 pygidium) (with *E. bornholmensis, L. abnormis, L. angustatus*), ATN-177 (cranidium) (with *L. angustatus*), ATN-217 (7 cranidia, >8 free cheeks) (with *E. bornholmensis, L. abnormis*), ATN-227 (10 cranidia, 1 free cheek), ATN-232 (3 cranidia, 5 free cheeks, 3 pygidia) (with *L. abnormis*), ATN-233 (1 free cheek) (with *L. angustatus*), ATN-237 (free cheek), ATN-241 (cranidium, 1 free cheek, 1 hypostome?) (with *L. abnormis*), ATN-242 (cranidium), ATN-243 (cranidium, 12 free cheeks, 2 pygidia) (with *L. abnormis*), ATN-244 (4 cranidia, 3 free cheeks), ATN-249 (cranidium), ATN-251 (3 cranidia, 7 free cheeks) (with *E. bornholmensis, L. abnormis, L. angustatus*), ATN-252 (cranidium) (with *L. abnormis, L. angustatus, L. crassicornis*), ATN-253 (cranidium) (with *L. angustatus*), ATN-254 (3 cranidia) (with *L. angustatus?, L. abnormis*), ATN-260 (3 cranidia, 1 free cheek) (with *L. abnormis, L. angustatus, E. bornholmensis*), ATN-261 (2 cranidia, >13 free cheeks, 1 pygidium) (with *L. abnormis, L. angustatus*), ATN-262 (3 cranidia, 4 free cheeks) (with *E. bornholmensis, L. abnormis*), ATN-263 (6 cranidia, >7 free cheeks, 3 pygidia) (with *L. abnormis, L. angustatus, L. crassicornis*), ATN-265 (3 cranidia, 2 free cheeks, 2 pygidia?) (with *E. bornholmensis, L. abnormis, L. angustatus, L. crassicornis*), ATN-269 (free cheek) (with *L. angustatus*), ATN-270 (3 cranidia, 4 free cheeks, 1 pygidium) (with *L. abnormis*), ATN-271 (2 cranidia, 2 free cheeks) (with *E. bornholmensis, L. abnormis*), ATN-276 (11 cranidia, >14 free cheeks, 3 pygidia) (with E. bornholmensis, *L. abnormis, L. crassicornis, L. angustatus*), ATN-277 (2 cranidia, 7 free cheeks) (with *E. bornholmensis, L. abnormis, L. angustatus*), ATN-278 (free cheek) (with *E. bornholmensis, L. abnormis, L. angustatus, L. crassicornis*), ATN-283 (cranidium) (with *L. abnormis*), ATN-288 (3 cranidia, 6 free cheeks) (with *L. abnormis, L. angustatus*), ATN-290 (4 cranidia), ATN-291 (2 cranidia, 1 free cheek), ATN-292 (free cheek) (with *E. bornholmensis, L. angustatus*), ATN-293 (cranidium, 5 free cheeks) (with *L. abnormis, L. angustatus, L. crassicornis?*), ATN-296 (cranidium) (with *E. latum*), ATN-299 (free cheek) (with *E. bornholmensis, L. angustatus*), ATN-301 (2 free cheeks) (with *L. abnormis, L. angustatus*), ATN-302 (1 free cheek, 2 pygidia) (with *L. abnormis*), ATN-304 (2 cranidia, >10 free cheeks, 3 pygidia) (with *E. bornholmensis, L. abnormis, L. angustatus, L. crassicornis*), ATN-306 (2 cranidia, >8 free cheeks, 1 pygidium) (with *E. bornholmensis, L. abnormis*), ATN-307 (3 cranidia, 9 free cheeks) (with *E. bornholmensis, L. abnormis*), ATN-328 (8 cranidia, 11 free cheeks, 2 pygidia) (with *E. bornholmensis, L. abnormis, L. angustatus, L. crassicornis*), ATN-329 (20 cranidia, 9 free cheeks) (with *E. bornholmensis*), ATN-331 (3 cranidia, 3 free cheeks) (with *L. abnormis, L. angustatus*), ATN-332 (5 cranidia, 1 pygidium) (with *L. abnormis, L. angustatus*), ATN-333 (5 free cheeks) (with *E. bornholmensis*),

ATN-335 (cranidium, 1 free cheek) (with *L. abnormis, L. angustatus*), ATN-336 (2 free cheeks) (with *E. bornholmensis, L. abnormis, L. angustatus*), ATN-338 (2 cranidia, 2 free cheeks) (with *L. abnormis*), ATN-339 (7 cranidia) (with *E. bornholmensis, L. abnormis*), ATN-340 (cranidium, >2 free cheeks) (with *E. bornholmensis, L. angustatus, L. abnormis*), ATN-341 (6 cranidia, >2 free cheeks) (with *L. abnormis, L. angustatus*), ATN-342 (9 cranidia, 3 free cheeks) (with *E. bornholmensis, L. abnormis*), ATN-343 (cranidium) (with *E. bornholmensis, L. abnormis, L. angustatus*), ATN-345 (3 cranidia), ATN-346 (9 cranidia, >14 free cheeks) (with *E. bornholmensis, L. abnormis, L. angustatus*), ATN-347 (5 cranidia, 8 free cheeks) (with *L. abnormis, L. angustatus*), ATN-348 (7 cranidia, 7 free cheeks) (with *L. abnormis, L. crassicornis*), L126 (5 cranidia, >10 free cheeks) (with *E. bornholmensis, L. abnormis*), GM 1870-847 (6 cranidia) (with *L. angustatus*), GM 1870-848 (cranidium, 2 free cheeks) (with *L. angustatus, L. crassicornis*), GM 1870-850 (3 cranidia, 2 free cheeks) (with *L. crassicornis*), GM 1871-607 (cranidium) (with *E. bornholmensis, L. angustatus*), GM 1888-289A (cranidium) (with *L. angustatus, L. crassicornis*), GM 1888-289D (cranidium), (with *L. angustatus, L. crassicornis*), GM 1902-1199 (cranidium), GM 1902-1200 (2 cranidia, 1 free cheek), GM 1902-1201 (cranidium) (with *L. abnormis*), GM 1902-1202 (cranidium, 2 free cheeks), GM 1902-1204 (2 free cheeks), GM 1902-1207 (cranidium, 3 free cheeks), GM 1922-138D (22 cranidia, 27 free cheeks, 1 pygidium) (*E. bornholmensis, L. abnormis, L. crassicornis*), GM 1922-138F (6 cranidia, 2 free cheeks), GM 1922-139B (4 cranidia, 2 free cheeks, 1 pygidium) (with *L. angustatus, L. crassicornis*), GM 1922-139E (4 cranidia, 5 free cheeks, 1 pygidium) (with *E. bornholmensis, L. abnormis, L. angustatus, L. crassicornis*), GM 1922-139G (cranidium, free cheek) (with *E. bornholmensis, L. angustatus*), GM 1930-99/100 (21 cranidia, 6 free cheeks) (with *E. bornholmensis, L. angustatus*), GM 2019-88 (3 cranidia, 2 free cheeks) (with *L. abnormis*), GM 2019-89 (7 cranidia, 4 free cheeks, 1 pygidium) (with *L. abnormis*), GM 2019-90 (9 cranidia, 8 free cheeks, 2 pygidia) (with *E. bornholmensis, L. abnormis, L. angustatus*).

Leptoplastus stenotus Angelin, 1854. *142 cranidia, 12 free cheeks and 5 pygidia.* Samples ATN-168 (21 cranidia), ATN-182 (3 cranidia), ATN-199 (6 cranidia, 2 free cheeks, 1 pygidium), ATN-255 (11 cranidia), ATN-257 (60 cranidia), ATN-266 (9 cranidia), L125 (20 cranidia), GM 1902-1205 (cranidium, external mould of free cheek), GM 1922-139F (4 cranidia, 1 juvenile cranidium, free cheek, pygidium) (incl. MGUH 1986), GM 1922-152 (6 cranidia, 8 free cheeks, 3 pygidia).

Eurycare bornholmensis (Poulsen, 1923). *2 more or less complete specimens, 123 cranidia (incl. one with 13 and one with 14 contiguous thoracic segments), 8 free cheeks, one hypostome (tentatively assigned) and 7 pygidia.* Samples ATN-106 (cranidium) (with *L. ovatus*), ATN-108 (4 cranidia) (with *L. ovatus*), ATN-110 (cranidium) (with *L. angustatus, L. crassicornis*), ATN-118 (cranidium with 13 thoracic segments) (with *L. angustatus, L. ovatus*), ATN-119 (2 cranidia) (with *L. abnormis, L. ovatus*), ATN-120 (complete specimen, 1 cranidium) (with *L. ovatus*), ATN-122 (5 cranidia, 1 external mould of cranidium) (with *L. abnormis, L. ovatus*), ATN-123 (2 cranidia, 1 pygidium) (with *P. leptoplastorum*?), ATN-124 (5 cranidia, 1 free cheek) (with *L. abnormis, L. angustatus, L. ovatus*), ATN-129 (2 external moulds of cranidium) (with *L. abnormis, L. angustatus, L. ovatus*), ATN-136 (3 cranidia incl. one with 14 thoracic segments, the other with 8 thoracic segments; counter piece of ATN-333) (with *L. angustatus*), ATN-154 (2 cranidia) (with *L. abnormis, L. ovatus*), ATN-156 (5 cranidia) (with *L. abnormis, L. angustatus, L. ovatus*), ATN-157 (2 cranidia, 1 external mould cranidium, 2 free cheeks, external mould of pygidium) (with *L. abnormis, L. angustatus, L. ovatus*), ATN-170 (cranidium) (with *L. abnormis, L. angustatus, L. ovatus*), ATN-176 (2 cranidia, 2 free cheeks) (with *L. abnormis, L. angustatus, L. ovatus*), ATN-216 (cranidium) (with *L. angustatus, L. crassicornis*), ATN-217 (3 cranidia) (with *L. abnormis, L. ovatus*), ATN-224 (2 cranidia) (with *L. angustatus*), ATN-248 (2 cranidia), ATN-251 (free cheek) (with *L. abnormis, L. angustatus, L. ovatus*), ATN-260 (cranidium) (with *L. angustatus, L. ovatus, L. abnormis*), ATN-262 (cranidium) (with *L. abnormis, L. ovatus*), ATN-265 (external mould of cranidium) (with *L. abnormis, L. angustatus, L. crassicornis, L. ovatus*), ATN-271 (external mould of cranidium) (with *L. abnormis, L. ovatus*), ATN-275 (2 cranidia) (with *L. abnormis, L. angustatus*), ATN-276 (cranidium) (with *L. abnormis, L. angustatus, L. crassicornis, L. ovatus*), ATN-277 (external moulds of 3 cranidia, 1 cranidium) (with *L. abnormis, L. angustatus, L. ovatus*), ATN-278 (cranidium) (with *L. abnormis, L. angustatus, L. crassicornis, L. ovatus*), ATN-292 (cranidium) (with *L. angustatus, L. ovatus*), ATN-299 (cranidium) (with *L. angustatus, L. ovatus*), ATN-304 (4 cranidia, 4 external moulds of cranidia, 1 pygidium) (with *L. abnormis, L. angustatus, L. crassicornis, L. ovatus*), ATN-306 (4 cranidia, 1 external mould of cranidium, 1 pygidium) (with *L. ovatus*), ATN-307 (1 external mould of cranidium, 1 free cheek) (with *L. abnormis, L. ovatus*), ATN-328 (3 cranidia) (with *L. abnormis, L. angustatus, L. crassicornis, L. ovatus*), ATN-329 (almost complete specimen, 3 cranidia) (with *L. angustatus, L. crassicornis, L. ovatus*), ATN-333 (counter piece to ATN-136) (with *L. ovatus*), ATN-336 (cranidium) (with *L. abnormis, L. angustatus, L. ovatus*), ATN-339 (4 cranidia, 3 external moulds of cranidia, 2 pygidia) (with *L. abnormis, L. ovatus*), ATN-340 (cranidium) (with *L. abnormis, L. angustatus, L. ovatus*), ATN-342 (2 cranidia) (with *L. abnormis, L. ovatus*), ATN-343 (cranidium) (with *L. abnormis, L. angustatus, L. ovatus*), ATN-346 (pygidium) (with *L. abnormis, L. angustatus, L. ovatus*), L126 (2 cranidia, 1 possible hypostome) (with *L. abnormis, L. ovatus*), GM 1871-607 (cranidium) (with *L. angustatus, L. ovatus*), GM 1881-1784 (2 cranidia), GM 1922-138D (small cranidium) (with *L. abnormis, L. crassicornis, L. ovatus*), GM 1922-139A (5 cranidia) (with *L. angustatus*), GM 1922-139E (cranidium) (with *L. abnormis, L. angustatus, L. ovatus*), GM 1930-99/100 (4 cranidia, 1 free cheek?) (with *L. angustatus, L. ovatus*), GM 1922-139G incl. MGUH 1964 (external mould of cranidium) (with *L. angustatus, L. ovatus*), GM 2019-90 (cranidium) (with *L. abnormis, L. angustatus, L. ovatus*).
.

Eurycare brevicauda Angelin, 1854. *1 cranidium*, sample ATN-280 (with *E. latum*).

Eurycare latum **(Boeck, 1838).** *156 cranidia including one with 6 continuous thoracic segments, 23 free cheeks and 18 pygidia.* Samples ATN-114 (13 cranidia, 1 free cheek, 3 pygidia, 2 external moulds of pygidia), ATN-150 (15 cranidia incl. one with 11 contiguous thoracic segments, 2 free cheeks, 3 pygidia), ATN-159 (21 cranidia, 3 free cheeks), ATN-231 (3 cranidia, 2 free cheeks), ATN-250 (7 cranidia, 3 free cheeks, 1 pygidium), ATN-268 (7 cranidia), ATN-272 (5 cranidia, 1 free cheek), ATN-273 (cranidium, 1 pygidium) (with *L. crassicornis*), ATN-279 (2 cranidia, 1 pygidium), ATN-280 (3 cranidia, 1 free cheek) (with *E. brevicauda*), ATN-282 (10 cranidia, 1 pygidium), ATN-284 (4 cranidia, 1 pygidium) (with *L. crassicornis*), ATN-286 (2 cranidia, 1 pygidium), ATN-287 (7 cranidia, 1 pygidium), ATN-294 (6 cranidia, >10 external moulds of cranidia, 3 free cheeks, 1 pygidium), ATN-296 (9 cranidia) (with *L. ovatus*), ATN-300 (8 cranidia, >2 external moulds of cranidia, 2 free cheeks, 1 pygidium), GM 1922-138A (3 cranidia), GM 1922-138B (5 cranidia, 1 free cheek, 1 pygidium), GM 1922-138C (4 cranidia, 1 free cheek), GM 1922-138E (4 cranidia, 3 free cheeks) (including MGUH 1961), GM 1922-138G (4 cranidia).

Ctenopyge (Ctenopyge) affinis **Westergård, 1922.** *222 cranidia incl. 13 external moulds, and 15 free cheeks (tentatively assigned).* Samples ATN-103 (12 cranidia, 3 free cheeks) (with *Peltura cf. minor, S. alatus*), ATN-113 (51 cranidia, 3 external moulds of cranidia, 3 free cheeks) (with *C. magna* n.sp., *C. ahlbergi, P. minor, S. alatus),* ATN-116 (5 cranidia, 1 free cheek?) (with *C. magna* n.sp., *C. ahlbergi, Peltura cf. minor, S. alatus*), ATN-117 (17 cranidia) (with *C. ahlbergi, S. magna* n.sp., *S. alatus*), ATN-127 (2 cranidia, 2 external moulds of cranidia) (with *C. ahlbergi, P. minor, S. alatus*), ATN-130 (4 cranidia) (with *C. magna* n.sp., *S. alatus),* ATN-132 (12 cranidia, free cheek?) (with *P. minor, C. ahlbergi, S. alatus*), ATN-133 (6 cranidia) (with *C. magna* n.sp., *C. ahlbergi, P. minor, S. alatus),* ATN-134 (12 cranidia, 1 external mould of cranidum, 1 free cheek?) (with *C. magna* n.sp., *C. ahlbergi, Peltura* sp., *S. alatus),* ATN-137 (cranidium) (with *C. magna* n.sp., *S. alatus*), ATN-139 (7 cranidia) (with *S. alatus, P. minor*), ATN-146 (9 cranidia, 2 free cheeks?) (with *C. magna* n.sp., *C. ahlbergi, S. alatus*), ATN-147 (5 cranidia, 1 free cheek?) (with *C. magna* n.sp., *S. alatus*), ATN-169 (3 cranidia, 1 external mould of cranidium, 2 external moulds of free cheeks) (with *C. magna* n.sp, *S. alatus*), ATN-173 (cranidium, 1 external mould of cranidium) (with *C. ahlbergi, C. magna* n.sp..*S. alatus*), ATN-191 (cranidium) (with *S. alatus*), ATN-192 (cranidium, 2 external moulds of cranidia) (with *S. alatus*), ATN-205 (external mould of cranidium) (with *C. ahlbergi, S. alatus*), ATN-222 (17 cranidia, 1 free cheek) (with *C. ahlbergi, S. alatus*), ATN-246 (11 cranidia, 2 external moulds of cranidia) (with *C. magna* n.sp., *S. alatus*). ATN-330 (5 cranidia including a juvenile) (with *C. magna* n.sp., *C. ahlbergi, S. alatus*), L76 (2 cranidia, 3 external moulds) (with *S. magna* n.sp*., S. ahlbergi, S. alatus*), L77 (cranidium, 1 external mould of cranidium) (with *C. ahlbergi, S. alatus* and unknown species?), L84 (6 cranidia) (with *C. magna* n.sp., *S. alatus*), L93 (2 cranidia) (with *C. magna* n.sp., *S. alatus*), GM 1902-1208 (2 cranidia) (with *S. alatus*), GM 1902-1209 (3 cranidia) (with *C. magna* n.sp., *C. ahlbergi, C. affinis, S. alatus*), GM 1902-1210 (7 cranidia) (with *C. magna* n.sp., *C. ahlbergi, S. alatus*), GM 1902-1212 (3 cranidia, 1 free cheek?, external mould of 1 free cheek?) (with *C. magna* n.sp., *C. ahlbergi, S. alatus*),

Ctenopyge (Ctenopyge) ahlbergi **Clarkson, Ahlgren & Taylor, 2004.** *38 cranidia incl. 2 external moulds of cranidia and 7 free cheeks.* Samples ATN-113 (3 cranidia, 3 free cheeks) (with *C. magna* n.sp., *C. affinis, P. minor, S. alatus),* ATN-116 (disarticulated thoracic segment) (with *C. magna* n.sp., *C. affinis, Peltura cf. minor, S. alatus*), ATN-117 (2 cranidia, 1 free cheek, disarticulated thoracic segment?) (with *C. affinis, S. magna* n.sp., *S. alatus*), ATN-127 (cranidium) (with *C. affinis, P. minor, S. alatus*), ATN-132 (2 cranidia, 1 external mould of cranidium, disarticulated thoracic segment?) (with *C. affinis, P. minor, S. alatus*), ATN-133 (cranidium, disarticulated thoracic segment?) (with *C. magna* n.sp., *C. affinis, P. minor, S. alatus),* ATN-134 (6 cranidia, 1 free cheek, disarticulated thoracic segments?) (with *C. magna* n.sp., *C. affinis, Peltura* sp., *S. alatus*), ATN-146 (cranidium, 1 free cheek) (with C. *magna* n.sp., *C. affinis, S. alatus*), ATN-148 (cranidium) (with *S. alatus, Peltura cf. minor*), ATN-173 (cranidium, 1 fragmentary free cheek, 1 thoracic segment) (with *C. affinis, C. magna* n.sp., *S. alatus*), ATN-205 (cranidium) (with *C. affinis**, S. alatus*), ATN-222 (poor cranidium) (with *C. affinis, S. alatus*), ATN-330 (3 cranidia) (with *C. magna* n.sp., *C. affinis, S. alatus*), L76 (cranidium, external mould of cranidium, disarticulated thoracic segments) (with *C. magna* n.sp., *C. affinis, S. alatus*), L77 (cranidium) (with *C. affinis, S. alatus*, unknown species?) GM 1902-1209 (9 cranidia, disarticulated thoracic segments?) (with *C. magna* n.sp., *C. affinis, S. alatus*), GM 1902-1210 (cranidium, disarticulated thoracic segment) (with *C. magna* n.sp., *C. affinis, S. alatus*), GM 1902-1212 (cranidium, fragmentary) (with *C. magna* n.sp., *C. affinis, S. alatus*).

Ctenopyge (Ctenopyge) bisulcata **(Phillips, 1848).** *6 cranidia.* Samples (in shale): GM 1922-142R (2 cranidia), GM 1922-143 (3 cranidia) (with *Ctenopyge fletcheri*), MGUH 1974 (cranidium).

Ctenopyge (Ctenopyge) fletcheri **(Matthew 1901).** *41 cranidia and 15 free cheeks.* Samples GM 1881-337A (5 cranidia, 2 free cheeks) (with *T. humilis*), GM 1922-143 (31 cranidia, 5 free cheeks) (with *Peltura* sp., *Ctenopyge bisulcata*), GM 1881-337B (5 cranidia, 8 free cheeks incl. MGUH 1978).

Ctenopyge (Ctenopyge) linnarssoni **Westergård, 1922.** *38 cranidia and 2 free cheeks.* Samples L17 (12 cranidia) (with *C. tenuis, P. scarabaeoides, T. humilis*), L38 (2 cranidia) (with *C. pecten, C. tenuis, C. teretifrons, Peltura* sp*., T. humilis*), L50 (2 cranidia) (with *Peltura* sp*., T. humilis*), L52 (1 small cranidium) (with *C. pecten, C. tenuis*), GM 1871-647 (cranidium) (with *Peltura* sp., *P. scarabaeoides, T.*

humilis), GM 1871-657 (free cheek?) (with *C. tenuis, T. humilis*), GM 1871-666 (free cheek), GM 1871-675A (cranidium) (with *T. humilis*), GM 1877-2000 (2 cranidia) (with *Peltura* sp., *T. humilis*), GM 1881-1805 (cranidium) (with *C. tenuis, C. teretifrons, Peltura* sp., *P. scarabaeoides, T. humilis*), GM 1922-142B (cranidium) (with *C. pecten, C. tenuis, C. teretifrons, Peltura* sp., *P. scarabaeoides, T. humilis*), GM 1922-142C (cranidium) (with *C. tenuis, C. teretifrons, Peltura* sp., *P. scarabaeoides, T. humilis*), GM 1922-142E (cranidium) (with *C. tenuis, C. teretifrons, Peltura* sp., *P. scarabaeoides, T. humilis*), GM 1922-142H (cranidium) (with *C. tenuis, C. teretifrons, Peltura* sp., *T. humilis*), GM 1922-142I (cranidium) (with *C. pecten, C. tenuis, C. teretifrons, Peltura* sp., *P. scarabaeoides, T. humilis*), GM 1922-142K (cranidium) (with *C. teretifrons, Peltura* sp., *P. scarabaeoides, T. humilis*), GM 1922-142L (cranidium), GM 1922-142M (cranidium) (with *C. tenuis, C. teretifrons, Peltura* sp., *P. scarabaeoides, T. humilis*), GM 1922-142N (4 cranidia) (with *C. tenuis, C. teretifrons, P. scarabaeoides, T. humilis*), GM 1922-142U (3 cranidia) (with *C. tenuis, Peltura scarabaeoides, Peltura* sp., *T. humilis*), MGUH 1970 (cranidium).

***Ctenopyge (Ctenopyge) magna* n.sp.**. *41 cranidia incl. 10 external moulds, 2 free cheeks? and 1 hypostome*. Samples ATN-113 (5 cranidia) (with *C. ahlbergi, C. affinis, S. alatus, P. minor*), ATN-116 (3 cranidia, 1 free cheek?) (with *C. ahlbergi, C. affinis, Peltura cf. minor, S. alatus*), ATN-117 (cranidium) (with *C. affinis, C. ahlbergi, S. alatus*), ATN-130 (cranidium) (with *C. affinis, S. alatus*), ATN-133 (cranidium) (with *C. ahlbergi, C. affinis, P. minor, S. alatus*), ATN-134 (2 cranidia, external mould of cranidium) (with *C. ahlbergi, C. affinis, Peltura* sp., *S. alatus*), ATN-137 (cranidium) (with *C. affinis, S. alatus*), ATN-146 (2 cranidia) (with *C. ahlbergi, C. affinis, S. alatus*), ATN-147 (cranidium) (with *C. affinis, S. alatus*), ATN-169 (fragmentary cranidium) (with *C. affinis, S. alatus*), ATN-173 (2 cranidia, 2 external moulds of cranidia, 1 fragmentary free cheek?) (with *C. affinis, C. ahlbergi, S. alatus*), ATN-246 (external mould of cranidium) (with *C. affinis, S. alatus*), ATN-330 (cranidium) (with *C. ahlbergi, C. affinis, S. alatus*), L76 (external mould of cranidium) (with *S. ahlbergi, S. affinis, S. alatus*), L84 (2 cranidia) (with *C. affinis, S. alatus*), L93 (fragment of cranidium) (with *C. affinis, S, alatus*), GM 1922-142S (cranidium) (with *T. humilis, C. tenuis, C. teretifrons, P. scarabaeoides*), GM 1902-1209 (4 cranidia incl. MGUH 1975) (with *C. ahlbergi, C. affinis, S. alatus*), GM 1902-1210 (1 cranidium, 4 external moulds of cranidia) (with *C. ahlbergi, C. affinis, S. alatus*), GM 1902-1212 (cranidium, 1 external mould of cranidium) (with *C. ahlbergi, C. affinis, S. alatus*).

***Ctenopyge (Ctenopyge) pecten* (Salter, 1864).** *21 cranidia*. Samples L38 (1 external mould of cranidium) (with *C. linnarssoni, C. tenuis, C. teretifrons, Peltura* sp., *T. humilis*), L43 (cranidium) (with *C. tenuis, C. teretifrons, P. scarabaeoides, T. humilis*, L52 (1 small cranidium) (with *C. linnarssoni, C. tenuis*), GM 1871-651B (cranidium) (with *T. humilis*), GM 1871-655 (2 cranidia) (with *C. tenuis, Peltura* sp, *T. humilis*), GM 1871-674 (cranidium) (with *T. humilis, P. scarabaeoides*), GM 1874-27 (2 cranidia) (with *C. tenuis, C. teretifrons, Peltura* sp., *P. scarabaeoides, T. humilis*), GM 1874-28 (cranidium) (with *C. tenuis, Peltura* sp., *T. humilis*), GM 1881-1802 (2 cranidia?) (with *C. teretifrons, P. scarabaeoides, T. humilis*), GM 1922-142A (cranidium?) (with *C. tenuis, C. teretifrons, Peltura* sp., *P. scarabaeoides, T. humilis*), GM 1922-142B (3 cranidia) (with *C. tenuis, C. linnarssoni, C. teretifrons, Peltura* sp., *P. scarabaeoides, T. humilis*), GM 1922-142D (cranidium) (with *C. tenuis, C. teretifrons, Peltura* sp., *P. scarabaeoides, T. humilis*), GM 1922-142I (cranidium) (with *C. linnarssoni, C. tenuis, C. teretifrons, Peltura* sp., *P. scarabaeoides, T. humilis*). GM 1922-142T (2 cranidia) (with *C. tenuis, C. teretifrons, Peltura* sp., *T. humilis*), GM 2019-99 (cranidium) (with *C. tenuis, Peltura* sp., *P. scarabaeoides, T. humilis*).

***Ctenopyge (Ctenopyge) tenuis* Poulsen, 1963**. *327 cranidia, 7 free cheeks, thorax with 4-5 contiguous segments and 24 pygidia with up to 9 attached thoracic segments attached*. Samples L17 (cranidium) (with *C. linnarssoni, Peltura* sp., *P. scarabaeoides, T. humilis*), L38 (2 cranidia, 2 external moulds of cranidia, 2 pygidia) (with *C. linnarssoni, C. pecten, C. teretifrons, Peltura* sp., *T. humilis*), L41 (3 cranidia) (with *C. teretifrons, Peltura* sp., *P. scarabaeoides, T. humilis*), L43 (11 cranidia, 1 poor pygidium) (with *C. pecten, C. teretifrons, P. scarabaeoides, T. humilis*), L44 (cranidium) (with *Peltura* sp., *P. scarabaeoides, T. humilis*), L45 (2 cranidia) (with *P. scarabaeoides, T. humilis*), L46 (9 cranidia) (with *C. teretifrons, Peltura* sp., *P. scarabaeoides, T. humilis*), L47 (cranidium) (with *P. scarabaeoides*), L48 (7 cranidia, 2 external moulds of cranidia, free cheek) (with *T. humilis*), L52 (5 cranidia, 2 external moulds of cranidia) (with *C. linnarssoni, C. pecten*), GM 1871-611 (cranidium) (with *Peltura* sp., *P. scarabaeoides, T. humilis*), GM 1871-612 (14 cranidia, 2 external moulds of cranidia, pygidium) (with *C. teretifrons, Peltura* sp., *T. humilis*), GM 1871-617 (cranidium) (with *Peltura* sp.), GM 1871-636 (5 continuous thoracic segments, 1 pygidium) (with *Peltura* sp.), GM 1871-655 (2 cranidia?) (with *C. pecten, Peltura* sp, *T. humilis*), GM 1871-657 (cranidium, 2 free cheeks) (with *C. linnarssoni?, T. humilis*), GM 1871-661 (5 cranidia) (with *Peltura* sp., *T. humilis*), GM 1871-672 (5 cranidia) (with *Peltura* sp., *T. humilis*), GM 1871-673 (cranidium) (with *Peltura scarabaeoides, Peltura* sp.), GM 1874-27 (13 cranidia, 2 external moulds of cranidia) (with *C. pecten, C. teretifrons, Peltura* sp., *P. scarabaeoides, T. humilis*), GM 1874-28 (3 cranidia, free cheek, 2 pygidia) (with *C. pecten, Peltura* sp., *T. humilis*), GM 1874-30 (4 cranidia) (with *Peltura* sp., *P. scarabaeoides, T. hunilis*), GM 1874-661 (2 cranidia) (with *Peltura* sp., *T. humilis*), GM 1881-1796 (including MGUH 1973) (2 cranidia, 1 pygidium with 5 continuous thoracic segments) (with *C. teretifrons, Peltura* sp., *T. humilis*), GM 1881-1797 (cranidium, 1 pygidium with 9 continuous thoracic segments) (including MGUH 1972) (with *T. humilis*), GM 1881-1804 (2 cranidia) (with *Peltura* sp., *T. humilis*), GM 1881-1805 (3 cranidia) (with *C. linnarssoni, C. teretifrons, Peltura* sp., *P. scarabaeoides, T. humilis*), GM 1883-341A (2 cranidia) (with *C. teretifrons, Peltura* sp., *T. humilis*), GM 1883-341B (4 cranidia) (with *Peltura* sp., *T. humilis*), GM 1886-199 (3 cranidia, 1 pygidium) (with *Peltura* sp.), GM 1922-142A (42 cranidia, 1 pygidium, 2 external moulds of pygidia) (with *C. teretifrons, Peltura* sp., *P. scarabaeoides, T. humilis*), GM 1922-142B (17 cranidia, 1 pygidium) (with *C. pecten, C. linnarssoni, C. teretifrons, Peltura* sp., *P. scarabaeoides, T. humilis*), GM 1922-142C (11 cranidia) (with *C. linnarssoni, C. teretifrons, Peltura* sp., *P. scarabaeoides, T. humilis*),

GM 1922-142D (6 cranidia, 1 pygidium) (with *C. pecten, C. teretifrons, Peltura* sp., *P. scarabaeoides, T. humilis*), GM 1922-142E (7 cranidia) (with *C. linnarssoni, C. teretifrons, Peltura* sp., *P. scarabaeoides, T. humilis*), GM 1922-142F (2 cranidia) (with *Peltura* sp., *P. scarabaeoides, T. humilis*), GM 1922-142H (13 cranidia, 1 pygidium, 1 external mould of pygidium) (with with *C. linnarssoni, C. teretifrons, Peltura* sp., *T. humilis*), GM 1922-142I (45 cranidia, 2 pygidia of which one has 3 thoracic segments attached) (with *C. linnarssoni, C. pecten, C. teretifrons, Peltura* sp., *P. scarabaeoides, T. humilis*), GM 1922-142J (11 cranidia, 2 free cheeks) (with *C. teretifrons, Peltura* sp., *P. scarabaeoides, T. humilis*), GM 1922-142M (3 cranidia, 2 pygidia) (with *C. linnarssoni, C. teretifrons, Peltura* sp., *P. scarabaeoides, T. humilis*), GM 1922-142N (7 cranidia, 1 pygidium) (with *C. linnarssoni, C. teretifrons, P. scarabaeoides, T. humilis*), GM 1922-142O (4 cranidia) (with *C. teretifrons, Peltura* sp., *P. scarabaeoides, T. humilis*), GM 1922-142P (4 cranidia) (including MGUH 1971) (with *Peltura* sp., *T. humilis*), GM 1922-142Q (including MGUH 1976) (cranidium) (with *C. teretifrons, Peltura* sp., *T. humilis*), GM 1922-142S (3 cranidia, 1 free cheek) (with *T. humilis, C. magna n.sp., C. teretifrons, P. scarabaeoides*), GM 1922-142T (5 cranidia) (with *C. pecten, C. teretifrons, Peltura* sp., *T. humilis*), GM 2019-7 (cranidium) (with *Peltura* sp., *T. humilis*), GM 2019-8 (2 cranidia, 2 pygidia) (with *Peltura* sp., *P. scarabaeoides*), GM 2019-9 (2 cranidia) (with *Peltura* sp.), GM 2019-10 (3 cranidia of which one is juvenile) (with *Peltura* sp.), GM 2019-11 (3 cranidia) (with *C. teretifrons, Peltura* sp., *T. humilis*), GM 2019-12 (2 cranidia) (with *Peltura* sp., *T. humilis*), GM 2019-13 (3 cranidia), GM 2019-14 (cranidium) (with *Peltura* sp., *T. humilis*), GM 2019-15 (11 cranidia) (with *C. teretifrons, Peltura* sp., *T. humilis*), GM 2019-16 (cranidium) (with *Peltura* sp., *T. humilis*), GM 2019-99 (5 cranidia, 2 external moulds of cranidia) (with *C. pecten, Peltura* sp., *P. scarabaeoides, T. humilis*).

Ctenopyge (Ctenopyge) teretifrons (**Angelin, 1854**). *71 cranidia.* Samples L38 (4 cranidia) (with *C. pecten, C. tenuis, C. linnarssoni, Peltura* sp., *T. humilis*), L39 (2 cranidia) (with *Peltura* sp., *T. humilis*), L41 (cranidium) (with *C. tenuis, Peltura* sp., *P. scarabaeoides, T. humilis*), L42 (cranidium) (with *Peltura* sp., *T. humilis*), L43 (cranidium, 1 external mould of cranidium) (with *C. pecten, C. tenuis, P. scarabaeoides, T. humilis*), L46 (2 cranidia) (with *C. tenuis, P. scarabaeoides, T. humilis*), L49 (cranidium) (with *Peltura* sp., *T. humilis*), GM 1874-27 (cranidium) (with *C. pecten, C. tenuis, Peltura* sp., *P. scarabaeoides, T. humilis*), GM 1871-612 (2 cranidia) (with *C. tenuis, Peltura* sp., *T. humilis*), GM 1871-648 (cranidium) (with *Peltura* sp., *T. humilis*), GM 1871-658 (cranidium), GM 1871-662 (cranidium), GM 1871-664 (cranidium) (with *T. humilis*), GM 1871-665 (2 cranidia) (with *T. humilis*), GM 1871-667 (cranidium) (with *P. scarabaeoides, T. humilis*), GM 1871-675B (cranidium) (with *T. humilis*), GM 1877-1999 (cranidium) (with with *Peltura* sp., *P. scarabaeoides, T. humilis*), GM 1881-1796 (2 cranidia) (with *C. tenuis, Peltura* sp., *T. humilis*), GM 1881-1802 (2 cranidia) (with *C. pecten, P. scarabaeoides, T. humilis*), GM 1881-1805 (cranidium) (with *C. linnarssoni, C. tenuis, Peltura* sp., *P. scarabaeoides, T. humilis*), GM 1883-341A (cranidium) (with *C. tenuis, Peltura* sp., *T. humilis*), GM 1922-142A (3 cranidia) (with *C. tenuis, Peltura* sp., *P. scarabaeoides, T. humilis*), GM 1922-142B (cranidium) (with *C. linnarssoni, C. pecten, C. tenuis, Peltura* sp., *P. scarabaeoides, T. humilis*), GM 1922-142C (6 cranidia) (with *C. linnarssoni, C. tenuis, Peltura* sp., *P. scarabaeoides, T. humilis*), GM 1922-142D (4 cranidia) (with *C. pecten, C. tenuis, Peltura* sp., *P. scarabaeoides, T. humilis*), GM 1922-142E (cranidium) (with *C. linnarssoni, C. tenuis, Peltura* sp., *P. scarabaeoides, T. humilis*), GM 1922-142H (3 cranidia) (with *C. linnarssoni, C. tenuis, Peltura* sp., *T. humilis*), GM 1922-142I (3 cranidia) (with *C. linnarssoni, C. pecten, C. tenuis, Peltura* sp., *P. scarabaeoides, T. humilis*), GM 1922-142J (cranidium) (with *C. tenuis, Peltura* sp., *P. scarabaeoides, T. humilis*), GM 1922-142K (2 cranidia) (with *C. linnarssoni, Peltura* sp., *P. scarabaeoides, T. humilis*), GM 1922-142M (cranidium) (with *C. linnarssoni, C. tenuis, Peltura* sp., *P. scarabaeoides, T. humilis*), GM 1922-142N (2 cranidia) (with *C. linnarssoni, C. tenuis, P. scarabaeoides, T. humilis*), GM 1922-142O (3 cranidia) (including MGUH 1969) (with *C. tenuis, Peltura* sp., *P. scarabaeoides, T. humilis*), GM 1922-142Q (2 cranidia) (with *C. tenuis, Peltura* sp., *T. humilis*), GM 1922-142S (cranidium) with *T. humilis, C. magna n.sp., C. tenuis, P. scarabaeoides*), GM 1922-142T (2 cranidia) (with *C. pecten, C. tenuis, Peltura* sp., *T. humilis*), GM 2019-11 (cranidium) (with *C. tenuis, Peltura* sp., *T. humilis*), GM 2019-15 (3 cranidia) (with *C. tenuis, Peltura* sp., *T. humilis*), GM 2019-97 (cranidium) (with *Peltura* sp., *T. humilis*).

Ctenopyge (Mesoctenopyge) tumida **Westergård, 1922**. *141 cranidia and 9 free cheeks.* Samples ATN-112 (6 cranidia) (with *S. alatus*), ATN-121 (2 cranidia) (with *S. angustus*), ATN-126 (8 cranidia, 2 external moulds) (with *S. alatus*), ATN-138 (5 cranidia, 2 free cheeks) (with *S. alatus*), ATN-151 (7 cranidia) (with *S. angustus*), ATN-171 (5 cranidia, 1 external mould of cranidium) (with *S. alatus*), ATN-175 (2 cranidia) (with *S. alatus*), ATN-188 (2 cranidia, 1 external mould of cranidium) (with *S. alatus*), ATN-193 (6 cranidia, 1 free cheek) (with *S. alatus*), ATN-197 (13 cranidia, 2 external moulds of cranidia, 1 free cheek) (with *S. alatus, C. tumidoides*), ATN-208 (2 cranidia, free cheek?) (with *S. alatus*), ATN-238 (3 cranidia, 1 external mould of cranidium, 1 free cheek) (with *S. alatus*), ATN-239 (4 cranidia) (with *S. alatus*), L53 (cranidium) (with *S. alatus*), L59 (2 cranidia) (with *S. alatus*), L61 (6 cranidia, 4 external moulds of cranidia) (with *S. alatus*), L64 (cranidium) (with *S. alatus*), L65 (cranidium) (with *C. tumidoides, S. angustus*), L67 (cranidium) (with *S. angustus*), L78 (cranidium, one external mould of cranidium, 1 free cheek) (with *S. alatus*), L81 (2 cranidia) (with *S. alatus*), L88 (external mould of cranidium) (with *S. angustatus*), L89 (cranidium) (with *S. alatus*), GM 1922-141A (cranidium) (with *C. tumidoides, S. angustus*), GM 1922-141C (cranidium,) (with *C. tumidoides, S. angustus*), GM 1922-141G (2 cranidia?) (with *C. tumidoides, S. angustus*), GM 1922-141H (2 cranidia) (with *S. alatus*), GM 1922-141J (2 cranidia) (with *C. tumidoides, S. angustus*), GM 1922-141K (3 cranidia including MGUH 1967) (with *C. tumidoides, S. angustus*), GM 1922-141N (2 cranidia) (with C. *tumidoides, S. angustus*), GM 1922-141P (2 cranidia) (with *C. tumidoides, S. angustus*), GM 1930-101/102 (10 cranidia) (with *C. tumidoides, S. angustus*), GM 2019-17 (11 cranidia, 3 external moulds of cranidia, 1 thoracic segment) (with *S. angustus*), GM 2019-18 (6 cranidia) (with *S. alatus*), GM 2019-21 (free cheek) (with *S. alatus*), GM 2019-25 (cranidium) (with *S. alatus*).

Ctenopyge (Mesoctenopyge) tumidoides **Henningsmoen, 1957.** *141 cranidia, 11 free cheeks.* Samples ATN-111 (cranidium, 3 external moulds of cranidia) (with *P. acutidens, S. angustatus*), ATN-115 (cranidium) (with *S. angustus*), ATN-135 (3 cranidia) (with *S. angustus*), ATN-145 (2 cranidia) (with *P. planicauda, S. angustus*), ATN-190 (4 cranidia) (with *S. angustus*), ATN-197 (5 cranidia, 2 external moulds of cranidia) (with *S. alatus, C. tumida*), ATN-211 (4 cranidia, 1 free cheek) (with *S. angustus*), ATN-218 (2 external moulds of cranidia) (with *S. angustus*), ATN-225 (cranidium) (with *S. angustus*), ATN-226 (6 cranidia, 2 external moulds of cranidia, 1 free cheek) (with *S. angustus*), ATN-258 (cranidium) (with *S. angustus*), ATN-327 (cranidium, 1 external mould of cranidium) (with *P. acutidens, S. angustus*), L55 (3 cranidia) (with *S. angustus*), L56 (6 cranidia) (with *S. angustus*), L57 (3 cranidia) (with *S. angustus*), L58 (cranidium) (with *S. angustus*), L60 (2 poor cranidia) (with *S. angustus*), L62 (cranidium, 2 external moulds of cranidia) (with *S. angustus*), L63 (3 cranidia) (with *S. angustus*), L65 (external mould of cranidium) (with *C. tumida, S. angustus*), L71 (cranidium) (with *S. angustus*), L73 (cranidium) (with *S. angustus*), L75 (cranidium) (with *S. angustus*), L80 (2 cranidia) (with *S. angustus*), L87 (11 cranidia, 2 external moulds of cranidia, 2 free cheeks, 1 external mould of free cheek, 1 thoracic segment) (with *S. angustus*), L92 (2 cranidia) (with *S. angustus*), L124 (1 cranidium) (with *S. angustus*), GM 1922-141A (6 cranidia) (with *C. tumida, S. angustus*), GM 1922-141C (4 cranidia, external mould of free cheek?) (with *C. tumida, S. angustus*), GM 1922-141D (cranidium, 3 external moulds of cranidia) (with *S. angustus*), GM 1922-141G (8 cranidia and 2 external moulds of cranidia) (with *C. tumida?, S. angustus*), GM 1922-141J (cranidium) (with *C. tumida, S. angustus*), GM 1922-141K (cranidium) (with *C. tumida, S. angustus*), GM 1922-141N (5 cranidia, 1 external mould of cranidium) (with *C. tumida, S. angustus*), GM 1922-141P (6 cranidia and 1 external mould of a cranidium) (with *C. tumida, S. angustus*), GM 1930-101/102 (16 cranidia, 2 external moulds of cranidia, 5 free cheeks) (with *C. tumida, S. angustus*), GM 2019-19 (cranidium, 1 external mould of cranidium) (with *S. angustus*), GM 2019-20 (cranidium) (with *S. angustus*), GM 2019-22 (external mould of cranidium) (with *S. angustus*), GM 2019-23 (external mould of cranidium) (with *S. angustus*), GM 2019-26 (cranidium).

Sphaerophthalmus alatus **(Boeck, 1838)**. *Cranidia are extremely abundant of which most are not registered (>> 1000 specimens); ~1011 cranidia, 23 free cheeks, 1 hypostome? and 2 pygidia.* Samples ATN-103 (>20 cranidia) (with *C. affinis, Peltura cf. minor*), ATN-112 (>40 cranidia) (with *C. tumida*), ATN-113 (>30 cranidia, 1 pygidium) (with *C. magna n.sp., C. ahlbergi, C. affinis, P. minor*), ATN-116 (>20 cranidia) (with *C. magna n.sp., C. ahlbergi?, C. affinis, Peltura cf. minor*), ATN-117 (>40 cranidia) (with *C. ahlbergi, C. affinis, S. magna n.sp.*), ATN-126 (c. 15 cranidia) (with *C. tumida*), ATN-127 (10 cranidia) (with *C. ahlbergi, C. affinis, P. minor*), ATN-130 (10 cranidia) (with *C. magna n.sp., C. affinis*), ATN-132 (>20 cranidia) (with *C. ahlbergi, C. affinis, P. minor*), ATN-133 (>20 cranidia) (with *C. magna n.sp., C ahlbergi, C. affinis, P. minor*), ATN-134 (>30 cranidia, 3 free cheeks) (with *C. magna n.sp., C. ahlbergi, C. affinis, Peltura* sp.), ATN-137 (6 cranidia) (with *C. magna n.sp., C. affinis*), ATN-138 (>20 cranidia) (with *C. tumida*), ATN-139 (>30 cranidia) (with *C. affinis, P. minor*), ATN-146 (> 20 cranidia, 1 free cheek) (with *C. magna n.sp., C. ahlbergi, C. affinis*), ATN-147 (> 10 cranidia) (with *C. magna n.sp., C. affinis*), ATN-148 (>20 cranidia) (with *C. ahlbergi, Peltura cf. minor*), ATN-164 (>20 cranidia), ATN-169 (>30 cranidia) (with *C. affinis, C. magna* n.sp.), ATN-171 (>20 cranidia, 1 pygidium) (with *C. tumida*), ATN-173 (>20 cranidia) (with *C. affinis, C. ahlbergi, C. magna* n.sp.), ATN-175 (>20 cranidia, 1 free cheek) (with *C. tumida*), ATN-180 (2 cranidia), ATN-188 (10 cranidia, 1 free cheek) (with *C. tumida*), ATN-191 (>10 cranidia) (with *C. affinis*), ATN-192 (>20 cranidia) (with *C. affinis*), ATN-193 (>30 cranidia) (with *C. tumida*), ATN-197 (>20 cranidia, 2 free cheeks) (with *C. tumida, C. tumidoides*), ATN-205 (>30 cranidia) (with *C. ahlbergi, C. affinis*), ATN-208 (>20 cranidia, 2 free cheeks) (with *C. tumida*), ATN-209 (>20 cranidia), ATN-222 (>30 cranidia) (with *C. affinis, C. ahlbergi*), ATN-236 (>10 cranidia), ATN-238 (>20 cranidia, 3 free cheeks) (with *C. tumida*), ATN-239 (>10 cranidia) (with *C. tumida*), ATN-246 (>20 cranidia) (with *C. affinis, C. magna* n.sp.), ATN-330 (>10 cranidia) (with *C. magna n.sp., C. ahlbergi, C. affinis*), L53 (>20 cranidia) (with *C. tumida*), L59 (5 cranidia) (with *C. tumida*), L61 (>15 cranidia, 1 free cheek) (with *C. tumida*), L64 (5 cranidia) (with *C. tumida*), L76 (>20 cranidia) (with *C. magna n.sp., C. ahlbergi, C. affinis*), L77 (6 cranidia) (with *C. affinis, C. ahlbergi,* unknown species?), L78 (cranidium, 1 free cheek) (with *C. tumida*), L81 (9 cranidia, 4 free cheeks) (with *C. tumida*), L84 (>20 cranidia) (with *C. affinis, C. magna* n.sp.), L86 (10 cranidia), L89 (8 cranidia, 2 free cheeks) (with *C. tumida*), L93 (8 cranidia) (with *C. affinis, C. magna* n.sp.), L94 (10 cranidia), GM 1870-944 (4 cranidia) (shale), GM 1870-945 (6 cranidia) (shale), GM 1870-947 (>8 cranidia) (shale), GM 1902-1208 (>5 cranidia) (with *C. affinis*), GM 1902-1209 (>20 cranidia) (with *C. magna n.sp., C. ahlbergi, C. affinis, S. alatus*), GM 1902-1210 (> 20 cranidia) (with *C. magna n.sp., C. ahlbergi, C. affinis*), GM 1902-1211 (4 cranidia), GM 1902-1212 (> 20 cranidia) (with *C. magna n.sp., C. ahlbergi, C. affinis*), GM 1922-141B (>15 cranidia), GM 1922-141E (10 cranidia, 1 free cheek), GM 1922-141F (10 cranidia, hypostome), GM 1922-141H (~20 cranidia) (with *C. tumida*), GM 1922-141L (4 cranidia) (including MGUH 1968), GM 2019-18 (>10 cranidia) (with *C. tumida*), GM 2019-21 (5 cranidia) (with *C. tumida*), GM 2019-24 (2 cranidia, 1 free cheek), GM 2019-25 (cranidium) (with *C. tumida*), GM 2019-27 (cranidium).

Sphaerophthalmus angustus **(Westergård, 1922)**. *>911 cranidia and >23 free cheeks.* Samples ATN-111 (>50 cranidia, >5 free cheeks) (with *C. tumidoides, P. acutidens*), ATN-115 (2 cranidia) (with *C. tumidoides*), ATN-121 (c. 10 cranidia) (with *C. tumida*), ATN-135 (>30 cranidia) (with *C. tumidoides*), ATN-145 (>12 cranidia, 2 free cheeks) (with *C. tumidoides, P. planicauda*), ATN-151 (>50 cranidia) (with *C. tumida*), ATN-183B (23 cranidia, 1 free cheek), ATN-190 (> 20 cranidia) (with *C. tumidoides*), ATN-211 (> 20 cranidia) (with *C. tumidoides*), ATN-218 (> 30 cranidia) (with *C. tumidoides*), ATN-225 (>15 cranidia) (with *C. tumidoides*), ATN-226 (>30 cranidia) (with *C. tumidoides*), ATN-240 (>20 cranidia), ATN-258 (3 cranidia) (with *C. tumidoides*), ATN-327 (>10 cranidia) (with *C. tumidoides,*

P. acutidens), L55 (>25 cranidia) (with *C. tumidoides*), L56 (>10 cranidia) (with *C. tumidoides*), L57 (>10 cranidia) (with *C. tumidoides*), L58 (>10 cranidia) (with *C. tumidoides*), L60 (6 cranidia, 1 free cheek) (with *C. tumidoides?*), L62 (>5 cranidia) (with *C. tumidoides*), L63 (>20 cranidia) (with *C. tumidoides*), L65 (>10 cranidia, 1 free cheek) (with *C. tumida, C. tumidoides*), L67 (7 cranidia) (with *C. tumida*), L70 (6 cranidia), L71 (3 cranidia) (with *C. tumidoides*), L73 (>20 cranidia) (with *C. tumidoides*), L75 (5 cranidia) (with *C. tumidoides*), L79 (7 cranidia), L80 (3 cranidia, 1 free cheek) (with *C. tumidoides*), L82 (8 cranidia, 1 free cheek) (with *Peltura cf. acutidens*), L83 (>20 cranidia), L85 (>20 cranidia), L87 (>20 cranidia) (with *C. tumidoides*), L88 (7 cranidia) (with *C. tumida*), L90 (>15 cranidia), L91 (10 cranidia, 2 free cheeks), L92 (11 cranidia, 2 free cheeks) (with *C. tumidoides*), L124 (> 10 cranidia) (with *C. tumidoides*), GM 1888-290 (>20 cranidia), GM 1922-141A (>40 cranidia) (with *C. tumida, C. tumidoides*), GM 1922-141C (>30 cranidia) (with *C. tumida, C. tumidoides*), GM 1922-141D (>50 cranidia) (with *C. tumidoides*), GM 1922-141G (>30 cranidia) (with *C. tumida?, C. tumidoides*), GM 1922-141I (c. 25 cranidia), GM 1922-141J (>20 cranidia) (with *C. tumida C. tumidoides*), GM 1922-141K (>10 cranidia) (with *C. tumida, C. tumidoides*), GM 1922-141M (7 cranidia, 1 free cheek, 1 hypostome) (including MGUH 1982), GM 1922-141N (7 cranidia, 3 free cheek (MGUH 1983)) (with *C. tumida, C. tumidoides*), GM 1922-141P (>100 cranidia, 4 free cheeks) (with *C. tumida, C. tumidoides*), GM 1930-101/102 (>40 cranidia) (with *C. tumida, C. tumidoides*), GM 2019-17 (>20 cranidia) (with *C. tumida*), GM 2019-19 (3 cranidia) (with *C. tumidoides*), GM 2019-20 (cranidium) (with *C. tumidoides*), GM 2019-22 (2 cranidia) (with *C. tumidoides*), GM 2019-23 (2 cranidia) (with *C. tumidoides*), GM 2019-96 (cranidium).

Sphaerophthalmus drytonensis **(Cobbold, 1934).** *One external mould of semi-complete specimen, 486 cranidia including 1 specimen with 7–8 contiguous thoracic segments and 114 free cheeks.* Samples ATN-105 (29 cranidia, 6 free cheeks) (with *P. praecursor, S. flagellifer*), ATN-107 (cranidium) (with *S. flagellifer*), ATN-125 (4 cranidia, 3 free cheeks) (with *S. flagellifer*), ATN-128 (5 cranidia, 3 free cheeks) (with *S. flagellifer*),
ATN-131 (14 cranidia, 3 free cheek) (with *S. flagellifer*), ATN-144 (7 cranidia) (with *S. flagellifer*, problematicum), ATN-166 (4 cranidia, 2 free cheeks) (with *S. flagellifer*), ATN-181 (9 cranidia, 5 free cheeks) (with *S. flagellifer*), ATN-215 (c. 30 cranidia, 10 free cheeks) (with *S. flagellifer*), ATN-256 (25 cranidia, 5 free cheeks) (with *S. flagellifer*), L19 (25 cranidia, 2 free cheeks) (with *S. flagellifer*), L20 (8 cranidia, 2 free cheeks) (with *S. flagellifer*), L21 (14 cranidia, 4 free cheeks) (with *S. flagellifer*), L22 (14 cranidia, 1 free cheek) (with *S. flagellifer*), L23 (22 cranidia, 4 free cheek) (with *S. flagellifer*), L24 (18 cranidia, 4 free cheeks) (with *S. flagellifer*), L25 (24 cranidia, 7 free cheeks) (with *S. flagellifer*), L26 (11 cranidia, 4 free cheeks) (with *S. flagellifer*), L27 (external mould of nearly complete specimen, 20 cranidia, 7 free cheeks) (with *S. flagellifer*), L28 (27 cranidia, 4 free cheeks), L29 (28 cranidia, 6 free cheeks) (with *S. flagellifer*), L30 (6 cranidia, 4 free cheeks) (with *S. flagellifer*), L66 (2 cranidia, 1 free cheek), L72 (16 cranidia, 2 free cheeks) (with *S. flagellifer?*), L74 (free cheek) (with *S. flagellifer*), GM 1897 (7 cranidia, 2 free cheeks), GM 1922-140B (54 cranidia, 13 free cheeks) (with *S. flagellifer*), GM 1922-140C (12 cranidia, 7 free cheeks) (with *S. flagellifer*), GM 1922-140D (9 cranidia, including one (?) with 7 thoracic segments [MGUH 1965], 2 free cheeks) (with *S. flagellifer*), GM 1922-140E (24 cranidia including MGUH 1966) (with *S. flagellifer*), GM 1922-140F (17 cranidia) (with *S. flagellifer*).

Undetermined ***Sphaerophthalmus drytonensis*** **(Cobbold, 1934) OR** *Sphaerophthalmus flagellifer* **Angelin, 1854,** most of them preserved in shale.
49 cranidia including 2 with 7-8 contiguous thoracic segments, 3 hypostomes, 1 free cheek and 1 contiguous thorax. Samples ATN-125 (hypostome) (with problematicum), ATN-128 (hypostome, 1 contiguous thorax), GM 1871-882 (2 cranidia), GM 1871-883 (cranidium, 1 free cheek), GM 1871-884 (2 cranidia), GM 1871-885 (cranidium), GM 1871-886 (cranidium), GM 1871-888 (6 cranidia), GM 1871-890 (cranidium), GM 1871-891 (cranidium), GM 1871-898 (cranidium), GM 1871-893 (2 cranidia), GM 1871-895 (5 cranidia), GM 1871-896 (3 cranidia), GM 1871-897 (cranidium), GM 1872-1070 (2 cranidia, incl. one with 8 contiguous thoracic segments), GM 1874-26 (8 cranidia, incl. one with 7 contiguous thoracic segments), GM 1922-140A (12 cranidia), GM 1922-140C (hypostome)

Sphaerophthalmus flagellifer **Angelin, 1854**. *207 cranidia and 41 free cheeks.* Samples ATN-105 (11 cranidia, 2 free cheeks) (with *P. praecursor, S. drytonensis*), ATN-107 (6 cranidia, 4 free cheeks) (with *S. drytonensis*), ATN-125 (3 cranidia) (with *S. drytonensis*), ATN-128 (4 cranidia, 1 free cheek) (with *S. drytonensis*), ATN-131 (11 cranidia) (with *S. drytonensis*), ATN-144 (6 cranidia, 1 free cheek) (with *S. drytonensis*), ATN-166 (cranidium) (with *S. drytonensis*), ATN-181 (cranidium, 1 free cheek) (with *S. drytonensis*), ATN-215 (c. 30 cranidia, 6 free cheeks), ATN-256 (7 cranidia, 1 free cheek) (with *S. drytonensis*), L19 (12 cranidia) (with *S. drytonensis*), L20 (4 cranidia) (with *S. drytonensis*), L21 (5 cranidia) (with *S. drytonensis*), L22 (5 cranidia, 2 free cheeks) (with *S. drytonensis*), L23 (15 cranidia, 2 free cheeks) (with *S. drytonensis*), L24 (19 cranidia) (with *S. drytonensis*), L25 (7 cranidia, 1 free cheek) (with *S. drytonensis*), L26 (2 cranidia, 3 free cheeks) (with *S. drytonensis*), L27 (7 cranidia, 2 free cheeks) (with *S. drytonensis*), L28 (4 cranidia, 3 free cheeks) (with *S. drytonensis*), L29 (3 cranidia, 1 free cheek) (with *S. drytonensis*), L30 (3 cranidia) (with *S. drytonensis*), L72 (1 free cheek?) (with *S. drytonensis*), L74 (cranidium) (with *S. drytonensis*), GM 1897 (4 cranidia, 2 free cheeks) (with *S. drytonensis*), GM 1922-140B (17 cranidia, 6 free cheeks) (with *S. drytonensis*), GM 1922-140C (5 cranidia, 1 free cheek) (with *S. drytonensis*), GM 1922-140D (2 cranidia) (with *S. drytonensis*), GM 1922-140E (7 cranidia, 1 free cheek) (with *S. drytonensis*), GM 1922-140F (5 cranidia) (with *S. drytonensis*).

Triangulopyge humilis (**Phillips, 1848**). *Cranidia are extremely abundant of which most are not registered (>> 1000 specimens). 610 cranidia, 5 free cheek and 8 pygidia.* Samples L17 (2 cranidia, 1 free cheek) (with *C. linnarssoni*, *Peltura* sp., *P. scarabaeoides*), L38 (8 cranidia, 1 pygidium) (with *C. linnarssoni*, *C. pecten*, *C. tenuis*, *C. teretifrons*, *Peltura* sp.), L39 (7 cranidia) (with *C. teretifrons*, *Peltura* sp.), L40 (5 cranidia) (with *Peltura* sp., *P. scarabaeoides*), L41 (3 cranidia, 1 pygidium) (with *C. tenuis*, *C. teretifrons*, *Peltura* sp., *P. scarabaeoides*), L42 (cranidium) (with *C. teretifrons*, *Peltura* sp.), L43 (cranidium) (with *C. pecten*, *C. tenuis*, *C. teretifrons*, *P. scarabaeoides*), L44 (10 cranidia) (with *C. tenuis*, *Peltura* sp., *P. scarabaeoides*), L45 (6 cranidia) (with *C. tenuis*, *P. scarabaeoides*), L46 (20 cranidia) (with *C. tenuis*, *C. teretifrons*, *Peltura* sp., *P. scarabaeoides*), L48 (pygidium) (with *C. tenuis*), L49 (cranidium) (with *C. teretifrons*, *Peltura* sp.), L50 (2 cranidia) (with *C. linnarssoni*, *Peltura* sp.), GM 1871-611 (9 cranidia) (with *C. tenuis*, *Peltura* sp., *P. scarabaeoides*), GM 1871-612 (6 cranidia) (with *C. tenuis*, *Peltura* sp.), GM 1871-619 (5 cranidia) (with *Peltura* sp., *P. scarabaeoides*), GM 1871-625 (7 cranidia) (with *Peltura* sp., *P. scarabaeoides*), GM 1871-626 (6 cranidia) (with *Peltura* sp., *P. scarabaeoides*), GM 1871-647 (8 cranidia) (with *C. linnarssoni*, *Peltura* sp., *P. scarabaeoides*), GM 1871-648 (7 cranidia) (with *C. teretifrons*, *Peltura* sp.), GM 1871-649 (3 cranidia) (with *Peltura* sp.), GM 1871-651A (4 cranidia) (with *Peltura* sp.), GM 1871-651B (cranidium) (with *C. pecten*), GM 1871-652 (3 cranidia) (with *P. scarabaeoides*), GM 1871-653 (cranidum) (with *Peltura* sp.), GM 1871-655 (5 cranidia) (with *C. pecten*, *C. tenuis*, *Peltura* sp.), GM 1871-661 (2 cranidia) (with *C. tenuis*, *Peltura* sp.), GM 1871-657 (2 cranidia) (with *C. linnarssoni?*, *C. tenuis*), GM 1871-663 (cranidium), GM 1871-664 (cranidium) (with *C. teretifrons*), GM 1871-665 (10 cranidia) (with *C. teretifrons*, *P. scarabaeoides*), GM 1871-667 (20 cranidia) (with *C. teretifrons*, *P. scarabaeoides*), GM 1871-671 (4 cranidia) (with *Peltura* sp.), GM 1871-672 (5 cranidia) (with *C. tenuis*, *Peltura* sp.), GM 1871-673 (2 cranidia) (with *Peltura* sp.), GM 1871-674 (5 cranidia, 1 pygidium) (with *C. pecten*, *P. scarabaeoides*), GM 1871-675A (2 cranidia) (with *C. linnarssoni*), GM 1871-675B (2 cranidia) (with *C. teretifrons*), GM 1871-868 (2 cranidia) (shale), GM 1871-871 (2 cranidia) (shale), GM 1871-872 (6 cranidia) (shale), GM 1871-874 (cranidium) (shale), GM 1871-876 (cranidium) (shale), GM 1874-27 (14 cranidia) (with *C. pecten*, *C. tenuis*, *C. teretifrons*, *Peltura* sp., *P. scarabaeoides*), GM 1874-28 (2 cranidia) (with *C. pecten*, *C. tenuis*, *Peltura* sp.), GM 1874-30 (2 cranidia) (with *C. tenuis*, *Peltura* sp., *P. scarabaeoides*), GM 1874-661 (2 cranidia) (with *C. tenuis*, *Peltura* sp.), GM 1877-1999 (3 cranidia) (with *C. tenuis*, *Peltura* sp., *P. scarabaeoides*), GM 1877-2000 (4 cranidia) (with *C. linnarssoni*, *Peltura* sp.), GM 1881-337A (11 cranidia) (with *C. fletcheri*), GM 1881-1802 (>30 cranidia, 1 pygidium) (with *C. pecten*, *C. teretifrons*, *P. scarabaeoides*), GM 1881-1804 (3 cranidia) (with *C. tenuis*, *Peltura* sp.), GM 1881-1805 (21 cranidia) (with *C. linnarssoni*, *C. tenuis*, *C. teretifrons*, *Peltura* sp., *P. scarabaeoides*), GM 1881-1796 (3 cranidia) (with *C. tenuis*), GM 1881-1797 (3 cranidia) (with *C. tenuis*), GM 1881-1802 (11 cranidia) (with *C. pecten*, *Peltura* sp.), GM 1883-341A (4 cranidia) (with *C. tenuis*, *C. teretifrons*, *Peltura* sp.), GM 1883-341B (2 cranidia) (with *C. tenuis*, *Peltura* sp.), GM 1884-1828 (5 cranidia) (with *Peltura* sp.), GM 1884-1830 (2 cranidia), GM 1922-142A (30 cranidia, 2 free cheeks, 1 pygidium) (with *C. tenuis*, *C. teretifrons*, *Peltura* sp., *P. scarabaeoides*), GM 1922-142B (35 cranidia) (with *C. linnarssoni*, *C. pecten*, *C. tenuis*, *C. teretifrons*, *Peltura* sp., *P. scarabaeoides*), GM 1922-142C (32 cranidia) (with *C. linnarssoni*, *C. tenuis*, *C. teretifrons*, *Peltura* sp., *P. scarabaeoides*), GM 1922-142D (9 cranidia) (with *C. pecten*, *C. tenuis*, *C. teretifrons*, *Peltura* sp., *P. scarabaeoides*), GM 1922-142E (8 cranidia) (with *C. linnarssoni*, *C. tenuis*, *C. teretifrons*, *Peltura* sp., *P. scarabaeoides*), GM 1922-142F (4 cranidia) (with *C. tenuis*, *Peltura* sp., *P. scarabaeoides*), GM 1922-142G (2 cranidia) (with *Peltura* sp.), GM 1922-142H (2 cranidia) (with *C. linnarssoni*, *C. tenuis*, *C. teretifrons*, *Peltura* sp.), GM 1922-142I (14 cranidia, 2 free cheeks) (with *C. linnarssoni*, *C. pecten*, *C. tenuis*, *C. teretifrons*, *Peltura* sp., *P. scarabaeoides*), GM 1922-142J (17 cranidia, 1 pygidium) (with *C. tenuis*, *C. teretifrons*, *Peltura* sp., *P. scarabaeoides*), GM 1922-142K (3 cranidia) (with *C. teretifrons*, *Peltura* sp., *P. scarabaeoides*), GM 1922-142M (4 cranidia) (with *C. linnarssoni*, *C. tenuis*, *C. teretifrons*, *Peltura* sp., *P. scarabaeoides*), GM 1922-142N (10 cranidia, 1 pygidium) (with *C. linnarssoni*, *C. tenuis*, *C. teretifrons*, *P. scarabaeoides*), GM 1922-142O (4 cranidia) (with *C. tenuis*, *C. teretifrons*, *Peltura* sp., *P. scarabaeoides*), GM 1922-142P (5 cranidia) (with *C. tenuis*, *Peltura* sp.), GM 1922-142Q (3 cranidia) (with *C. tenuis*, *C. teretifrons*, *Peltura* sp.), GM 1922-142S (25 cranidia) (with *P. scarabaeoides*, *C. magna n.sp.*, *C. tenuis*, *C. teretifrons*), GM 1922-142T (19 cranidia) (with *C. pecten*, *C. teretifrons*, *C. tenuis*, *Peltura* sp.), GM 1922-142U (16 cranidia) (with *C. linnarssoni*, *C. tenuis*, *P. scarabaeoides*, *Peltura* sp.), GM 2019-7 (5 cranidia) (with *Peltura* sp.), GM 2019-11 (5 cranidia) (with *C. teretifrons*, *C. tenuis*, *Peltura* sp.), GM 2019-12 (3 cranidia) (with *C. tenuis*, *Peltura* sp.), GM 2019-14 (3 cranidia) (with *C. tenuis*, *Peltura* sp.), GM 2019-15 (7 cranidia) (with *C. tenuis*, *C. teretifrons*, *Peltura* sp.), GM 2019-16 (2 cranidia) (with *C. tenuis*, *Peltura* sp.), GM 2019-97 (cranidium) (with *C. teretifrons*, *Peltura* sp.), GM 2019-99 (21 cranidia) (with *C. pecten*, *C. tenuis*, *Peltura* sp., *P. scarabaeoides*).
.

Protopeltura planicauda (**Brøgger, 1882**). *One pygidium*, sample ATN-145 (with *C. tumidoides*, *S. angustus*).

Protopeltura praecursor (**Westergård, 1909**). *One pygidium*, sample ATN-105 (with *S. drytonensis*, *S. flagellifer*).

Peltura acutidens **Brøgger, 1882**. *One pygidium and 1 free cheek (?).* Samples ATN-111 (external mould of pygidium, counter piece of ATN-327) (with *C. tumidoides*, *S. angustus*), ATN-327 (pygidium, counter piece of ATN-111) (with *S. angustus*, *C. tumidoides*), L82 (with *S. angustus*)

Peltura minor (**Brøgger, 1882**). *4 cranidia (tentatively assigned), 1 free cheek (tentatively assigned), 1 external mould of free cheek (tentatively assigned) and 6 pygidia incl. one with 9 thoracic segments attached.* Samples ATN-103 (cranidium) with *C. affinis*, *S. alatus*), ATN-113 (pygidium) (with *C. affinis*, *C. ahlbergi*, *C. magna n.sp.*, *S. alatus*), ATN-116 (cranidium, 1 free cheek) (with *C. ahlbergi*, *C.*

affinis, C. magna n.sp., *S. alatus*), ATN-127 (cranidium, 2 pygidia) (with *C. ahlbergi, C. affinis, S. alatus*), ATN-132 (pygidium) (with *C. ahlbergi, C. affinis, S. alatus*), ATN-133 (pygidium) (with *C. magna n.sp., C. ahlbergi, C. affinis, S. alatus*), ATN-139 (pygidium with 9 thoracic segments) (with *C. affinis, S. alatus*), ATN-148 (cranidium, 1 external mould of free cheek) (with *C. ahlbergi, S. alatus*).

Peltura scarabaeoides **(Wahlenberg, 1818)**. *One almost complete specimen, 84 pygidia, incl. one with 8 contiguous thoracic segments, 3 hypostomes, 112 free cheeks, and 160 cranidia, including one with 10 contiguous thoracic segments (cranidia and free cheeks are registered as* Peltura *sp.).* Samples L17 (3 cranidia, 7 pygidia) (with *C. linnarssoni, T. humilis*), L39 (cranidium?) (with *C. teretifrons, T. humilis*), L40 (2 cranidia, 3 pygidia) (with *T. humilis*), L41 (3 cranidia, 1 pygidium) (with *C. tenuis, C. teretifrons, T. humilis*), L43 (external mould of free cheek) (with *C. pecten, C. tenuis, C. teretifrons, T. humilis*), L44 (4 cranidia, 1 pygidium) (with *C. tenuis, T. humilis),* L45 (free cheek) (with *C. tenuis, T. humilis*), L46 (4 cranidia, 1 pygidium) (with *C. tenuis, C. teretifrons, T. humilis*), L47 (free cheek) (with *C. tenuis*), L51 (free cheek) (with *T. humilis*), GM 1871-611 (cranidium, 2 free cheeks, 3 pygidia) (with *C. tenuis, T. humilis*), GM 1871-619 (1 free cheek, 1 pygidium) (with *T. humilis*), GM 1871-621 (pygidium), GM 1871-625 (cranidium, 4 free cheeks, 2 pygidia) (with *T. humilis*), GM 1871-626 (cranidium, 1 free cheek, 2 pygidia) (with *T. humilis*), GM 1871-647 (free cheek, 3 pygidia) (with *C. linnarssoni, T. humilis*), GM 1871-652 (pygidium) (with *T. humilis*), GM 1871-665 (pygidium) (with *C. teretifrons, T. humilis*), GM 1871-667 (3 pygidia) (*C. teretifrons, T. humilis*), GM 1871-671 (hypostome?) (with *T. humilis*), GM 1871-673 (3 cranidia, 1 hypostome) (with *C. tenuis*), GM 1871-674 (hypostome) (with *C. pecten, T. humilis*), GM 1874-27 (cranidium, 2 free cheeks, 1 pygidium) (with *C. pecten, C. tenuis, C. teretifrons, T. humilis*), GM 1874-30 (cranidium, 1 free cheek, 1 pygidium with 8 thoracic segments) (with *C. tenuis, T. humilis*), GM 1877-1999 (cranidium, 3 free cheeks, 1 pygidium) (with *C. tenuis, T. humilis*), GM 1881-1802 (6 cranidia, 10 free cheeks, 3 pygidia, incl. MGUH 1977) (with *C. pecten, C. teretifrons, T. humilis*), GM 1881-1805 (1 complete specimen, 9 cranidia, 3 free cheeks, 1 pygidium) (with *C. linnarssoni, C. tenuis, C. teretifrons, T. humilis*), GM 1922-142A (9 cranidia incl. one with 10 thoracic segments, 2 free cheeks, 2 pygidia) (with *C. tenuis, C. teretifrons, T. humilis*), GM 1922-142B (4 cranidia, 9 free cheeks, 2 pygidia) (with *C. linnarssoni, C. pecten, C. tenuis, C. teretifrons, T. humilis*), GM 1922-142C (6 cranidia, 8 free cheeks, 6 pygidia) (with *C. linnarssoni, C. tenuis, C. teretifrons, T. humilis*), GM 1922-142D (5 cranidia, 2 free cheeks, 2 pygidia) (with *C. pecten, C. tenuis, C. teretifrons, T. humilis*), GM 1922-142E (19 cranidia, 8 free cheeks, 4 pygidia) (with *C. linnarssoni, C. tenuis, C. teretifrons, T. humilis*), GM 1922-142F (8 cranidia, 3 free cheeks, 1 pygidium) (with *C. tenuis, T. humilis*), GM 1922-142I (10 cranidia, 11 free cheeks, 6 pygidia) (with *C. linnarssoni, C. pecten, C. tenuis, C. teretifrons, T. humilis*), GM 1922-142J (10 cranidia, 11 free cheeks, 4 pygidia) (with *C. tenuis, C. teretifrons, T. humilis*), GM 1922-142K (3 cranidia, 1 pygidium) (with *C. linnarssoni C. teretifrons, T. humilis*), GM 1922-142M (6 cranidia, 2 free cheeks, 3 pygidia) (with *C. linnarssoni, C. tenuis, C. teretifrons, T. humilis*), GM 1922-142N (5 cranidia, 4 free cheeks, 2 pygidia) (with *C. linnarssoni, C. tenuis, C. teretifrons, T. humilis*), GM 1922-142O (4 cranidia, 1 pygidium) (with with *C. tenuis, C. teretifrons, T. humilis*), GM 1922-142S (10 cranidia, 13 free cheeks, 6 pygidia) (with *T. humilis, C. magna n.sp., C. tenuis, C. teretifrons*), GM 1922-142U (2 cranidia, 1 pygidium) (with *C. linnarssoni, C. tenuis, T. humilis*), GM 2019-8 (11 cranidia, 1 free cheek, 5 pygidia) (with *C. tenuis*), GM 2019-99 (7 cranidia, 6 free cheeks, 1 pygidium) (with *C. pecten, C. tenuis, T. humilis*).

Peltura westergaardi **Henningsmoen, 1957**. *25 pygidia, 1 cephalon, 12 free cheeks, 2 hypostomes and 116 tentatively assigned cranidia (registered as* Peltura *sp.).* Samples L4 (pygidium), L9 (3 cranidia, 1 pygidium), L10 (external mould of pygidium) (with *P. lobata praecurrens*), L11 (2 pygidia) (with *P. lobata praecurrens*), L12 (cranidium, 1 pygidium) (with *P. lobata praecurrens*), L13 (pygidium), L14 (4 cranidia, 3 pygidia) (with *P. lobata praecurrens*), L15 (2 cranidia, 1 free cheek, 1 pygidium), L16 (3 cranidia, 1 pygidium) (with *P. lobata praecurrens*, orthid brachiopod), GM 2019-93 (1 cephalothorax, 18 cranidia (several juvenile), 3 free cheeks, 3 pygidia), GM 2019-94 (32 cranidia (most of them juvenile), 1 hypostome, 4 free cheeks, 6 pygidia), GM 2019-95 (38 cranidia (most of them juvenile), 1 hypostome, 1 free cheek, 4 pygidia), sample 2019-101 (incl. MGUH 1987) (4 juvenile cranidia), sample 2019-104 (incl. MGUH 1988) (8 cranidia of which 5 are juvenile), 2019-105 (incl. MGUH 1989) (3 juvenile cranidia, 3 free cheeks).

Orusia lenticularis **(Wahlenberg, 1821) (brachiopod).** Specimens not counted; the species is extremely common. Samples ATN-104, ATN-140, ATN-141, ATN-143, ATN-165, ATN-179, ATN-183A, ATN-184, ATN-185, ATN-186, ATN-187, ATN-189, ATN-194, ATN-195, ATN-198, ATN-200, ATN-201, ATN-202, ATN-203, ATN-204, ATN-206, ATN-207, ATN-210, ATN-212, ATN-213, ATN-214, ATN-221, ATN-235, ATN-245

Other samples (Miaolingian samples, lithology samples, samples without determinable fossils). ATN-161, ATN-196, ATN-229, ATN-230, ATN-267, ATN-308, ATN-309, ATN-310, ATN-311, ATN-312, ATN-313, ATN-314, ATN-315, ATN-316, ATN-317, ATN-318, ATN-319, ATN-321, L5, L6, L7, L8, L34, L35, L36, L37, L68, L69, L96, L97, L102, L06, L107, L109, L110, L113, L114, L116, L117, L120, L121, L122, L123.

On the genus *Vanikoropsis* Meek, 1876 (Gastropoda, Caenogastropoda) from the Paleocene of Denmark and West Greenland with descriptions of three new species

KAI INGEMANN SCHNETLER & MOGENS STENTOFT NIELSEN

DGF

The predominantly Cretaceous gastropod genus *Vanikoropsis* Meek, 1876 is represented in the Paleocene of Denmark and West Greenland by four species, of which three are established herein as new, *viz. Vanikoropsis mortenseni* n. sp., *Vanikoropsis* (s.l.) *jakobseni* n. sp. and *Vanikoropsis* (s.l.) *bashforthi* n. sp. The Danish species was found in a boulder of Kerteminde Marl (Selandian, middle Paleocene) from Gundstrup, while the species from West Greenland were found in the localities Sonja Lens and Qaarsutjægerdal on the Nuussuaq peninsula (late Danian, early Paleocene). The Danish species extends the stratigraphic range of the genus into the middle Paleocene and supports the affinities of the Kerteminde Marl fauna to the Paleocene fauna of West Greenland.

Keywords: Gastropoda, Vanikoridae, *Vanikoropsis*, Danian, Selandian, Paleocene, Kerteminde Marl, Denmark, Nuussuaq, West Greenland.

Kai Ingemann Schnetler [i.schnetler@mail.dk], Fuglebakken 14, Stevnstrup, DK-8870 Langå, Denmark. Mogens Stentoft Nielsen [rimo@mail.dk], Dankvart Drejers Vej 42, DK-5230, Odense M, Denmark.

The genus *Vanikoropsis* Meek, 1876 is represented in the Danish Kerteminde Marl Formation (Selandian, middle Paleocene) by a new species, which seems to represent the youngest occurrence of the genus. Stilwell *et al.* (2004) recorded *Vanikoropsis arktowskiana* (Wilckens, 1910) from the Sobral Formation of Antarctica and presumed it to be of Selandian age, but both Bowman *et al.* (2014) and Montes *et al.* (2019) suggested a Danian age.

The late Danian (early Paleocene) gastropod fauna from the Nuussuaq peninsula, West Greenland, contains three species of the genus *Vanikoropsis*, of which *Vanikoropsis skoui* was established by Rosenkrantz (1970). Two other representatives of the genus were mentioned in open nomenclature by Kollmann & Peel (1983) and illustrated. The gastropod fauna was recorded by Kollmann & Peel (1983) and contains at least 257 gastropod species, of which some families have already been revised (Merle & Pacaud 2004; Pacaud & Schnetler 1999; Schnetler & Petit 2010). The species from the Kerteminde Marl and the two undescribed species from West Greenland are established herein as new species. An overview of the stratigraphic record of *Vanikoropsis* is given.

Geological setting and stratigraphy

Denmark

The Danish Basin is situated between the Sorgenfrei–Tornquist Zone to the north and the Ringkøbing Fyn High to the south (Fig. 1). The Danian and Selandian deposits are thin over this high and thick in the Danish Basin (Sorgenfrei & Buch 1964; Clausen & Huuse 1999; Clemmensen & Thomsen 2005), having their maximum thickness of more than 350 m and 150 m, respectively (Gry 1935; Thomsen 1995).

The Danian deposits consist of carbonates, while the Selandian deposits are mainly clastic (Gry 1935; Heilmann-Clausen 1985, 1995; Clemmensen & Thom-

sen 2005). Three facies groups are recognised in the Danish Basin: the Lellinge Greensand, Kerteminde Marl and Æbelø Formations (Fig. 1). The Lellinge Greensand is strongly calcareous and glauconitic and is known from Sjælland and the margins of the Ringkøbing–Fyn High (Gry 1935; Foged *et al.* 1995; Clemmensen & Thomsen 2005). It has a thickness of less than 10 m and was presumably deposited in an inner shelf environment (Gry 1935; Schnetler 2001). Laterally towards the depocenter and upwards, the Lellinge Greensand grades into the fine-grained Kerteminde Marl Formation (Clemmensen & Thomsen 2005). The maximum thickness of this unit is controlled by Quaternary erosion and seems to have been more than 100 m. King (1994, 2015) presumed a deposition in a middle to outer neritic environment. The calcium carbonate content is composed of calcare-

ous nannofossils and varies between 50 % and 70 % in the Lellinge Greensand and the Kerteminde Marl (Gry 1935; Foged *et al.* 1995). The overlying, slightly calcareous to non-calcareous Æbelø Formation was apparently deposited in the bathyal depth zone (King 1994, 2015).

Lithostratigraphical and biostratigraphical correlations

The Kerteminde Marl falls within the dinoflagellate zone 2 sensu Nøhr-Hansen & Heilmann-Clausen (2000). The age is early Selandian and the dinoflagellates indicate an open marine environment (Heilmann-Clausen pers. comm. 2003). Heilmann-Clausen (2006, p. 195) stated that the silicified boulders from the gravel-pit Gundstrup are coarser than the typical Kerteminde Marl and have a higher content of ben-
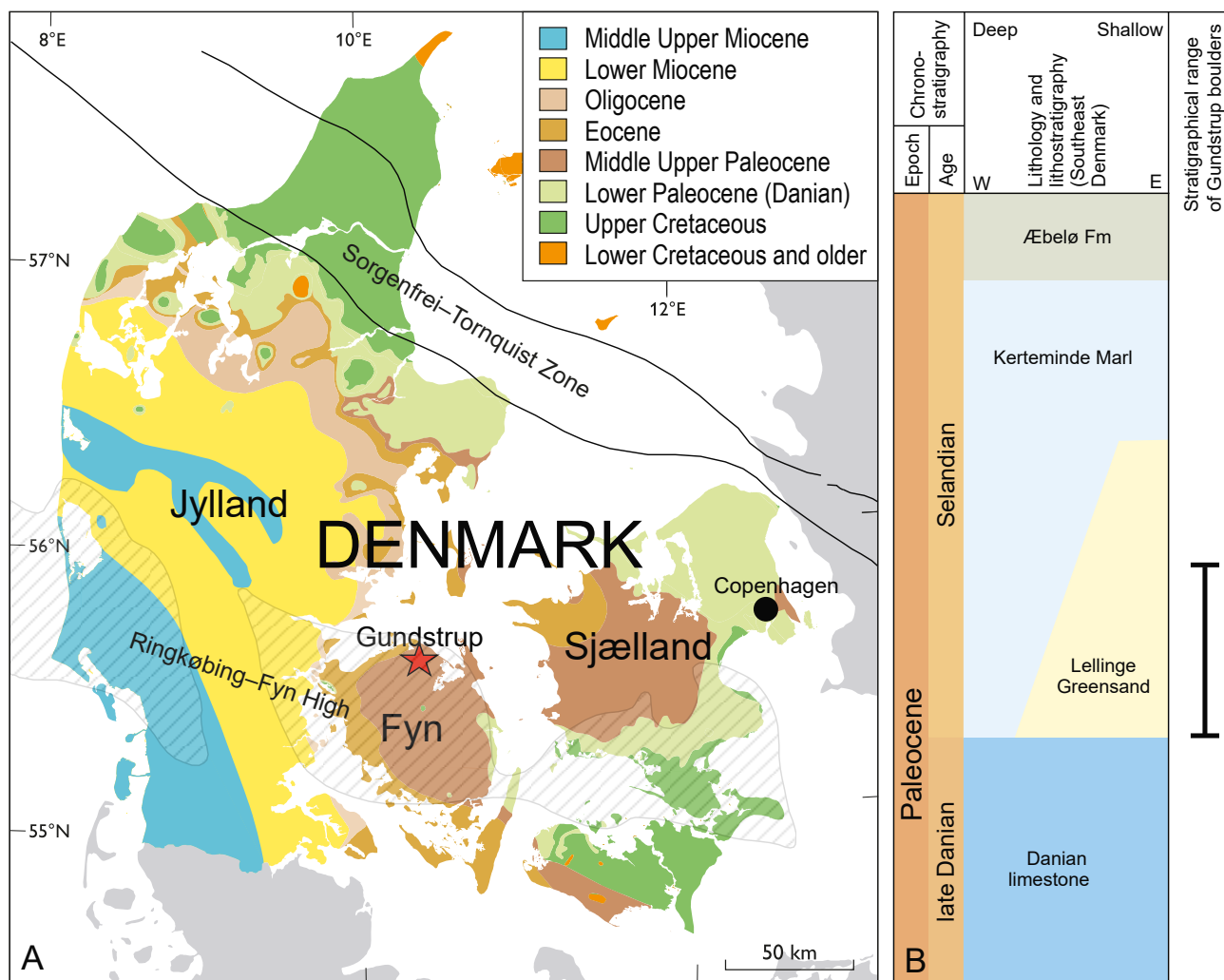
Fig. 1. A: Pre-Quaternary geological map of Denmark showing the location of the Gundstrup gravel pit on the island of Fyn (55.56°N, 10.35°E). Modified from Håkansson & Pedersen (1992). The gravel pit contains fossil-rich, glacially derived fragments of the Kerteminde Marl. **B:** Schematic representation of the Upper Danian – Selandian stratigraphy of south-eastern Denmark. Modified from Clemmensen & Thomsen (2005).

thic fossils. Thomsen (pers. comm., 2016) analysed the calcareous nannofossils in five Paleocene boulders retrieved from Quaternary deposits in the gravel pit at Gundstrup, north Fyn and found that the boulders could be correlated with the lowermost Selandian immediately above the Danian-Selandian boundary (Thomsen 1994; Clemmensen & Thomsen 2005). Thus, the samples could be correlated with the lower part of the Lellinge Greensand and the lowermost part of the Kerteminde Marl.

West Greenland

The geological setting of the West Greenland continental margin has been described by Rosenkrantz *et al.* (1974), Dam & Sønderholm (1994), Nøhr-Hansen & Dam (1997), Dam *et al.* (1998), Dam (2002), Nøhr-Hansen *et al.* (2002) and Dam *et al.* (2009). This margin was developed in connection with the extensional opening of the Labrador Sea during the late Mesozoic to early Cenozoic. Exposures of rocks and sediments from Cretaceous (Albian) to Paleocene (?Selandian) ages are found onshore on Baffin Island and in the Nuussuaq Basin, where they are overlain by Palaeogene basalts (Clarke & Pedersen 1976; Henderson *et al.* 1976; Burden & Langille 1990). The exposed succession of the Nuussuaq Basin consists of 2.5 km Albian to Paleocene sediments overlain by 3–5 km of Paleocene and Early Eocene hyaloclastites and basalts (Dam *et al.* 1998). From the late Albian, siliciclastic sandstones and shales were deposited in fluvial and deltaic settings on eastern Disko and central Nuussuaq, whereas the delta fanned into deeper marine, partly turbidic, environments towards the western and northern Nuussuaq. The Nuus-suaq Basin underwent major rifting from the Albian to early Paleocene. At least three phases of rifting, major uplift and erosion and infilling of subaerial valleys and submarine canyons resulted in basin-wide unconformities in the late Maastrichtian to early Paleocene interval (Dam *et al.* 1998; Dam & Sønderholm 1998; Sørensen *et al.* 2017). The deposition of marine sediments of the Kangilia Formation was recorded by the first of these rifting events. The younger tectonic phases gave rise to the mudstone dominated Eqalulik and Agatdal Formations in deeper marine settings towards the northwest and the fluviatile incised valley fills of the Quikavsak Formation in the southern part of the basin (Dam 2002). The deposition of the marine sediments was followed by the extrusion of a thick succession of volcanic rocks of the Vaigat and Maligât Formations (Pedersen *et al.* 2006; Hjuler *et al.* 2016; Larsen *et al.* 2016; Fig. 2).

Lithostratigraphical and biostratigraphical correlations

Rosenkrantz (1970) referred the Agatdal Formation to the Upper Danian. The dinoflagellate cysts from the pre-volcanic Paleocene mudstone succession and the intrabasaltic Paleocene sediments at Nuussuaq were studied by Hansen (1980), Piacecki *et al.* (1992), Nøhr-Hansen (1996, 1997a, 1997b), Nøhr-Hansen & Dam (1997), Nøhr-Hansen & Heilmann-Clausen (2000) and Nøhr-Hansen *et al.* (2002). Nannoplankton assemblages have been studied by Perch-Nielsen (1973), Jürgensen & Mikkelsen (1974) and Nøhr-Hansen & Sheldon (2000). Perch-Nielsen (1973) dated samples from the Sonja Lens of the Sonja Member at Agatkløft as upper Zone NP3 based on nannofossils. Jürgensen & Mikkelsen (1974) dated samples from Marraat Killiit
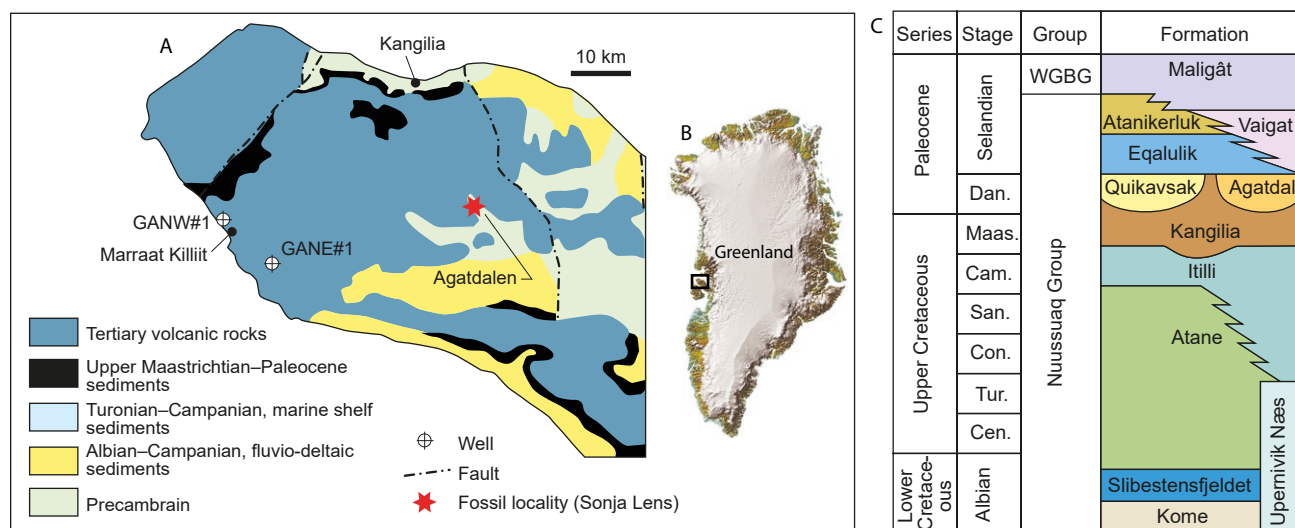

Fig. 2. A: Strongly simplified geological map of the western part of Nuussuaq. Modified from Sheldon (2003). **B:** Map of Greenland showing the location of Nuussuaq (rectangle). **C:** Lithostratigraphic scheme of the Nuussuaq Group and the lowermost part of the West Greenland Basalt Group (WGBG). Modified from Hjuler *et al.* (2017).

on the south-west coast of Nuussuaq and Kangilia on the north coast and placed them into Zone NP3, while Nøhr-Hansen & Sheldon (2000) referred the Equalik and Kangilia Formations to the upper NP3 to lower NP4 zones. Sheldon (2003) recorded an assemblage containing *Neochiastozygus perfectus* from the Eqalulik Formation of the GANE#1 and GANW#1 wells of western Nuussuaq, indicating correlation with the upper NP4 (Danian) or NP5 (Selandian) zones. Hansen (1980) dated the lower and upper part of the Paleocene mudstone succession at Nuussuaq as early and middle Paleocene, based upon dinoflagellate cysts, and correlated the lower part with nannoplankton zones NP3-NP4 and the upper part with NP5-NP6 (Martini, 1971). Jürgensen & Mikkelsen (1974), however, dated the upper part of the Kangilia Formation (now Eqalulik Formation) to NP3 (late Danian). Piasecki *et al.* (1992) suggested a late Danian to Thanetian age (NP zones 4-8). Nøhr-Hansen (1997a, 1997b) and Christiansen *et al.* (1997) dated dinoflagellate cyst assemblages from the Paleocene sediments in four wells and suggested a Selandian age (NP5-NP6) for the upper part of the succession. Nøhr-Hansen & Dam (1997) suggested an early Danian age (NP1-NP3?) for the oldest Paleocene on Nuussuaq. However, palaeomagnetic studies (Riisager & Abrahamsen 1999) correlated the lowermost volcanic Anaanaa Member with the late Danian. The correlation with NP5-NP6 suggested by Piasecki *et al.* (1992), Nøhr-Hansen (1997a, b) and Christiansen *et al.* (1997) was based on the presence of a dinoflagellate cyst species similar to the Selandian marker species *Isabelidinium viborgense*, previously only recorded from NP5 and NP6 in Denmark (Heilmann-Clausen 1985). Later examination, however, proved this species to be previously undescribed (Nøhr-Hansen & Heilmann-Clausen 2000), and its first occurrence was correlated with NP3 (middle Danian). Nøhr-Hansen *et al.* (2002) established a detailed zonation of the Lower Paleocene succession in the Nuussuaq Basin, based on dinoflagellate cyst and nannofossil data. They referred the Kangilia Formation in Central Nuussuaq to Danian

(NP1-NP4) and the overlying Eqalulik Formation to NP4-NP5. Hjuler *et al.* (2017), Christiansen *et al.* (2020) and Nøhr-Hansen (pers. comm., 2020) referred the Agatdal Formation to the Danian (Fig. 1).

Material and methods

The gravel-pit of Alex Andersen A/S is situated near the village Gundstrup, *c.* 20 km north of Odense on Fyn and is remarkable by its very high content of glacially transported Paleocene boulders, which have yielded a rich and diverse molluscan fauna (Schnetler & Nielsen 2018). The bulk of the molluscs from the Kerteminde Marl is generally preserved as external impressions and internal moulds. As the boulders are consolidated, the making of silicone latex casts of fine quality is possible with SILASTIC® 9161 RTV Silicone Elastomer (product information sheet in the references). This process was described in detail by Schnetler & Nielsen (2018). The material has been collected by the junior author and Peter Tang Mortensen, who collected the boulder with the only *Vanikoropsis* specimen known from Denmark.

The mollusc material from Nuussuaq was collected by the late professor Alfred Rosenkrantz and his co-workers in the years between 1938 and 1968 (Kollmann & Peel 1983, Dam *et al.* 2009). In 1948 Sonja Hansen found fossiliferous sandstone in a riverbed in Agatdalen (Fig. 2) and four years later this rock type was found *in situ*. It was a sand lens with a length of 7 m and a thickness of only 0.7 m, according to Rosenkrantz (1970). The specimens of *Vanikoropsis* from the Nuussuaq have been collected at the localities Sonja Lens and Qaarsutjægerdal, east of Turritellakløft, Nuussuaq in 1953, 1956 and 1958 (Table 1). The locality Sonja Lens is a very loose sandstone and has yielded thousands of fossils, mainly gastropods, which have been found by washing and sieving the loose sediment (Rosenkrantz 1970, Kollmann & Peel 1983). The shells are

Table 1. West Greenland specimens of *Vanikoropsis* (*V.* in the table)

SNM no.[1]	Rkz no.[2]	Species Kollmann & Peel (1983)	Species this study	Locality	Year collected	Remarks
MGUH 10807	MS 144	*V. skoui* Rosenkrantz, 1970	*V.* (s.l.) *skoui* Rosenkrantz, 1970	Sonja Lens	1958	Holotype
MGUH 15744	MS 322B	*V. skoui* Rosenkrantz, 1970	*V.* (s.l.) *skoui* Rosenkrantz, 1970	Sonja Lens	1958	Paratype
MGUH 15745	MS 140	*V.* sp. 1	*V.* (s.l.) *jakobseni* n. sp.	Qaarsutjægerdal	1953	Holotype
MGUH 15746	MS 315	*V.* sp. 2	*V.* (s.l.) *bashforthi* n. sp.	Qaarsutjægerdal	1958	Holotype
GM 1977.1181/8	MS 228	cf. *Coptostoma*	*V.* (s.l.) *bashforthi* n. sp.	Sonja Lens	1956	Paratype
GM 1977.1296	MS 315	*V.* sp. 2	*V.* (s.l.) *bashforthi* n. sp.	Qaarsutjægerdal	1953	Paratype
GM 1977.1308	MS 322	*V. skoui* Rosenkrantz, 1970	*V.* (s.l.) *skoui* Rosenkrantz, 1970	Sonja Lens	1958	Additional specimen

[1]SNM no.: number in the type collection of SNM, [2] Rkz no.: number in the Rosenkrantz collection of drawings

often somewhat worn, due to the transport by water. Stratigraphically, the lens is part of the Sonja Member at the base of the Agatdal Formation. The locality is the most significant in West Greenland for aragonitic molluscs preserved, but ammonites are found in the late Cretaceous Itilli Formation (Rasmussen, pers. comm. 2009).

Rosenkrantz organized the gastropods from Nuussuaq into species. The species were documented in many pencil drawings by artists, working under the supervision of Rosenkrantz, and some photos. All illustrations are stored in folders in the Rosenkrantz Collection in Natural History Museum of Denmark (SNM), Copenhagen. The bivalves were described by Petersen & Vedelsby (2000). The gastropods have been treated by Rosenkrantz (1970), Kollmann & Peel (1983), Pacaud & Schnetler (1999), Merle & Pacaud (2004), and Schnetler & Petit (2010). According to Kollmann & Peel (1983), the species from Nuussuaq were not arranged systematically, but were given current working numbers in a series from 1 to 340. However, a later revision of these species resulted in a lower number, as Kollmann & Peel (1983) documented only 254 taxa and concluded that Rosenkrantz had used a too narrow species concept. For their paper they selected numerous drawings from the Rosenkrantz files of drawings and arranged them in two folders. All illustrations are stored in folders in the Rosenkrantz Collection in Natural History Museum of Denmark (SNM), Copenhagen. Rosenkrantz used several numbers for species of *Vanikoropsis* in the drawings (Table 1), and we may conclude that he assumed a higher number of *Vanikoropsis* species. Kollmann & Peel (1983) recognized two further species of *Vanikoropsis* in Rosenkrantz' material.

Kollmann & Peel (1983) also discussed the gastropod fauna in detail and stated that the fauna of the Kangilia Formation was derived from a single environment, whereas the fauna of the overlying Agatdal Formation originated from a mixture of environments. Many specimens demonstrate signs of transport, and the composition of the gastropods indicates that they originate from different ecological niches. Kollmann & Peel (1983) concluded that the gastropods in the Agatdal Formation were transported to their present juxtaposition from different biocoenoses into a deeper part of the basin.

Abbreviations

SNM: Natural History Museum of Denmark, Copenhagen.
DK: Acronym for specimens housed in the Danekræ collection, SNM.

GM: Registered material housed in SNM.
ISL: Material housed in the collection of the senior author (only a silicone rubber cast of *Vanikoropsis mortenseni* n. sp., described herein).
MGUH: Type collection in SNM.
MNO: Material housed in the collection of the junior author (only a silicone rubber cast of *Vanikoropsis mortenseni* n. sp., described herein).
MS: Acronym for drawings in the folders of drawings in the Rosenkrantz collection in SNM.
Rkz no.: Number in the Rosenkrantz collection of drawings.

Systematic Palaeontology

Class Gastropoda Cuvier, 1797

Subclass Caenogastropoda Cox, 1960

Order Littorinimorpha Golikov & Starobogatov, 1975

Superfamily Vanikoroidea Gray, 1840

Family ? Vanikoridae Gray, 1840

[= Naricidae Récluz, 1845 = Merriidae Hedley, 1918].

Wenz (1941, p. 885, fig. 2694) gave a short diagnosis of the family Vanikoridae. According to this, species of this family have a depressed globose outline (like *Natica*) with a depressed, in rare cases a projecting spire. The protoconch is small, with a projecting tip. The last whorl is large, with an umbilicus and spiral ornament and more or less prominent prosocline axial folds. The aperture is large, oblique, and rounded. His diagnosis of *Vanikoro* Quoy & Gaimard, 1832, the type genus of the family, stated a medium-sized to small, rather thin-shelled shell with a depressed spherical outline, a short apex, convex whorls separated by a deep suture, prosocline axial ribs, spiral cords, a wide, rounded and obliquely placed aperture and a slightly concave columella. Cossmann (1925) described the protoconch of vanikorids as smooth, slender, and pointed. However, Bandel & Kowalke (1997, pl. 2, figs 1-9; pl. 3, figs 1-9) and Bandel (2006, pl. 2, figs. 8, 10) illustrated different types of protoconchs of Vanikoridae.

Genus *Vanikoropsis* Meek, 1876

Type species. Natica tuomeyana Meek & Hayden, 1856 by original designation. (1876, p. 270). Maastrichtian, USA.

Diagnosis. Sohl (1967, p. B 22) gave this diagnosis of the genus *Vanikoropsis*: Medium-sized thick naticiform shells. Sculpture dominated by strong broad spiral ribbons with transverse sculpture absent or as low and broad collabral rugosities. Umbilicus narrow.

Discussion. The genus *Vanikoropsis* was proposed by Meek (1876) for thick-walled unumbilicate shells with strong growth rugae. He provisionally placed the genus in the family Vanikoridae Gray, 1840 on the basis of the similarity with *Vanikoro* Quoy & Gaimard, 1832, the type genus of the family. Meek founded *Vanikoropsis* on the holotype of *Natica tuomeyana* Meek & Hayden, 1856. This holotype was illustrated by Wenz (1941, p. 1024, fig. 2935), who reproduced the illustration in Meek (1876), and it is a defective specimen with a worn spire and the body whorl broken back for about one half whorl. Wenz observed no umbilicus on this illustration, but a better illustration by Sohl (1967, pl. 5, figs. 15, 16) of the holotype showed its narrow umbilicus. Because of similarities in outline, sculpture, thickness of the shell and presence of an umbilicus Sohl (1967) included the type species, *Fossar? nebrascensis* (Meek & Hayden, 1860)*, Natica haydeni* Cossmann, 1899 and *Natica praenominata* Cossmann,1920 in the genus *Vanikoropsis*.

The family Vanikoroidae was given a short diagnosis by Wenz (1940, p. 885): Shell white, more or less depressed spherical (*Natica*-like), mostly with a low spire, rarely with a raised spire. Protoconch small, smooth, somewhat projecting, last whorl large with umbilicus, with a spiral ornament and more or less distinct axial ribs. Aperture very large, rounded, and oblique. Species of the genus *Vanikoro* (type species

Vanikoro cancellata (Lamarck, 1822)) are rather thin-shelled and have a stratigraphic range from late Jurassic (Portlandian = Tithonian) to Recent.

The taxonomic classification of the genus *Vanikoropsis* has been discussed since the establishing of the genus. The *Natica*-like outline for some species and the more or less visible umbilicus have caused assignments to Naticidae Guilding, 1834 or Ampullinidae Cossmann, 1918. Wenz (1941, p. 1024) placed *Vanikoropsis* next to *Ampullonatica* Sacco, 1890. Other authors suggesting this classification are White (1889), Cossmann (1907, 1925), Cossmann & Peyrot (1919), Pchelintsev (1927), Beisel (1983), and Caze *et al.* (2011). Cossmann (1907, 1925) and Cossmann & Peyrot (1919) found that the thick shell, broad aperture, inner-lip callus, and closed umbilicus do not match the diagnosis of Vanikoridae.

Sohl (1967) found *Vanikoropsis* and *Vanikoro cancellata* rather similar, as the former differed only in having a thicker shell, a lower spire, and a rounded aperture and placed *Vanikoropsis* in the Vanikoridae. This classification was followed by *e.g.* Thomson (1971), Erickson (1974), Kase (1984), Stilwell & Henderson (2002), and Kollmann (2005). Stilwell *et al.* (2004) referred *Vanikoropsis arktowskiana* (Wilckens, 1910) from the Paleocene of Antarctica to the family Vanikoridae. Crame *et al.* (2014) and Harper *et al.* (2019) however, revert to the original placement by Wilckens (1910), partly based on co-occurrence with drill holes, favored a naticid affinity and Crame *et al.* (2014) suggested that in the future the taxon could be placed in a new genus of the family Naticidae. However, there is no evidence of a similar association in the material from neither Denmark nor West Greenland. Beu (2009) assigned *Vanikoropsis arktowskiana* to the genus *Littorina* Férussac, 1822 (s.l.), because of similarities in outline and spiral ornament and the thickened lips meeting in a clearly defined angle at the top of the aperture.

Cataldo (2017) concluded that the shell outline and

Table 2. Measurements of West Greenland and Danish specimens of *Vanikoropsis (V.)*

SNM no.[1]	Rkz no.[2]	Species this study	Remarks	Height	Width	Height/ width ratio	Last whorl	LW/H ratio	Aperture	A/H ratio
MGUH 10807	MS 144	*V.* (s.l.) *skoui* Rosenkrantz, 1970	Holotype	13.8	15.7	0.88	11.5	0.83	7.1	0.51
MGUH 15744	MS 322B	*V.* (s.l.) *skoui* Rosenkrantz, 1970	Paratype	3.3	3.8	0.87	3.3	1.0	2.8	0.85
MGUH 15745	MS 140	*V.* (s.l.) *jakobseni* n. sp.	Holotype	11.9	11.4	1.04	11.0	0.92	7.7	0.65
MGUH 15746	MS 315	*V.* (s.l.) *bashforthi* n. sp.	Holotype	15.2	14.3	1.06	6.9	0.45	9.8	0.64
GM 1977.1181/8	MS 228	*V.* (s.l.) *bashforthi* n. sp.	Paratype	7.8	6.7	1.16	6.8	0.87	4.9	0.63
GM 1977.1296	MS 315	*V.* (s.l.) *bashforthi* n. sp.	Paratype	18.8	17.7	1.06	15.1	0.80	11.5	0.61
GM 1977.1308	MS 322	*V.* (s.l.) *skoui* Rosenkrantz, 1970	Additional specimen	3.9	4.2	0.67	3.4	0.87	2.9	0.74
MGUH 33950		*Vanikoropsis mortenseni* n. sp.	Holotype	24.1	22.8	1.06	21.5	0.89	13.7	0.61

[1]SNM no.: number in the type collection of SNM, [2]Rkz no.: number in the Rosenkrantz collection of drawings

sculpture in *Vanikoropsis* are evidently convergent with other gastropod taxa and emphasized further studies of the protoconch morphology for a safer suprageneric placement. The protoconch of *V. nebrascensis* from the Maastrichtian of Wyoming, USA was described by Sohl (1967) and Erickson (1974) as dome-shaped, paucispiral and smooth. Judging from the illustration of the holotype the protoconch of *V. demipleura* Stilwell & Henderson, 2002 (fig. 5-2) from the Cenomanian of Australia also is paucispiral.

The protoconchs of the West Greenland species, described herein, are all paucispiral and depressed, with 1¼ to 1½ planispiral, smooth whorls. As this protoconch type is not known from other *Vanikoropsis* species, we use the denomination *Vanikoropsis* (s.l.) for the West Greenland species. The species from the Kerteminde Marl apparently has a dome-like paucispiral protoconch, which is also known from other *Vanikoropsis* species, *e.g., V.? leviplicata* Cataldo, 2017, *V. nebrascensis* (Meek & Hayden, 1860) and *V. demipleura* Stilwell & Henderson, 2002.

In our opinion especially the thick-walled shell, the strong varices and the undulating suture contradict an assignment of the species described herein to the families Naticidae and Ampullinidae. We agree with Sohl (1967) and Cataldo (2017) and tentatively include *Vanikoropsis* in the family Vanikoridae.

Vanikoropsis mortenseni n. sp.
Fig. 3; Fig. 7i–j; Fig. 8a

Type material. Fig. 3a–f; Fig. 7i–j; Fig. 8a, MGUH 33950 (silicone latex cast of holotype MGUH 33950A and MGUH 33950B (ex DK 1133)). Casts in ISL and MNO.

Etymology. This species is named after Peter Tang Mortensen, who collected the only specimen found.

Type locality. Gravel-pit at Gundstrup, north of Odense, Fyn, Denmark.

Type strata. Kerteminde Marl, Selandian, middle Paleocene.

Diagnosis. A rather large, naticiform and moderately thick-walled *Vanikoropsis* with a H/W ratio at almost 1.1, a slightly undulating suture and numerous spiral ribbons. Secondary spirals are inserted from the first teleoconch whorl. Protoconch paucispiral and dome-like.

Measurements. See Table 2.
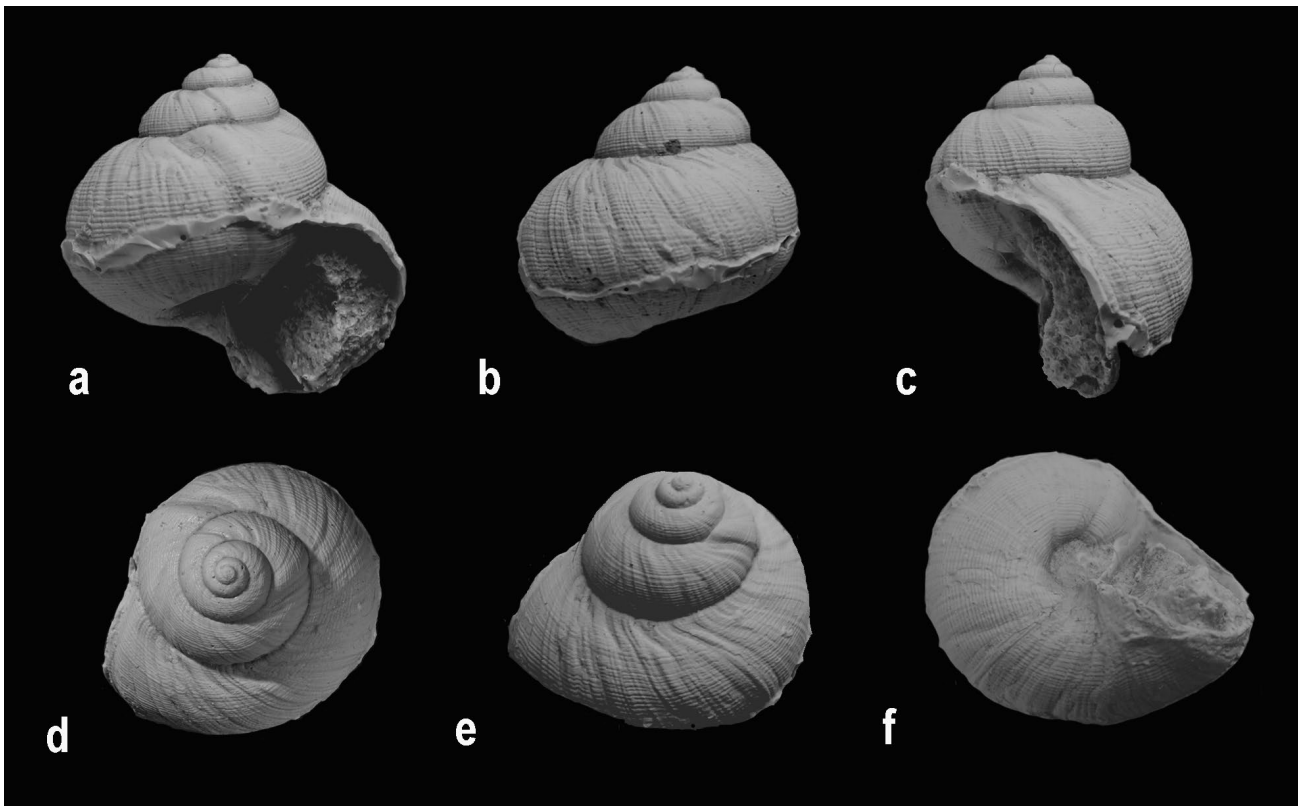
Fig. 3. a-f: *Vanikoropsis mortenseni* n. sp. Silicone latex cast of holotype MGUH 33950A and MGUH 33950B, ex DK 1133. Height 24.1 mm, width 22.8 mm. **a:** apertural view, **b:** rear view, **c:** lateral view, **d:** apical view, **e:** oblique apical view, **f:** umbilical view.

Description. The shell is medium sized, naticiform and moderately thick-walled, with a H/W ratio of 1.1. The only specimen has 5 whorls, of which the first 1¼ belongs to the protoconch. The whorls are medium convex and separated by a deep to slightly caniculate and a slightly undulating suture. The body whorl equals 0.92 of the total shell height. The aperture equals 0.47 of the total shell height and is obliquely ovate, well rounded anteriorly, subangulate posteriorly. The labium is concave and partly covered by a thin callus, which also covers part of the parietal wall. The labrum is thickened and prosocline, inclined about 20° to the axis of coiling. There is a narrow, but rather deep umbilicus. The rather badly preserved protoconch is paucispiral and dome-like, consisting of 1¼ whorls. The teleoconch whorls are completely covered by numerous spiral ribbons, which are separated by narrow interspaces. The spiral ribbons on the abapical part of the whorls are wider than the adapical ribbons. Two spiral ribbons situated a little above the middle of the whorls are a little more prominent than the others. The number of spiral ribbons is 8 on the first teleoconch and secondary spirals are inserted from the first teleoconch whorl. On the penultimate whorl there are almost 30 spiral ribbons. The axial sculpture consists of prosocline growth lines or broad discontinuous swellings, which get more close-set before the aperture. Three old apertures are visible as indistinctively demarcated swellings. They have distances from 0.25 whorl to 0.75 whorl in abapical direction.

Discussion. We assign the new species to *Vanikoropsis* because of the general outline, the spiral ornament, the prosocline axial folds, and the rather thick-walled shell with varices. The apparently dome-like paucispiral protoconch is also known on other species of *Vanikoropsis*. *Vanikoropsis* (s.l.) *skoui* Rosenkrantz, 1970 is considerably more thick-walled and has a coarser spiral ornament. The whorls have a narrow adapical ramp and more coarse axial folds and more prominent varices and the protoconch is planispiral and depressed. Kollmann & Peel (1983, p. 65, figs 131A-D) illustrated the holotype and an additional juvenile specimen, which is more low-spired. *Vanikoropsis* (s.l.) *jakobseni* n. sp. (Kollmann & Peel 1983, p. 65, figs 132A, B) has a lower spire and stronger and less numerous spiral cords. The suture is caniculate and there is a narrow subsutural ramp. The protoconch is planispiral and depressed. *Vanikoropsis* (s.l.) *bashforthi* n. sp. (Kollmann & Peel 1983, p. 66, fig. 133) has an outline rather similar to the new species, but a lower number of spiral cords, which are wider and very weak on the body whorl. Furthermore, this species has a considerably more thick-walled shell, less convex

whorls, and a more concave parietal wall. The axial folds are more prominent and cause a much more undulating suture. The protoconch is planispiral and depressed. *Vanikoropsis nebrascensis* (Meek & Hayden, 1860) from the Maastrichtian of Wyoming, USA has a higher spire and a lower number of spiral cords, which are wider. *Vanikoropsis? leviplicata* Cataldo, 2017 from the Lower Cretaceous of Argentina differs by having a closed umbilicus partially covered by the callus, a lower number of wider spiral ribbons and a subangular periphery. However, the protoconch is dome-like and is reminiscent of the protoconch of the Danish species.

Vanikoropsis (s.l.) *skoui* Rosenkrantz, 1970
Fig. 4a–e, f–h; Fig. 7f–h; Fig. 8b

1970 *Vanikoropsis skoui* Rosenkrantz, p. 438, text-figs 13, 14a-b.
1983 *Vanikoropsis skoui* Rosenkrantz – Kollmann & Peel, p. 65, figs 131A-D.

Type material. Holotype Fig. 4a–e, Fig. 8b, MGUH 10807, *Vanikoropsis skoui* Rosenkrantz (1970, p. 438, text-figs 13, 14a–b); Kollmann & Peel (1983, p. 65, figs 131A, B); additional specimen Fig. 4f–h, MGUH 15744 (Kollmann & Peel 1983, p. 65, figs 131C, D).

Additional material. Fig. 7f–h, MGUH 33953 (ex 1977.1308), Sonja Lens, 1 juvenile specimen.

Type locality. Sonja Lens, east of Turritellakløft, Nuussuaq peninsula, West Greenland.

Type strata. Agatdal Formation, late Danian, early Paleocene.

Measurements. See Table 2.

Description. The shell is small and naticiform, height/width ratio *c.* 0.9. The shell is rather thick-shelled with strongly convex whorls, which are regularly increasing in diameter. The whorls are separated by a deep to caniculate, undulating suture. The protoconch is planispiral, consisting of *c.* 1¼ whorls, which are laying deeper than the following whorls. There are *c.* four teleoconch whorls. Last whorl equals 0.8 of the total shell height, the aperture *c.* 0.5 of the total shell height. The last whorl is large and swollen, wider than tall, with its maximum diameter at almost mid-whorl. The umbilicus is narrow, and the innerlip callus partly covers it. The aperture is holostomate and prosocline, with a deviation from the axis, the peristome round to slightly ovate, with an anterior spout near the columella, rounded abapically. The

labrum is strongly thickened and inclined about 15° to the axis of coiling. The inner lip is flat to slightly concave on parietal area and the callus thick and narrow. The columella is concave. The spiral ornament consists of low, band-like cords, which are separated by narrower spiral striae. The cords are twice as broad as the striae, nearly 20 on last whorl; the growth lines are prosocline and straight. There are growth rugae on last and penultimate whorl. They are irregular, parallel to growth lines, accentuated on adapical third of whorls. Old apertures are visible as swellings in distances of half a whorl. These swellings cause an undulating suture. The periphery is inconspicuous. The base is convex with spiral cords and growth lines.

Discussion. Rosenkrantz (1970, p. 438) gave no diagnosis and only a few descriptive remarks. He stated that the diagnosis given by Sohl (1967, p. 22) covers the thick-shelled naticiform new species completely and that the species in shape and height of the spire matches the holotype of *Vanikoropsis tuomeyana* (Meek & Hayden, 1860), the type species of *Vanikoropsis*. He stated that his new species has a finer spiral sculpture like *Vanikoropsis nebrascensis* (Meek & Hayden, 1860). However, he noted that this species has a much higher spire than the species from West Greenland. Rosenkrantz mentioned a few specimens of *V. skoui* but only illustrated the holotype. However, he obviously may have recognized further different *Vanikoropsis* species, as he supervised drawings of the specimens, by Kollmann & Peel (1983) interpreted as *Vanikoropsis* sp. 1 and sp. 2, and the additional specimens of *Vanikoropsis* (s.l.) *skoui* and *Vanikoropsis* (s.l.) *bashforthi* n. sp., illustrated herein.
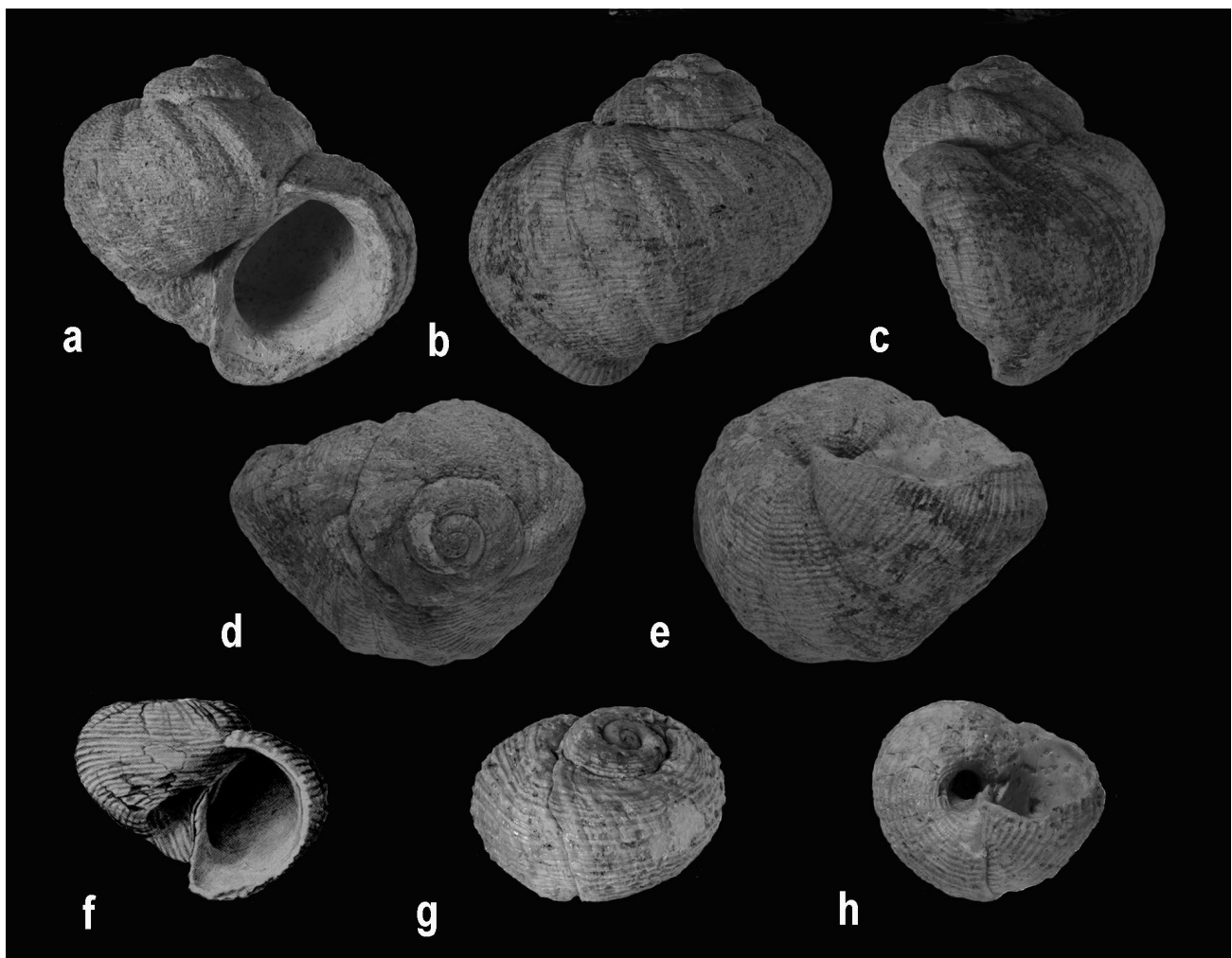
Fig. 4. a-e. *Vanikoropsis* (s.l.) *skoui* Rosenkrantz, 1970. Holotype MGUH 10807. Height 13.8 mm, width 15.7 mm. **a:** apertural view, **b:** rear view, **c:** lateral view, **d:** apical view, **e:** umbilical view. **f-h.** *Vanikoropsis* (s.l.) *skoui* Rosenkrantz, 1970. MGUH 15744. Height 3.3 mm, width 3.8 mm. **f:** apertural view (reproduced from Kollmann & Peel 1983, p. 65, fig. 131D), **g:** oblique apical view, **h:** umbilical view.

Vanikoropsis (s.l.) jakobseni n. sp.
Fig. 5a–e; Fig. 8c

1983 *Vanikoropsis* sp. 1 – Kollmann & Peel, p. 65, figs 132A-B.

Type material. Holotype Fig. 5a–e, Fig. 8c, MGUH 15745.

Etymology. This species is named after Sten Lennart Jakobsen, Geomuseum Faxe, for his great help doing the greater part of the photographical work in SNM.

Type locality. Qaarsutjægerdal, east of Turritellakløft, Nuussuaq peninsula, West Greenland.

Type strata. Agatdal Formation, late Danian, early Paleocene.

Diagnosis. A low-spired *Vanikoropsis* with a rather coarse spiral ornament, a narrow umbilicus, and a narrow adapical ramp.

Measurements. See Table 2.

Description. The only specimen is naticiform and low-spired and provides three and a half whorls, which are separated by a canaliculate suture, and the protoconch. The whorls are medium convex and have a rather narrow adapical ramp. The last whorl equals 0.9 of the total shell height, the aperture 0.6. The aperture is ovate and oblique to the axis, with an anterior spout adaxially. The interior side of the thickened labrum is smooth. The labium is concave, and a thin callus partly covers the narrow umbilicus. The labrum is thickened and inclined *c.* 15° to the axis of coiling. The paucispiral protoconch is planispiral, consisting of *c.* 1½ whorls, which are laying deeper than the following teleoconch whorls. The protoconch whorls are more convex than on *Vanikoropsis* (s.l.) *skoui* and *Vanikoropsis* (s.l.) *bashforthi* n. sp. (described herein). On the first teleoconch whorl a keel appears near the adapical suture and is situated above the protoconch. This keel demarcates a narrow adapical ramp with indistinct spiral ribs. On the abapical part of the whorl there are 7-8 spiral cords of varying strength and on the body whorl weaker secondary spirals are inserted. There are irregularly placed axial rugae, which are most prominent adapically.

Discussion. The species especially differs from *Vanikoropsis* (s.l.) *skoui* by its lower apex and lower number of spiral cords. Kollmann & Peel interpreted it as a possible variation of *Vanikoropsis* (s.l.) *skoui*, but because of the mentioned differences in outline and spiral ornament we interpret it as not conspecific with *Vanikoropsis* (s.l.) *skoui*.
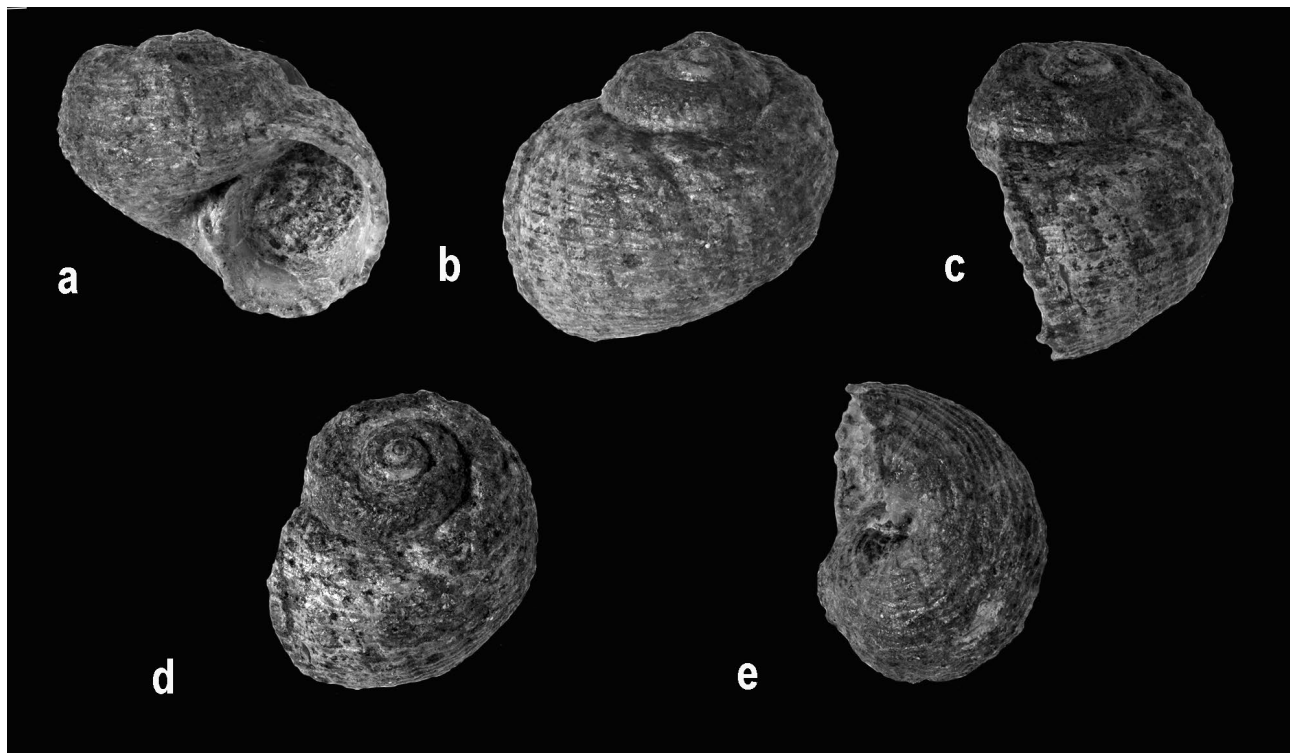
Fig. 5. *Vanikoropsis* (s.l.) *jakobseni* n. sp. Holotype MGUH 15745. Height 11.9 mm, width 11.4 mm. **a:** apertural view, **b:** rear view, **c:** lateral view, **d:** apical view, **e:** umbilical view.

Vanikoropsis (s.l.) bashforthi n. sp.
Fig. 6a–e, f–j; Fig. 7a–e; Fig. 8d

1983 *Vanikoropsis* sp. 2 – Kollmann & Peel, p. 66, figs 133A-B.

Type material. Holotype Fig. 6a–e; Fig. 8d, MGUH 15746. Paratypes Fig. 6f–j, MGUH 33951 (ex GM 1977.1296); Fig. 7a–e, MGUH 33952 (ex GM 1977.1181/8).

Etymology. This species is named after Arden Roy Bashforth, SNM, Copenhagen, for his great help with locating of the material in the Rosenkrantz collection in SNM.

Type locality. Qaarsutjægerdal, east of Turritellakløft, Nuussuaq peninsula, West Greenland.

Type strata. Agatdal Formation, late Danian, early Paleocene.

Diagnosis. A relatively high-spired *Vanikoropsis* with a spiral ornament of delicate spiral threads, which cover the entire shell. The spiral ornament gradually becomes weaker on the body whorl. The whorls are slightly to medium convex, and the shell is thick-walled. The umbilicus is narrow. Old apertures are visible as swellings at intervals of half a whorl. The paucispiral protoconch is planispiral and depressed.
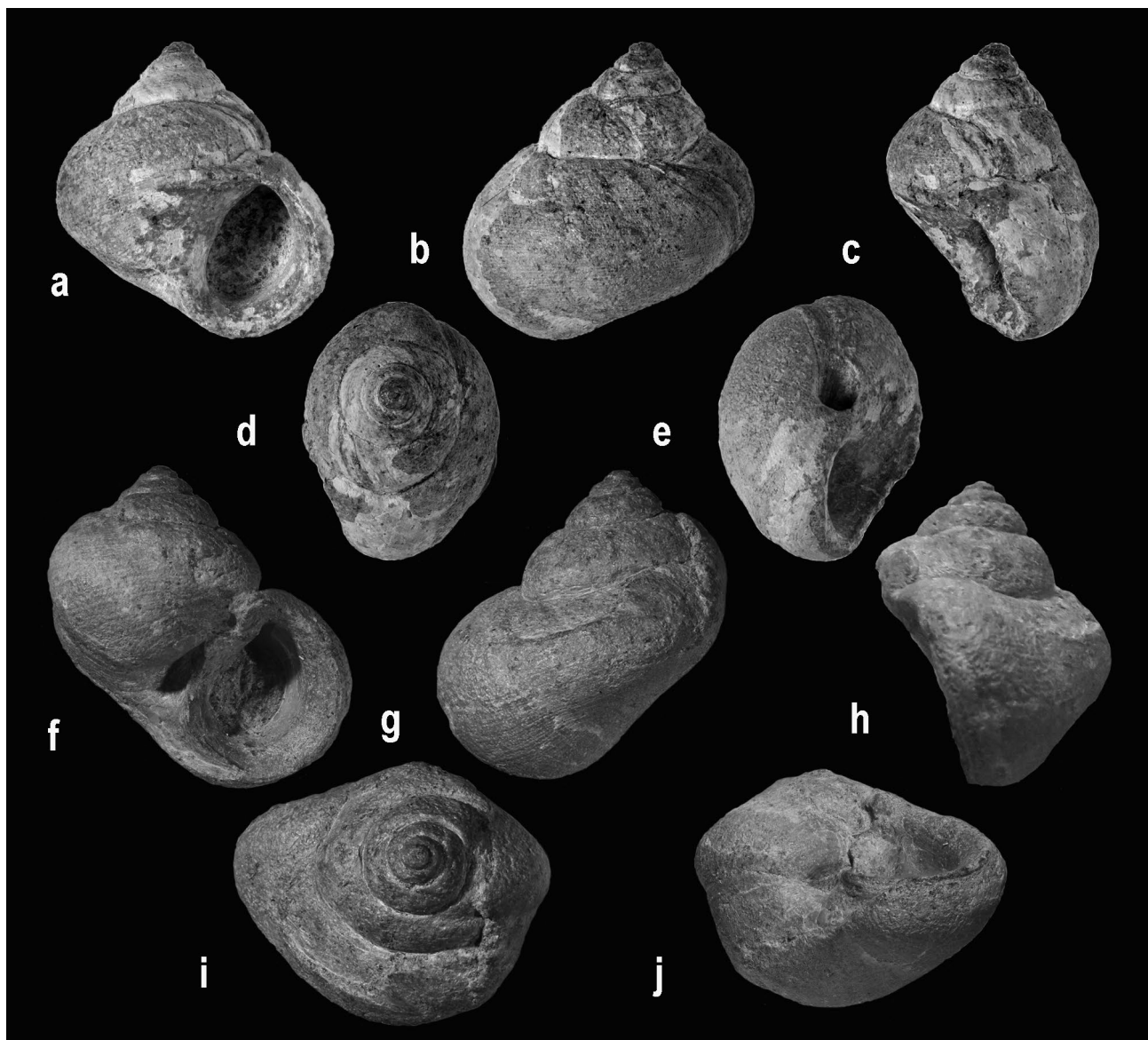
Fig. 6. a-e: *Vanikoropsis* (s.l.) *bashforthi* n. sp. Holotype MGUH 15746. Height 15.2 mm, width 14.3 mm. **a:** apertural view, **b:** rear view, **c:** lateral view, **d:** apical view, **e:** umbilical view. **f-j:** *Vanikoropsis* (s.l.) *bashforthi* n. sp. Paratype MGUH 33951, ex GM 1977.1296. Height 18.8 mm, width 17.7 mm. **f:** apertural view, **g:** rear view, **h:** lateral view, **i:** apical view, **j:** umbilical view.
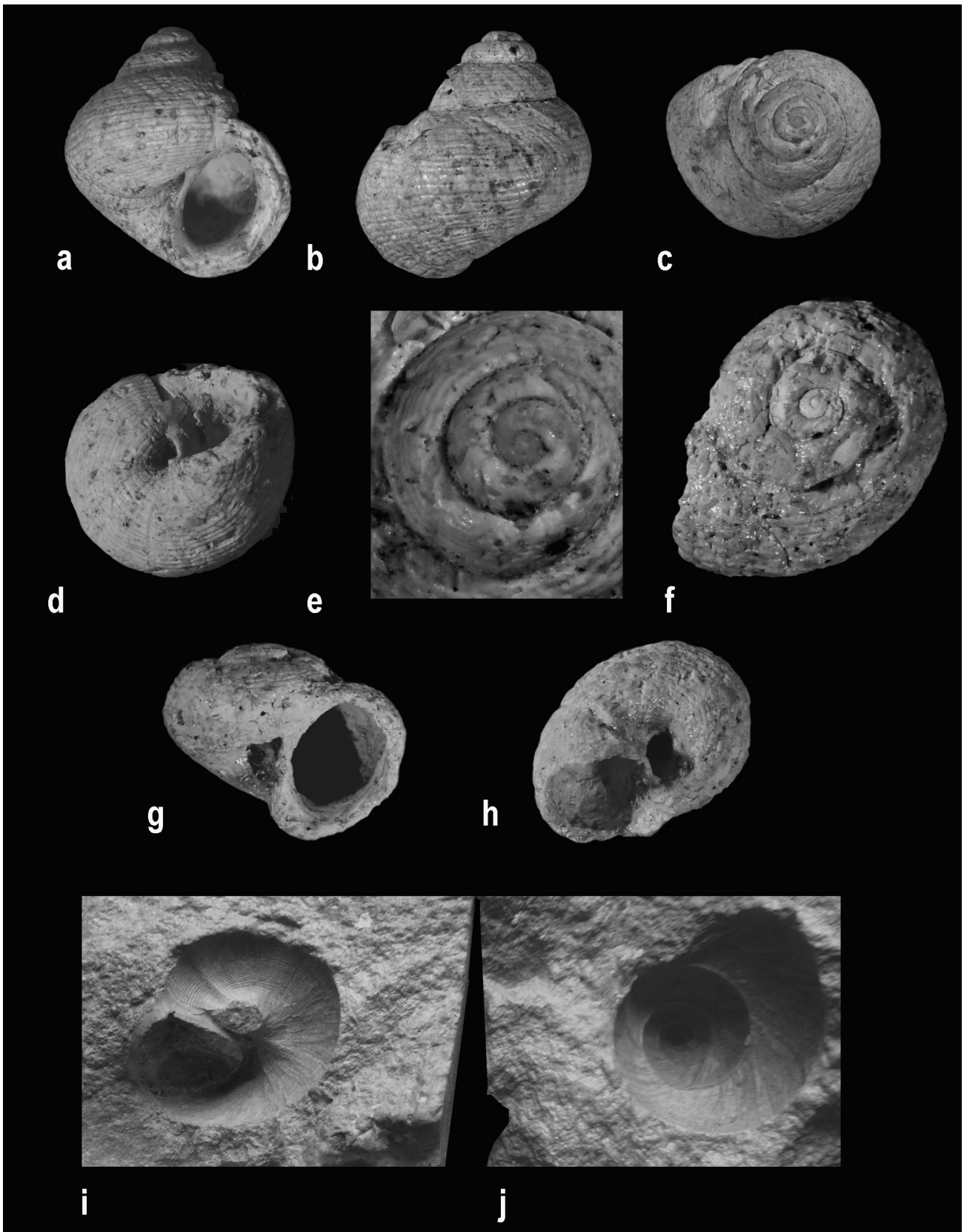
Fig. 7. a-e: *Vanikoropsis* (s.l.) *bashforthi* n. sp. Paratype MGUH 33952, ex GM 1977.1181/8. Height 7.8 mm, width 6.7 mm. **a:** apertural view, **b:** rear view, **c:** apical view, **d:** umbilical view, **e:** protoconch and first teleoconch whorls. **f-h:** *Vanikoropsis* (s.l.) *skoui* Rosenkrantz, 1970. MGUH 33953, ex GM 1977.1308. Height 3.9 mm, width 4.2 mm. **f:** protoconch and first teleoconch whorls, **g:** apertural view, **h:** umbilical view. **i-j:** *Vanikoropsis mortenseni* n. sp. Holotype MGUH 33950A and MGUH 33950B (ex DK 1133). Impressions in slabs of Kerteminde Marl. Length 69 mm, height 27 mm.

Measurements. See Table 2.

Description. The material includes the three illustrated specimens only. The holotype was illustrated by Kollmann & Peel (1983). The paratype MGUH 33952 was found by the senior author (2005) in the sample GM 1977.1181, by Kollmann & Peel (1983, p. 94) labelled "cf. *Coptostoma* sp.". As a matter of fact, the senior author found eight different taxa in this sample, including a juvenile specimen, which he labelled "*Vanikoropsis* sp." and gave the number GM 1977.1181/8. The paratype MGUH 33951 (ex GM 1977.1296) is a larger specimen. The rather small turbiniform shell provides the protoconch and four slightly to medium convex whorls, which are separated by a distinct and highly undulating suture. The width/height ratio is *c.* 1.1. The body whorl equals 0.76-0.85 of the total shell height, the aperture 0.44-0.59. The aperture is rounded ovate, and the callus partly covers the narrow umbilicus. The shell is very thick-walled. The protoconch could be studied on the specimen 1977.1181/8. It consists of 1½ planispiral smooth whorls, which lay lower than the first teleoconch whorl. The transition into the teleoconch is indicated by a change in color. There are 10 fine spirals on the first teleoconch whorl, separated by fine furrows. The abapical spirals are stronger than the adapical spirals. On the following whorls secondary spirals are inserted and the entire shell is covered of these spirals, which are of slightly varying width. The aperture is rounded ovate and obliquely placed to the axis. The labrum is thickened and inclined about 30° to the axis of coiling. The thin callus partly covers the narrow umbilicus. Old apertures are visible as thickenings with intervals of half a whorl, which cause an undulating suture. In apical view the adult shell has a subovate outline.

Discussion. The species differs from the two other species from West Greenland by its spiral ornament of fine spirals and its more high-spired outline. It comes closer to the species from Denmark with regards to outline and ornament but has a different protoconch. *Vanikoropsis arktowskiana* (Wilckens, 1910) from the Danian of Antarctica has a similar outline, but a spiral ornament of fewer and coarser cords. Kollmann & Peel (1983) noted that *Littorina* sp. indet. in Krach (1963, p. 49; pl. 4, fig. 4; pl. 17, fig. 8) seemed to be related. This species has a rather similar outline, but a coarser spiral ornament.
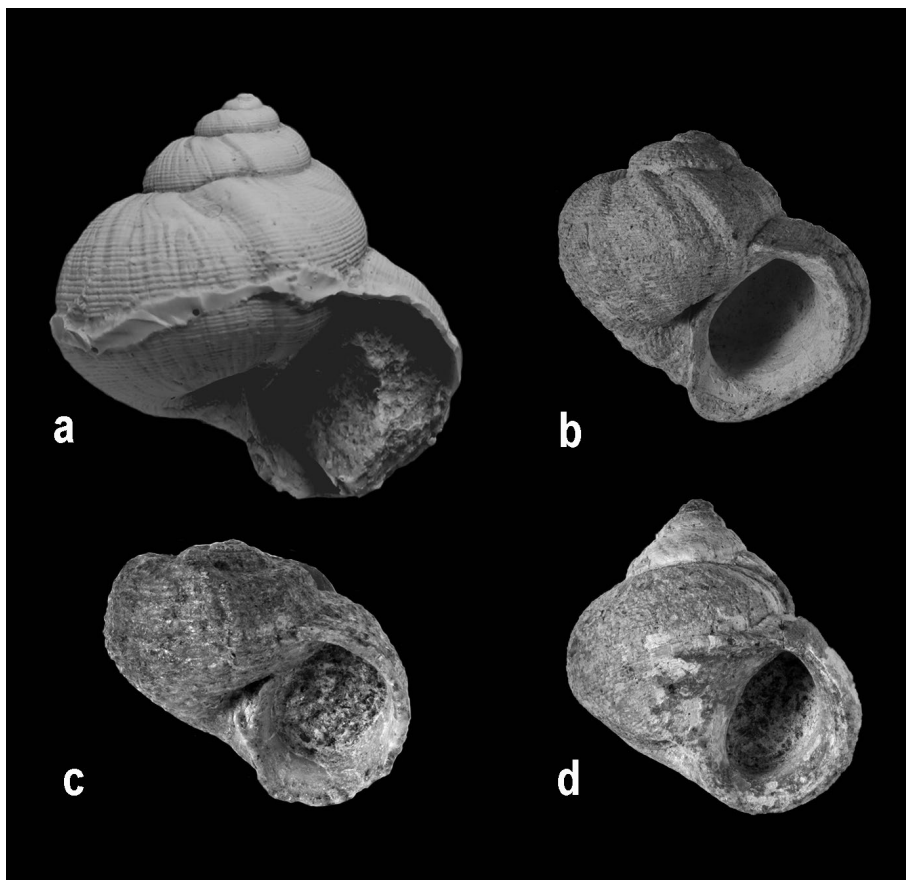
Fig. 8. a: *Vanikoropsis mortenseni* n. sp. Silicone latex cast of holotype MGUH 33950A and MGUH 33950B. Impressions in slabs of Kerteminde Marl. Height 24.1 mm, width 22.8 mm. **b:** *Vanikoropsis* (s.l.) *skoui* Rosenkrantz, 1970. Holotype MGUH 10807. Height 13.8 mm, width 15.7 mm. **c:** *Vanikoropsis* (s.l.) *jakobseni* n. sp. Holotype MGUH 15745. Height 11.9 mm, width 11.4 mm. **d:** *Vanikoropsis* (s.l.) *bashforthi* n. sp. Holotype MGUH 15746. Height 15.2 mm, width 14.3 mm.

Table 3. Stratigraphical records of *Vanikoropsis (V.)*, based on references in literature

Species	Country	Series/Epoch	Stage/Age	Reference
V. neritoides (Trautschold, 1866)	Russia	Upper Jurassic/ Lower Cretaceous		Gerasimov (1992)
V. minuta Pan, 1977	China	Middle Jurassic	Bajocian/Bathonian	Stilwell *et al.* (2004)
V. suciensis White, 1889	US	Cretaceous		Sohl (1967)
V. decussata (Deshayes in Leymerie, 1842)	France	Lower Cretaceous	Albian	Stilwell & Henderson (2002)
V. decussata (Deshayes in Leymerie, 1842)	Japan	Lower Cretaceous	Barremian	Stilwell & Henderson (2002)
V. exerta Cossmann, 1907	France	Lower Cretaceous	Barremian	Cossmann (1925)
V. houdardi Cossmann, 1925	France	Lower Cretaceous	Albian	Cossmann (1925)
V. borissjaki Pchelintsev, 1927	Ukraine	Lower Cretaceous	Albian	Pchelintsev (1927)
V. communis Pchelintsev, 1927	Ukraine	Lower Cretaceous	Albian	Pchelintsev (1927)
V. multistriata Pchelintsev, 1927	Ukraine	Lower Cretaceous	Albian	Pchelintsev (1927)
Vanikoropsis? sp.	Antarctica	Lower Cretaceous		Thomson (1971)
Vanikoro? sp.	Argentina	Lower Cretaceous	Barremian	Stanton (1901)
V? leviplicata Cataldo, 2017	Argentina	Lower Cretaceous	Upper Hauterivian	Cataldo (2017)
V. valanginensis Beisel, 1983	Sibiria	Lower Cretaceous	Valangian	Beisel (1983)
V. jackii Etheridge in Jack & Etheridge, 1892	Australia	Lower Cretaceous		Etheridge (1920)
V? stuarti Etheridge, 1902	Australia	Lower Cretaceous		Etheridge (1902)
V. decussata Etheridge, 1920 (non Deshayes in Leymerie, 1842)	Australia	Lower Cretaceous		Etheridge (1920)
V. demipleura Stilwell & Henderson, 2002	Australia	Upper Cretaceous	Cenomanian	Stilwell & Henderson (2002)
V. cassisiana (d'Orbigny, 1842)	Serbia	Upper Cretaceous	Lower Cenomanian	Ayoub-Hannaa *et al.* (2015)
V. nebrascensis (Meek & Hayden, 1860)	USA	Upper Cretaceous	Maastrichtian	Sohl (1967)
Vanikoro kiliani Wilckens, 1910	Antarctica	Upper Cretaceous		Wilckens (1910)
V. arktowskiana (Wilckens, 1910)	Antarctica	Lower Paleocene	Danian	Stilwell *et al.* (2004)
Vanikoropsis skoui Rosenkrantz, 1970	Greenland	Lower Paleocene	Danian	Rosenkrantz (1970)
Vanikoropsis? bashforthi n. sp.	Greenland	Lower Paleocene	Danian	Schnetler & Nielsen (this study)
Vanikoropsis? jakobsen n. sp.	Greenland	Lower Paleocene	Danian	Schnetler & Nielsen (this study)
Vanikoropsis mortenseni n. sp.	Denmark	Middle Paleocene	Selandian	Schnetler & Nielsen (this study)

Distribution of the genus *Vanikoropsis*

According to Wenz (1941, p. 1024) the genus has a stratigraphical range from upper Jurassic (Portlandian = Tithonian) to upper Cretaceous. Cataldo (2017, p. 428–429), in her discussion of the new species *Vanikoropsis? leviplicata*, discussed records of *Vanikoropsis* species in literature. We have checked the references but are not convinced that all these species in fact can be assigned to *Vanikoropsis*. In some cases, especially in older references, the illustrations and/or the material are rather poor, and the members of this group show a considerable variation in outline, sculpture, aperture and umbilicus. Thus, the group is most probably polyphyletic. As the present paper is not intended to be a revision of the genus *Vanikoropsis*, we prefer to list the records in Table 3, which is mainly based on Cataldo (2017).

Conclusions

The predominantly Cretaceous genus *Vanikoropsis* Meek, 1876 is represented by one species in the Danish Selandian (middle Paleocene) and three species in the Danian (early Paleocene) of West Greenland. Three new species are described, viz. *Vanikoropsis mortenseni* n. sp., *Vanikoropsis* (s.l.) *jakobseni* n. sp. and *Vanikoropsis* (s.l.) *bashforthi* n. sp. The protoconchs of the species from West Greenland are all paucispiral and depressed, whereas the species from Denmark apparently has a dome-like protoconch. The genus *Vanikoropsis* is tentatively included in the family Vanikoridae. The occurrences support the affinities between the Danish and the West Greenland Paleocene, which were discussed by Schnetler & Nielsen (2018). *Vanikoropsis mortenseni* n. sp. is probably the youngest record of *Vanikoropsis*.

References

Ayoub-Hannaa, W., Radulovic, V.J. & Fürsich, F.T. 2015: Gastropods from the Lower Cenomanian of Koracica (Kosmaj Mountain, central Serbia). Neues Jahrbuch für Geologie und Paläontologie, Abhandlungen 276, 27–62. https://doi.org/10.1127/njgpa/2015/0474

Bandel, K. & Kowalke, T. 1997: Systematíc value of the larval shell of fossil and modern Vanikoridae, Pickworthiidae and the genus *Fossarus* (Caenogastropoda, Mollusca). Berliner geowissenschaftliche Abhandlungen E25, 3–29.

Bandel, K. 2006: Families of the Cerithioidea and related superfamilies (Palaeo-Caenogastropoda; Mollusca) from the Triassic to the Recent characterized by protoconch morphology, including the description of new taxa. Paläontologie, Stratigraphie, Fazies. Freiberger Forschungshefte C 511, 59–138.

Beisel, A.L. 1983: [Late Jurassic and early Cretaceous Gastropods of the North of Middle Siberia (systematic composition, paleoecology, stratigraphic and paleogeographic significance)]. Trudy Instytut Geologii i Geofizika Akademiya Nauk SSSR 484, 1–94. [in Russian].

Beu, A.G. 2009: Before the ice: Biogeography of Antarctic Paleogene molluscan faunas. Palaeogeography, Palaeoclimatology, Palaeoecology 284, 191–226. https://doi.org/10.1016/j.palaeo.2009.09.025

Bowman, V., Francis, J. & Askin, R. 2014: Latest Cretaceous–earliest Paleogene vegetation and climate change at the high southern latitudes: palynological evidence from Seymour Island, Antarctic Peninsula. Palaeogeography, Palaeoclimatology, Palaeoecology, 408, 26-47. https://doi.org/10.1016/j.palaeo.2014.04.018

Burden, E.T. & Langille, A.B. 1990: Stratigraphy and sedimentology of Cretaceous and Paleocene strata in half-grabens on the southeast coast of Baffin Island, Northwest Territories. Canada Petroleum Geology Bulletin 38, 185–195. https://doi.org/10.1080/01916122.1991.9989392

Cataldo, C.S. 2017: New records of marine gastropods from the Lower Cretaceous of west-central Argentina. Ameghiniana 54, 405–440. https://doi.org/10.5710/amgh.14.12.2016.3053

Caze, B., Merle, D., Le Meur, M., Pacaud, J.-M., Ledon, D. & Saint Martin, J.-P. 2011: Taxonomic implications of the residual colour patterns of ampullinid gastropods and their contribution to the discrimination from naticids. Acta Palaeontologica Polonica 56, 329–347. https://doi.org/10.4202/app.2009.0084

Christiansen, F.G., Bojesen-Koefoed, J.A., Dam, G., Laier, T., & Salehi, S. 2020: A review of oil and gas seepage in the Nuussuaq Basin, West Greenland – implications for petroleum exploration. GEUS Bulletin 44, 4567. https://doi.org/10.34194/geusb.v44.4567

Christiansen, F.G., Dam, G., Larsen, L.M., Nøhr-Hansen, H., Pedersen, A.K., Boserup, J., Bojesen-Kofoed, J., Laier, T. & Pulvertaft, T.C. 1997: Stratigraphy, sedimentology and geochemistry of cores and other samples from the GANW#1 well, Nuussuaq, West Greenland. Danmarks og Grønlands Geologiske Undersøgelse Rapport 1997/36, 52 pp.

Clarke, D.B. & Pedersen, A.K. 1976: Tertiary volcanic province of West Greenland. In: Escher, A. & Watt, W.S. (eds): Geology of Greenland, 365–387. Copenhagen: The Geological Survey of Greenland.

Clausen, O.R. & Huuse, M. 1999: Topography of the Top Chalk surface, on- and offshore Denmark. Marine and Petroleum Geology 16, 677–691. https://doi.org/10.1016/s0264-8172(99)00003-3

Clemmensen, A. & Thomsen, E. 2005: Palaeoenvironmental changes across the Danian–Selandian boundary in the North Sea Basin. Palaeogeography Palaeoclimatology Palaeoecology 19, 351–394. https://doi.org/10.1016/j.palaeo.2005.01.005

Cossmann, M. 1899: Essais de paléoconchologie comparée 3, 201 pp. Published by the author. https://doi.org/10.5962/bhl.title.52314

Cossmann, M. 1907: Description des gastropodes et pélécypodes. In: Pellat, E. & Cossmann, M. (eds): Le Barrémien supérieur à facies urgonien de Brouzet-les-Alais (Gard). Mémoires de la Société Géologique de France 37, 6–42. https://doi.org/10.5962/bhl.title.13768

Cossmann, M. 1918: Essais de paléoconchologie comparée 11, 388 pp. Published by the author. https://doi.org/10.5962/bhl.title.53878

Cossmann, M. 1925: Essais de paléoconchologie comparée 13, 345 pp. Paris: Les Presses Universitaires de France. https://doi.org/10.5962/bhl.title.52314

Cossmann, M., & Peyrot, A. 1919: Conchologie néogénique de l'Aquitaine. Actes de la Société Linnéenne de Bordeaux 70, 181–356. https://doi.org/10.5962/bhl.title.165529

Cox, L.R. 1960: Gastropoda. In: Moore, R.C. (ed.): Treatise on invertebrate paleontology I: Mollusca 1, 85–169. The Geological Society of America and the University of Kansas Press.

Crame, J.A., Beu, A.G., Ineson, J.R., Francis, J.E., Whittle, R.J. & Bowman, V.C. 2014: The early origin of the Antarctic marine fauna and its evolutionary implications. PLoS ONE 9, e114732. https://doi.org/10.1371/journal.pone.0114743

Cuvier, G. 1797: Tableau élémentaire de l'histoire naturelle des animaux, 710 pp. https://doi.org/10.5962/bhl.title.45918

Dam, G. 2002: Sedimentology of magmatically and structurally controlled outburst valleys along rifted volcanic margins: examples from the Nuussuaq Basin, West Greenland. Sedimentology 49, 505–532. https://doi.org/10.1046/j.1365-3091.2002.00457.x

Dam, G. & Sønderholm, M. 1994: Lowstand slope channels of the Itilli succession (Maastrichtian – Lower Paleocene), Nuussuaq, West Greenland. Sedimentary Geology 94, 49–71. https://doi.org/10.1016/0037-0738(94)90146-5

Dam, G. & Sønderholm, M. 2021: Tectonostratigraphic evolution, palaeogeography and main petroleum plays of the Nuussuaq Basin: An outcrop analogue for the Cretaceous–Palaeogene rift basins offshore West Greenland. Marine and Petroleum Geology 129, 105047. https://doi.org/10.1016/j.marpetgeo.2021.105047

Dam, G., Larsen, M. & Sønderholm, M. 1998: Sedimentary response to mantle plumes: Implications from Paleocene onshore successions, West and East Greenland. Geology 26, 207–210. https://doi.org/10.1130/0091-7613(1998)026<0207:srtmpi>2.3.co;2

Dam, G., Pedersen, G.K., Sønderholm, M., Midtgaard, H., Larsen, L.M., Nøhr-Hansen, H. & Pedersen, A.K. 2009: Lithostratigraphy of the Cretaceous–Paleocene Nuussuaq Group, Nuussuaq Basin, West Greenland. Geological Survey of Denmark and Greenland Bulletin 19, 171 pp. https://doi.org/10.34194/geusb.v19.4886

Deshayes, G.P. in Leymerie, M.A. 1842: Suite du Mémoire sur le Terrain Crétacé du Departement de l'Aube, Seconde Partie. Mémoires de la Société Géologique de France 5, 1–34. https://doi.org/10.2113/gssgfbull.s5-xiii.7-9.343

Erickson, J.M. 1974: Revision of the Gastropoda of the Fox Hills Formation, Upper Cretaceous (Maestrichtian) of North Dakota. Bulletins of American Paleontology 66, 132–253.

Etheridge, R. 1902: A monograph of the Cretaceous invertebrate fauna of New South Wales. Memoirs of the Geological Survey of New South Wales 11, 1–98.

Etheridge, R. 1907: Lower Cretaceous fossils from the sources of the Barcoo, Ward and Nive Rivers, south central Queensland. Part I. Annelida, Pelecypoda and Gasteropoda. Records of the Australian Museum 6, 317–329. https://doi.org/10.3853/j.0067-1975.6.1907.1016

Etheridge, R. 1920: Small Gasteropoda from the Lower Cretaceous of Queensland. Publications of the Geological Survey of Queensland 269, 8–21.

Etheridge, R. in Jack, R.L. & Etheridge, R. 1892: The geology and paleontology of Queensland and New Guinea, 808 pp. London: Government Printer, Brisbane and Dulau & Co.

Férussac, A.E.J.P.F. d'Audebard 1822: Tableaux systématiques des animaux mollusques classés en familles naturelles, dans lesquels on a établi la concordance de tous les systèmes; suivis d'un prodrome général pour tous les mollusques terrestres ou fluviatiles, vivants ou fossils. 110 pp. https://doi.org/10.5962/bhl.title.124941

Foged, N., Larsen, G., Larsen, B. & Thomsen, E. 1995: An overview on engineering geological conditions at Storebælt. Dansk Geoteknisk Forening Bulletin 11, 5.7–5.30.

Gerasimov, P.A. 1992: [Gastropods from the Jurassic and Lower Cretaceous of European Russia], 190 pp. Moscow: Rossiyskaja Akademija Nauk. [in Russian].

Golikov, A. N. & Ya. I. Starobogatov, 1989 ["1988"]: Voprosy filogenii i sistemy perednezhabernykh briukhonogikh molliuskov. [Problems of phylogeny and system of the prosobranchiate gastropods]. Trudy Zoologicheskogo Instituta 187, 4–77. [in Russian] [Volume 187 on title page of volume; vol. 176 in error on running title of article; published after 27 December 1988, before 7 August 1989].

Gray, J.E. 1840: Shells of molluscous animals. In: British Museum (Corporate author), Synopsis of the contents of the British Museum, Forty-second edition, Second impression, 106–156. London: Woodfall and Son.

Gry, H. 1935: Petrology of the Paleocene sedimentary rocks of Denmark. Danmarks Geologiske Undersøgelse II. Række 61, 172 pp. https://doi.org/10.34194/raekke2.v61.6849

Hansen, H.J. 1970: Danian foraminifera from Nûgssuaq, West Greenland. Bulletin Grønlands Geologiske Undersøgelse 93, 132 pp. https://doi.org/10.34194/bullggu.v93.6633

Harper, E.M., Crame, J.A. & Pullen, A.M. 2019: The fossil record of durophagous predation in the James Ross Basin over the last 125 million years. Advances in Polar Science 30, 199–209. https://doi.org/10.13679/j.advps.2019.0001

Hedley, C. 1918: A checklist of the marine fauna of New South Wales. Part 1. Journal and Proceedings of the Royal Society of New South Wales. 51: M1-M120.

Hedley, C. 1918: A checklist of the marine fauna of New South Wales, part 1. Journal and Proceedings of the Royal Society of New South Wales 51, M1–M120.

Heilmann-Clausen, C. 1985: Dinoflagellate stratigraphy of the uppermost Danian to Ypresian in the Viborg 1 borehole, central Jylland, Denmark. Danmarks Geologiske Undersøgelse Serie A 7, 69 pp. https://doi.org/10.34194/seriea.v7.7026

Heilmann-Clausen, C. 1995: Palæogene aflejringer over danskekalken. In: Nielsen, O.B. (ed.): Danmarks geologi fra Kridt til i dag, 69–114. Aarhus: Geologisk Institut, Aarhus Universitet.

Heilmann-Clausen, C. 2006: Koralrev og lerhav, Palæogen. In: Larsen, G. (ed.): Naturen i Danmark, Geologien, 181–226. Copenhagen: Gyldendal.

Henderson, G., Rosenkrantz, A. & Schiener, E.J. 1976: Cretaceous-Tertiary sedimentary rocks of West Greenland. In: Escher, A. & Watt, W.S. (eds): Geology of Greenland, 341–362. Copenhagen: Geological Survey of Greenland.

Hjuler, M.L., Schovsbo, N.H., Pedersen, G.K. & Hopper, J.R. 2017: Potential hydrocarbon reservoirs of Albian–Paleocene age in the Nuussuaq Basin, West Greenland. Geological Survey of Denmark and Greenland Bulletin 38, 49–52. https://doi.org/10.34194/geusb.v38.4408

Jürgensen, T. & Mikkelsen, N. 1974: Coccoliths from volcanic sediments (Danian) in Nûgssuaq, West Greenland. Geological Society of Denmark Bulletin 23, 225–230.

Kase, T. 1984: Early Cretaceous marine and brackish-water Gastropoda from Japan. National Science Museum Monographs 1, 263 pp.

Kase, T. & Maeda, H. 1980: Early Cretaceous Gastropoda from the Choshi District, Chiba Prefecture, Central Japan. Transactions and Proceedings of the Palaeontological Society of Japan, New Series 118, 291–324.

King, C. 1994: Late Paleocene microfaunas of the Harre borehole (North Jylland, Denmark). In: Nielsen, O.B. (ed.): Lithostratigraphy and biostratigraphy of the Tertiary sequence from Harra Borehole, Denmark. Aarhus Geoscience 1, 65–72.

King, C. 2016: A revised correlation of Tertiary rocks of the British Isles and adjacent areas of NW Europe. Geological Society of London Special Report 27, 724 pp. https://doi.org/10.1144/sr27.15

Kollmann, H.A. 2005: Révision critique de la Paléontologie Française d'Alcide d'Orbigny Volume 3: Gastropodes Crétacés, 239 pp. Leiden: Backhuys Publishers. https://doi.org/10.1016/j.annpal.2007.06.001

Kollmann, H.A. & Peel, J.S. 1983: Paleocene gastropods from Nûgssuaq, West Greenland. Bulletin Grønlands Geologiske Undersøgelse 146, 1–115. https://doi.org/10.34194/bullggu.v146.6688

Krach, W. 1963: Mollusca of the Babica Clays (Paleocene) of the middle Carpathians. Part 1: Gastropoda. Studia Geologica Polonica 14, 128 pp.

Lamarck, J.-B. 1822: Histoire Naturelle des Animaux sans Vertèbres, Tome Sixième, 2me. Partie, 232 pp. Printed by the author, Paris. https://doi.org/10.1017/cbo9781139567442.005

Larsen, L.M., Pedersen, A.K, Tegner, C., Duncan, R.A., Hald, N. & Larsen, J.G. 2016: Age of Tertiary volcanic rocks on the West Greenland continental margin: volcanic evolution and event correlation to other parts of the North Atlantic Igneous Province. Geological Magazine 153, 487–511. https://doi.org/10.1017/s0016756815000515

Martini, E. 1971: Standard Tertiary and Quaternary calcareous nannoplankton zonation. In: Fainacci, A. (ed.): Proceedings of the II Planktonic Conference, Roma 1970, 739–785. Rome: Tecnoscienza.

Meek, F.B. 1864: Check list of invertebrate fossils of North America; Cretaceous and Jurassic. Smithsonian Miscellaneous Collection 7(177), 1–40. https://doi.org/10.5962/bhl.title.140016

Meek, F.B. 1876: A report on the invertebrate cretaceous and Tertiary Fossils of the upper Missouri country. Report of the United States Geological Survey of the Territories, Washington. Government Printing Office, vol. 9, 629 pp. https://doi.org/10.3133/70038959

Meek, F.B., & Hayden, F.V. 1856: Descriptions of new fossil species of Mollusca collected by Dr. F. V. Hayden, in Nebraska Territory; together with a complete catalogue of all the remains of invertebrata hitherto described and identified from the Cretaceous and Tertiary formations of that region. Proceedings of the National Academy of Sciences, Philadelphia 8, 265–286.

Meek, F.B. & Hayden, F.V. 1860: Descriptions of new organic remains from the Tertiary, Cretaceous and Jurassic rocks of Nebraska. Proceedings of the National Academy of Sciences of Philadelphia 12, 175–185.

Merle, D. & Pacaud, J.-M. 2004: New species of *Eocithara* Fischer, 1883 (Mollusca, Gastropoda, Harpidae) from the Early Paleogene with phylogenetic analysis of the Harpidae. Geodiversitas 26, 61–87. https://doi.org/10.5252/geodiversitas2020v42a29

Montes, M., Beamud, E., Nozal, F. & Satillana, S. 2019: Late Maastrichtian–Paleocene chronostratigraphy from Seymour Island (James Ross Basin, Antarctic Peninsula): Eustatic controls on sedimentation. Advances in Polar Science 30, 303–327. https://doi.org/10.13679/j.advps.2018.0045

Nøhr-Hansen, H. 1997a: Palynology of the boreholes GANE#1, GANK#1 and GANT#1, Nuussuaq, West Greenland. Danmarks og Grønlands Geologiske Undersøgelse Rapport 1997/89, 22 pp.

Nøhr-Hansen, H. 1997b: Palynology of the GRO#3 well, Nuussuaq, West Greenland. Danmarks og Grønlands Geologiske Undersøgelse Rapport 1997/151, 19 pp.

Nøhr-Hansen, H. & Dam, G. 1997: Palynology and sedimentology across a new marine Cretaceous–Tertiary boundary section on Nuussuaq, West Greenland. Geology 25, 851–854. https://doi.org/10.1130/0091-7613(1997)025<0851:pasaan>2.3.co;2

Nøhr-Hansen, H. & Heilmann-Clausen, C. 2000: *Cerodinium kangiliense* sp. nov. and *Senegalinium iterlaaense* sp. nov. two new, stratigraphic important Paleocene species from West Greenland and Denmark. Neues Jahrbuch für Paläontologie. Abhandlungen 219, 153–170. https://doi.org/10.1127/njgpa/219/2001/153

Nøhr-Hansen, H. & Sheldon, E. 2000: Palyno- and nannostratigraphic dating of the marine Paleocene succession in the Nuussuaq Basin, West Greenland. Geologiska Föreningens i Stockholm Förhandlinger 122, 115–116. https://doi.org/10.1080/11035890001221115

Nøhr-Hansen, H., Sheldon, E. & Dam, G. 2002: A new biostratigraphic scheme for the Paleocene onshore West Greenland and its implications for the timing of the pre-volcanic evolution. In: Jolley, D.W. & Bell, B.R. (eds): The North Atlantic Igneous Province: Stratigraphy, Tectonic, Volcanic and Magmatic Processes. Geological Society, London, Special Publications 197, 111–156. https://doi.org/10.1144/gsl.sp.2002.197.01.06

Pacaud, J.-M. & Schnetler, K.I., 1999: Revision of the gastropod family Pseudolividae from the Paleocene of West Greenland and Denmark. Bulletin of the Geological Society of Denmark 46, 53–67. https://doi.org/10.37570/bgsd-1999-46-06

Pan, H.-Z. 1977: Mesozoic and Cenozoic fossil Gastropoda from Yunnan. Mesozoic fossils from Yunnan 2, 83–152. Beijing: Science Press.

Pchelintsev, V.F. 1927: [The Jurassic and Lower Cretaceous fauna of the Crimea and the Caucasus]. Trudy eologicheskogo Komiteta Novaya seriya 172, 367 pp. [in Russian].

Pedersen, A.K., Larsen, L.M. & G.K. 2017: Lithostratigraphy, geology and geochemistry of the volcanic rocks of the Vaigat Formation on Disko and Nuussuaq, Paleocene of West Greenland. Geological Survey of Denmark and Greenland Bulletin 39, 244 pp. https://doi.org/10.34194/geusb.v39.4354

Pedersen, A.K., Larsen, L.M. & G.K. 2018: Lithostratigraphy, geology and geochemistry of the volcanic rocks of the Maligât Formation and associated intrusions on Disko and Nuussuaq,

Paleocene of West Greenland. Geological Survey of Denmark and Greenland Bulletin 40, 239 pp. https://doi.org/10.34194/geusb.v40.4326

Perch-Nielsen, K. 1973: Danian/Maastrichtian coccoliths from Nûgssuaq, West Greenland. Bulletin of the Geological Society of Denmark 22, 79–82.

Perch-Nielsen, K. 1979: Calcareous nannofossil zonation at the Cretaceous/Tertiary boundary in Denmark. In: Birkelund, T. & Bromley, R.G. (eds): Proceedings Cretaceous–Tertiary Boundary Events Symposium, vol. 1, 115–135. Copenhagen University. https://doi.org/10.1111/let.1979.12.2.188

Pedersen, A.K., Larsen, L.M., Pedersen, G.K. & Dueholm, K.S. 2006: Five slices through the Nuussuaq Basin, West Greenland. Geological Survey of Greenland and Denmark Bulletin 10, 53–56. https://doi.org/10.34194/geusb.v10.4909

Petersen, G.H. & Vedelsby, A. 2000: An illustrated catalogue of the Paleocene Bivalvia from Nuussuaq, Northwest Greenland: Their paleoenvironments and the paleoclimate. Steenstrupia 25, 25–120.

Piasecki, S., Larsen, L.M., Pedersen, A.K. & Pedersen, G.K. 1992: Palynostratigraphy of the Lower Tertiary volcanics and marine clastic sediments in the southern part of West Greenland Basin: implications for the timing and duration of the volcanism. Rapport Grønlands Geologiske Undersøgelse 154, 13–31. https://doi.org/10.34194/rapggu.v154.8166

Récluz, C.A. 1845 [October]: Monographie du genre *Narica*. Magasin de Zoologie, ser. 2, 7, 72 pp.

Riisager, P. & Abrahamsen, N. 1999: Magnetostratigraphy of Palaeocene basalts from the Vaigat Formation of West Greenland. Geophysical Journal International 137, 774–782. https://doi.org/10.1046/j.1365-246x.1999.00830.x

Rosenkrantz, A. 1970: Marine Upper Cretaceous and lowermost Tertiary deposits in West Greenland. Meddelelser fra Dansk Geologisk Forening 19, 406–453.

Rosenkrantz, A., Münther, V. & Henderson, G. 1974: Geological map of Greenland, 1:100 000, Agatdal, 70 V.1 Nord. Copenhagen: Geological Survey of Greenland.

Sacco, F. 1890: I molluschi dei terreni terziarii del Piemonte e della Liguria. Parte VIII. Galeodoliidae, Doliidae, Ficulidae, Naticidae. Bollettino dei Musei di Zoologia ed Anatomia comparata della R. Universita di Torino. 5, 22–43. https://doi.org/10.5962/bhl.part.27225

Schnetler, K.I. & Nielsen, M.S. 2018: A Palaeocene (Selandian) molluscan fauna from boulders of Kerteminde Marl in the gravel-pit at Gundstrup, Fyn, Denmark. Cainozoic Research 18, 3–81.

Schnetler, K.I. & Petit, R.E. 2010: Revision of the gastropod family Cancellariidae from the Paleocene of Nuussuaq, West Greenland. Cainozoic Research 7, 3–26.

Schnetler, K.I., Lozouet, P. & Pacaud, J.-M. 2001: Revision of the gastropod family Scissurellidae from the Middle Danian (Paleocene) of Denmark. Bulletin of the Geological Society of Denmark 48, 79–90. https://doi.org/10.37570/bgsd-2001-48-04

Sheldon, E. 2003: New nannofossil dating of the initial Early Paleocene volcanism in Nuussuaq, central West Greenland. Courier Forschungs-Institut Senckenberg 244, 37–45.

SILASTIC® 9161 RTV Silicone Elastomer, product information sheet: http://docs-europe.electrocomponents.com/webdocs/114b/0900766b8114b68a.pdf.

Sohl, N.F. 1967: Upper Cretaceous gastropods from the Pierre Shale at Red Bird, Wyoming. U.S. Geological Survey Professional Paper 393B, 1–46. https://doi.org/10.3133/pp393b

Sørensen, E.V., Hopper, J.R., Pedersen, G.K., Nøhr-Hansen, H., Guarnieri, P., Pedersen, A.K. & Christiansen, F.G. 2017: Inversion structures as potential petroleum exploration targets on Nuussuaq and Northern Disko, onshore West Greenland. Geological Survey of Denmark and Greenland Bulletin 38, 45–48. https://doi.org/10.34194/geusb.v38.4406

Sorgenfrei, Th. & Buch, A. 1964: Deep tests in Denmark 1935-1959. Danmarks Geologiske Undersøgelser III Række 36, 146 pp. https://doi.org/10.34194/raekke3.v36.6941

Stanton, T.W. 1901: Volume IV, Palaeontology I, part I, The marine Cretaceous Invertebrates. In: Scott, W.B. (ed.): Reports of the Princeton University Expeditions to Patagonia, 1896–1899, J.B. Hatcher in charge. The University of Princeton, Princeton and Schweizerbart'sche, Sttutgart p. 1–43. https://doi.org/10.5962/bhl.title.12486

Stilwell, J.D. & Henderson, R.A. 2002: Description and paleobiogeographic significance of a rare Cenomanian molluscan faunule from Bathurst Island, Northern Australia. Journal of Paleontology 76, 447–471. https://doi.org/10.1666/0022-3360(2002)076<0447:dapsoa>2.0.co;2

Stilwell, J.D., Zinsmeister, W.J. & Oleinik, A.E. 2004: Early Paleocene mollusks of Antarctica: Systematics, paleoecology and paleobiogeographic significance. Bulletins of American Paleontology 367, 89 pp.

Thomsen, E. 1994: Calcareous nannofossil stratigraphy across the Danian-Selandian boundary in Denmark. GFF 116, 65–67. https://doi.org/10.1080/11035899409546160

Thomsen, E. 1995: Kalk og kridt i den danske undergrund. In: Nielsen, O.B. (ed.): Danmarks geologi fra Kridt til i dag, 32–67. Aarhus: Geologisk Institut, Aarhus Universitet.

Thomson, M.R.A. 1971: Gastropoda from the Lower Cretaceous sediments of south-eastern Alexander Island. British Antarctic Survey Bulletin 25, 45–58.

Trautschold, H. 1866: Zur Fauna des russischen Jura. Bulletin de la Societé Impériale des Naturalistes de Moscou 39, 1–24. https://doi.org/10.1515/9783112371701-059

Wenz, W. 1938–1944: Gastropoda, Teil I: Allgemeiner Teil und Prosobranchia. In: Schindewolf, O.H. (ed.): Handbuch der Paläozoologie, Band 6, 1639 pp. Berlin: G. Bornträger. https://doi.org/10.1017/s0016756800072459

White, C.A. 1889: On invertebrate fossils from the Pacific coast. Bulletin of the United States Geological Survey 51, 9–63. https://doi.org/10.3133/b51

Wilckens, O. 1910: Die Anneliden, Bivalven und Gastropoden der Antarktischen Kredieformation. Wissenschaftliche Ergebnisse der Schwedischen Südpolar-Expedition, 1901–1903, 3(12), 42 pp. https://doi.org/10.5962/bhl.title.6756

The K–T boundary strata north of Korsnæb, Stevns Klint, Denmark – evolution and geometry revealed in a long, horizontal profile

ALFRED ROSENKRANTZ †, FINN SURLYK*, KRESTEN ANDERSKOUV, PETER FRYKMAN, LARS STEMMERIK & NICOLAS THIBAULT

A 460 m long profile of the Cretaceous–Paleogene (K–T) boundary strata at Stevns Klint was measured by the late Professor A. Rosenkrantz probably in 1944. The measured profile was inherited by Finn Surlyk around 1974 together with other original boundary data. This material was dug up in a long-forgotten drawer in connection with detailed field work by the co-authors on the boundary succession in the late spring and summer of 2021. The profile illustrates the stratigraphy, geometry and palaeotopography of the boundary strata in unprecedented detail. The part of the cliff illustrated in the profile is today partly covered by beach ridges composed of flint rubble but is situated below the finest section of the lower Danian bryozoan mounds exposed at Stevns Klint. This coastal section is situated immediately adjacent to a large limestone quarry and was planned to be quarried away around 1937, but was saved by A. Rosenkrantz who demonstrated its great scientific and educational value to the authorities.

Alfred Rosenkrantz †
Finn Surlyk [finns@ign.ku.dk], Department of Geosciences and Natural Resource Management, University of Copenhagen, Øster Voldgade 10, DK-1350 Copenhagen K, Denmark. Kresten Anderskouv [ka@ign.ku.dk], Department of Geosciences and Natural Resource Management, University of Copenhagen, Øster Voldgade 10, DK-1350 Copenhagen K, Denmark. Peter Frykman [pfr@geus.dk], GEUS, Øster Voldgade 10, DK-1350 Copenhagen K, Denmark. Lars Stemmerik [ls@geus.dk], GEUS, Øster Voldgade 10, DK-1350 Copenhagen K, Denmark. Nicolas Thibault [nt@ign.ku.dk], Department of Geosciences and Natural Resource Management, University of Copenhagen, Øster Voldgade 10, DK-1350 Copenhagen K, Denmark.

† Deceased 1974

Corresponding author: Finn Surlyk

A full description, including a new lithostratigraphy of the Maastrichtian–Danian succession exposed in the 14.5 km long coastal cliff, Stevns Klint (Fig. 1) based on stereo-photogrammetric mapping was provided by Surlyk *et al.* (2006). The nature of the Cretaceous–Paleogene (K–T, K–Pg) boundary which is well exposed in the cliff has a long history of investigation. The boundary succession is rather complex partly due to the development of low bryozoan chalk mounds in the uppermost Maastrichtian Højerup Member. The boundary clay, the Fiskeler Member was only deposited in the small basins between the mounds. It passes upwards into the Cerithium Limestone Member and an erosion surface truncates the top of the Cerithium Limestone and the intervening crests of the Maastrichtian mounds. The layers beneath the erosion

surface were lithified to form a complex hardground, comprising the Cerithium Limestone and the top of the Maastrichtian mounds. The true stratigraphic nature of the boundary was first unravelled in a short, seminal paper by Alfred Rosenkrantz in 1924, who in contrast to previous workers distinguished carefully between lithified topmost Maastrichtian and similarly lithified lowermost Danian Cerithium Limestone during fossil collection. He discovered that the two superficially similar rock types contained remarkably different faunas (e.g. Rosenkrantz 1939, 1966) – an early indication of the K–T boundary mass extinction, first clearly recognized many years later (e.g. Alvarez *et al.* 1980, 1984a, b, c and references therein).

A field sketch book inherited by FS after the death of A. Rosenkrantz in 1974 was dug up in a long-forgot-
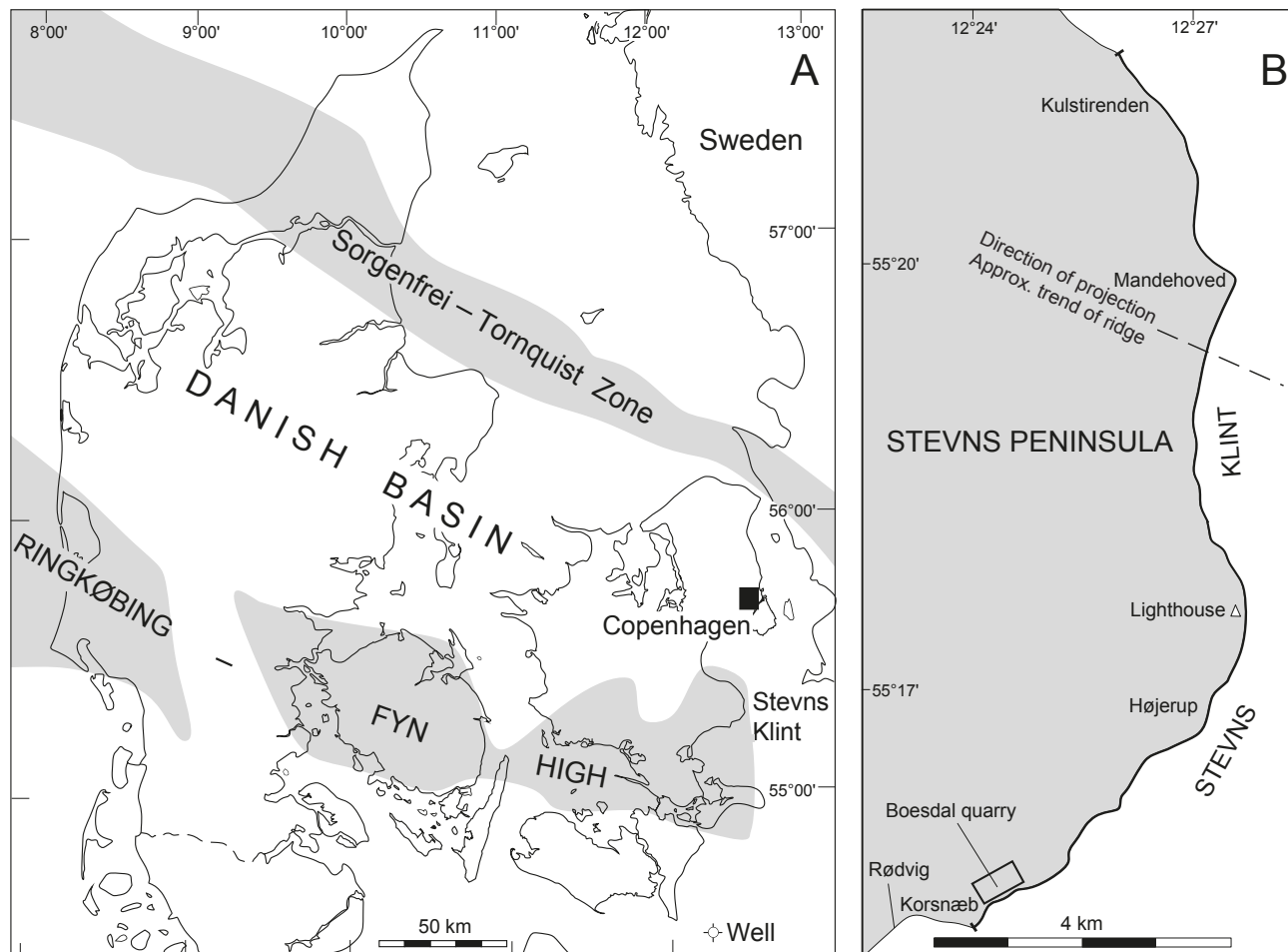
Fig. 1. A: Map of Denmark, showing the major structural elements. From Lykke-Andersen & Surlyk (2004) and Surlyk *et al.* (2006). B. Map of the Stevns peninsula showing important localities along the cliff. The profile measured by Rosenkrantz was measured along the cliff N of Korsnæb. Dashed line indicates the approximate orientation of late Maastrichtian sea floor ridges and valleys identified on seismic data by Lykke-Andersen & Surlyk (2004) and shown in cross section in figure 6.
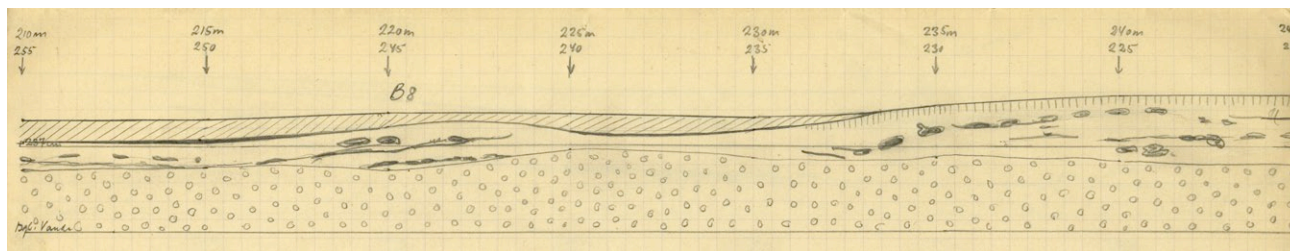
Fig. 2. Example of part of the profile measured by A. Rosenkrantz, probably in 1944.

ten drawer in connection with detailed field work on the boundary strata by the co-authors of to this article (Fig. 2). It contains a 460 m long horizontal profile of the boundary strata measured in great detail by A. Rosenkrantz in a stretch of the cliff from Korsnæb and farther north (Figs 1, 3). It is not indicated in the note book when the profile was measured but the best guess is 1944 where a large block indicated on the profile was excavated for exhibition at the Geological Museum of the University of Copenhagen. Today, the boundary strata are mostly covered by beach ridges composed of flint rubble along the measured stretch of the cliff. The succession is overlain by some of the most well exposed, and easily accessible lower Danian bryozoan mounds exposed along the 14.5 km long cliff (Surlyk 1997) and is visited by numerous researchers, student field trips, amateur palaeontologists and tourists every year. This coastal exposure is situated immediately adjacent to the large Boesdal limestone quarry, and it was only through a thorough demonstration to the authorities by A. Rosenkrantz of the great scientific value of the profile that it was saved from being quarried away.

Stevns Klint became a UNESCO World Heritage Site in 2014 (Damholt & Surlyk 2012), and the exhibition centre highlighting the significance of the boundary strata is at the time of writing under construction in the now abandoned quarry.

The boundary succession has been studied by a large number of workers focusing on foraminifers (Schmitz *et al.* 1992; Hart *et al.* 2005; Rasmussen *et al.* 2005), organic-walled dinocysts (Hansen 1977, 1979; Kjellström & Hansen 1981; FitzPatrick *et al.* 2018), calcareous dinocysts (Leighton *et al.* 2011), coccoliths (Thomsen 1975; Perch-Nielsen 1979a, b, c), bivalves (Heinberg 1976, 1978, 1979a, b, 1989, 1993, 1999b),
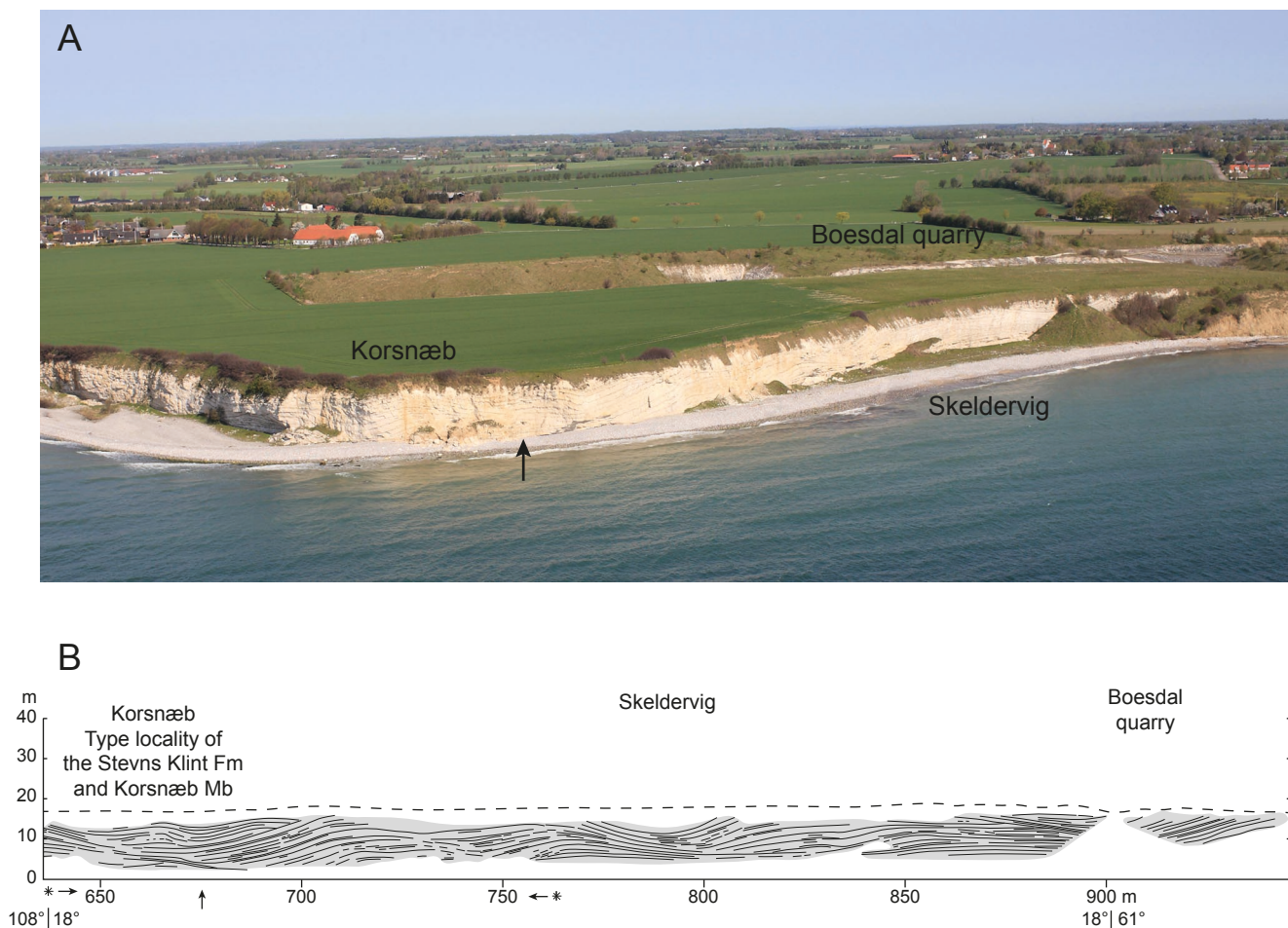
Fig. 3. A: Aerial photograph of the southern part of Stevns Klint showing the position of Korsnæb and the bay Skeldervig where the profile shown in figures 5–7 was measured by A. Rosenkrantz, probably in 1944. The 0 m starting point of the profile is immediately below the word 'Korsnæb'. The K–T boundary strata are exposed at the arrow. It is mainly covered by the beach ridge in the rest of the profile. Photo from Pedersen (2011). B: Photogrammetric profile of the part of Stevns Klint where the profile was measured. The southern starting point indicated with an arrow. The profile extends northwards over 460 m, but northern end of the profile is today covered by scree or quarried away.

gastropods (Hansen 2019), brachiopods Surlyk (1979, 1984), ammonites (Birkelund 1993; Surlyk & Nielsen 1999; Machalski & Heinberg 2005), trace fossils (Ekdale & Bromley 1984), inorganic geochemistry including stable isotopes (Christensen *et al.* 1973; Alvarez *et al.* 1980; Schmitz 1985; Schmitz *et al.* 1988, 1992; Elliot *et al.* 1989; Frei & Frei 2002; Hart *et al.* 2004; Drits *et al.* 2004; Gilleaudeau *et al.* 2018) and organic geochemistry (Sepúlveda *et al.* 2009). However, it is remarkable that only very few precise and detailed sections through the succession have been published. Many are misleading or outright wrong and Rosenkrantz' old profile and sections are in our opinion the most precise yet produced and records the nature of the K–T boundary over a long stretch of the cliff in unprecedented detail.

We have thus felt it highly relevant and timely to publish Rosenkrantz' old profile documented with photographs and comments.

Geological setting and stratigraphy

The coastal cliff, Stevns Klint is 14.5 km long, up to 41 m high, and roughly N–S-oriented with an E–W-bend at the southern end from Rødvig to Korsnæb. It is situated over the eastern end of the Ringkøbing–Fyn High which forms the southern border of the Danish Basin (Fig. 1). It was described and illustrated along its length based on stereo-photogrammetric mapping accompanied by a new lithostratigraphic subdivision by Surlyk *et al.* (2006). The Tor Formation of that paper was subsequently changed to the Møns Klint Formation based on a fully cored borehole by Surlyk *et al.* (2013). The stratigraphic evolution across the K–T boundary was unravelled by Rosenkrantz (1924). A detailed subdivision of the boundary clay, the Fiskeler Member of the Rødvig Formation was first established by Christensen *et al.* (1973). Sequence stratigraphic analyses of the succession were presented first by Thomsen (1995) and in more detail by Surlyk (1997).

The succession exposed in the cliff encompasses the following units and key surfaces from below (Figs 4–6; Surlyk 1997; Surlyk *et al.* 2006, 2013):

1. Gently mound-bedded upper Maastrichtian chalk (Surlyk *et al.* 2006; Anderskouv *et al.* 2007), passing upwards into horizontally bedded chalk, both belonging to the Sigerslev Member (Møns Klint Formation) with about 32 m exposed in the cliff.

3. Two incipient hardgrounds 10–25 cm apart, the upper one defining the top of the Sigerslev Member. A prominent band of large black flint nodules occurs 30–50 cm below the upper hardground and forms a

clearly visible marker bed along the whole length of the cliff.

4. Up to 4–5 m of bryozoan chalk deposited in low, asymmetric mounds forming the uppermost Maastrichtian Højerup Member, Møns Klint Formation (Svendsen 1975; Surlyk 1997; Larsen & Håkansson 2000). The member thins towards the north and is only about 1 m thick at Kulstirenden at the northern end of the cliff (Fig. 1B).

5. The basal Danian Fiskeler Member (Rødvig Formation) is a mainly 5–10 cm thick clay-marl layer, comprising at least three sublayers (Christensen *et al.* 1973; Ekdale & Bromley 1984; Surlyk *et al.* 2006). It reaches a maximum thickness of 30–45 cm to the north at Kulstirenden. The sublayer of black clay at the base contains the famous iridium anomaly discovered by Alvarez *et al.* (1980). The Fiskeler Member is restricted to the central parts of the basins between the mound crests of the Højerup Member and wedges out towards the basin margins.

Chrono-strati-graphy		Lithostratigraphy			Biostratigraphy		
					Foraminifers	Nannofossils	
					(Rasmussen *et al.* 2005; Stenestad 1979)	(Perch-Nielsen 1979a, b)	(Thomsen 1995)
Palaeogene	Danian		Stevns Klint Fm	Korsnæb Mb	P1c	D4	
		Chalk Group				D3	3
					P1b	D2	2
			Rødvig Fm	Cerithium Limestone Mb	P1a	D1	1
					Pα		
				Fiskeler Mb	P0		
Cretaceous	Maastrichtian		Møns Klint Fm	Højerup Mb	*Stensioeina esnehensis*	*Nephrolithus frequens*	
				Sigerslev Mb	*Pseudotextularia elegans*		

Fig. 4. Stratigraphic scheme of the Cretaceous–Paleogene (K–T) boundary strata at Stevns Klint. The profile measured by A. Rosenkrantz (Fig. 5) includes the top of the Højerup Member, the Rødvig Formation and the lowermost Korsnæb Member. NP 1–4 are standard nannoplankton zones, whereas coccolith zones 1–3 are local zones of Thomsen (1995).

6. The Fiskeler Member passes gradationally or in some case abruptly upwards into the partly cemented, strongly burrowed and up to mainly 30–60 cm thick lower Danian Cerithium Limestone Member, which, however, reaches 80 cm at some basins north of Rødvig and 120 cm at Kulstirenden (Hart *et al.* 2005; Surlyk *et al.* 2006). It oversteps the Fiskeler along the margins of the basins and onlap the basin margins along a shallow-dipping disconformity, separating it from the top of the Højerup Member.

7. The Cerithium Limestone and the intervening cemented crests of the topmost Maastrichtian mounds of the Højerup Member are truncated by a prominent erosion surface along the length of the cliff. The complex hardground topped by the erosion surface is double at the northernmost locality, Kulstirenden where a second minor hardground occurs about 10 cm above the main hardground (probably first recognised by C. Heinberg, quoted by Hart *et al.* (2005) as Heinberg (1999a) but not mentioned in the latter publication). The position of the erosion surface varies from about 5 m below to about 30 m above present-day sea level and forms a series of highs and lows which were earlier interpreted to represent anticlines and synclines formed by post-depositional folding (Rosenkrantz 1937). However, seismic data clearly show that the wavy relief represents the original sea-floor topography formed by persistent WNW-flowing bottom currents (Lykke-Andersen & Surlyk 2004; Surlyk & Lykke-Andersen 2007).

8. The top Cerithium Limestone hardground forms the basis for the growth of prominent lower Danian

bryozoan mounds of the Korsnæb Member, Stevns Klint Formation (Figs 3B, 5, 6A) (e.g. Surlyk 1997; Surlyk *et al.* 2006; Bjerager & Surlyk 2007a, b).

Rosenkrantz' profile from Stevns Klint

A detailed 460 m long horizontal profile was measured by Alfred Rosenkrantz probably in 1944 from just north of Korsnæb and northwards along the bay, Skeldervig (Figs 1, 3, 7, 8). Stratigraphically, the profile comprises up to 5 m of Maastrichtian chalk (top Sigerslev Member overlain by the Højerup Member), measured from the daily mean sea level and upwards, but the lowest metres were covered by flint rubble at the time when the profile was measured. The exposed chalk belongs to the mound-bedded, bryozoan-rich Højerup Member. Up to three bands of large black flint nodules occur in the chalk and outlines the mounded geometries of the bryozoan chalk. The upper nodule band is the most prominent and is situated about 1 m below the top Cerithium Limestone erosion surface. In addition, scattered thin sheet flints occur along the length of the profile. The Højerup Member is overlain by the Fiskeler Member, the Cerithium Limestone Member and the lowest metre or so of the Korsnæb Member. The profile includes a total of 13 Fiskeler–Cerithium Limestone basins (B1–13; Fig. 7).

One of the basins, B7 was truncated along the basin margin where the Fiskeler is absent and only Ce-
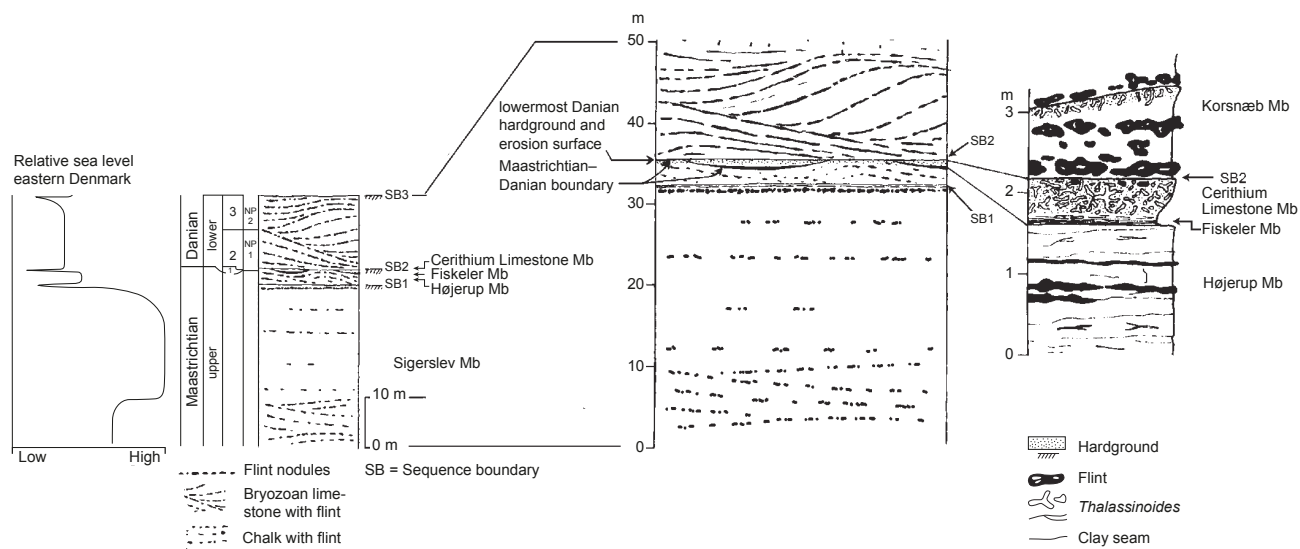

Fig. 5. Schematic sections showing the stratigraphic evolution, sequence boundaries and interpreted relative sea-level curve across the Maastrichtian–Danian boundary at Stevns Klint. The indicated sequence boundaries (SB1–3) are marked by erosion caused by relative sea-level falls. Partly after Surlyk (1997).
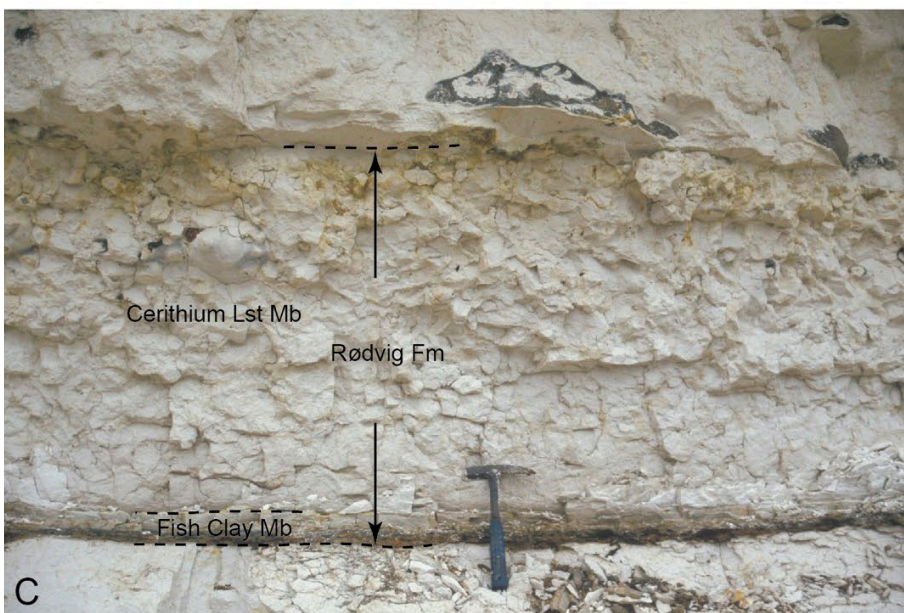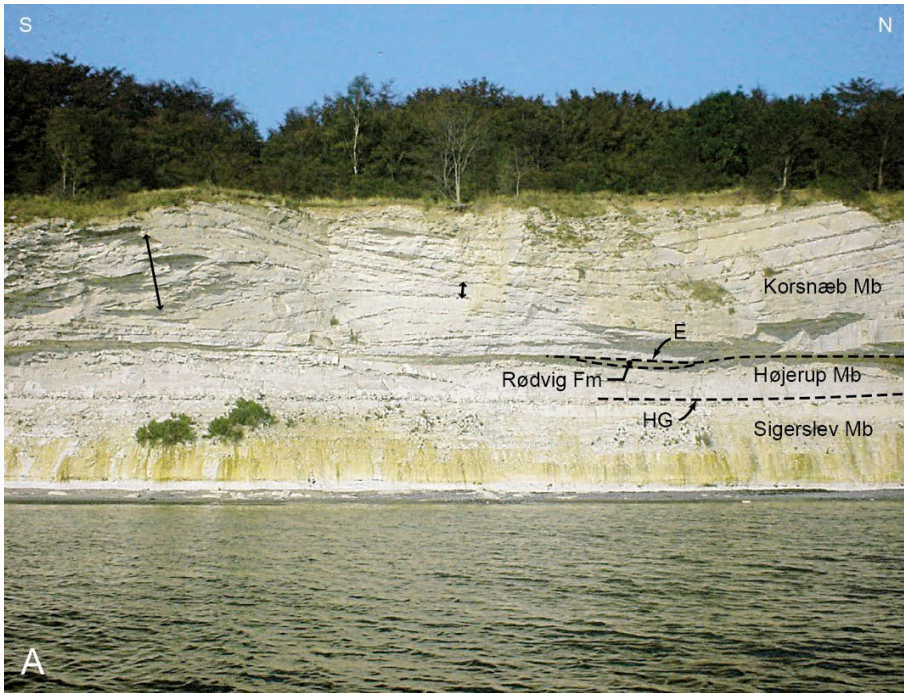
Fig. 6. Photographs of the K–T boundary strata at Stevns Klint (Fig. 1B). **A:** Cliff section showing the stratigraphic units across the K–T boundary north of the old church at Højerup. The Rødvig Formation was deposited in small basins formed between the mound crests of the uppermost Maastrichtian Højerup Member, and includes the lowermost Danian Fiskeler Member overlain by the Cerithium Limestone Member. E indicates the top Cerithium Limestone erosion surface. **B:** The boundary strata immediately south of the old church. Note that the Fiskeler Member wedges out towards the margins of the small basin. **C:** Type locality of the Rødvig Formation west of Korsnæb (Figs 1B, 3) immediately west of the profile measured by A. Rosenkrantz (Fig. 5). The yellow stained top of the Rødvig Formation is the top Cerithium Limestone hardground. Hammer is 33 cm long.
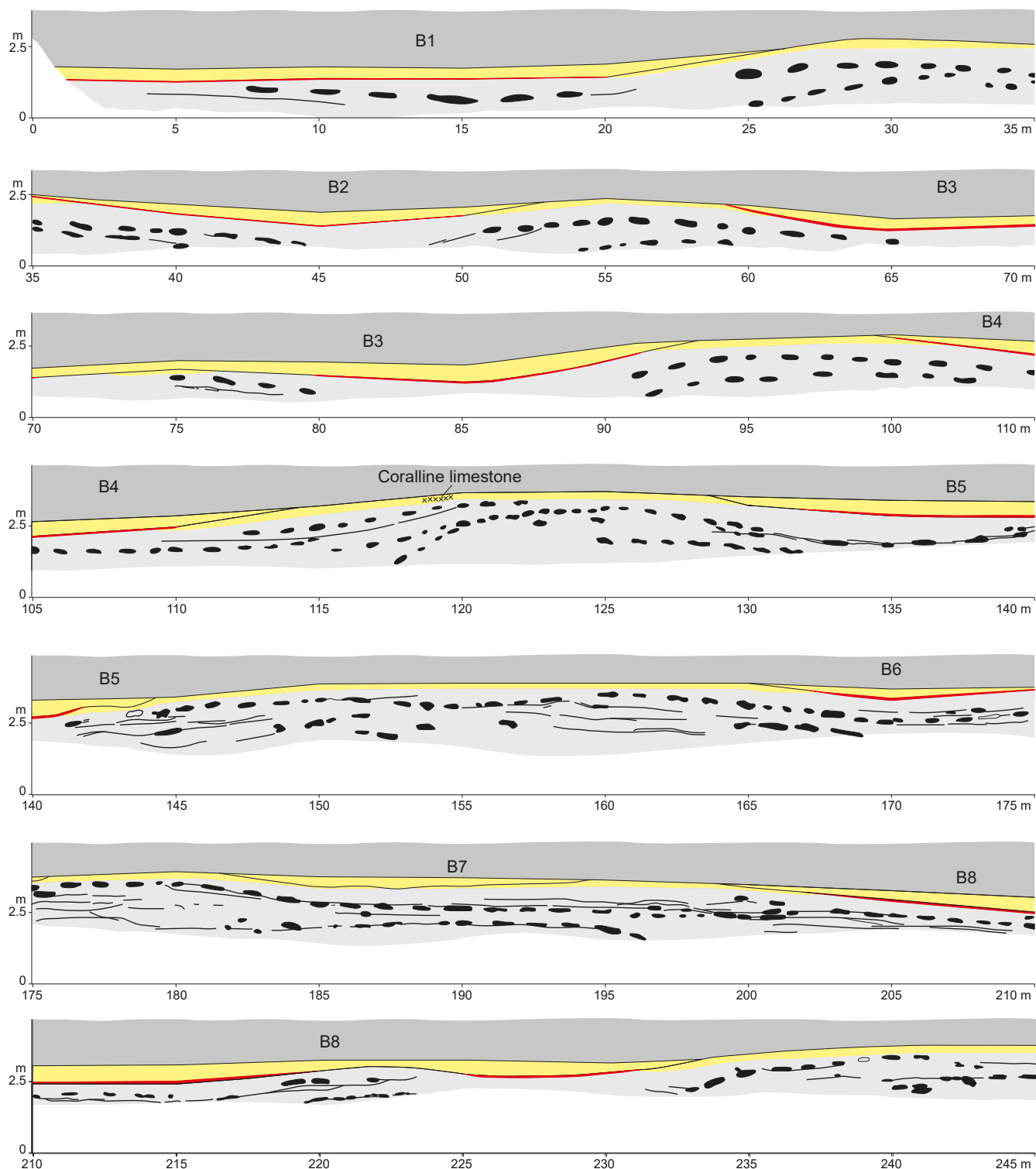
▲▼ Fig. 7. The 460 m long horizontal profile measured by A. Rosenkrantz, probably in 1944 in the area from Korsnæb and northwards along the Skeldervig bay (Fig. 1B). The complex hardground (yellow signature) includes the lithified lower Danian Cerithium Limestone and the intervening crests of the mounds in the uppermost Maastrichtian Højerup Member. The erosion surface topping the hardground has a slightly wavy geometry, being lower over the Cerithium Limestone than over the adjacent top Maastrichtian mounds, partly reflecting compaction of the Fiskeler Member.
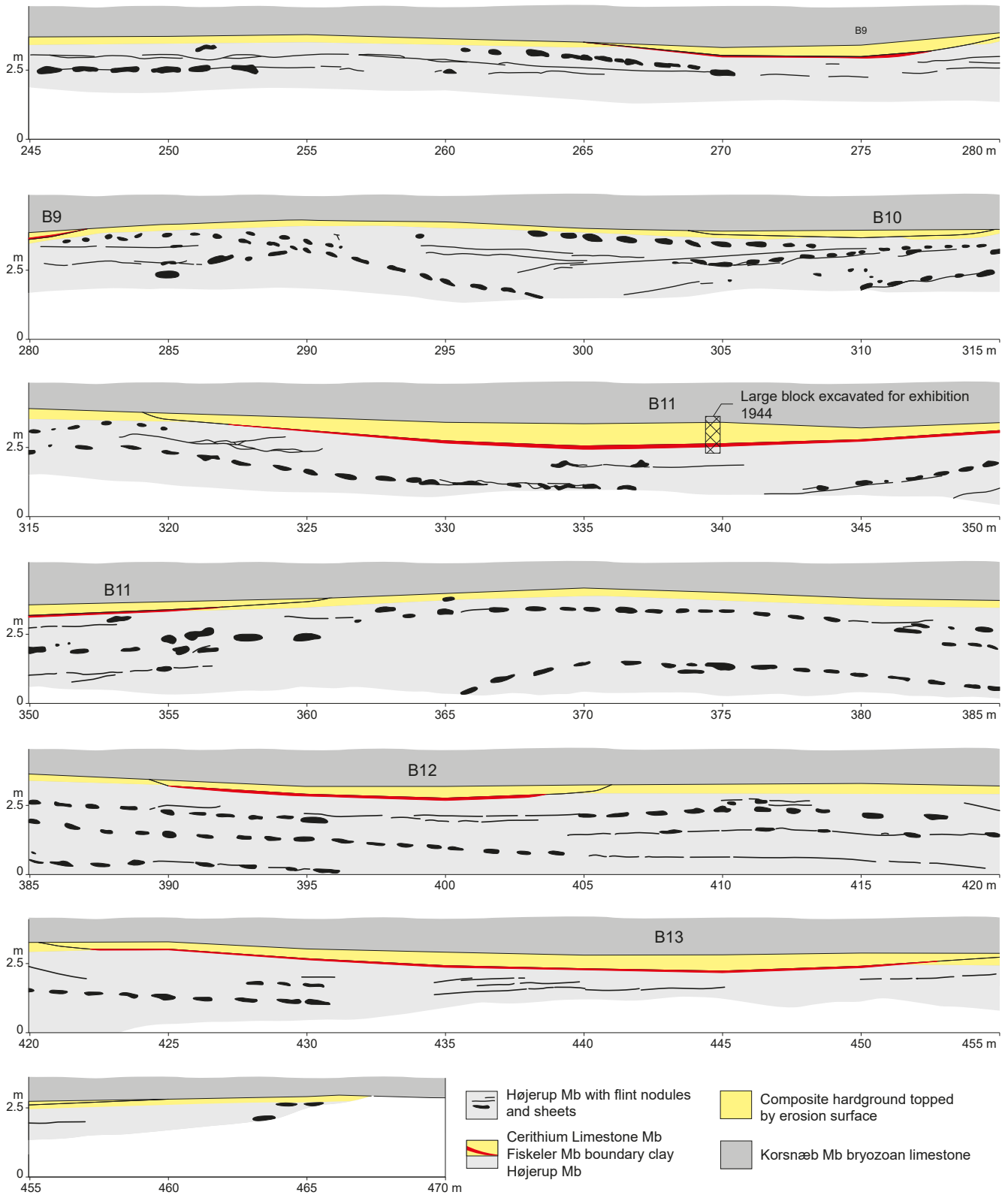
Fig. 7. Continued from previous page.
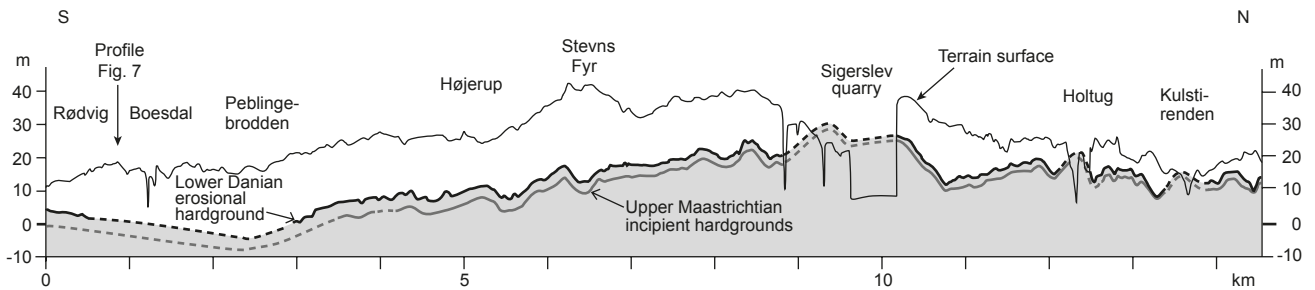
Fig. 8. Profile of Stevns Klint showing the present-day land surface and the position of top Cerithium Limestone erosion surface. The location of the profile described here (Fig. 7) is indicated with an arrow. Modified from Surlyk *et al.* (2006).

rithium Limestone is exposed in this section. Another basin, B8 is subdivided into two sub-basins by a low bryozoan mound, which probably was cut laterally to the culmination of the crest.

The height of the base of the Fiskeler varies between 1.3 and 2.5 m above daily sea level and the top of the erosion surface truncating the Cerithium Limestone and the top of the Maastrichtian mounds varies in height between 1.8 and 3.9 m. The erosion surface reaches its lowest position at 1.8 m above sea level at the 5 m mark at the southern start of the profile and the highest at the 370 m mark in the northern end (Fig. 7). It is in general situated at a lower level above the Cerithium Limestone than above the bryozoan chalk of the Højerup Member, probably reflecting the greater erodibility of the Cerithium Limestone than the cemented crests of the Maastrichtian chalk mounds and compaction of the Fiskeler Member. The amplitude of the erosion surface reaches 2.1 m even over the relatively short distance of 460 m. This should be compared with the maximum amplitude of about 35 m along the 14.5 km long cliff as seen in the long profile of Surlyk *et al.* (2006). The erosion surface in the present profile occupies a position close to the main valley formed by bottom currents in the top Maastrichtian chalk surface (Fig. 8). The profile of Rosenkranz (Fig. 7) thus illustrates important aspects of the K–T boundary at Stevns Klint and is in our opinion the most detailed section measured at the whole length of the cliff. It is thus not only of historical interest but shows the nature of the boundary over a long stretch in unprecedented detail.

Conclusions

- A detailed, 460 m long profile covering the K–T boundary strata north of Korsnæb in the southern part of Stevns Klint was measured by the late Alfred Rosenkrantz probably in 1944.

- The boundary strata include mounded bryozoan chalk of the uppermost Maastrichtian Højerup Member, the lowermost Danian Fiskeler and Cerithium Limestone Members and the mounded bryozoan limestone of the lower Danian Korsnæb Member.
- The profile shows 13 Fiskeler basins and intervening cemented mound crests of the Højerup Member.
- One basin is exposed in a basin margin position, where the Fiskeler is absent and the section thus only exposes the Cerithium Limestone.
- Another basin is double as it is subdivided into two by a mound which appears to have been cut marginal to the crest in the measured profile.
- The amplitude of the erosion surface truncating the Cerithium Limestone and the intervening mound crests is 2.1 m with the lowest position at the southern end of the profile.
- The erosion surface cuts deeper into the Cerithium Limestone than over the Højerup Member.
- The amplitude of the erosion surface along the whole 14.5 km length of the cliff is about 35 m, reflecting the action of a persistent WNW-flowing bottom current system which sculpted the top Maastrichtian surface into large valleys and ridges.
- The profile occupies a position in the deepest valley formed by late Maastrichtian bottom currents.

Acknowledgements

References

Anderskouv, K., Damholt, T. & Surlyk, F. 2007: Late Maastrichtian chalk mounds, Stevns Klint, Denmark—combined physical and biogenic structures. Sedimentary Geology 200, 57–72. https://doi.org/10.1016/j.sedgeo.2007.03.005

Alvarez, L.W., Alvarez, W., Asaro, F. & Michel, H.V. 1980: Extraterrestrial cause for the Cretaceous–Tertiary extinction. Science 208, 1095–1108. https://doi.org/10.1126/science.208.4448.1095

Alvarez, W., Alvarez, L.W., Asaro, F. & Michel, H.V. 1984a: The end of the Cretaceous: Sharp boundary or gradual transition? Science 223, 1183–1186. https://doi.org/10.1126/science.223.4641.1183

Birkelund, T. 1979: The last Maastrichtian ammonites. In: Birkelund, T. & Bromley, R.G: (eds): Cretaceous–Tertiary boundary events. I. The Maastrichtian and Danian of Denmark, 51–57. Copenhagen: University of Copenhagen.

Birkelund, T. 1993: Ammonites form the Maastrichtian White Chalk of Denmark. Bulletin of the Geological Society of Denmark 40, 33–81. https://doi.org/10.37570/bgsd-1994-40-02

Bjerager, M. & Surlyk, F. 2007a: Danian cool-water bryozoan mounds at Stevns Klint, Denmark – a new class of noncemented skeletal mounds. Journal of Sedimentary Research 77, 634–660. https://doi.org/10.2110/jsr.2007.064

Bjerager, M. & Surlyk, F. 2007b: Benthic palaeoecology of Danian deep-shelf bryozoan mounds in the Danish Basin. Palaeogeography, Palaeoclimatology, Palaeoecology 250, 184–215. https://doi.org/10.1016/j.palaeo.2007.03.008

Christensen, L., Fregerslev, S., Simonsen, A. & Thiede, J. 1973: Sedimentology and depositional environment of lower Danian Fish Clay from Stevns Klint, Denmark. Bulletin of the Geological Society of Denmark 2, 193–212.

Damholt, T. & Surlyk, F. 2012. Nomination of Stevns Klint for inclusion in the World Heritage List, 160 pp. St. Heddinge: Østsjællands Museum.

Drits, V.A., Lindgreen, H., Sakharov, B.A., Jakobsen, H.J. & Zviagina, B.B. 2004: The detailed structure and origin of clay minerals at the Cretaceous/Tertiary boundary in Denmark; implications for the causes of the terminal Cretaceous extinction. Journal of Sedimentary Research 54, 681–703.

Ekdale, A.A. & Bromley, R.G. 1984: Sedimentology and ichnology of the Cretaceous–Tertiary boundary in Denmark: Implications for the causes of the terminal Cretaceous extinction. Journal of Sedimentary Petrology 54, 3, 681–703. https://doi.org/10.1306/212F84D6-2B24-11D7-8648000102C1865D

Elliot, W.C., Aronson, J.L., Millard, H.T. & Gierlowski-Kordesch, E. 1989: The origin of the clay minerals at the Cretaceous/Tertiary boundary in Denmark. Geological Society of America Bulletin 101, 702–710. https://doi.org/10.1130/0016-606(1989)101<0702:TOOTCM>2.3.CO;2

FitzPatrick, M.E.J., Forber, D.A. & Hart, M.B. 2018: Dinocyst stratigraphy and palaeoenvironmental of the Cretaceous/Paleogene boundary at Stevns Klint, Denmark. Cretaceous Research 87, 408–421. https://doi.org/10.1016/j.cretres.2017.09.001

Frei, R. & Frei, K.M. 2002: A multi-isotopic and trace element investigation of the Cretaceous–Tertiary boundary layer at Stevns Klint, Denmark; inferences for the origin and nature of siderophile and lithophile element geochemical anomalies. Earth and Planetary Science Letters 203, 691–708. https://doi.org/10.1016/S0012-821X(02)00865-8

Gilleaudeau, G.J., Voegelin, A.R., Thibault, N., Moreau, J., Ullman, C.V., Klaebe, R.M., Korte, C. & Frei, R. 2018: Stable isotope records across the Cretaceous–Paleogene transition, Stevns Klint, Denmark: New insights from the chromium isotope system. Geochimica et Cosmochimica Acta 235, 305–332. https://doi.org/10.1016/j.gca.2018.04.028

Hansen, J.M. 1977: Dinoflagellate stratigraphy and echinoid distribution in Upper Maastrichtian and Danian deposits from Denmark. Bulletin of the Geological Society of Denmark 26, 1–26.

Hansen, J.M. 1979: Dinoflagellate zonation around the boundary. In: Birkelund, T. & Bromley, R.G: (eds): Cretaceous–Tertiary boundary events. I. The Maastrichtian and Danian of Denmark, 136–141. Copenhagen: University of Copenhagen.

Hansen, T. 2019: Gastropods from the Cretaceous-Palaeogene boundary in Denmark. Zootaxa 4654, 1–196. https://doi.org/10.11646/zootaxa.4654.1.1

Hart, M.B., Feist, S.E., Price, G.D. & Leng, M. 2004: Reappraisal of the K–T boundary at Stevns Klint, Denmark. Journal of the Geological Society, London 161, 885–892. https://doi.org/10.1144/0016-764903-071

Hart, M.B., Feist, S.E., Håkansson, E., Heinberg, C., Price, G.D., Leng, M.J. & Watkinson, M.P. 2005: The Cretaceous–Palaeogene boundary succession at Stevns Klint, Denmark: Foraminifers and stable isotope stratigraphy. Palaeogeography, Palaeoclimatology, Palaeoecology 224, 6–26. https://doi.org/10.1016/j.palaeo.2005.03.029

Heinberg, C. 1976: Bivalves from the white chalk (Maastrichtian) of Denmark: Limopsidae. Bulletin of the Geological Society of Denmark 25, 57–70.

Heinberg, C. 1978: Bivalves from the white chalk (Maastrichtian) of Denmark, II: Arcoida. Bulletin of the Geological Society of Denmark 27, 105–116.

Heinberg, C. 1979a: Evolutionary ecology of nine sympatric species of the pelecypod *Limopsis* in Cretaceous chalk. Lethaia 12, 325–340. https://doi.org/10.1111/j.1502-3931.1979.tb01018.x

Heinberg, C. 1979b: Bivalves from the white chalk (Maastrichtian) of Denmark, III: Cuspidariidae. Bulletin of the Geological Society of Denmark 28, 39–45.

Heinberg, C. 1989: Bivalves from the white chalk (Maastrichtian) of Denmark, IV: Nucoloida. Bulletin of the Geological Society of Denmark 37, 227–236. https://doi.org/10.37570/bgsd-1988-37-18

Heinberg, C. 1993: *Birkelundita*, a new genus (Bivalvia, Cardiacea) from the Upper Cretaceous white chalk of Europe. Bulletin of the Geological Society of Denmark 40, 185–195. https://doi.org/10.37570/bgsd-1993-40-09

Heinberg, C. 1999a: Depositional setting of the K/T boundary clay, and its implications for the interpretation of the biological turnover, Stevns Klint, Denmark. 19th Regional

European Meeting of Sedimentology, Copenhagen 1999, Abstracts, p. 108.

Heinberg, C. 1999b: Lower Danian bivalves, Stevns Klint, Denmark: Continuity across the K/T boundary. Palaeogeography, Palaeoclimatology, Palaeoecology 154, 87–106. https://doi.org/10.1016/S0031-0182(99)00088-7

Kaminski, M.A. & Malmgren, B.A. 1989: Stable isotope and trace element stratigraphy across the Cretaceous Tertiary boundary in Denmark. Geologiska Föreningens i Stockholm Förhandlingar 111, 305–312. https://doi.org/10.1080/11035898909453128

Kjellström, G.J & Hansen, J.M. 1981: Dinoflagellate biostratigraphy of the Cretaceous–Tertiary boundary in southern Scandinavia. Geologiska Föreningens i Stockholm Förhandlingar 103, 211–228. https://doi.org/10.1080/11035898109454523

Larsen, N. & Håkansson, E. 2000: Microfacies mosaics across latest Maastrichtian bryozoan mounds in Denmark. 11th International Bryozoology Association Conference 272–281.

Leighton, A.D., Hart, M.B., Smart, C.W. 2011: A preliminary investigation into calcareous dinoflagellate cysts and problematic microfossils from an expanded Cretaceous/Paleogene boundary section at Kulstirenden, Stevns Klint, Denmark. Cretaceous Research, 32, 606–617. https://doi.org/10.1016/j.cretres.2011.05.011

Lykke-Andersen, H. & Surlyk, F. 2004: The Cretaceous–Palaeogene boundary at Stevns Klint, Denmark: inversion tectonics or sea-floor topography. Journal of the Geological Society, London 161, 343–352. https://doi.org/10.1144/0016-764903-021

Machalski, M. & Heinberg, C. 2005: Evidence for ammonite survival into the Danian (Paleogene) from the Cerithium Limestone at Stevns Klint, Denmark. Bulletin of the Geological Society of Denmark 52, 97–111. https://doi.org/10.37570/bgsd-2005-52-08

Pedersen, S.A.S. 2011: Rockfalls at Stevns Klint. Landslide hazard assessment based on photogrammetrical supported geological analysis of the limestone cliff Stevns Klint in eastern Denmark. GEUS rapport 2011/93, 25 pp.

Perch-Nielsen, K. 1979a: Calcareous nannofossil zonation at the Cretaceous/Tertiary boundary in Denmark. In: Birkelund, T. & Bromley, R.G: (eds): Cretaceous–Tertiary boundary events. I. The Maastrichtian and Danian of Denmark, 115–135. Copenhagen: University of Copenhagen.

Perch-Nielsen, K. 1979b: Calcareous nannofossils in Cretaceous/Tertiary boundary sections in Denmark. In: Christensen, W.K. & Birkelund, T. (eds): Cretaceous–Tertiary boundary events. II. Proceedings, 120–126. Copenhagen: University of Copenhagen.

Perch-Nielsen, K., Ulleberg, K. & Evensen, J.A., 1979: Comments on the terminal Cretaceous event. In: Christensen, W.K. & Birkelund, T. (eds): Cretaceous–Tertiary boundary events. II. Proceedings, 106–111. Copenhagen: University of Copenhagen.

Rasmussen, J.A., Heinberg, C. & Håkansson, E. 2005: Planktonic foraminifers, biostratigraphy and the diachronous nature of the lowermost Danian Cerithium Limestone at Stevns Klint, Denmark Bulletin of the Geological Society of Denmark 52,

113–131. https://doi.org/10.37570/bgsd-2005-52-09

Rosenkrantz, A. 1924: Nye Iagttagelser over Cerithiumkalken i Stevns Klint med bemærkninger om Grænsen mellem Kridt og Tertiær. Meddelelser fra Dansk Geologisk Forening 6, 28–31.

Rosenkrantz, A. 1937: Bemærkninger om det østsjællandske Daniens stratigrafi og tektonik. Meddelelser fra Dansk Geologisk Forening 10 152–158.

Rosenkrantz, A. 1939: Faunaen i Cerithiumkalken og det hærdnede Skrivekridt i Stevns Klint. Meddelelser fra Dansk Geologisk Forening 9, 4, 509–514.

Rosenkrantz, A. 1966: Die Senon/Dan Grenze in Dänemark. Ber. Deutsch. Ges. Geol. Wiss. A. 11, 721–727.

Schmitz, B. 1985: Metal precipitation in the Cretaceous–Tertiary boundary clay at Stevns Klint, Denmark. Geochimica et Cosmochimica Acta 49, 2361–2370. https://doi.org/10.1016/0016-7037(85)90236-4

Schmitz, B., Andersson, P. & Dahl, J. 1988: Iridium, sulfur isotopes and rare earth elements in the Cretaceous–Tertiary boundary clay at Stevns Klint, Denmark. Geochimica et Cosmochimica Acta 52, 229–236. https://doi.org/10.1016/0016-7037(88)90072-5

Schmitz, B., Keller, G. & Stenvall, O. 1992: Stable isotopes and foraminiferal changes across the Cretaceous–Tertiary boundary at Stevns Klint, Denmark: Arguments for long-term oceanic instability before and after bolide-impact event. Palaeogeography, Palaeoclimatology, Palaeoecology 96, 233–260. https://doi.org/10.1016/0031-0182(92)90104-D

Sepúlveda, J., Wendler, J.E., Summons, R.E., Hinrichs, K.-U. 2009: Rapid Resurgence of Marine Productivity After the Cretaceous-Paleogene Mass Extinction. Science, 326(5949), 129–132. https://doi.org/10.1126/science.1176233

Surlyk, F. 1979: Maastrichtian brachiopods from Denmark. In: Birkelund, T. & Bromley, R.G: (eds): Cretaceous–Tertiary boundary events. I. The Maastrichtian and Danian of Denmark, 45–50. Copenhagen: University of Copenhagen.

Surlyk, F. 1984: The Maastrichtian Stage in NW Europe, and its brachiopod zonation. Bulletin of the Geological Society of Denmark 33, 217–223. https://doi.org/10.37570/bgsd-1984-33-20

Surlyk, F. 1997: A cool-water carbonate ramp with bryozoan mounds: Late Cretaceous – Danian of the Danish Basin. In James, N.P. & Clarke, J.A.D. (eds), Cool-water carbonates. SEPM Special Publication 56, 293–307. https://doi.org/10.2110/pec.97.56.0293

Surlyk, F., Damholt, T. & Bjerager, M. 2006: Stevns Klint, Denmark: Uppermost Maastrichtian chalk, Cretaceous–Tertiary boundary, and lower Danian bryozoan mound complex. Bulletin of the Geological Society of Denmark 54, 1–48. https://doi.org/10.37570/bgsd-2006-54-01

Surlyk, F. & Lykke-Andersen, H. 2007: Contourite drifts, moats and channels in the Upper Cretaceous chalk of the Danish Basin. Sedimentology 54, 405–422. https://doi.org/10.1111/j.1365-3091.2006.00842.x

Surlyk, F. & Nielsen, J.M. 1999: The last ammonite? Bulletin of the Geological Society of Denmark 46, 115–119. https://doi.org/10.37570/bgsd-1999-46-10

Surlyk, F., Rasmussen, S.L., Boussaha, M., Schiøler, P., Schovsbo, N.H., Sheldon, E., Stemmerik, L. & Thibault, N. 2013. Upper Campanian – Maastrichtian holostratigraphy of the eastern Danish Basin. Cretaceous Research 46, 232–256. https://doi.org/10.1016/j.cretres.2013.08.006

Svendsen, N. 1975: Carbonat-sedimentologiske studier af to profiler 300 m nord for Højerup Kirke. Unpublished MSc Thesis, 68 pp, University of Copenhagen, Copenhagen.

Thomsen, E. 1975: Kalk og kridt i den danske undergrund. In: Nielsen, O.B. (ed.): Danmarks geologi fra Kridt til i dag. Aarhus Geokompendier 1, 31–67.

Zhao, M. & Bada, J.L. 1989: Extraterrestrial amino acids in Cretaceous/Tertiary boundary sediments at Stevns Klint, Denmark. Nature 339, 463–465. https://doi.org/10.1038/339463a0

Instructions to authors

See also www.2dgf.dk/publikationer/bulletin/vejledning.html

The Bulletin publishes articles normally not exceeding 30 printed pages, and short contributions not longer than 4 pages. Longer articles and monographs are also published, but in this case it is advisable to consult the chief editor before submitting long manuscripts. Short contributions may be comments on previously published articles, presentation of current scientific activities, short scientific notes, or book reviews.

Manuscripts with complete sets of illustrations, tables, captions, etc., should be submitted electronically to the chief editor (obe@geus.dk). The **main text** with references and figure captions should be in Word format, figures should be in either pdf, jpeg, or tiff format, and tables should be in Excel or Word format. Word tables should be ordinary text files with tab spacing between table columns; Word's 'table function' is discouraged. Compare published articles for table layout.

Manuscripts will be reviewed by two referees; suggestions of referees are welcome. The final decision on whether or not a manuscript will be accepted for publication rests with the chief editor, acting on the advice of the scientific editors. Articles will be published in the order in which they are accepted and produced for publication.

Manuscript

Language – Manuscripts should be in English. Authors who are not proficient in English should ask an English-speaking colleague for assistance before submission of the manuscript.

Title – Titles should be short and concise, with emphasis on words useful for indexing and information retrieval. An abbreviated title to be used as running title may also be submitted.

Abstract – An abstract in English must accompany all papers. It should be short, factual, and stress new information and conclusions rather than describing the contents of the manuscript. Conclude the abstract with a list of key words.

Main text – Use 1.5 or double spacing throughout, and leave wide margins. Italics should be used only in generic and species names and in some Latin abbreviations (e.g. c, *et al.*, ibid., op. cit).

Spelling – Geological units named after localities in Greenland, formal lithostratigraphical units and intrusions named after localities in Greenland remain unchanged even if the eponymous locality names have since been changed in accordance with modern Greenlandic orthography.

References to figures, tables and papers – References to figures and tables in the text should have the form: Fig. 1, Figs 1–3, Table 3 or as (Smith 1969, fig. 3) when the reference is to a figure in a cited paper.

References to papers are given in the form Smith (1969) or (Smith 1969). Combined citations by different authors are separated by a semicolon; two or more papers by same author(s) are separated by commas. Citations are mentioned chronologically and then alphabetically. Use 'et al.' for three or more authors, e.g. Smith *et al.* (1985).

Reference list

Use the following style:

Smith, A.A. 1989: Geology of the Bulbjerg Formation. Bulletin of the Geological Society of Denmark 38, 119–144. [Note that name of journal is given in full].

Smith, A.A., Jensen, B.B. & MacStuff, C.C. 1987: Sandstones of Denmark, 2nd edition, 533 pp. New York: Springer Verlag. [For more than 10 authors, use first author followed by *et al.*].

Smith, A.A., Jensen, B.B. & MacStuff, C.C. 1992: Characterization of Archean volcanic rocks. In: Hansen, D.D. *et al.* (eds): Geology of Greenland. Geological Survey of Denmark and Greenland Bulletin 40, 1397–1438. [More than three editors – therefore *et al.* form is used].

Sorting – Danish letters æ, ø and å (aa) are treated as ae, o and a (aa), respectively.

References are sorted by:

1) Alphabetically by the first author's surname. 2) Papers by one author: two or more papers are arranged chronologically. 3) Papers by two authors: alphabetically after second author's name. Two or more papers by the same two authors: chronologically. 4) Papers by three or more authors: chronologically. Papers from the same year are arranged alphabetically after second, third, etc. author's name. Authors themselves are responsible for the accuracy and completeness of their references. The reference list must include all, and only, the references cited in the paper (including figures, tables etc).

CrossRef

Please add hyperlinks to Crossref DOI when you create your citation list whenever possible.

Illustrations

May be prepared in either black and white or colour. There is no colour charge. Horizontal illustrations are much to be preferred. Size of smallest letters in illustrations should not be less than 5.5 pt. Remember scale.

All figures (including photographs) should be submitted in electronic form ready for direct reproduction, i.e. having the dimensions of the final figure with a standard resolution of 300 dpi for photographs. Preferred formats are pdf, tiff and jpg.

Size – Width: All widths up to full page width (170 mm) are accepted. Maximum height is 223 mm. Design figure contents to match the preferred figure size.

Captions – Captions to figures and plates must be delivered on separate pages, preferably at the end of the manuscript.

Supplementary data files

Supplementary files are accepted. Such files may provide e.g. analytical data tables, detailed data documentation, illustrations with special effects, or videos.

Proofs

Authors receive page proofs of the article after technical production. The cost of any alterations against the final manuscript will be charged to the author.

Content, vol. 69

Instructions to authors:
See inside the back cover and also www.2dgf.dk/publikationer/bulletin/vejledning.html